UNCLASSIFIED

AD NUMBER

AD826319

NEW LIMITATION CHANGE

TO

Approved for public release, distribution unlimited

FROM

Distribution authorized to U.S. Gov't. agencies and their contractors; Administrative/Operational Use; MAY 1967. Other requests shall be referred to Air Force Flight Dynamics Lab., Research and Technology Div., Wright-Patterson AFB, OH 45433.

AUTHORITY

AFSC/DOOS[WPAFB]Ltr, dtd 30 Jul 1991

THIS PAGE IS UNCLASSIFIED

THIS REPORT HAS BEEN DELIMITED
AND CLEARED FOR PUBLIC RELEASE
UNDER DOD DIRECTIVE 5200.20 AND
NO RESTRICTIONS ARE IMPOSED UPON
ITS USE AND DISCLOSURE.

DISTRIBUTION STATEMENT A

APPROVED FOR PUBLIC RELEASE;
DISTRIBUTION UNLIMITED.

U

67-050161
AFFDL-TR-66-195-Volume I

WAD: R 005-[illegible]

AD826319

FOR OFFICIAL USE ONLY

THE X-19 V/STOL TECHNOLOGY - A CRITICAL REVIEW

Wright Aeronautical Division
Curtiss-Wright Corporation
Wood-Ridge, New Jersey 07075

TECHNICAL REPORT AFFDL-TR-66-195
May 1967

Air Force Flight Dynamics Laboratory
Research and Technology Division
Air Force Systems Command
Wright-Patterson Air Force Base, Ohio

Each transmittal of this document outside the agencies of the U.S. Government must have prior approval of the Air Force Flight Dynamics Laboratory, V/STOL Technology Division (FDV), Wright-Patterson Air Force Base, Ohio 45433.

355

When Government drawings, specifications, or other data are used for any purpose other than in connection with a definitely related Government procurement operation, the United States Government thereby incurs no responsibility nor any obligation whatsoever; and the fact that the Government may have formulated, furnished, or in any way supplied said drawings, specifications, or other data, is not to be regarded by implication or otherwise as in any manner licensing the holder or any other person or corporation, or conveying any rights or permission to manufacture, use, or sell any patented invention that may in any way be related thereto.

3

Copies of this report should not be returned to the Research and Technology Division unless return is required by security considerations, contractural obligations or notice on a specific document.

AFFDL-TR-66-195-Volume I

Copy 58 of 100

THE X-19 V/STOL TECHNOLOGY - A CRITICAL REVIEW

Harold Fluk
"et al"

Each transmittal of this document outside the agencies of the U.S. Government must have prior approval of the Air Force Flight Dynamics Laboratory, V/STOL Technology Division (FDV), Wright-Patterson Air Force Base, Ohio 45433.

FOREWORD

The purpose of this report is to present a critical review and summary of the V/STOL technology involved in the development, component testing, ground testing, and flight testing of the X-19 aircraft. It is the final report of work accomplished by Curtiss-Wright Corporation, VTOL Systems Division, located at Caldwell, New Jersey, under Contract Number AF 33(615)-3940. The contract was administered under the direction of Captain R. M. Berg and Mr. B. Lindenbaum, FDV, Air Force Flight Dynamics Laboratory, (RTD), Wright-Patterson AFB, Ohio.

The following Curtiss-Wright Corporation personnel made the principal contributions to this report:

H. V. Borst, Chief Engineer - Technical Services
W. F. Meyer, Chief of Structures
W. Amott, Mechanical Systems Group Leader - Structures
H. Fluk, Flight Loads Group Leader - Aerodynamics
J. H. Barker, Stability and Control Group Leader - Aerodynamics
E. L. Hassell, X-19 Performance Group Leader - Aerodynamics
E. J. Tursich, Project Engineer, P.D. - Aerodynamics

Because of the breadth of material required to be treated by the contract statement of work, each of the thirteen sections has been treated as an entity. Thus, each section has its own nomenclature, text, figures, and references. In some instances, nomenclature has been written into the text for convenience. Otherwise, it appears on the reverse side of the section divider page. The separation of nomenclature by section is intended to prevent confusion over the duplicity of meanings attached to given symbols by the different disciplines treated in the report.

It is to be noted that some of the material contained in this report is proprietary to Curtiss-Wright and is so stamped. The report is releasable only to agencies of the United States Government. Release of the report to any other organizations or individuals must have the approval of Curtiss-Wright.

Information in this report is embargoed under the Department of State International Traffic In Arms Regulations. This report, or information extracted from it, may be released to foreign governments by departments or agencies of the U. S. Government subject to approval of The Air Force Flight Dynamics Laboratory, or higher authority within the Department of the Air Force. Private individuals or firms require a Department of State export license.

Publication of this report does not constitute Air Force approval of the reports findings or conclusions. It is published only for the exchange and stimulation of ideas.

WILLIAM E. LAMAR
Deputy Director
Air Force Flight Dynamics Laboratory

ABSTRACT

This report contains a condensed description of the X-19 V/STOL Technolo[illegible] . The broad categories discussed, include in Section I, a review of the developments leading up to the X-19 program. Sections II through VI are devoted entirely to the propellers, and the considerations involved in design. The Radial Force principle is postulated in Section II. Interference effects on the wings due to the propellers are discussed in Section III. The propeller aerodynamic design in hover and cruise is presented in Section IV. Section V is devoted to the structure and control mechanisms of the propeller. Section VI relates to the use of propellers as an airplane control device. The tandem wing principle is discussed in Section VII covering stability, control, and drag. Section VIII is devoted solely to Ground Effects. The sizable wind tunnel research activity leading up to the X-19 is presented in Section IX. The structural loads in hover, transition and cruise are discussed in Section X. Section XI presents information pertinent to landing procedures in hover or cruise in the event of power failure. A summary of the flight test program is given in Section XII, including aircraft and hardware performance characteristics. Finally, Section XIII is devoted to a general discussion and assessment of the aircraft's unorthodox features.

TABLE OF CONTENTS

SECTION		PAGE
I	REVIEW OF DEVELOPMENTS LEADING TO THE X-19 PROGRAM	1
	1. REPORT OBJECTIVE	1
	2. BACKGROUND HISTORY	1
	3. X-100 AIRPLANE	2
	4. M-200 OPERATIONAL AIRCRAFT	6
	a. Initial Design Objectives	6
	(1) Tandem Wing Design Considerations	6
	(2) Turbo-Prop System	8
	(3) Selection of Hover Disk Loading	8
	(4) Selection of Fixed Wing System	9
	(5) Selection of Tandem Wing Four Propeller Configuration	9
	5. TRI-SERVICE X-19 (CW MODEL 200 DIMENSIONS AND GENERAL DATA)	10
	REFERENCES	17
II	RADIAL FORCE PRINCIPLE	19
	1. INTRODUCTION	19
	2. THEORY AND METHOD FOR COMPUTING PROPELLER FORCES	19
	a. General	19
	b. Theory of Normal Force and Yawing Moment	25
	3. APPLICATION OF PROPELLER RADIAL LIFT TO V/STOL AIRCRAFT	35
	a. General	35
	b. Application in Cruise	37
	c. Application in Transition	38
	d. Summary	43
	4. CORRELATION OF CALCULATED AND TEST RESULTS	43
	REFERENCES	51
III	WING-PROPELLER INTERFERENCE EFFECTS	53
	1. INTRODUCTION	53
	2. LIFT LOSS IN HOVER	53
	a. Theory	53
	b. Download Test Data	54
	c. Predicted Download	73
	3. PERIODIC FORCES ON WINGS AND PROPELLERS IN HOVER	73
	4. SUMMARY OF FORCES ON WINGS AND PROPELLERS	74
	a. Wings and Propellers out of Ground Effect	74
	b. Wings and Propellers in Ground Effect	97
	c. Net Forces in and out of Ground Effect	116
	5. FLAP DEFLECTION INTERFERENCE EFFECTS IN TRANSITION	120
	REFERENCES	121

TABLE OF CONTENTS (CONT'D)

SECTION PAGE

IV PROPELLER AERODYNAMIC DESIGN 123
1. BLADE GEOMETRIC CHARACTERISTICS 123
2. AERODYNAMIC DESIGN 130
3. HOVER PERFORMANCE AS MEASURED AND CALCULATED 131
4. CRUISE PERFORMANCE MAPS 138
5. EFFECTS OF TIP SPEED AND BLADE TWIST IN HOVER AND CRUISE 138
6. HOVER POWER HISTOGRAMS 149
REFERENCES 155

V PROPELLER STRUCTURE AND CONTROL MECHANISM 157
1. MECHANICAL DESIGN INCLUDING PHILOSOPHY, RELIABILITY, WEIGHT AND MAINTENANCE 157
    a. General Description 157
    b. Component Descriptions 157
    c. Blade Maintenance 162
    d. Reliability 167
    e. Propeller Weight 168
2. BLADE STRUCTURAL DESIGN 168
    a. General 168
    b. Blade Design 171
    c. Design Details - 13166A10P3 190
    d. Design Details - 13166A12P3 Design 199
    e. Structural Analysis 199
    f. Full Scale Blade Testing 210
3. PROPELLER DESIGN LOADING THEORY AND TEST 228
    a. General 228
    b. Theoretical Propeller Loading 228
    c. Propeller Test Loads 233
4. WEIGHT COMPARISON OF X-19 FIBERGLASS PROPELLER 238
    a. Blade Weight Studies 238
    b. Hub Weight Studies 238
5. PROPELLER STRUCTURAL PROBLEMS 242
    a. Blades 242
    b. Blade Shank 243
    c. Hubs 245
    d. Blade Pitch Control 245
    e. Propeller Housing 246
6. PROPELLER INDUCED LOADS 247
    a. Theoretical Loads 247
    b. Airframe Test Results 248
7. PROPELLER TESTING 254
    a. Propeller Hub Static Test 254
    b. Laboratory Whirl Test 257
    c. Electric Motor Whirl Test of X-19 Propeller 265
    d. 1 X P Gyroscopic Endurance 272
    e. Half Systems Rig Testing 276
REFERENCES 282

TABLE OF CONTENTS (CONT'D)

SECTION PAGE

VI AIRCRAFT CONTROL BY PROPELLER THRUST MODULATION 283
1. INTRODUCTION 283
2. CONTROL POWERS 300
3. TIME CONSTANT FOR PROPELLER FORCES 296
4. PROPELLER POWER INCREMENTS DUE TO CONTROL APPLICATION 299
5. CONTROL COUPLING AND RESPONSE 299
6. PROPELLER CONTRIBUTION TO CENTER OF GRAVITY MOMENTS - TRANSITION 301
7. CONTROL DEFICIENCIES AND ACTIONS 310
8. PROPELLER POWER PENALTIES DUE TO CONTROL INPUT DEVIATIONS 313
REFERENCES 318

VII TANDEM WING AIRPLANE 319
1. FLIGHT CONTROL OF TANDEM WING AIRCRAFT 319
  a. Transition Flight Regime 319
    (1) Introduction 319
    (2) Assumptions 319
    (3) Stability 319
    (4) Control and Control Systems 321
  b. Cruise Flight Regime 335
    (1) Introduction 335
    (2) Assumptions 335
    (3) Stability 335
    (4) Controls and Control Systems 349
    (5) Maneuvering Flight 351
2. AERODYNAMIC CHARACTERISTICS (DRAG) OF TANDEM-WING SYSTEM 360
  a. Basic Data 360
  b. Drag Estimate 361
  c. Propellers off - Incompressible Profile Drag 361
  d. Effects of Lift, Power, and Compressibility 361
  e. Lift/Drag Ratio 366
3. TEST AND THEORY COMPARISON OF AERODYNAMIC AND FLIGHT CONTROL CHARACTERISTICS 366
  a. Aerodynamic 366
  b. Flight Control 370
4. AIRCRAFT BEHAVIOR IN GROUND EFFECT 370
5. FLIGHT CONTROL DEFICIENCIES 370
  a. Transition Flight Regime 370
    (1) Introduction 370
    (2) Stability 371
    (3) Control 372
  b. Cruise Flight Regime 372
    (1) Introduction 372

TABLE OF CONTENTS (CONT'D)

SECTION PAGE

(2) Stability 373
(3) Control 375
6. AVAILABLE C.G. RANGE 376
7. TILT, FLAP AND BLADE ANGLE PHASING 378
a. Nacelle Tilt Phasing 378
b. Flap and Collective Aileron Phasing 379
c. Propeller Blade Angle Phasing 381
(1) Auto Trim Schedule 381
(2) Pitch Gain Schedule 381
(3) Roll Gain Schedule 386
(4) Yaw Gain Schedule 386
8. CONTROL MIXING 386
REFERENCES 389

VIII GROUND EFFECTS 391
1. INTRODUCTION 391
2. GROUND EFFECTS UPON STABILITY AND CONTROL 391
3. FLOW FIELD RECIRCULATION - ENGINE INLET 393
4. HOVER POWER REQUIREMENT WITH GROUND HEIGHT 394
REFERENCES 398

IX WIND TUNNEL TESTS 399
1. INTRODUCTION 399
2. TESTS IN SUPPORT OF X-19 AND X-100 AIRCRAFT 399
a. General 399
b. Test Models 400
c. Test Uses of Models 400
d. Model Variations 401
e. Wind Tunnel Test Facilities Used 402
f. Other Applicable Test Programs 427
3. TESTS IN SUPPORT OF ADVANCED TANDEM WING CONCEPTS 431
4. TRANSITION WIND TUNNEL WALL CORRECTIONS 432
5. CORRECTIONS OF MODEL PROPELLERS TO FULL SCALE RESULTS 433
REFERENCES 444

X STRUCTURAL LOADS 447
1. INTRODUCTION 447
2. CRUISE LOADS 447
a. General 447
b. Propeller-off Distributions 447
c. Effects of Power 448
d. Effects of Mach Number 448
e. Effects of Reynolds Number 463
f. Effects of Aeroelastic Twist 463
g. Drag Distribution 464
h. Flight Envelope 465

TABLE OF CONTENTS (CONT'D)

SECTION PAGE

i. Symmetrical Gust Envelopes 465
j. Balance Equations 467
k. Load Breakdowns 471
l. Spanwise Lift Distribution 471
3. HOVER LOADS 481
a. General 481
b. Symmetrical Trimmed Thrusts 481
c. Trim Button 483
d. Throttle and Control Excursions 488
e. Design Criteria 488
4. TRANSITION LOADS 489
a. General 489
b. Airplane Characteristics 489
c. Design Control Loads Criteria 495
d. Design Maneuvers and Flight Envelopes 505
e. Design Gust Loads Criteria 505
5. DESIGN GROUND LOADS CRITERIA 514
REFERENCES 515

XI POWER-OFF CONSIDERATIONS 517
1. SAFE OPERATING ENVELOPE 517
2. ENGINE FAILURE CONSIDERATIONS 517
3. POWER-OFF CHARACTERISTICS VS SPEED AND ALTITUDE (WIND MILLING) 519
4. AUTOROTATIVE CHARACTERISTICS 529

XII FLIGHT TEST SUMMARY 535
1. INTRODUCTION 535
2. HISTORY OF X-19 TEST FLIGHTS 536
a. Historical Progression 536
b. Simplified Flight Test Schedule at Curtiss Wright 536
c. Flight Test Schedule at NAFEC 545
d. Aircraft used in Flight Tests 548
3. AIRCRAFT CONFIGURATION VS TIME 564
a. Aircraft at Beginning of Flight No. 8 564
b. Configuration Changes During Test Program 565
c. Configuration at Flight No. 50 571
d. Flight Test Instrumentation Thru Flight No. 37 571
e. Flight Test Instrumentation at NAFEC 571
4. AIRCRAFT PERFORMANCE RESULTS USING STEADY STATE DATA 575
a. Overall Airplane Performance From Flight Tests 575
b. Hovering Performance 575
c. Conversion/Reconversion Flight Maneuvers 575
d. Power Required 575

TABLE OF CONTENTS (CONT'D)

SECTION		PAGE
	e. Thrust-Power Download	582
	f. Ground Effect	583
	g. System Thrust Response to Power Excursions	587
	h. Fuel Consumption	587
	5. AIRCRAFT STABILITY AND CONTROL	592
	a. Initial Hover Stability and Control Results	592
	b. Pilot Operation Rating	592
	c. Flight Tests With S.A.S. Inoperative	592
	d. STOL Operations	602
	REFERENCES	603
XIII	ASSESSMENT OF RESULTS AND CONCLUSIONS	605
	1. INTRODUCTION	605
	2. OVERALL X-19 CONCEPT AND ITS DERIVATION	605
	a. Radial Lift Propellers	605
	b. Tilt Propeller, Fixed Wing Configuration	606
	c. Tandem Wing Configuration	608
	d. Control Power	612
	e. Transmission Design Philosophy	613
	f. Gust Sensitivity	615
	g. Propeller Control Problems	615
	3. OPERATIONAL FLIGHT CONSIDERATIONS	617
	a. Engine-out Safety	617
	b. Cruise Stall Characteristics	617

LIST OF ILLUSTRATIONS (CONT'D)

FIGURE NO.		PAGE
39	X-19, thrust coefficient as a function of thrust axis angle of attack.	82
40	Propeller 156109, thrust coefficient as a function of power parameter.	84
41	Propeller 156109, thrust coefficient as a function of power parameter.	85
42	X-19, variation of front propeller lift and thrust coefficient with thrust axis angle of attack.	86
43	X-19, variation of rear propeller lift and thrust coefficient with thrust axis angle of attack.	87
44	X-19, variation of front wing lift coefficient with nacelle tilt angle.	89
45	X-19, variation of rear wing lift coefficient with nacelle tilt angle.	90
46	X-19, variation of front wing drag coefficient with nacelle tilt angle.	91
47	X-19, variation of rear wing drag coefficient with nacelle tilt angle.	92
48	X-19, incremental front wing lift coefficient, due to front propeller wash, with variation in thrust axis angle of attack.	93
49	X-19, incremental rear wing lift coefficient, due to all wash, with variation in rear thrust axis angle of attack.	94
50	X-19, incremental front wing thrust coefficient, due to front propeller wash, with variation in thrust axis angle of attack.	95
51	X-19, incremental rear wing thrust coefficient, due to all wash, with variation in rear thrust axis angle of attack.	96
52	X-19, installed rear wing lift curve.	98
53	X-19, installed rear wing spanwise lift distribution, propellers off.	99
54	X-19, installed rear wing spanwise lift distribution.	100
55	X-19, installed rear wing spanwise lift distribution.	101
56	X-19, installed rear wing spanwise lift distribution.	102
57	X-19, installed rear wing lift curve.	103
58	X-19, installed rear wing spanwise lift distribution, propellers off.	104
59	X-19, installed rear wing spanwise lift distribution.	105
60	X-19, installed rear wing spanwise lift distribution.	106

LIST OF ILLUSTRATIONS (CONT'D)

FIGURE NO.		PAGE
61	X-19, installed rear wing spanwise lift distribution.	107
62	X-19, installed rear wing lift curve.	108
63	X-19, installed rear wing spanwise lift distribution.	109
64	X-19, installed rear wing lift curve.	110
65	X-19, installed rear wing spanwise lift distribution.	111
66	X-19, front propeller thrust coefficient.	112
67	X-19, rear propeller thrust coefficient.	113
68	X-19, front propeller power coefficient.	114
69	X-19, rear propeller power coefficient	115
70	X-19, airplane lift characteristics, ground effects.	117
71	X-19, airplane drag characteristics, ground effects.	118
72	X-19, airplane moment characteristics, ground effects; c.g. @ 42.8% lift chord and W.L. 123.8 inches.	119
	SECTION IV	123
73	Blade characteristics of the Curtiss-Wright X-100 propeller 3(X100188) blade; Dia. = 10 ft., AF = 188, IC_{Li} = 0.068.	124
74	Blade characteristics of the X-19 propeller 3(130168) blade; Dia. = 13 ft., AF = 168, IC_{Li} = 0.057.	125
75	Power loading as a function of disk loading on a static isolated propeller; density ratio $\sigma = 1.0$.	126
76	Typical drag polar as a function of design C_L.	128
77	Blade angle and thrust coefficient as a function of power coefficient, static performance, 3(X100188) blade, 500 to 800 πnD.	132
78	Thrust coefficient as a function of power coefficient, static whirl test dated 7/19/60, WPAFB whirl rig No. 2; Model 138592/10188A2F, Dia. = 10 ft., AF = 188, IC_{Li} = 0.068; 1000 horsepower, NACA 64 section series.	133
79	Blade angle as a function of power coefficient, static whirl test dated 7/9/60, WPAFB whirl rig No. 2; Model 138542/10188A2F, Dia. = 10 ft., AF = 188, IC_{Li} = 0.068; 1000 horsepower.	134
80	X-19 thrust coefficient as a function of power coefficient, static, Wright Field whirl rig No. 2; 3(1368A10P3), Dia. = 13 ft., AF = 168, IC_{Li} = 0.057, NACA 64 Series sections, 1000 horsepower.	135

LIST OF ILLUSTRATIONS (CONT'D)

FIGURE NO. PAGE

81 X-19, propeller blade angle as a function of power coefficient, static, Wright Field Whirl Rig. No. 2; 3(13168A10P3), Dia. = 13 ft. AF = 168, IC_{L_i} = 0.057, NACA 64 Series sections, 1000 horsepower. 133

82 X-19, Figure of Merit as a function of power coefficient, static, Wright Field Whirl Rig. No. 2; 3 (13168A10P3), Dia. = 13 ft., AF = 168, IC_{L_i} = 0.057, NACA 64 series sections, 1000 horsepower. 137

83 X-19, thrust coefficient versus power coefficient, static; 3(13168A10P3) blade, Curtiss Wright Whirl Test Rig. 139

84 X-19, propeller blade angle versus power coefficient, static; 3(13168A10P3) blade, Curtiss Wright Whirl Test Rig. 140

85 Propeller cruise efficiency map, Curtiss-Wright X-100 propeller, 3(X100188); AF = 188 Dia. = 10 ft., IC_{L_i} = 0.057, forward Mach No. 0.3 or less. 141

86 X-19, propeller cruise efficiency map, 3(13168A10P3) blade; AF = 168, Dia. = 13 ft., IC_{L_i} = 0.057, forward Mach No. = 0.3 or less. 142

87 X-19, propeller cruise efficiency map, 3(13168A10P3) blade; AF = 168, Dia. = 13 ft., IC_{L_i} = 0.057, forward Mach No. = 0.4. 143

88 X-19, propeller cruise efficiency map, 3(13168A10P3) blade; AF = 168, Dia. = 13 ft., IC_{L_i} = 0,057, forward Mach No. = 0.5. 144

89 X-19, propeller cruise efficiency map, 3(13168A10P3) blade; AF = 168, Dia. = 13 ft., IC_{L_i} = 0.057, forward Mach No. = 0.6. 145

90 X-19, propeller cruise efficiency map, 3(13168A10P3) blade; AF = 168, Dia. = 13 ft., IC_{L_i} = 0.057, forward Mach No. = 0.7. 146

91 X-19, propeller cruise efficiency map, 3(13168A10P3) blade; AF = 168, Dia. = 13 ft., IC_{L_i} = 0.057, forward Mach No. 0.8. 147

92 Blade characteristics of the Curtiss-Wright 109652 propeller blade; Dia. = 15 ft., AF = 115, IC_{L_i} = 0.5, NACA 65 section series. 148

93 Figure of merit of the Curtiss-Wright 109652 propeller blade as a function of power coefficient measured on Curtiss-Wright Test Rig. 150

94 Effect of blade retwist on the Figure of Merit; 3(109652) blade, 900 πnD, three blades. 151

95 X-19, histogram of transverse shaft loading flight No. 31, 12/23/64. 152

LIST OF ILLUSTRATIONS (CONT'D)

FIGURE NO.		PAGE
96	X-19 histogram of transverse shaft loading, flight No. 35, 1/7/65.	153
	SECTION V	157
97	X-19, schematic assembly of the blade pitch change mechanism.	158
98	Blade schematic illustrating the typical construction of the lightweight fiberglass blade.	163
99	Fiberglass blade repair chart illustrating the type of repair that can be performed in the field.	165
100	X-19, experimental program as scheduled for the airplane, subsystems and components.	169
101	Strength to weight comparison between fiberglass and other common structural materials.	172
102	Fiberglass propeller blades which have been built and tested. From left to right: 10'-10" diameter used on X-100 aircraft, 13'-0" diameter used on X-19 aircraft, 13'-6" diameter used in static thrust testing, 13'-6" designed/for T-64 engine tested to 4000 HP, 15'-6" designed for T-64 tested to 4400 HP.	173
103	Sectioned fiberglass propeller blade showing the steel shank, fiberglass shell, and foam filler.	174
104	Epoxy fiberglass, ultimate tensile stress and tensile modulus, variation with temperature, 1 layer Stanpreg VET 181 per CPS 5037, 3 layers Stanpreg VET 43 per CPS 5038, 17 ply thickness: ASTM: D638-60T.	175
105	Epoxy fiberglass, ultimate flexural stress and modulus variation with temperature, 1 layer Stanpreg VET 181 per CPS 5037, 3 layers Stanpreg VET 43 per CPS 5038, 17 ply thickness: ASTM: D790-59T.	176
106	Epoxy fiberglass, typical tensile stress strain curve longitudinal direction, 1 layer Stanpreg VET 181 per CPS 5037, 3 layers Stanpreg VET 43 per CPS 5038, 17 ply thickness: ASTM: D638-60T.	177
107	Epoxy fiberglass, tensile stress rupture, standard room temperature, standard humidity and 100% humidity, 1 layer Stanpreg VET 181 per CPS 5037, 3 layers Stanpreg VET 43 per CPS 5038, 17 ply thickness: ASTM: D674-56.	178
108	Epoxy fiberglass, creep rupture curve longitudinal tension, tensile stress = 75000 psi. 1 layer Stanpreg VET 181 per CPS 5037, 3 layers Stanpreg VET 43 per CPS 5038, 17 ply thickness: ASTM: 674-56.	179

LIST OF ILLUSTRATIONS (CONT'D)

FIGURE NO.		PAGE
109	Epoxy figerblass, interlaminar shear variation with temperature, 1 layer Stanpreg VET 181 per CPS 5037, 3 layers Stanpreg VET 43 per CPS 5038, 17 ply thickness: Fed. Test Method Std. 406.	180
110	Epoxy fiberglass, flexural fatigue S-N curves for smooth and notched longitudinal specimens and smooth transverse specimens at room temperature, 1 layer Stanpreg VET 181 per CPS 5037, 3 layers Stanpreg VET 43 per CPS 5038, 17 ply thickness: ASTM: D671-517.	181
111	Epoxy fiberglass, modified Goodman diagram with longitudinal and transverse directions, 1 layer Stanpreg VET 181 per CPS 5037, 3 layers Stanpreg VET 43 per CPS 5038, 17 ply thickness : ASTM: D671-51T.	182
112	Epoxy fiberglass, design modified Goodman diagram as established for propeller blades, 1 layer Stanpreg VET 181 per CPS 5037, 3 layers Stanpreg VET 43 per CPS 5038.	183
113	Comparative erosion resistance of various coating materials on fiberglass.	184
114	The effect of immersion in various solvents for 7 days on the ultimate tensile strength of epoxy fiberglass with and without urethane coating.	185
115	The strength characteristics of the various adhesives selected for use in the manufacture of fiberglass reinforced plastic blades.	186
116	Typical properties of foam plastic filler as used in the fiberglass foam plastic blade. Polyether base - freon blown, A = 7.0 lbs per ft^3, B = 5.0 lb per ft^3.	188
117	Steel shank as designed for the 13166A10P3 blade. AMS 6415 vacuum melt steel, RC 42-46.	189
118	Typical shank end cracks which occurred during fabrication and which were attributed to hydrogen embrittlement.	191
119	The 13166A10P3 blade steady stress distribution for a pitching maneuver during transition flight; 927HP, 1065 rpm, 80 knots.	203
120	The 13166A10P3 blade vibratory stress distribution for a pitching maneuver during transition flight; 927HP, 1065 rpm, V = 80 knots.	204
121	Comparison of the calculated and measured steady stress distribution around the 11 in. station in the 13166A10P3 blade. Centrifugal load = 46,000 lb, bending moment = 24000 in. lb.	207

LIST OF ILLUSTRATIONS (CONT'D)

FIGURE NO. PAGE

122 Comparison of the calculated and measured vibratory stress distribution around the 11 in. station on the 13166A10P3 blade. Bending moment = ± 66,000 in.-lbs. 208

123 Calculated fixed root resonant frequencies of the 13166A10P3 fiberglass propeller blade. 209

124 Laboratory test set up for endurance testing propeller blades in the free-free mode. 211

125 Typical blade failure obtained in free-free endurance testing. This blade completed 10 X 10^6 cycles at each of ± 8000, ± 9000, ± 10,000, and ± 11,000 psi. Failure occurred at 1.2 X 10^6 cycles at the ± 12,000 psi level. 214

126 Laboratory test set up for fixed root endurance testing of propeller blades. 216

127 Typical blade fatigue failure obtained during fixed root endurance testing of the X-19 propeller blade. 217

128 Laboratory test set up for free-free torsion endurance testing of propeller blades. 218

129 Fatigue failure on blade P42-6 after 1.0 X 10^6 cycles of torsional endurance testing on blade P42-6. 220

130 Laboratory test set up for static tension test of the X-19 propeller unbonded blade shank. 222

131 X-19, propeller unbonded blade shank failure. Ultimate load was 128,000 lbs. 223

132 Blade retention, laboratory fatigue test set up. This facility simultaneously applies centrifugal force, steady bending moment, and vibratory bending moment. 224

133 Typical fatigue failure of the X-19 blade shank. 227

134 Basic velocity components at the disk of a tilted propeller disk. 229

135 Comparison of the propeller yawing and pitching moment coefficients at flow angularities close to 90°, and at low advance ratios, $\beta_{.75R} = 15°$. 235

136 Comparison of propeller normal and side force coefficients at flow angularities close to 90° at low advance ratios, $\beta_{.75R} = 15°$. 236

137 Comparison of calculated and measured blade vibratory shank stress for equilibrium transition flight of the X-19 aircraft. 237

LIST OF ILLUSTRATIONS (CONT'D)

FIGURE NO.		PAGE
138	Relative blade weight comparison considering various materials for the design of a hypothetical VTOL/STOL propeller; 15'-0" diameter, 120 A.F., 1000 HP @ 1146 rpm.	239
139	Relative blade weight comparison considering various materials for the design of a typical turboprop installation; 13'-6" diameter, 150 A.F., 4000 HP @ 1160 rpm.	240
140	Variation of blade weight with 1 X P excitation factor, Aq, for hollow steel and fiberglass blades on a typical turboprop installation; 13'-6" diameter, 165 A.F., 4500 HP 1020 rpm.	241
141	The 2 X P component of blade stress as measured during flight test on the X-19 aircraft showing a resonant trend with rpm.	250
142	Variation of the 2 X P blade stress component with rpm as measured during a ground vibration survey on the X-19 aircraft.	251
143	Variation of the 2 X P blade stress as measured during flight test of the X-19 aircraft as a function of the theoretical 2 X P parameter, $(V \sin\phi)^2 \sin\beta$.	253
144	Laboratory test facility for the static testing of propeller hubs under simulated flight steady and vibratory loading.	255
145	Stress coat patterns appearing on the X-19 propeller hub under a simulated design steady/vibratory load condition.	256
146	Location of wire strain gages around outer circumference of barrels of X-19 propeller hub 162595 during static testing in hub tension machine.	258
147	Location of wire strain gages around inner and outer periphery of ring of X-19 propeller hub 162595 during static testing in hub tension machine.	259
148	Location of wire strain gages on inner and outer surfaces of rear extension of X-19 propeller hub 162595 during static testing in hub tension machine.	260
149	X-19, propeller hub showing typical location of strain gages during static test.	261
150	Laboratory whirl test facility for qualifying the propeller nacelle assembly under simulated loading.	263
151	Maximum composite blade stress taken during propeller thrust calibration on WPAFB Electric Whirl Rig.	269

LIST OF ILLUSTRATIONS (CONT'D)

FIGURE NO.		PAGE
152	Blade stress monitoring curve taken during propeller endurance test on WPAFB electric whirl rig.	270
153	Curtiss gyroscopic test facility for qualifying full scale propellers under simulated steady and vibratory loading.	273
154	X-19 blade modified Goodman diagram showing design and gyroscopic test points.	275
155	X-19 blade vibratory stresses as monitored during the gyroscopic endurance testing.	278
156	Curtiss half systems test rig for qualifying the propulsion system of the X-19.	279
	SECTION V1	283
157	X-19, block diagram of the propeller thrust modulation system.	284
158	X-19, coordinator output stroke as a function of pitch control deflection or SAS motion.	285
159	X-19, coordinator output stroke as a function of pilot pitch trim actuator displacement.	286
160	X-19, coordinator output stroke as a function of roll control deflection or SAS motion.	287
161	X-19, coordinator output stroke as a function of yaw control (pedal) deflection.	288
162	X-19, coordinator output stroke as a function of tilt angle (auto-trim schedule).	289
163	X-19, propeller pitch control gain as a function of tilt angle (pitch-gain schedule).	291
164	X-19. propeller roll control gain as a function of tilt angle (roll-gain schedule).	292
165	X-19, propeller yaw control gain as a function of tilt angle (yaw-gain schedule).	293
166	X-19, coordinator output stroke as a function of governor collective shaft displacement.	294
167	X-19, nacelle input arm position as a function of coordinator output stroke.	295
168	X-19, propeller blade angle as a function of nacelle input arm position.	297
169	X-19, hover control moment response due to a pilot commanded step input of pitch, roll or yaw control.	298
170	X-19, propeller blade angle relationships due to control column application.	300
171	X-19, roll coupling generated by a yaw control input.	302
172	X-19, pitch coupling generated by roll or yaw control input; V = 0 fps.	303

LIST OF ILLUSTRATIONS (CONT'D)

FIGURE NO. PAGE

173 X-19, distribution of forces due to a roll control input (maximum aileron). 304

174 X-19, distribution of forces due to a yaw control input (maximum rudder). 305

175 X-19, aircraft pitching moment characteristics at $\phi_F = 20°$, including airframe and propeller contributions; c.g. = 42.8% lift chord. 306

176 X-19, aircraft pitching moment characteristics at $\phi_F = 40°$, including airframe and propeller contributions; c.g. = 42.8% lift chord. 307

177 X-19, aircraft pitching moment characteristics at $\phi_F = 60°$, including airframe and propeller contributions; c.g. = 42.8% lift chord. 308

178 X-19, aircraft pitching moment characteristics at $\phi_F = 82.5\%$, including airframe and propeller contributions; c.g. = 42.8% lift chord. 309

179 X-19, time history of hover thrust response to a step power lever input, original and modified system. 314

SECTION VII 319

180 X-19, damping characteristics of the longitudinal short period mode through transition with SAS off; W = 12,300 lb., Height = Sea Level. 330

181 X-19, damping characteristics of the Dutch Roll mode through transition with SAS off; W = 12,300 lb., Height = Sea Level. 331

182 X-19, migration of the longitudinal short period mode roots through transition with SAS off; W = 12,300 lb., Height = Sea Level, Start cruise/end transition c.g. = 42% lift chord. 332

183 X-19, migration of the longitudinal phugoid mode roots through transition with SAS off; W = 12,300 lb., Height = Sea Level. Start cruise/end transition c.g. = 42% lift chord. 333

184 X-19, migration of the roots of the lateral directional modes through transition with SAS off; W = 12,300 lb., Height = Sea Level. Start cruise/end transition c.g. = 42% lift chord. 334

185 X-19, variation of available pitch control power and required trim moments through transition. 336

186 X-19, variation of available roll control power through transition. 337

187 X-19, variation of available yaw control power through transition. 338

LIST OF ILLUSTRATIONS (CONT'D)

FIGURE NO.		PAGE
188	X-19, power-on lift and pitching moment characteristics in cruise configuration based on wind tunnel data; c.g. = 42.9% lift chord.	340
189	X-19, power-on sideforce characteristics in cruise configuration based on wind tunnel data; $\alpha_{fus} = 0°$.	341
190	X-19, power-on yawing moment characteristics in cruise configuration based on wind tunnel data; c.g. = 42.9% lift chord, $\alpha_{fus} = 0°$.	342
191	X-19, power-on rolling moment characteristics in cruise configuration based on wind tunnel data; c.g. = 42.9% lift chord, $\alpha_{fus} = 0°$.	343
192	X-19, damping characteristics of the longitudinal short period mode in cruise; W = 12,300 lb., Height = Sea Level.	344
193	X-19, damping characteristics of the longitudinal short period mode in cruise; W = 12,300 lb., Height = 15,000 ft.	345
194	X-19, damping characteristics of the Dutch Roll mode in cruise; W = 12,300 lb., Height = Sea Level.	346
195	X-19, damping characteristics of the Dutch Roll mode in cruise; W = 12,300 lb., Height = 15,000 ft.	347
196	X-19, damping characteristics of the Dutch Roll mode in cruise; W = 12,300 lb., Height = 25,000 ft.	348
197	X-19, elevator hinge moment characteristics in cruise.	350
198	X-19, aileron hinge moment characteristics in cruise; $\alpha_{fus} = 0°$.	352
199	X-19, rudder hinge moment characteristics in cruise; $\alpha_{fus} = 0°$.	353
200	X-19, cruise elevator trim settings in level flight at 15,000 ft; W = 12,300 lb. and 13,500 lb., c.g. = 39%, 42% lift chord.	354
201	X-19, cruise elevator angle per 'g' at 15,000 ft; W = 12,300 lb., 13,500 lb., c.g. = 39% and 42% lift chord.	356
202	X-19, roll performance in cruise; steady roll rate and wing tip helix angle with a stick force of 25 lb.	357
203	X-19, roll performance in cruise; bank angle attained one second after an instantaneous aileron deflection with a stick force of 25 lb.	358
204	X-19, roll performance in cruise; roll time constant.	359

LIST OF ILLUSTRATIONS (CONT'D)

FIGURE NO. PAGE

205 X-19, effect of power and trim on the induced drag factor ($\partial C_D / \partial C_L^2$) in cruise. 364
206 X-19, effect of Mach Number and altitude on minimum cruise drag coefficient. 365
207 X-19, components of total cruise drag coefficient. 367
208 X-19, effect of speed and altitude on cruise lift-drag ratio; W = 13,660 lb. 368
209 X-19, effect of weight and altitude on cruise lift-drag ratio; V = 300 knots TAS. 369
210 Horizontal c.g. envelope for the basic 13,660 lb. design gross weight aircraft. 377
211 X-19, recommended tilt velocity schedule. 380
212 X-19, flap deflection schedule, forward lift strut. 382
213 X-19, collective aileron schedule, rear lift strut. 383
214 X-19, coordinator auto-trim schedule. 384
215 X-19, coordinator pitch-gain schedule. 385
216 X-19, coordinator roll-gain schedule. 387
217 X-19, coordinator yaw-gain schedule. 388

SECTION VIII 391

218 Estimated hover ground effect pressure distribution for the X-200 configuration. 395
219 Comparison of ground effect augmentation of hover lift of two different types of VTOL testbed aircraft. 397

SECTION IX 399

220 0.12 scale model of the Curtiss-Wright X-19 configuration mounted in the NACAL wind tunnel. 403

221 Longitudinal aerodynamic characteristics of the 0.12 scale model of the Curtiss-Wright X-19, power on and power off, MIT-1019 runs 28 and 100. 408

LIST OF ILLUSTRATIONS (CONT'D)

FIGURE NO.		PAGE
222	Drag characteristics of the 0.12 scale model of the Curtiss-Wright X-19.	409
223	Directional and lateral stability characteristics of the 0.12 scale model X-19 in MIT-1019 cruise simulation.	410
224	NACAL low speed tunnel X-19 type model installation for NACAL-93 wind tunnel tests.	415
225	NACAL-93 test data to demonstrate the effect of propeller and propeller speed in pitch, X-19 cruise configuration.	417
226	NACAL-93 test data to demonstrate the effect of propeller and propeller speed in pitch, X-19 transition configuration.	418
227	NACAL-93 test data to demonstrate the effect of propeller and propeller speed in yaw, X-19 cruise configuration.	419
228	NACAL-93 test data to demonstrate the effect of propeller and propeller speed in yaw, X-19 transition configuration.	420
229	NACAL low speed tunnel X-19 model installation for NACAL-120 wind tunnel tests.	421
230	NACAL-120 test data to demonstrate the effect of ground plane presence on longitudinal characteristics in hover of the X-19 model.	423
231	NACAL-120 test data to demonstrate the effect of nacelle angle on lateral-directional characteristics in hover of the X-19 model.	424
232	Curtiss-Wright test facility for the investigation of over-water aspects of high disk loading VTOL airplanes.	428
233	Installation of the X-100 research aircraft on the NASA 40 x 80 wind tunnel mounts at Ames Research Center.	430
234	Comparison of similar test configurations of the 0.12 scale X-19 model in three different wind tunnels-C_L vs α_{fus}, power off.	434
235	Comparison of similar test configurations of the 0.12 scale X-19 model in three different wind tunnels - C_D vs α_{fus}, power off.	435
236	Comparison of similar test configurations of the 0.12 scale X-19 model in three different wind tunnels - C_M vs α_{fus}, power off.	436
237	Comparison of similar test configurations of the 0.12 scale X-19 model in three different wind tunnels - C_l vs ψ, power off.	437
238	Comparison of similar test configurations of the 0.12 scale X-19 model in three different wind tunnels - C_n vs ψ, power off.	438

LIST OF ILLUSTRATIONS (CONT'D)

FIGURE NO. PAGE

239 Comparison of similar test configurations of the 0.12 scale X-19 model in three different wind tunnels - C_y vs ψ, power off. 439

240 Comparison of calculated and test data of X-100 propeller blade angle and thrust coefficient versus power coefficient at static condition. 441

241 Comparison of X-100 full scale and model propeller data in terms of C_T and C_P. 442

242 X-100 maximum values of propeller figure of merit at various reynolds numbers based on full-scale and model test data. 443

SECTION X 447

243 X-19, fuselage lift coefficient characteristics; S_{ref} = 154.6 sq. ft. 449

244 X-19, exposed front wing lift coefficient; Sref = 154.6 sq. ft. 450

245 X-19, exposed rear wing lift coefficient; S_{ref} = 154.6 sq. ft., (external to BL 16.7 inches). 451

246 X-19, nacelle lift coefficients; S_{ref} = 154.6 sq. ft. 452

247 X-19, lift coefficient of complete airplane-propellers off; S_{ref} = 154.6 sq. ft. 453

248 X-19, pitching moment coefficient of fuselage alone about the 42.9 percent c.g.; S_{ref} = 154.6 sq. ft., $\bar{c}$ = 2.875 ft. 454

249 X-19, exposed front and rear wing pitching moments about respective quarter chords; S_{ref} = 154.6 sq. ft., $\bar{c}$ = 2.875 ft. 455

250 X-19, nacelle pitching moments about respective wing quarter chords; S_{ref} = 154.6 sq. ft., $\bar{c}$ = 2.875 ft. 456

251 X-19, pitching moment of complete airplane about the 42.9 percent c.g., propellers off; S_{ref} = 154.6 sq. ft., $\bar{c}$ = 2.875 ft. 457

252 X-19, propeller lift coefficients, front and rear; S_{ref} = 154.6 sq. ft. 458

253 X-19, propeller pitching moment coefficients front and rear; S_{ref} = 154.6 sq. ft., $\bar{c}$ = 2.875 ft. 459

254 X-19, propeller side force and yawing moment coefficient, S_{ref} = 154.6 sq. ft., $\bar{c}$ = 2.875 ft. 460

255 Propeller sign convention. 461

256 X-19, aeroelastic wing and propeller twist derivatives. 462

LIST OF ILLUSTRATIONS (CONT'D)

FIGURE NO. PAGE

257 X-19, V-n diagram, W = 13,660 pounds. 466

258 X-19, gust envelope; W = 13,660 pounds. 468

259 Diagrammatic representation of aerodynamic cruise loads. 469

260 X-19, rear wing lift coefficients based on S = 85.74 sq. ft. (exposed) area; NACA 64_3-418 airfoil modified. 472

261 X-19, rear wing spanwise lift distribution - propellers off. 473

262 Effects of fuselage upon the wing $\partial C_L/\partial \alpha$; wing located along fuselage x/L; various body width ratios; based on clear through wing area; z/h = 0.907. 476

263 Effects of fuselage upon wing angle of zero lift; parameters: x/L, b/W, z/h = 0.907. 477

264 X-19, fuselage and nacelle wash effects upon the rear wing at 77 percent chord position. 478

265 X-19, rear wing chordwise pressure distribution-propellers off; ϕ_F = -3 degrees. 479

266 X-19, rear wing chordwise pressure distributions-propellers off; ϕ_F = -3 degrees, α_{fus} = +2 degrees. 480

267 X-19, fuselage induced wash derivative on rear wing due to sideslip, at 77 percent chord position. 482

268 X-19, center of gravity envelope, based on empty weight. 484

269 X-19, hover transmission limit - allowable forward center of gravity position at thrust to weight = 1.0. 485

270 X-19, propeller horsepower histogram (hover). 486

271 X-19, tee-box horsepower histogram (hover). 487

272 X-19, transition lift coefficient characteristics; ϕ_F = 82.5°, V = 49 knots, 819 πnD, neutral stick. 490

273 X-19, transition lift coefficient characteristics; ϕ_F = 82.5°, V = 49 knots, 725 πnD, neutral stick. 491

274 X-19, transition lift coefficient characteristics; ϕ_F = 60°, V = 85 knots, 725 πnD , neutral stick. 492

275 X-19, transition lift coefficient characteristics; ϕ_F = 40°, V = 102 knots, 725 πnD , neutral stick. 493

276 X-19, transition lift coefficient characteristics; ϕ_F = 20°, V = 120 knots, 725 πnD , neutral stick. 494

277 X-19, transition drag coefficient characteristics; ϕ_F = 82.5°, V = 49 knots, 819 πnD, neutral stick. 496

278 X-19, transition drag coefficient characteristics; ϕ_F = 82.5°, V = 49 knots, 725 πnD , neutral stick. 497

279 X-19, transition drag coefficient characteristics; ϕ_F = 60°, V = 85 knots, 725 πnD , neutral stick. 498

LIST OF ILLUSTRATIONS (CONT'D)

FIGURE NO. PAGE

280 X-19, transition drag coefficient characteristics; $\phi_F = 40°$, V = 102 knots, 725 πnD , neutral stick. 499

281 X-19, transition drag coefficient characteristics; $\phi_F = 20°$, V = 120 knots, 725 πnD , neutral stick. 500

282 X-19, transition pitching moment coefficient characteristics; $\phi_F = 82.5°$, V = 49 knots, c.g. = 42.8%, neutral stick, 725 and 819 πnD. 501

283 X-19, transition pitching moment coefficient characteristics; $\phi_F = 60°$, V = 85 knots, c.g. = 42.8%, neutral stick, 725 πnD. 502

284 X-19, transition pitching moment coefficient characteristics; $\phi_F = 40°$, V = 102 knots, c.g. = 42.8%, neutral stick, 725 πnD. 503

285 X-19, transition pitching moment coefficient characteristics; $\phi_F = 20°$, V = 120 knots, c.g. = 42.8%, neutral stick, 725 πnD. 504

286 X-19, transition front and rear propelier trim powers; $\phi_F = 82.5°$, V = 49 knots, 725 πnD , c.g. = 42.8%. 506

287 X-19, transition front and rear propeller trim powers; $\phi_F = 60°$, V = 85 knots, 725 πnD , c.g. = 42.8%. 507

288 X-19, transition front and rear propeller trim powers; $\phi_F = 40°$. V = 102 knots, 725 πnD , c.g. = 42.8%. 508

289 X-19, transition front and rear propeller trim powers; $\phi_F = 20°$, V = 120 knots, 725 πnD, c.g. = 42.8%. 509

290 X-19, effects of c.g. location on stick position; $\phi_F = 60°$, πnD = 725, V = 85 knots, W = 13,660 pounds. 510

291 X-19, effects of πnD variation upon trim; $\phi_F = 60°$, V = 85 knots, W = 13,660 pounds, c.g. = 41%. 511

292 X-19, effects of πnD variation upon trim; $\phi_F = 40°$, W = 12,300 pounds, V = 102 knots, c.g. = 42.8%. 512

293 X-19, effects of c.g. location upon trim; $\phi_F = 40°$, πnD = 725, V = 102 knots. 513

LIST OF ILLUSTRATIONS (CONT'D)

FIGURE NO. SECTION XI PAGE

294 X-19, hover operating envelope, single engine failure. 518

295 X-19, cruise windmilling descent, trim characteristics; W = 12,300 pounds, c.g. = 42.9 percent; $\phi_F = 16.3^\circ$, $\beta_{.75R} = 51$ degrees. 521

296 X-19, cruise windmilling descent angle; W = 12,300 pounds, c.g. = 42.9 percent, $\phi_F = 16.3^\circ$, $\beta_{.75R} = 51$ degrees. 522

297 X-19, cruise windmilling rate of descent flares; W = 12,300 pounds, c.g. = 42.9 percent, $\phi_F = 16.3$ degrees, $\beta_{.75R} = 51$ degrees. 523

298 X-19, cruise windmilling flared flight paths; W = 12,300 pounds, c.g. = 42.9 percent, $\phi_F = 16.3^\circ$, $\beta_{.75R} = 51^\circ$, $\alpha_{fus} = 14.4^\circ$. 525

299 X-19, windmilling lift coefficient characteristics at $\phi_F = 16.25^\circ$, $S_{ref} = 154.6$ sq. ft., $\delta_F = 23.2^\circ$, $\delta_{a_{coll}} = 21.5^\circ$. 526

300 X-19, windmilling drag coefficient characteristics at $\phi_F = 16.25^\circ$, $S_{ref} = 154.6$ sq. ft., $\delta_F = 23.2^\circ$, $\delta_{a_{coll}} = 21.5^\circ$. 527

301 X-19, windmilling moment coefficient characteristics at $\phi_F = 16.25^\circ$; $S_{ref} = 154.6$ sq. ft., c.g. = 42.9%, $\delta_F = 23.2^\circ$, $\delta_{a_{coll}} = 21.5^\circ$. 528

302 Thrust coefficient characteristics at tilt angle of 140°, CWC blade 3(156109), AF 115, $IC_{L_i} = 0.482$. 531

303 Thrust coefficient characteristics at tilt angle of 160°, CWC blade 3(156109), AF 115, $IC_{L_i} = 0.482$. 532

304 Thrust coefficient characteristics at tilt angle of 180°, CWC blade 3(156109), AF 115, $IC_{L_i} = 0.482$. 533

305 Blade characteristics of CWC 3(156109); AF 109, $IC_{L_i} = 0.482$. 534

SECTION XII 535

306 Flight test schedule, X-19 S/N 62-12197. 543

307 X-19 flight No. 50, track velocity history (theodolite digital data). 549

308 X-19 flight No. 50, altitude time history (theodolite digital data). 551

309 X-19 flight No. 50, climb velocity vs. time (theodolite digital data). 553

310 X-19 flight No. 50, resultant velocity vs. time (theodolite digital data). 554

LIST OF ILLUSTRATIONS (CONT'D)

FIGURE NO.		PAGE
311	X-19 flight No. 50, in-flight acceleration vs. time (theodolite digital data).	555
312	X-19 flight No. 50, vertical acceleration vs. time (theodolite digital data).	556
313	X-19 flight No. 50, bank angle (theodolite film data).	557
314	X-19 flight No. 50, pitch angle and component of yaw angle (theodolite film data).	558
315	X-19 flight No. 50, roll and pitch rate (theodolite film data).	559
316	X-19 flight No. 50, front and rear nacelle angles (theodolite film data).	560
317	X-19 flight No. 50, excess thrust horsepower absorbed (average theodolite trace and digital data).	561
318	X-19 S/N 62-12197 in conversion flight at 90 kts.	562
319	X-19 S/N 62-12197 in hover flight.	563
320	X-19, flight speed range tested for steady level flight, test velocity vs. schedule velocity.	577
321	X-19, test power required for steady level flight, PIW_N vs. VIW.	579
322	X-19, test front nacelle power required for steady level flight, PIW_{N_F} vs. VIW.	580
323	X-19, test rear nacelle power required for steady level flight, PIW_{N_R} vs. VIW.	581
324	X-19, ground run No. 96, thrust coefficient and blade angle vs. power coefficient.	584
325	X-19, flights Nos. 8 thru 22, thrust coefficient vs. power coefficient for steady hover and translational flight.	585
326	X-19, test installation for ground effect tuft study.	586
327	X-19, ground run No. 97, thrust transient following throttle chop.	588
328	Estimated descent velocity vs. time following a single engine failure in hover (based on X-19 ground run No. 97).	589
329	Estimated altitude lost vs. time following a single engine failure in hover (based on X-19 ground run No. 97).	590
330	Estimated descent velocity vs. altitude lost following a single engine failure in hover (based on X-19 ground run No. 97).	591
331	X-19, category I flight test program. Scope of configuration testing thru January 1965.	594

LIST OF ILLUSTRATIONS (CONT'D)

FIGURE NO.		PAGE
332	X-19, low speed longitudinal handling qualities, with S.A.S. "off" in both axes (pilot: J. V. Ryan).	595
333	X-19, low-speed lateral handling qualities, with S.A.S. "off" in both axes (pilot: J. V. Ryan).	596
334	X-19, pilot opinion rating as a function of airspeed; pitch axis. Electronic pitch S.A.S. "on."	598
335	X-19, pilot opinion rating as a function of airspeed; roll axis. Electronic roll S.A.S. "on."	599
336	X-19, pilot opinion rating as a function of airspeed; yaw axis. No stability augmentation.	600
337	X-19, pilot opinion rating as a function of airspeed; height control. Height control system "on."	601

LIST OF TABLES

TABLE		PAGE
I	X-100 VTOL airplane characteristics.	33
II	Comparison between calculated and test values of radial force, R.	44
III	X-19, rear wing download test conditions.	61
IV	Blade design 13166A10P3; general design data and summary.	192
V	Blade design 13166A10P3; blade section characteristics data.	193
VI	Blade design 13166A10P3; summary of blade structural and mass section properties (equivalent to fiberglass).	195
VII	Blade design 13166A12P3: summary of blade structural and mass section properties (equivalent to fiberglass).	200
VIII	Design propeller shaft loads 13166A10P3 blade, X-19 aircraft.	201
IX	Summary, structural analysis; 13166A10P3 blade design, design loads for 12,300 lb. airplane G.W.	205
X	Tabulation of endurance history; 13166A10P3 blades.	212
XI	Maximum composite stresses in X-19 propeller hub 162595.	262
XII	Gage layout.	268
XIII	Vibratory and steady stress summary, X-19 blades.	277
XIV	X-19 PFVT, 13,660 lb. gross weight flight cycle.	281
XV	Stick - fixed equations of motion.	320
XVI	Formulae for the X-19 stability derivitives.	322
XVII	Incompressible power-off profile drag breakdown.	362
XVIII	Historical breakdown X-19 S/N 62-12197.	537
XIX	Typical multiplexed temperature record schedule.	572
XX	Typical test instrumentation oscillograph schedule.	573
XXI	Typical X-19 S/N 62-12197 photo panel parameter schedule.	574
XXII	Cooper Rating Scale	597

SECTION I

REVIEW OF DEVELOPMENTS LEADING TO THE X-19 PROGRAM

SECTION I NOMENCLATURE

A = shaft angle of attack

C_g = center of gravity

C_L = lift coefficient

D = drag

I_x = polar moment of inertia - roll

I_v = polar moment of inertia - pitch

I_z = polar moment of inertia - yaw

HP = horsepower

L = lift

M = mach number

MAC = mean aerodynamic chord

MPH = miles per hour

SLSD = sea level standard day

SECTION I

REVIEW OF DEVELOPMENTS LEADING TO THE X-19 PROGRAM

1. REPORT OBJECTIVE

During the time period of 1957 to 1966 the Curtiss-Wright Corporation was engaged in a major effort in the development of tilt propeller VTOL Aircraft. This work ceased after termination of the flight test contract for the X-19 Aircraft. To assess the program and make available the important technical results, an Air Force Contract AF33(651)-3940 was negotiated with Curtiss-Wright, to prepare a report covering the major achievements of the effort. It is the objective of this report to conduct a thorough assessment and to critically review the positive as well as the negative results of the X-19 technology effort.

2. BACKGROUND HISTORY

The conventional propeller and turbine engine appeared to be a very promising way to obtain hover lift and high thrust performance in the cruise flight condition. As propeller manufacturers, we had the opportunity to observe the difficulty in meeting the required take-off performance and good cruise efficiency requirements of VTOL aircraft. This problem was particularly apparent with those companies developing the tilt-wing and deflected slipstream types of VTOL aircraft. The propeller manufacturer was consulted for design information and data long after those aircraft configurations were frozen, with the result that propeller diameters were too small and disk loadings too high. At that time, disk loading was chosen for reasons other than wing stall, such as propeller spacing, weight, etc.

Because a VTOL aircraft depends on the propeller for lift and control during a major portion of the early low-speed flight, it appeared that a better solution to the problem of vertical take-off and landing could be obtained by designing the aircraft from the propeller designer's point of view. This idea led to examination of the propeller operating at the full range of shaft angles and the associated effects on the over-all airplane. When the propeller was sized to produce the required level of take-off or hover thrust, it became apparent that a secondary in-plane force would produce sufficient lift to be of real significance. This in-plane force is known as side force, or radial force and as shown in Chapter II is a function of propeller diameter and blade area. Since the propeller radial force is large, it was found that an aircraft could be designed to fly without wings using propeller radial force and thrust in all flight modes. Flight without wings was a stimulating idea to management; it was decided to pursue this notion further.

However, the lift-drag ratio of a lifting propeller is poor unless the angle of attack of the propeller is small. This is apparent, since

$$L/D = \frac{1}{\tan A} = 57.3 \text{ at } A = 1 \text{ degree}$$

where L = the lift component of radial force
D = the drag component
A = the shaft angle

Although the lift-drag ratio is high at small angles, the actual level of radial force is low. Thus the initial studies indicated that some wing area would be required. Instead of a wingless aircraft, area was added to obtain maximum lift-drag ratio at the cruise flight condition. It was found that the wing could be sized for maximum efficiency in cruise, since the radial force, thrust and wing lift, were adequate to meet the other flight conditions. At the transition flight conditions, lift-drag ratio of the airplane is low; this was considered to be unimportant. The idea began to gel. An efficient cruise aircraft with good lift in hover appeared to be possible.

3. X-100 AIRPLANE

The ground work had been laid. It was decided to build an aircraft to investigate and demonstrate the radial force principle. This effort is documented in references (1) through (4).

The X-100 airplane is a two-place, 3,500 pound, single-engine aircraft. The general characteristics are shown on Table I and Figures 1 and 2. The aircraft was completed late in 1958, and ground/flight tested during 1959 and 1960. A total time of 220 hours on the ground and 10 flight hours was accumulated. In addition, the X-100 airplane was used for ground erosion tests at Langley Field;and further, was tested in the 40 by 80 ft. NASA Ames wind tunnel. The purpose of the wind tunnel test was twofold: to confirm the results obtained in flight, and to obtain data on propeller loading when operating at high angles of tilt.

The flight tests of the X-100 airplane proved that radial force tilt propellers could be flown from hover to cruise without encountering adverse effects. Furthermore, the stability, control and performance of the X-100 were equal to or better than that predicted. The success of the X-100 tests was encouraging enough to initiate the next effort. Design of the Model 200 was begun.

Table I. X-100 VTOL airplane characteristics.

Airplane Type: 2 place VTOL

No. of Engines and Type: 1 Lycoming YT-53

Engine Rating Military: 825 HP

No. of Propellers and Type: 2 three-blade 10' 0" diameter propellers

Gross Weight: 3500 pounds plus

Polar Moments of Inertia: I_x = 1300 slug feet^2 - - roll
I_y = 2151 slug feet^2 - - pitch
I_z = 3200 slug feet^2 - - yaw

Wing Area = 22.5 square feet

Horizontal Tail Area = 23 square feet

Vertical Tail Area = 18.75 square feet

Length = 28.3 feet

Overall Width = 25 feet

Height = 10.75 feet

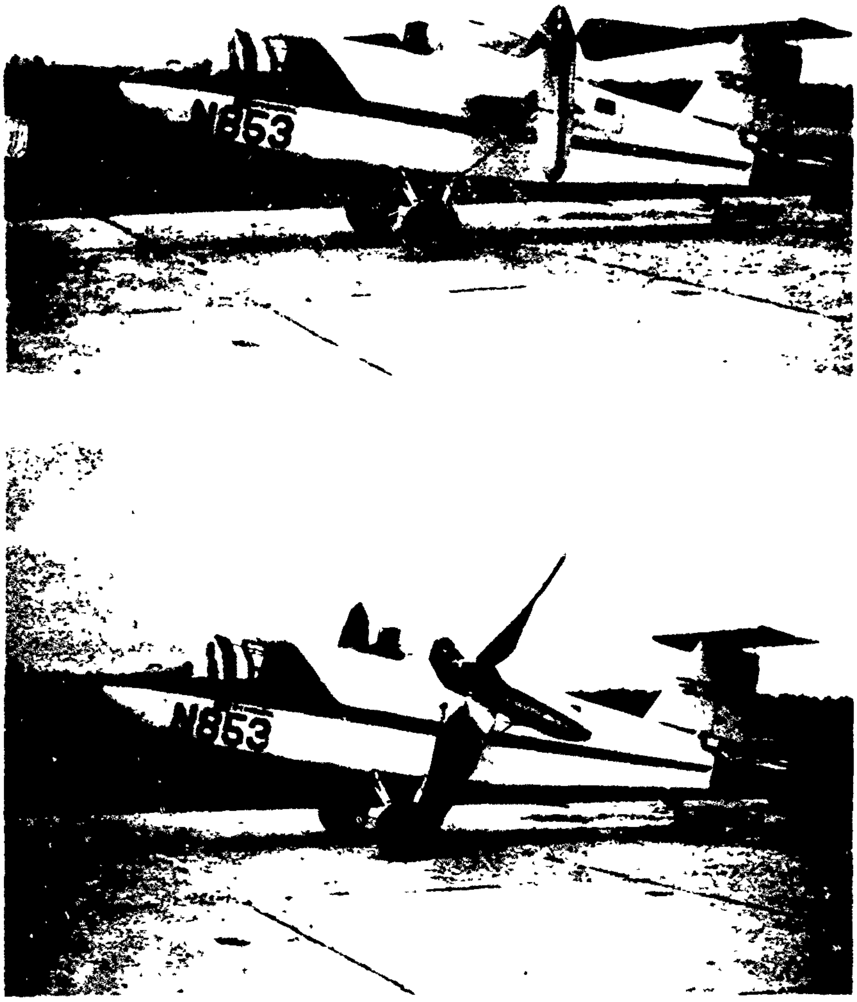

Figure 1. X-100 in the hover and cruise nacelle position.

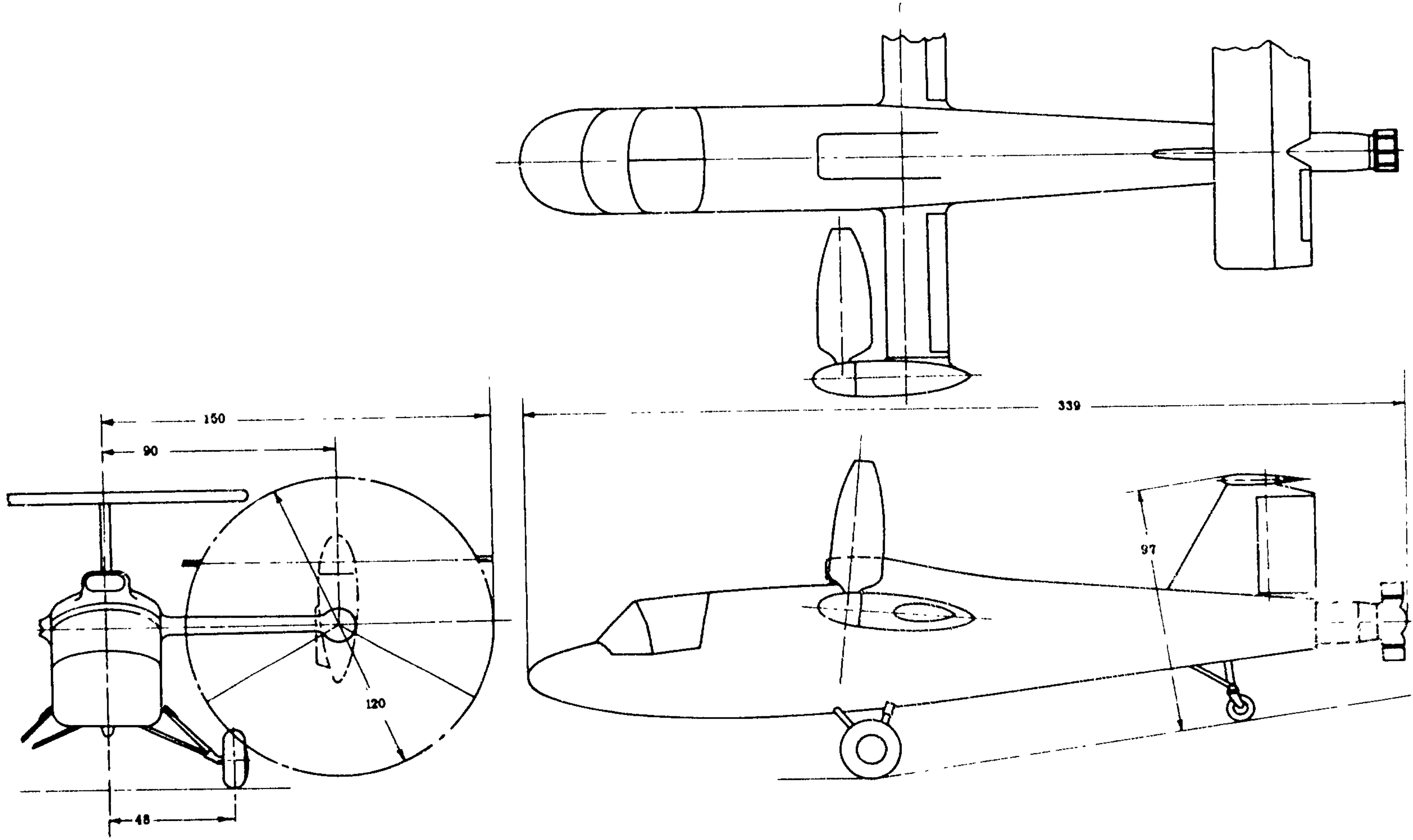
150
90
120
48
339
97

Figure 2. X-100 three view drawing (dimensions in inches).

4. M-200 OPERATIONAL AIRCRAFT

a. Initial Design Objectives

The X-19 airplane is based on the Curtiss-Wright model M-200. It was originally designed to be a corporate executive transport incorporating the W.A.D. rotating combustion engine. The M-200 aircraft was to be a six-place machine with four rotating-combustion (R/C) engines each rated at 580 HP at 5,000 ft. and 100°F. It was intended to provide vertical take-off and landing on a hot day with the aircraft capable of remaining airborne in case of the failure of one engine. The aircraft was to have a range of 900 to 1150 miles with a maximum level speed of 400 mph at 16,000 feet. Further, the design was to conform to FAA regulations, have all-weather flying capability, and be quiet as a result of the use of lightly loaded propellers operating at low tip speed and free from vibration. The gross weight projected for this aircraft was 10,000 pounds.

With the Curtiss-Wright management change, it was decided that the aircraft designed around the R/C (rotating combustion) engine had little hope for success. A new airplane with new-type engines, both untried, could not hope to be successful. While the aircraft with the R/C engines was being designed, studies were conducted to determine the possibility of using two turbine engines. This effort resulted in the turbine version of the aircraft.

The Curtiss-Wright Model 200 was then redesigned to use two T-55 engines instead of the four rotating combustion engines. This reduced the problems considerably, as engine cooling was no longer necessary. The same design performance objectives were retained; however, instead of designing for the commercial market, the machine was pointed toward military applications. The major objective of hovering out-of-ground effect was retained, but with much reduced altitude and temperature accountability. This reduction of one engine out performance could not be avoided when going from the four to two engine configuration; the fact that turbine engines are more sensitive in power to outside air temperature than the rotating combustion engine was another reason.

The design objectives of the Model 200 airplane were developed mainly by Curtiss, as no military specification or requirement was available. Performance-wise the idea was to carry as much payload as possible, as far as possible, and still retain the engine-out feature. This was to be done with gear box operational-limit envelopes, the same as were originally set up for the 10,000 pound aircraft.

(1) Tandem-Wing Design Considerations

During the flight testing of the X-100 aircraft, it was observed that the aircraft had the following undesirable characteristics:

(a) Insufficient hover control power
(b) Roll yaw coupling at hover
(c) High pitch-up moments as a function of forward speed

All these factors made the low-speed flight characteristics unsatisfactory, especially in gusty air. An increase in control power, especially in pitch, was deemed necessary to solve the problem. To obtain the required control power and tilt moments for the pitch control of a tilt propeller a large pitching moment is required. The thrust at the tail of the airplane required to produce this moment can be generated by the use of propellers, ducted fans or jets. The power necessary to generate the thrust is of course dependent on disk loading of the device used. The solution ultimately devised for the X-100 aircraft was a controllable air-deflection cascade system mounted in the tail section and powered by engine exhaust which provided pitch and yaw thrust as needed. It was considered to be undesirable to use a separate device for the generation of a moment for pitch control which is necessary at hover and low forward speeds as additional drives, clutches and controls would be required which added to the overall weight and complexity of the aircraft.

One of the main difficulties encountered with the two propeller VTOL aircraft is the roll yaw coupling problem. To overcome this problem large amounts of control power are needed to counteract the torque change induced due to a roll input. When the airplane is holding in a side wind, for instance, the lee prop is absorbing more power than the upwind prop. If the props are rotating up past the wing, necessary in the case of the fixed wing configuration, the power difference tends to turn the machine so the tail weathervanes into the wind. This must be prevented to provide the control characteristics necessary for a hovering aircraft. As the aircraft design evolved to larger proportions the propeller size appeared to be a limiting factor. Propellers in excess of 20 feet diameter, were envisioned; but sooner or later as the aircraft grew in size at least four propellers would be required. In arranging these on such an aircraft it was thought that the control problems at hover could be solved and the wing size could be kept to a minimum if the tandem configuration was adopted. Also the tandem arrangement appeared to offer the possibility of higher wing loading with the desired low disk loading for hover. If, however, the propellers are disposed along a single wing the download losses of the two inboard units would be higher than if they were placed at the wing tip. Furthermore, with the single wing configuration a tail fan or a Jetavator-type system must be used to provide pitch control in hover and low speed flight conditions. As a result, on a single-wing design five propellers are needed together with the necessary equipment for starting and stopping the tail propeller. A tail propeller could also be used to obtain yaw control but probably differential tilting of the outboard props would be preferrable to the complication of the fifth propeller. For these reasons, and the need for uncoupled flight controls in hover and low speed flight, the four-propeller tandem configuration was chosen for the X-19 configuration.

(2) Turboprop System

The turboprop system was selected to provide the following:

(a) Objective was to cover approximately 0-400 MPH (M 0.65) speed range, and have up to 25,000 ft. altitude capability.

(b) Superior propulsion system efficiencies of turboprop in selected speed-altitude regime.

(c) Excellent performance flexibility of conventional propeller between static and selected high speed conditions.

(d) Capability of the propeller to provide needed radial force for smooth transition flight characteristics.

(3) Selection of Hover Disk Loading

Disk loading was selected from the following point of view:

(a) Good from ground disturbance point of view.

(b) Near lowest possible disk loading with conventional aircraft propellers considering combined aerodynamic/structural aspects. At lower disk loadings difficulty with blade dynamics was a concern.

(c) High static thrust performance (about 6.0 lbs/HP at SLSD and 25 lb/ft^2 disk loading) to minimize installed power requirements.

(d) Peak static thrust performance from propeller obtained at reasonable tip speeds of approximately 820 feet per second at this disk loading, giving low noise characteristics.

(e) Light weight blade construction methods available - a fundamental keystone as conventional blade methods of construction result in propeller weights unacceptability high.

(f) Confidence in the design feasibility of large diameter conventional propellers for large aircraft.

(g) Ability to hold high propeller cruise flight efficiencies approximately 80% using the speed variation capability of gas-coupled shaft turbine engines.

(4) Selection of Non Tilting Wing System

The airframe geometry was based on the following:

(a) Selection of the non tilting wing system was fundamentally hinged on the moderate hover disk loading selection, i.e., 15 to 30 lbs per square foot.

(b) Recognition that if a tilting wing were used, the wing would have to be carefully slatted and flapped to avoid stall at high transition angle of attack conditions. Also, there was great concern that the slipstream dynamic pressures associated with the selected low disk loading propellers would be inadequate to cope with the problem, even with efficient slats and flaps incorporated. The above-noted advantages of low disk loading should not be sacrificed by increasing disk loading merely to make the tilting wing feasible.

(5) Selection of Tandem-Wing Four Propeller Configuration

(a) The tandem wing arrangement allowed the use of low or moderate propeller disk loadings and high wing loadings without resorting to the use of long narrow wings or intermeshing propellers. In the case of a four propeller tandem wing airplane the propellers mounted at the wing tips would have a lower download than is possible with a single wing airplane.

(b) Tandem wings with tip-mounted propellers kept a large part of the wings from beneath the propeller, thus minimizing thrust losses due to slipstream blowdown.

(c) Tandem wings allowed use of four propellers, thus minimizing size of individual propellers for the selected disk loading and aircraft weight.

(d) The configuration allows full exploitation of the concept of a continuously running propulsion system. An auxiliary system to provide a control force at hover and low forward speeds is not required.

(e) A tandem aircraft configuration is easily controlled at hover and at the low speed flight conditions as large control moments can be generated by the use of propeller collective pitch controls.

5. TRI-SERVICE X-19 (CW MODEL 200) DIMENSIONS AND GENERAL DATA
(Refer to Figure 3 for general arrangement)

Wings:

Span: (to nacelle centerlines)	Fwd. wing 19.5 ft. Aft. wing 21.5 ft.
Areas:	Fwd. wing 56.1 Aft. wing 98.5 sq. ft.

Chord: (constant along span)

Fwd. wing	34.5 inches
Aft. wing	55.0 inches
Lift chord	274.0 inches

Airfoil section designation and thickness (percent chord)
constant along span....... fwd. wing NACA 2421 Modified-21%
aft. wing NACA 64_3-418 Modified-18%

Incidence (degrees):

	FWD WING	AFT WING
At root	0	0
At construction tip	0	0
Sweepback, degrees	0	0
Dihedral, degrees	0	0
Aspect Ratio	6.8	4.7

Ailerons: Outboard on Aft wing only

Area (both)	14.44 sq. ft.
Span	54 inches
Chord (average percent aft wing chord, aft of hinge	35%
Distance from plane of symmetry to centroid of aileron area	93.5 inches

Tab -- NONE

Flaps: On Forward wing only

Area (both)	15.16 sq. ft.
Type - Plain	
Span, exclusive of cutouts	78.05 inches
Chord, (average percent front wing chord, aft of hinge)	40.5%

Elevators: On Aft wing only

Area (both)	12.85 sq. ft.
Span (each)	48.0 inches
Chord (average percent aft wing chord, aft of hinge	35.0%

Tab -- NONE

Horizontal Tail: - See aft wing

Vertical Tail:

Area (Excl. Dorsal)		46.18 sq. ft.
Span		117.0 inches
Chord	Root	74.32 inches
	Tip	39.42 inches
Airfoil section designation and thickness	NACA 0012 W L. 136.75	12%
	NACA 0010 W.L. 250.75	10%
Tab dimensions	Length =	28.18 inches
Chord:	Top	4.195 inches
	Bottom	4.70 inches
Tab Location		W.L. 167.00 to W.L. 195.18
Incidence, normal		0°
Sweep of leading edge, degrees		32° 6 minutes
Dihedral, degrees		0°
Adjustment each side of neutral		0°
Aspect ratio		2.05

Fuselage:

Length of fuselage	42.08 ft.
Net wetted area of fuselage	631.8 sq. ft.
Maximum cross-sectional area	26.6 sq. ft.
Area of engine air inlet:	1.67 sq. ft.
Cabin length	14.8 ft.
Cabin width	4.33 ft.

Propeller Nacelles:

Length of front nacelles		6.41 ft.
Maximum diameter of front nacelles		1.375 ft.
Net wetted area of two front nacelles		45.7 sq. ft.
Cruise inclination of front nacelles relative to fuselage datum		-3.0°
Length of rear nacelles		7.50 ft.
Diameter of rear nacelles		1.375 ft.
Tilt Angles	Front	97° to -3°
	Rear	81° to -3°

Net wetted area of two rear nacelles	47.6 sq. ft.
Cruise inclination of rear nacelles relative to fuselage datum	-2.54°

Total aircraft:

Total aircraft wetted area	1090.5 sq. ft.
Height over highest fixed part of aircraft (Vertical Tail) Reference line level (reference is to ground level)	17' 1/4"
Height over highest part of tail, reference line level	17' 1/4"
Length, maximum: Reference line level	44' 5"
Distance from fwd. wing quarter chord point to aft wing quarter chord point	23' 4-1/8"
Distance from aft wing quarter chord point to vertical tail MAC quarter chord point	28.58 inches
Angle between fuselage reference line and wing zero-lift line	Fwd. -2.3° as installed Aft -0.9°
Ground angle, degrees	0

Propeller:

Propeller diameter	13.0 ft.
Blade Area	8.4 sq. ft.
No. of propellers per aircraft	4
No. of blades per propeller	3
Blade designation	13168A10P3(Modified)
Activity Factor	168
Integrated Design C_L	0.057
Blade Characteristics	(See Figure 74)
Airfoil Section Type	NACA 64

Alighting gear:

Wheel size:	
Main wheels	24 x 7.7
Nose wheel	6.00 x 6.0
Tire size:	
Main wheels	24 x 7.7
Nose wheel	6.00 x 6.0
Tread of main wheels	6.0 feet 8.0 inches
Wheel base	22.0 feet
Vertical travel of axle from extended to fully compressed position:	
Main wheels	8.0 inches
Nose wheel	6.0 inches
Distance from main wheel contact point to center of gravity:	
Horizontal Distance:	
At most forward permissible cruise c.g.	45.4 inches
At most aft permissible cruise c.g.	35.4 inches

Vertical Distance:

At most forward c.g. 59.4 inches at 13,660 pounds gross weight

At most aft c.g. 59.2 inches at 13,660 pounds gross weight

Engines:

2 Lycoming T55-L-5

Direct Drive

CONTROL MOVEMENT AND CORRESPONDING CONTROL SURFACE MOVEMENTS

Control and control surface movements on each side of neutral position for full movement, as limited by stops.

Rudder 33 degrees right, 33 degrees left.

Rudder pedals 3 inches forward, 3 inches aft.

Rudder tab 8 degrees right, 8 degrees left.

Rudder tab control actuated by electrical switch.

Elevator 20 degrees above, 15 degrees below.

Elevator control stick 5.42 inches aft, 4.06 inches forward.

Ailerons 15 degrees above, 11 degrees below.

Aileron control stick 4 inches right, 4 inches left.

Aileron droop (maximum) 60 degrees.

Forward wing flap (maximum) 60 degrees nominal movement.

Flap and aileron droop positions are mechanically coordinated with nacelle position.

GENERAL FEATURES OF DESIGN AND CONSTRUCTION

The aircraft is a tandem high wing airplane with propellers mounted on nacelles at each wing tip, as shown in Figure 3. The nacelles tilt from horizontal to vertical approximately 100 degrees. Power is provided by two turbo-shaft engines contained within the fuselage. Conventional aircraft construction techniques and materials are used throughout.

GENERAL INTERIOR ARRANGEMENT

The interior arrangement consists of a cockpit and a passenger/cargo compartment.

The pilot's compartment contains two crew seats, all the controls, switches, instruments and other equipment required to operate the airplane from either the left or right seat.

The passenger/cargo compartment has provisions for 4 passenger seats, but can be re-arranged for cargo carriage as well.

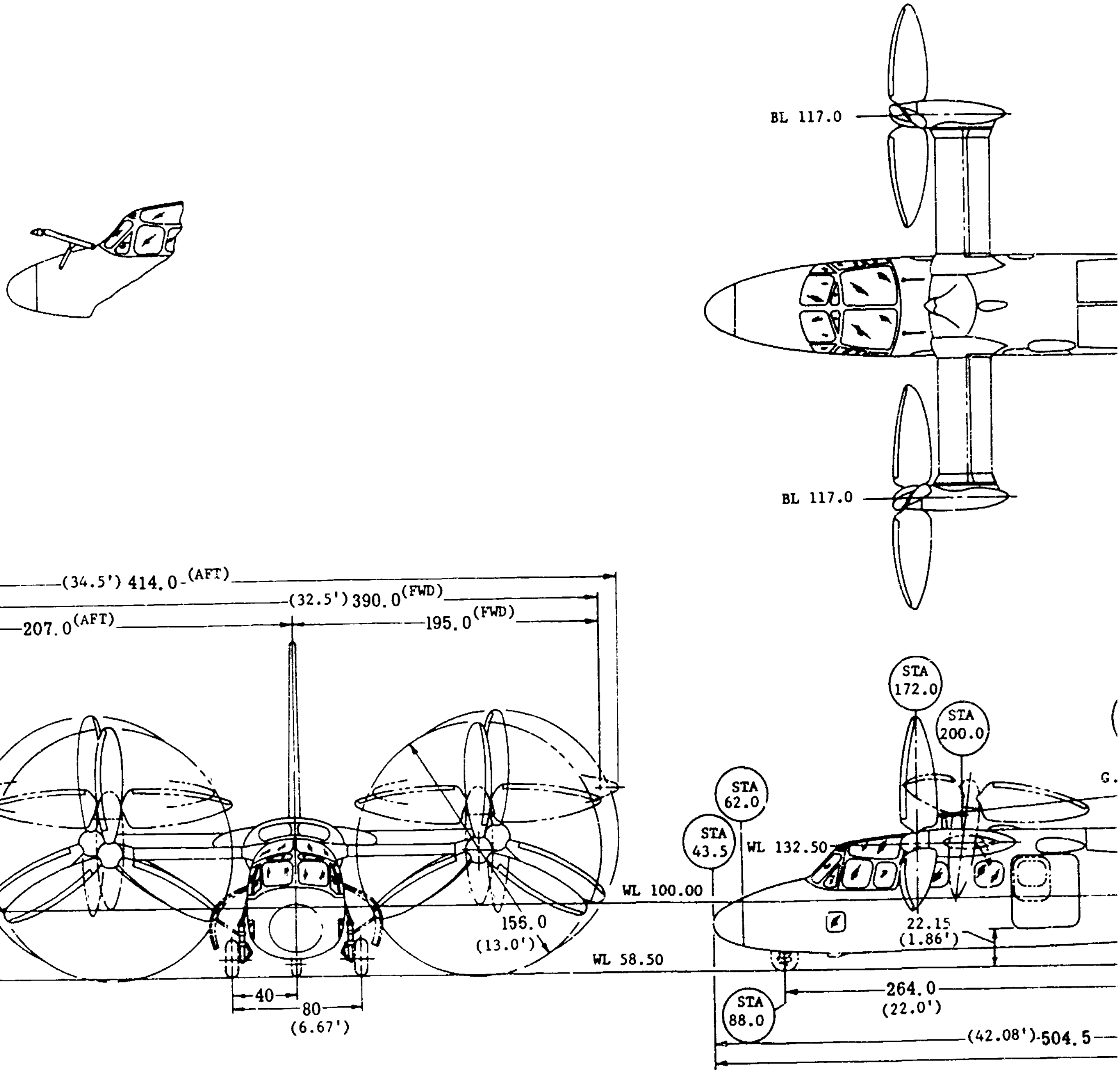
BL 117.0
BL 117.0
(34.5') 414.0 (AFT)
(32.5') 390.0 (FWD)
207.0 (AFT)
195.0 (FWD)
156.0
(13.0')
WL 100.00
WL 58.50
40
80
(6.67')
STA 172.0
STA 200.0
STA 62.0
STA 43.5
WL 132.50
G.
22.15
(1.86')
264.0
(22.0')
STA 88.0
(42.08') 504.5

A

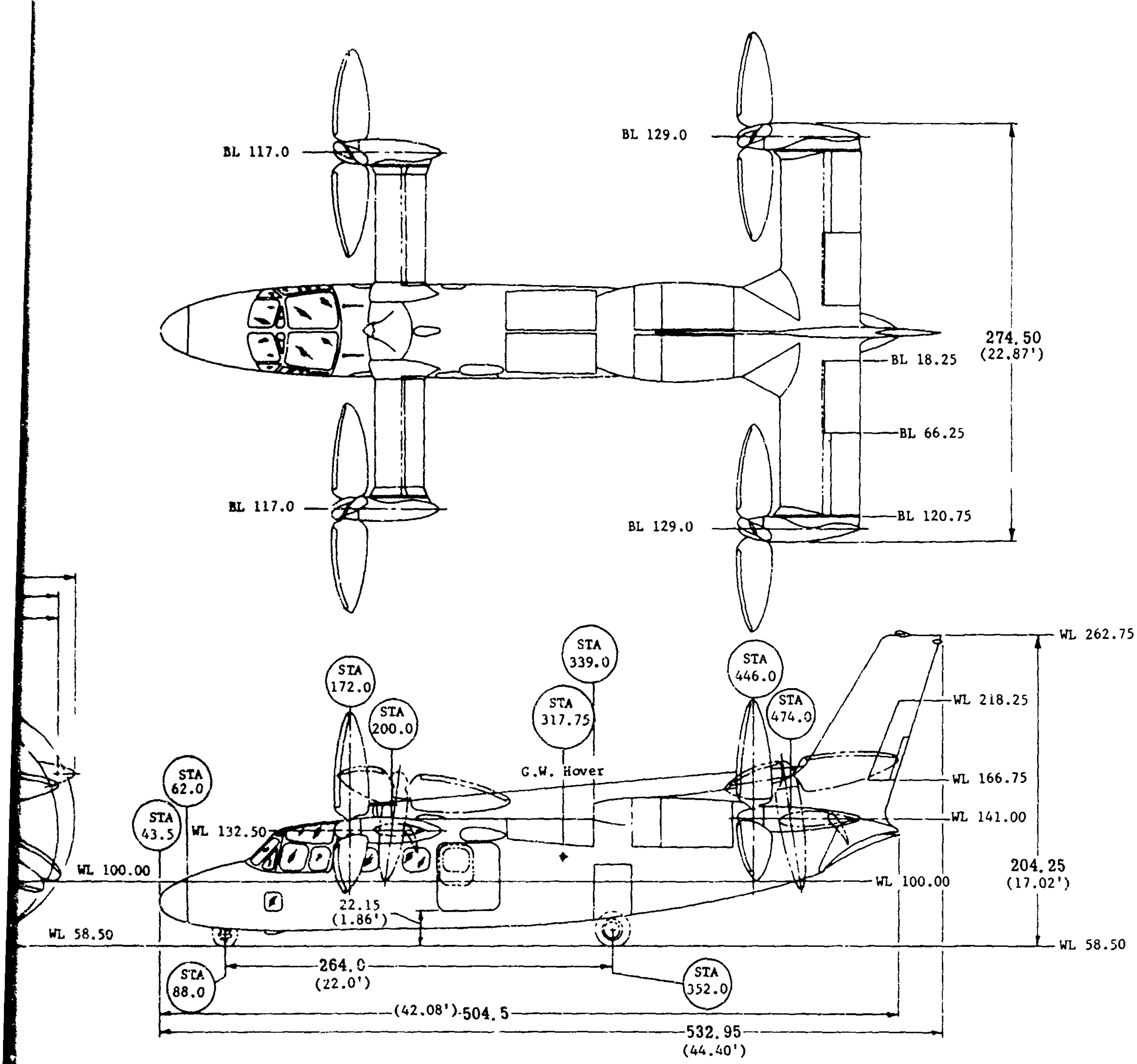
BL 117.0
BL 129.0
274.50
(22.87')
BL 18.25
BL 66.25
BL 117.0
BL 129.0
BL 120.75
WL 262.75
STA 339.0
STA 172.0
STA 446.0
STA 200.0
STA 317.75
STA 474.0
WL 218.25
STA 62.0
G.W. Hover
WL 166.75
STA 43.5
WL 132.50
WL 141.00
WL 100.00
204.25
(17.02')
WL 100.00
22.15
(1.86')
WL 58.50
WL 58.50
264.0
(22.0')
STA 88.0
STA 352.0
(42.08')-504.5
532.95
(44.40')

Figure 3. X-19 three view drawing.

B

REFERENCES

1. H. Borst, Feasibility Study of a New Type of VTOL Aircraft, Curtiss-Wright Report No. C-2725, dated 20 Dec. 1957.

2. H. Borst, Design and Performance of the Lifting Propeller X-100 VTOL Airplane, Curtiss-Wright Report No. C-2798, dated 8 October 1959.

3. H. Borst, Flight Test of the Curtiss-Wright X-100 VTOL Aircraft, Curtiss-Wright Report No. C-2846, dated 21 March 1961.

4. E. Sand, Design Report Curtiss-Wright X-100 VTOL Aircraft, Curtiss-Wright Report No. C-2843, dated 10 January 1961.

SECTION II

RADIAL FORCE PRINCIPLE

1. INTRODUCTION

It is well known that the conventional propeller is an highly efficient device for converting shaft power to thrust. Propellers have demonstrated a figure of merit of the order of 80 to 82 percent at the static or hover condition, and well designed propellers have demonstrated efficiencies as high as 90 percent at the cruise speeds of 200 to 400 knots. For instance, the propeller designed for the Lockheed 1049C using three number 109652 blades operated at a cruising efficiency of 89% and demonstrated a Figure of Merit of 80% at the static condition or zero velocity condition, reference 9.1. The Figure of Merit of 80% was obtained at a power coefficient of 0.05 well below the normal take-off power coefficient of the 1049C airplane, which is approximately 0.1. Thus, the propeller is a suitable device for providing lift at the hover condition as well as propelling an airplane at the cruise condition. To accomplish this dual purpose it is necessary that the propeller be tilted through 90 degrees between the hover condition and the cruise condition. During this conversion portion of the flight the propeller will be operating with its shaft at a high angle of attack. At an angle of attack the force along the shaft of the propeller, generally defined as thrust, can be broken down into two forces, a lift force and a force in the direction of flight (Figure 4).

When the propeller is operating with its shaft at an angle of tilt there is, in addition to the thrust force, a secondary force produced which acts in the plane of the disk of the propeller. This force is known as propeller normal or radial force and is a function of the propeller size, the shaft angle of attack of the propeller, and the operating speed of the propeller. The propeller normal force, known as side force to those doing stability and control calculations, is also illustrated in Figure 4. It will be noted that this force, like the normal force produced by a wing, can be broken into two components --- lift and drag. In the case of conventional aircraft, the normal force produced by the propeller is small compared with the overall forces produced. In the case of propellers used on VTOL aircraft, the diameter and blade area necessary are larger than would be used for conventional airplanes as the blade sections must operate below stall at the static or hover flight conditions to obtain high values of figure of merit. The propellers will also operate through a high angle of attack range during conversion. Since the propeller normal force is directly dependent on the shaft angle with respect to the airflow, the blade area, and the propeller diameter squared, the normal force has been observed to be a very significant parameter affecting the overall characteristics of the VTOL propeller airplane.

2. THEORY AND METHOD FOR COMPUTING PROPELLER FORCES

a. General

To show how a propeller produces the radial force and the associated moment, indicated in Figure 4, it is necessary to examine the

FURNISHED UNDER UNITED STATES GOVERNMENT CONTRACT No. AF33(615)-3940. SHALL NOT BE EITHER RELEASED OUTSIDE THE GOVERNMENT, OR USED, DUPLICATED, OR DISCLOSED IN WHOLE OR IN PART FOR MANUFACTURE OR PROCUREMENT, WITHOUT THE WRITTEN PERMISSION OF CURTISS-WRIGHT CORPORATION, EXCEPT FOR (I) EMERGENCY REPAIR OR OVERHAUL WORK BY OR FOR THE GOVERNMENT, WHERE THE ITEM OR PROCESS IS NOT OTHERWISE REASONABLY AVAILABLE TO ENABLE TIMELY PERFORMANCE OF THE WORK, OR (II) RELEASE TO A FOREIGN GOVERNMENT AS THE INTERESTS OF THE UNITED STATES MAY REQUIRE; PROVIDED THAT IN EITHER CASE THE RELEASE, USE, DUPLICATION OR DISCLOSURE HEREOF SHALL BE SUBJECT TO THE FOREGOING LIMITATIONS. THIS LEGEND SHALL BE MARKED ON ANY REPRODUCTION HEREOF IN WHOLE OR IN PART.

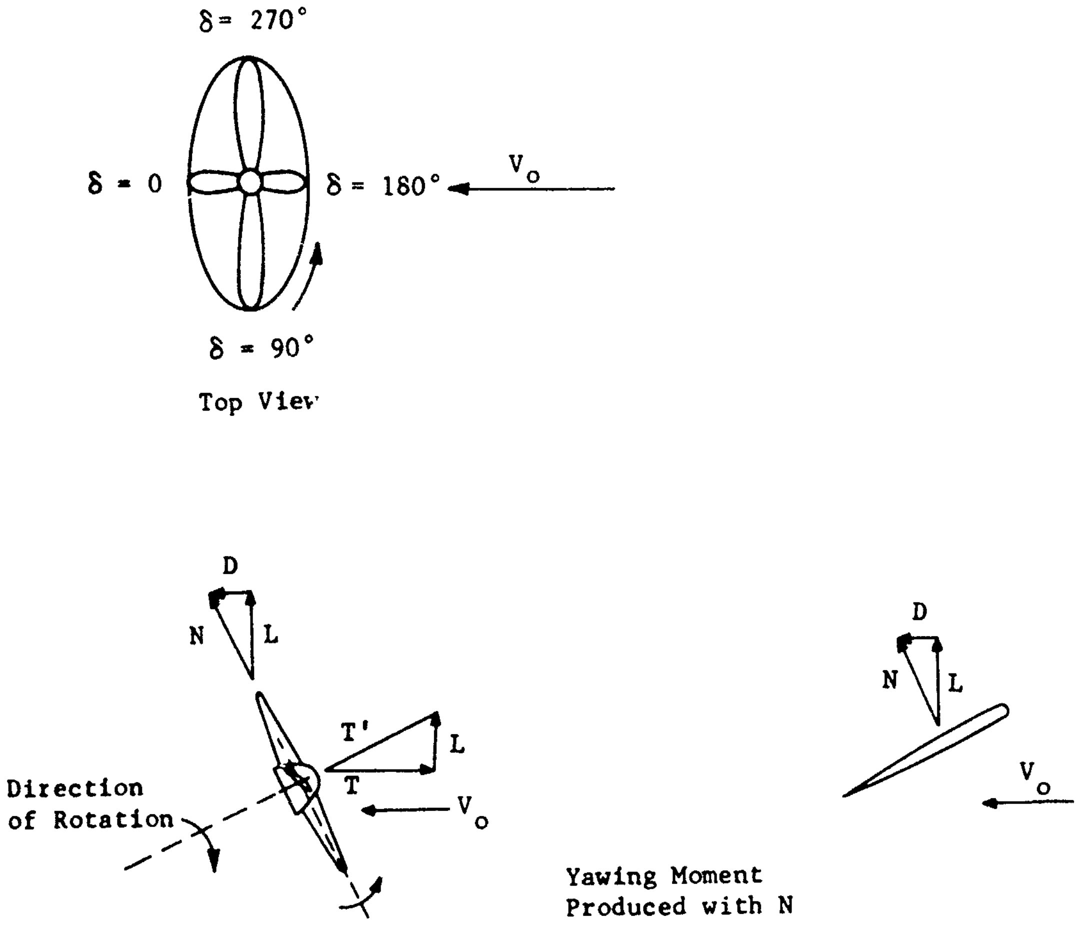
δ= 270°
δ = 0
δ = 180°
V$_o$
δ = 90°
Top View
D
N
L
T'
L
T
V$_o$
Direction of Rotation
D
N
L
V$_o$
Yawing Moment Produced with N

Figure 4. Comparison of normal force produced by wings and propellers.

"FURNISHED UNDER UNITED STATES GOVERNMENT CONTRACT No. AF33(615)-3940. SHALL NOT BE EITHER RELEASED OUTSIDE THE GOVERNMENT, OR USED, DUPLICATED, OR DISCLOSED IN WHOLE OR IN PART FOR MANUFACTURE OR PROCUREMENT, WITHOUT THE WRITTEN PERMISSION OF CURTISS-WRIGHT CORPORATION, EXCEPT FOR (I) EMERGENCY REPAIR OR OVERHAUL WORK BY OR FOR THE GOVERNMENT, WHERE THE ITEM OR PROCESS IS NOT OTHERWISE REASONABLY AVAILABLE TO ENABLE TIMELY PERFORMANCE OF THE WORK, OR (II) RELEASE TO A FOREIGN GOVERNMENT, AS THE INTERESTS OF THE UNITED STATES MAY REQUIRE; PROVIDED THAT IN EITHER CASE THE RELEASE, USE, DUPLICATION OR DISCLOSURE HEREOF SHALL BE SUBJECT TO THE FOREGOING LIMITATIONS. THIS LEGEND SHALL BE MARKED ON ANY REPRODUCTION HEREOF IN WHOLE OR IN PART."

detailed forces on each blade section as a blade rotates through a full revolution. Consider a three-blade propeller operating at a forward velocity V_0 at a shaft angle of attack equal to A. Let equal the azimuth angle of the blade measured in the counterclockwise direction from the vertical position, as viewed from in front of the propeller. Thus, when the blade is on the down stroke and is horizontal, δ will be equal to 90°. On Figure 5 the velocity components are shown for the propeller at angles of δ equal to 0, 90, 270°.

The blade section rotation velocity is πnDx, where x is the fractional radius. This rotational velocity adds vectorially to the forward velocity component, giving a resultant velocity W as shown on Figure 5. At the 90° and 270° blade position the section experiences the full value of forward velocity V_0. Whereas at 0 and 180° the section is influenced by $V_0 \cos A$ velocity component plus the rotational velocity πnDx. At any azimuth position the component of forward velocity affecting the section will be:

$$V\sqrt{(\sin^2 A)\sin^2 \delta + \cos^2 A}$$

The lift forces produced by a typical blade section of a propeller operating at a shaft angle of attack are shown on Figure 6 as a function of azimuth angle.

Each blade section will also be affected by a change in apparent angle of attack as it rotates, in addition to the change of the sectional velocity as determined by the above equation. The change in velocity and section angle of attack will cause a variation of lift produced as the blade rotates. When the propeller is operating at low shaft angles of attack, A, and the blade section is properly loaded so that positive or negative section stall is not encountered, the lift will vary approximately "sinusoidally" as the blade rotates through a complete revolution, see Figure 7. The drag of the propeller blade section will also vary. The manner in which the drag varies depends on the portion of the drag curve at which the section is operating. If the section angle of attack is high, variation of drag approaches a "sinusoidal" shape above and below the initial value; whereas, if the drag varies from the minimum value, the variation is sinusoidal shape, but will never go below the initial value.

The change in lift such as shown on Figure 7 resolved in the propeller plane adds vectorially and gives the in-plane force known as both "Radial force" or "Side force." The variation in blade section lift force such as shown on Figure 6, when resolved in the propeller thrust direction, results in a couple. If the propeller shaft angle is at a positive angle of attack, this couple is a yawing moment, its sign depending on the direction of rotation. A propeller rotating clockwise, i.e., viewed from the rear, a right hand propeller, will produce a yawing moment to the left when the shaft is at a positive angle of attack, see Figure 7.

FURNISHED UNDER UNITED STATES GOVERNMENT CONTRACT No AF33(615)-3940 SHALL NOT BE EITHER RELEASED OUTSIDE THE GOVERNMENT, OR USED, DUPLICATED, OR DISCLOSED IN WHOLE OR IN PART FOR MANUFACTURE OR PROCUREMENT, WITHOUT THE WRITTEN PERMISSION OF CURTISS-WRIGHT CORPORATION, EXCEPT FOR (I) EMERGENCY REPAIR OR OVERHAUL WORK BY OR FOR THE GOVERNMENT, WHERE THE ITEM OR PROCESS IS NOT OTHERWISE REASONABLY AVAILABLE TO ENABLE TIMELY PERFORMANCE OF THE WORK, OR (II) RELEASE TO A FOREIGN GOVERNMENT, AS THE INTERESTS OF THE UNITED STATES MAY REQUIRE; PROVIDED THAT IN EITHER CASE THE RELEASE, USE, DUPLICATION OR DISCLOSURE HEREOF SHALL BE SUBJECT TO THE FOREGOING LIMITATIONS. THIS LEGEND SHALL BE MARKED ON ANY REPRODUCTION HEREOF IN WHOLE OR IN PART."

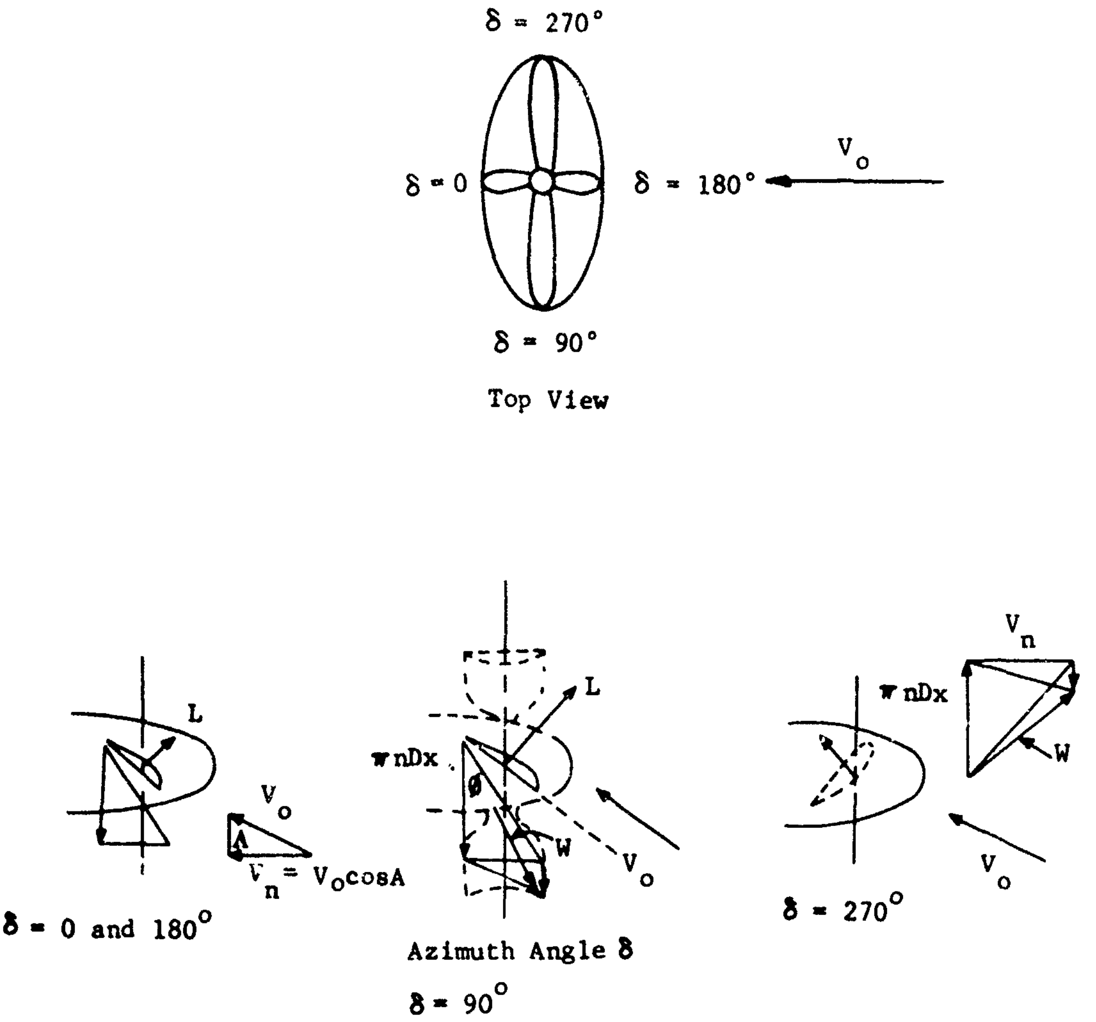

Top View

Azimuth Angle δ

Figure 5. Propeller inflow velocity components.

"FURNISHED UNDER UNITED STATES GOVERNMENT CONTRACT No. AF33(615)-3940. SHALL NOT BE EITHER RELEASED OUTSIDE THE GOVERNMENT, OR USED, DUPLICATED, OR DISCLOSED IN WHOLE OR IN PART FOR MANUFACTURE OR PROCUREMENT, WITHOUT THE WRITTEN PERMISSION OF CURTISS-WRIGHT CORPORATION, EXCEPT FOR (I) EMERGENCY REPAIR OR OVERHAUL WORK BY OR FOR THE GOVERNMENT, WHERE THE ITEM OR PROCESS IS NOT OTHERWISE REASONABLY AVAILABLE TO ENABLE TIMELY PERFORMANCE OF THE WORK, OR (II) RELEASE TO A FOREIGN GOVERNMENT, AS THE INTERESTS OF THE UNITED STATES MAY REQUIRE. PROVIDED THAT IN EITHER CASE THE RELEASE, USE, DUPLICATION OR DISCLOSURE HEREOF SHALL BE SUBJECT TO THE FOREGOING LIMITATIONS. THIS LEGEND SHALL BE MARKED ON ANY REPRODUCTION HEREOF IN WHOLE OR IN PART."

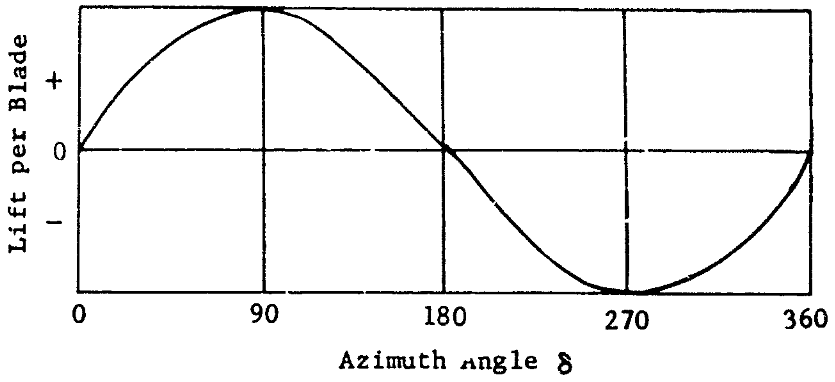

Figure 6. Approximate blade lift variation with rotational position.

"FURNISHED UNDER UNITED STATES GOVERNMENT CONTRACT No. AF33(615)-3940 SHALL NOT BE EITHER RELEASED OUTSIDE THE GOVERNMENT, OR USED, DUPLICATED, OR DISCLOSED IN WHOLE OR IN PART FOR MANUFACTURE OR PROCUREMENT, WITHOUT THE WRITTEN PERMISSION OF CURTISS-WRIGHT CORPORATION, EXCEPT FOR (i) EMERGENCY REPAIR OR OVERHAUL WORK BY OR FOR THE GOVERNMENT, WHERE THE ITEM OR PROCESS IS NOT OTHERWISE REASONABLY AVAILABLE TO ENABLE TIMELY PERFORMANCE OF THE WORK, OR (ii) RELEASE TO A FOREIGN GOVERNMENT AS THE INTERESTS OF THE UNITED STATES MAY REQUIRE. PROVIDED THAT IN EITHER CASE THE RELEASE, USE, DUPLICATION OR DISCLOSURE HEREOF SHALL BE SUBJECT TO THE FOREGOING LIMITATIONS. THIS LEGEND SHALL BE MARKED ON ANY REPRODUCTION HEREOF IN WHOLE OR IN PART."

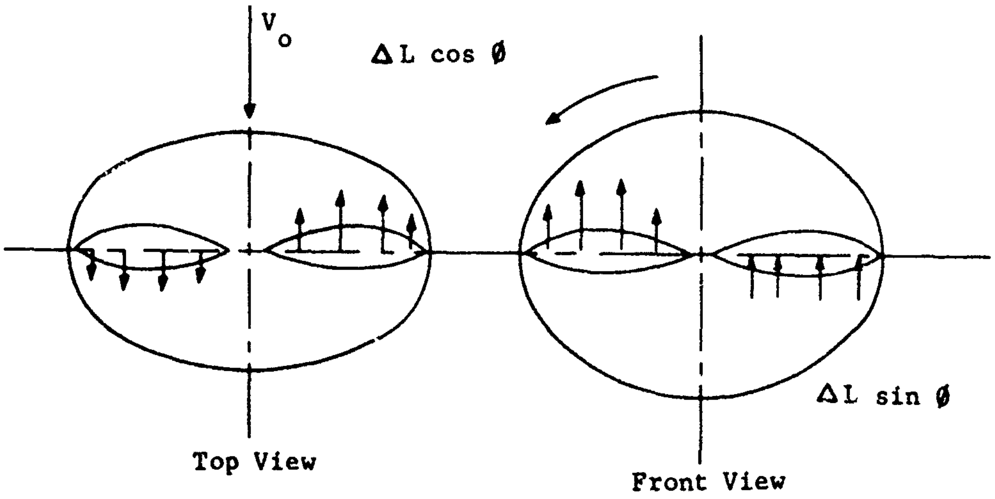

Figure 7. Incremental force variation due to propeller angle of attack, A.

"FURNISHED UNDER UNITED STATES GOVERNMENT CONTRACT No. AF33(615)-3940. SHALL NOT BE EITHER RELEASED OUTSIDE THE GOVERNMENT, OR USED, DUPLICATED, OR DISCLOSED IN WHOLE OR IN PART FOR MANUFACTURE OR PROCUREMENT, WITHOUT THE WRITTEN PERMISSION OF CURTISS-WRIGHT CORPORATION, EXCEPT FOR (i) EMERGENCY REPAIR OR OVERHAUL WORK BY OR FOR THE GOVERNMENT, WHERE THE ITEM OR PROCESS IS NOT OTHERWISE REASONABLY AVAILABLE TO ENABLE TIMELY PERFORMANCE OF THE WORK; OR (ii) RELEASE TO A FOREIGN GOVERNMENT, AS THE INTERESTS OF THE UNITED STATES MAY REQUIRE; PROVIDED THAT IN EITHER CASE THE RELEASE, USE, DUPLICATION OR DISCLOSURE HEREOF SHALL BE SUBJECT TO THE FOREGOING LIMITATIONS. THIS LEGEND SHALL BE MARKED ON ANY REPRODUCTION HEREOF IN WHOLE OR IN PART."

A left hand propeller will produce a yawing moment to the right when the shaft is at a positive angle of attack.

If the advance ratio and forward velocity are determined based on the velocity normal to the propeller disc, V_n, the power absorbed is nearly independent of the shaft angle. This is true as long as the propeller is operating near peak efficiency, blade sections do not stall, and the shaft angle of attack is less than approximately 5 degrees. Even if the mean drag is above the initial value when the propeller is operating at an angle of attack less than five degrees the overall efficiency is only slightly influenced as the power required for drag is only 5 to 15% of the total power used. As the shaft angle of attack is increased the drag variation as the blade rotates starts to become significant and the power increases with a corresponding drop of efficiency. The propeller data of reference 9 indicates that the thrust and power coefficients as measured along the shaft axis do not change in the range of shaft angle between 0 and 15°. Thus the loss of propeller efficiency at the shaft angle of 15 degrees is equal to the one minus cosine of the angle or 3.4%. This is considered of great importance as when the propeller is used to produce lift for cruise flight using radial force, it would be operating at a shaft angle of 3 to 4° with a corresponding loss of efficiency due to non-linear effects of less than 1%.

b. Theory of Normal Force and Yawing Moment

The radial force and yawing moment of an inclined propeller can be calculated by the method of strip analysis in the same manner as determining the thrust and torque of uninclined propellers. The main difficulty in analyzing the forces and moments produced by the inclined propeller is determining the inflow velocity at each azimuth position. Unlike a propeller operating with a zero shaft angle of attack where the wake is uniform, the inclined propeller has a wake that is varying in strength. This non-uniform wake is caused by the variation of circulation of lift produced as the propeller rotates in the inclined flow position. For this reason, when determining the inflow velocity at each position the local conditions cannot be used with conventional inflow calculations as this assumes that the wake is uniform and at a strength equal to that of the local conditions.

To calculate the inflow velocity and angle of an inclined propeller axis at the various blade azimuth positions, it was assumed that the strength of wake varied directly as the change in section

"FURNISHED UNDER UNITED STATES GOVERNMENT CONTRACT No. AF33(615)-3940. SHALL NOT BE EITHER RELEASED OUTSIDE THE GOVERNMENT, OR USED, DUPLICATED, OR DISCLOSED IN WHOLE OR IN PART FOR MANUFACTURE OR PROCUREMENT, WITHOUT THE WRITTEN PERMISSION OF CURTISS-WRIGHT CORPORATION, EXCEPT FOR (i) EMERGENCY REPAIR OR OVERHAUL WORK BY OR FOR THE GOVERNMENT, WHERE THE ITEM OR PROCESS IS NOT OTHERWISE REASONABLY AVAILABLE TO ENABLE TIMELY PERFORMANCE OF THE WORK. OR (ii) RELEASE TO A FOREIGN GOVERNMENT, AS THE INTERESTS OF THE UNITED STATES MAY REQUIRE: PROVIDED THAT IN EITHER CASE THE RELEASE, USE, DUPLICATION OR DISCLOSURE HEREOF SHALL BE SUBJECT TO THE FOREGOING LIMITATIONS. THIS LEGEND SHALL BE MARKED ON ANY REPRODUCTION HEREOF IN WHOLE OR IN PART."

lift as shown on Figure 6. The load distribution at each azimuth position and radial station was approximated by assuming steady state condition. Analysis could then be made by strip calculations, (5) and (6), to determine the load distribution and thus the strength of the wake at each azimuth position and downstream position from the propeller. Thus, knowing the characteristics of the wake behind the propeller, it is possible to find the inflow velocity at each position using the solution of the Biot Savart law given in (7). The procedure for calculating the inflow velocity is given as follows:

From Figure 8,

$$V_n = V_o \cos A$$

$$V_t = V_o \sin A$$

$$\tan \phi_o = \frac{V_o \cos A}{\pi n D x + (V_o \sin A) \sin \delta} = \frac{V_n}{\pi n D x + V_t \sin \delta}$$

$$J_{Local} = \pi x \tan \phi_o$$

δ = reference angle on the propeller disk[1]

V_o = forward velocity

The strength of circulation, Γ, is found for various values of ϕ_o, where

$$\Gamma = \frac{b\, C_L\, V_o}{2 \sin \phi_o}$$

It is desired to obtain the axial inflow-velocity, u, from (7) thus:

$$u = - \frac{1}{4 \pi R} \int_0^1 \sum_{p=0}^{p=B-1} \sum_0^{\infty} \frac{d\Gamma}{dx} \cdot \frac{1}{x} \Delta I dx$$

where p = blade number, from 0 to (B-1), and where δ increments of 45° were taken.

---

[1] Note that (7) refers to δ as ϕ.

"FURNISHED UNDER UNITED STATES GOVERNMENT CONTRACT No. AF33(615)-3940 SHALL NOT BE EITHER RELEASED OUTSIDE THE GOVERNMENT, OR USED, DUPLICATED, OR DISCLOSED IN WHOLE OR IN PART FOR MANUFACTURE OR PROCUREMENT, WITHOUT THE WRITTEN PERMISSION OF CURTISS-WRIGHT CORPORATION, EXCEPT FOR (I) EMERGENCY REPAIR OR OVERHAUL WORK BY OR FOR THE GOVERNMENT, WHERE THE ITEM OR PROCESS IS NOT OTHERWISE REASONABLY AVAILABLE TO ENABLE TIMELY PERFORMANCE OF THE WORK, OR (II) RELEASE TO A FOREIGN GOVERNMENT, AS THE INTERESTS OF THE UNITED STATES MAY REQUIRE. PROVIDED THAT IN EITHER CASE THE RELEASE, USE, DUPLICATION OR DISCLOSURE HEREOF SHALL BE SUBJECT TO THE FOREGOING LIMITATIONS. THIS LEGEND SHALL BE MARKED ON ANY REPRODUCTION HEREOF IN WHOLE OR IN PART."

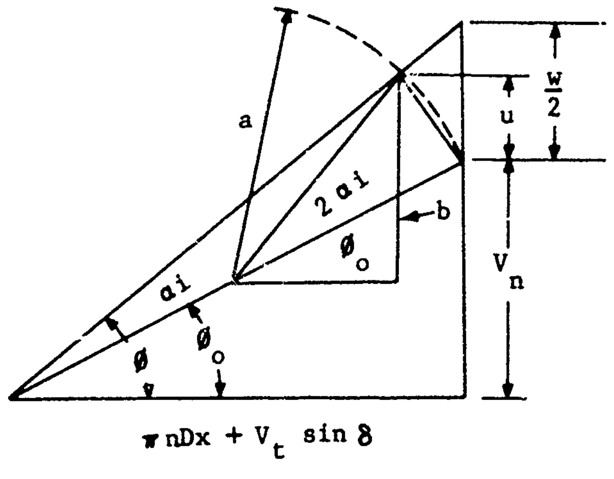

Figure 8. Propeller blade velocity components.

FURNISHED UNDER UNITED STATES GOVERNMENT CONTRACT No. AF33(615)-3940. SHALL NOT BE EITHER RELEASED OUTSIDE THE GOVERNMENT, OR USED, DUPLICATED, OR DISCLOSED IN WHOLE OR IN PART FOR MANUFACTURE OR PROCUREMENT, WITHOUT THE WRITTEN PERMISSION OF CURTISS-WRIGHT CORPORATION, EXCEPT FOR (I) EMERGENCY REPAIR OR OVERHAUL WORK BY OR FOR THE GOVERNMENT, WHERE THE ITEM OR PROCESS IS NOT OTHERWISE REASONABLY AVAILABLE TO ENABLE TIMELY PERFORMANCE OF THE WORK, OR (II) RELEASE TO A FOREIGN GOVERNMENT, AS THE INTERESTS OF THE UNITED STATES MAY REQUIRE. PROVIDED THAT IN EITHER CASE THE RELEASE, USE, DUPLICATION OR DISCLOSURE HEREOF SHALL BE SUBJECT TO THE FOREGOING LIMITATIONS. THIS LEGEND SHALL BE MARKED ON ANY REPRODUCTION HEREOF IN WHOLE OR IN PART."

$I = I_{@30^\circ} - I_{@45^\circ}$ or $I_{@45^\circ} - I_{@90^\circ}$ . . .

and $\frac{d\Gamma}{dx}$ is read at δ of 22.5° or 67.5° . . .

For a complete analysis this procedure for calculating u must be carried out for each station along the blade for varying δ and blade position.

A convenient way of comparing the results obtained as a propeller rotates is to evaluate $\bar{w}$, the ratio of the displacement velocity of the vortex sheet at infinity to the forward velocity of the airplane. For the case of the inclined propeller, the forward velocity is taken as the normal velocity $V_n = V_0 \cos A$. Calculations were made for the 0.7 radius where the propeller was at the reference angle of 0 and 90°. The following is the method used to calculate $\bar{w}$ once u has been determined. (See Figure 8.)

$$a = \frac{\sqrt{(\pi nDx + V_t \sin\delta)^2 + V_n^2}}{2}$$

$$b = u + \frac{V_n}{2}$$

$$\phi = \frac{\sin^{-1} b/a + \phi_0}{2}$$

$$\bar{w} = \frac{2u}{V_n \cos^2 \phi}$$

The following shows the results calculated at 0.7 radius for a three-blade propeller using blades with a 132 Activity Factor and IC_{Li} of 0.239. The propeller is inclined at an angle of 10° and operating at $J = 2.3$, $M_0 = 0.263$ and $\beta_{0.7R} = 50°.4$:

	For a Varying Wake (Actual Conditions)	For a Uniform Wake
δ_0	$\bar{w}$	$\bar{w}_{strip}$
0	.236	.171
90	.228	.288

FURNISHED UNDER UNITED STATES GOVERNMENT CONTRACT No. [illegible] SHALL NOT BE EITHER RELEASED OUTSIDE THE GOVERNMENT, OR USED, DUPLICATED, OR DISCLOSED IN WHOLE OR IN PART FOR MANUFACTURE OR PROCUREMENT, WITHOUT THE WRITTEN PERMISSION OF CURTISS WRIGHT CORPORATION, EXCEPT FOR (I) EMERGENCY REPAIR OR OVERHAUL WORK BY OR FOR THE GOVERNMENT, WHERE THE ITEM OR PROCESS IS NOT OTHERWISE REASONABLY AVAILABLE TO ENABLE TIMELY PERFORMANCE OF THE WORK, OR (II) RELEASE TO A FOREIGN GOVERNMENT, AS THE INTERESTS OF THE UNITED STATES MAY REQUIRE, PROVIDED THAT IN EITHER CASE THE RELEASE, USE, DUPLICATION OR DISCLOSURE HEREOF SHALL BE SUBJECT TO THE FOREGOING LIMITATIONS. THIS LEGEND SHALL BE MARKED ON ANY REPRODUCTION HEREOF IN WHOLE OR IN PART.

The displacement velocity, $\bar{V}$, is very nearly constant at $\delta_0 = 0°$ and 90° for the actual wake conditions, indicating a constant value over the entire disk. For the case where the wake is assumed uniform, based on the loadings at the azimuth angle under consideration, large differences in the displacement velocity ratio are observed for the $\delta_0 = 0$ and 90°. Because the wake is changing as a function of time, this assumption is believed to be wrong and is therefore discarded. It was investigated, as early theories made the assumption of the loading only influencing the wake and thus the inflow velocity.

These assumptions are:

(1) The change in induced angle at various azimuth positions is negligible.

(2) The slope of the lift curve is constant and has the value for the mean value of C_L (obtained from ordinary strip calculation).

(3) $\sin \phi = \sin \phi_o$ Light loading assumption

(4) The radial force contribution of blade section drag is negligible.

The local lift contribution for a station is

$$dL = 1/2 \rho W_o^2 \, b \, C_L \, dr \tag{1}$$

The local incremental lift contribution for a station is then

$$\Delta dL = \tfrac{1}{2} \rho b \left[(W_o + \Delta W)^2 (C_L + \Delta C_L) - W_o^2 C_L \right] dr \tag{2}$$

$$\Delta dL = \tfrac{1}{2} \rho b \Big[2W_o \Delta W C_L + \Delta W^2 C_L + 2W_o \Delta W a \Delta \alpha + \Delta W a^2 \Delta \alpha + \cdots + W_o^2 a \Delta \alpha \Big] dr \tag{3}$$

$$= \tfrac{1}{2} \rho b \Delta W^2 \left[C_L \left(\frac{2W_o}{\Delta W} + 1 \right) + a \Delta \alpha \left(\frac{W_o}{W} + 1 \right)^2 \right] dr \tag{4}$$

From Figure 9(c) the following relations are formed:

$$\cot \phi_o = \frac{\pi n D x}{V_o \cos A}$$

$$\cot \phi_o' = \frac{\pi n D x + V_o \sin A \sin \delta}{V_o \cos A} = \cot \phi_o + \tan A \sin \delta$$

$$W_o = V_o \cos A \csc \phi_o$$

FURNISHED UNDER UNITED STATES GOVERNMENT CONTRACT No. [illegible] SHALL NOT BE EITHER RELEASED OUTSIDE THE GOVERNMENT, OR USED, DUPLICATED, OR DISCLOSED IN WHOLE OR IN PART FOR MANUFACTURE OR PROCUREMENT, WITHOUT THE WRITTEN PERMISSION OF CURTISS WRIGHT CORPORATION EXCEPT FOR (1) EMERGENCY REPAIR OR OVERHAUL WORK BY OR FOR THE GOVERNMENT, WHERE THE ITEM OR PROCESS IS NOT OTHERWISE REASONABLY AVAILABLE TO ENABLE TIMELY PERFORMANCE OF THE WORK, OR (2) RELEASE TO A FOREIGN GOVERNMENT, AS THE INTERESTS OF THE UNITED STATES MAY REQUIRE; PROVIDED THAT IN EITHER CASE THE RELEASE, USE, DUPLICATION OR DISCLOSURE HEREOF SHALL BE SUBJECT TO THE FOREGOING LIMITATIONS. THIS LEGEND SHALL BE MARKED ON ANY REPRODUCTION HEREOF IN WHOLE OR IN PART.

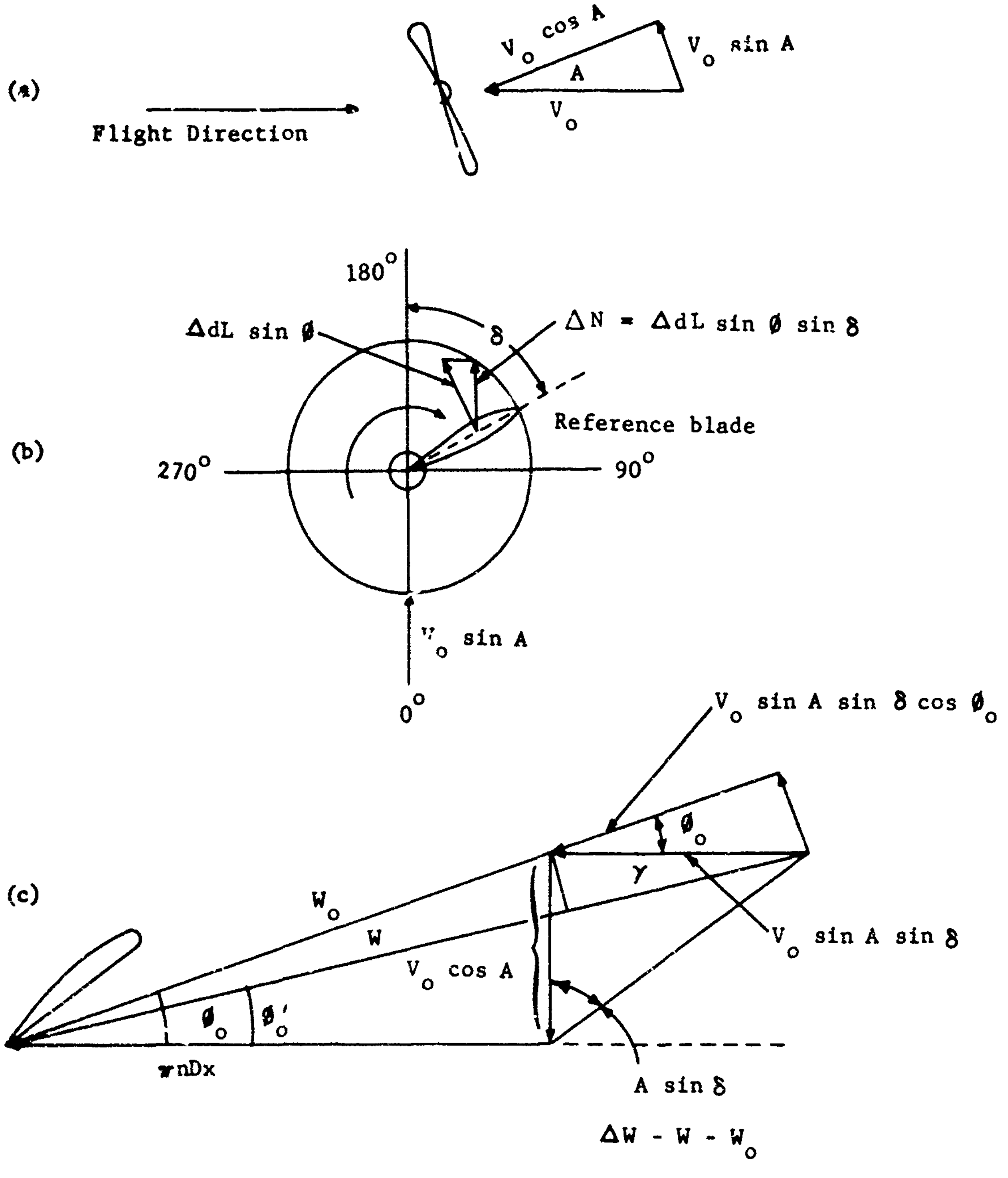
(a)
Flight Direction
$V_o \cos A$
$V_o \sin A$
A
V_o
(b)
180°
$\Delta dL \sin \phi$
δ
$\Delta N = \Delta dL \sin \phi \sin \delta$
Reference blade
270°
90°
$V_o \sin A$
0°
(c)
$V_o \sin A \sin \delta \cos \phi_o$
ϕ_o
γ
W_o
W
$V_o \sin A \sin \delta$
$V_o \cos A$
ϕ_o
ϕ_o'
πnDx
$A \sin \delta$
$\Delta W - W - W_o$

Figures 9. Three dimensional distribution of velocity components.

FURNISHED UNDER UNITED STATES GOVERNMENT CONTRACT No AF33(6.5)-3940. SHALL NOT BE EITHER RELEASED OUTSIDE THE GOVERNMENT, OR USED, DUPLICATED, OR DISCLOSED IN WHOLE OR IN PART FOR MANUFACTURE OR PROCUREMENT, WITHOUT THE WRITTEN PERMISSION OF CURTISS-WRIGHT CORPORATION, EXCEPT FOR (I) EMERGENCY REPAIR OR OVERHAUL WORK BY OR FOR THE GOVERNMENT WHERE THE ITEM OR PROCESS IS NOT OTHERWISE REASONABLY AVAILABLE TO ENABLE TIMELY PERFORMANCE OF THE WORK. OR (II) RELEASE TO A FOREIGN GOVERNMENT, AS THE INTERESTS OF THE UNITED STATES MAY REQUIRE. PROVIDED THAT IN EITHER CASE THE RELEASE, USE, DUPLICATION OR DISCLOSURE HEREOF SHALL BE SUBJECT TO THE FOREGOING LIMITATIONS. THIS LEGEND SHALL BE MARKED ON ANY REPRODUCTION HEREOF IN WHOLE OR IN PART.

$$W = V_o \cos A \csc \phi'_o$$

$$\Delta W = W - W_o$$

$$\Delta W = V_o \cos A (\csc\phi'_o - \csc \phi_o)$$

$$\frac{2W_o}{\Delta W} + 1 = \frac{\csc\phi'_o + \csc\phi_o}{\csc\phi'_o - \csc\phi_o}$$

$$\frac{W_o}{\Delta W} + 1 = \frac{\csc\phi'_o}{\csc\phi'_o - \csc\phi_o}$$

$$\Delta\alpha = \phi_o - \phi'_o$$

Substituting these values into equation (4) gives

$$\Delta dL = \tfrac{1}{2}\rho b \left\{V_o \cos A \left[\csc \phi'_o - \csc \phi_o\right]\right\}^2 \left\{C_L\left[\frac{\csc\phi'_o + \csc\phi_o}{\csc\phi'_o - \csc\phi_o}\right] + \right.$$

$$\left. \cdots \quad + a(\phi_o - \phi'_o)\left[\frac{\csc\phi'_o}{\csc\phi'_o - \csc\phi_o}\right]\right\} dr$$

$$\Delta dL = qb \cos^2 A \left[C_L \ (\csc^2\phi'_o - \csc^2\phi_o) + a(\phi_o - \phi'_o)(\csc^2\phi'_o)\right] dr$$

$$\Delta dL = qb \frac{\cos^2 A}{\sin^2\phi'_o}\left[C_L(1- \frac{\sin^2\phi'_o}{\sin^2\phi_o}) + a(\phi_o - \phi'_o)\right] dr \qquad (5)$$

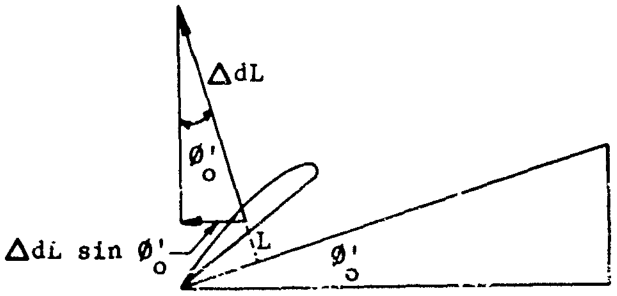

From Figure 9, the radial force component in the propeller plane is seen to be $\Delta dL \sin\phi'_o$. And From Figure 9(b), the incremental normal force is seen as $\Delta dL \sin \phi'_o \sin \delta$. By substitution in Equation (5),

$$\Delta F_N = qb \frac{\cos^2 A \sin \delta}{\sin \phi'_o}\left[C_L(1 - \frac{\sin^2\phi'_o}{\sin^2\phi_o}) + a(\phi_o - \phi'_o)\right] dr \qquad (6)$$

FURNISHED UNDER UNITED STATES GOVERNMENT CONTRACT No. AF33(615)-3940. SHALL NOT BE EITHER RELEASED OUTSIDE THE GOVERNMENT, OR USED, DUPLICATED, OR DISCLOSED IN WHOLE OR IN PART FOR MANUFACTURE OR PROCUREMENT, WITHOUT THE WRITTEN PERMISSION OF CURTISS-WRIGHT CORPORATION, EXCEPT FOR (i) EMERGENCY REPAIR OR OVERHAUL WORK BY OR FOR THE GOVERNMENT, WHERE THE ITEM OR PROCESS IS NOT OTHERWISE REASONABLY AVAILABLE TO ENABLE TIMELY PERFORMANCE OF THE WORK, OR (ii) RELEASE TO A FOREIGN GOVERNMENT, AS THE INTERESTS OF THE UNITED STATES MAY REQUIRE, PROVIDED THAT IN EITHER CASE THE RELEASE, USE, DUPLICATION OR DISCLOSURE HEREOF SHALL BE SUBJECT TO THE FOREGOING LIMITATIONS. THIS LEGEND SHALL BE MARKED ON ANY REPRODUCTION HEREOF IN WHOLE OR IN PART."

$$N = \sum_{\delta}^{\delta + \frac{B-1}{B} 2\pi} \int_{x}^{1} \Delta F_n R dx$$

$$N_{AV.} = \frac{B}{2\pi} \int_{\delta}^{\delta + \frac{2\pi}{B}} F_n d\delta$$

This section will consist of a simplification of the method formed in the previous section. From this section a plot of dL versus "δ" showed that the variation was approximately sinusoidal. By making the following assumptions, a shorter, but still accurate method for finding radial force will be developed.

Assumptions:

(a) ΔdL varies sinusoidally during a revolution.

(b) All of the lift curve slopes may be represented by a single value.

(c) Small angles may be approximated by their tangents.

(d) Products of differentials are negligible.

By removing higher order differentials from Equation (3), the equation becomes

$$\Delta dL = 1/2 \, \rho b \left\{ 2W_o \Delta C_L + W_o^2 a \Delta \alpha \right\} dr \qquad (7)^{2}$$

From Figure 9c the following is obtained:

$$W_o = \frac{V_o \cos A}{\sin \phi_o}$$

$$W \cong V \sin A \cos \gamma$$

$$\tan\Delta\alpha = \frac{V \sin A \sin \phi_o}{W_o + V \sin A \cos \phi_o} \cong \Delta\alpha$$

The following are obtained by combining terms.

$$W_o^2 \Delta\alpha = \frac{V \sin A \sin \phi_o W_o^2}{W_o + V \sin A \cos \phi_o} = \frac{V^2 \left(\frac{\sin 2A}{2}\right)}{1 + \tan\left(\frac{A \sin 2\phi_o}{\gamma}\right)}$$

---

[2] Note that sin δ is omitted from these equations; this is so because only the peak value at 90° is used and sin 90° = 1.

FURNISHED UNDER UNITED STATES GOVERNMENT CONTRACT No. AF33(616)-3945 SHALL NOT BE EITHER RELEASED OUTSIDE THE GOVERNMENT, OR USED, DUPLICATED, OR DISCLOSED IN WHOLE OR IN PART FOR MANUFACTURE OR PROCUREMENT, WITHOUT THE WRITTEN PERMISSION OF CURTISS-WRIGHT CORPORATION EXCEPT FOR (i) EMERGENCY REPAIR OR OVERHAUL WORK BY OR FOR THE GOVERNMENT, WHERE THE ITEM OR PROCESS IS NOT OTHERWISE REASONABLY AVAILABLE TO ENABLE TIMELY PERFORMANCE OF THE WORK, OR (ii) RELEASE TO A FOREIGN GOVERNMENT, AS THE INTERESTS OF THE UNITED STATES MAY REQUIRE; PROVIDED THAT IN EITHER CASE THE RELEASE, USE, DUPLICATION OR DISCLOSURE HEREOF SHALL BE SUBJECT TO THE FOREGOING LIMITATIONS. THIS LEGEND SHALL BE MARKED ON ANY REPRODUCTION HEREOF IN WHOLE OR IN PART.

$$W_o \, \Delta W = \frac{V \cos A \; V \sin A \cos \gamma}{\sin \phi_o} = \frac{V^2 (\frac{\sin 2A}{2}) \cos \gamma}{\sin \phi_o}$$

By substituting these quantities into Equation (7), dL is obtained

$$\Delta dL_{90^\circ} = qb \, \frac{\sin 2A}{2} \left\{ 2C_L \left(\frac{\cos \gamma}{\sin \phi_o}\right) \frac{a}{1 + \tan(\frac{A \sin 2\phi_o}{2})} \right\} dr$$

From Assumption 1, $\Delta dL = \Delta dL_{90^\circ} \sin \delta$, and

from Figure 9(b), $\Delta N = (\Delta dL_{90^\circ} \sin \delta) \sin \phi \sin \delta$

$$\Delta N_{av.} = \Delta dL_{90^\circ} \sin \phi \int_0^{2\pi} \frac{\sin^2 \delta \, d\delta}{2\pi} = \frac{\Delta dL_{90^\circ} \sin \phi}{2}$$

$$dN = \tfrac{1}{2} qBb \, \frac{\sin 2A}{2} \left\{ 2\left(\frac{C_L \sin \phi \cos \gamma}{\sin \phi_o}\right) + \frac{a \sin \phi}{1 + (\frac{\tan A \sin 2\phi_o}{2})} \right\} dr \qquad (8)$$

The final equation has a factor of 0.95 to insure conservative values

$$N = 0.95 \, \frac{B}{2} \, qR \, \frac{\sin 2A}{2} \sum_{0}^{x=1} b \left\{ \frac{2C_L \sin \phi \cos \gamma}{\sin \phi_o} + \frac{a \sin \phi}{1 + \frac{\tan A \sin 2\phi_o}{2}} \right\} \Delta x \qquad (9)$$

Note that although the blade chord is a function of x for a given blade the value of N is constant as long as $b \Delta x$ remains constant.

The above equation has been programmed on IBM equipment.

In a similar manner the shaft moment (yawing) generated by the propeller operating at an angle of attack can be derived.

The equation is:

$$M = 0.95 \, \frac{B}{2} \, qR \, \frac{\sin 2A}{2} \sum_{x=0}^{1} br \left\{ \frac{2C_L \cos \phi}{\sin \phi_o} + \frac{a \cos \phi}{1 + \frac{\tan A \sin 2\phi_o}{2}} \right\} \Delta x \qquad (10)$$

"FURNISHED UNDER UNITED STATES GOVERNMENT CONTRACT No AF33(615)-3940. SHALL NOT BE EITHER RELEASED OUTSIDE THE GOVERNMENT, OR USED, DUPLICATED, OR DISCLOSED IN WHOLE OR IN PART FOR MANUFACTURE OR PROCUREMENT, WITHOUT THE WRITTEN PERMISSION OF CURTISS-WRIGHT CORPORATION, EXCEPT FOR (I) EMERGENCY REPAIR OR OVERHAUL WORK BY OR FOR THE GOVERNMENT, WHERE THE ITEM OR PROCESS IS NOT OTHERWISE REASONABLY AVAILABLE TO ENABLE TIMELY PERFORMANCE OF THE WORK OR (II) RELEASE TO A FOREIGN GOVERNMENT, AS THE INTERESTS OF THE UNITED STATES MAY REQUIRE. PROVIDED THAT IN EITHER CASE THE RELEASE, USE, DUPLICATION OR DISCLOSURE HEREOF SHALL BE SUBJECT TO THE FOREGOING LIMITATIONS. THIS LEGEND SHALL BE MARKED ON ANY REPRODUCTION HEREOF IN WHOLE OR IN PART."

It can be shown that for small values of A, Equations (9) and (10) can be reduced to

$$F_n = \frac{K^1 BAq(AF)D^2}{K_1} \sin\beta_{0.7} \left(a_{0.7} + 2C_{L_{0.7}} \cot\beta_{0.7}\right) \tag{11}$$

$$M = \frac{K^1 BAq(AF)D^3}{K_1} \cos\beta_{0.7} \left(a_{0.7} + 2C_{L_{0.7}} \cot\beta_{0.7}\right) \tag{12}$$

where

K^1 = 1.1
AF = activity factor
D = propeller diameter
$\beta_{0.7}$ = blade angle measured at the 0.7 blade radius
C_L = operating lift coefficient
K_1 = 450,000

The torque and thrust of propellers operating at an angle of attack can be calculated by the method and data given in (5) and (6). The induced effects are determined by the advance ratio, normal to the propeller disk and the given power coefficient or

$$J_n = J \cos A$$

The theory developed on the preceeding pages assumes that all sections of the propeller are operating on the straight portion of the lift curve and below the positive and negative stall angle. Further the theory assumes that the drag is small in comparison to the lift and can be neglected. For these reasons the theory outlined is considered to be accurate only up to a shaft angle of approximately 30 to 45 degrees; at higher angles it is necessary to use test data, and this is what was done in determining the performance, loads, and stability of X-100 and X-19 aircraft. It is recognized that this situation is unsatisfactory, but satisfactory theories and section test data were not available.

Although it was necessary to make several assumptions in the course of the development of a theory for calculating propeller radial force and some of these assumptions may appear to

FURNISHED UNDER UNITED STATES GOVERNMENT CONTRACT No. AF33([illegible])-[illegible]40 SHALL NOT BE EITHER RELEASED OUTSIDE THE GOVERNMENT, OR USED, DUPLICATED, OR DISCLOSED IN WHOLE OR IN PART FOR MANUFACTURE OR PROCUREMENT, WITHOUT THE WRITTEN PERMISSION OF CURTISS-WRIGHT CORPORATION, EXCEPT FOR (I) EMERGENCY REPAIR OR OVERHAUL WORK BY OR FOR THE GOVERNMENT WHERE THE ITEM OR PROCESS IS NOT OTHERWISE REASONABLY AVAILABLE TO ENABLE TIMELY PERFORMANCE OF THE WORK, OR (II) RELEASE TO A FOREIGN GOVERNMENT, AS THE INTERESTS OF THE UNITED STATES MAY REQUIRE; PROVIDED THAT IN EITHER CASE THE RELEASE, USE, DUPLICATION OR DISCLOSURE HEREOF SHALL BE SUBJECT TO THE FOREGOING LIMITATIONS. THIS LEGEND SHALL BE MARKED ON ANY REPRODUCTION HEREOF IN WHOLE OR IN PART.

be crude, the results of the calculations in general agree very closely with test data, see Figures 13 to 18 and Table II. The largest difference between the calculated and test data occurs at a 15 degrees where the calculated level of radial force coefficient is 10 to 15% above the measured level. At the higher shaft angle of attack better agreement is obtained. It is believed that since good agreement was obtained with other test data at the lower angles, Table II, that the test data at the 15° angle for the X-100 propeller is in error.

At the time of the development of the X-19 and X-100 airplanes methods were not available for calculating propeller radial force at shaft angles above 45° as the position and shape of the vortex shed in the wake could not be found. Since the shed vortices and their strength determine the inflow velocity and thus, the angle of attack of the blade section, it is apparent that the radial force could not be calculated at these high angles. This difficulty has been one of the major problems with propellers and rotary wing aircraft, and the problem is now in process of solution.

3. APPLICATION OF PROPELLER RADIAL LIFT TO V/STOL AIRCRAFT

a. General

The radial lift developed by propellers must be properly accounted for in the early design phase of any aircraft, and especially an airplane where the propellers operate through a high range of tilt angles. By the proper application of propeller radial lift a VTOL aircraft can be improved whether it be a tilt propeller single wing, a tilt wing, a tandem tilt propeller or a deflected propeller slipstream type. An improvement in performance will be obtained as the propeller supplies lift due to radial force which reduces wing stall tendencies. The advantages of radial force have been studied only for the tilt propeller fixed wing type. Therefore the application of radial force and the methods of optimization apply only to this type aircraft.

When an airplane is configured as a VTOL vehicle the wing is no longer primarily needed for lift at the take-off and landing conditions. Thus it can be optimized only for the other critical flight conditions.

If the aircraft is of the transport category the wing would normally be optimized for operation at the primary design cruise condition in accordance with classical aerodynamic techniques. Items such as weight, aspect ratio and wing area would be considered in such an optimization procedure.

"FURNISHED UNDER UNITED STATES GOVERNMENT CONTRACT No. AF33([illegible])-3940. SHALL NOT BE EITHER RELEASED OUTSIDE THE GOVERNMENT, OR USED, DUPLICATED, OR DISCLOSED IN WHOLE OR IN PART FOR MANUFACTURE OR PROCUREMENT, WITHOUT THE WRITTEN PERMISSION OF CURTISS-WRIGHT CORPORATION, EXCEPT FOR (I) EMERGENCY REPAIR OR OVERHAUL WORK BY OR FOR THE GOVERNMENT, WHERE THE ITEM OR PROCESS IS NOT OTHERWISE REASONABLY AVAILABLE TO ENABLE TIMELY PERFORMANCE OF THE WORK, OR (II) RELEASE TO A FOREIGN GOVERNMENT, AS THE INTERESTS OF THE UNITED STATES MAY REQUIRE; PROVIDED THAT IN EITHER CASE THE RELEASE, USE, DUPLICATION OR DISCLOSURE HEREOF SHALL BE SUBJECT TO THE FOREGOING LIMITATIONS. THIS LEGEND SHALL BE MARKED ON ANY REPRODUCTION HEREOF IN WHOLE OR IN PART."

To generate the required thrust at hover even with high levels of Figure of Merit, the propellers used on tilt wing and tilt propeller V/STOL aircraft will be larger than for the same weight conventional airplane. The propellers of V/STOL aircraft will operate at section lift coefficients near the optimum (and have large blade areas) whereas the propellers of conventional aircraft operate at overloaded conditions and high section lift coefficients. Since the propeller can be used to generate lift at the cruise flight condition, some of the wing area of the airplane normally chosen for peak cruise performance can be eliminated. With a fixed propeller geometry the lift produced is a function of the flight dynamic pressure, "q", and the propeller shaft angle of tilt A. The propeller blade stress is also proportional to "Aq" and as a result this has been an important design parameter for conventional propellers. At any flight condition the lift and drag developed by the propeller operating at a positive angle of attack is found from the equations:

$$L = N \text{ Cos } A + A \, T_n \text{Sin } A \qquad (13)$$

$$D = N \text{ Sin } [illegible] \; T_n \, (1 - \text{Cos } A) \qquad (14)$$

where

N = the ra [illegible] force - the actual in plane force

T_n = the p [illegible] r thrust normal to the propeller disk.

Equation 13 and [illegible] ume that the loss of thrust due to the shaft angle inclination [illegible] well as the inclination of the normal force in the direction o [illegible] e drag is charged to drag. Propeller thrust must be used to overcome the drag. The lift drag ratio of the propeller operating at an angle of attack is then from equations 13 and 14

$$\frac{L}{D} = \frac{N \text{ cos } A + T_n \text{ Sin } A}{N \text{ Sin } A + T_n \, (1 - \text{Cos } A)} \qquad (15)$$

At low shaft angle this equation shows that the L/D becomes very high and even approaches infinity as a limit as A approaches 0. Of course N approaches 0 as A approaches 0 so this is of importance only at finite values of N. Thus by choosing the proper shaft angle, the propeller can be made to operate at any desired value of lift-drag ratio desired. However, as the shaft angle is reduced the radial force becomes smaller since, by Equation (11) N is a direct function of A.

"FURNISHED UNDER UNITED STATES GOVERNMENT CONTRACT No. AF33(615)-1960. SHALL NOT BE EITHER RELEASED OUTSIDE THE GOVERNMENT, OR USED DUPLICATED, OR DISCLOSED IN WHOLE OR IN PART FOR MANUFACTURE OR PROCUREMENT, WITHOUT THE WRITTEN PERMISSION OF CURTISS-WRIGHT CORPORATION, EXCEPT FOR (I) EMERGENCY REPAIR OR OVERHAUL WORK BY OR FOR THE GOVERNMENT, WHERE THE ITEM OR PROCESS IS NOT OTHERWISE REASONABLY AVAILABLE TO ENABLE TIMELY PERFORMANCE OF THE WORK, OR (II) RELEASE TO A FOREIGN GOVERNMENT, AS THE INTERESTS OF THE UNITED STATES MAY REQUIRE. PROVIDED THAT IN EITHER CASE THE RELEASE, USE, DUPLICATION OR DISCLOSURE HEREOF SHALL BE SUBJECT TO THE FOREGOING LIMITATIONS. THIS LEGEND SHALL BE MARKED ON ANY REPRODUCTION HEREOF IN WHOLE OR IN PART."

b. Application In Cruise

To obtain the maximum lift-drag ratio with minimum wing area, the propellers on the tilt-prop fixed-wing type V/STOL aircraft should operate at a shaft angle that gives a L/D equal to that of the wing When the wing area is reduced by the use of radial lift the propellers serve two purposes which help keep the weight empty of the aircraft low. Also, improved vertical take-off performance is obtained as the download losses are reduced due to the reduction of area under the propeller.

In determining the proper wing area and aspect ratio to be used with propellers producing radial lift many other factors must be considered and all the important flight conditions must be analyzed where high lift-drag ratio must be obtained.

For instance when reducing the wing area to a minimum the wing structure can become a problem as the spar box depth becomes limited by the wing thickness ratio necessary to obtain low drag and high values of critical Mach number. In the case of the X-19 the thickness ratios of the front and rear wings were 21 and 18%, respectively, and obtaining a good structure became a major problem. On the front wing it was necessary to use 1/4 inch skins of aluminum alloy to obtain the required characteristics.

With small wings, problems are also encountered in providing the necessary area or lift coefficient range for the flight control surfaces. In the case of the X-19 the area available for the elevators and ailerons was marginal and still have an adequate structure. If it had been necessary to increase the control power on this airplane, considerable difficulty would have been encountered. The wings of the X-19 were designed with a high loading as the airplane was originally intended to operate at high speeds and fairly low altitude.

The X-19 wing loading based on a weight of 13,660 lb. was approximately 85 psf considering the area of both the front and rear wings. At the design cruise condition of 271 knots EAS the front propellers are designed to operate at a shaft angle of 2.8° which gives an L/D of 29 for the propellers. Even at a speed of 230 knots EAS the propellers operate at a lift drag ratio of 12 which is above the maximum of the entire aircraft. Note that at the 230 knot condition a reduction of the propeller tilt angle would reduce the propeller lift slightly and improve the overall L/D. It would therefore appear that it should be possible to select the propeller shaft angle at any flight condition to obtain the maximum performance.

'FURNISHED UNDER UNITED STATES GOVERNMENT CONTRACT No. AF33(615)-3940. SHALL NOT BE EITHER RELEASED OUTSIDE THE GOVERNMENT, OR USED, DUPLICATED, OR DISCLOSED IN WHOLE OR IN PART FOR MANUFACTURE OR PROCUREMENT, WITHOUT THE WRITTEN PERMISSION OF CURTISS-WRIGHT CORPORATION, EXCEPT FOR (I) EMERGENCY REPAIR OR OVERHAUL WORK BY OR FOR THE GOVERNMENT, WHERE THE ITEM OR PROCESS IS NOT OTHERWISE REASONABLY AVAILABLE TO ENABLE TIMELY PERFORMANCE OF THE WORK. OR (II) RELEASE TO A FOREIGN GOVERNMENT, AS THE INTERESTS OF THE UNITED STATES MAY REQUIRE: PROVIDED THAT IN EITHER CASE THE RELEASE, USE, DUPLICATION OR DISCLOSURE HEREOF SHALL BE SUBJECT TO THE FOREGOING LIMITATIONS. THIS LEGEND SHALL BE MARKED ON ANY REPRODUCTION HEREOF IN WHOLE OR IN PART.'

c. Application in Transition

The wing configuration chosen for high performance at the cruise flight conditions must be adequate to handle the lift requirements at the other flight conditions. One criteria that may affect the wing area requirements is the speed at which the propeller must be tilted down and locked. No specification has been established to define such a speed and there does not appear to be any factor other than mechanical that should establish such a limitation. In the case of the X-19 the speed for conversion was 160 knots, and at a gross weight of 13,660 lb. the angle of attack required was 13.5°. It is believed that the speed for conversion should have been higher with a corresponding lower angle of attack.

Unlike a conventional airplane where the wings supply all the necessary lift for flight, a VTOL airplane must have direct lift produced from the expenditure of power to supplement the wing lift. This lift must be supplied in ever increasing amounts as the speed is reduced toward zero until at hover all the lift is supplied by a direct conversion of power and thrust.

When the propeller is tilted up the required lift, over and above that supplemented by the wing, is obtained from the thrust and the radial force vector. The variation with speed of the wing lift, thrust and radial force is shown on Figure 10 for the X-100, a VTOL aircraft with a wing loading of 160 psf. At the low flight speeds, high tilt angles must be maintained so that the required lift can be generated by the propeller thrust. As the wings pick up lift from forward motion of the aircraft, the tilt angle can be reduced so that the propellers start to generate lift through radial force. This builds up to a peak of approximately 26% of the required lift at 160 MPH.

The variation of lift between the front and rear propellers and wings is shown for an equilibrium transition of the X-19 on Figure 11. As in the case of the X-100 the propellers are supplying a large portion of the lift requirement from radial force at speeds of 100 to 160 knots.

For lifting-propeller VTOL aircraft the tilt angle necessary at any given speed will be dependent on the following: -

(1) Wing loading
(2) Propeller disk loading
(3) Radial propeller force
(4) Power
(5) Aircraft angle of attack
(6) Acceleration

At a given speed and tilt angle, an increase in propeller radial lift will reduce the wing area required, or the aircraft angle of attack, or the propeller tilt angle while increasing the power.

"FURNISHED UNDER UNITED STATES GOVERNMENT CONTRACT No. AF33(615)-3940 SHALL NOT BE EITHER RELEASED OUTSIDE THE GOVERNMENT, OR USED, DUPLICATED, OR DISCLOSED IN WHOLE OR IN PART FOR MANUFACTURE OR PROCUREMENT, WITHOUT THE WRITTEN PERMISSION OF CURTISS-WRIGHT CORPORATION, EXCEPT FOR (I) EMERGENCY REPAIR OR OVERHAUL WORK BY OR FOR THE GOVERNMENT, WHERE THE ITEM OR PROCESS IS NOT OTHERWISE REASONABLY AVAILABLE TO ENABLE TIMELY PERFORMANCE OF THE WORK OR (II) RELEASE TO A FOREIGN GOVERNMENT AS THE INTERESTS OF THE UNITED STATES MAY REQUIRE. PROVIDED THAT IN EITHER CASE THE RELEASE, USE, DUPLICATION OR DISCLOSURE HEREOF SHALL BE SUBJECT TO THE FOREGOING LIMITATIONS. THIS LEGEND SHALL BE MARKED ON ANY REPRODUCTION HEREOF IN WHOLE OR IN PART."

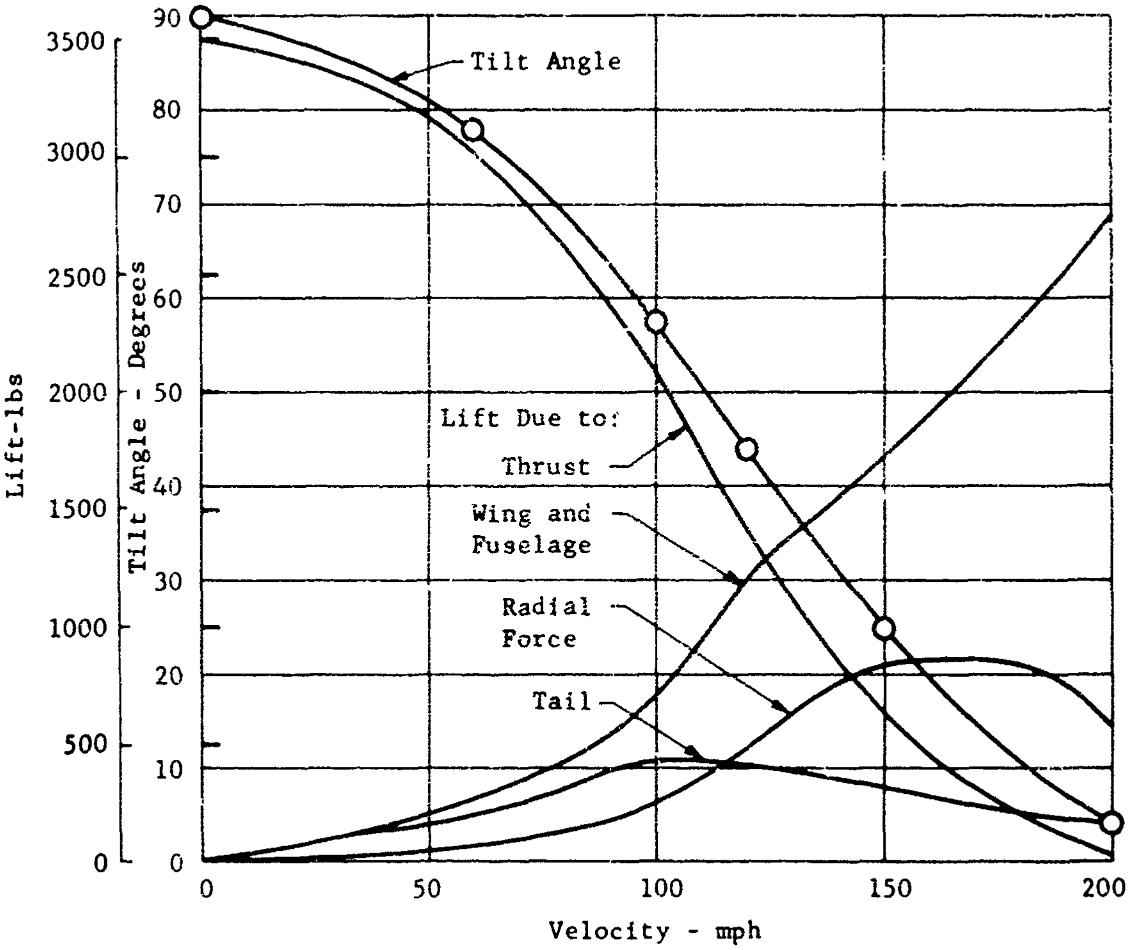

Figure 10. Curtiss-Wright X-100 distribution of propeller and airplane component lift distributions through equilibrium transition; G.W. 3500 lbs., 1240 RPM, $\alpha_{fus} = 5^{\circ}$. Determined from model wing tunnel test data.

"FURNISHED UNDER UNITED STATES GOVERNMENT CONTRACT No. AF33(615)-3940 SHALL NOT BE EITHER RELEASED OUTSIDE THE GOVERNMENT, OR USED, DUPLICATED, OR DISCLOSED IN WHOLE OR IN PART FOR MANUFACTURE OR PROCUREMENT, WITHOUT THE WRITTEN PERMISSION OF CURTISS-WRIGHT CORPORATION, EXCEPT FOR (i) EMERGENCY REPAIR OR OVERHAUL WORK BY OR FOR THE GOVERNMENT, WHERE THE ITEM OR PROCESS IS NOT OTHERWISE REASONABLY AVAILABLE TO ENABLE TIMELY PERFORMANCE OF THE WORK OR (ii) RELEASE TO A FOREIGN GOVERNMENT, AS THE INTERESTS OF THE UNITED STATES MAY REQUIRE: PROVIDED THAT IN EITHER CASE THE RELEASE, USE, DUPLICATION OR DISCLOSURE HEREOF SHALL BE SUBJECT TO THE FOREGOING LIMITATIONS. THIS LEGEND SHALL BE MARKED ON ANY REPRODUCTION HEREOF IN WHOLE OR IN PART."

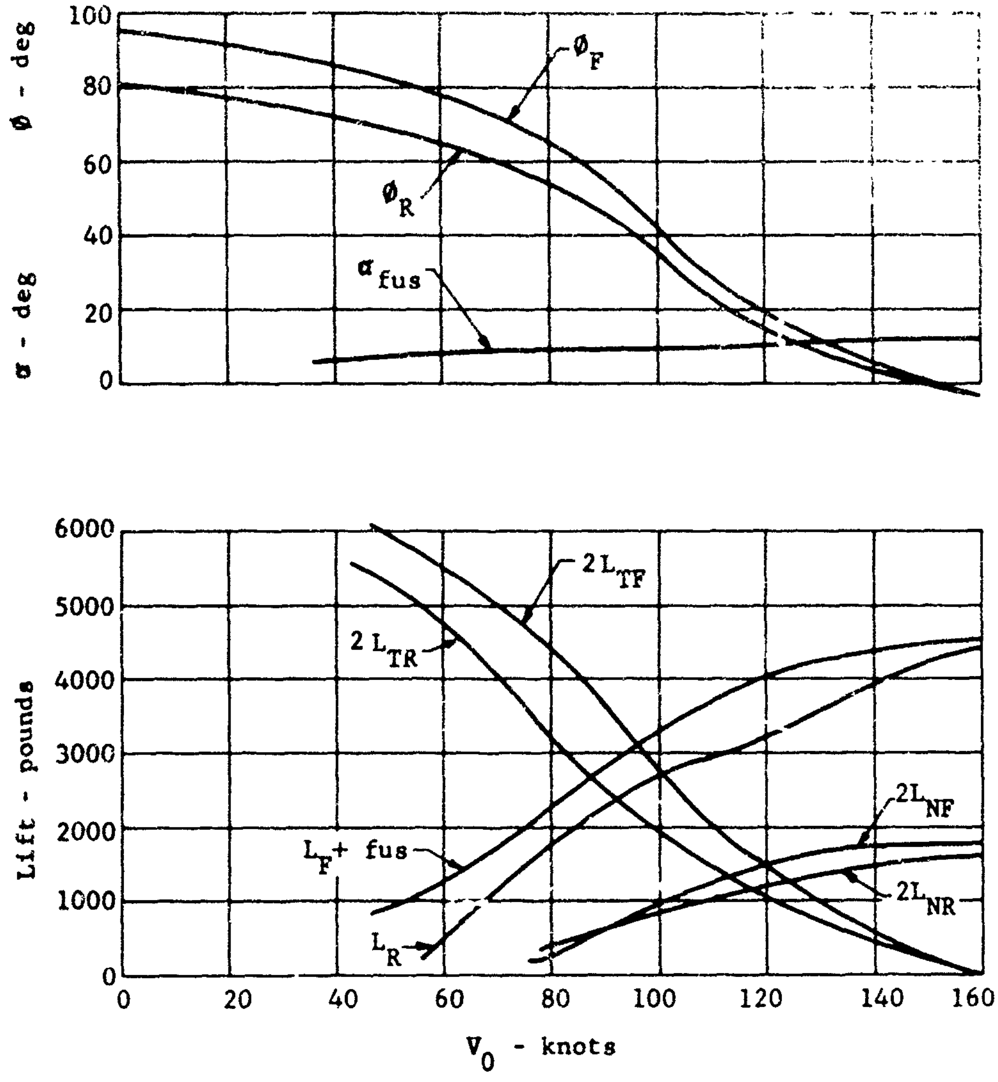

Figure 11. X-19, distribution of propeller and airplane component lift distributions through equilibrium transition; G.W. 12300 lbs. Determined from powered model wind tunnel test data.

"FURNISHED UNDER UNITED STATES GOVERNMENT CONTRACT No. AF33(615)-3941 SHALL NOT BE EITHER RELEASED OUTSIDE THE GOVERNMENT OR USED, DUPLICATED, OR DISCLOSED IN WHOLE OR IN PART FOR MANUFACTURE OR PROCUREMENT, WITHOUT THE WRITTEN PERMISSION OF CURTISS-WRIGHT CORPORATION, EXCEPT FOR (i) EMERGENCY REPAIR OR OVERHAUL WORK BY OR FOR THE GOVERNMENT, WHERE THE ITEM OR PROCESS IS NOT OTHERWISE REASONABLY AVAILABLE TO ENABLE TIMELY PERFORMANCE OF THE WORK, OR (ii) RELEASE TO A FOREIGN GOVERNMENT, AS THE INTERESTS OF THE UNITED STATES MAY REQUIRE, PROVIDED THAT IN EITHER CASE THE RELEASE, USE, DUPLICATION OR DISCLOSURE HEREOF SHALL BE SUBJECT TO THE FOREGOING LIMITATIONS. THIS LEGEND SHALL BE MARKED ON ANY REPRODUCTION HEREOF IN WHOLE OR IN PART."

Since the power required is less than that necessary for hovering, the increased radial lift is more than needed. By increasing the drag vector the power can be added to increase thrust and therefore lift, and so in a secondary way the radial force drag component is important in supplying lift to the overall configuration.

It should be realized that at low speeds, when the propeller is producing high radial force at a high angle of attack, the L/D of the propeller is poor. For instance at 45° the L/D of the propeller radial force is only one. However, during the conversion maneuver the lift that can be produced is much more important than L/D since little time, and therefore fuel, is required.

It is apparent that if the schedule of shaft angle of attack and α were properly chosen, the conversion could be accomplished without the wing. The speed at which conversion would be completed would be high; of course trim moments still have to be provided. The wing then does not have to be chosen to provide lift, if the propellers can be operated at any Aq. This is the problem, as the stresses in the blades are a direct function of the Aq encountered (see Section 5.0).

It is therefore necessary to examine the wing area and propeller Aq in combination to be sure that the total wing lift is adequate to keep the propeller lift and stress requirements within bounds.

The propeller forces produced during the conversion conditions can be reduced for coefficients similar to lift and drag instead of the usual propeller thrust and normal force coefficients as follows:

$$C_{L_p} = \frac{T \sin A + N \cos A}{q S_p}$$

and

$$C_{X_p} = \frac{T \cos A - N \sin A}{q S_p}$$

where T = shaft thrust; N = normal force; q = dynamic pressure, $1/2 \rho V_o^2$; S_p = prop disk area; and A = shaft angle of attack.

At a given propeller advance ratio, C_{L_p} and C_{X_p} can be plotted against shaft angle of attack in a manner similar to that of a wing (Figure 12). Unlike a wing, however, the variation of the propeller lift and total thrust forces have no sudden force breaks. For this reason it is believed that with a properly designed VTOL aircraft the propellers will not cause any sudden breaks in the lift at any flight conditions. As a result the conversion characteristics should be smooth for the tilt propeller V/STOL

"FURNISHED UNDER UNITED STATES GOVERNMENT CONTRACT No. AF33(616)-5940. SHALL NOT BE EITHER RELEASED OUTSIDE THE GOVERNMENT, OR USED, DUPLICATED, OR DISCLOSED IN WHOLE OR IN PART FOR MANUFACTURE OR PROCUREMENT, WITHOUT THE WRITTEN PERMISSION OF CURTISS-WRIGHT CORPORATION, EXCEPT FOR (I) EMERGENCY REPAIR OR OVERHAUL WORK BY OR FOR THE GOVERNMENT, WHERE THE ITEM OR PROCESS IS NOT OTHERWISE REASONABLY AVAILABLE TO ENABLE TIMELY PERFORMANCE OF THE WORK, OR (II) RELEASE TO A FOREIGN GOVERNMENT, AS THE INTERESTS OF THE UNITED STATES MAY REQUIRE. PROVIDED THAT IN EITHER CASE THE RELEASE, USE, DUPLICATION OR DISCLOSURE HEREOF SHALL BE SUBJECT TO THE FOREGOING LIMITATIONS. THIS LEGEND SHALL BE MARKED ON ANY REPRODUCTION HEREOF IN WHOLE OR IN PART."

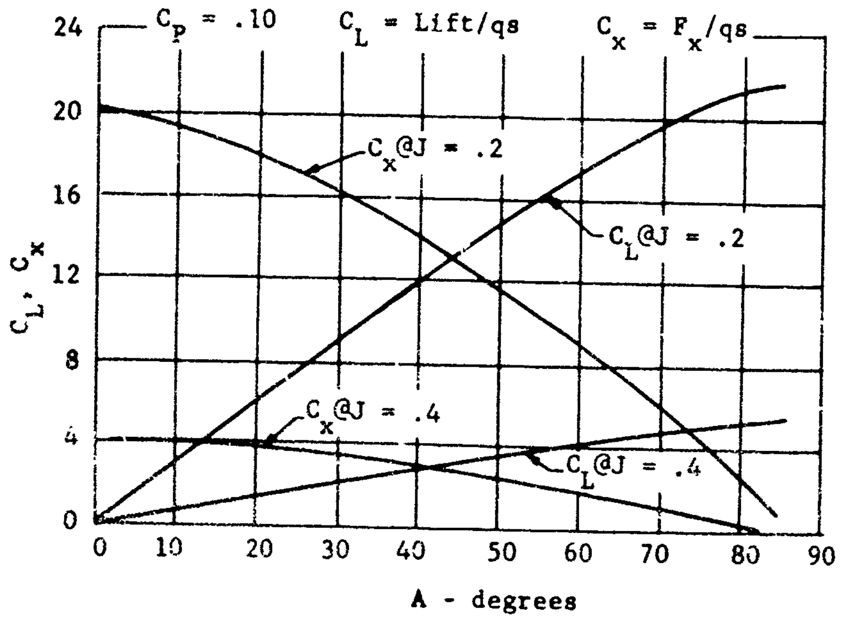

Figure 12. Propeller lift and accelerating thrust variation with "A" angle; wind axis coordinates.

FURNISHED UNDER UNITED STATES GOVERNMENT CONTRACT No AF33(615)-3940 SHALL NOT BE EITHER RELEASED OUTSIDE THE GOVERNMENT, OR USED DUPLICATED, OR DISCLOSED IN WHOLE OR IN PART FOR MANUFACTURE OR PROCUREMENT, WITHOUT THE WRITTEN PERMISSION OF CURTISS-WRIGHT CORPORATION, EXCEPT FOR (I) EMERGENCY REPAIR OR OVERHAUL WORK BY OR FOR THE GOVERNMENT, WHERE THE ITEM OR PROCESS IS NOT OTHERWISE REASONABLY AVAILABLE TO ENABLE TIMELY PERFORMANCE OF THE WORK OR (II) RELEASE TO A FOREIGN GOVERNMENT, AS THE INTERESTS OF THE UNITED STATES MAY REQUIRE. PROVIDED THAT IN EITHER CASE THE RELEASE, USE, DUPLICATION OR DISCLOSURE HEREOF SHALL BE SUBJECT TO THE FOREGOING LIMITATIONS. THIS LEGEND SHALL BE MARKED ON ANY REPRODUCTION HEREOF IN WHOLE OR IN PART."

aircraft. This was demonstrated with the X-100 aircraft.

d. Summary

In summary the propeller operating with radial force makes it possible to design a VTOL airplane incorporating the wing area necessary for optimum cruise flight at any condition or series of conditions. This, coupled with the stall free characteristics with changes in shaft angle, make the high radial lift propeller a useful and efficient device for V/STOL airplanes.

4. CORRELATION OF CALCULATED AND TEST RESULTS

Using the theory given in (6) the radial force was calculated for a number of points as shown in Table II and compared to the test data of (8) and (9). As noted from Table II fair agreement between the test and calculated points are obtained for shaft angles up to 20°. Further comparisons between the data obtained with the X-100 propeller, (9), are shown on Figures 13 to 18. From these comparisons it appears that fairly good accuracy is obtained by calculation up to angles of 45°. At angles above 45° the tests indicate higher levels of radial force than calculated.

Although good success was obtained in the calculation of radial force, it was still not possible to calculate the level of force at angles above 45° with any degree of accuracy. For this reason when determining the performance of the X-19, propeller test data were used.

FURNISHED UNDER UNITED STATES GOVERNMENT CONTRACT No. AF33(615)-3940 SHALL NOT BE EITHER RELEASED OUTSIDE THE GOVERNMENT, OR USED, DUPLICATED, OR DISCLOSED IN WHOLE OR IN PART FOR MANUFACTURE OR PROCUREMENT, WITHOUT THE WRITTEN PERMISSION OF CURTISS-WRIGHT CORPORATION, EXCEPT FOR (I) EMERGENCY REPAIR OR OVERHAUL WORK BY OR FOR THE GOVERNMENT, WHERE THE ITEM OR PROCESS IS NOT OTHERWISE REASONABLY AVAILABLE TO ENABLE TIMELY PERFORMANCE OF THE WORK, OR (II) RELEASE TO A FOREIGN GOVERNMENT, AS THE INTERESTS OF THE UNITED STATES MAY REQUIRE. PROVIDED THAT IN EITHER CASE THE RELEASE, USE, DUPLICATION OR DISCLOSURE HEREOF SHALL BE SUBJECT TO THE FOREGOING LIMITATIONS. THIS LEGEND SHALL BE MARKED ON ANY REPRODUCTION HEREOF IN WHOLE OR IN PART."

Table II. Comparison between calculated and test values of radial force, N.

10-(3) (062)-045 Blade B = 3 D = 10'0"

400 πnD

J	Cp	A°	N, IBM	N, Test
2.3	.248	10°	403	410
1.15	.129	10°	82.2	88
1.15	.129	20°	161	193
1.15	.247	10°	97.5	102
1.15	.247	20°	193	224
2.3	.210	10°	396	444
2.3	.210	20°	767	975
2.3	.248	10°	403	453
2.3	.248	20°	783	995
3.46	.248	10°	964	1090
3.46	.248	20°	1881	2395
3.46	.438	10°	997	1125
3.46	.438	20°	1957	2455

"FURNISHED UNDER UNITED STATES GOVERNMENT CONTRACT No. AF33(615)-3940. SHALL NOT BE EITHER RELEASED OUTSIDE THE GOVERNMENT, OR USED, DUPLICATED, OR DISCLOSED IN WHOLE OR IN PART FOR MANUFACTURE OR PROCUREMENT, WITHOUT THE WRITTEN PERMISSION OF CURTISS-WRIGHT CORPORATION, EXCEPT FOR (I) EMERGENCY REPAIR OR OVERHAUL WORK BY OR FOR THE GOVERNMENT, WHERE THE ITEM OR PROCESS IS NOT OTHERWISE REASONABLY AVAILABLE TO ENABLE TIMELY PERFORMANCE OF THE WORK, OR (II) RELEASE TO A FOREIGN GOVERNMENT, AS THE INTERESTS OF THE UNITED STATES MAY REQUIRE. PROVIDED THAT IN EITHER CASE THE RELEASE, USE, DUPLICATION OR DISCLOSURE HEREOF SHALL BE SUBJECT TO THE FOREGOING LIMITATIONS. THIS LEGEND SHALL BE MARKED ON ANY REPRODUCTION HEREOF IN WHOLE OR IN PART."

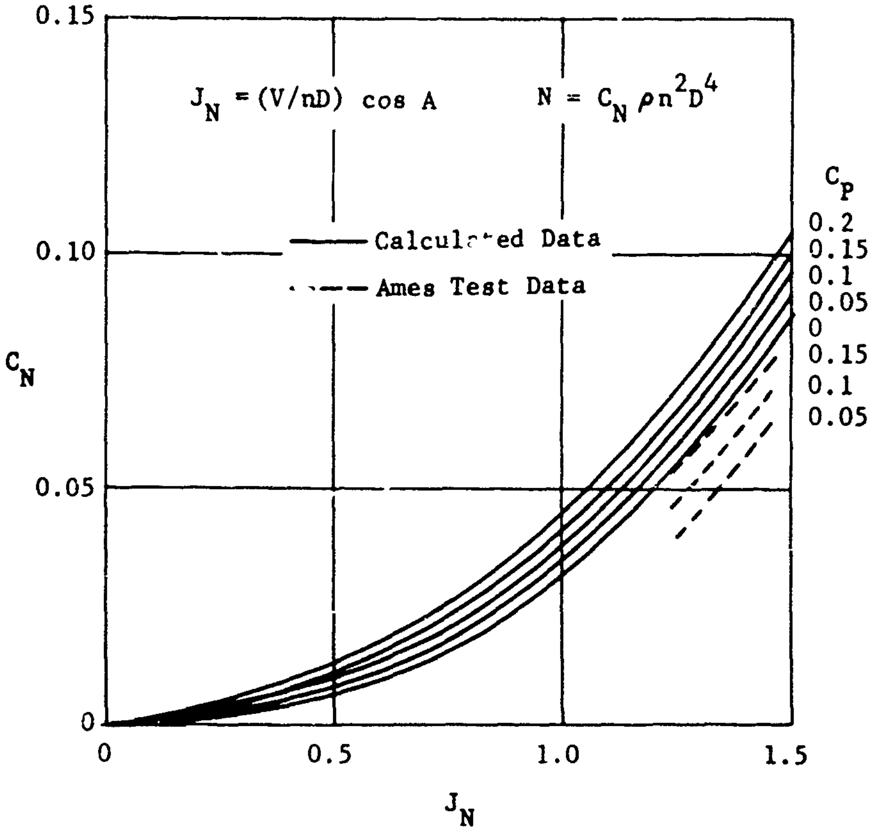

Figure 13. Normal force coefficient as a function of advance ratio perpendicular to the propeller disk; 3(X100188) blade, dia. = 10 ft. AF = 188, IC_{L_i} = 0.068; A = 15°.

FURNISHED UNDER UNITED STATES GOVERNMENT CONTRACT No. AF33(615)-1940. SHALL NOT BE EITHER RELEASED OUTSIDE THE GOVERNMENT, OR USED, DUPLICATED, OR DISCLOSED IN WHOLE OR IN PART FOR MANUFACTURE OR PROCUREMENT, WITHOUT THE WRITTEN PERMISSION OF CURTISS-WRIGHT CORPORATION, EXCEPT FOR (I) EMERGENCY REPAIR OR OVERHAUL WORK BY OR FOR THE GOVERNMENT, WHERE THE ITEM OR PROCESS IS NOT OTHERWISE REASONABLY AVAILABLE TO ENABLE TIMELY PERFORMANCE OF THE WORK, OR (II) RELEASE TO A FOREIGN GOVERNMENT, AS THE INTERESTS OF THE UNITED STATES MAY REQUIRE. PROVIDED THAT IN EITHER CASE THE RELEASE, USE, DUPLICATION OR DISCLOSURE HEREOF SHALL BE SUBJECT TO THE FOREGOING LIMITATIONS. THIS LEGEND SHALL BE MARKED ON ANY REPRODUCTION HEREOF IN WHOLE OR IN PART."

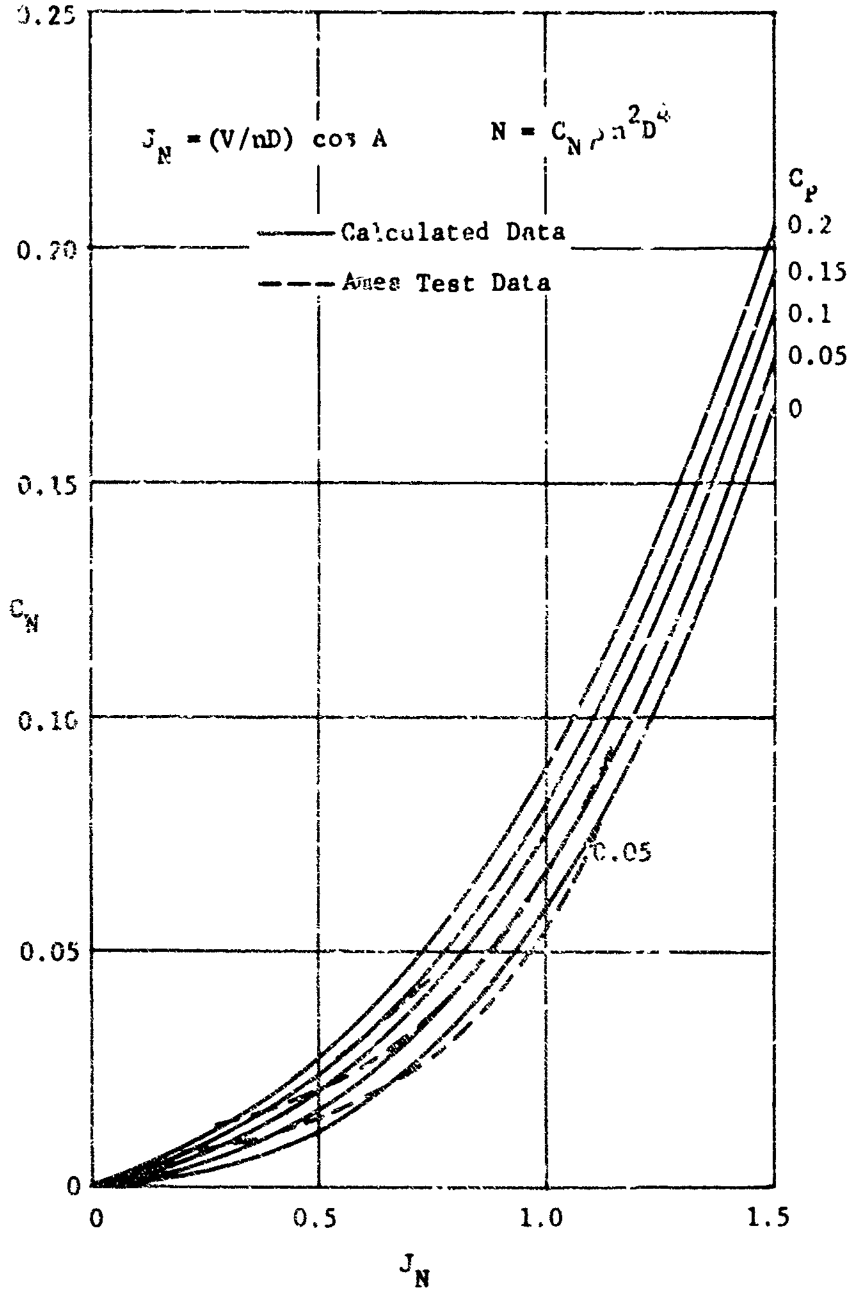

Figure 14. Normal force coefficient as a function of advance ratio perpendicular to the propeller disk; 3(X100188) blade, dia. = 10 ft. AF = 188, IC_{L_i} = 0.068; A = 30°.

"FURNISHED UNDER UNITED STATES GOVERNMENT CONTRACT No. AF33(615)-3940. SHALL NOT BE EITHER RELEASED OUTSIDE THE GOVERNMENT, OR USED, DUPLICATED, OR DISCLOSED IN WHOLE OR IN PART FOR MANUFACTURE OR PROCUREMENT, WITHOUT THE WRITTEN PERMISSION OF CURTISS-WRIGHT CORPORATION, EXCEPT FOR (I) EMERGENCY REPAIR OR OVERHAUL WORK BY OR FOR THE GOVERNMENT, WHERE THE ITEM OR PROCESS IS NOT OTHERWISE REASONABLY AVAILABLE TO ENABLE TIMELY PERFORMANCE OF THE WORK, OR (II) RELEASE TO A FOREIGN GOVERNMENT, AS THE INTERESTS OF THE UNITED STATES MAY REQUIRE. PROVIDED THAT IN EITHER CASE THE RELEASE, USE, DUPLICATION OR DISCLOSURE HEREOF SHALL BE SUBJECT TO THE FOREGOING LIMITATIONS. THIS LEGEND SHALL BE MARKED ON ANY REPRODUCTION HEREOF IN WHOLE OR IN PART."

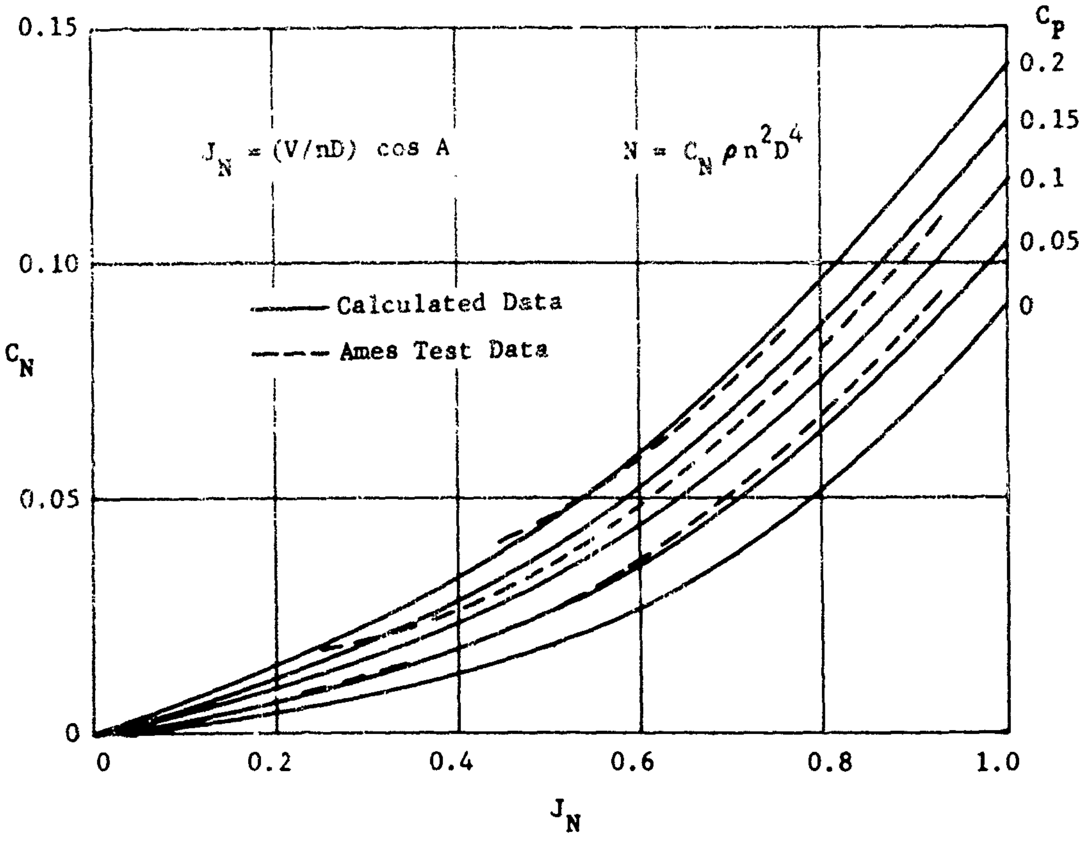

Figure 15. Normal force coefficient as a function of advance ratio perpendicular to the propeller disk; 3(X100188) blade, dia. = 10 ft. AF = 188, IC_{L_i} = 0.068; A = 45°.

"FURNISHED UNDER UNITED STATES GOVERNMENT CONTRACT No AF33(615)-3940 SHALL NOT BE EITHER RELEASED OUTSIDE THE GOVERNMENT, OR USED, DUPLICATED, OR DISCLOSED IN WHOLE OR IN PART FOR MANUFACTURE OR PROCUREMENT, WITHOUT THE WRITTEN PERMISSION OF CURTISS-WRIGHT CORPORATION, EXCEPT FOR (i) EMERGENCY REPAIR OR OVERHAUL WORK BY OR FOR THE GOVERNMENT, WHERE THE ITEM OR PROCESS IS NOT OTHERWISE REASONABLY AVAILABLE TO ENABLE TIMELY PERFORMANCE OF THE WORK, OR (ii) RELEASE TO A FOREIGN GOVERNMENT, AS THE INTERESTS OF THE UNITED STATES MAY REQUIRE. PROVIDED THAT IN EITHER CASE THE RELEASE, USE, DUPLICATION OR DISCLOSURE HEREOF SHALL BE SUBJECT TO THE FOREGOING LIMITATIONS. THIS LEGEND SHALL BE MARKED ON ANY REPRODUCTION HEREOF IN WHOLE OR IN PART."

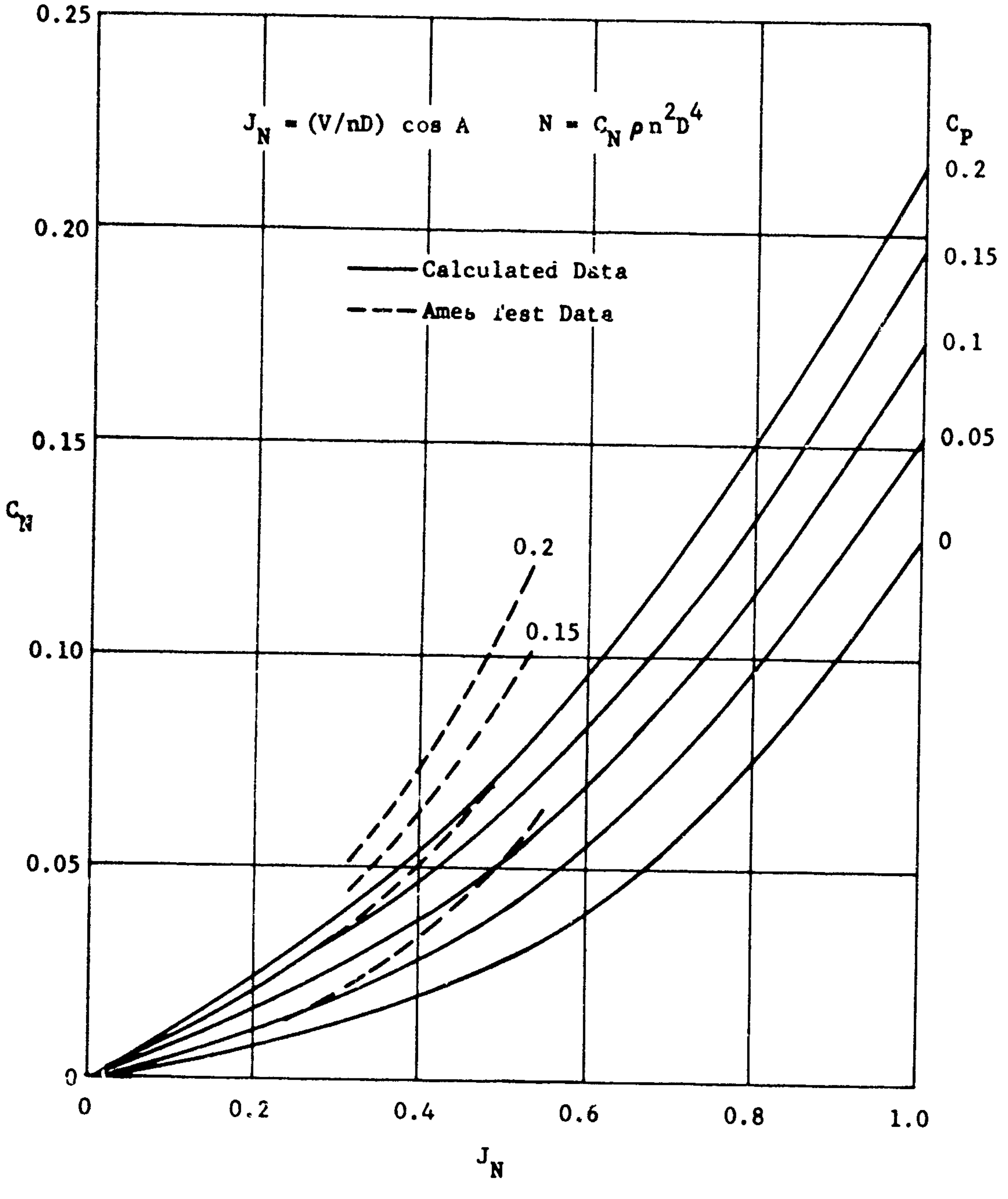

Figure 16. Normal force coefficient as a function of advance ratio perpendicular to the propeller disk; 3(X100188) blade, dia. = 10 ft. AF = 188, IC_{L_i} = 0.068; A = 60°.

"FURNISHED UNDER UNITED STATES GOVERNMENT CONTRACT No. AF33(615)-3940. SHALL NOT BE EITHER RELEASED OUTSIDE THE GOVERNMENT, OR USED, DUPLICATED, OR DISCLOSED IN WHOLE OR IN PART FOR MANUFACTURE OR PROCUREMENT, WITHOUT THE WRITTEN PERMISSION OF CURTISS-WRIGHT CORPORATION, EXCEPT FOR (I) EMERGENCY REPAIR OR OVERHAUL WORK BY OR FOR THE GOVERNMENT, WHERE THE ITEM OR PROCESS IS NOT OTHERWISE REASONABLY AVAILABLE TO ENABLE TIMELY PERFORMANCE OF THE WORK, OR (II) RELEASE TO A FOREIGN GOVERNMENT, AS THE INTERESTS OF THE UNITED STATES MAY REQUIRE. PROVIDED THAT IN EITHER CASE THE RELEASE, USE, DUPLICATION OR DISCLOSURE HEREOF SHALL BE SUBJECT TO THE FOREGOING LIMITATIONS. THIS LEGEND SHALL BE MARKED ON ANY REPRODUCTION HEREOF IN WHOLE OR IN PART."

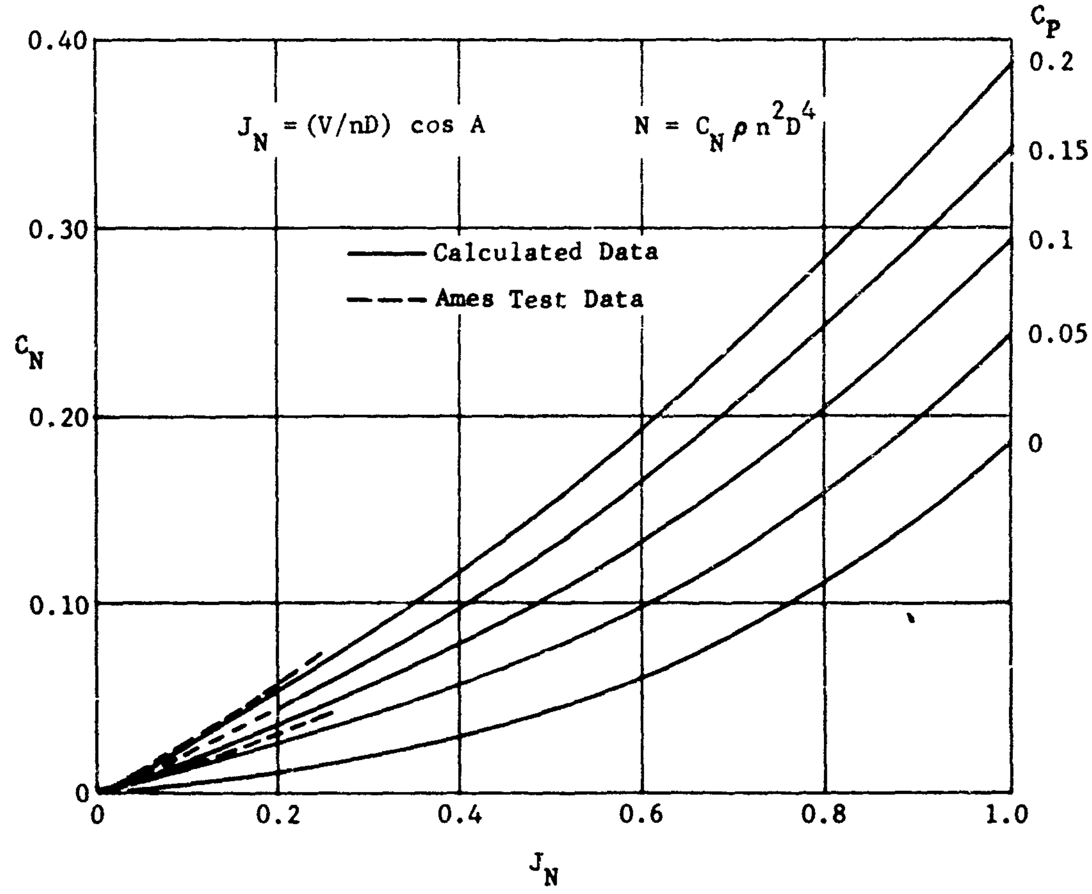

Figure 17. Normal force coefficient as a function of advance ratio perpendicular to the propeller disk; 3(X100188)blade, dia. = 10 ft. AF = 188, IC_{L_i} = 0.068; A = 75°.

"FURNISHED UNDER UNITED STATES GOVERNMENT CONTRACT No. AF33(615)-1940. SHALL NOT BE EITHER RELEASED OUTSIDE THE GOVERNMENT, OR USED, DUPLICATED, OR DISCLOSED IN WHOLE OR IN PART FOR MANUFACTURE OR PROCUREMENT, WITHOUT THE WRITTEN PERMISSION OF CURTISS-WRIGHT CORPORATION, EXCEPT FOR (I) EMERGENCY REPAIR OR OVERHAUL WORK BY OR FOR THE GOVERNMENT, WHERE THE ITEM OR PROCESS IS NOT OTHERWISE REASONABLY AVAILABLE TO ENABLE TIMELY PERFORMANCE OF THE WORK. OR (II) RELEASE TO A FOREIGN GOVERNMENT, AS THE INTERESTS OF THE UNITED STATES MAY REQUIRE: PROVIDED THAT IN EITHER CASE THE RELEASE, USE, DUPLICATION OR DISCLOSURE HEREOF SHALL BE SUBJECT TO THE FOREGOING LIMITATIONS. THIS LEGEND SHALL BE MARKED ON ANY REPRODUCTION HEREOF IN WHOLE OR IN PART."

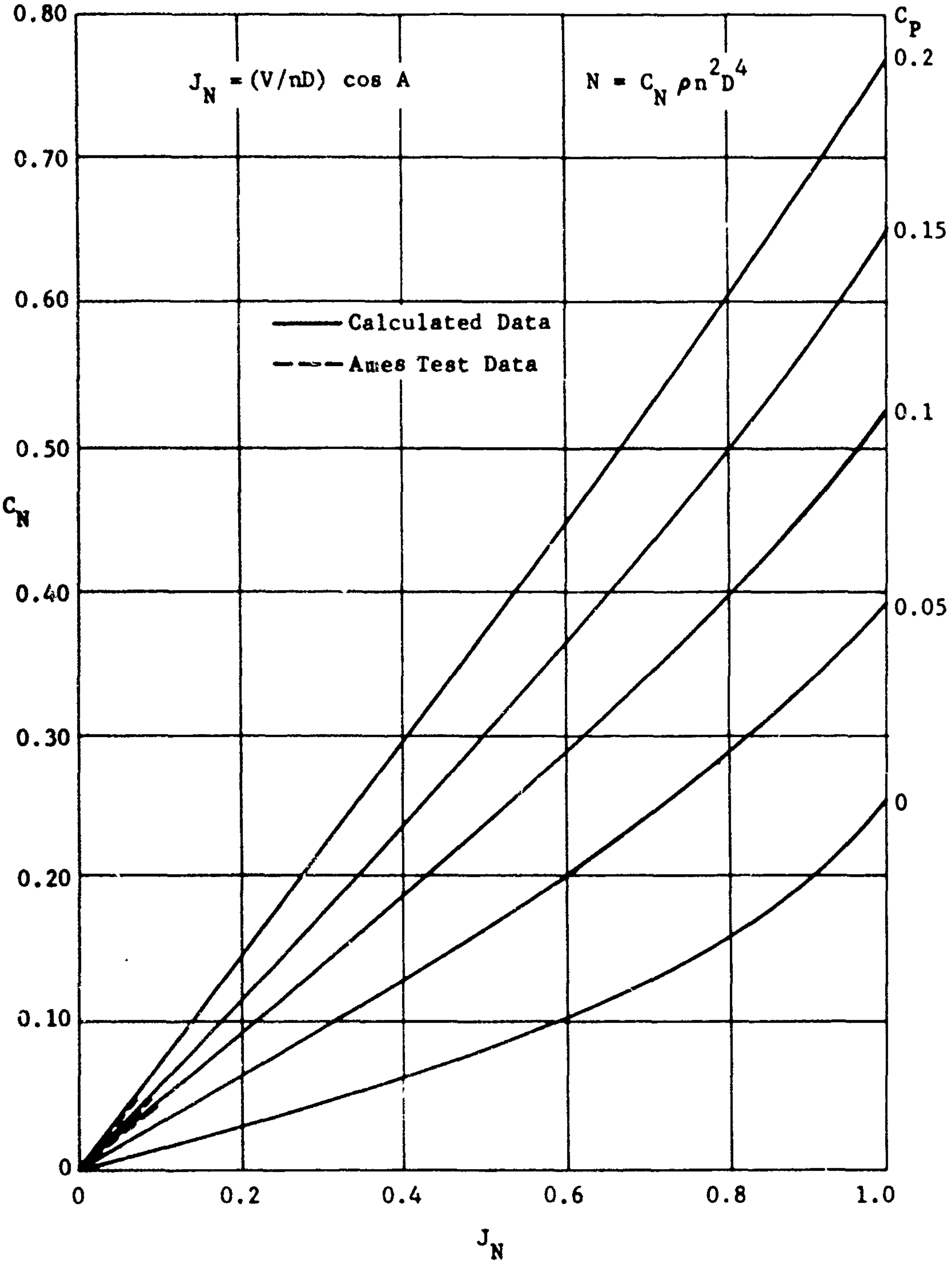

Figure 18. Normal force coefficient as a function of advance ratio perpendicular to the propeller disk; 3(X100188) blade, dia. = 10 ft. AF = 188, IC_{L_i} = 0.068; A = 85°.

"FURNISHED UNDER UNITED STATES GOVERNMENT CONTRACT No. AF33(615)-1940 SHALL NOT BE EITHER RELEASED OUTSIDE THE GOVERNMENT OR USED, DUPLICATED, OR DISCLOSED IN WHOLE OR IN PART FOR MANUFACTURE OR PROCUREMENT, WITHOUT THE WRITTEN PERMISSION OF CURTISS-WRIGHT CORPORATION, EXCEPT FOR (i) EMERGENCY REPAIR OR OVERHAUL WORK BY OR FOR THE GOVERNMENT, WHERE THE ITEM OR PROCESS IS NOT OTHERWISE REASONABLY AVAILABLE TO ENABLE TIMELY PERFORMANCE OF THE WORK, OR (ii) RELEASE TO A FOREIGN GOVERNMENT, AS THE INTERESTS OF THE UNITED STATES MAY REQUIRE. PROVIDED THAT IN EITHER CASE THE RELEASE, USE, DUPLICATION OR DISCLOSURE HEREOF SHALL BE SUBJECT TO THE FOREGOING LIMITATIONS. THIS LEGEND SHALL BE MARKED ON ANY REPRODUCTION HEREOF IN WHOLE OR IN PART."

REFERENCES

5. Glover, L.S., Borst, H.V., Application of Theodorsen's Theory to Strip Analysis Procedure for Single Rotation Propellers, Curtiss Report C-2070, 1945

6. Glover, L.S., Borst, H.V., A Method of Strip Analysis for a Dual Rotation Propeller, Curtiss Report C-2085

7. Borst, H.V., The Vortex Theory of Propellers in a Compressible Fluid, Curtiss Report C-2518, 1951

8. McLemore, H.C., Cannon, M.D., Aerodynamic Investigation of a Four-Blade Propeller Operating through an Angle-of-Attack Range from 0° to 180°, NACA TN 3228, 1954

9.a Yaggy, Paul F., Wind-Tunnel Investigation of Three Propellers Through an Angle-Of-Attack Range from 0° to 85°, NASA TN D-318, 1960

9.b Borst, H. V. & Ladden, R. M., Propeller Testing At Zero Velocity, Curtiss-Wright Corporation, Wood-Ridge, N. J., Cornell Aero Lab AVLABS Symposium, June 1966

SECTION III

WING-PROPELLER INTERFERENCE EFFECTS

SECTION III NOMENCLATURE

A	propeller thrust line angle of attach = $\theta + \alpha_f$,	degrees
C	wing Chord	ft
C_D	drag coefficient in wind axes = D/qS_w	
C_{do}	wing drag coefficient	
C_L	lift coefficient in wind axes = L/qS_w	
C_m	pitching moment coefficient	
$C_{m\alpha}$	slope of pitching moment coefficient versus α_f	
C_P	power coefficient = $550HP/\rho n^3 D_p^5$	
C_T	thrust coefficient = $T/\rho\, n^2 D_p^4$	
$C_X = -C_D$	force coefficient in wind axes equal to C_D but with positive orientation opposite to C_D	
D	drag of airplane or wing in presence of propeller,	lb
D_e	effective wing drag,	lb
D_p	propeller diameter,	ft
D_w	slipstream diameter in final wake,	ft
h/D_p	height above ground in propeller diameters	
HP	horsepower	
J_o	propeller advance ratio in the wind axes = V/nD_p	
K_1	D_w/D_p	
K_2	T_o/T	
L	lift,	lb
n	propeller speed,	rps
q	dynamic pressure = $\frac{1}{2}\rho v^2$,	lb/ft^2
R_e	Reynold's Number	
S_p	propeller disk area,	ft^2
s_w	wing area washed by propeller,	ft^2
S_w	wing area,	ft^2
T_c	thrust coefficient in propeller axes = T/qS_p	
T	propeller axial thrust,	lb
T_l	propeller axial thrust in influence of Wing	
v	average axial velocity through propeller,	ft/sec
v'	average axial velocity in fully developed wake	ft/sec
V	velocity,	ft/sec
X'	average axial velocity on final wake,	ft/sec
α_f	fuselage angle of attack (Referenced to WL 100),	degrees
β	propeller blade angle of attack at .691 propeller radius,	degrees
η	propeller efficiency	
ρ	air density,	$lb\text{-}sec^2/ft^4$
ϕ	propeller tilt angle (Referenced to WL 100),	degrees
δt	flap angle	degrees
Z	distance from propeller disk to wing surface	inches

Subscripts

F	front Propeller
R	rear Propeller
O	free Air
ℓ	in presence of wing

SECTION III

WING-PROPELLER INTERFERENCE EFFECTS

1. INTRODUCTION

One of the most serious hover problems encountered with fixed wing tilt propeller VTOL Aircraft is the lift loss due to the high slipstream velocity of the propeller impinging on the wing. This causes a high wing drag which reduces the overall lift generated by the propeller. Since the lift loss is caused by drag, it is a function of the slipstream velocity (and thus the propeller loading), the projected wing area in the slipstream, drag coefficient of the wing and the distance of the wing aft of the propeller disk. In addition since the wing produces blockage of the propeller slipstream it can also affect the overall propeller thrust which is an important factor when determining the download by test.

2. LIFT LOSS IN HOVER

a. Theory

Consider a propeller mounted above a wing as shown in Figure 19.

By the simple momentum theory

$$T = \rho S_P \frac{v'}{2} v' \quad ; \quad \text{since } v' = 2v \tag{1}$$

$$\rho \frac{(v')^2}{2} = \frac{T}{S_p} = q \tag{2}$$

Now the drag on the section in the prop wake is assuming a rectangular wing.

$$D = C_{D_o} q\, s_w \tag{3}$$

$$D = C_{D_o} \frac{T_1}{S_P} C \frac{D_w}{2} \tag{4}$$

$$\frac{D}{T_1} = C_{D_o} \frac{C}{S_P} \frac{D_P}{2} K_1 \tag{5}$$

For the X-19,

$$\left.\begin{aligned} D/T_1 &= .18\ C_{Do}\ \text{(rear wing-X-19)} \\ D/T_1 &= .112\ C_{Do}\ \text{(front wing-X-19)} \\ D/_{T_1} &= .102\ C_{Do}\ \text{(front wing-X-100)} \end{aligned}\right\} \qquad (6)$$

The drag coefficient used in Equation (5) and (6) is a function of the following parameter:

a) Aspect ratio of immersed body (prop radius to chord ratio).

b) The flap deflection angle δ_f.

The wing can cause considerable blockage of the propeller wake which influences the performance. Therefore when calculating the effective download D/T_o the change in the propeller performance due to the presence of the wing must be considered.

Tests at the static condition by the NACA reference 13.b have indicated that the blockage causes an increase of thrust which helps reduce the overall download. If K_2 is the ratio of the in-increase of thrust then the effective loss due to download is expressed by the equation

$$D_e = T_o \frac{K_2}{T_1} \left(D - \frac{T_1}{K_2} (K_2 - 1) \right) \qquad (7)$$

The factor K_2 is dependent on the area and distance of the blockage from the propeller disk.

b. Download Test Data

The drag coefficient of the wing and blockage effect on the propeller performance must be determined from test data, so that the effective download performance can be calculated. The only data available is that given in (10) and (11). These data were used to estimate the download loss for the X-100 airplane. Download data were determined from tests of the 15% scale model and full scale airplane and are obtained from a combination of unpublished information and data appearing in (12). These test data are summarized on Figure 20 and indicate the download was higher than the predicted value. The data measured on the full scale X-100 airplane were obtained by measuring the total thrust with the wing chord parallel and normal to the direction of the slipstream velocity vector. When the wing was perpendicular to the stream vector the flap was deflected 45° to determine the effects of flap angle on the download loss.

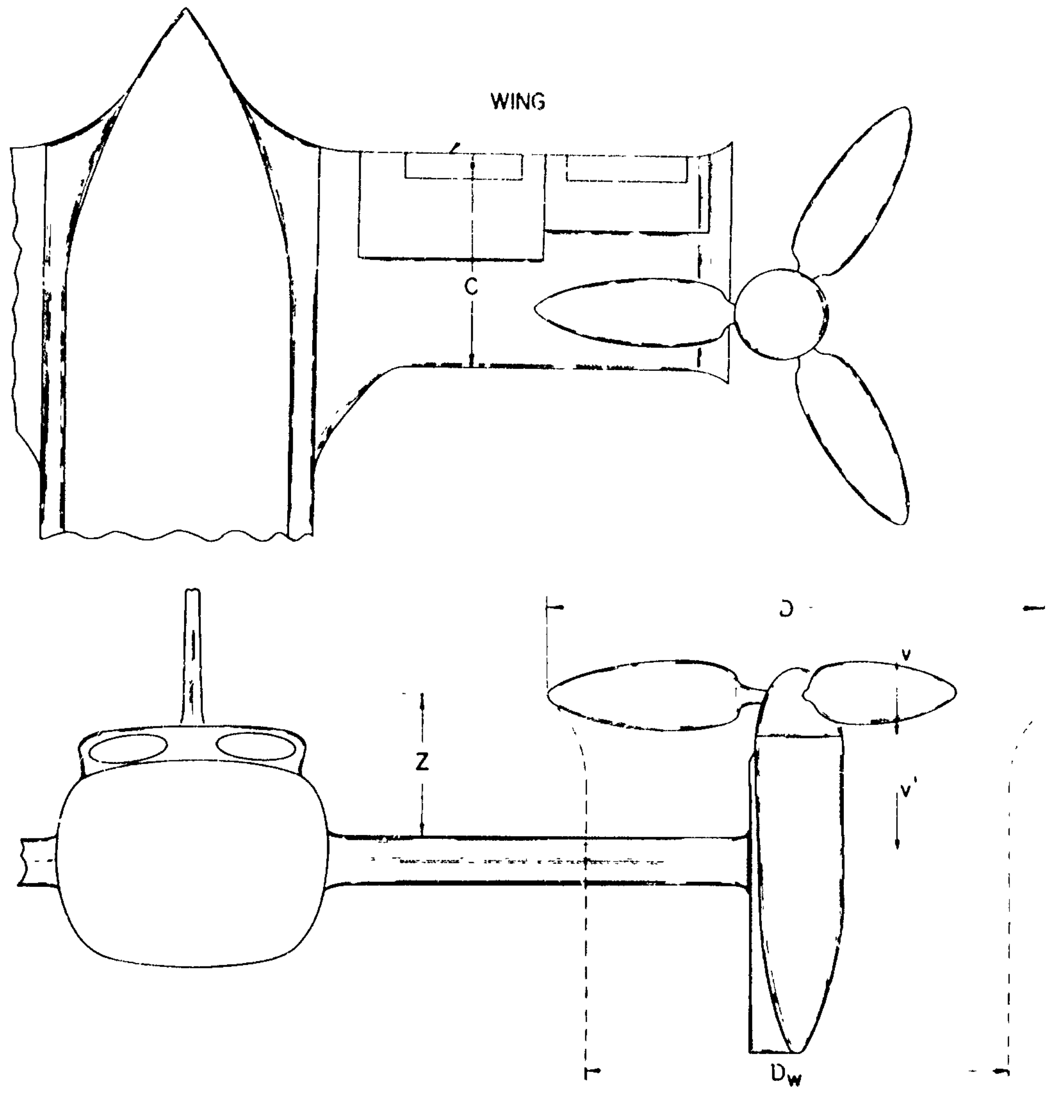
WING
C
D
v
v'
Z
D_w

Figure 19. X-19, rear wing nomenclature.

The result of these tests are shown on Figure 20 as D_e/T_1. The actual magnitude of the drag is not known as the value of K_2 was not determined. The data from the model tests appear to agree quite well with the full scale results in spite of the large change in Reynolds Number and disk loading between the two tests. In the range of disk loading of 16 to 22 psf. the download ratio appears to be nearly constant. Also deflection of the flap has a large affect on the magnitude of the download as was indicated in the XV-3 testing (11).

To determine the download losses, full scale pressure measurements were taken on the port rear wing of the No. 1 X-19 aircraft during Ground Run No. 244. The pressure pick-up system consisted of multitube straps adhered, chordwise, to the wing surface at five spanwise locations.

Figure 21 shows these locations and their positions in terms of propeller radius, R, and Figure 22 shows the corresponding chordwise location of the pressure holes. The tests were conducted with the propeller operating at approximately a diameter off the ground, Figure 23.

Atmospheric conditions were recorded manually and transverse shaft torque, net thrust component, propeller speed, blade angle, rear nacelle tilt angle and control surface deflections were recorded on the aircraft oscillographs.

All the testing was done with only the rear propellers operating; but the test did cover a range of tilt angles and disk loadings. See Table III. At a disk loading of 18.72 the propeller is producing the required thrust for hover at a 40% C.G. location and 12,300 lbs gross weight.

The test indicated that the lower surface pressure distribution is basically rectangular in shape throughout, with the wing pressure coefficient never exceeding approximately 0.40. These results are in agreement, with a uniform flow field around a two-dimensional airfoil section over a range of angles of attack from 0° to 180°.

The upper surface pressure distribution over the undeflected portion of the wing has a characteristic shape whose magnitude changes with the distance from the propeller shaft. Within the propeller sweep these surface pressures are greater than ambient and reflect the propeller slipstream dynamic pressure.

The distributions outside of the propeller sweep are probably generated by a combination of spanwise and chordwise flows, a detailed examination of which, at this stage, appears unnecessary.

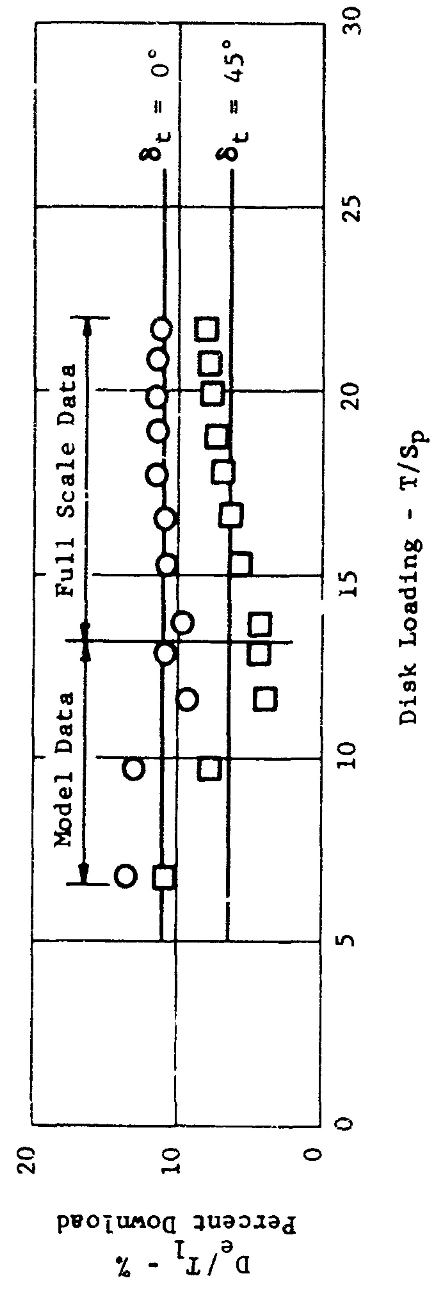

Figure 20. X-100, download variation with disk loading.

FURNISHED UNDER UNITED STATES GOVERNMENT CONTRACT No AF33(615)-3940 SHALL NOT BE EITHER RELEASED OUTSIDE THE GOVERNMENT OR USED, DUPLICATED, OR DISCLOSED IN WHOLE OR IN PART FOR MANUFACTURE OR PROCUREMENT, WITHOUT THE WRITTEN PERMISSION OF CURTISS-WRIGHT CORPORATION, EXCEPT FOR (i) EMERGENCY REPAIR OR OVERHAUL WORK BY OR FOR THE GOVERNMENT, WHERE THE ITEM OR PROCESS IS NOT OTHERWISE REASONABLY AVAILABLE TO ENABLE TIMELY PERFORMANCE OF THE WORK, OR (ii) RELEASE TO A FOREIGN GOVERNMENT, AS THE INTERESTS OF THE UNITED STATES MAY REQUIRE PROVIDED THAT IN EITHER CASE THE RELEASE, USE, DUPLICATION OR DISCLOSURE HEREOF SHALL BE SUBJECT TO THE FOREGOING LIMITATIONS THIS LEGEND SHALL BE MARKED ON ANY REPRODUCTION HEREOF IN WHOLE OR IN PART.'

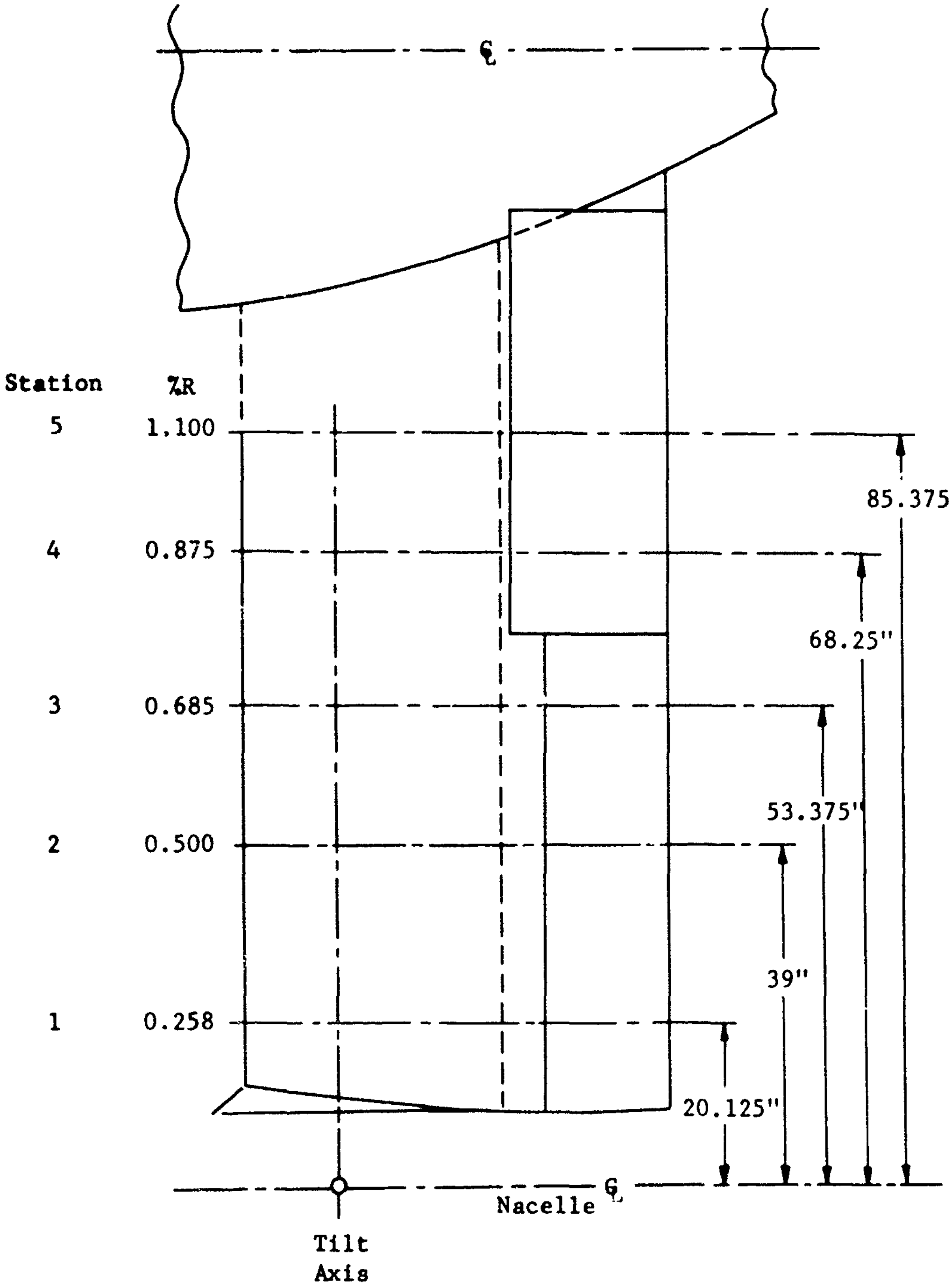
℄
Station
%R
5
1.100
4
0.875
3
0.685
2
0.500
1
0.258
85.375"
68.25"
53.375"
39"
20.125"
Nacelle ℄
Tilt
Axis

Figure 21. X-19, rear wing download test; locations of spanwise pressure stations.

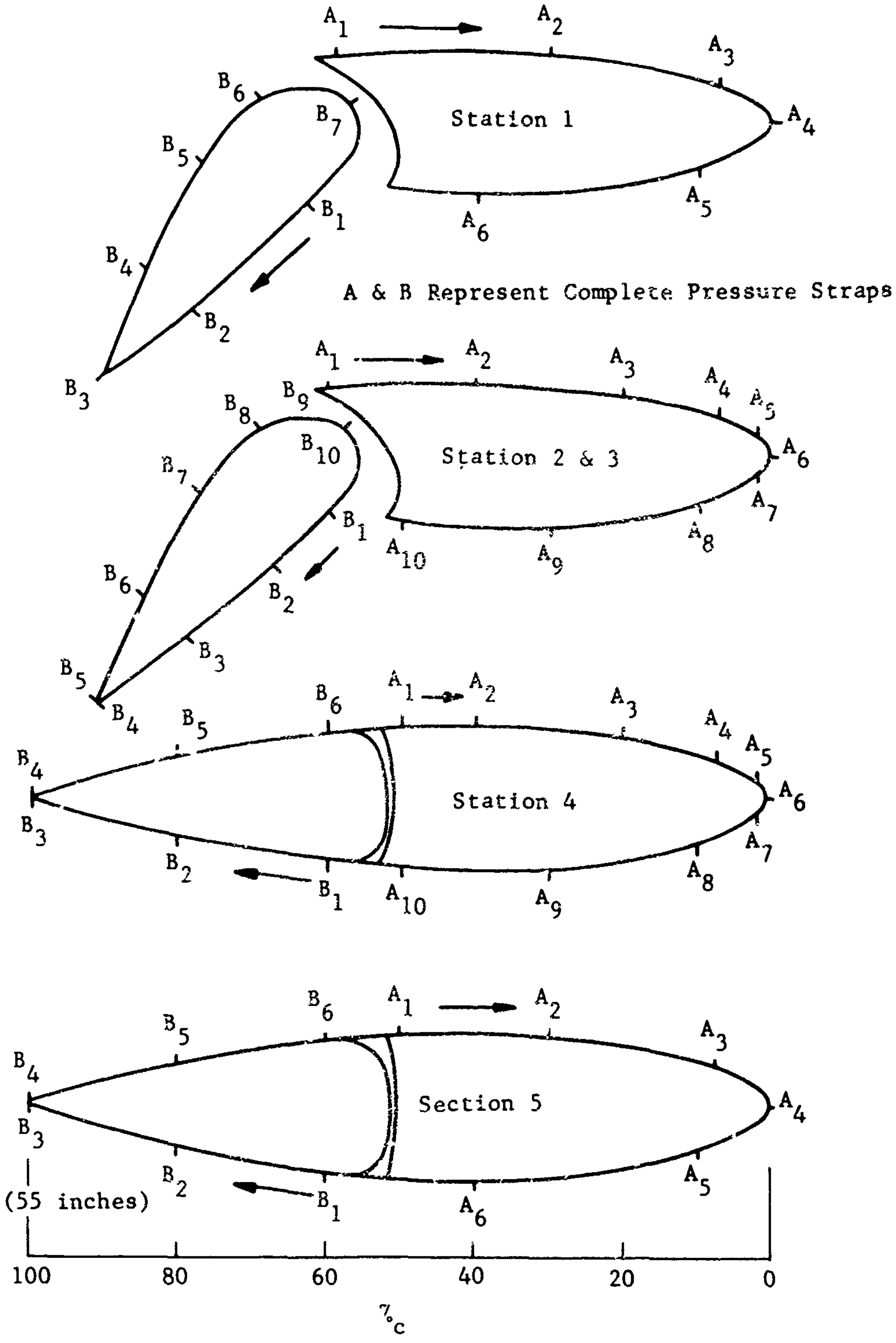
A & B Represent Complete Pressure Straps
Station 1
A_1 A_2 A_3 A_4 A_5 A_6
B_1 B_2 B_3 B_4 B_5 B_6 B_7
Station 2 & 3
A_1 A_2 A_3 A_4 A_5 A_6 A_7 A_8 A_9 A_{10}
B_1 B_2 B_3 B_4 B_5 B_6 B_7 B_8 B_9 B_{10}
Station 4
A_1 A_2 A_3 A_4 A_5 A_6 A_7 A_8 A_9 A_{10}
B_1 B_2 B_3 B_4 B_5 B_6
Section 5
A_1 A_2 A_3 A_4 A_5 A_6
B_1 B_2 B_3 B_4 B_5 B_6
(55 inches)
100
80
60
40
20
0
%c

Figure 22. X-19, rear wing download test; locations of chordwise pressure stations.

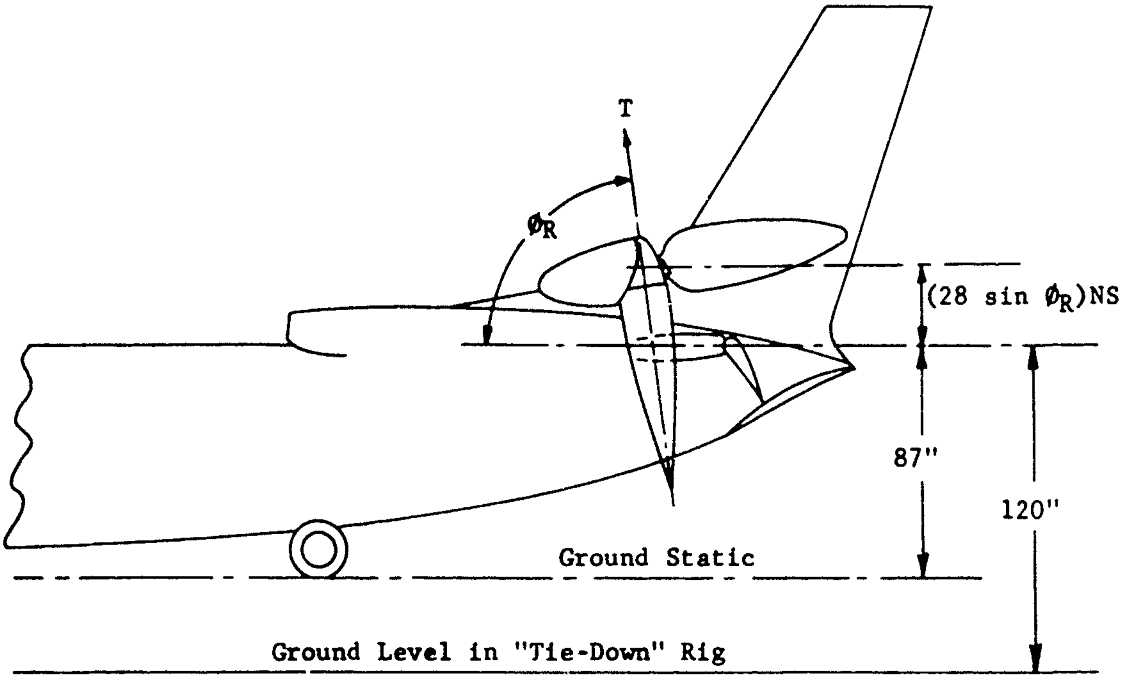
T
ϕ_R
$(28 \sin \phi_R)$NS
87"
120"
Ground Static
Ground Level in "Tie-Down" Rig

Figure 23. X-19, ground clearances on the "tie-down" rig.

Table III. X-19, rear wing download test conditions.

Test Condition	Nacelle Angle (deg)	Aileron Angle (deg)	Blade Angle (deg)	C_P	C_T	Disk Loading T/S_P - lb/ft^2
1	81.5	57.0	3.1	0.0181	0.0411	4.55
2	81.5	57.0	13.1	0.0682	0.1503	18.72
3	75.0	53.9	11.0	0.0544	0.1241	15.90
4	70.0	51.9	10.4	0.0515	0.1195	15.23
5	81.5	57.0	10.8	0.0518	0,1208	15.05

However, some thought may be given to the distribution around the 50% chord, Figure 24 for the inboard station. At that station the upper and lower surface pressures try to balance out through the gap between elevator and wing, whereas at station 4 (per Figure 21) there is an additional effect, due probably to a carry-over of the suction peaks from the deflected aileron.

Figure 25 shows typical spanwise load distribution obtained from integration of the pressures.

For comparison with propeller wake dynamic pressure predictions, Figure 26 presents the wing upper surface pressure along the spanwise line through the propeller axis. This shows that although the correlation achieved is not absolute, it is sufficient to show that the propeller wake dynamic pressure properties are the major factors affecting both the distribution and magnitude of the download on this surface.

Ground effects on the download are not yet fully understood, but it is most likely that the under surface of the aircraft (and hence wings) will be subjected to the most influence. This influence depends upon the aircraft height above the ground; for these tests height is shown in Figure 23.

The download on the X-19 is composed of contributions from the fuselage and wings. Because the download is a result of propeller wash and related aircraft interferences, the major contribution to this download comes from the wings, and in particular from those portions of the wings swept by the propellers.

To obtain an indication of the download generated by the wings the spanwise loadings were integrated from wing tip to wing root and the results plotted in Figure 27 as a percentage of actual thrust measured along the propeller axis. It must be emphasized that these values are in ground effect and represent exposed wing contributions only. The total download must be obtained by integrating from wing tip to fuselage centerline.

The download values, given in Figure 27 for upper and lower surfaces, diminish for disk loadings greater than approximately 14 lb./sq.ft. As escribed elsewhere herein, this is of doubtful validity since it represents the sum of two conflicting items (i.e. ground effect and download) which at this stage cannot be investigated separately. As a partial step toward this separation of effects, the upper surface pressures only were integrated to find that surface's contribution to the download. This is because it comes primarily from direct propeller wash impingement and thus would be less affected by the ground effects.

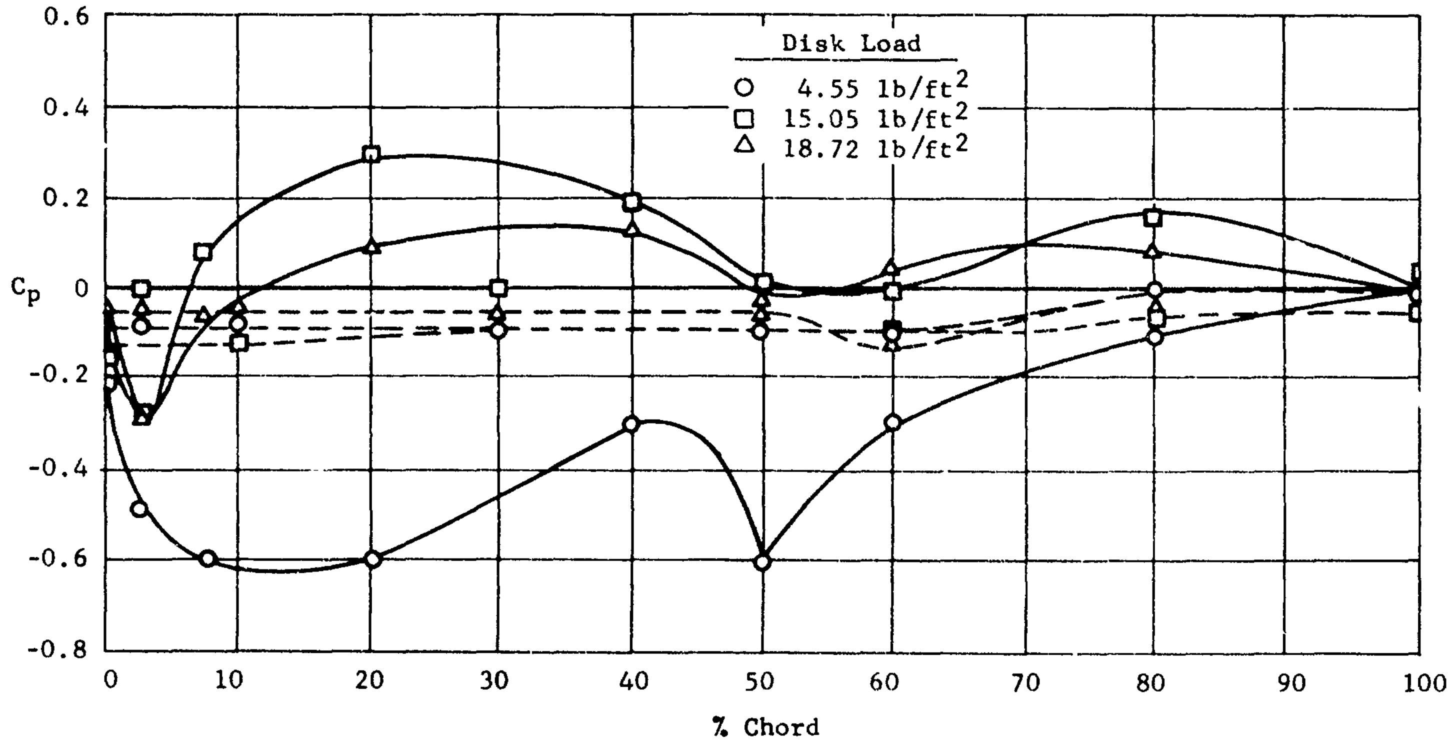

Figure 24. X-19, effect of disk loading on the rear wing - station 4.

"FURNISHED UNDER UNITED STATES GOVERNMENT CONTRACT No. AF33(615)-3940 SHALL NOT BE EITHER RELEASED OUTSIDE THE GOVERNMENT, OR USED, DUPLICATED, OR DISCLOSED IN WHOLE OR IN PART FOR MANUFACTURE OR PROCUREMENT, WITHOUT THE WRITTEN PERMISSION OF CURTISS-WRIGHT CORPORATION, EXCEPT FOR (I) EMERGENCY REPAIR OR OVERHAUL WORK BY OR FOR THE GOVERNMENT, WHERE THE ITEM OR PROCESS IS NOT OTHERWISE REASONABLY AVAILABLE TO ENABLE TIMELY PERFORMANCE OF THE WORK: OR (II) RELEASE TO A FOREIGN GOVERNMENT, AS THE INTERESTS OF THE UNITED STATES MAY REQUIRE PROVIDED THAT IN EITHER CASE THE RELEASE, USE, DUPLICATION OR DISCLOSURE HEREOF SHALL BE SUBJECT TO THE FOREGOING LIMITATIONS. THIS LEGEND SHALL E MARKED ON ANY REPRODUCTION HEREOF IN WHOLE OR IN PART."

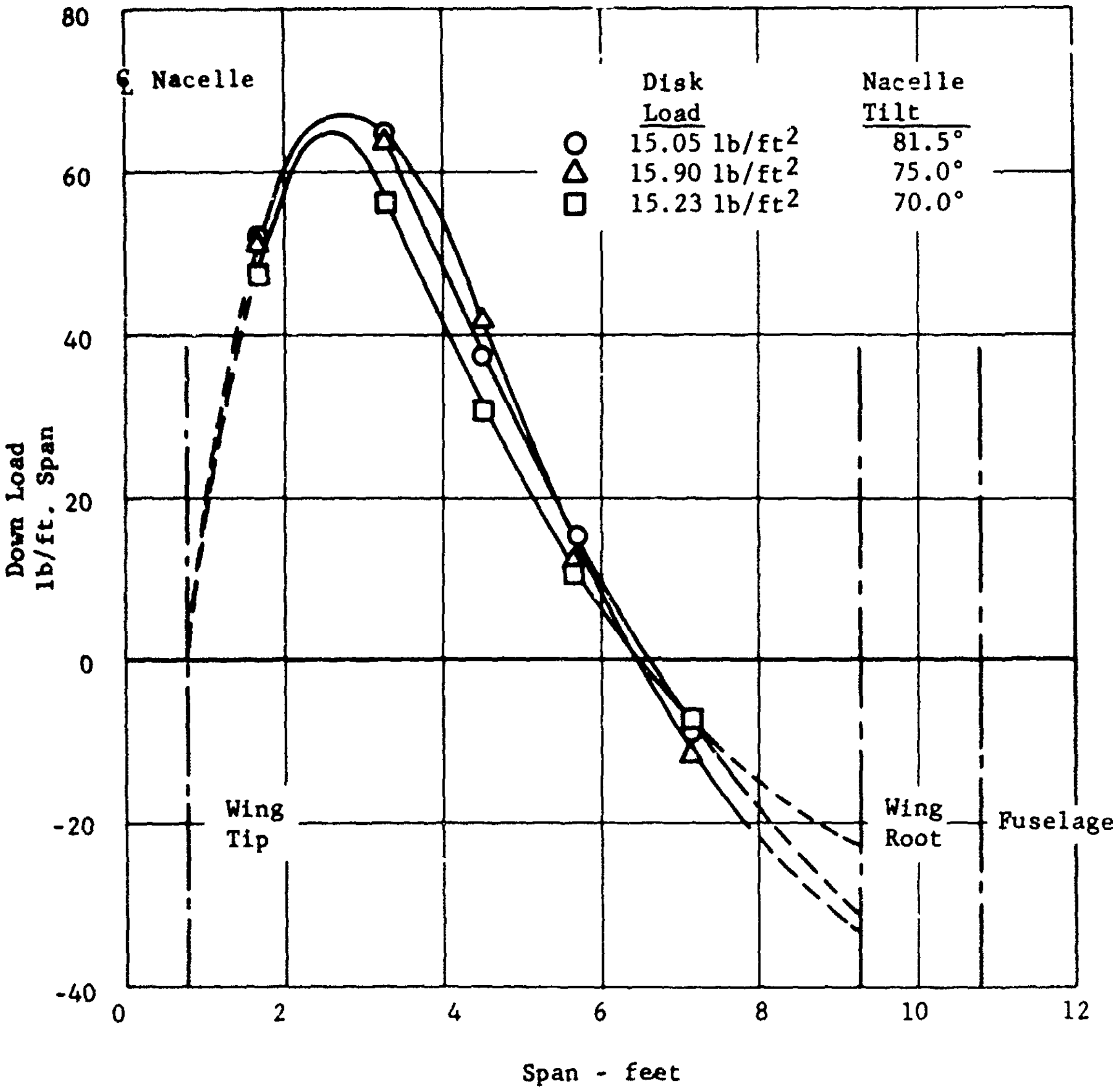

Figure 25. X-19, effect of nacelle tilt angle on the spanwise loading, rear wing, static propeller.

"FURNISHED UNDER UNITED STATES GOVERNMENT CONTRACT No. AF33(615)-3940 SHALL NOT BE EITHER RELEASED OUTSIDE THE GOVERNMENT, OR USED, DUPLICATED, OR DISCLOSED IN WHOLE OR IN PART FOR MANUFACTURE OR PROCUREMENT, WITHOUT THE WRITTEN PERMISSION OF CURTISS-WRIGHT CORPORATION, EXCEPT FOR (i) EMERGENCY REPAIR OR OVERHAUL WORK BY OR FOR THE GOVERNMENT, WHERE THE ITEM OR PROCESS IS NOT OTHERWISE REASONABLY AVAILABLE TO ENABLE TIMELY PERFORMANCE OF THE WORK. OR (ii) RELEASE TO A FOREIGN GOVERNMENT, AS THE INTERESTS OF THE UNITED STATES MAY REQUIRE: PROVIDED THAT IN EITHER CASE THE RELEASE, USE, DUPLICATION OR DISCLOSURE HEREOF SHALL BE SUBJECT TO THE FOREGOING LIMITATIONS. THIS LEGEND SHALL BE MARKED ON ANY REPRODUCTION HEREOF IN WHOLE OR IN PART."

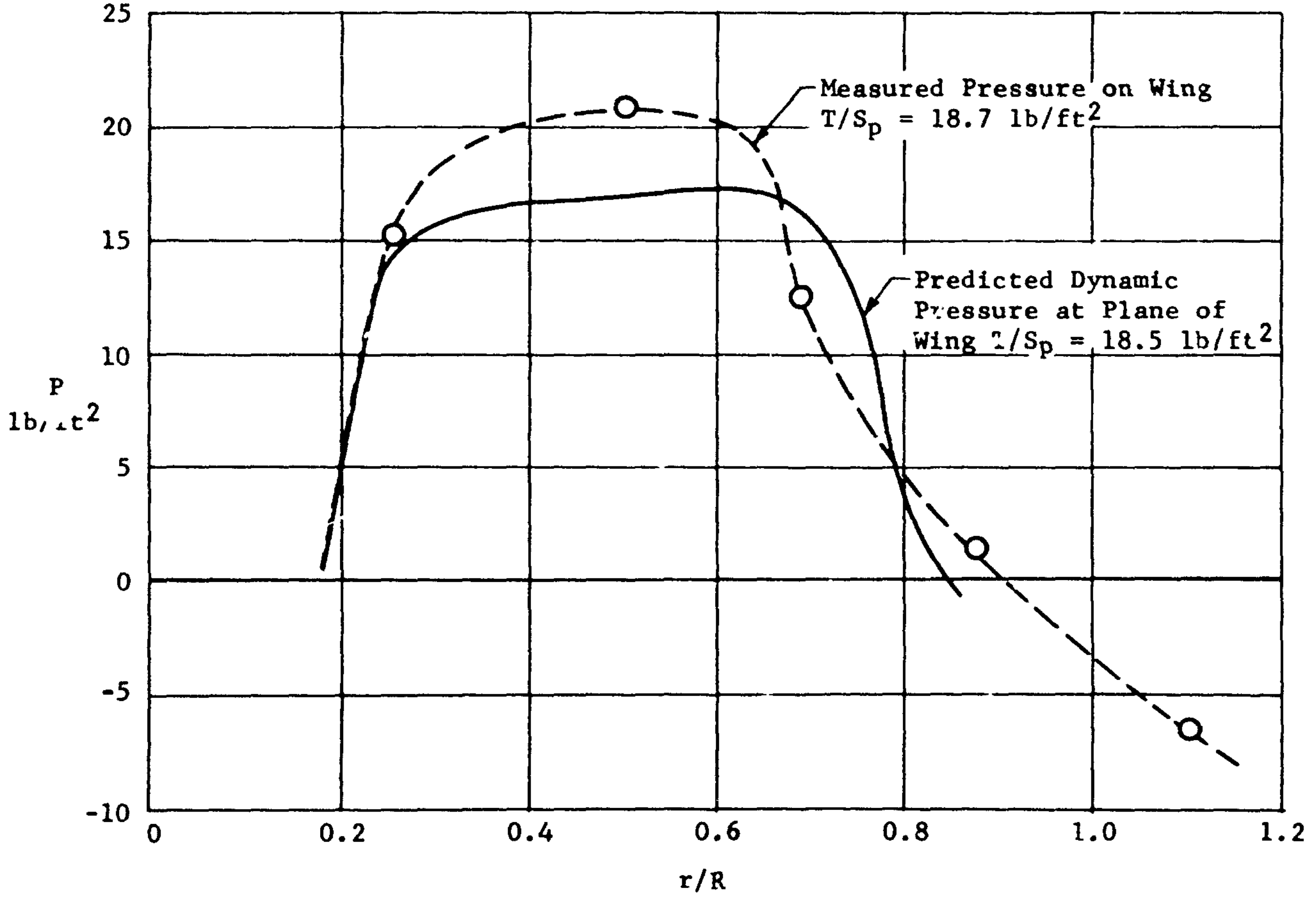

Figure 26. X-19, rear wing pressure in the propeller wake, static propeller.

"FURNISHED UNDER UNITED STATES GOVERNMENT CONTRACT No. AF33(615)-3940. SHALL NOT BE EITHER RELEASED OUTSIDE THE GOVERNMENT, OR USED, DUPLICATED, OR DISCLOSED IN WHOLE OR IN PART FOR MANUFACTURE OR PROCUREMENT, WITHOUT THE WRITTEN PERMISSION OF CURTISS-WRIGHT CORPORATION, EXCEPT FOR (i) EMERGENCY REPAIR OR OVERHAUL WORK BY OR FOR THE GOVERNMENT, WHERE THE ITEM OR PROCESS IS NOT OTHERWISE REASONABLY AVAILABLE TO ENABLE TIMELY PERFORMANCE OF THE WORK: OR (ii) RELEASE TO A FOREIGN GOVERNMENT, AS THE INTERESTS OF THE UNITED STATES MAY REQUIRE. PROVIDED THAT IN EITHER CASE THE RELEASE, USE, DUPLICATION OR DISCLOSURE HEREOF SHALL BE SUBJECT TO THE FOREGOING LIMITATIONS. THIS LEGEND SHALL BE MARKED ON ANY REPRODUCTION HEREOF IN WHOLE OR IN PART."

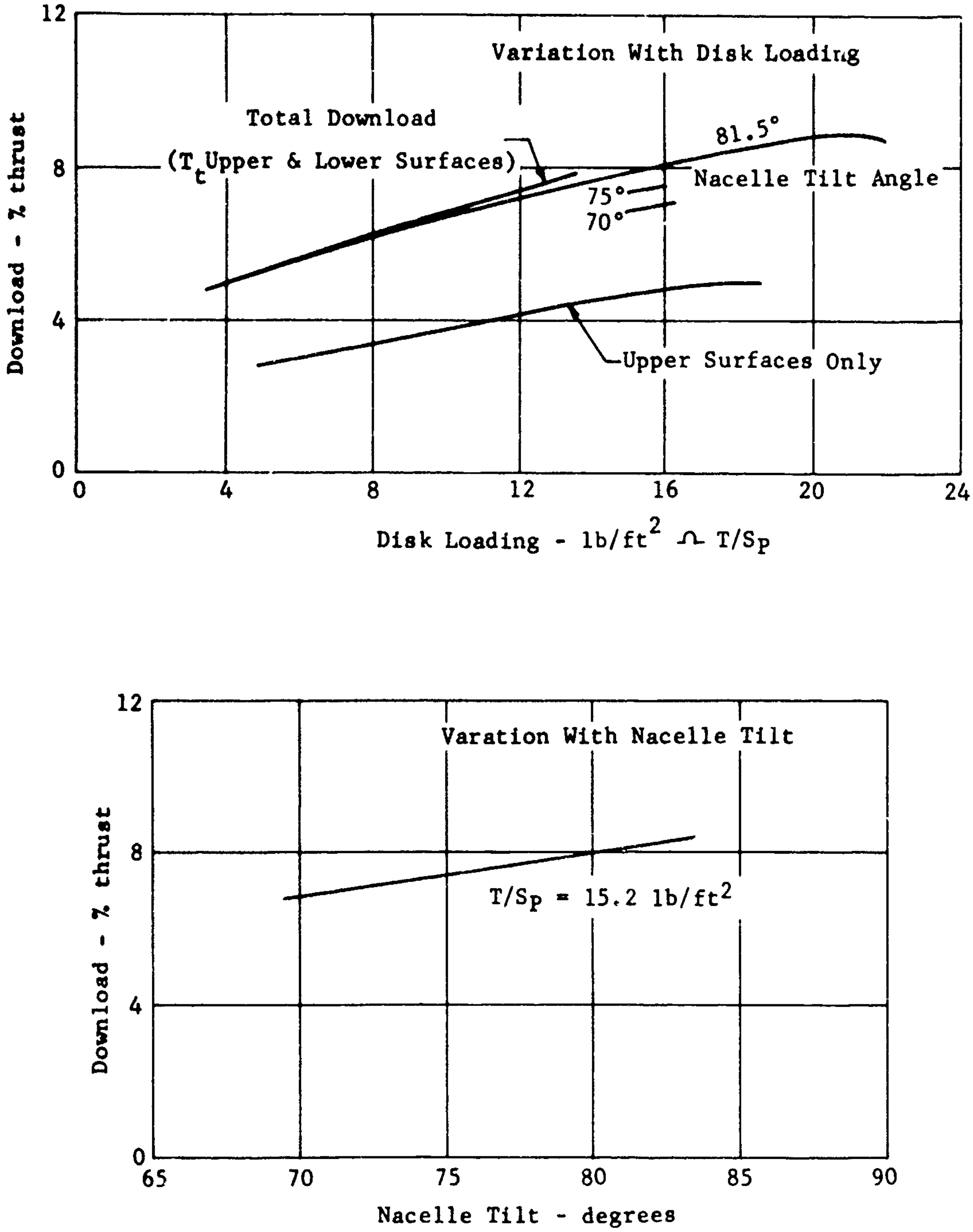

Figure 27. X-19, download on the rear wing.
Out of ground effect.

"FURNISHED UNDER UNITED STATES GOVERNMENT CONTRACT No AF33(615)-3940 SHALL NOT BE EITHER RELEASED OUTSIDE THE GOVERNMENT, OR USED, DUPLICATED, OR DISCLOSED IN WHOLE OR IN PART FOR MANUFACTURE OR PROCUREMENT, WITHOUT THE WRITTEN PERMISSION OF CURTISS-WRIGHT CORPORATION, EXCEPT FOR (I) EMERGENCY REPAIR OR OVERHAUL WORK BY OR FOR THE GOVERNMENT, WHERE THE ITEM OR PROCESS IS NOT OTHERWISE REASONABLY AVAILABLE TO ENABLE TIMELY PERFORMANCE OF THE WORK; OR (II) RELEASE TO A FOREIGN GOVERNMENT, AS THE INTERESTS OF THE UNITED STATES MAY REQUIRE. PROVIDED THAT IN EITHER CASE THE RELEASE, USE, DUPLICATION OR DISCLOSURE HEREOF SHALL BE SUBJECT TO THE FOREGOING LIMITATIONS. THIS LEGEND SHALL BE MARKED ON ANY REPRODUCTION HEREOF IN WHOLE OR IN PART."

The download on the upper surface is seen from Figure 27 to represent approximately half of the measured total. The trends of download losses with variations of disk loading should not be taken as absolute; further work is necessary to check this. The variation of download with propeller tilt at small angles is slight but possesses the expected trend of reduction with diminishing propeller tilt angle.

Since the download is generated mainly within the propeller swept area, it was considered possible that alleviating devices might produce noticeable reductions in wing downloads. These devices are employed to equalize the upper and lower surface pressures by channelling the upper surface air of high pressure to the subambient lower surface.

To measure the download losses over a greater range of conditions and out of the influences of the ground, tests were conducted on the Curtiss static thrust test rig described in (13). The rig was modified so that the thrust of the propeller could be measured in the presence of the wing. The total wing forces produced by the propeller slipstream were also measured.

Tests were run to investigate if various combinations of flaps and slots could be used to reduce the download losses. The planned tests were not completed but enough testing was done simulating the rear wing and propeller to provide useful data; see Figures 28 through 32.

The effect of disk loading, tilt angle, and aileron angle are shown in Figures 28 and 29 for nacelle angles of 80° and 90°. The results indicate that the gross download ratio, the actual measured drag over the actual measured thrust is nearly independent of the disk loading for the range of T/S_p of 10 to 25 psf. As might be expected the difference in download due to changes of nacelle tilt angle are small. The download loss is reduced considerably by deflection of the flap, Figures 28 to 30. This would be expected due to the reduction of wing area normal to the propeller wake. The peak download reduction occurs at a δ_f of 90° although the difference between 60 and 90° is very small.

A comparison of the performance of the propeller operating with and without the blockage produced by the rear wing of the X-19 is shown on Figure 31. Sufficient data were not obtained to fully define the trend. A relatively large increase in thrust due to blockage is evident. The trend shown for changes in flap angle and disk loading are not necessarily conclusive, as the data are too meager to fully substantiate such a trend. Presumably the blockage does increase the thrust at a given power in a manner similar to that in which ground effect increases thrust. This effect results in a thrust 3 or 4% higher than would be measured without blockage. This increase in thrust has been observed in the static testing of propellers and is discussed in (13). Further testing is required to more fully

"FURNISHED UNDER UNITED STATES GOVERNMENT CONTRACT No. AF33(615)-3940. SHALL NOT BE EITHER RELEASED OUTSIDE THE GOVERNMENT, OR USED, DUPLICATED, OR DISCLOSED IN WHOLE OR IN PART FOR MANUFACTURE OR PROCUREMENT, WITHOUT THE WRITTEN PERMISSION OF CURTISS-WRIGHT CORPORATION, EXCEPT FOR (i) EMERGENCY REPAIR OR OVERHAUL WORK BY OR FOR THE GOVERNMENT, WHERE THE ITEM OR PROCESS IS NOT OTHERWISE REASONABLY AVAILABLE TO ENABLE TIMELY PERFORMANCE OF THE WORK, OR (ii) RELEASE TO A FOREIGN GOVERNMENT, AS THE INTERESTS OF THE UNITED STATES MAY REQUIRE. PROVIDED THAT IN EITHER CASE THE RELEASE, USE, DUPLICATION OR DISCLOSURE HEREOF SHALL BE SUBJECT TO THE FOREGOING LIMITATIONS. THIS LEGEND SHALL BE MARKED ON ANY REPRODUCTION HEREOF IN WHOLE OR IN PART."

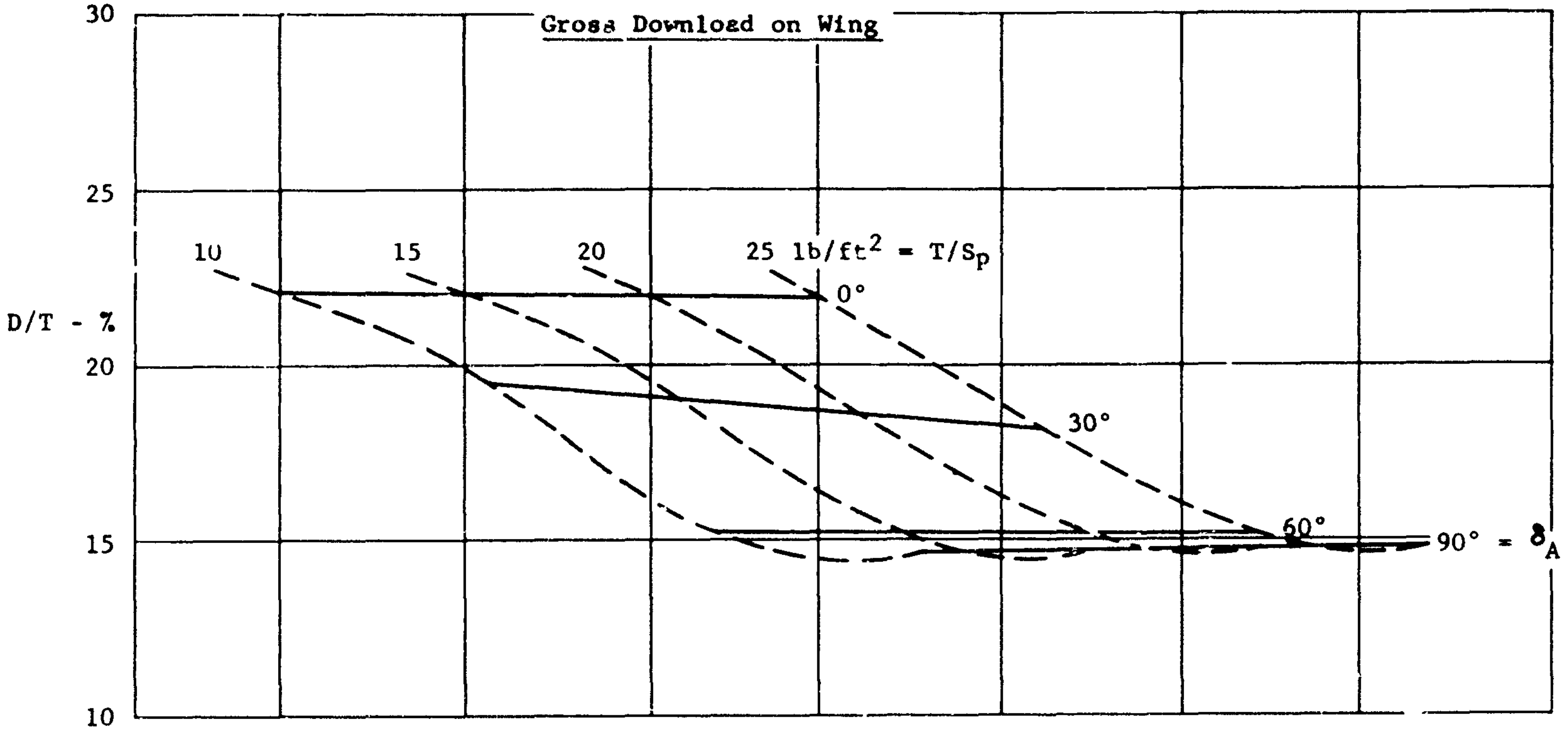

Figure 28. X-19, effects of disk loading and collective aileron angle on the rear wing download. $\phi_R = 80°$, $\delta_e = 0°$, $z = 28$ in.

"FURNISHED UNDER UNITED STATES GOVERNMENT CONTRACT No. AF33(615)-3940. SHALL NOT BE EITHER RELEASED OUTSIDE THE GOVERNMENT, OR USED, DUPLICATED, OR DISCLOSED IN WHOLE OR IN PART FOR MANUFACTURE OR PROCUREMENT, WITHOUT THE WRITTEN PERMISSION OF CURTISS-WRIGHT CORPORATION, EXCEPT FOR (I) EMERGENCY REPAIR OR OVERHAUL WORK BY OR FOR THE GOVERNMENT, WHERE THE ITEM OR PROCESS IS NOT OTHERWISE REASONABLY AVAILABLE TO ENABLE TIMELY PERFORMANCE OF THE WORK. OR (II) RELEASE TO A FOREIGN GOVERNMENT, AS THE INTERESTS OF THE UNITED STATES MAY REQUIRE. PROVIDED THAT IN EITHER CASE THE RELEASE, USE, DUPLICATION OR DISCLOSURE HEREOF SHALL BE SUBJECT TO THE FOREGOING LIMITATIONS. THIS LEGEND SHALL BE MARKED ON ANY REPRODUCTION HEREOF IN WHOLE OR IN PART.

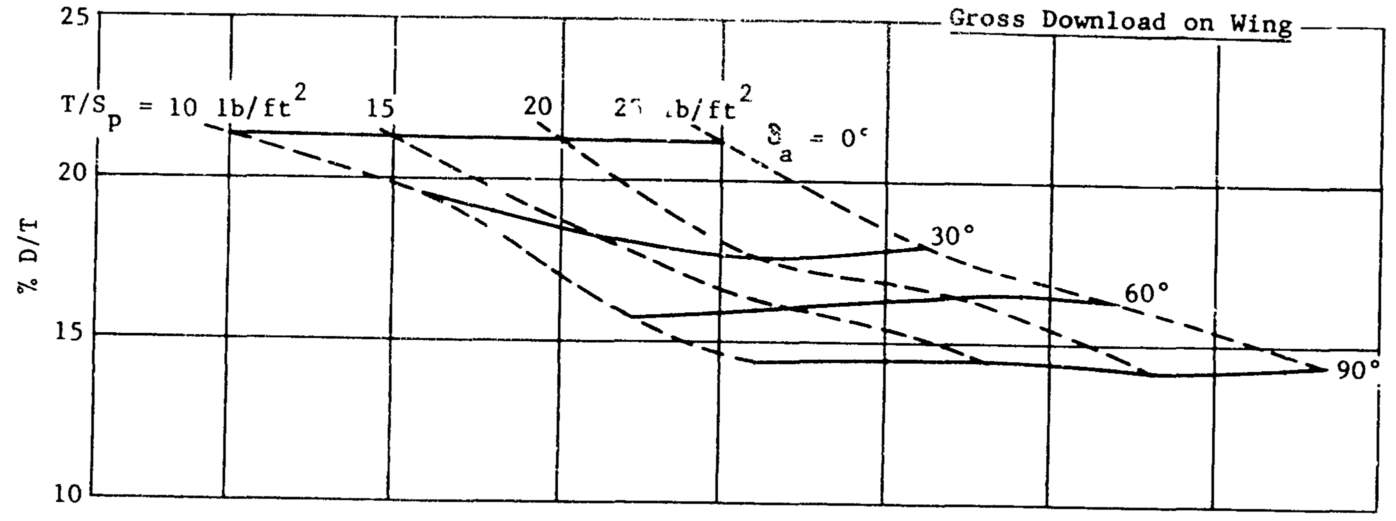

Figure 29. X-19, effects of disk loading and collective aileron angle on the rear wing download; $\phi_R = 90^{\circ}$, $\delta_e = 0^{\circ}$, z = 28 in.

FURNISHED UNDER UNITED STATES GOVERNMENT CONTRACT No. AF33(615)-3940 SHALL NOT BE EITHER RELEASED OUTSIDE THE GOVERNMENT, OR USED, DUPLICATED, OR DISCLOSED IN WHOLE OR IN PART FOR MANUFACTURE OR PROCUREMENT, WITHOUT THE WRITTEN PERMISSION OF CURTISS-WRIGHT CORPORATION, EXCEPT FOR (I) EMERGENCY REPAIR OR OVERHAUL WORK BY OR FOR THE GOVERNMENT, WHERE THE ITEM OR PROCESS IS NOT OTHERWISE REASONABLY AVAILABLE TO ENABLE TIMELY PERFORMANCE OF THE WORK, OR (II) RELEASE TO A FOREIGN GOVERNMENT, AS THE INTERESTS OF THE UNITED STATES MAY REQUIRE; PROVIDED THAT IN EITHER CASE THE RELEASE, USE, DUPLICATION OR DISCLOSURE HEREOF SHALL BE SUBJECT TO THE FOREGOING LIMITATIONS. THIS LEGEND SHALL BE MARKED ON ANY REPRODUCTION HEREOF IN WHOLE OR IN PART."

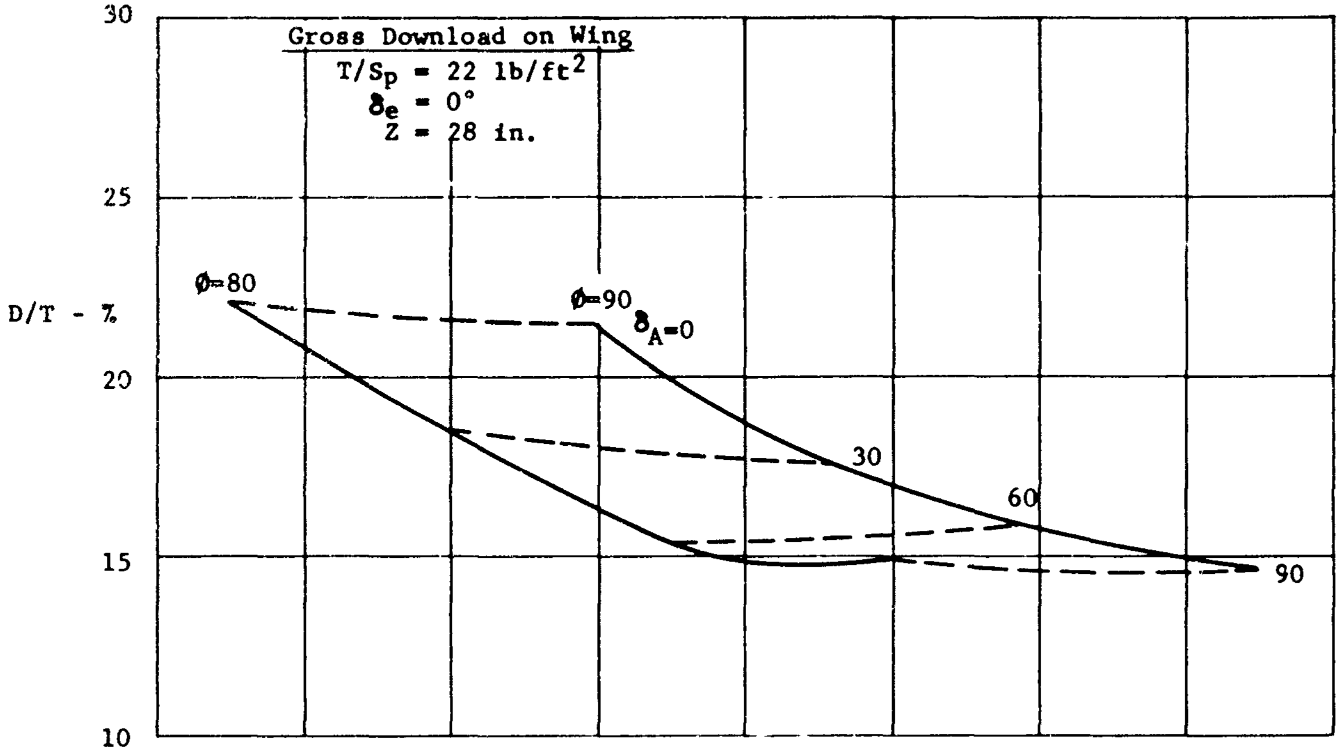

Figure 30. X-19, effects of nacelle tilt angle and collective aileron angle on the rear wing download.

FURNISHED UNDER UNITED STATES GOVERNMENT CONTRACT No. AF33(615)-1940 SHALL NOT BE EITHER RELEASED OUTSIDE THE GOVERNMENT, OR USED, DUPLICATED, OR DISCLOSED IN WHOLE OR IN PART FOR MANUFACTURE OR PROCUREMENT, WITHOUT THE WRITTEN PERMISSION OF CURTISS-WRIGHT CORPORATION, EXCEPT FOR (I) EMERGENCY REPAIR OR OVERHAUL WORK BY OR FOR THE GOVERNMENT, WHERE THE ITEM OR PROCESS IS NOT OTHERWISE REASONABLY AVAILABLE TO ENABLE TIMELY PERFORMANCE OF THE WORK, OR (II) RELEASE TO A FOREIGN GOVERNMENT, AS THE INTERESTS OF THE UNITED STATES MAY REQUIRE. PROVIDED THAT IN EITHER CASE THE RELEASE, USE, DUPLICATION OR DISCLOSURE HEREOF SHALL BE SUBJECT TO THE FOREGOING LIMITATIONS. THIS LEGEND SHALL BE MARKED ON ANY REPRODUCTION HEREOF IN WHOLE OR IN PART."

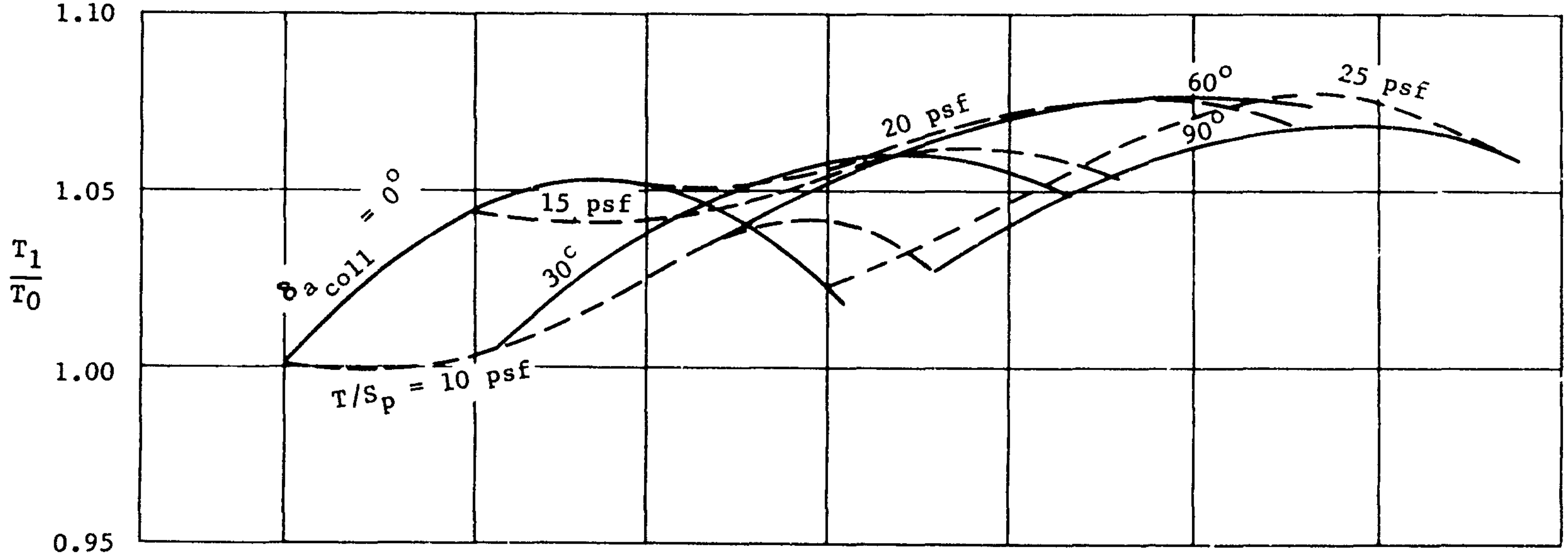

Figure 31. X-19, effect of rear wing interference on the rear propeller thrust; $\phi_R = 80^\circ$, $\delta_e = 0^\circ$, $z = 28$ in.

"FURNISHED UNDER UNITED STATES GOVERNMENT CONTRACT No AF33(615)-3940. SHALL NOT BE EITHER RELEASED OUTSIDE THE GOVERNMENT, OR USED, DUPLICATED, OR DISCLOSED IN WHOLE OR IN PART FOR MANUFACTURE OR PROCUREMENT, WITHOUT THE WRITTEN PERMISSION OF CURTISS-WRIGHT CORPORATION, EXCEPT FOR (i) EMERGENCY REPAIR OR OVERHAUL WORK BY OR FOR THE GOVERNMENT, WHERE THE ITEM OR PROCESS IS NOT OTHERWISE REASONABLY AVAILABLE TO ENABLE TIMELY PERFORMANCE OF THE WORK, OR (ii) RELEASE TO A FOREIGN GOVERNMENT, AS THE INTERESTS OF THE UNITED STATES MAY REQUIRE PROVIDED THAT IN EITHER CASE THE RELEASE, USE, DUPLICATION OR DISCLOSURE HEREOF SHALL BE SUBJECT TO THE FOREGOING LIMITATIONS THIS LEGEND SHALL BE MARKED ON ANY REPRODUCTION HEREOF IN WHOLE OR IN PART."

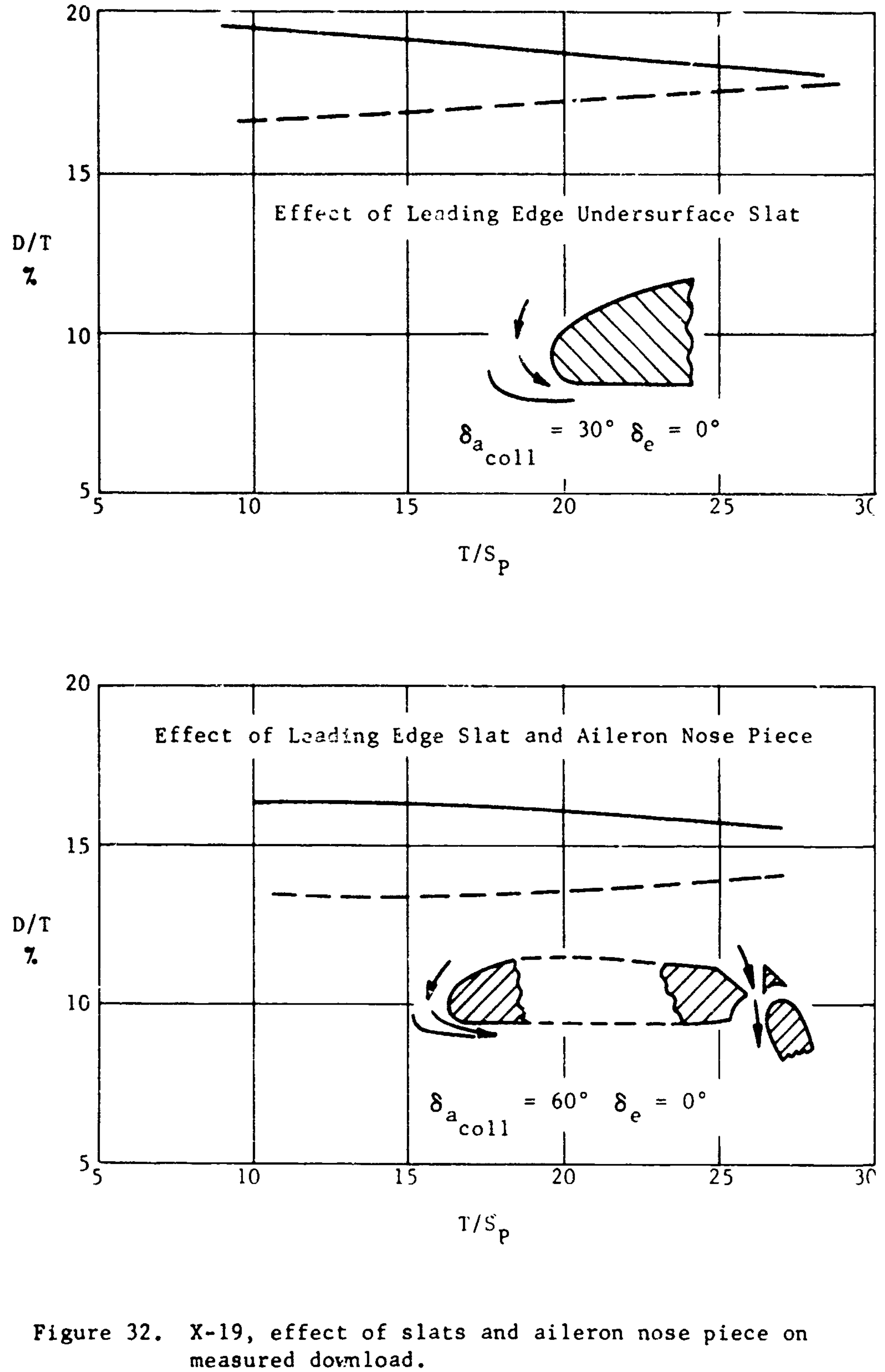

Figure 32. X-19, effect of slats and aileron nose piece on measured download.

FURNISHED UNDER UNITED STATES GOVERNMENT CONTRACT No. AF33(615)-3740 SHALL NOT BE EITHER RELEASED OUTSIDE THE GOVERNMENT, OR USED, DUPLICATED, OR DISCLOSED IN WHOLE OR IN PART FOR MANUFACTURE OR PROCUREMENT, WITHOUT THE WRITTEN PERMISSION OF CURTISS-WRIGHT CORPORATION, EXCEPT FOR (I) EMERGENCY REPAIR OR OVERHAUL WORK BY OR FOR THE GOVERNMENT, WHERE THE ITEM OR PROCESS IS NOT OTHERWISE REASONABLY AVAILABLE TO ENABLE TIMELY PERFORMANCE OF THE WORK, OR (II) RELEASE TO A FOREIGN GOVERNMENT, AS THE INTERESTS OF THE UNITED STATES MAY REQUIRE PROVIDED THAT IN EITHER CASE THE RELEASE, USE, DUPLICATION OR DISCLOSURE HEREOF SHALL BE SUBJECT TO THE FOREGOING LIMITATIONS THIS LEGEND SHALL BE MARKED ON ANY REPRODUCTION HEREOF IN WHOLE OR IN PART."

understand its meaning and effects on the download problem

The increased thrust caused by blockage helps to reduce the download losses. For example, let us say that the thrust increase is 4%. Therefore, $K_2 = 1.04$, and the effective download for the rear wing of the X-19 becomes approximately 10.5% at a flap angle of 60° rather than 15% as indicated by the direct measurements.

c. Predicted Download

The method used and the download losses predicted for the X-100 airplane are given in (10) and (11). An adjustment was made in the data to agree with published XV-3 test data. The effects of propeller blockage are not considered in these data. Based on the test data run full scale with the X-100 airplane and shown on Figure 20, the original predicted download losses appeared much too low. The test data indicate a loss of 11% with no flap deflection compared with the predicted value of 7.7%. With the flap deflected 45° the test shows a loss of 6% in contrast with a predicted loss of 3.4% with a flap setting of 60°.

The predicted download loss on the X-19 airplane was based on the data given in Figure 20. It was assumed that the ratio of thrust increase due to blockage is the same for both front and rear wings. The predicted download loss for the front is 6.5% and the rear wing 9.5%, both with the flaps deflected to 60°. This gives an average loss due to download of 8.8% for the average take-off C.G. of 42.8%. The drag coefficient based on equation 5 for the rear wing was 0.58 and the corresponding coefficient for the front wing is 0.53. The difference in drag coefficient is due to the size of the flap on the front wing which results in less area for blockage, and consequently reduces the download.

3. PERIODIC FORCES ON WINGS AND PROPELLERS IN HOVER

The wing operating in the slipstream of the propeller will experience periodic forces due to the unsteady nature of the flow. When the airplane is hovering it is expected the forces would peak. The periodic forces are a function of the variation of velocity due to the presence of the propeller blades, as contrasted with a true disk. The frequency of the variation of force would be three times propeller rotational speed for the three-blade propeller used on the X-19. The variation of velocity from the mean was measured with a hot film anemometer as reported in (13). These measurements indicated the velocity peaks were approximately 10% above the minimum level and are quite abrupt in character. The measurements with pressure tubes on the rear wing showed little variation of pressure, which tends to confirm the hot film data.

From the test results it is expected the periodic forcing function would be small and be important only in creating a resonance condition in the structure of the movable control surfaces. This situation was encountered

FURNISHED UNDER UNITED STATES GOVERNMENT CONTRACT No AF33(615)-3940 SHALL NOT BE EITHER RELEASED OUTSIDE THE GOVERNMENT, OR USED, DUPLICATED, OR DISCLOSED IN WHOLE OR IN PART FOR MANUFACTURE OR PROCUREMENT, WITHOUT THE WRITTEN PERMISSION OF CURTISS-WRIGHT CORPORATION, EXCEPT FOR (I) EMERGENCY REPAIR OR OVERHAUL WORK BY OR FOR THE GOVERNMENT, WHERE THE ITEM OR PROCESS IS NOT OTHERWISE REASONABLY AVAILABLE TO ENABLE TIMELY PERFORMANCE OF THE WORK. OR (II) RELEASE TO A FOREIGN GOVERNMENT, AS THE INTERESTS OF THE UNITED STATES MAY REQUIRE PROVIDED THAT IN EITHER CASE THE RELEASE, USE, DUPLICATION OR DISCLOSURE HEREOF SHALL BE SUBJECT TO THE FOREGOING LIMITATIONS. THIS LEGEND SHALL BE MARKED ON ANY REPRODUCTION HEREOF IN WHOLE OR IN PART "

with the X-19 aircraft where trouble was experienced with a bracket holding the aileron. The difficulty was fixed by detuning the bracket from the 3XP periodic force. In the investigation of this problem, measurements of the frequency were made at the supporting bracket, confirming the 3XP frequency of periodic force.

The effect of the wing on the propeller when the aircraft is hovering was found to be small, from analysis of flight test records. Outboard on the blade a 1XP blade stress was measured of $\pm$ 600 psi, whereas the allowable is over 4,000 psi. A shank 1XP stress of $\pm$3,000 psi was measured whereas the allowable is 20,000 psi.

From the results of the download tests it will be noted that the propeller indicates an increase of thrust due to the wing blockage, as on Figure 31. For this reason it appears reasonable that the wing could induce a 1XP stress in the blades while the airplane is hovering. This stress is of little importance to the design of the propeller.

4. SUMMARY OF FORCES - WINGS AND PROPELLERS

a. Wings and Propellers - Out of Ground Effect

A reasonable determination of wing, propeller and fuselage interference effects for the X-19 has been obtained from (14). The wind tunnel data proved difficult to analyze for power effects; therefore, a suitable parameter was employed to linearize all data at a given "A" angle.

The propeller thrust coefficient (T_C) proved to be the device for providing a single effective function with reasonable data scatter. The data were collected at "A_F" angles from 16° to 90° for the lift coefficient (C_L) of the front and rear wing plus the propellers. These are plotted vs. T_C. In addition, C_L of the props was plotted for corresponding "A" angles.

The drag coefficient was handled in a similar manner. A consistent grouping of data was obtained to facilitate fairing slopes or curves. Where noted, data were taken at two velocities. In these instances, a R_e effect could be expected. The shaded points of the higher velocity appear higher at $A_F = 76°$; however, there aren't enough corroborating facts at other "A" angles to support a definite R_e effect. Figures 33 through 36 are selected curves from which one can see the nature of these effects.

FURNISHED UNDER UNITED STATES GOVERNMENT CONTRACT No AF33(615)-1940 SHALL NOT BE EITHER RELEASED OUTSIDE THE GOVERNMENT, OR USED, DUPLICATED, OR DISCLOSED IN WHOLE OR IN PART FOR MANUFACTURE OR PROCUREMENT, WITHOUT THE WRITTEN PERMISSION OF CURTISS-WRIGHT CORPORATION, EXCEPT FOR (I) EMERGENCY REPAIR OR OVERHAUL WORK BY OR FOR THE GOVERNMENT, WHERE THE ITEM OR PROCESS IS NOT OTHERWISE REASONABLY AVAILABLE TO ENABLE TIMELY PERFORMANCE OF THE WORK, OR (II) RELEASE TO A FOREIGN GOVERNMENT, AS THE INTERESTS OF THE UNITED STATES MAY REQUIRE. PROVIDED THAT IN EITHER CASE THE RELEASE, USE, DUPLICATION OR DISCLOSURE HEREOF SHALL BE SUBJECT TO THE FOREGOING LIMITATIONS. THIS LEGEND SHALL BE MARKED ON ANY REPRODUCTION HEREOF IN WHOLE OR IN PART."

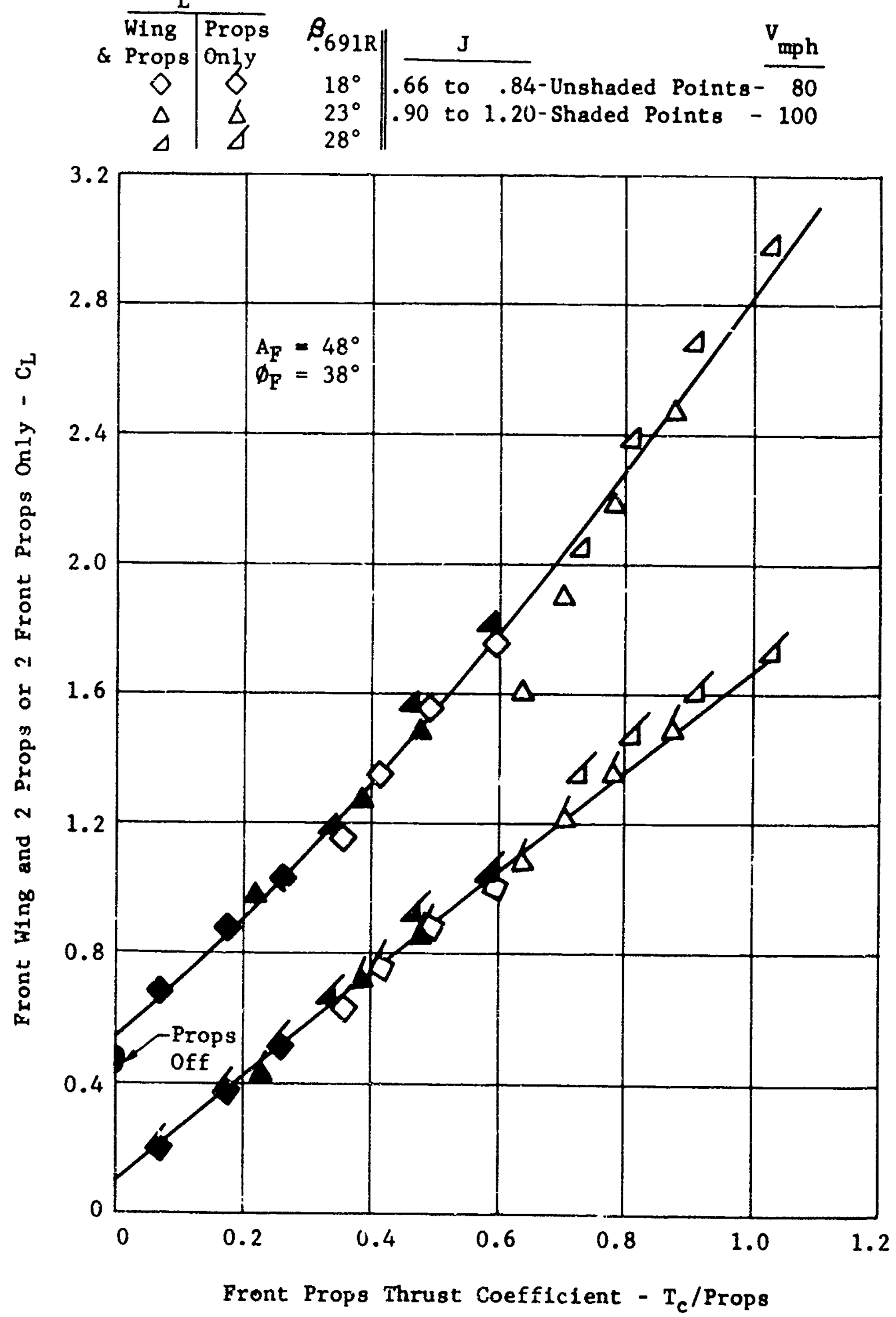

Figure 33. X-19, lift coefficient of front propellers and front wing plus propellers as a function of thrust coefficient.

FURNISHED UNDER UNITED STATES GOVERNMENT CONTRACT No AF33(615)-3940 SHALL NOT BE EITHER RELEASED OUTSIDE THE GOVERNMENT, OR USED, DUPLICATED, OR DISCLOSED IN WHOLE OR IN PART FOR MANUFACTURE OR PROCUREMENT, WITHOUT THE WRITTEN PERMISSION OF CURTISS-WRIGHT CORPORATION, EXCEPT FOR (I) EMERGENCY REPAIR OR OVERHAUL WORK BY OR FOR THE GOVERNMENT, WHERE THE ITEM OR PROCESS IS NOT OTHERWISE RESONABLY AVAILABLE TO ENABLE TIMELY PERFORMANCE OF THE WORK OR (II) RELEASE TO A FOREIGN GOVERNMENT, AS THE INTERESTS OF THE UNITED STATES MAY REQUIRE PROVIDED THAT IN EITHER CASE THE RELEASE, USE, DUPLICATION OR DISCLOSURE HEREOF SHALL BE SUBJECT TO THE FOREGOING LIMITATIONS. THIS LEGEND SHALL BE MARKED ON ANY REPRODUCTION HEREOF IN WHOLE OR IN PART."

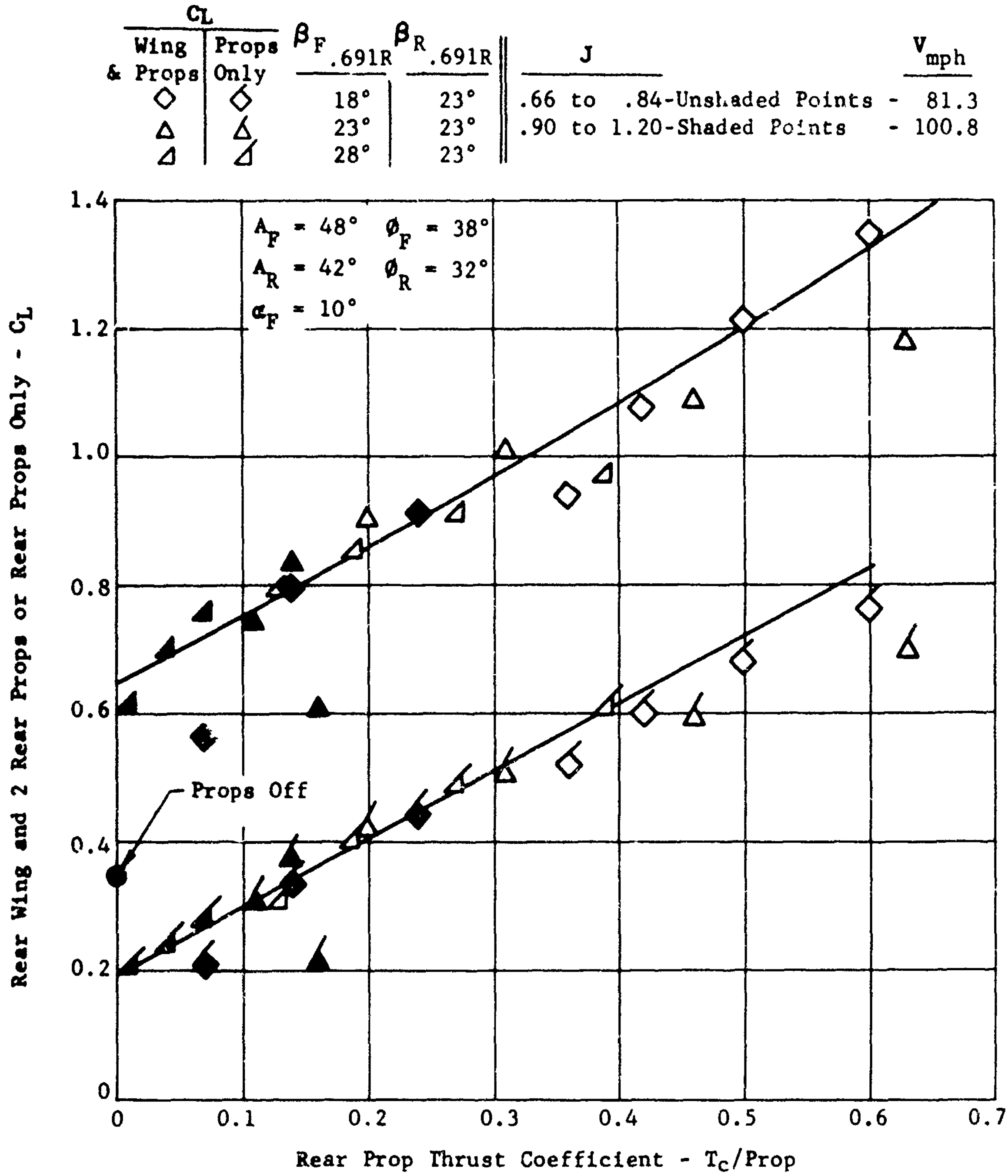

Figure 34. X-19, lift coefficient of rear propellers and rear wing in present of front wing plus front propellers as a function of thrust coefficient.

"FURNISHED UNDER UNITED STATES GOVERNMENT CONTRACT No AF33(615)-1940 SHALL NOT BE EITHER RELEASED OUTSIDE THE GOVERNMENT, OR USED, DUPLICATED, OR DISCLOSED IN WHOLE OR IN PART FOR MANUFACTURE OR PROCUREMENT, WITHOUT THE WRITTEN PERMISSION OF CURTISS-WRIGHT CORPORATION, EXCEPT FOR (I) EMERGENCY REPAIR OR OVERHAUL WORK BY OR FOR THE GOVERNMENT, WHERE THE ITEM OR PROCESS IS NOT OTHERWISE REASONABLY AVAILABLE TO ENABLE TIMELY PERFORMANCE OF THE WORK. OR (II) RELEASE TO A FOREIGN GOVERNMENT, AS THE INTERESTS OF THE UNITED STATES MAY REQUIRE. PROVIDED THAT IN EITHER CASE THE RELEASE, USE, DUPLICATION OR DISCLOSURE HEREOF SHALL BE SUBJECT TO THE FOREGOING LIMITATIONS. THIS LEGEND SHALL BE MARKED ON ANY REPRODUCTION HEREOF IN WHOLE OR IN PART."

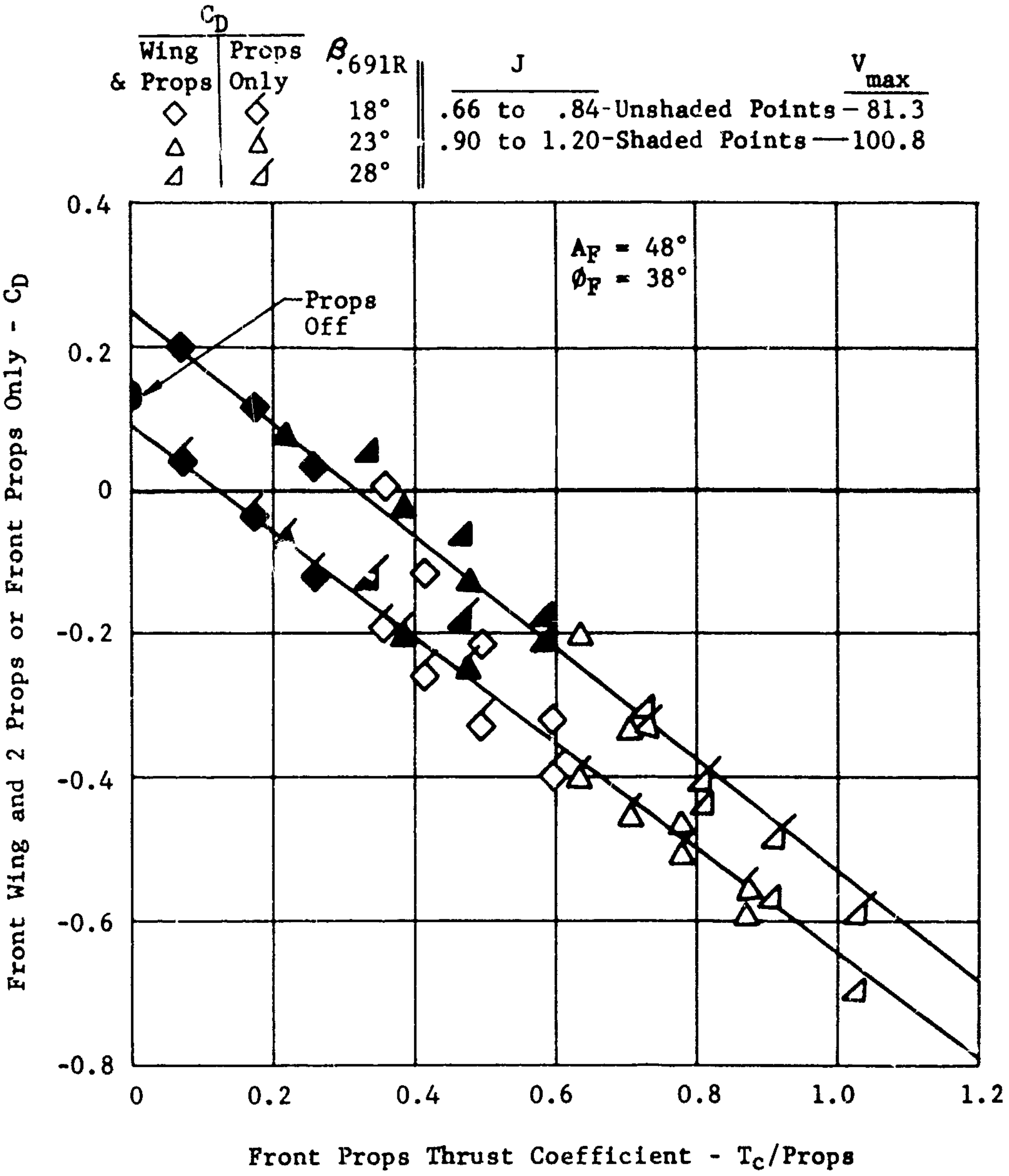

Figure 35. X-19, drag coefficient of front propellers and front wing plus propellers as a function of thrust coefficient.

FURNISHED UNDER UNITED STATES GOVERNMENT CONTRACT No. AF33(615)-3940. SHALL NOT BE EITHER RELEASED OUTSIDE THE GOVERNMENT, OR USED, DUPLICATED, OR DISCLOSED IN WHOLE OR IN PART FOR MANUFACTURE OR PROCUREMENT, WITHOUT THE WRITTEN PERMISSION OF CURTISS-WRIGHT CORPORATION, EXCEPT FOR (I) EMERGENCY REPAIR OR OVERHAUL WORK BY OR FOR THE GOVERNMENT, WHERE THE ITEM OR PROCESS IS NOT OTHERWISE RESONABLY AVAILABLE TO ENABLE TIMELY PERFORMANCE OF THE WORK. OR (II) RELEASE TO A FOREIGN GOVERNMENT, AS THE INTERESTS OF THE UNITED STATES MAY REQUIRE PROVIDED THAT IN EITHER CASE THE RELEASE, USE, DUPLICATION OR DISCLOSURE HEREOF SHALL BE SUBJECT TO THE FOREGOING LIMITATIONS THIS LEGEND SHALL BE MARKED ON ANY REPRODUCTION HEREOF IN WHOLE OR IN PART."

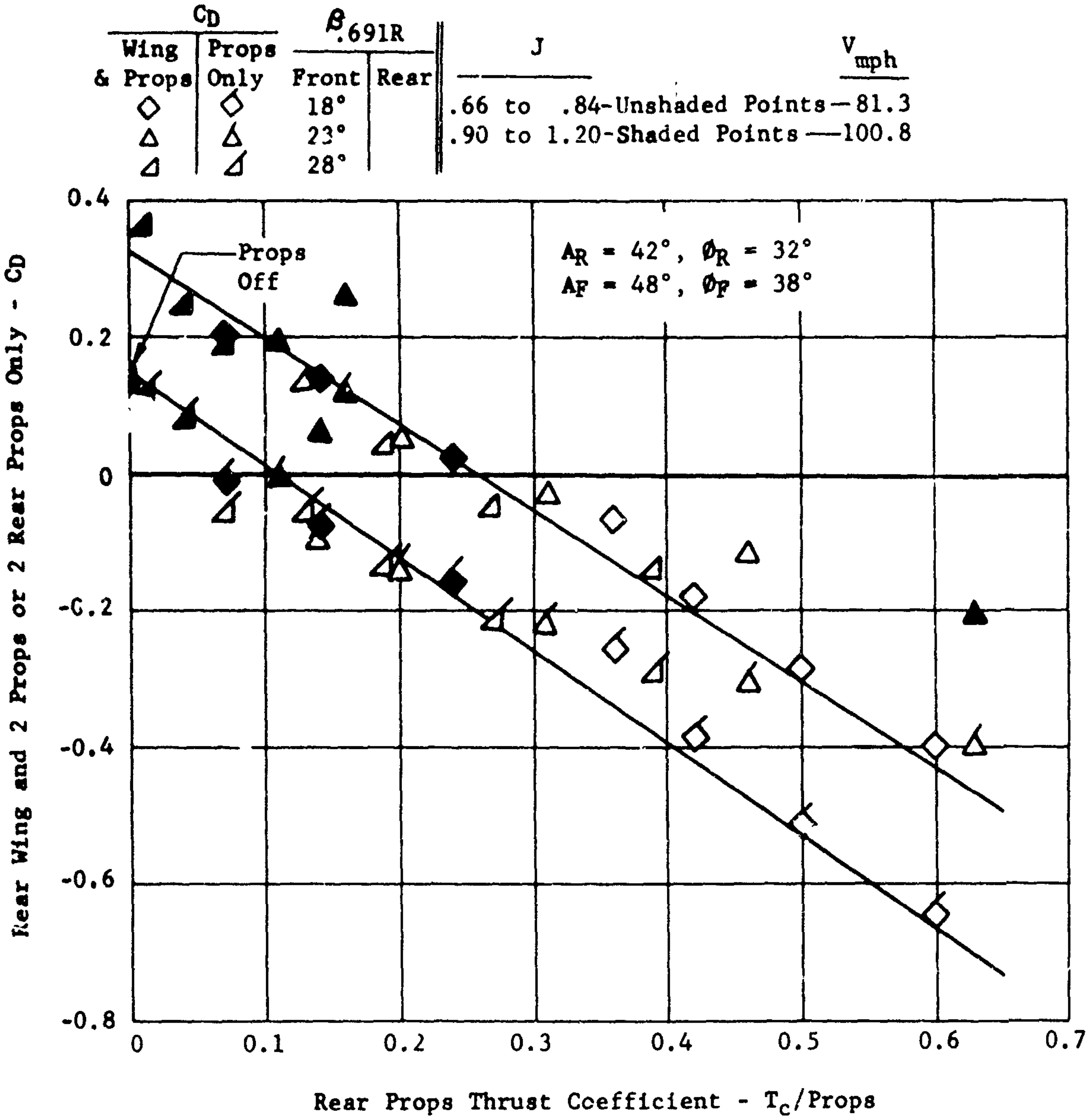

Figure 36. X-19, drag coefficient of rear propellers and rear wing plus propellers as a function of thrust coefficient.

FURNISHED UNDER UNITED STATES GOVERNMENT CONTRACT No. AF33(615)-3940. SHALL NOT BE EITHER RELEASED OUTSIDE THE GOVERNMENT, OR USED, DUPLICATED, OR DISCLOSED IN WHOLE OR IN PART FOR MANUFACTURE OR PROCUREMENT, WITHOUT THE WRITTEN PERMISSION OF CURTISS-WRIGHT CORPORATION, EXCEPT FOR (I) EMERGENCY REPAIR OR OVERHAUL WORK BY OR FOR THE GOVERNMENT, WHERE THE ITEM OR PROCESS IS NOT OTHERWISE REASONABLY AVAILABLE TO ENABLE TIMELY PERFORMANCE OF THE WORK, OR (II) RELEASE TO A FOREIGN GOVERNMENT, AS THE INTERESTS OF THE UNITED STATES MAY REQUIRE. PROVIDED THAT IN EITHER CASE THE RELEASE, USE, DUPLICATION OR DISCLOSURE HEREOF SHALL BE SUBJECT TO THE FOREGOING LIMITATIONS. THIS LEGEND SHALL BE MARKED ON ANY REPRODUCTION HEREOF IN WHOLE OR IN PART."

To provide a more common device for comparison, derivation of a suitable power parameter was accomplished as follows.

$$\frac{TV}{550\eta} = \text{HP (Horse Power)}$$

$$\frac{T_c\ (\frac{1}{2}\rho V^2)\ S_p\ V}{550\eta} = \frac{C_p\ \rho\ n^3 D_p{}^5}{550}$$

$$T_c = K\,\eta\,(C_p/J^3)$$

Where $K = 8/\pi$

This relationship of T_c and $(C_p\ /\ J^3)$ was used to parameterize the thrust and power data. Figures 37 and 38 contain plots of these parameters at constant "A" angles, and show relatively small data scatter. Therefore a relationship is apparent for the tilted propeller which ties the estimation of lift and drag power effects to these parameters. Figure 39 is a cross plot of the two previous curves. This form is of considerable interest, in that it describes a simple picture of the front wash effect upon the rear propeller. Note that the parameter, $(C_p\ /\ J^3)$, is proportional to HP $/V^3$. Thus for a fixed horsepower and velocity, one can see how the thrust (proportional to T_C) varies with "A" angle. On the front propeller, thrust increases rapidly at "A" angles above 45° while on the rear, only small changes occur. From the stability consideration, this is undesirable; however, it is common to all tandem lifting bodies and cannot be completely avoided. It is this characteristic which has been found to be responsible for the unstable C_{m_α} (per wind tunnel results) of the X-19 at the high tilt angles and low advance ratios.

During flight test, there was little indication of static instability in the region indicated by tunnel tests ($\phi_F = 82.5°$, $V = 50$ knots). However, specific tests to determine this were not performed. Consequently, a correlation between model and full scale characteristics was never established.

Later data of (15) indicated that curves of T_c vs $(C_p/_J3)$ are not independent of β_{coll} at a given ϕ , α_f . This would suggest that some of the single line curves which appear to have scatter in the points should be several curves which are nearly colinear. (See Figures 37 and 38). It is also known that propeller lift efficiency varies widely with πnD_p at the higher "A" angles. Yet if a single curve is drawn for C_L vs. $(C_p/_J3)$ (at a given A angle)

FURNISHED UNDER UNITED STATES GOVERNMENT CONTRACT No. AF33(615)-3940 SHALL NOT BE EITHER RELEASED OUTSIDE THE GOVERNMENT, OR USED, DUPLICATED, OR DISCLOSED IN WHOLE OR IN PART FOR MANUFACTURE OR PROCUREMENT, WITHOUT THE WRITTEN PERMISSION OF CURTISS-WRIGHT CORPORATION, EXCEPT FOR (i) EMERGENCY REPAIR OR OVERHAUL WORK BY OR FOR THE GOVERNMENT, WHERE THE ITEM OR PROCESS IS NOT OTHERWISE REASONABLY AVAILABLE TO ENABLE TIMELY PERFORMANCE OF THE WORK, OR (ii) RELEASE TO A FOREIGN GOVERNMENT, AS THE INTERESTS OF THE UNITED STATES MAY REQUIRE. PROVIDED THAT IN EITHER CASE THE RELEASE, USE, DUPLICATION OR DISCLOSURE HEREOF SHALL BE SUBJECT TO THE FOREGOING LIMITATIONS. THIS LEGEND SHALL BE MARKED ON ANY REPRODUCTION HEREOF IN WHOLE OR IN PART.'

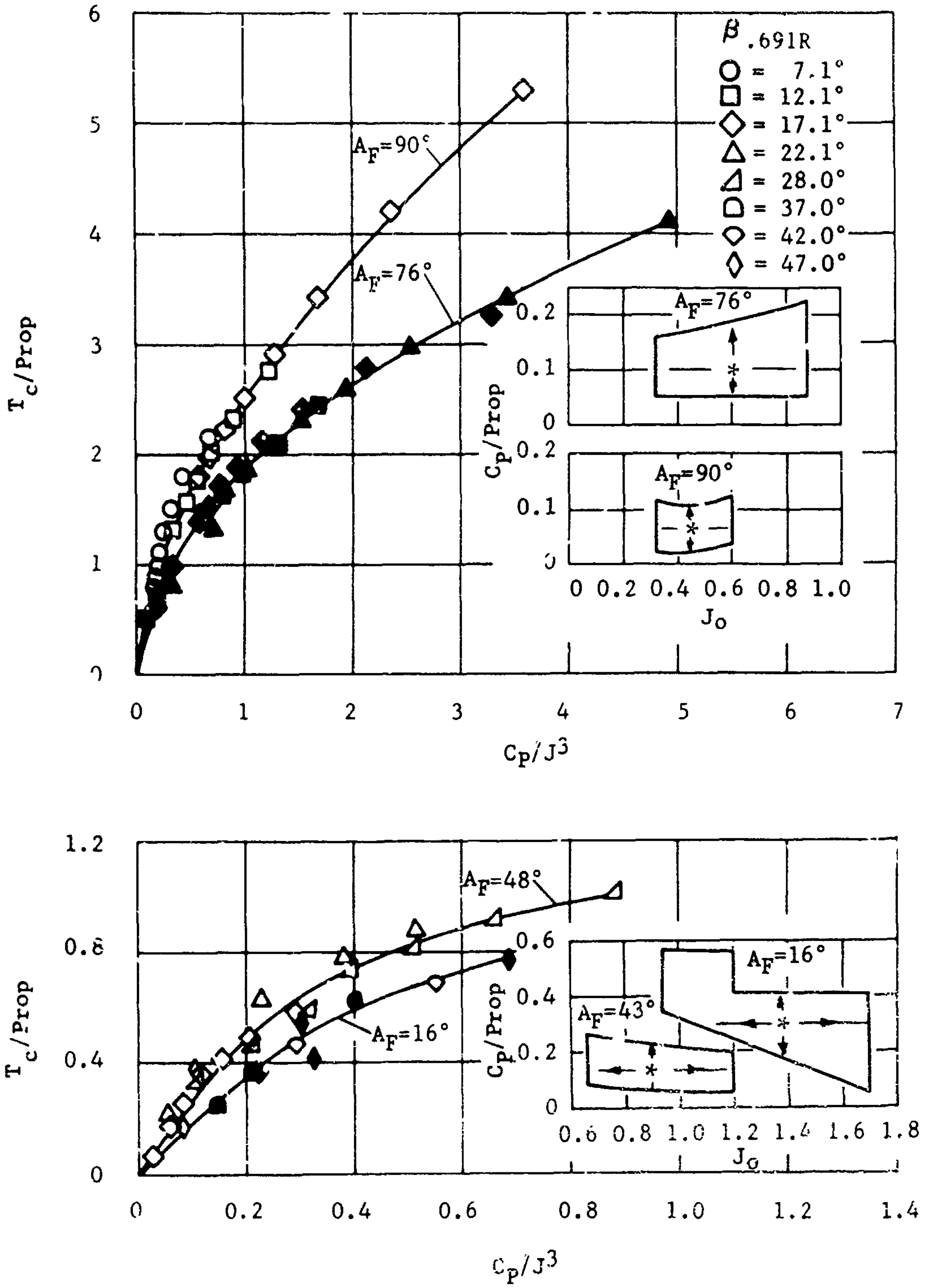

* Area covered by test points

Figure 37. X-19, front propeller thrust coefficient as a function of power parameter, C_p/J^3.

URNISHED UNDER UNITED STATES GOVERNMENT CONTRACT No. AF33(615)-19 SHALL NOT BE EITHER RELEASED OUTSIDE THE GOVERNMENT, OR USED, DUPLICATED, OR DISCLOSED IN WHOLE OR IN PART FOR MANUFACTURE OR PROCUREMENT, WITHOUT THE WRITTEN PERMISSION OF CURTISS-WRIGHT CORPORATION, EXCEPT FOR (I) EMERGENCY REPAIR OR OVERHAUL WORK BY OR FOR THE GOVERNMENT, WHERE THE ITEM OR PROCESS IS NOT OTHERWISE REASONABLY AVAILABLE TO ENABLE TIMELY PERFORMANCE OF THE WORK, OR (II) RELEASE TO A FOREIGN GOVERNMENT, AS THE INTERESTS OF THE UNITED STATES MAY REQUIRE, PROVIDED THAT IN EITHER CASE THE RELEASE, USE, DUPLICATION OR DISCLOSURE HEREOF SHALL BE SUBJECT TO THE FOREGOING LIMITATIONS. THIS LEGEND SHALL BE MARKED ON ANY REPRODUCTION HEREOF IN WHOLE OR IN PART.

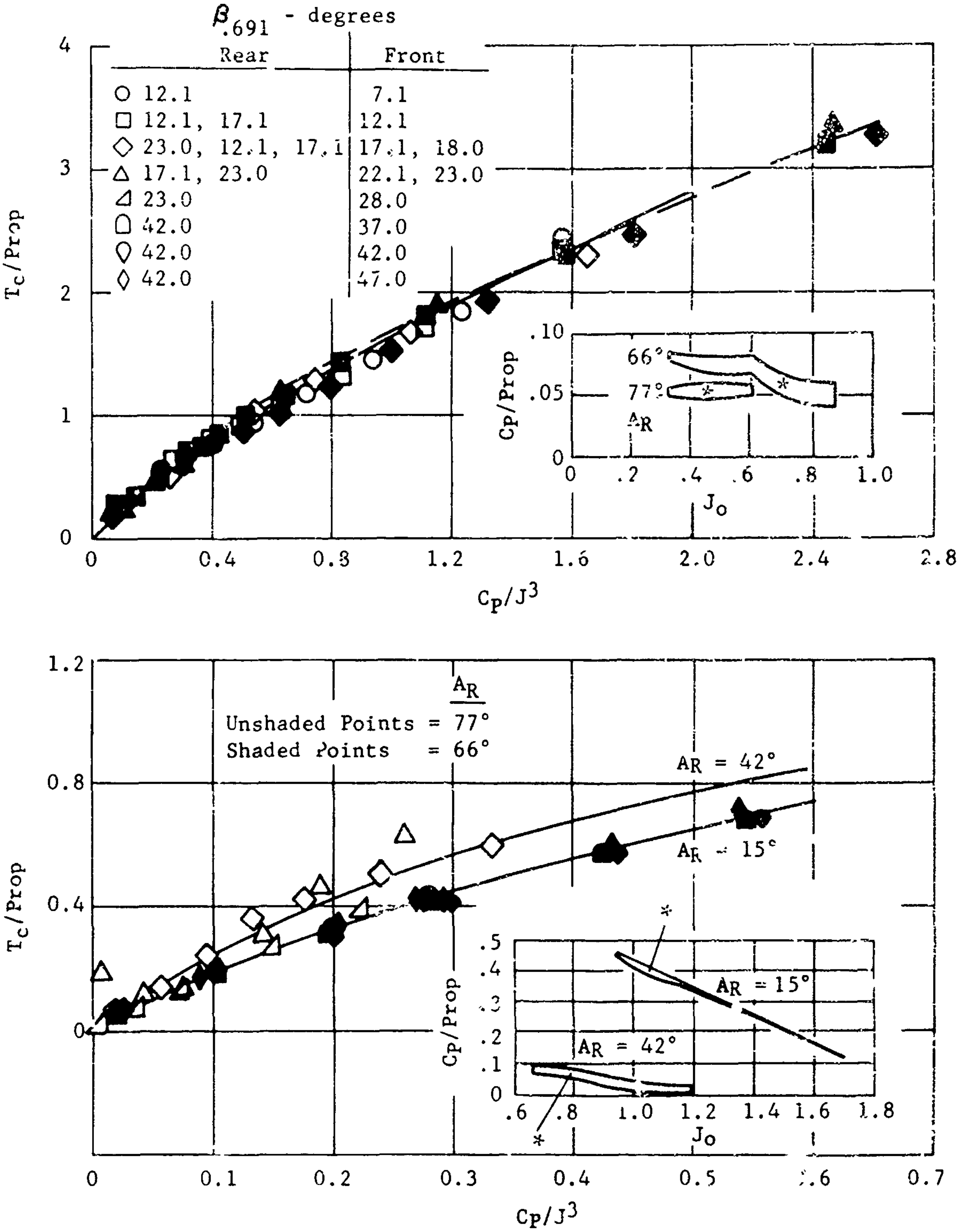

* Area covered by test points

Figure 38. X-19, rear propeller thrust coefficient as a function of power parameter.

FURNISHED UNDER UNITED STATES GOVERNMENT CONTRACT No. AF33(615)-3940 SHALL NOT BE EITHER RELEASED OUTSIDE THE GOVERNMENT, OR USED, DUPLICATED, OR DISCLOSED IN WHOLE OR IN PART FOR MANUFACTURE OR PROCUREMENT, WITHOUT THE WRITTEN PERMISSION OF CURTISS-WRIGHT CORPORATION, EXCEPT FOR (I) EMERGENCY REPAIR OR OVERHAUL WORK BY OR FOR THE GOVERNMENT WHERE THE ITEM OR PROCESS IS NOT OTHERWISE REASONABLY AVAILABLE TO ENABLE TIMELY PERFORMANCE OF THE WORK OR (II) RELEASE TO A FOREIGN GOVERNMENT, AS THE INTERESTS OF THE UNITED STATES MAY REQUIRE PROVIDED THAT IN EITHER CASE THE RELEASE, USE, DUPLICATION OR DISCLOSURE HEREOF SHALL BE SUBJECT TO THE FOREGOING LIMITATIONS. THIS LEGEND SHALL BE MARKED ON ANY REPRODUCTION HEREOF IN WHOLE OR IN PART."

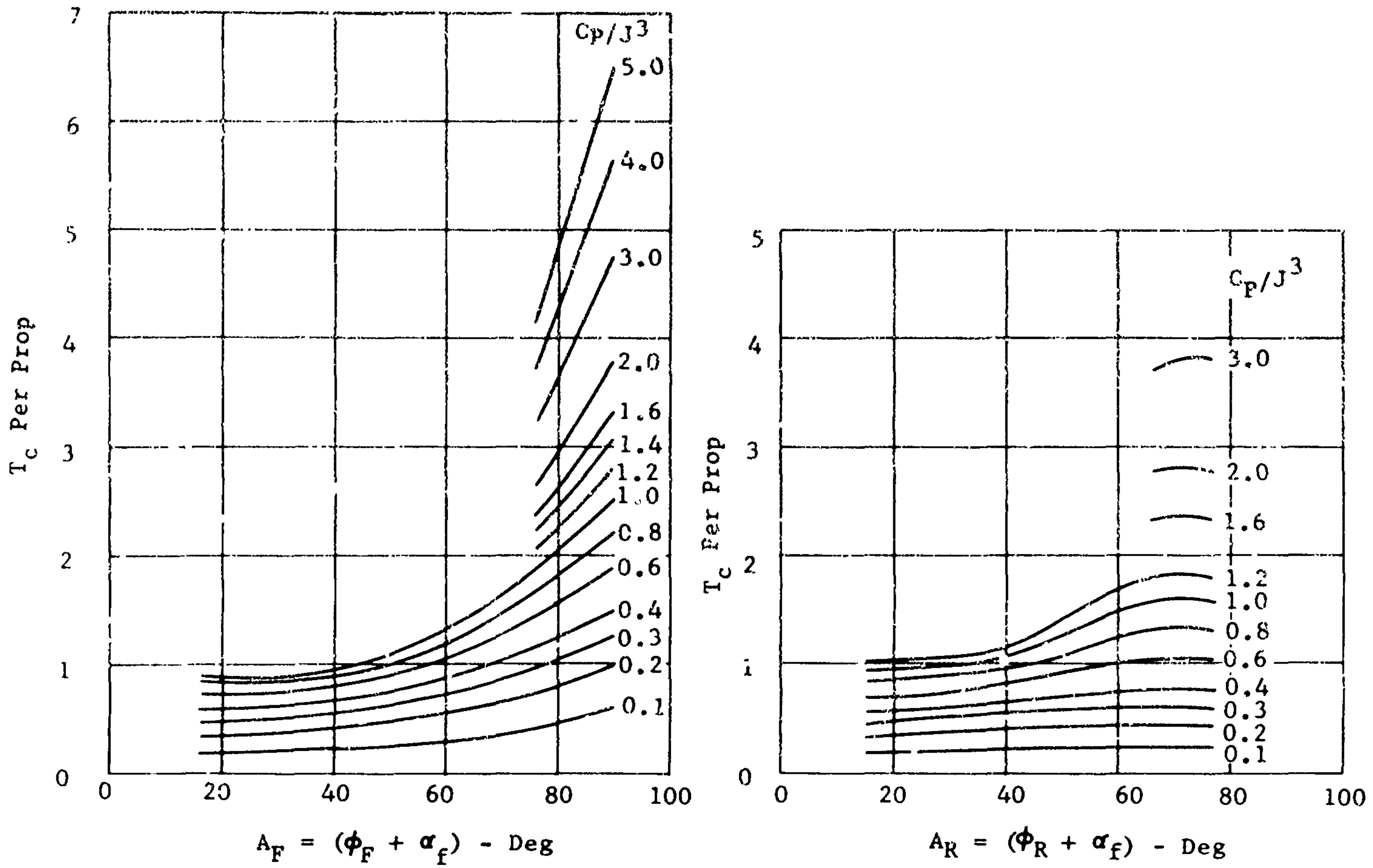

Figure 39. X-19, thrust coefficient as a function of thrust axis angle of attack.

"FURNISHED UNDER UNITED STATES GOVERNMENT CONTRACT No. AF33(615)-3940. SHALL NOT BE EITHER RELEASED OUTSIDE THE GOVERNMENT, OR USED, DUPLICATED, OR DISCLOSED IN WHOLE OR IN PART FOR MANUFACTURE OR PROCUREMENT, WITHOUT THE WRITTEN PERMISSION OF CURTISS-WRIGHT CORPORATION, EXCEPT FOR (I) EMERGENCY REPAIR OR OVERHAUL WORK BY OR FOR THE GOVERNMENT, WHERE THE ITEM OR PROCESS IS NOT OTHERWISE REASONABLY AVAILABLE TO ENABLE TIMELY PERFORMANCE OF THE WORK, OR (II) RELEASE TO A FOREIGN GOVERNMENT, AS THE INTERESTS OF THE UNITED STATES MAY REQUIRE; PROVIDED THAT IN EITHER CASE THE RELEASE, USE, DUPLICATION OR DISCLOSURE HEREOF SHALL BE SUBJECT TO THE FOREGOING LIMITATIONS. THIS LEGEND SHALL BE MARKED ON ANY REPRODUCTION HEREOF IN WHOLE OR IN PART."

the lift will be independent of $\pi n D_p$. Therefore, the single line can only be an approximation. (16) describes the most recent analysis of an isolated propeller plotted in the C_p/J^3 parameter. Figures 40 and 41 are taken from this report to illustrate the non-colinear characteristics. For practical considerations, in selecting the operating conditions of the propeller, one achieves a near optimum setting throughout the flight regime. Consequently, as one moves along the C_p/J^3 curve, T_c will fall close to the envelope curve (a single line). For this reason, the single line presentations shown in Figures 37 to 39 are quite indicative of the "trends" and general efficiency levels at which the propellers are operating.

Note further that this approximating technique has represented the entire T_c, A, J and C_p interrelationship regime on one sheet of curves (Figure 39).

Of more value, however, are the C_L and C_D (or $-C_x$) of the propellers. That information is given in Figures 42 and 43, where:

$$C_L = \left[T_c \sin(\phi + \alpha_f) + N_c \cos(\phi + \alpha_f)\right] \frac{\pi/4 \; D_p{}^2}{S}$$

$$C_X = -C_D = \left[T_c \cos(\phi + \alpha_f) - N_c \sin(\phi + \alpha_f)\right] \frac{\pi/4 \; D_p{}^2}{S}$$

The term, N_c, is the propeller normal force coefficient defined in the same manner as T_c. These data represent some of the earlier information obtained for the X-19 front and rear propellers. Some later propeller data have been obtained from recent wind tunnel tests; unfortunately, time did not permit correlation of these data with that shown here. In simple spot checks, it was found that the trends shown in Figure 39 are still valid. However, the absolute level of thrust (at fixed power) appears to be higher.

The wing forces are the next phase of this discussion. This is separately treated as the lift and drag of the wings without propellers, and the power effects of the propellers upon the wings.

The propeller-off wing forces are normally represented by a C_L and C_D vs α_f curve. However, the small size of the wings (lift struts) makes them sensitive to the presence of nearby bodies. The nacelles for one, are sufficiently large to cause considerable interference. Thus, curves of C_L and C_D are given as a function

"FURNISHED UNDER UNITED STATES GOVERNMENT CONTRACT No. AF33(615)-3940. SHALL NOT BE EITHER RELEASED OUTSIDE THE GOVERNMENT, OR USED, DUPLICATED, OR DISCLOSED IN WHOLE OR IN PART FOR MANUFACTURE OR PROCUREMENT, WITHOUT THE WRITTEN PERMISSION OF CURTISS-WRIGHT CORPORATION, EXCEPT FOR (I) EMERGENCY REPAIR OR OVERHAUL WORK BY OR FOR THE GOVERNMENT, WHERE THE ITEM OR PROCESS IS NOT OTHERWISE REASONABLY AVAILABLE TO ENABLE TIMELY PERFORMANCE OF THE WORK, OR (II) RELEASE TO A FOREIGN GOVERNMENT, AS THE INTERESTS OF THE UNITED STATES MAY REQUIRE. PROVIDED THAT IN EITHER CASE THE RELEASE, USE, DUPLICATION OR DISCLOSURE HEREOF SHALL BE SUBJECT TO THE FOREGOING LIMITATIONS. THIS LEGEND SHALL BE MARKED ON ANY REPRODUCTION HEREOF IN WHOLE OR IN PART."

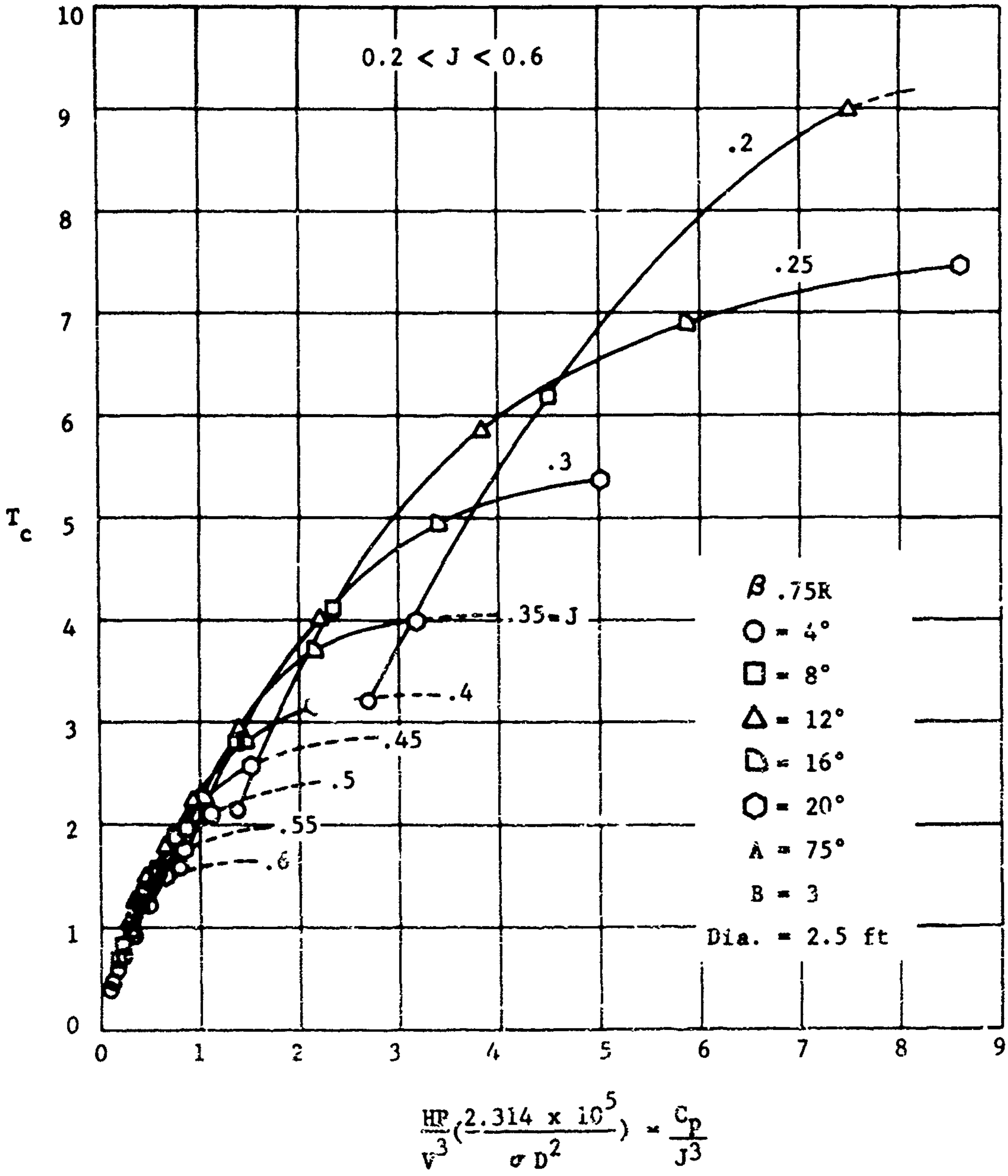

Figure 40. Propeller 156109, thrust coefficient as a function of power parameter. Tilt Angle A = 75°

"FURNISHED UNDER UNITED STATES GOVERNMENT CONTRACT No. AF33(615)-1940. SHALL NOT BE EITHER RELEASED OUTSIDE THE GOVERNMENT, OR USED, DUPLICATED, OR DISCLOSED IN WHOLE OR IN PART FOR MANUFACTURE OR PROCUREMENT, WITHOUT THE WRITTEN PERMISSION OF CURTISS-WRIGHT CORPORATION, EXCEPT FOR (I) EMERGENCY REPAIR OR OVERHAUL WORK BY OR FOR THE GOVERNMENT, WHERE THE ITEM OR PROCESS IS NOT OTHERWISE REASONABLY AVAILABLE TO ENABLE TIMELY PERFORMANCE OF THE WORK. OR (II) RELEASE TO A FOREIGN GOVERNMENT, AS THE INTERESTS OF THE UNITED STATES MAY REQUIRE. PROVIDED THAT IN EITHER CASE THE RELEASE, USE, DUPLICATION OR DISCLOSURE HEREOF SHALL BE SUBJECT TO THE FOREGOING LIMITATIONS. THIS LEGEND SHALL BE MARKED ON ANY REPRODUCTION HEREOF IN WHOLE OR IN PART."

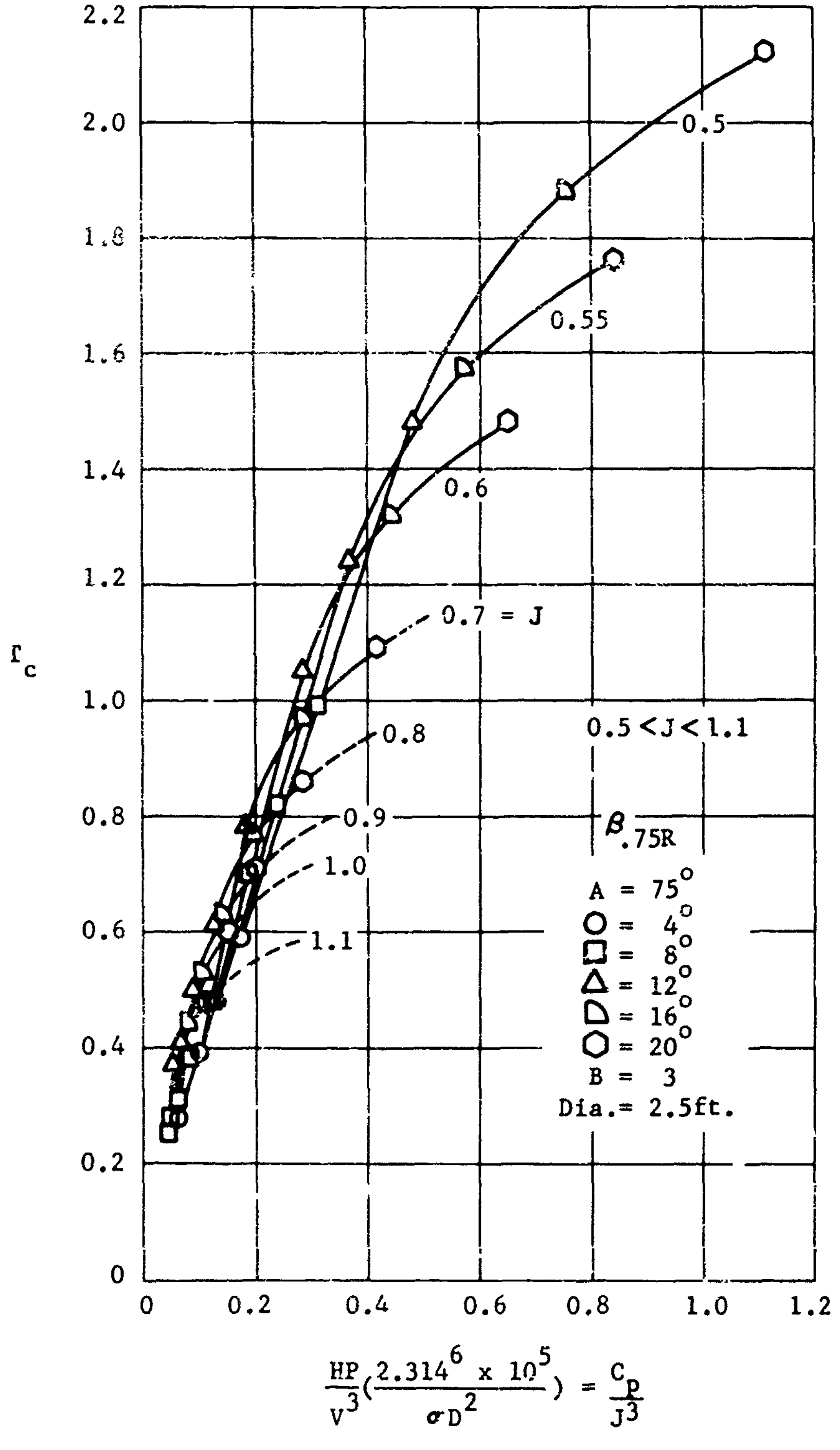

Figure 41. Propeller 156109, thrust coefficient as a function of power parameter. Tilt Angle A = 75°

"FURNISHED UNDER UNITED STATES GOVERNMENT CONTRACT No. AF33(615)-3940. SHALL NOT BE EITHER RELEASED OUTSIDE THE GOVERNMENT, OR USED, DUPLICATED, OR DISCLOSED IN WHOLE OR IN PART FOR MANUFACTURE OR PROCUREMENT, WITHOUT THE WRITTEN PERMISSION OF CURTISS-WRIGHT CORPORATION, EXCEPT FOR (I) EMERGENCY REPAIR OR OVERHAUL WORK BY OR FOR THE GOVERNMENT, WHERE THE ITEM OR PROCESS IS NOT OTHERWISE REASONABLY AVAILABLE TO ENABLE TIMELY PERFORMANCE OF THE WORK. OR (II) RELEASE TO A FOREIGN GOVERNMENT, AS THE INTERESTS OF THE UNITED STATES MAY REQUIRE PROVIDED THAT IN EITHER CASE THE RELEASE, USE, DUPLICATION OR DISCLOSURE HEREOF SHALL BE SUBJECT TO THE FOREGOING LIMITATIONS. THIS LEGEND SHALL BE MARKED ON ANY REPRODUCTION HEREOF IN WHOLE OR IN PART."

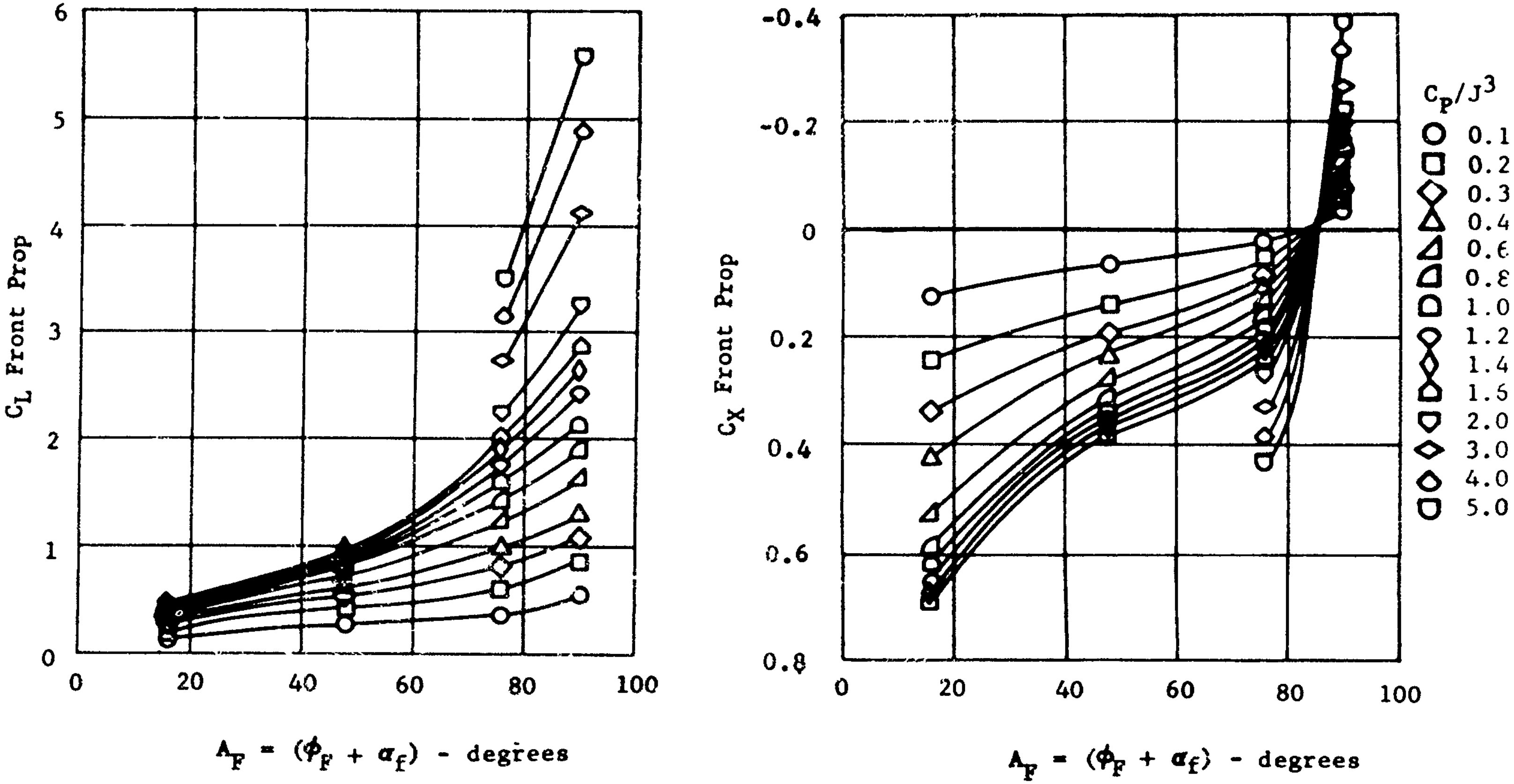

Figure 42. X-19, variation of front propeller lift and thrust coefficient with thrust axis angle of attack.

"FURNISHED UNDER UNITED STATES GOVERNMENT CONTRACT No. AF33(615)-3940. SHALL NOT BE EITHER RELEASED OUTSIDE THE GOVERNMENT, OR USED, DUPLICATED, OR DISCLOSED IN WHOLE OR IN PART FOR MANUFACTURE OR PROCUREMENT, WITHOUT THE WRITTEN PERMISSION OF CURTISS-WRIGHT CORPORATION, EXCEPT FOR (i) EMERGENCY REPAIR OR OVERHAUL WORK BY OR FOR THE GOVERNMENT, WHERE THE ITEM OR PROCESS IS NOT OTHERWISE REASONABLY AVAILABLE TO ENABLE TIMELY PERFORMANCE OF THE WORK, OR (ii) RELEASE TO A FOREIGN GOVERNMENT, AS THE INTERESTS OF THE UNITED STATES MAY REQUIRE. PROVIDED THAT IN EITHER CASE THE RELEASE, USE, DUPLICATION OR DISCLOSURE HEREOF SHALL BE SUBJECT TO THE FOREGOING LIMITATIONS. THIS LEGEND SHALL BE MARKED ON ANY REPRODUCTION HEREOF IN WHOLE OR IN PART."

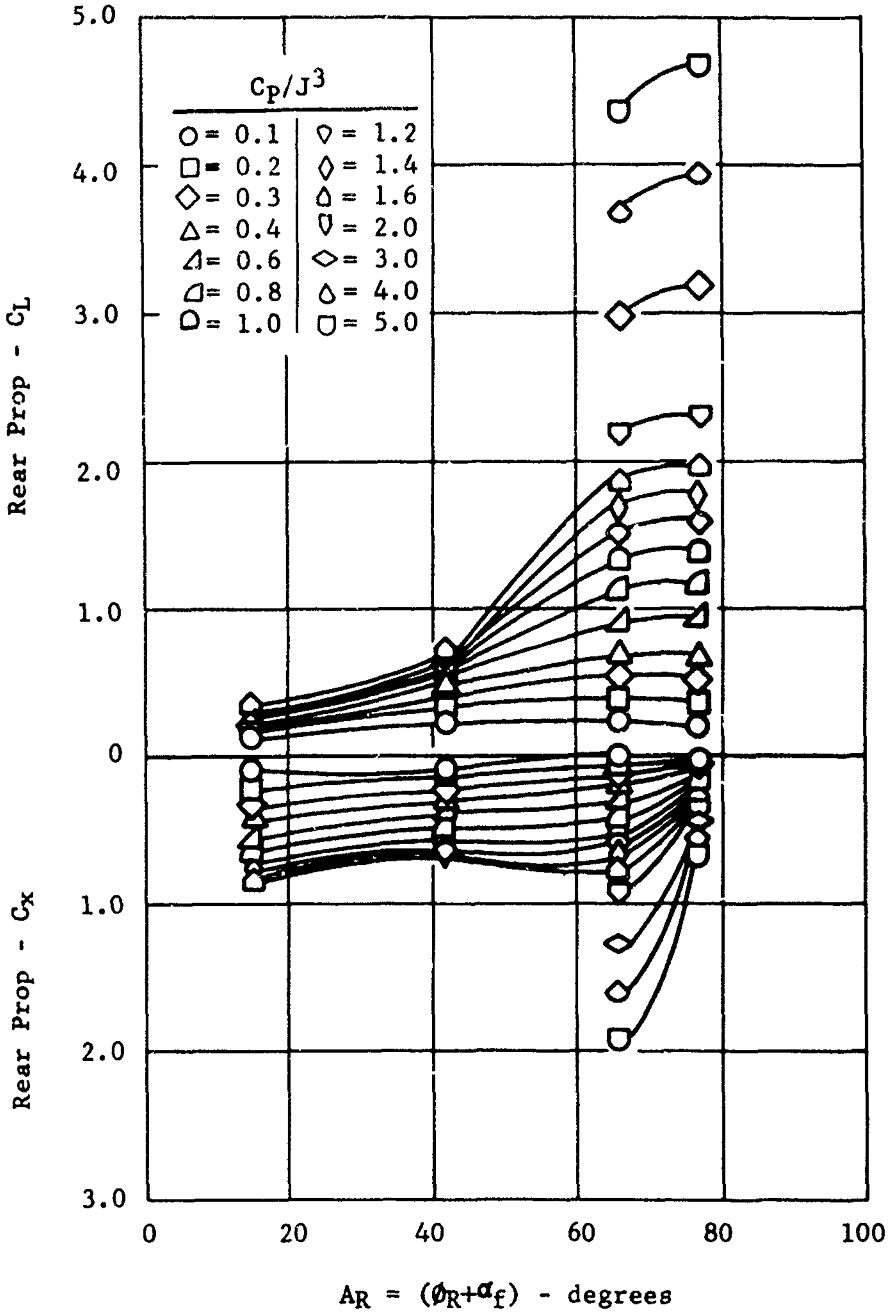

Figure 43. X-19, variation of rear propeller lift and thrust coefficient with thrust axis angle of attack.

"FURNISHED UNDER UNITED STATES GOVERNMENT CONTRACT No. AF33(615)-3940. SHALL NOT BE EITHER RELEASED OUTSIDE THE GOVERNMENT, OR USED, DUPLICATED, OR DISCLOSED IN WHOLE OR IN PART FOR MANUFACTURE OR PROCUREMENT, WITHOUT THE WRITTEN PERMISSION OF CURTISS-WRIGHT CORPORATION, EXCEPT FOR (I) EMERGENCY REPAIR OR OVERHAUL WORK BY OR FOR THE GOVERNMENT, WHERE THE ITEM OR PROCESS IS NOT OTHERWISE REASONABLY AVAILABLE TO ENABLE TIMELY PERFORMANCE OF THE WORK. OR (II) RELEASE TO A FOREIGN GOVERNMENT, AS THE INTERESTS OF THE UNITED STATES MAY REQUIRE. PROVIDED THAT IN EITHER CASE THE RELEASE, USE, DUPLICATION OR DISCLOSURE HEREOF SHALL BE SUBJECT TO THE FOREGOING LIMITATIONS. THIS LEGEND SHALL BE MARKED ON ANY REPRODUCTION HEREOF IN WHOLE OR IN PART."

of nacelle tilt angle and angle of attack in Figures 44 through 47. Note the diminished lift and increased drag at the high tilt angles. This is attributed to wing tip stall induced by the nacelle, as reported in (17) and (18), and shows that maximum C_{L_α} occurs in the vicinity of $10^\circ < \phi < 20^\circ$. Both wings are referenced to the airplane area rather than individual wing areas. Furthermore, both wings generate approximately the same lift; yet the rear wing is twice the size of the front. This merely reflects the large downwash to which the rear wing is subjected by the front wing and propeller when installed on the aircraft.

Included in these results is the fuselage-induced wash. This manifests itself as an upwash field on the front wing and a downwash field on the rear wing. A more comprehensive discussion of fuselage induced wash is given in Section X.2.k. Aileron and flap angles are zero throughout.

The effects of propeller wash upon the wings is highly pronounced and is clearly a function of propeller tilt angle (with respect to wing) and disk loading coefficient (T_c). The results are given in Figures 48 through 51. A look at Figure 48 presents some interesting perspective. A positive lift is shown acting on the wing which is equal to or greater than that of the wing, power off. The T_c was computed using tunnel data run at 40 mph with $.3 < J < .6$ For zero velocity, T_c would be infinite; however, the wing lift would be negative. Obviously somewhere between $0 < J < .3$ the prop wash shifts aft and the wing's lift goes from a download (negative) to a positive lift, and even a positive lift increment above the established C_{L_α} relationship. Therefore, these curves cannot be used in the immediate vicinity of the hover.

The rear wing experiences both a positive and negative lift increment depending on the tilt angle. Referring to Figure 49, note a large download at the high "A" angles. Investigation has shown that the incremental lifts, positive on the front wing and negative on the rear wing, contribute strongly to the aircraft's pitch-up moment (trim) progressing from hover to a finite forward velocity.

Both the front and rear wing (Figures 50 and 51) appear to experience a drag-power effect at the high tilt angles and a thrust at the low tilt angles. This would seem to imply high suctions on the leading edge. For practical purposes, this thrust is of small consequence because cruise values of T_c approach zero for speeds not much in excess of 160 knots. Also, at low tilt angles, the parameter ($\phi + \alpha_f$) does not clearly define the wash, as the power effects will vary both with ($\phi + \alpha_f$) and ϕ. However, the test data did not provide for both of these parameters to be varied.

"FURNISHED UNDER UNITED STATES GOVERNMENT CONTRACT No AF33(615)-1940. SHALL NOT BE EITHER RELEASED OUTSIDE THE GOVERNMENT, OR USED, DUPLICATED, OR DISCLOSED IN WHOLE OR IN PART FOR MANUFACTURE OR PROCUREMENT, WITHOUT THE WRITTEN PERMISSION OF CURTISS-WRIGHT CORPORATION, EXCEPT FOR (I) EMERGENCY REPAIR OR OVERHAUL WORK BY OR FOR THE GOVERNMENT, WHERE THE ITEM OR PROCESS IS NOT OTHERWISE RESONABLY AVAILABLE TO ENABLE TIMELY PERFORMANCE OF THE WORK; OR (II) RELEASE TO A FOREIGN GOVERNMENT, AS THE INTERESTS OF THE UNITED STATES MAY REQUIRE. PROVIDED THAT IN EITHER CASE THE RELEASE, USE, DUPLICATION OR DISCLOSURE HEREOF SHALL BE SUBJECT TO THE FOREGOING LIMITATIONS. THIS LEGEND SHALL BE MARKED ON ANY REPRODUCTION HEREOF IN WHOLE OR IN PART."

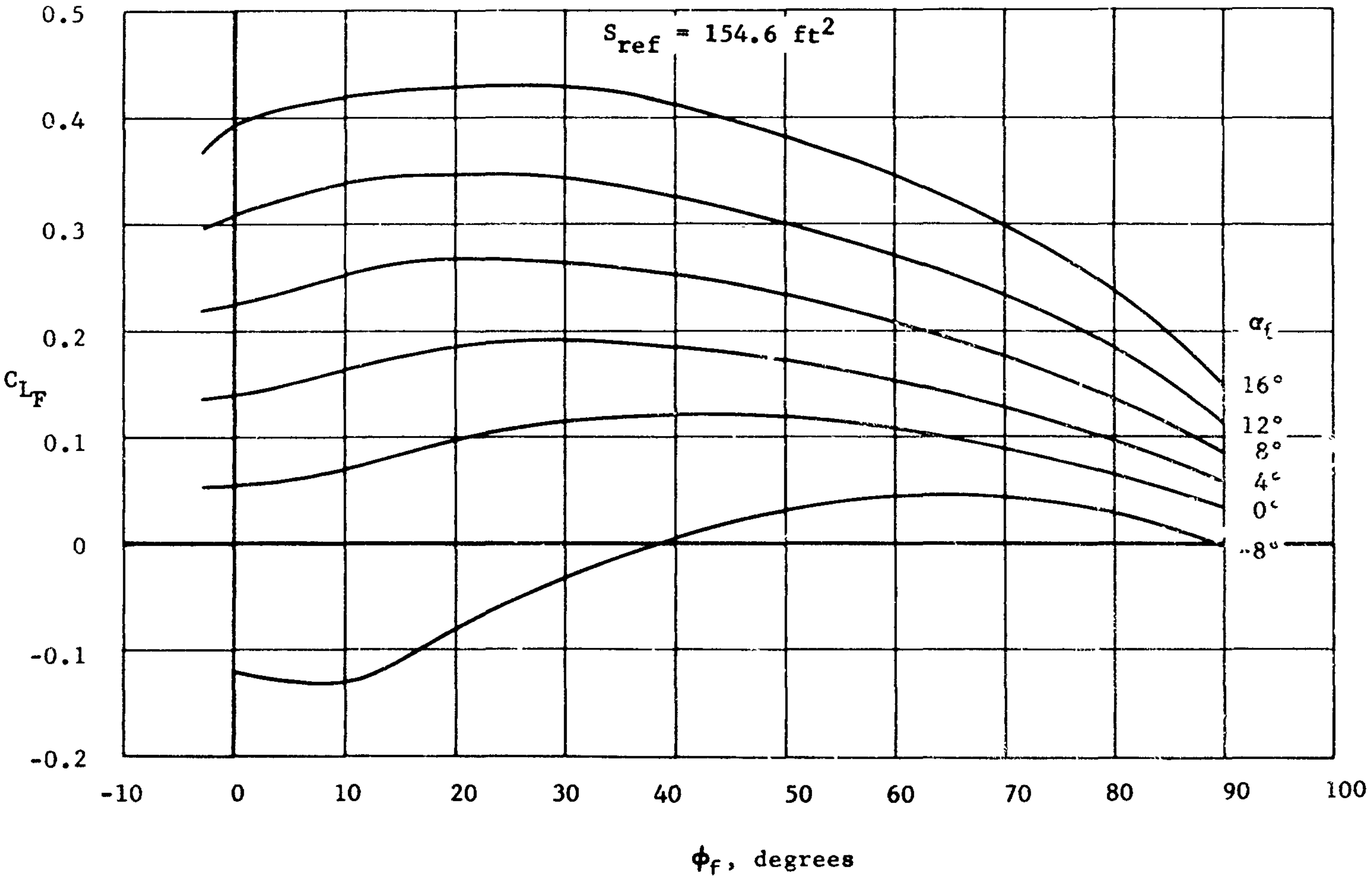

Figure 44. X-19, variation of front wing lift coefficient with nacelle tilt angle, propellers off.

"FURNISHED UNDER UNITED STATES GOVERNMENT CONTRACT No. AF33(615)-3940 SHALL NOT BE EITHER RELEASED OUTSIDE THE GOVERNMENT, OR USED, DUPLICATED, OR DISCLOSED IN WHOLE OR IN PART FOR MANUFACTURE OR PROCUREMENT, WITHOUT THE WRITTEN PERMISSION OF CURTISS-WRIGHT CORPORATION, EXCEPT FOR (I) EMERGENCY REPAIR OR OVERHAUL WORK BY OR FOR THE GOVERNMENT, WHERE THE ITEM OR PROCESS IS NOT OTHERWISE REASONABLY AVAILABLE TO ENABLE TIMELY PERFORMANCE OF THE WORK, OR (II) RELEASE TO A FOREIGN GOVERNMENT, AS THE INTERESTS OF THE UNITED STATES MAY REQUIRE, PROVIDED THAT IN EITHER CASE THE RELEASE, USE, DUPLICATION OR DISCLOSURE HEREOF SHALL BE SUBJECT TO THE FOREGOING LIMITATIONS. THIS LEGEND SHALL BE MARKED ON ANY REPRODUCTION HEREOF IN WHOLE OR IN PART."

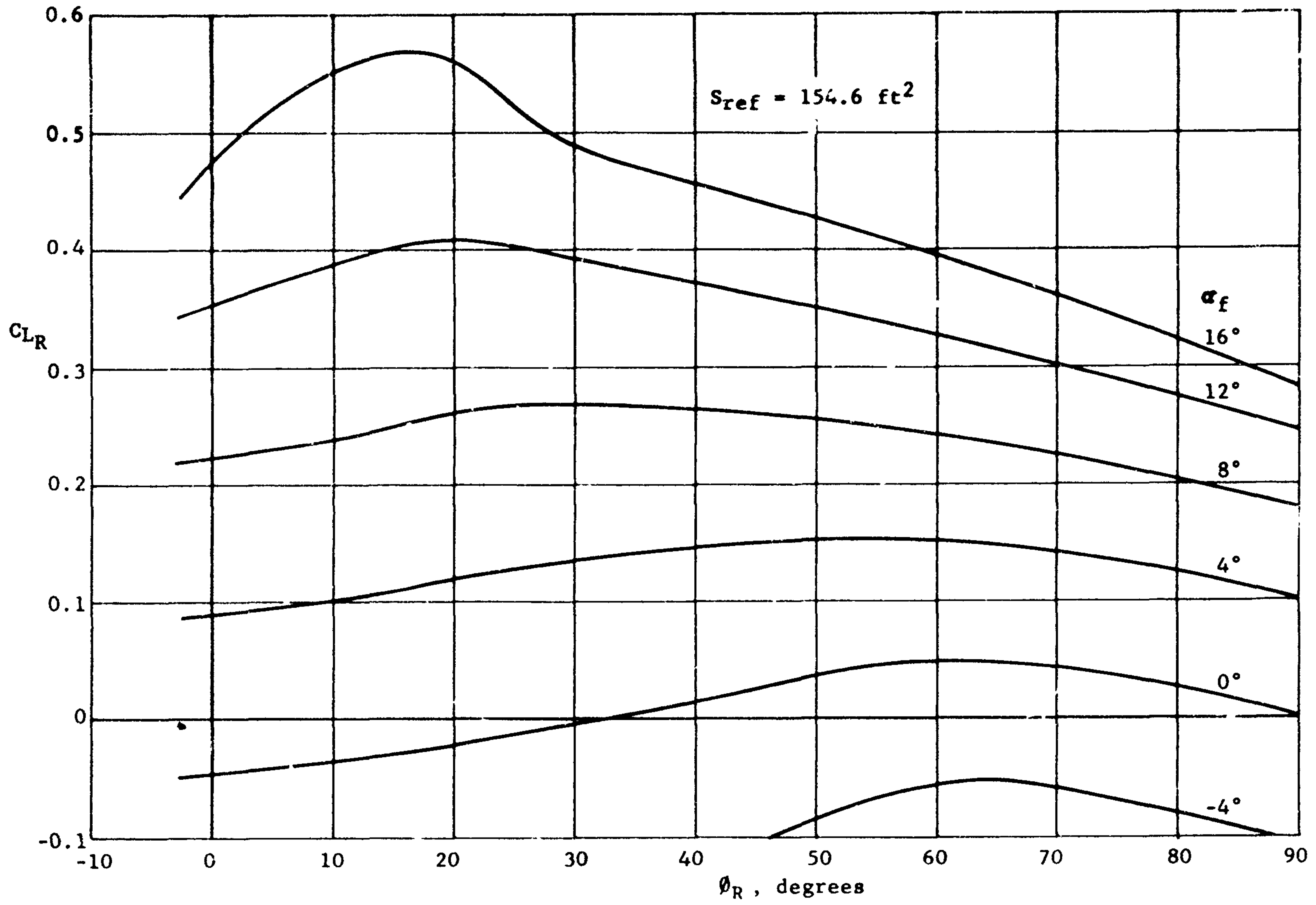

Figure 45. X-19, variation of rear wing lift coefficient with nacelle tilt angle, propellers off.

"FURNISHED UNDER UNITED STATES GOVERNMENT CONTRACT No AF33(615)-3940. SHALL NOT BE EITHER RELEASED OUTSIDE THE GOVERNMENT, OR USED, DUPLICATED, OR DISCLOSED IN WHOLE OR IN PART FOR MANUFACTURE OR PROCUREMENT, WITHOUT THE WRITTEN PERMISSION OF CURTISS-WRIGHT CORPORATION, EXCEPT FOR (I) EMERGENCY REPAIR OR OVERHAUL WORK BY OR FOR THE GOVERNMENT, WHERE THE ITEM OR PROCESS IS NOT OTHERWISE REASONABLY AVAILABLE TO ENABLE TIMELY PERFORMANCE OF THE WORK. OR (II) RELEASE TO A FOREIGN GOVERNMENT, AS THE INTERESTS OF THE UNITED STATES MAY REQUIRE. PROVIDED THAT IN EITHER CASE THE RELEASE, USE, DUPLICATION OR DISCLOSURE HEREOF SHALL BE SUBJECT TO THE FOREGOING LIMITATIONS. THIS LEGEND SHALL BE MARKED ON ANY REPRODUCTION HEREOF IN WHOLE OR IN PART."
]

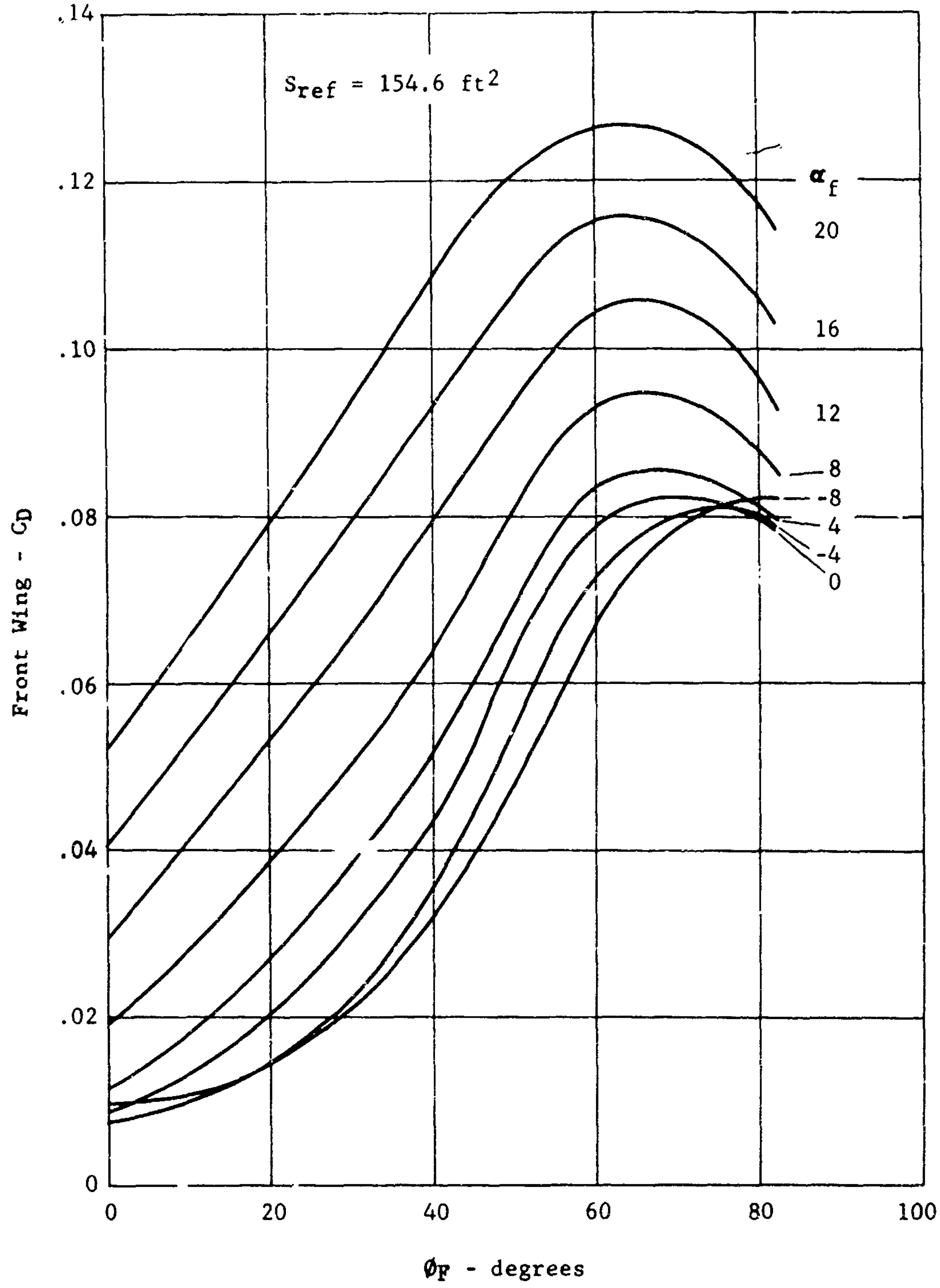

Figure 46. X-19, variation of front wing drag coefficient with nacelle tilt angle, propellers off.

"FURNISHED UNDER UNITED STATES GOVERNMENT CONTRACT No. AF33(615)-3940 SHALL NOT BE EITHER RELEASED OUTSIDE THE GOVERNMENT, OR USED, DUPLICATED, OR DISCLOSED IN WHOLE OR IN PART FOR MANUFACTURE OR PROCUREMENT, WITHOUT THE WRITTEN PERMISSION OF CURTISS-WRIGHT CORPORATION, EXCEPT FOR (1) EMERGENCY REPAIR OR OVERHAUL WORK BY OR FOR THE GOVERNMENT, WHERE THE ITEM OR PROCESS IS NOT OTHERWISE REASONABLY AVAILABLE TO ENABLE TIMELY PERFORMANCE OF THE WORK. OR (2) RELEASE TO A FOREIGN GOVERNMENT, AS THE INTERESTS OF THE UNITED STATES MAY REQUIRE. PROVIDED THAT IN EITHER CASE THE RELEASE, USE, DUPLICATION OR DISCLOSURE HEREOF SHALL BE SUBJECT TO THE FOREGOING LIMITATIONS. THIS LEGEND SHALL BE MARKED ON ANY REPRODUCTION HEREOF IN WHOLE OR IN PART."

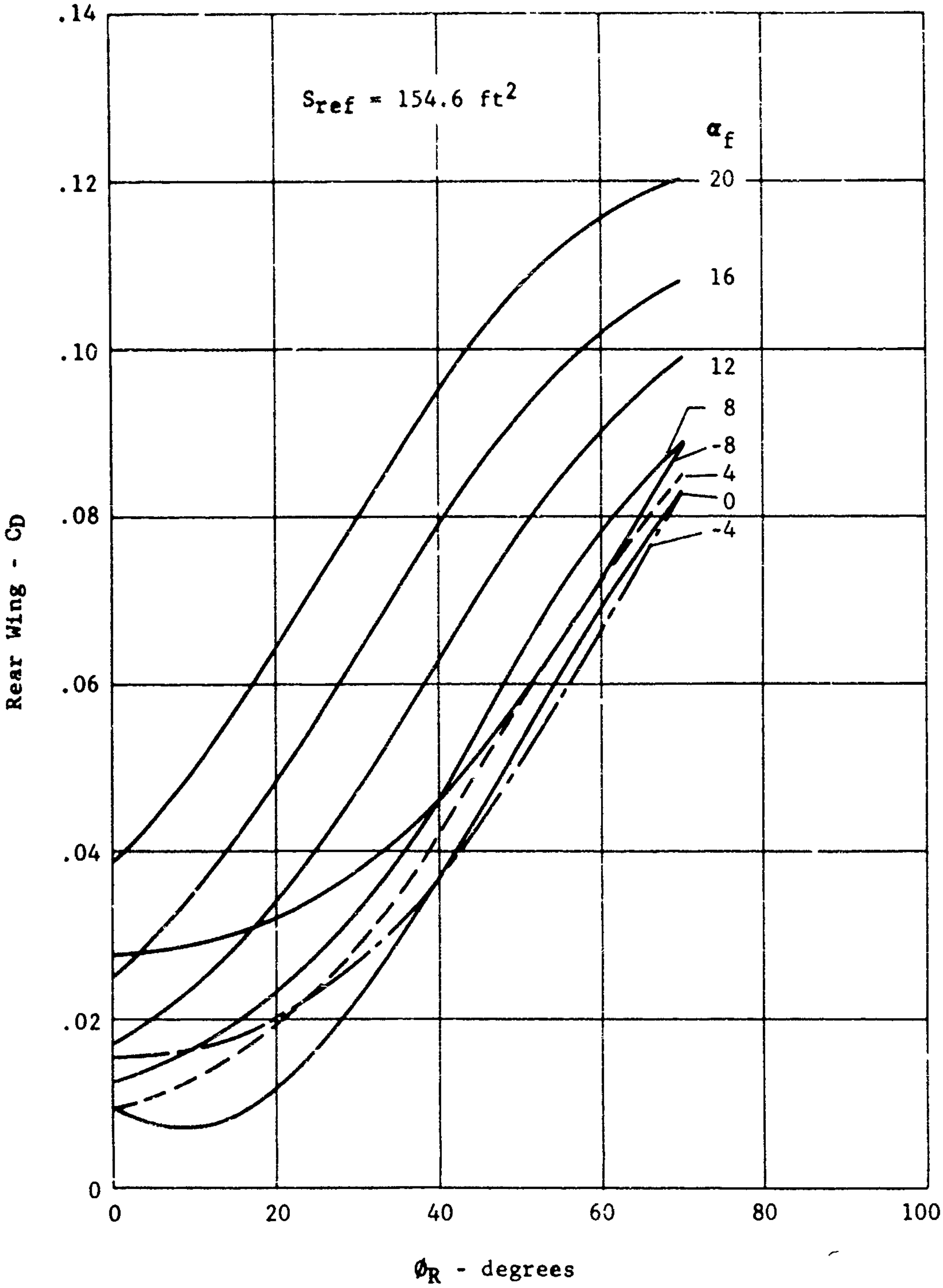

Figure 47. X-19, variation of rear wing drag coefficient with nacelle tilt angle, propellers off.

FURNISHED UNDER UNITED STATES GOVERNMENT CONTRACT No AF33(615)-1940 SHALL NOT BE EITHER RELEASED OUTSIDE THE GOVERNMENT, OR USED, DUPLICATED, OR DISCLOSED IN WHOLE OR IN PART FOR MANUFACTURE OR PROCUREMENT, WITHOUT THE WRITTEN PERMISSION OF CURTISS-WRIGHT CORPORATION EXCEPT FOR (I) EMERGENCY REPAIR OR OVERHAUL WORK BY OR FOR THE GOVERNMENT, WHERE THE ITEM OR PROCESS IS NOT OTHERWISE REASONABLY AVAILABLE TO ENABLE TIMELY PERFORMANCE OF THE WORK OR (II) RELEASE TO A FOREIGN GOVERNMENT, AS THE INTERESTS OF THE UNITED STATES MAY REQUIRE PROVIDED THAT IN EITHER CASE THE RELEASE, USE, DUPLICATION OR DISCLOSURE HEREOF SHALL BE SUBJECT TO THE FOREGOING LIMITATIONS. THIS LEGEND SHALL BE MARKED ON ANY REPRODUCTION HEREOF IN WHOLE OR IN PART."

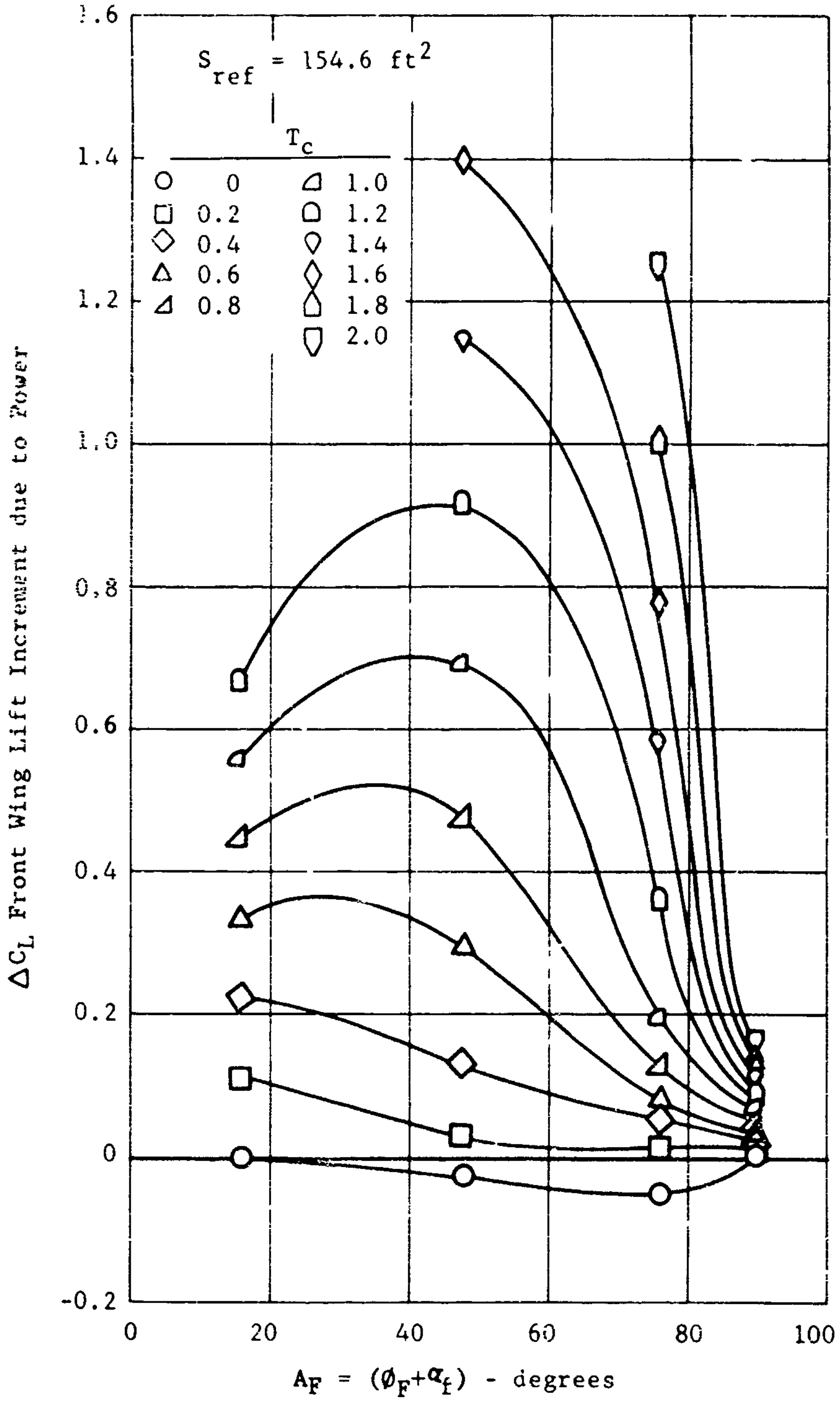

Figure 48. X-19, incremental front wing lift coefficient, due to front propeller wash, with variation in thrust axis angle of attack.

FURNISHED UNDER UNITED STATES GOVERNMENT CONTRACT No. AF33(615)-3940. SHALL NOT BE EITHER RELEASED OUTSIDE THE GOVERNMENT, OR USED, DUPLICATED, OR DISCLOSED IN WHOLE OR IN PART FOR MANUFACTURE OR PROCUREMENT, WITHOUT THE WRITTEN PERMISSION OF CURTISS-WRIGHT CORPORATION, EXCEPT FOR (i) EMERGENCY REPAIR OR OVERHAUL WORK BY OR FOR THE GOVERNMENT, WHERE THE ITEM OR PROCESS IS NOT OTHERWISE REASONABLY AVAILABLE TO ENABLE TIMELY PERFORMANCE OF THE WORK, OR (ii) RELEASE TO A FOREIGN GOVERNMENT, AS THE INTERESTS OF THE UNITED STATES MAY REQUIRE. PROVIDED THAT IN EITHER CASE THE RELEASE, USE, DUPLICATION OR DISCLOSURE HEREOF SHALL BE SUBJECT TO THE FOREGOING LIMITATIONS. THIS LEGEND SHALL BE MARKED ON ANY REPRODUCTION HEREOF IN WHOLE OR IN PART.

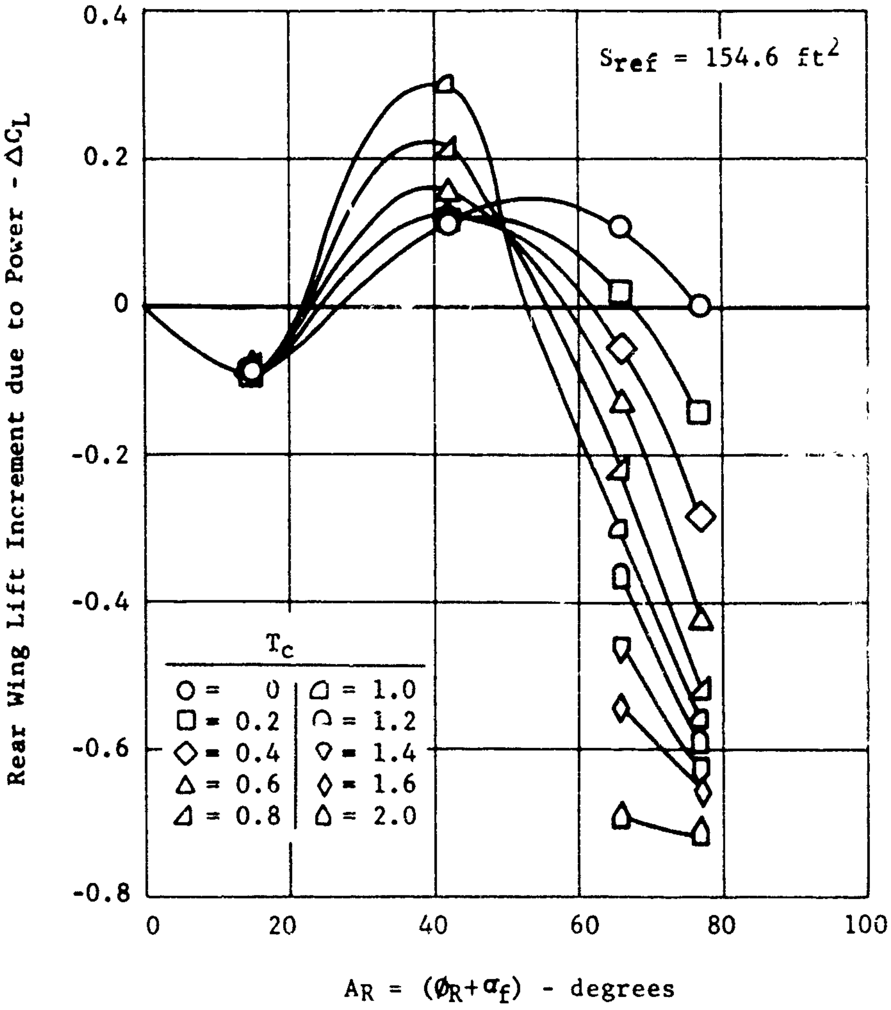

Figure 49. X-19, incremental rear wing lift coefficient, due to all wash, with variation in rear thrust axis angle of attack.

'FURNISHED UNDER UNITED STATES GOVERNMENT CONTRACT No. AF33(615)-3940. SHALL NOT BE EITHER RELEASED OUTSIDE THE GOVERNMENT, OR USED, DUPLICATED, OR DISCLOSED IN WHOLE OR IN PART FOR MANUFACTURE OR PROCUREMENT, WITHOUT THE WRITTEN PERMISSION OF CURTISS-WRIGHT CORPORATION, EXCEPT FOR (I) EMERGENCY REPAIR OR OVERHAUL WORK BY OR FOR THE GOVERNMENT, WHERE THE ITEM OR PROCESS IS NOT OTHERWISE REASONABLY AVAILABLE TO ENABLE TIMELY PERFORMANCE OF THE WORK, OR (II) RELEASE TO A FOREIGN GOVERNMENT, AS THE INTERESTS OF THE UNITED STATES MAY REQUIRE; PROVIDED THAT IN EITHER CASE THE RELEASE, USE, DUPLICATION OR DISCLOSURE HEREOF SHALL BE SUBJECT TO THE FOREGOING LIMITATIONS. THIS LEGEND SHALL BE MARKED ON ANY REPRODUCTION HEREOF IN WHOLE OR IN PART.'

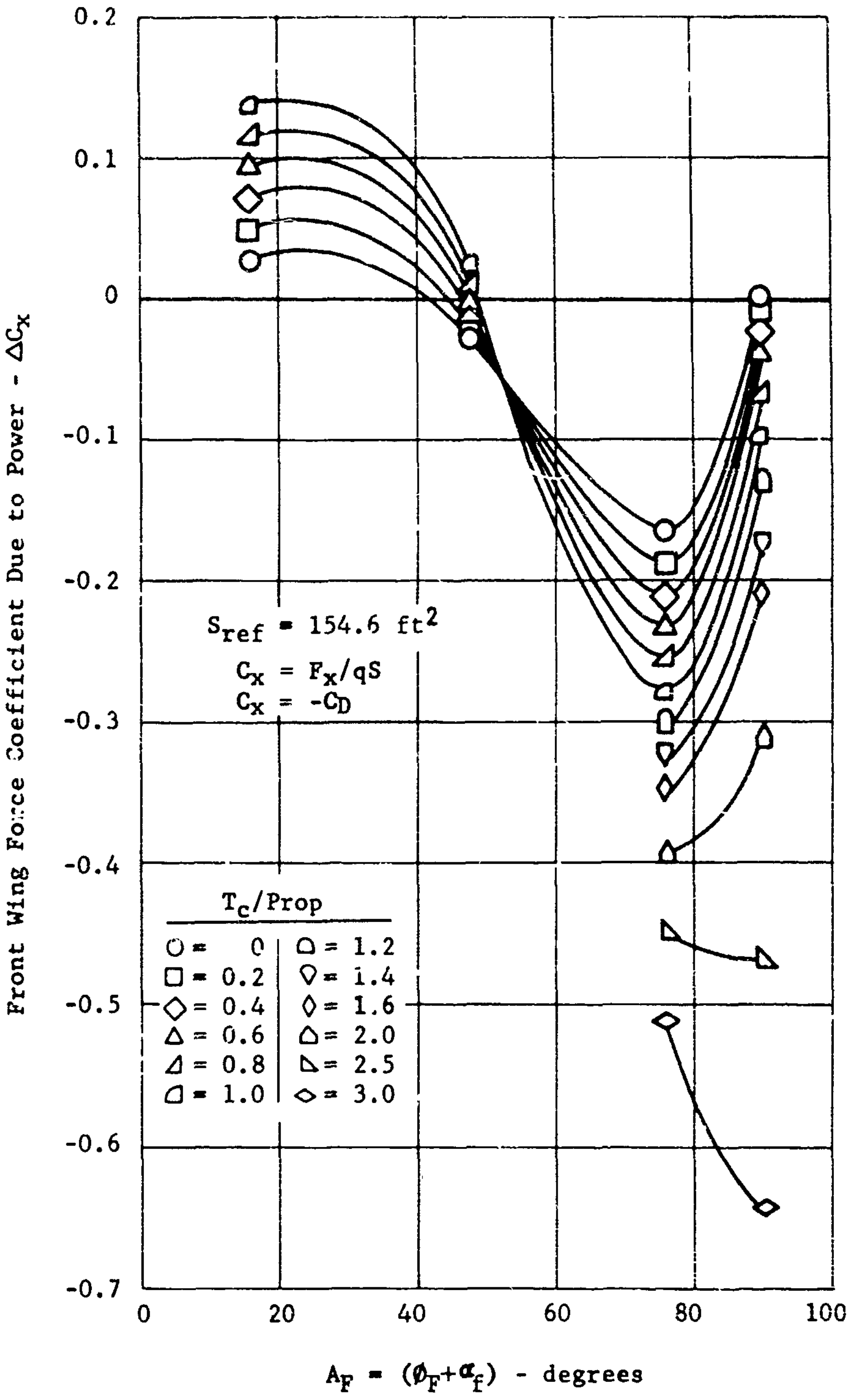

Figure 50. X-19, incremental front wing thrust coefficient, due to front propeller wash, with variation in thrust axis angle of attack.

FURNISHED UNDER UNITED STATES GOVERNMENT CONTRACT No. AF33(615)-3940. SHALL NOT BE EITHER RELEASED OUTSIDE THE GOVERNMENT, OR USED DUPLICATED, OR DISCLOSED IN WHOLE OR IN PART FOR MANUFACTURE OR PROCUREMENT, WITHOUT THE WRITTEN PERMISSION OF CURTISS-WRIGHT CORPORATION, EXCEPT FOR (I) EMERGENCY REPAIR OR OVERHAUL WORK BY OR FOR THE GOVERNMENT, WHERE THE ITEM OR PROCESS IS NOT OTHERWISE REASONABLY AVAILABLE TO ENABLE TIMELY PERFORMANCE OF THE WORK OR (II) RELEASE TO A FOREIGN GOVERNMENT, AS THE INTERESTS OF THE UNITED STATES MAY REQUIRE PROVIDED THAT IN EITHER CASE THE RELEASE, USE, DUPLICATION OR DISCLOSURE HEREOF SHALL BE SUBJECT TO THE FOREGOING LIMITATIONS. THIS LEGEND SHALL BE MARKED ON ANY REPRODUCTION HEREOF IN WHOLE OR IN PART."

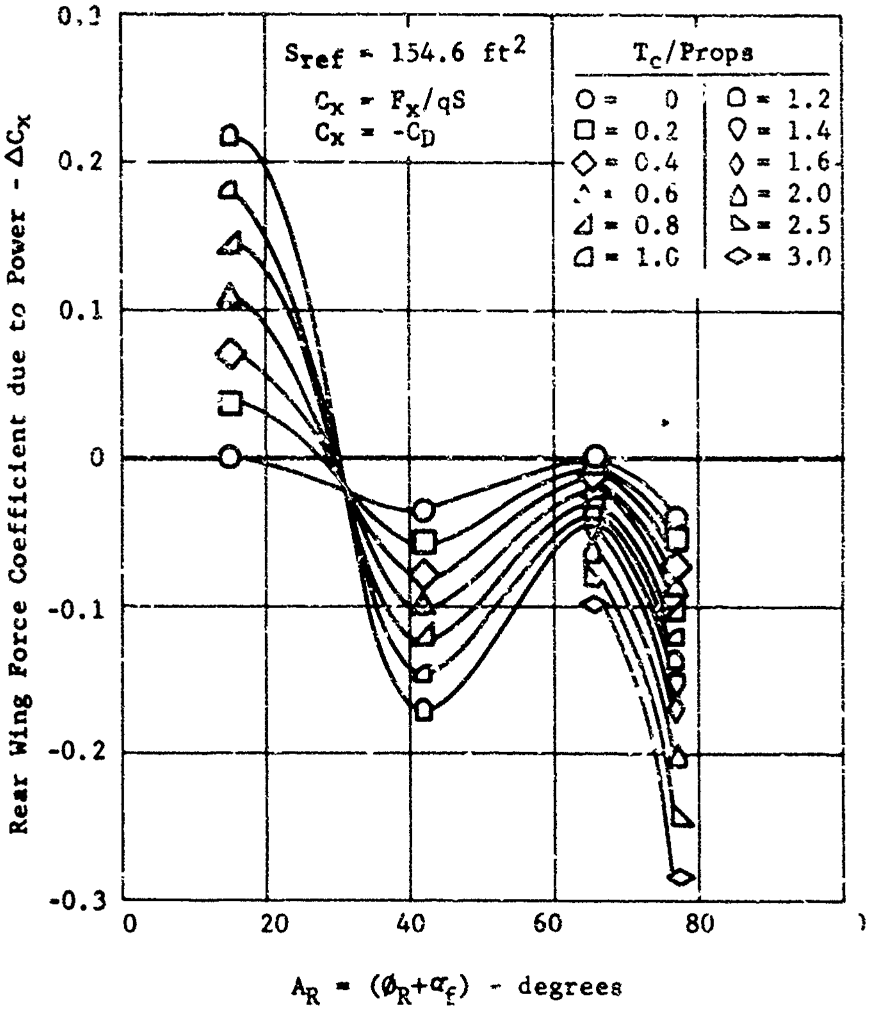

Figure 51. X-19, incremental rear wing thrust coefficient, due to all wash, with variation in rear thrust axis angle of attack.

"FURNISHED UNDER UNITED STATES GOVERNMENT CONTRACT No. AF33(615)-1940. SHALL NOT BE EITHER RELEASED OUTSIDE THE GOVERNMENT, OR USED, DUPLICATED, OR DISCLOSED IN WHOLE OR IN PART FOR MANUFACTURE OR PROCUREMENT, WITHOUT THE WRITTEN PERMISSION OF CURTISS-WRIGHT CORPORATION, EXCEPT FOR (I) EMERGENCY REPAIR OR OVERHAUL WORK BY OR FOR THE GOVERNMENT, WHERE THE ITEM OR PROCESS IS NOT OTHERWISE REASONABLY AVAILABLE TO ENABLE TIMELY PERFORMANCE OF THE WORK; OR (II) RELEASE TO A FOREIGN GOVERNMENT, AS THE INTERESTS OF THE UNITED STATES MAY REQUIRE; PROVIDED THAT IN EITHER CASE THE RELEASE, USE, DUPLICATION OR DISCLOSURE HEREOF SHALL BE SUBJECT TO THE FOREGOING LIMITATIONS. THIS LEGEND SHALL BE MARKED ON ANY REPRODUCTION HEREOF IN WHOLE OR IN PART."

The additional Figures 52 through 65 display both C_L vs α_f and spanwise lift distributions on the rear wing as functions of tilt angle and advance ratio. These curves have been prepared from pressure data extracted from (15). Figure 57 provides a check point against Figure 49. For example at $\phi_R = 16.9^{\circ}$, $\alpha_f = 0^{\circ}$, (Figure 57) the $\Delta C_L \approx -0.06$ due to power effects. Figure 49 would show a $\Delta C_L \simeq -0.07$ at $(\phi_R + \alpha_f) = 17^{\circ}$.

b. Wings and Propellers in Ground Effect

Figures 66 through 69 have been included to demonstrate the influence of the ground on the propellers. As the propeller blade angles are constant throughout this range of tests one finds that power absorption is influenced by the ground presence. At J's of 0.12 and 0.325, the front and rear propellers absorb less power as the ground is approached. At J = 0.54 however, a reversal occurs and the propellers absorb more power in the ground presence. A study of this phenomenon has not been pursued. However, it is believed to be related to the general inclination of the wake.

The general loading of the front propellers and unloading of the rear propellers with increasing angle of attack should be noted. This effect has been observed as well at tilt angles lower than the hover values for which these curves are plotted. Additionally a sharp increase in thrust and power on the rear propellers above angles of attack of twelve degrees was evidenced. Again, it is hypothesized that the rear propellers are passing beneath the main core of the front wake. The aircraft stability is expected to increase in this vicinity. This, in fact, is the case. Ground presence does not appear to alter the trend.

As the blade angles are held constant throughout the range of α_{fus} and J, a condition prevails which is equivalent to fixed collective pitch as well as stick position. It is obvious that total power, and its distribution, do not remain constant throughout even the α_{fus} range. To fully define the picture it would be necessary to run a range of collective and differential blade angles so that lines of constant power and stick deflection could be defined. Unfortunately, this was not within the scope of the test data. One additional comment is made concerning the thrust data; it does not always appear consistent with the power data. The tendency has been to favor the power data and to regard the thrust intercepts with suspicion. This problem has consistently reared itself throughout the testing, and serves to illustrate the caution required in data interpretation.

No data have been accumulated to determine the influence of ground

FURNISHED UNDER UNITED STATES GOVERNMENT CONTRACT No. AF33(615)-3940. SHALL NOT BE EITHER RELEASED OUTSIDE THE GOVERNMENT, OR USED, DUPLICATED OR DISCLOSED IN WHOLE OR IN PART FOR MANUFACTURE OR PROCUREMENT WITHOUT THE WRITTEN PERMISSION OF CURTISS-WRIGHT CORPORATION, EXCEPT FOR (I) EMERGENCY REPAIR OR OVERHAUL WORK BY OR FOR THE GOVERNMENT, WHERE THE ITEM OR PROCESS IS NOT OTHERWISE REASONABLY AVAILABLE TO ENABLE TIMELY PERFORMANCE OF THE WORK, OR (II) RELEASE TO A FOREIGN GOVERNMENT, AS THE INTERESTS OF THE UNITED STATES MAY REQUIRE, PROVIDED THAT IN EITHER CASE THE RELEASE, USE, DUPLICATION OR DISCLOSURE HEREOF SHALL BE SUBJECT TO THE FOREGOING LIMITATIONS. THIS LEGEND SHALL BE MARKED ON ANY REPRODUCTION HEREOF IN WHOLE OR IN PART.'

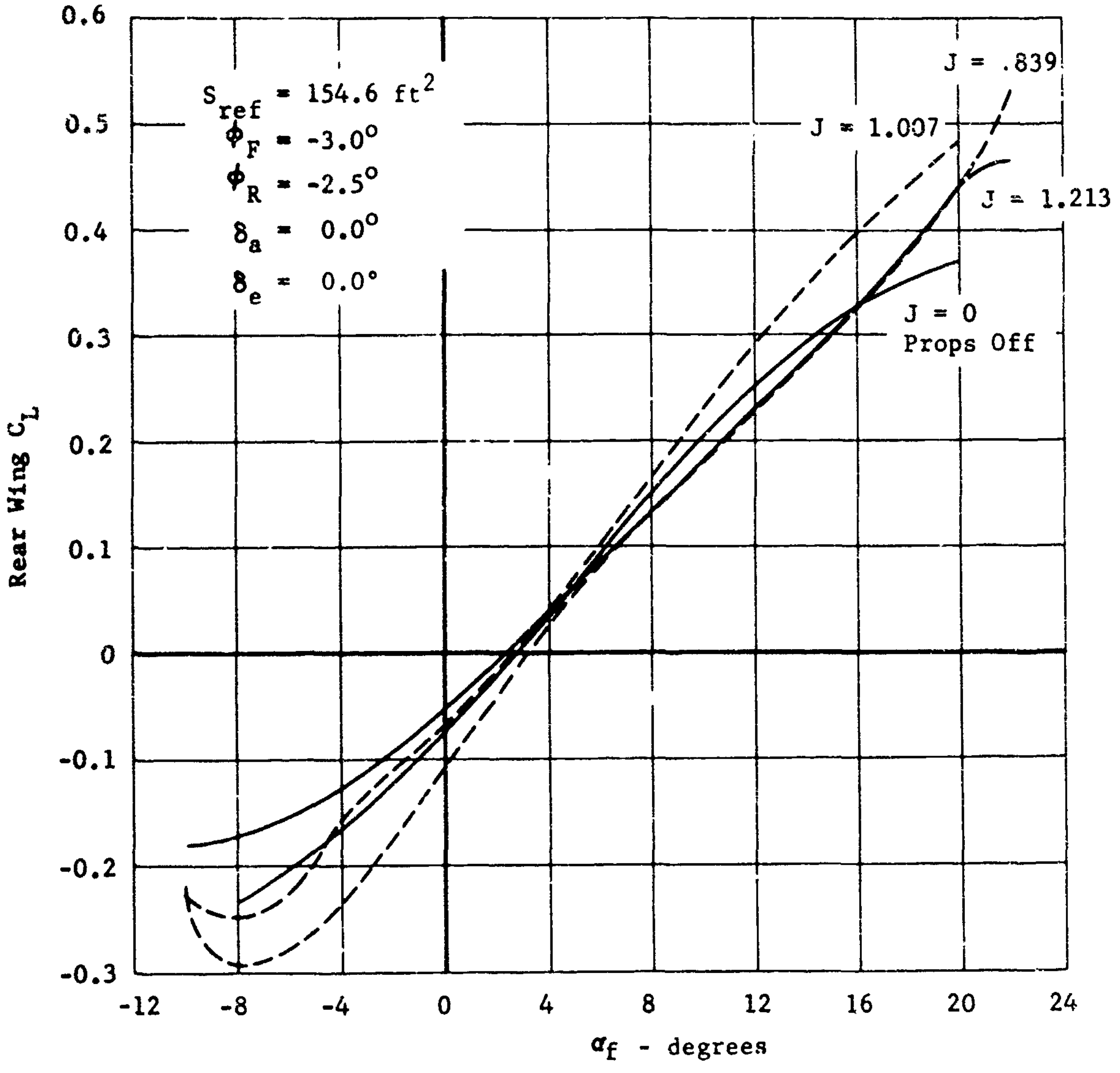

Figure 52. X-19, installed rear wing lift curve.

FURNISHED UNDER UNITED STATES GOVERNMENT CONTRACT No. AF33(615)-3940 SHALL NOT BE EITHER RELEASED OUTSIDE THE GOVERNMENT, OR USED, DUPLICATED, OR DISCLOSED IN WHOLE OR IN PART FOR MANUFACTURE OR PROCUREMENT, WITHOUT THE WRITTEN PERMISSION OF CURTISS-WRIGHT CORPORATION EXCEPT FOR (I) EMERGENCY REPAIR OR OVERHAUL WORK BY OR FOR THE GOVERNMENT, WHERE THE ITEM OR PROCESS IS NOT OTHERWISE REASONABLY AVAILABLE TO ENABLE TIMELY PERFORMANCE OF THE WORK OR (II) RELEASE TO A FOREIGN GOVERNMENT, AS THE INTERESTS OF THE UNITED STATES MAY REQUIRE PROVIDED THAT IN EITHER CASE THE RELEASE, USE, DUPLICATION OR DISCLOSURE HEREOF SHALL BE SUBJECT TO THE FOREGOING LIMITATIONS. THIS LEGEND SHALL BE MARKED ON ANY REPRODUCTION HEREOF IN WHOLE OR IN PART."

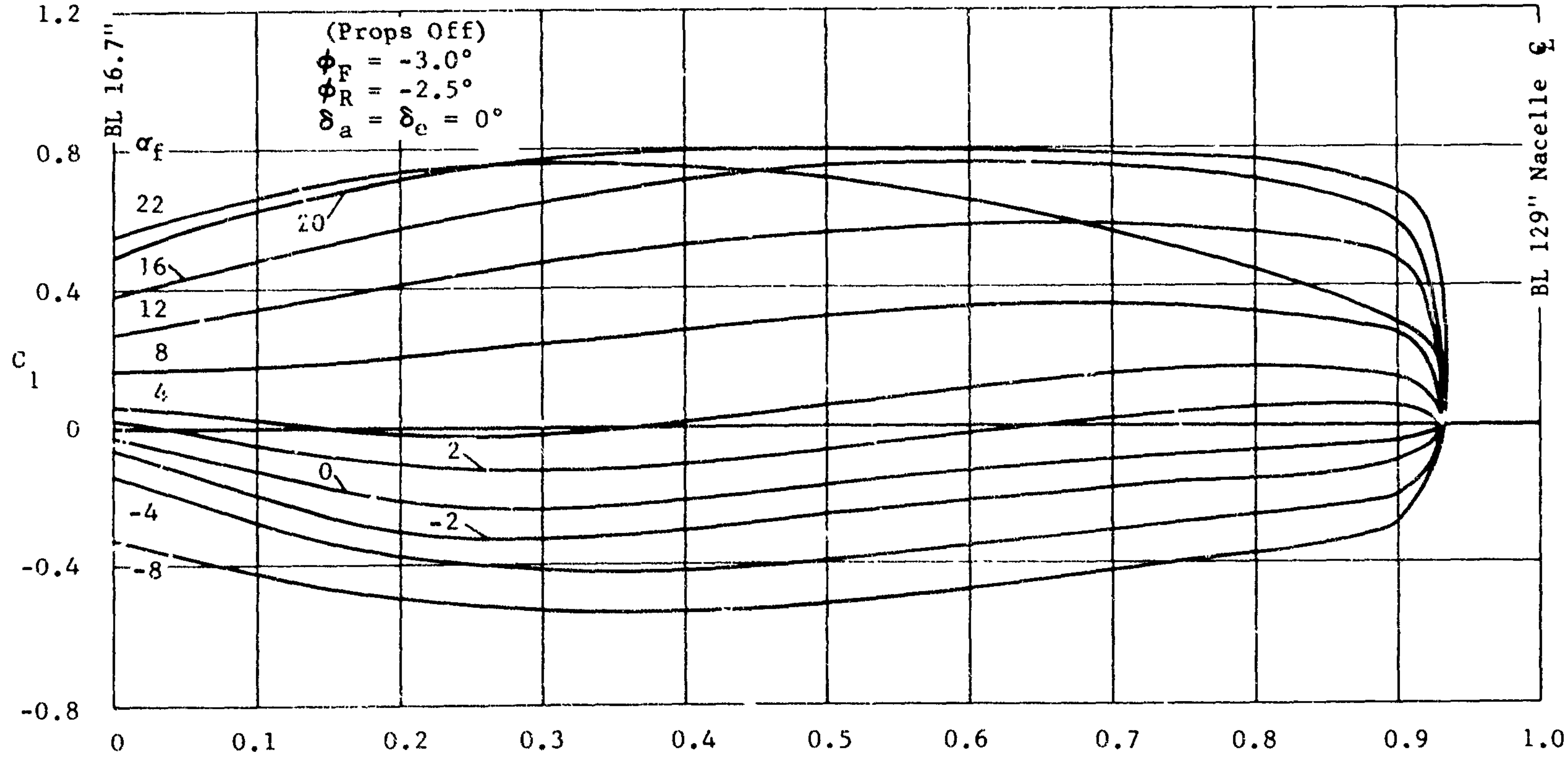

Figure 53. X-19, installed rear wing spanwise lift distribution, propellers off.

FURNISHED UNDER UNITED STATES GOVERNMENT CONTRACT No. AF33(615)-3940 SHALL NOT BE EITHER RELEASED OUTSIDE THE GOVERNMENT OR USED, DUPLICATED, OR DISCLOSED IN WHOLE OR IN PART FOR MANUFACTURE OR PROCUREMENT, WITHOUT THE WRITTEN PERMISSION OF CURTISS-WRIGHT CORPORATION, EXCEPT FOR (I) EMERGENCY REPAIR OR OVERHAUL WORK BY OR FOR THE GOVERNMENT, WHERE THE ITEM OR PROCESS IS NOT OTHERWISE REASONABLY AVAILABLE TO ENABLE TIMELY PERFORMANCE OF THE WORK OR (II) RELEASE TO A FOREIGN GOVERNMENT, AS THE INTERESTS OF THE UNITED STATES MAY REQUIRE PROVIDED THAT IN EITHER CASE THE RELEASE, USE, DUPLICATION OR DISCLOSURE HEREOF SHALL BE SUBJECT TO THE FOREGOING LIMITATIONS THIS LEGEND SHALL BE MARKED ON ANY REPRODUCTION HEREOF IN WHOLE OR IN PART "

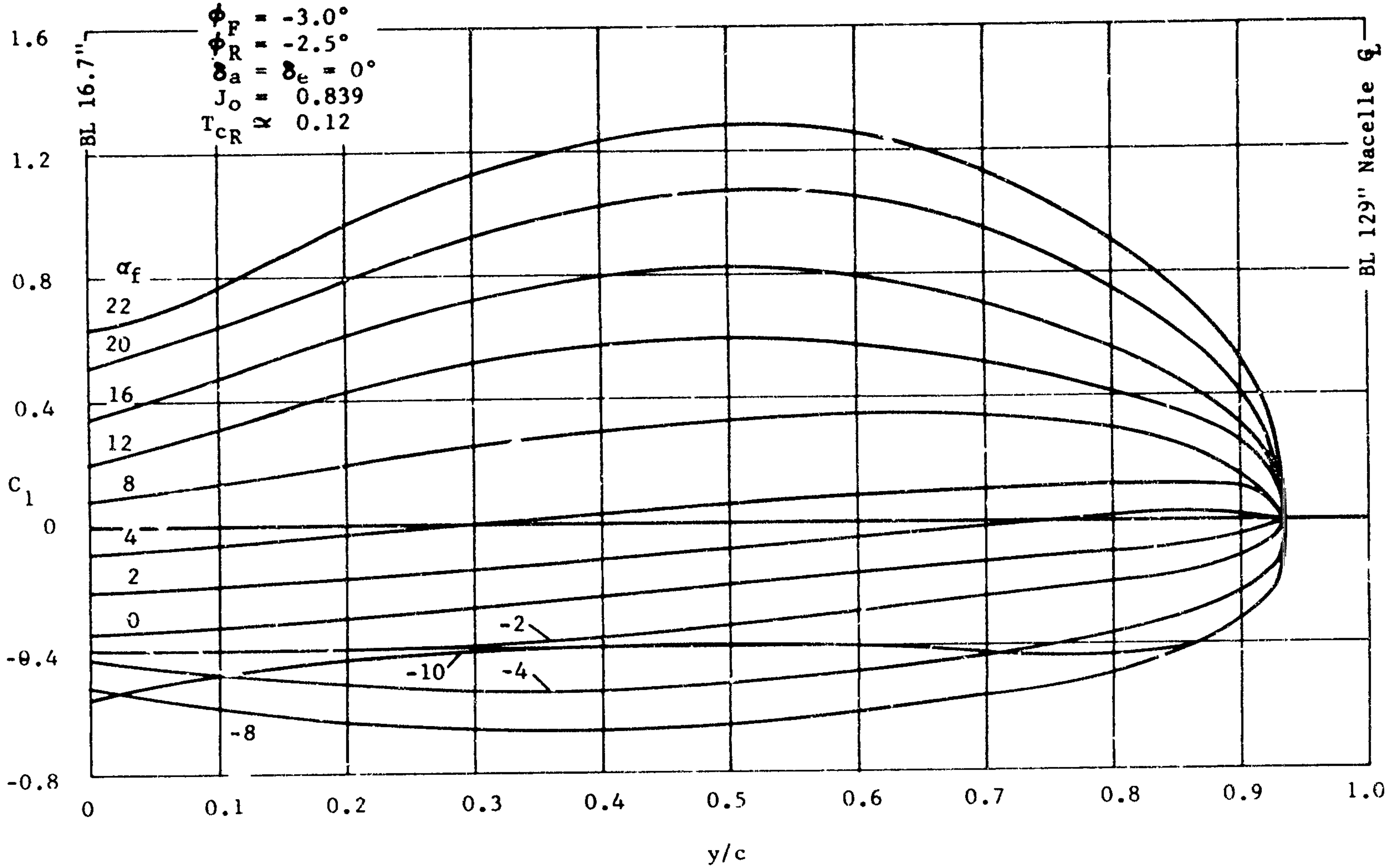

Figure 54. X-19, installed rear wing spanwise lift distribution propellers on.

"FURNISHED UNDER UNITED STATES GOVERNMENT CONTRACT No. AF33(615)-3940. SHALL NOT BE EITHER RELEASED OUTSIDE THE GOVERNMENT, OR USED, DUPLICATED, OR DISCLOSED IN WHOLE OR IN PART FOR MANUFACTURE OR PROCUREMENT, WITHOUT THE WRITTEN PERMISSION OF CURTISS-WRIGHT CORPORATION, EXCEPT FOR (I) EMERGENCY REPAIR OR OVERHAUL WORK BY OR FOR THE GOVERNMENT, WHERE THE ITEM OR PROCESS IS NOT OTHERWISE REASONABLY AVAILABLE TO ENABLE TIMELY PERFORMANCE OF THE WORK, OR (II) RELEASE TO A FOREIGN GOVERNMENT, AS THE INTERESTS OF THE UNITED STATES MAY REQUIRE; PROVIDED THAT IN EITHER CASE THE RELEASE, USE, DUPLICATION OR DISCLOSURE HEREOF SHALL BE SUBJECT TO THE FOREGOING LIMITATIONS. THIS LEGEND SHALL BE MARKED ON ANY REPRODUCTION HEREOF IN WHOLE OR IN PART."

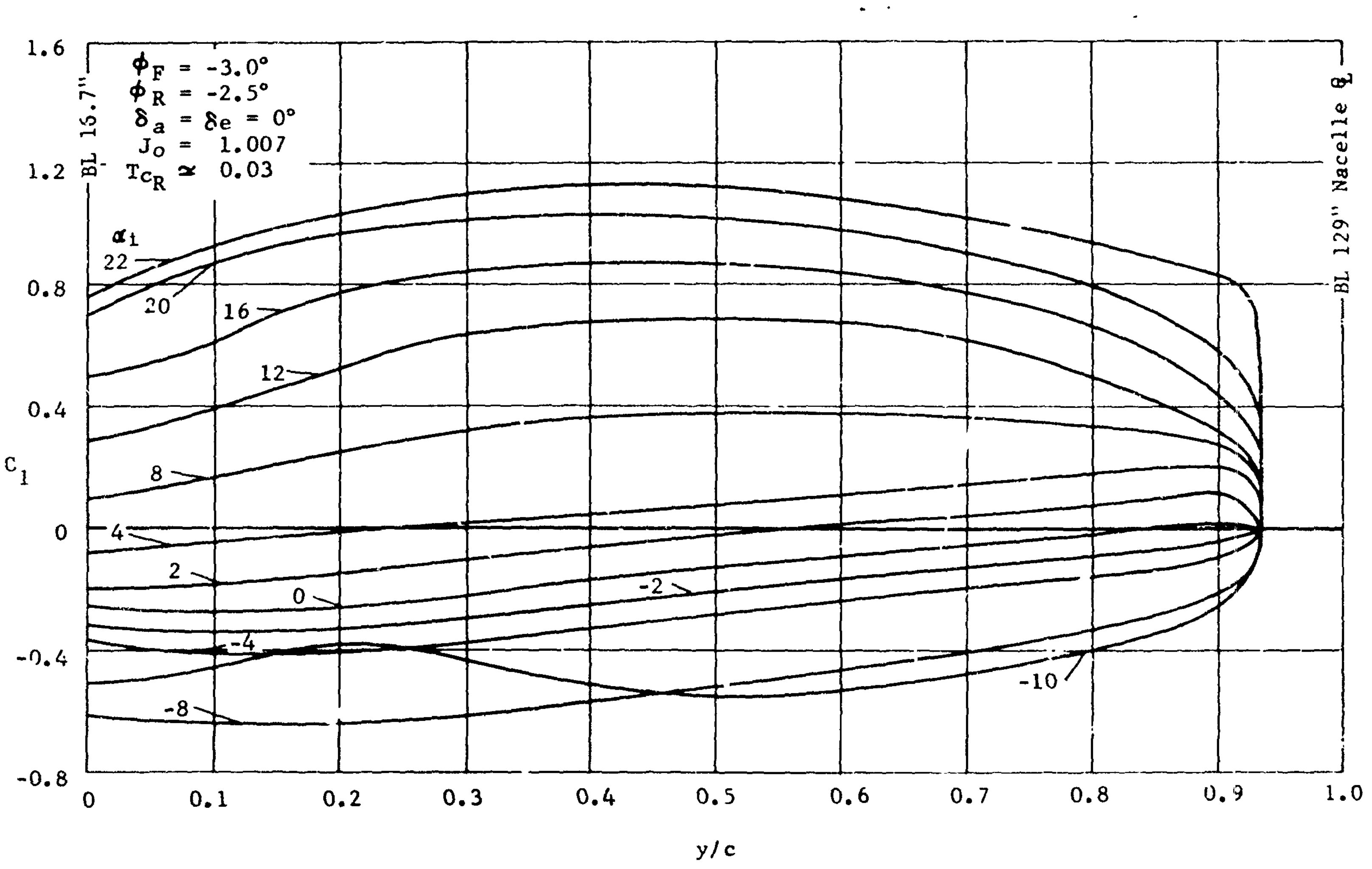

Figure 55. X-19, installed rear wing spanwise lift distribution propellers on.

FURNISHED UNDER UNITED STATES GOVERNMENT CONTRACT No. AF33(615)-3940. SHALL NOT BE EITHER RELEASED OUTSIDE THE GOVERNMENT, OR USED, DUPLICATED, OR DISCLOSED IN WHOLE OR IN PART FOR MANUFACTURE OR PROCUREMENT, WITHOUT THE WRITTEN PERMISSION OF CURTISS-WRIGHT CORPORATION, EXCEPT FOR (i) EMERGENCY REPAIR OR OVERHAUL WORK BY OR FOR THE GOVERNMENT WHERE THE ITEM OR PROCESS IS NOT OTHERWISE REASONABLY AVAILABLE TO ENABLE TIMELY PERFORMANCE OF THE WORK OR (ii) RELEASE TO A FOREIGN GOVERNMENT, AS THE INTERESTS OF THE UNITED STATES MAY REQUIRE. PROVIDED THAT IN EITHER CASE THE RELEASE, USE, DUPLICATION OR DISCLOSURE HEREOF SHALL BE SUBJECT TO THE FOREGOING LIMITATIONS. THIS LEGEND SHALL BE MARKED ON ANY REPRODUCTION HEREOF IN WHOLE OR IN PART.

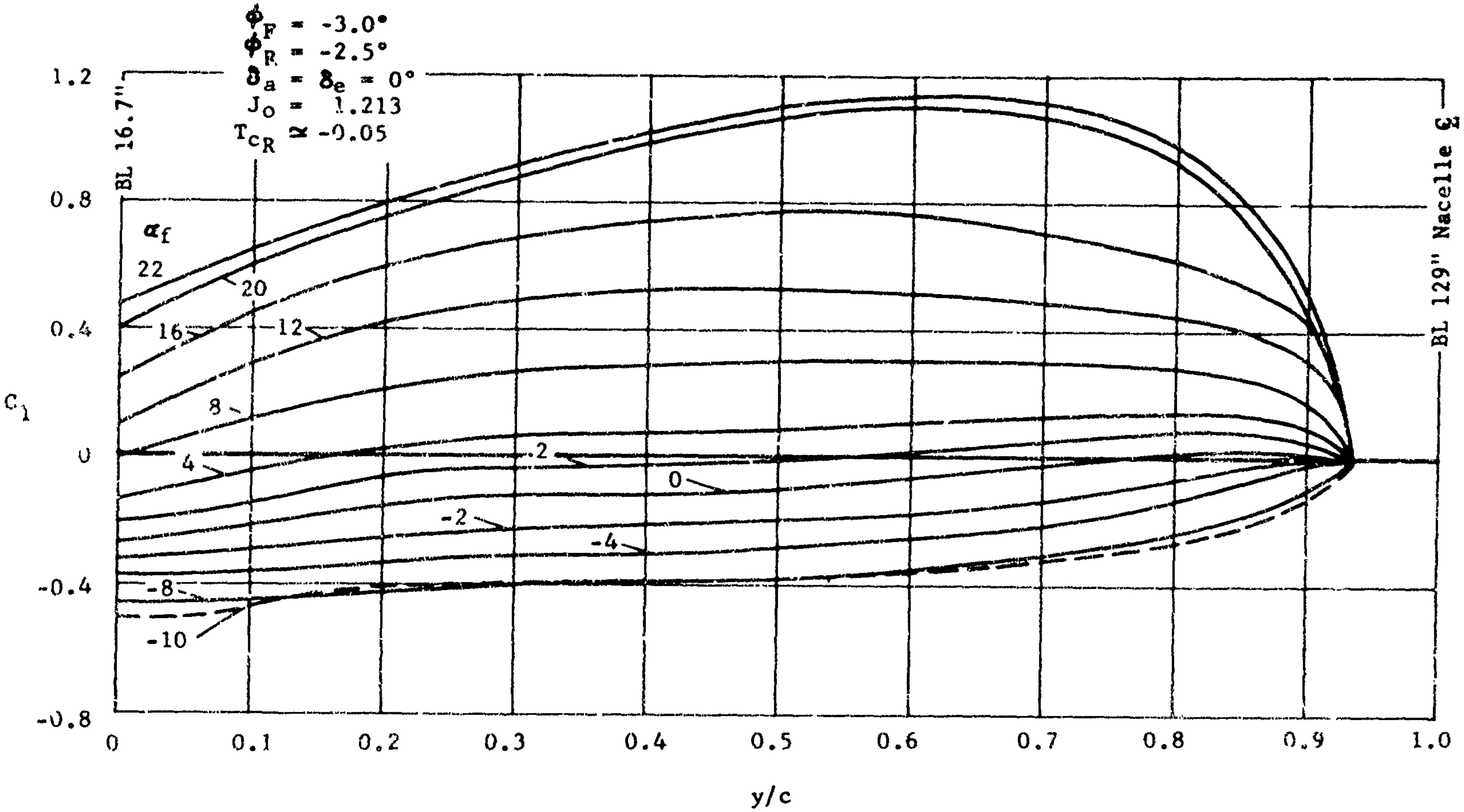

Figure 56. X-19, installed rear wing spanwise lift distribution.

FURNISHED UNDER UNITED STATES GOVERNMENT CONTRACT No. AF33(615)-1946 SHALL NOT BE EITHER RELEASED OUTSIDE THE GOVERNMENT, OR USED, DUPLICATED, OR DISCLOSED IN WHOLE OR IN PART FOR MANUFACTURE OR PROCUREMENT, WITHOUT THE WRITTEN PERMISSION OF CURTISS-WRIGHT CORPORATION, EXCEPT FOR (I) EMERGENCY REPAIR OR OVERHAUL WORK BY OR FOR THE GOVERNMENT, WHERE THE ITEM OR PROCESS IS NOT OTHERWISE REASONABLY AVAILABLE TO ENABLE TIMELY PERFORMANCE OF THE WORK, OR (II) RELEASE TO A FOREIGN GOVERNMENT, AS THE INTERESTS OF THE UNITED STATES MAY REQUIRE; PROVIDED THAT IN EITHER CASE THE RELEASE, USE, DUPLICATION OR DISCLOSURE HEREOF SHALL BE SUBJECT TO THE FOREGOING LIMITATIONS. THIS LEGEND SHALL BE MARKED ON ANY REPRODUCTION HEREOF IN WHOLE OR IN PART."

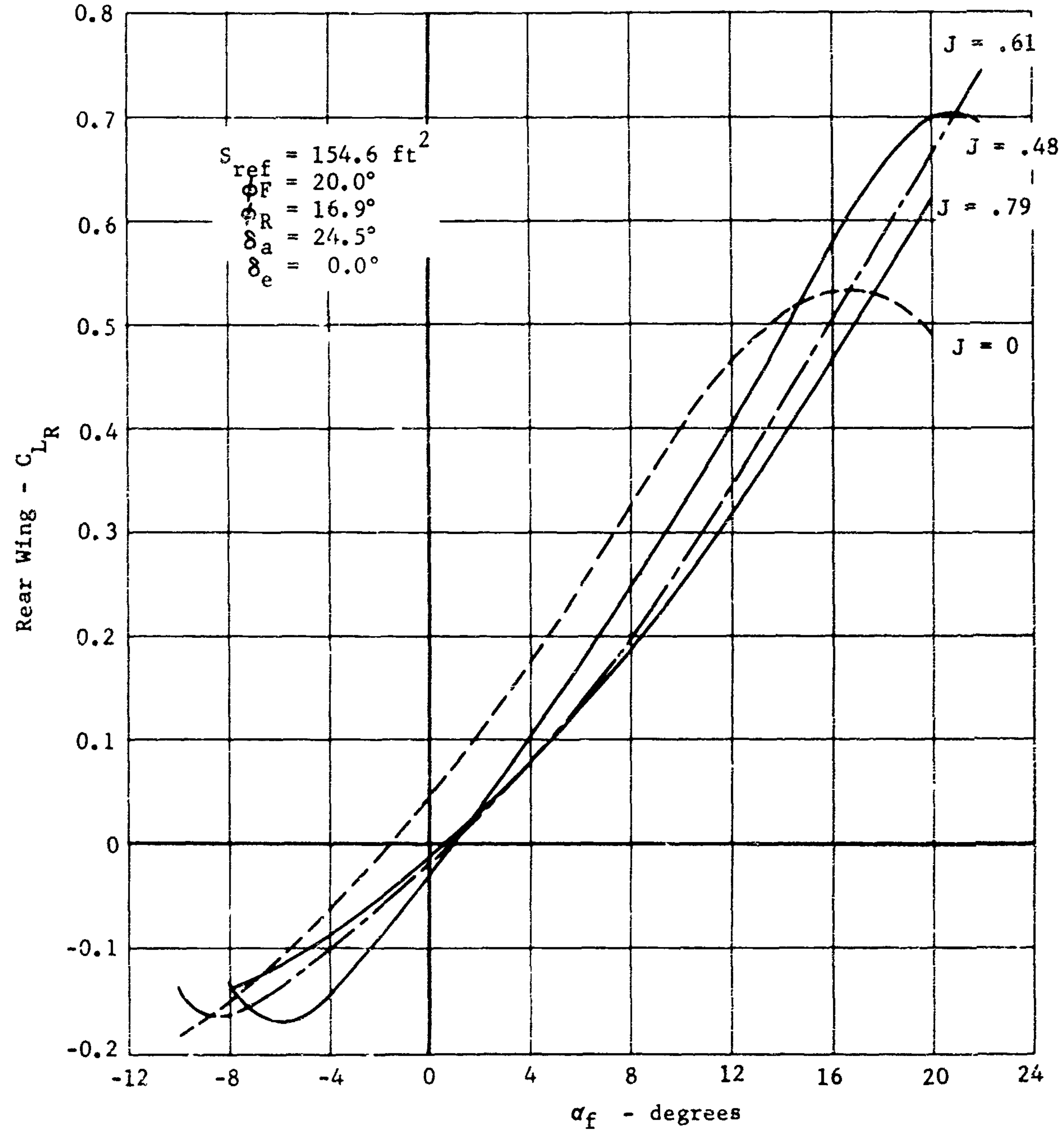

Figure 57. X-19, installed rear wing lift curve.

FURNISHED UNDER UNITED STATES GOVERNMENT CONTRACT No. AF33(615)-3940. SHALL NOT BE EITHER RELEASED OUTSIDE THE GOVERNMENT, OR USED, DUPLICATED, OR DISCLOSED IN WHOLE OR IN PART FOR MANUFACTURE OR PROCUREMENT, WITHOUT THE WRITTEN PERMISSION OF CURTISS-WRIGHT CORPORATION, EXCEPT FOR (I) EMERGENCY REPAIR OR OVERHAUL WORK BY OR FOR THE GOVERNMENT, WHERE THE ITEM OR PROCESS IS NOT OTHERWISE REASONABLY AVAILABLE TO ENABLE TIMELY PERFORMANCE OF THE WORK, OR (II) RELEASE TO A FOREIGN GOVERNMENT, AS THE INTERESTS OF THE UNITED STATES MAY REQUIRE; PROVIDED THAT IN EITHER CASE THE RELEASE, USE, DUPLICATION OR DISCLOSURE HEREOF SHALL BE SUBJECT TO THE FOREGOING LIMITATIONS. THIS LEGEND SHALL BE MARKED ON ANY REPRODUCTION HEREOF IN WHOLE OR IN PART."

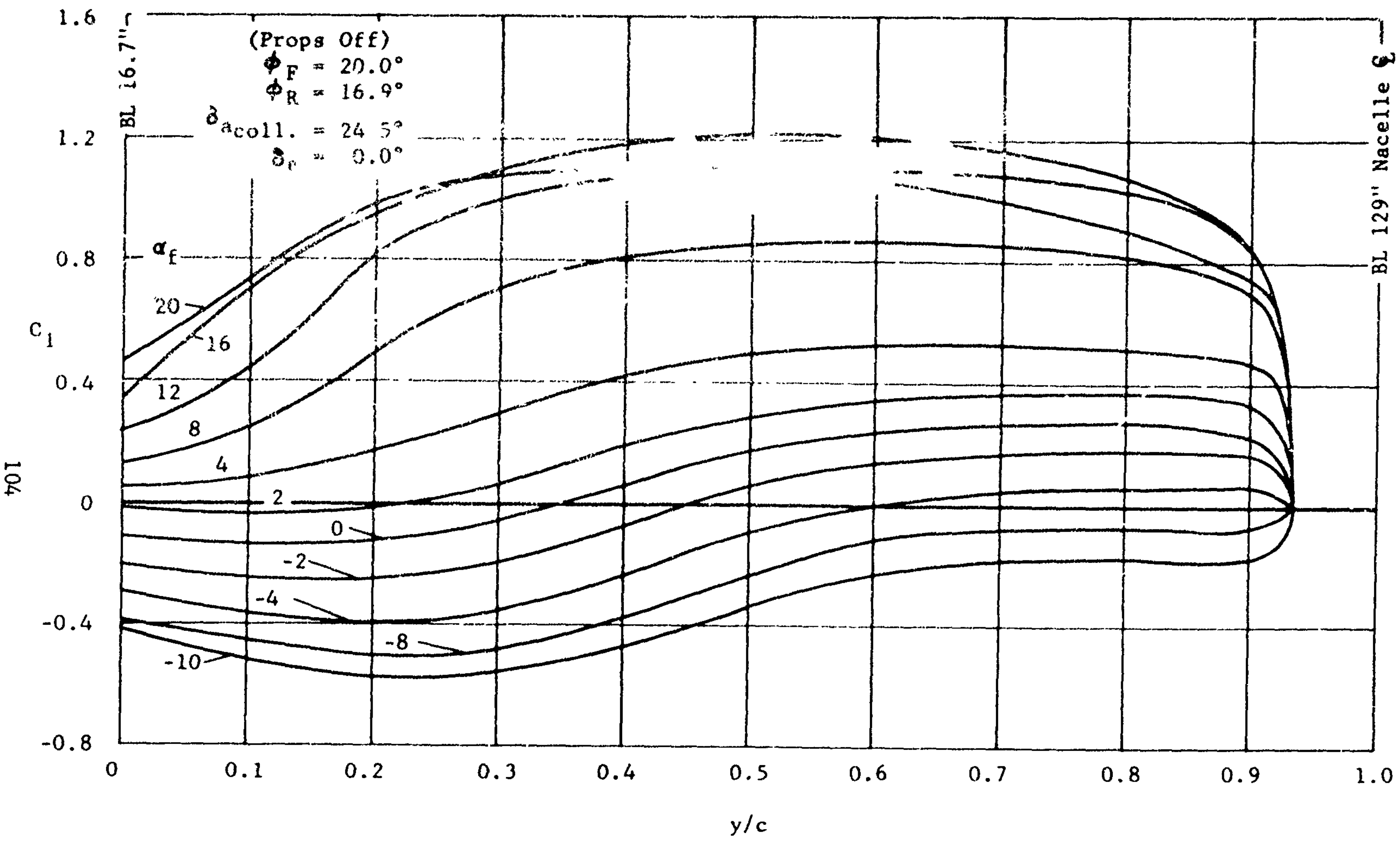

Figure 58. X-19, installed rear wing spanwise lift distribution, propellers off.

"FURNISHED UNDER UNITED STATES GOVERNMENT CONTRACT No. AF33(657)-1940. SHALL NOT BE EITHER RELEASED OUTSIDE THE GOVERNMENT, OR USED, DUPLICATED, OR DISCLOSED IN WHOLE OR IN PART FOR MANUFACTURE OR PROCUREMENT, WITHOUT THE WRITTEN PERMISSION OF CURTISS-WRIGHT CORPORATION, EXCEPT FOR (I) EMERGENCY REPAIR OR OVERHAUL WORK BY OR FOR THE GOVERNMENT, WHERE THE ITEM OR PROCESS IS NOT OTHERWISE REASONABLY AVAILABLE TO ENABLE TIMELY PERFORMANCE OF THE WORK, OR (II) RELEASE TO A FOREIGN GOVERNMENT, AS THE INTERESTS OF THE UNITED STATES MAY REQUIRE; PROVIDED THAT IN EITHER CASE THE RELEASE, USE, DUPLICATION OR DISCLOSURE HEREOF SHALL BE SUBJECT TO THE FOREGOING LIMITATIONS. THIS LEGEND SHALL BE MARKED ON ANY REPRODUCTION HEREOF IN WHOLE OR IN PART."

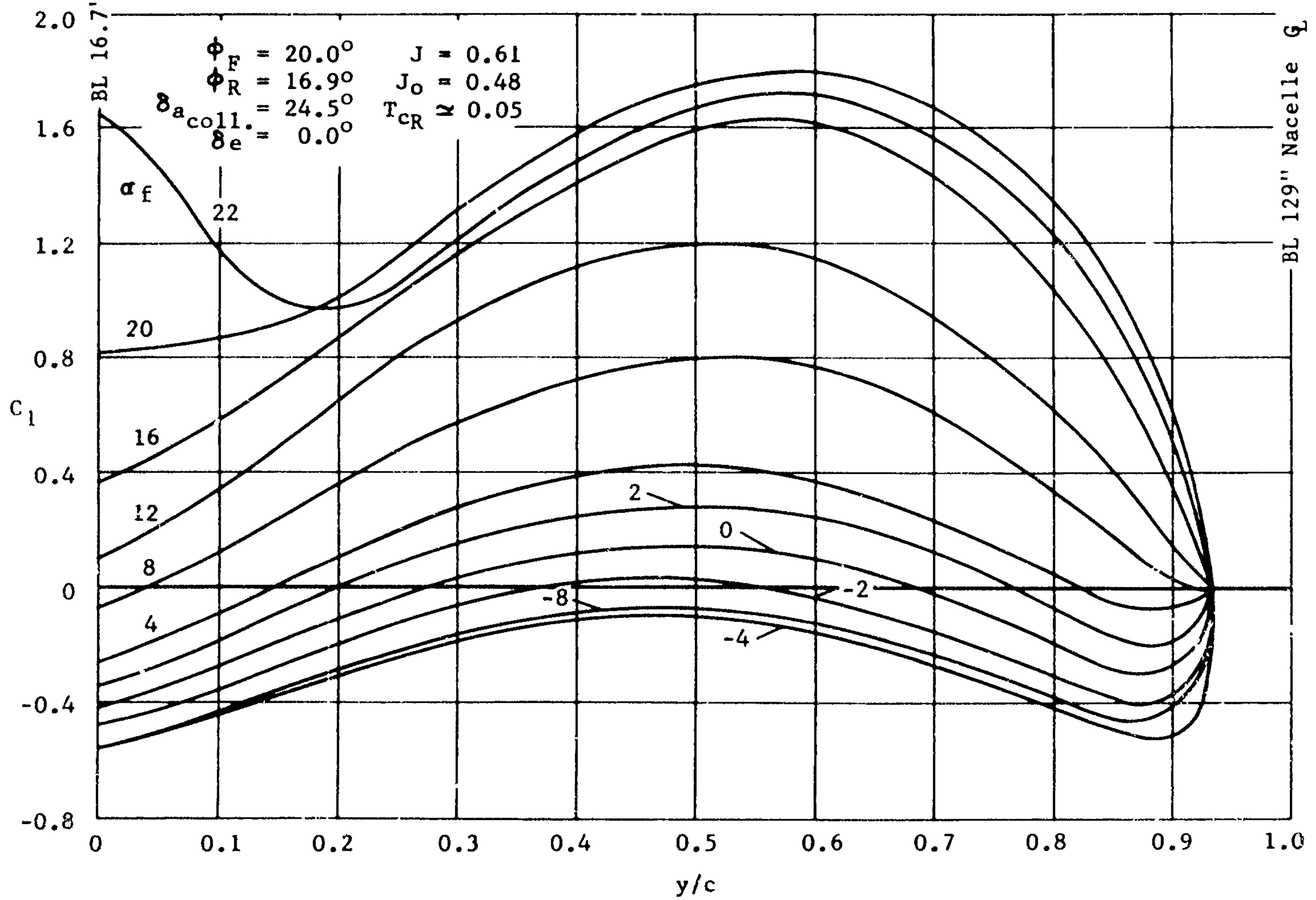

Figure 59. X-19, installed rear wing spanwise lift distribution.

"FURNISHED UNDER UNITED STATES GOVERNMENT CONTRACT No. AF33(615)-3940. SHALL NOT BE EITHER RELEASED OUTSIDE THE GOVERNMENT, OR USED, DUPLICATED, OR DISCLOSED IN WHOLE OR IN PART FOR MANUFACTURE OR PROCUREMENT, WITHOUT THE WRITTEN PERMISSION OF CURTISS-WRIGHT CORPORATION EXCEPT FOR (i) EMERGENCY REPAIR OR OVERHAUL WORK BY OR FOR THE GOVERNMENT, WHERE THE ITEM OR PROCESS IS NOT OTHERWISE REASONABLY AVAILABLE TO ENABLE TIMELY PERFORMANCE OF THE WORK, OR (ii) RELEASE TO A FOREIGN GOVERNMENT, AS THE INTERESTS OF THE UNITED STATES MAY REQUIRE. PROVIDED THAT IN EITHER CASE THE RELEASE, USE, DUPLICATION OR DISCLOSURE HEREOF SHALL BE SUBJECT TO THE FOREGOING LIMITATIONS. THIS LEGEND SHALL BE MARKED ON ANY REPRODUCTION HEREOF IN WHOLE OR IN PART."

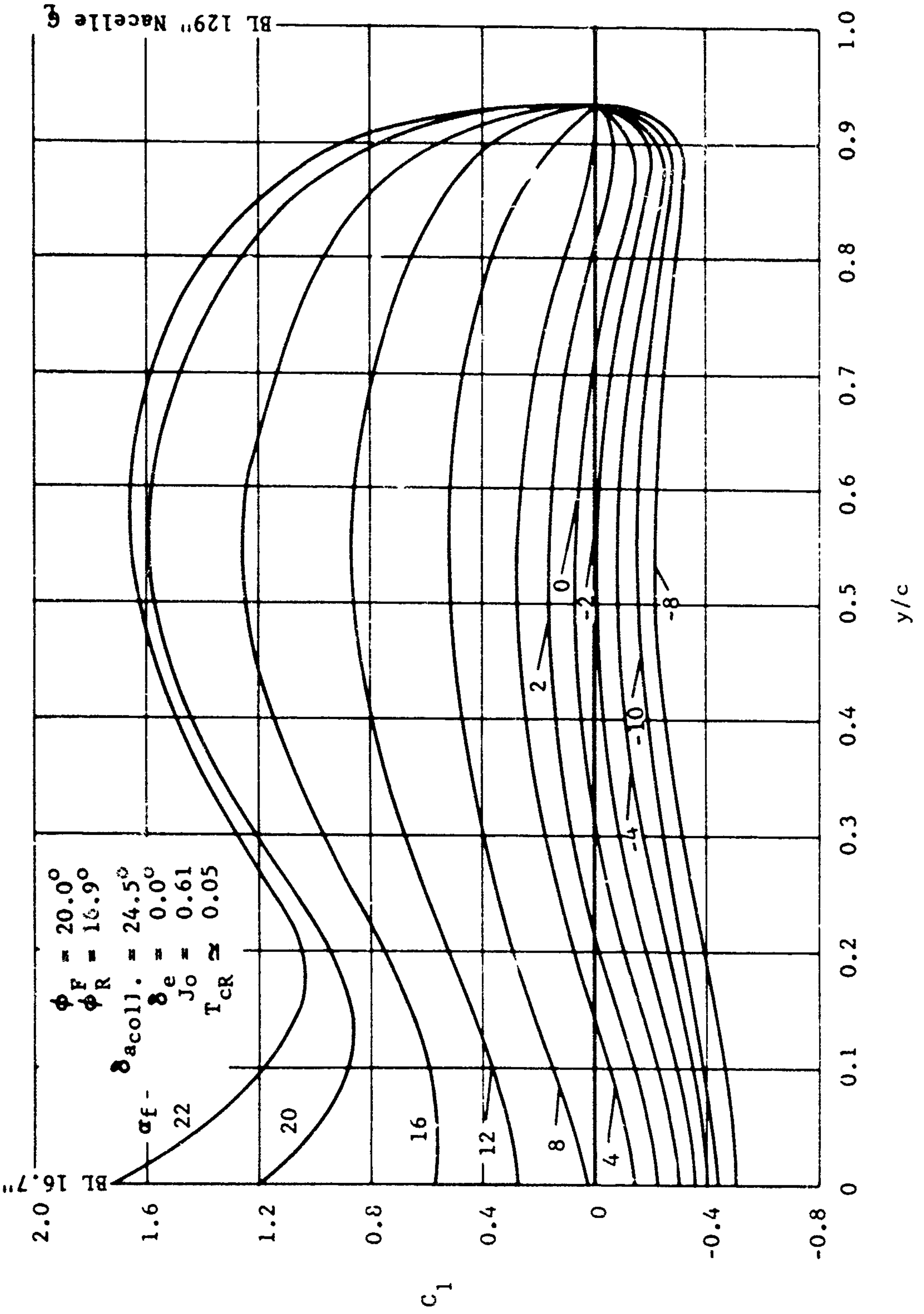

Figure 60. X-19, installed rear wing spanwise lift distribution.

FURNISHED UNDER UNITED STATES GOVERNMENT CONTRACT No. AF33(657)-3940. SHALL NOT BE EITHER RELEASED OUTSIDE THE GOVERNMENT, OR USED, DUPLICATED, OR DISCLOSED IN WHOLE OR IN PART FOR MANUFACTURE OR PROCUREMENT, WITHOUT THE WRITTEN PERMISSION OF CURTISS-WRIGHT CORPORATION, EXCEPT FOR (I) EMERGENCY REPAIR OR OVERHAUL WORK BY OR FOR THE GOVERNMENT, WHERE THE ITEM OR PROCESS IS NOT OTHERWISE REASONABLY AVAILABLE TO ENABLE TIMELY PERFORMANCE OF THE WORK, OR (II) RELEASE TO A FOREIGN GOVERNMENT, AS THE INTERESTS OF THE UNITED STATES MAY REQUIRE; PROVIDED THAT IN EITHER CASE THE RELEASE, USE, DUPLICATION OR DISCLOSURE HEREOF SHALL BE SUBJECT TO THE FOREGOING LIMITATION. THIS LEGEND SHALL BE MARKED ON ANY REPRODUCTION HEREOF IN WHOLE OR IN PART.

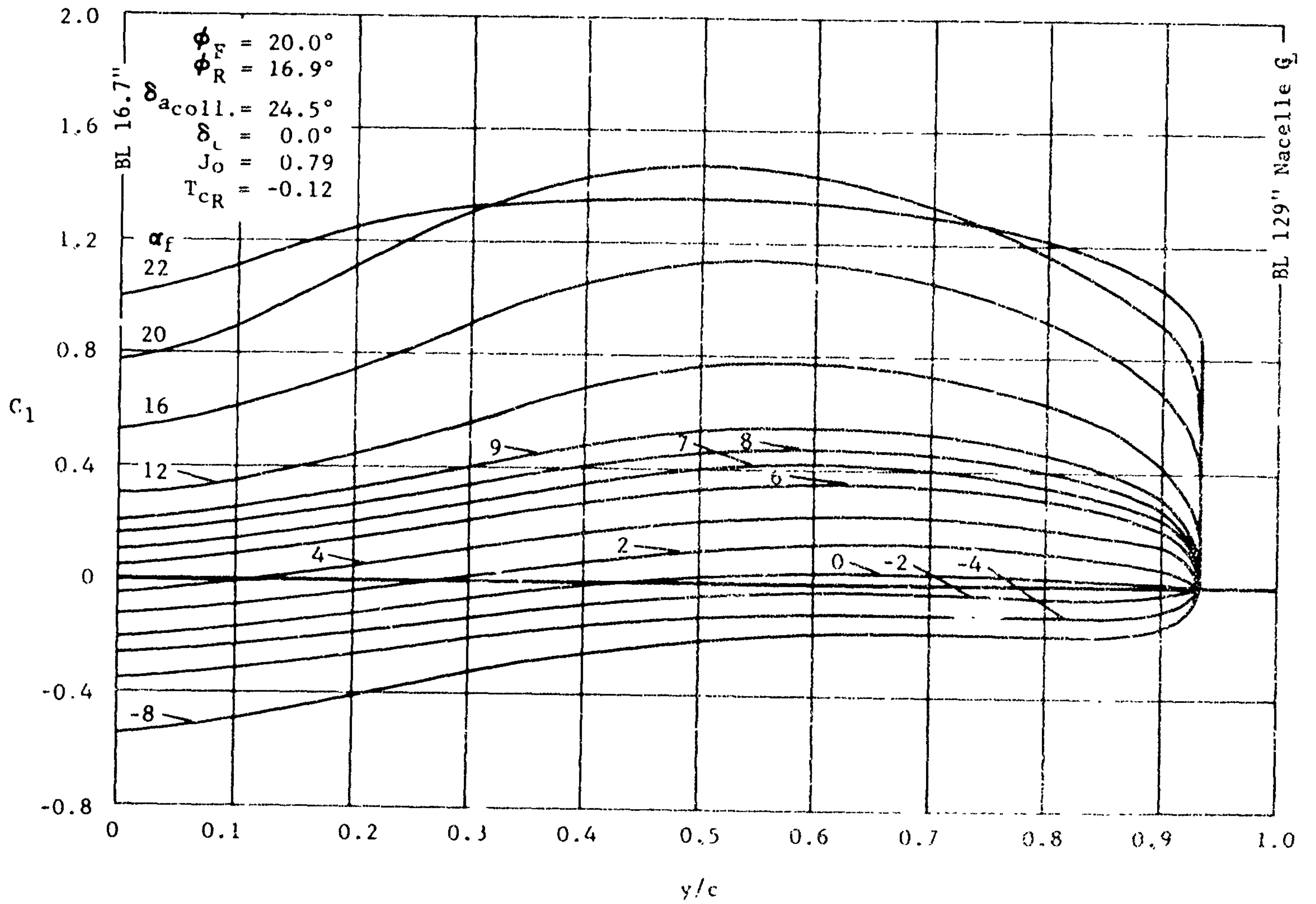

Figure 61. X-19, installed rear wing spanwise lift distribution.

"FURNISHED UNDER UNITED STATES GOVERNMENT CONTRACT No. AF33(615)-3940. SHALL NOT BE EITHER RELEASED OUTSIDE THE GOVERNMENT, OR USED, DUPLICATED, OR DISCLOSED IN WHOLE OR IN PART FOR MANUFACTURE OR PROCUREMENT, WITHOUT THE WRITTEN PERMISSION OF CURTISS-WRIGHT CORPORATION, EXCEPT FOR (I) EMERGENCY REPAIR OR OVERHAUL WORK BY OR FOR THE GOVERNMENT, WHERE THE ITEM OR PROCESS IS NOT OTHERWISE REASONABLY AVAILABLE TO ENABLE TIMELY PERFORMANCE OF THE WORK, OR (II) RELEASE TO A FOREIGN GOVERNMENT, AS THE INTERESTS OF THE UNITED STATES MAY REQUIRE. PROVIDED THAT IN EITHER CASE THE RELEASE, USE, DUPLICATION OR DISCLOSURE HEREOF SHALL BE SUBJECT TO THE FOREGOING LIMITATIONS. THIS LEGEND SHALL BE MARKED ON ANY REPRODUCTION HEREOF IN WHOLE OR IN PART."

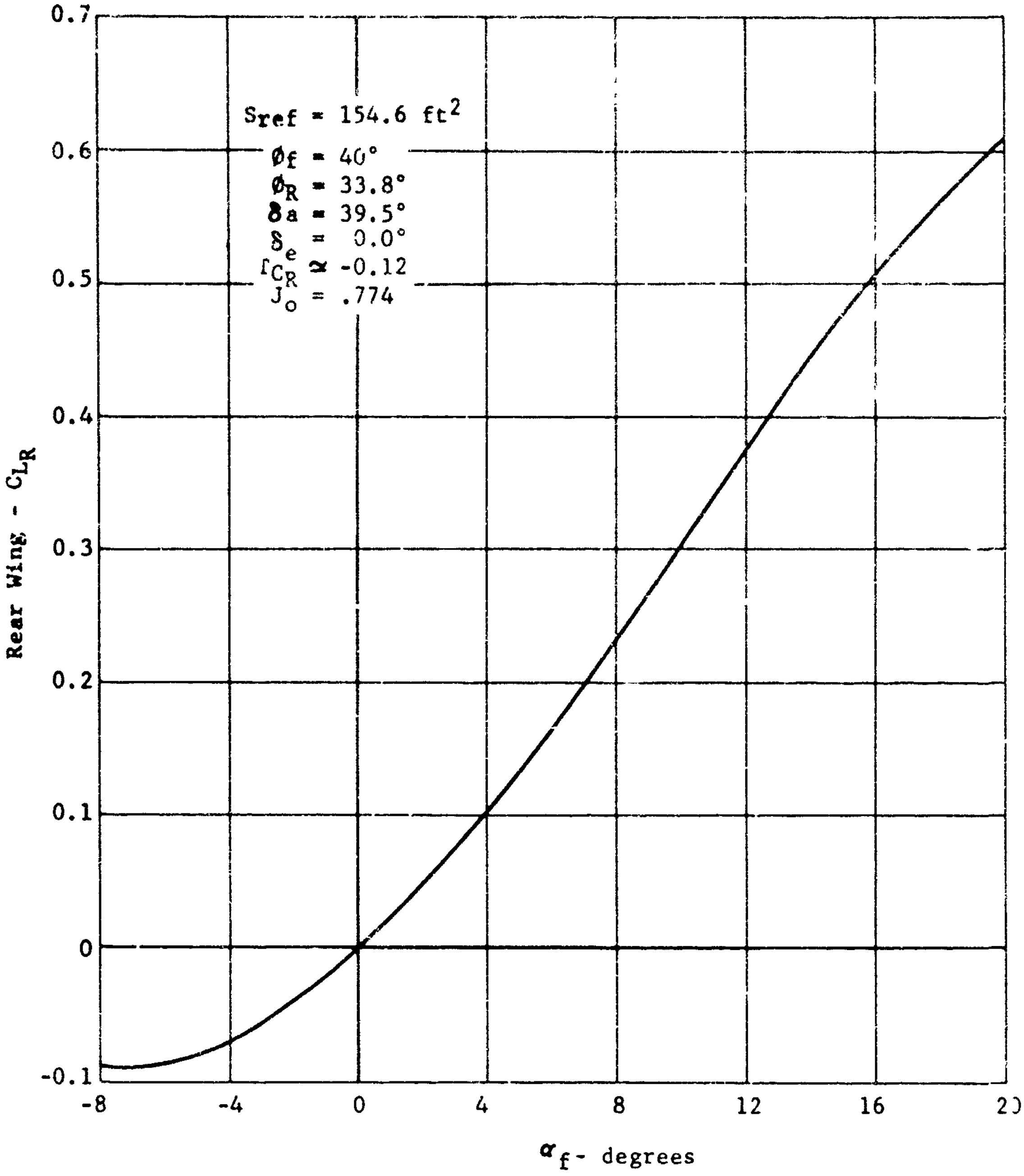

Figure 62. X-19, installed rear wing lift curve.

FURNISHED UNDER UNITED STATES GOVERNMENT CONTRACT No. AF33(615)-3940. SHALL NOT BE EITHER RELEASED OUTSIDE THE GOVERNMENT, OR USED, DUPLICATED, OR DISCLOSED IN WHOLE OR IN PART FOR MANUFACTURE OR PROCUREMENT, WITHOUT THE WRITTEN PERMISSION OF CURTISS-WRIGHT CORPORATION, EXCEPT FOR (i) EMERGENCY REPAIR OR OVERHAUL WORK BY OR FOR THE GOVERNMENT, WHERE THE ITEM OR PROCESS IS NOT OTHERWISE REASONABLY AVAILABLE TO ENABLE TIMELY PERFORMANCE OF THE WORK, OR (ii) RELEASE TO A FOREIGN GOVERNMENT, AS THE INTERESTS OF THE UNITED STATES MAY REQUIRE; PROVIDED THAT IN EITHER CASE THE RELEASE, USE, DUPLICATION OR DISCLOSURE HEREOF SHALL BE SUBJECT TO THE FOREGOING LIMITATIONS. THIS LEGEND SHALL BE MARKED ON ANY REPRODUCTION HEREOF IN WHOLE OR IN PART.

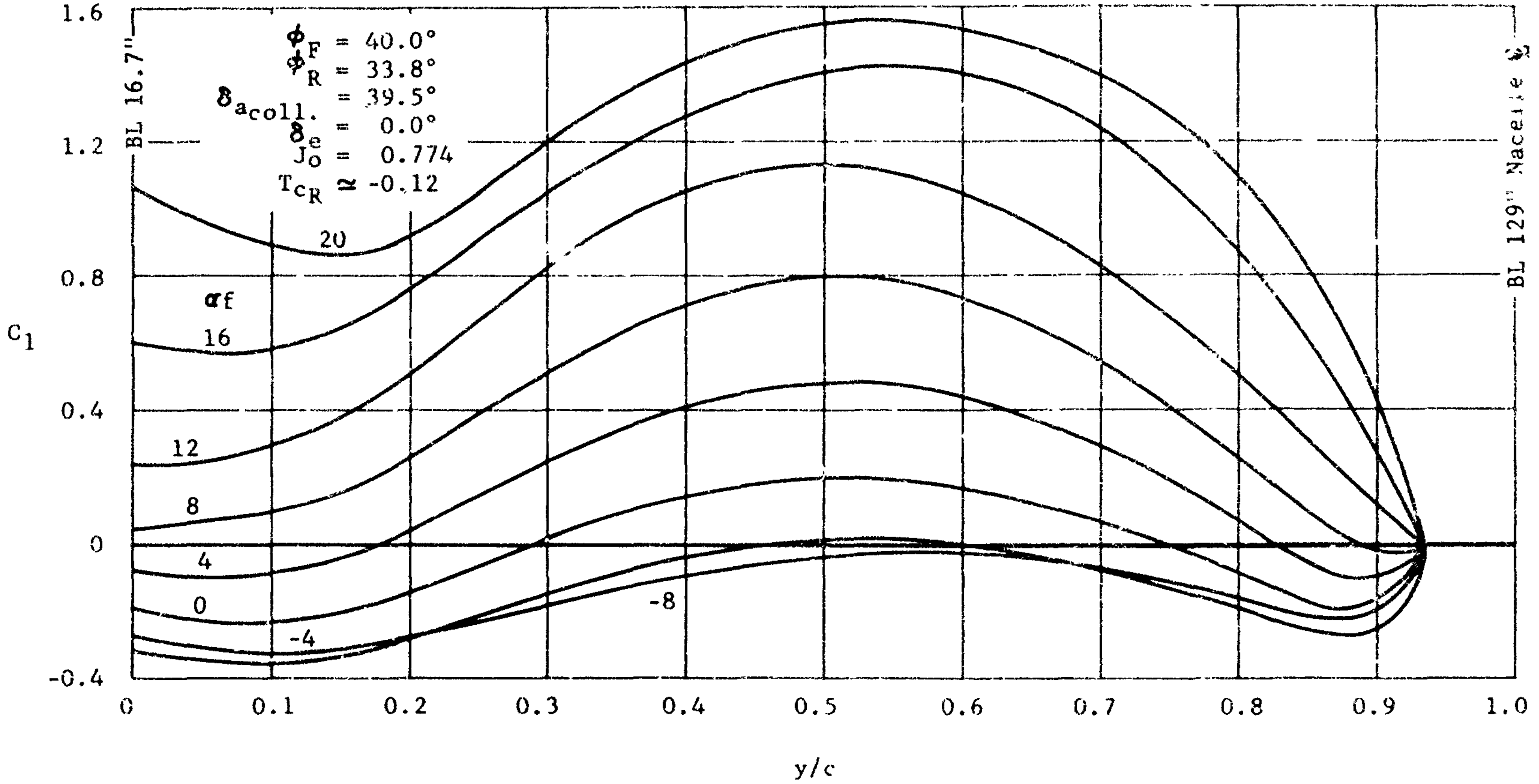

Figure 63. X-19, installed rear wing spanwise lift distribution.

"FURNISHED UNDER UNITED STATES GOVERNMENT CONTRACT No. AF33(615)-3940. SHALL NOT BE EITHER RELEASED OUTSIDE THE GOVERNMENT, OR USED, DUPLICATED, OR DISCLOSED IN WHOLE OR IN PART FOR MANUFACTURE OR PROCUREMENT, WITHOUT THE WRITTEN PERMISSION OF CURTISS-WRIGHT CORPORATION, EXCEPT FOR (i) EMERGENCY REPAIR OR OVERHAUL WORK BY OR FOR THE GOVERNMENT, WHERE THE ITEM OR PROCESS IS NOT OTHERWISE REASONABLY AVAILABLE TO ENABLE TIMELY PERFORMANCE OF THE WORK. OR (ii) RELEASE TO A FOREIGN GOVERNMENT, AS THE INTERESTS OF THE UNITED STATES MAY REQUIRE. PROVIDED THAT IN EITHER CASE THE RELEASE, USE, DUPLICATION OR DISCLOSURE HEREOF SHALL BE SUBJECT TO THE FOREGOING LIMITATIONS. THIS LEGEND SHALL BE MARKED ON ANY REPRODUCTION HEREOF IN WHOLE OR IN PART."

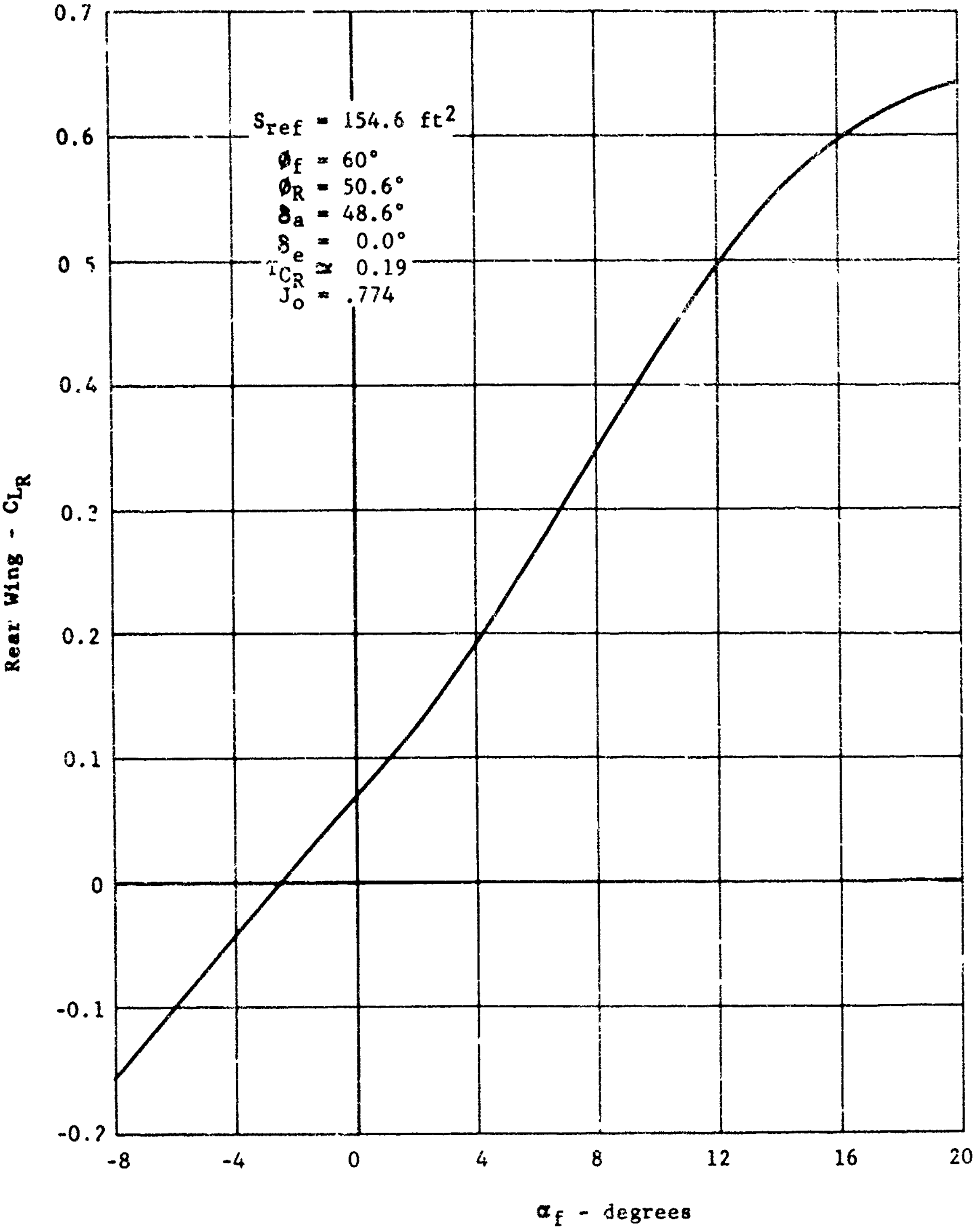

Figure 64. X-19, installed rear wing lift curve.

FURNISHED UNDER UNITED STATES GOVERNMENT CONTRACT No. AF33(615)-1940. SHALL NOT BE EITHER RELEASED OUTSIDE THE GOVERNMENT, OR USED, DUPLICATED, OR DISCLOSED IN WHOLE OR IN PART FOR MANUFACTURE OR PROCUREMENT, WITHOUT THE WRITTEN PERMISSION OF CURTISS-WRIGHT CORPORATION, EXCEPT FOR (I) EMERGENCY REPAIR OR OVERHAUL WORK BY OR FOR THE GOVERNMENT, WHERE THE ITEM OR PROCESS IS NOT OTHERWISE REASONABLY AVAILABLE TO ENABLE TIMELY PERFORMANCE OF THE WORK, OR (II) RELEASE TO A FOREIGN GOVERNMENT, AS THE INTERESTS OF THE UNITED STATES MAY REQUIRE; PROVIDED THAT IN EITHER CASE THE RELEASE, USE, DUPLICATION OR DISCLOSURE HEREOF SHALL BE SUBJECT TO THE FOREGOING LIMITATION. THIS LEGEND SHALL BE MARKED ON ANY REPRODUCTION HEREOF IN WHOLE OR IN PART.

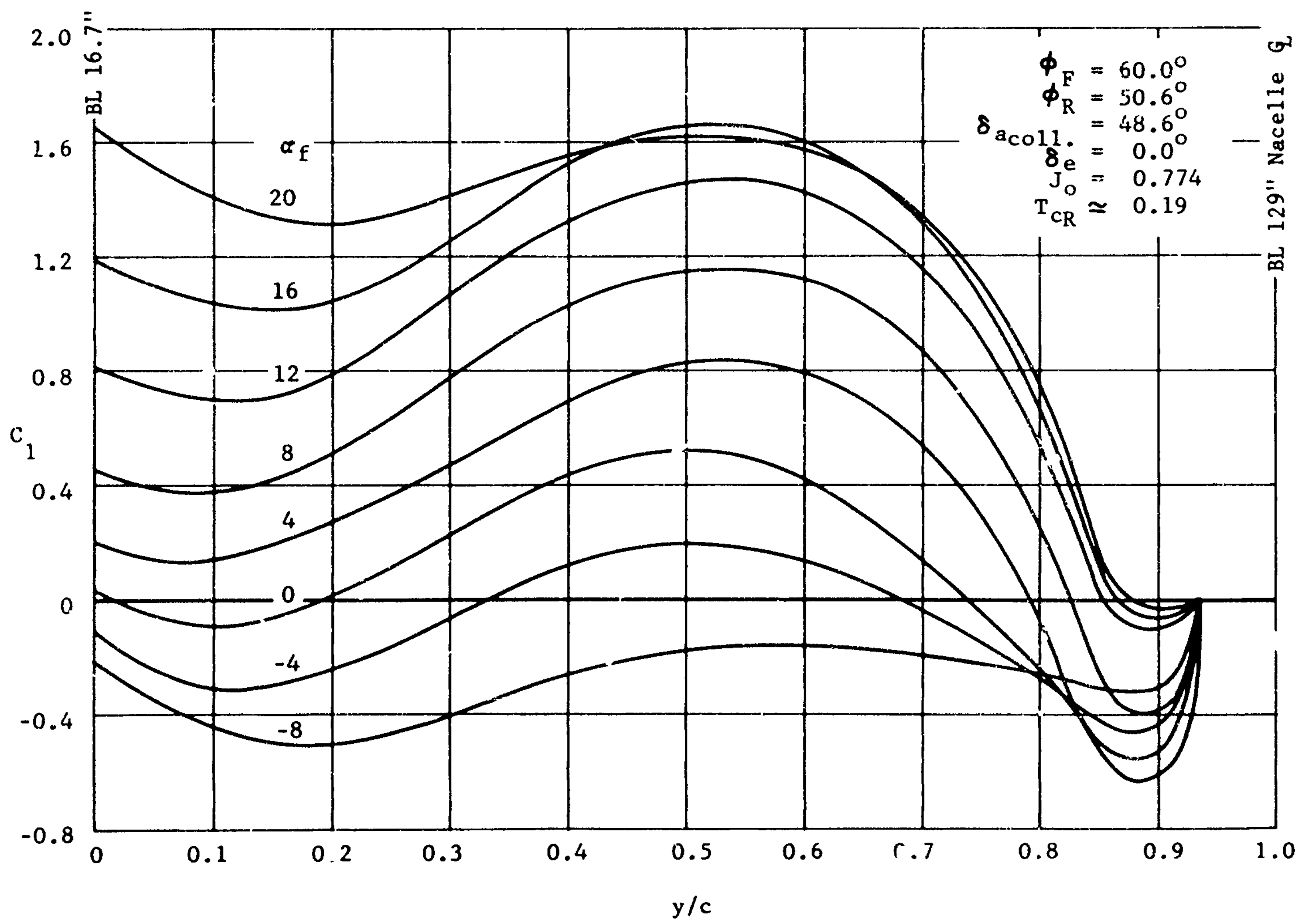

Figure 65. X-19, installed rear wing spanwise lift distribution.

FURNISHED UNDER UNITED STATES GOVERNMENT CONTRACT No. AF33(615)-3940. SHALL NOT BE EITHER RELEASED OUTSIDE THE GOVERNMENT, OR USED, DUPLICATED, OR DISCLOSED IN WHOLE OR IN PART FOR MANUFACTURE OR PROCUREMENT, WITHOUT THE WRITTEN PERMISSION OF CURTISS-WRIGHT CORPORATION, EXCEPT FOR (I) EMERGENCY REPAIR OR OVERHAUL WORK BY OR FOR THE GOVERNMENT, WHERE THE ITEM OR PROCESS IS NOT OTHERWISE REASONABLY AVAILABLE TO ENABLE TIMELY PERFORMANCE OF THE WORK, OR (II) RELEASE TO A FOREIGN GOVERNMENT, AS THE INTERESTS OF THE UNITED STATES MAY REQUIRE. PROVIDED THAT IN EITHER CASE THE RELEASE, USE, DUPLICATION OR DISCLOSURE HEREOF SHALL BE SUBJECT TO THE FOREGOING LIMITATIONS. THIS LEGEND SHALL BE MARKED ON ANY REPRODUCTION HEREOF IN WHOLE OR IN PART."

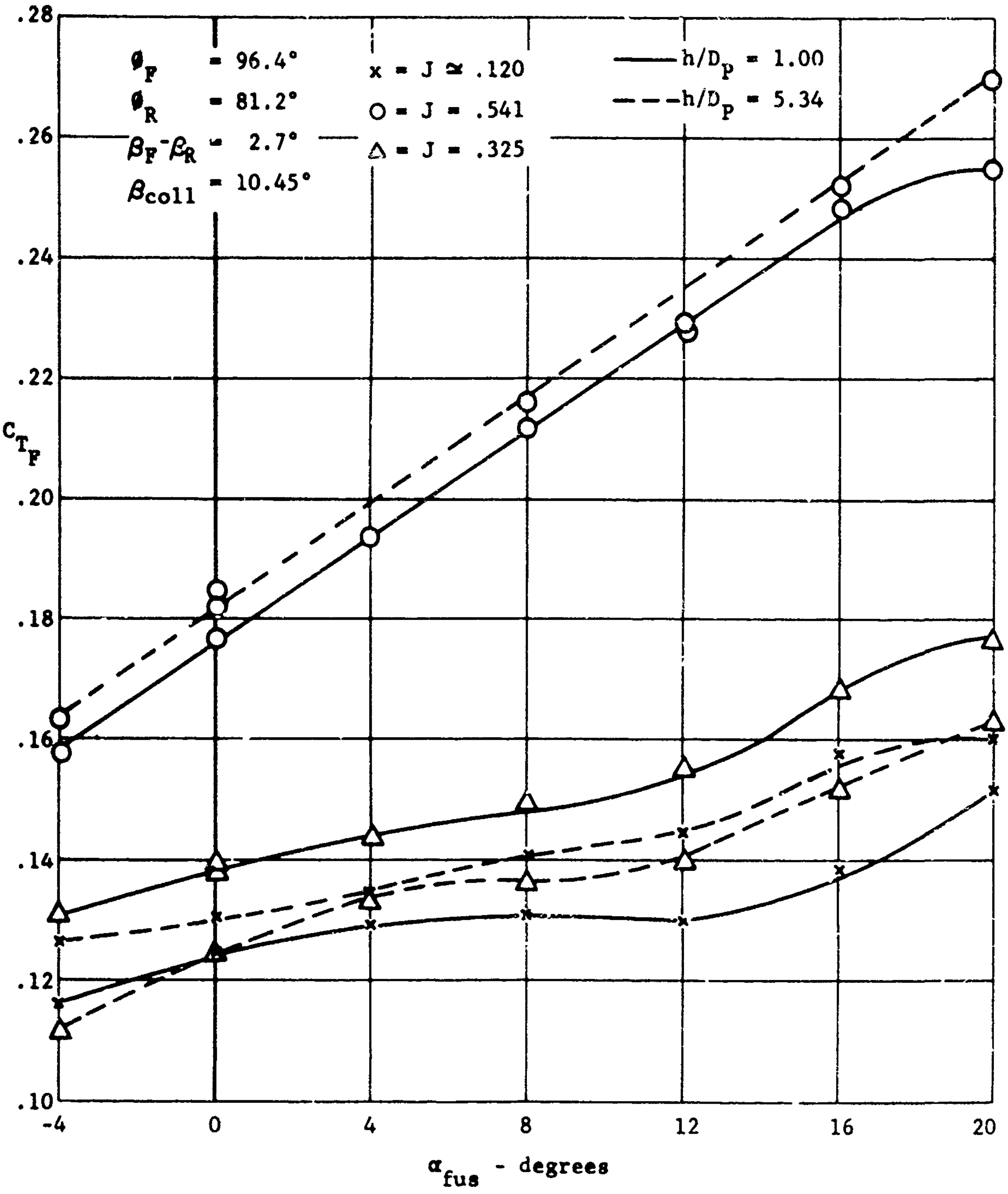

Figure 66. X-19 front propeller thrust coefficient.

FURNISHED UNDER UNITED STATES GOVERNMENT CONTRACT No. AF33(615)-[illegible] SHALL NOT BE EITHER RELEASED OUTSIDE THE GOVERNMENT, OR USED, DUPLICATED, OR DISCLOSED IN WHOLE OR IN PART FOR MANUFACTURE OR PROCUREMENT, WITHOUT THE WRITTEN PERMISSION OF CURTISS-WRIGHT CORPORATION, EXCEPT FOR (I) EMERGENCY REPAIR OR OVERHAUL WORK BY OR FOR THE GOVERNMENT, WHERE THE ITEM OR PROCESS IS NOT OTHERWISE REASONABLY AVAILABLE TO ENABLE TIMELY PERFORMANCE OF THE WORK, OR (II) RELEASE TO A FOREIGN GOVERNMENT, AS THE INTERESTS OF THE UNITED STATES MAY REQUIRE; PROVIDED THAT IN EITHER CASE THE RELEASE, USE, DUPLICATION OR DISCLOSURE HEREOF SHALL BE SUBJECT TO THE FOREGOING LIMITATIONS. THIS LEGEND SHALL BE MARKED ON ANY REPRODUCTION HEREOF IN WHOLE OR IN PART.

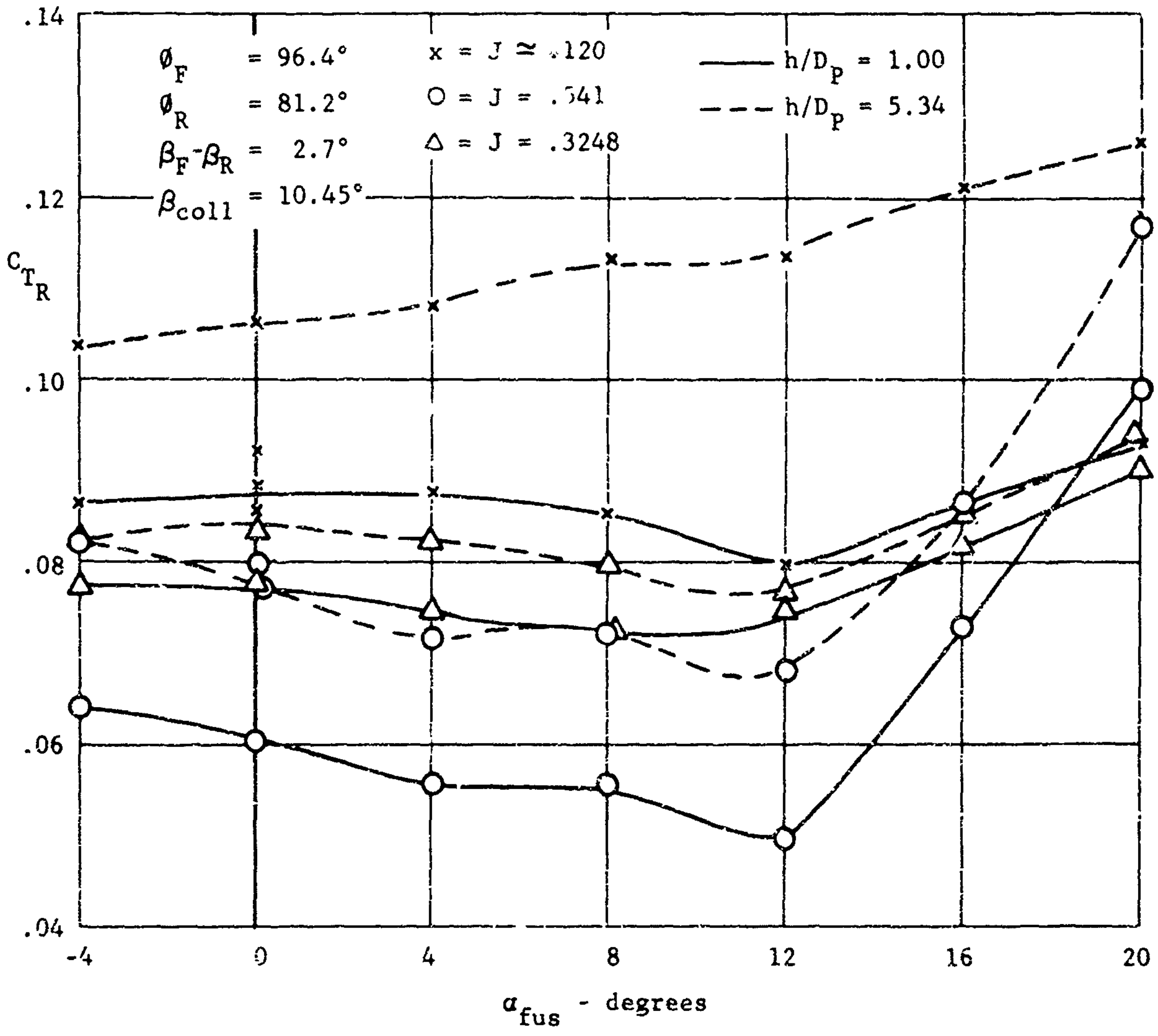

Figure 67. X-19, rear propeller thrust coefficient.

FURNISHED UNDER UNITED STATES GOVERNMENT CONTRACT No. AF33(615)-3940. SHALL NOT BE EITHER RELEASED OUTSIDE THE GOVERNMENT, OR USED, DUPLICATED, OR DISCLOSED IN WHOLE OR IN PART FOR MANUFACTURE OR PROCUREMENT, WITHOUT THE WRITTEN PERMISSION OF CURTISS-WRIGHT CORPORATION, EXCEPT FOR (I) EMERGENCY REPAIR OR OVERHAUL WORK BY OR FOR THE GOVERNMENT, WHERE THE ITEM OR PROCESS IS NOT OTHERWISE REASONABLY AVAILABLE TO ENABLE TIMELY PERFORMANCE OF THE WORK, OR (II) RELEASE TO A FOREIGN GOVERNMENT, AS THE INTERESTS OF THE UNITED STATES MAY REQUIRE. PROVIDED THAT IN EITHER CASE THE RELEASE, USE, DUPLICATION OR DISCLOSURE HEREOF SHALL BE SUBJECT TO THE FOREGOING LIMITATIONS. THIS LEGEND SHALL BE MARKED ON ANY REPRODUCTION HEREOF IN WHOLE OR IN PART."

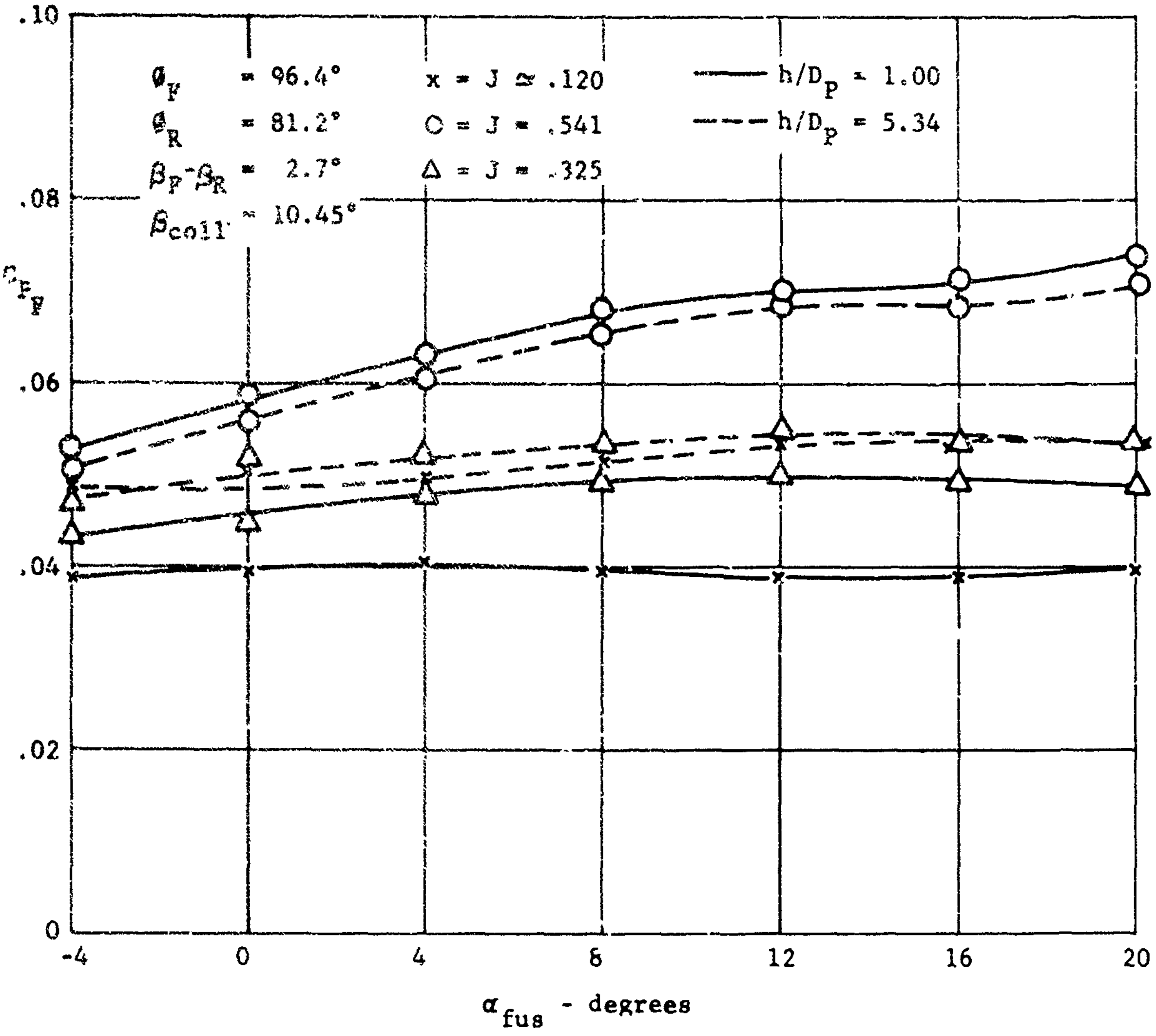

Figure 68. X-19, front propeller power coefficient.

FURNISHED UNDER UNITED STATES GOVERNMENT CONTRACT No. AF33(615)-3940 SHALL NOT BE EITHER RELEASED OUTSIDE THE GOVERNMENT OR USED DUPLICATED, OR DISCLOSED IN WHOLE OR IN PART FOR MANUFACTURE OR PROCUREMENT, WITHOUT THE WRITTEN PERMISSION OF CURTISS-WRIGHT CORPORATION EXCEPT FOR (I) EMERGENCY REPAIR OR OVERHAUL WORK BY OR FOR THE GOVERNMENT, WHERE THE ITEM OR PROCESS IS NOT OTHERWISE REASONABLY AVAILABLE TO ENABLE TIMELY PERFORMANCE OF THE WORK OR (II) RELEASE TO A FOREIGN GOVERNMENT, AS THE INTERESTS OF THE UNITED STATES MAY REQUIRE PROVIDED THAT IN EITHER CASE THE RELEASE, USE DUPLICATION OR DISCLOSURE HEREOF SHALL BE SUBJECT TO THE FOREGOING LIMITATIONS. THIS LEGEND SHALL BE MARKED ON ANY REPRODUCTION HEREOF IN WHOLE OR IN PART.

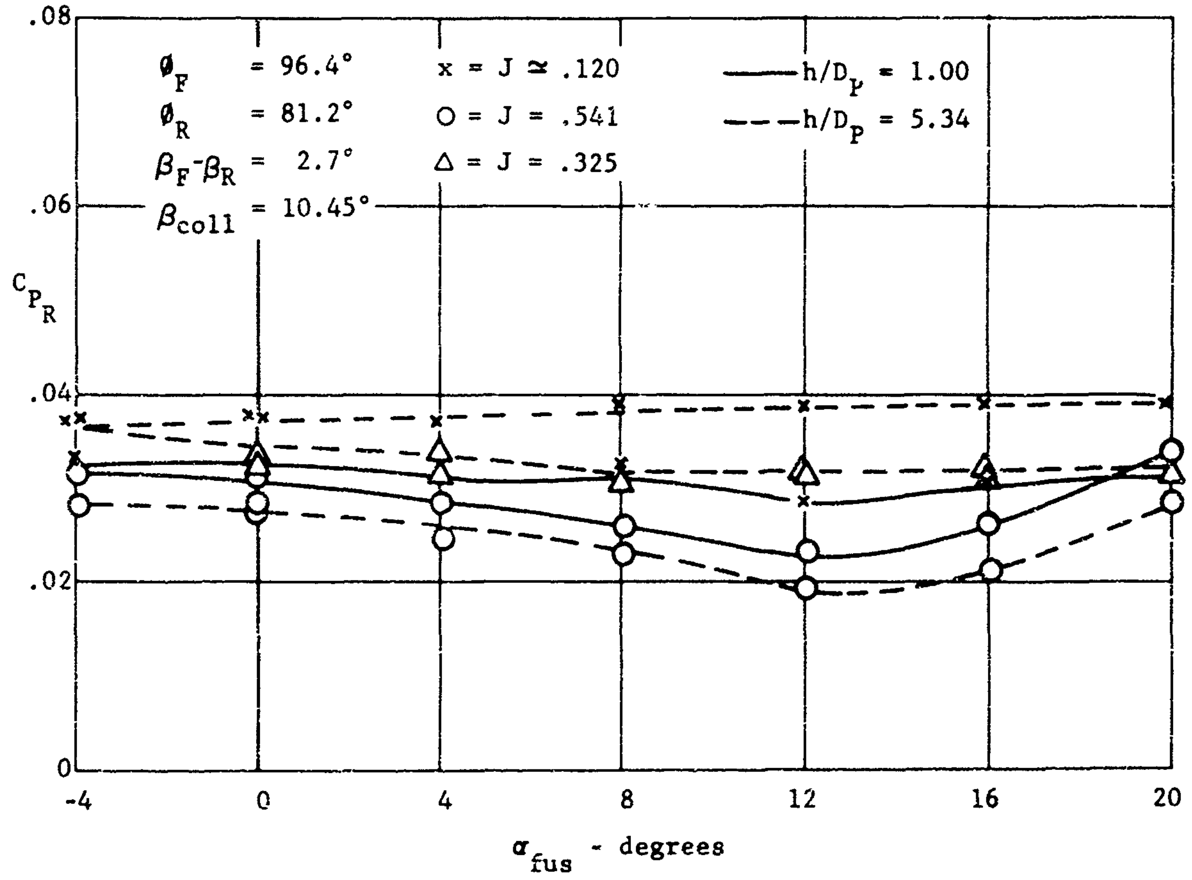

Figure 69. X-19, rear propeller power coefficient.

"FURNISHED UNDER UNITED STATES GOVERNMENT CONTRACT No. AF33(615)-1940. SHALL NOT BE EITHER RELEASED OUTSIDE THE GOVERNMENT, OR USED, DUPLICATED, OR DISCLOSED IN WHOLE OR IN PART FOR MANUFACTURE OR PROCUREMENT, WITHOUT THE WRITTEN PERMISSION OF CURTISS-WRIGHT CORPORATION EXCEPT FOR (i) EMERGENCY REPAIR OR OVERHAUL WORK BY OR FOR THE GOVERNMENT WHERE THE ITEM OR PROCESS IS NOT OTHERWISE REASONABLY AVAILABLE TO ENABLE TIMELY PERFORMANCE OF THE WORK. OR (ii) RELEASE TO A FOREIGN GOVERNMENT, AS THE INTERESTS OF THE UNITED STATES MAY REQUIRE. PROVIDED THAT IN EITHER CASE THE RELEASE, USE, DUPLICATION OR DISCLOSURE HEREOF SHALL BE SUBJECT TO THE FOREGOING LIMITATIONS. THIS LEGEND SHALL BE MARKED ON ANY REPRODUCTION HEREOF IN WHOLE OR IN PART."

presence on the wings. A reasonable assumption would be to suggest that it resembles the trends exhibited by the propellers, at least with respect to the intercepts.

c. Net Forces and Moments In and Out of Ground Effect

The source of transition ground effect data accumulated on the X-19 is given in (19). The information is based on 12% model scale and is quite limited in nature. For example, only one collective blade angle was run ($\beta_{coll} = 10.45^{\circ}$) for a range of fuselage attitudes and advance ratio (see Figures 70, 71 and 72). At first glance, one notes that C_L, C_D and C_m are strongly affected by the ground effect. A closer scrutiny indicates that power absorption has also changed, so that a collective change would be required to maintain constant power. As this is not available, the ratio of C_L/C_P has been formed; it is given in the following table:

h/D	J = 0.12	0.32	0.54
1.0	370	61.3	23.8
5.34	361	54.6	23.6

$$\left[C_L/C_P\right]_{\alpha_{fus} = 0}$$

Lift ground effect is thus shown to be about 12% at J = 0.32 and 1% at J = 0.541. The value at J = 0.12 is not quite correct as the IGE and OGE runs were made at slightly different J's. Small as the difference is, the slope C_L vs J is sufficiently large to cloud the comparison at this J. The predicted ground effect at $h/D_P = 1$, for static operation (J = 0) is 3.5%. By definition $h/D_P = 1$ means that wheel height is equal to one propeller diameter above the ground.

Another consideration in establishing the resultant ground effect upon power is the effect of h/D_P on the drag and consequent fuselage attitude. Thus, ground effect would result in a slight attitude change as well as a throttle change. Figure 71 shows a positive drag for the entire range of α_{fus} plotted. This can be corrected by nosing the fuselage to negative attitudes at J = 0.12, and by tilting to lower nacelle angles for the higher values of J. At negative values of α_{fus} the ground effect tends to decrease the drag. As it also increases the lift it may be concluded that for acceleration in ground effect (negative α_{fus}) both the lift and drag contributions are beneficial in helping to reduce power.

Unfortunately, the data have insufficient depth to fully define the resultant ground effects.

FURNISHED UNDER UNITED STATES GOVERNMENT CONTRACT No. AF33(615)-3940. SHALL NOT BE EITHER RELEASED OUTSIDE THE GOVERNMENT, OR USED, DUPLICATED, OR DISCLOSED IN WHOLE OR IN PART FOR MANUFACTURE OR PROCUREMENT, WITHOUT THE WRITTEN PERMISSION OF CURTISS-WRIGHT CORPORATION, EXCEPT FOR (i) EMERGENCY REPAIR OR OVERHAUL WORK BY OR FOR THE GOVERNMENT, WHERE THE ITEM OR PROCESS IS NOT OTHERWISE REASONABLY AVAILABLE TO ENABLE TIMELY PERFORMANCE OF THE WORK, OR (ii) RELEASE TO A FOREIGN GOVERNMENT, AS THE INTERESTS OF THE UNITED STATES MAY REQUIRE; PROVIDED THAT IN EITHER CASE THE RELEASE, USE, DUPLICATION OR DISCLOSURE HEREOF SHALL BE SUBJECT TO THE FOREGOING LIMITATIONS. THIS LEGEND SHALL BE MARKED ON ANY REPRODUCTION HEREOF IN WHOLE OR IN PART.

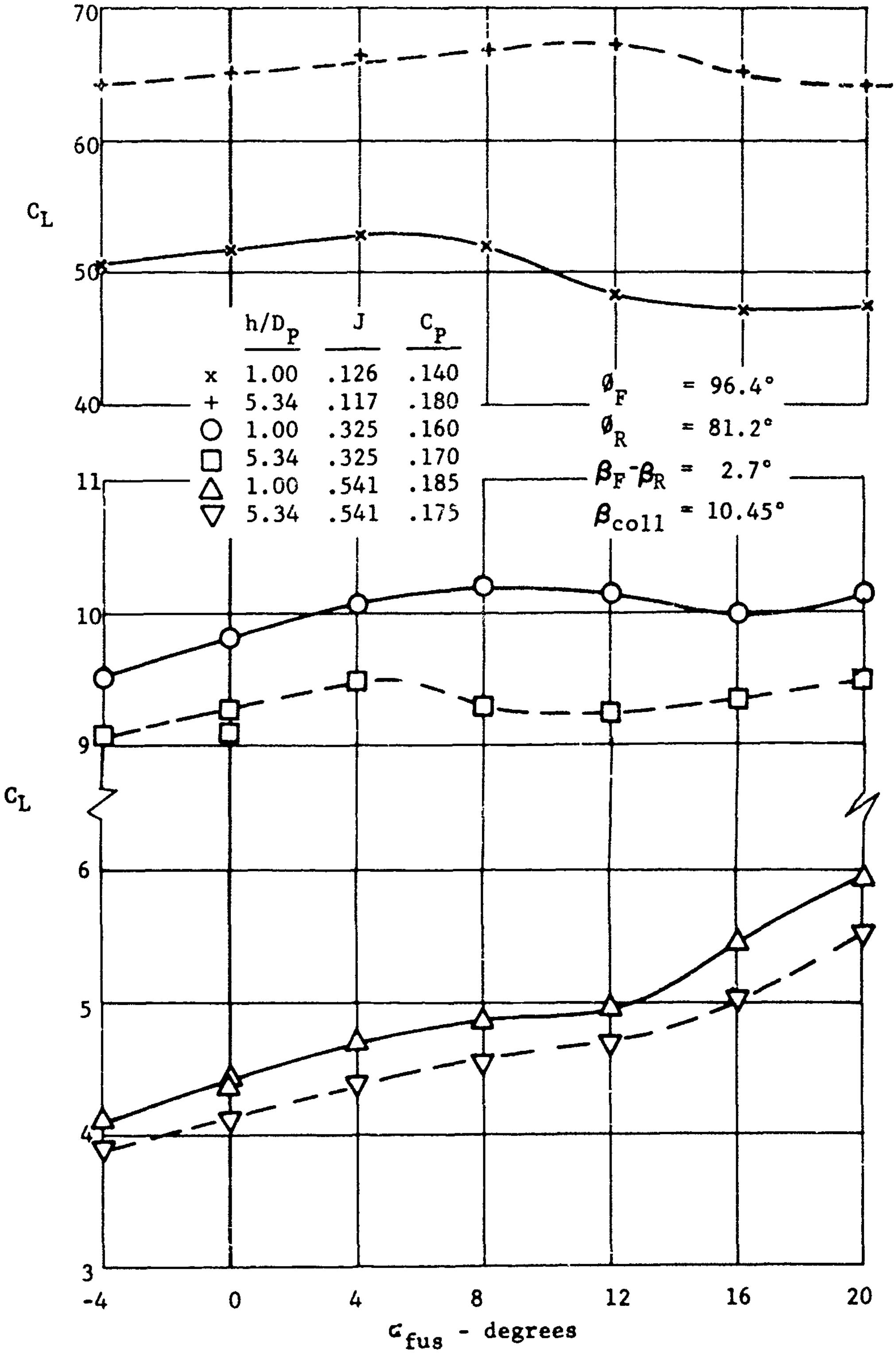

Figure 70. X-19, airplane lift characteristics, ground effects.

FURNISHED UNDER UNITED STATES GOVERNMENT CONTRACT No. AF33(615)-3940 SHALL NOT BE EITHER RELEASED OUTSIDE THE GOVERNMENT, OR USED, DUPLICATED, OR DISCLOSED IN WHOLE OR IN PART FOR MANUFACTURE OR PROCUREMENT, WITHOUT THE WRITTEN PERMISSION OF CURTISS-WRIGHT CORPORATION, EXCEPT FOR (I) EMERGENCY REPAIR OR OVERHAUL WORK BY OR FOR THE GOVERNMENT, WHERE THE ITEM OR PROCESS IS NOT OTHERWISE REASONABLY AVAILABLE TO ENABLE TIMELY PERFORMANCE OF THE WORK, OR (II) RELEASE TO A FOREIGN GOVERNMENT, AS THE INTERESTS OF THE UNITED STATES MAY REQUIRE PROVIDED THAT IN EITHER CASE THE RELEASE USE, DUPLICATION OR DISCLOSURE HEREOF SHALL BE SUBJECT TO THE FOREGOING LIMITATIONS THIS LEGEND SHALL BE MARKED ON ANY REPRODUCTION HEREOF IN WHOLE OR IN PART."

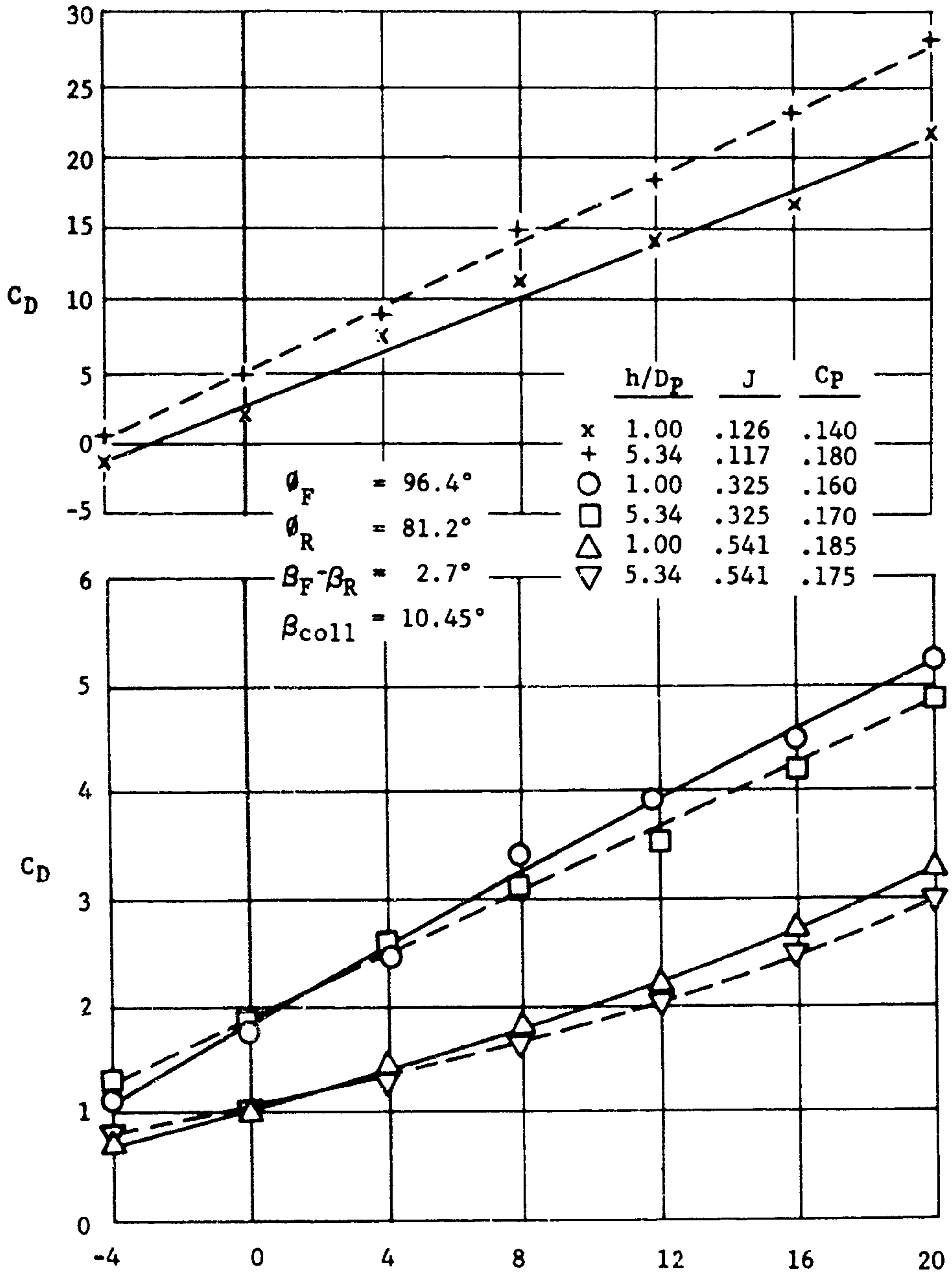

Figure 71. X-19, airplane drag characteristics, ground effects.

FURNISHED UNDER UNITED STATES GOVERNMENT CONTRACT No. AF33(615)-3940. SHALL NOT BE EITHER RELEASED OUTSIDE THE GOVERNMENT, OR USED, DUPLICATED, OR DISCLOSED IN WHOLE OR IN PART FOR MANUFACTURE OR PROCUREMENT, WITHOUT THE WRITTEN PERMISSION OF CURTISS-WRIGHT CORPORATION, EXCEPT FOR (i) EMERGENCY REPAIR OR OVERHAUL WORK BY OR FOR THE GOVERNMENT, WHERE THE ITEM OR PROCESS IS NOT OTHERWISE REASONABLY AVAILABLE TO ENABLE TIMELY PERFORMANCE OF THE WORK, OR (ii) RELEASE TO A FOREIGN GOVERNMENT, AS THE INTERESTS OF THE UNITED STATES MAY REQUIRE; PROVIDED THAT IN EITHER CASE THE RELEASE, USE, DUPLICATION OR DISCLOSURE HEREOF SHALL BE SUBJECT TO THE FOREGOING LIMITATIONS. THIS LEGEND SHALL BE MARKED ON ANY REPRODUCTION HEREOF IN WHOLE OR IN PART.

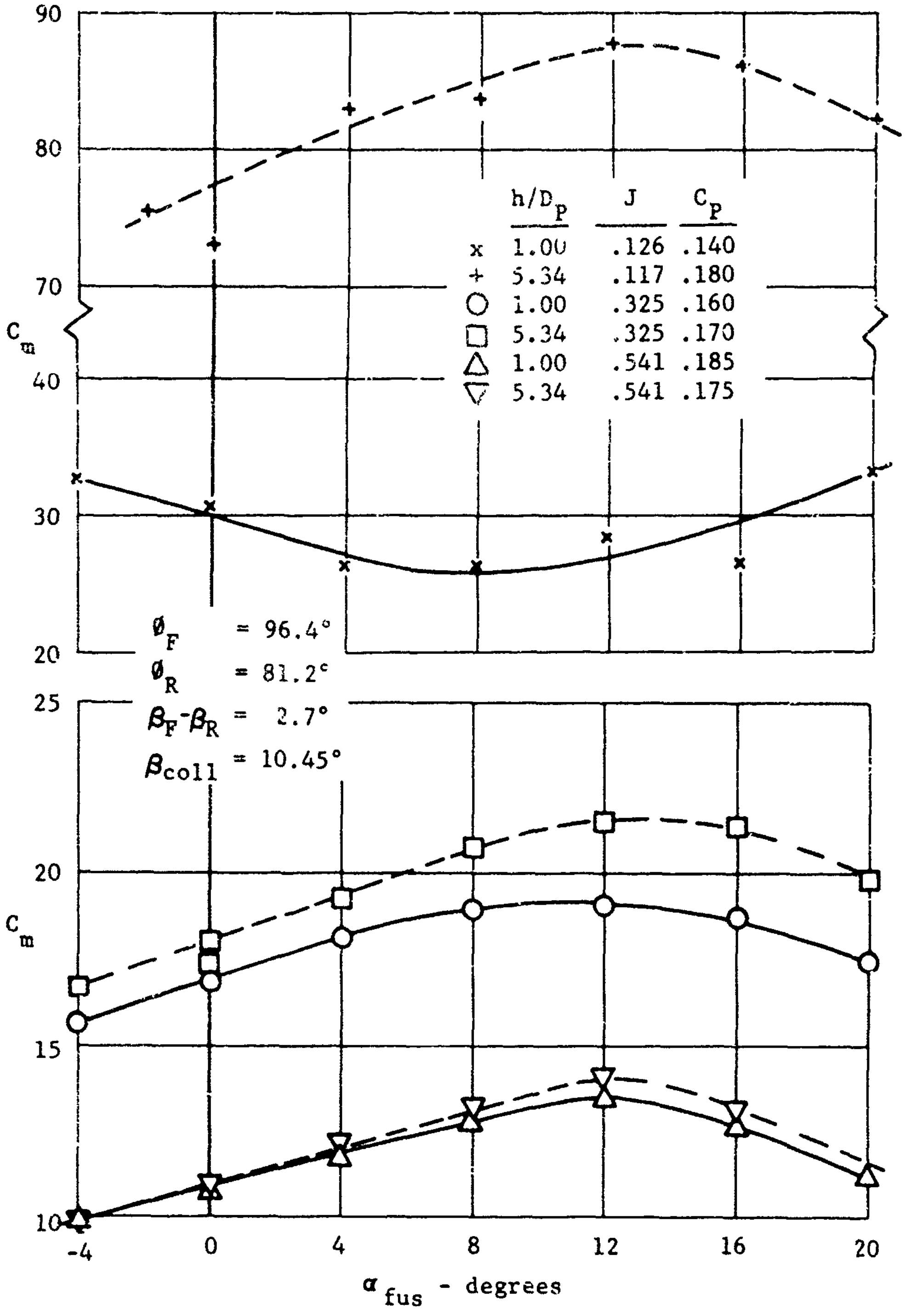

Figure 72. X-19, airplane moment characteristics, ground effects; c.g. at 42.8% lift chord and W.L. 123.8 inches.

FURNISHED UNDER UNITED STATES GOVERNMENT CONTRACT No AF33(6.5)-3940. SHALL NOT BE EITHER RELEASED OUTSIDE THE GOVERNMENT, OR USED, DUPLICATED OR DISCLOSED IN WHOLE OR IN PART FOR MANUFACTURE OR PROCUREMENT, WITHOUT THE WRITTEN PERMISSION OF CURTISS-WRIGHT CORPORATION, EXCEPT FOR (I) EMERGENCY REPAIR OR OVERHAUL WORK BY OR FOR THE GOVERNMENT, WHERE THE ITEM OR PROCESS IS NOT OTHERWISE REASONABLY AVAILABLE TO ENABLE TIMELY PERFORMANCE OF THE WORK, OR (II) RELEASE TO A FOREIGN GOVERNMENT, AS THE INTERESTS OF THE UNITED STATES MAY REQUIRE, PROVIDED THAT IN EITHER CASE THE RELEASE, USE, DUPLICATION OR DISCLOSURE HEREOF SHALL BE SUBJECT TO THE FOREGOING LIMITATIONS. THIS LEGEND SHALL BE MARKED ON ANY REPRODUCTION HEREOF IN WHOLE OR IN PART."

5. FLAP DEFLECTION INTERFERENCE EFFECTS IN TRANSITION

The bulk of the testing performed in the transition area concerns itself with propeller and model force readouts. There were no tests performed to establish interference effects of a flap or aileron upon its own propeller front or rear wing. The only testing done to determine effects of flap deflection was at the hover condition and was discussed previously.

REFERENCES

10. McKee, John W., and Naeseth, Roger L., Experimental Investigation of the Drag of Flat Plates and Cylinders in the Slipstream of a Hovering Rotor, NACA TN 4239, April 1958

11. "Proceedings Of The Fourteenth Annual National Forum," American Helicopter Society, April, 1958

12. Pope, A. "Forces and Moments Over a NACA 'Airfoil'," Aero Digest Vol. 58 No. 4 1945

13. Borst, H.V., and Ladden, R.M., "Propeller Testing at Zero Velocity," U. S. Army Aviation Material Laboratories and Cornell Aeronautical Laboratory, Inc. Symposium, June 1966

13.1 Salters, Leland B. Jr., and Norton, Harry T. Jr., "An Investigation of the Effects of the WADC 30,000 Horsepower Whirl Rig Upon the Static Characteristics of a Propeller", NACA RM SL52F20

14. Curtiss-Wright Corporation, Model X-200T Tandem, Front and Rear Propeller-Nacelle-Wing Characteristics in the Presence of the Fuselage, MIT Wind Tunnel Report No. 1003, Oct. 1960

15. K.J. Rogers, Low Speed Wind Tunnel Tests of a 0.12 Scale Model of the CW M-200 VTOL Airplane to Evaluate Longitudinal, Lateral and Directional Stability Characteristics, NAA Report No. NA62-H-719, dated Oct. 2, 1962. (NACAL 93)

16. H. Fluk, Isolated Model Propeller Characteristics 3(156109), Dia. 2.5 ft., Curtiss-Wright Report 001-67, Aug. 26, 1965

17. E.L. Hassell, Curtiss-Wright Corporation Wind Tunnel Tests on Half-Scale Wing Model, MIT Report No. 992, Nov. 1959

18. Granath, J.I., and Locklin R.G., Stability and Control Investigation of Curtiss Model X-200, MIT Wright Brothers Wind Tunnel Report No. 989, dated

19. K.J. Rogers, Low Speed Wind Tunnel Tests of A 0.12 Scale Model of the Curtiss-Wright X-19 Aircraft, NAA report NA64H-837, August 21, 1964 (NACAL 120)

20. K.J. Rogers, Curtiss-Wright Corporation M-200 Turbine Stability Model, MIT Report No. 1019, March 1962

21. K.J. Rogers, Low Speed Wind Tunnel Test of A 0.12 Scale Powered Model of the X-19 Aircraft to Determine the Optimum Propeller Tilt Schedule in Transition, North American Aviation, Inc. Report No. NA66H-43, February 25, 1966 (NACAL 142)

SECTION IV

PROPELLER AERODYNAMIC DESIGN

2

SECTION IV NOMENCLATURE

A = disk area = πR^2

AF = activity Factor = $\frac{100,000}{16} \int_{.2}^{1.0} (\frac{b}{D}) (\frac{r}{R})^3 \; d(\frac{r}{R})$

b = blade chord ft

C_{L_i} = section design lift coefficient

C_T = thrust coefficient = $\frac{T}{\rho n^2 D^2}$

C_P = power coefficient = $\frac{P}{\rho n^3 D^5}$

C_L = lift coefficient = L/qS

C_D = drag coefficient = D/qS

D = drag

FM = Figure of Merit = $.798 \frac{C_T^{3/2}}{C_P}$

H.P. = horsepower

h = section maximum thickness

IC_{L_i} = blade integrated design $C_L = 4 \int_{.2}^{1.0} C_{L_i} (\frac{r}{R})^3 \; d(\frac{r}{R})$

J = advance Ratio = V/nD

L = lift

n = RPS

N = RPM

Q = torque

r = blade radius along blade

R = propeller total radius

$B_{.75}$ = blade angle at .75 radius

$\beta 42''$ = blade angle at 42 inch station

σ = density ratio = ρ / ρ_o

ρ = air density

ρ_o = air density at sea level

SECTION IV

PROPELLER AERODYNAMIC DESIGN

1. BLADE GEOMETRIC CHARACTERISTICS

The propellers for the X-100 and X-19 airplanes feature wide chord blades that were configured to generate high values of radial force while maintaining high levels of operating efficiency at the take-off and cruise flight conditions. The detailed geometric characteristics of the blades are shown on Figures 73 and 74. In determining the detailed characteristics of the propeller blades the diameter was established by the disk loading requirements whereas the other aspects of the design were dictated by a compromise among cruise, take-off and radial lift performance requirements. Three-blade propellers were selected to obtain a wide chord blade which could be thick inboard and still maintain a thickness ratio of less than 30% at any blade station.

If two-blade propellers had been chosen, very high vibration forces would be generated when operating at high shaft angles which could only be eliminated by hinging the blades. The weight of three- and four-blade propellers was found to be nearly equal when designed to have the same total solidity. Since the performance difference at both the hover and cruise conditions was found to be small, the three-blade design was chosen for the improved structure possible with the wider chord design. It should be realized that with lightly loaded propellers the induced efficiency is already high so that a larger number of blades can not improve the efficiency level significantly. See reference 9.1.

For the X-100 airplane the required thrust to power level was established by the power available and the estimated weight. It was determined on this basis that a thrust to horsepower ratio of approximately 6.0 would be required. The disk loading necessary to obtain the required thrust to horsepower, at hover, is also dependent on the Figure of Merit. When the X-100 was designed, it was believed that Figure of Merit of 80% or over could be obtained. The theory of propellers operating at the static condition was presumed to be satisfactory and that a propeller could be designed to have this high level of performance. At a sea level standard day FM of 80% and a thrust to horsepower ratio of 6.0 resulted in a disk loading of 25 lb/ft^2 (Figure 75). For the X-100 airplane a disk loading of 25 resulted in an installed diameter of 10 feet and gave a level of thrust necessary for hover. Since the hover and operational characteristic of the X-100 airplane were satisfactory with this disk loading, this level was retained for the X-19. This resulted in a diameter of 13' 0" for the latter aircraft.

Results of single point calculations in (22) and (23) indicated that at a low value of integrated design C_L with 150 activity-factor blades would give the required performance at both the cruise and take-off operating conditions. By increasing the integrated design C_L the solidity could be reduced. The Figure of Merit at hover would be increased slightly, less than 2% 22 but the cruise efficiency would be decreased as the result of operating high integrated design lift blade at low values of operating lift coefficients However, this was considered to be undesirable, as it was shown by Equation (9) of Section II that the blade area must be large to obtain high values of radial force.

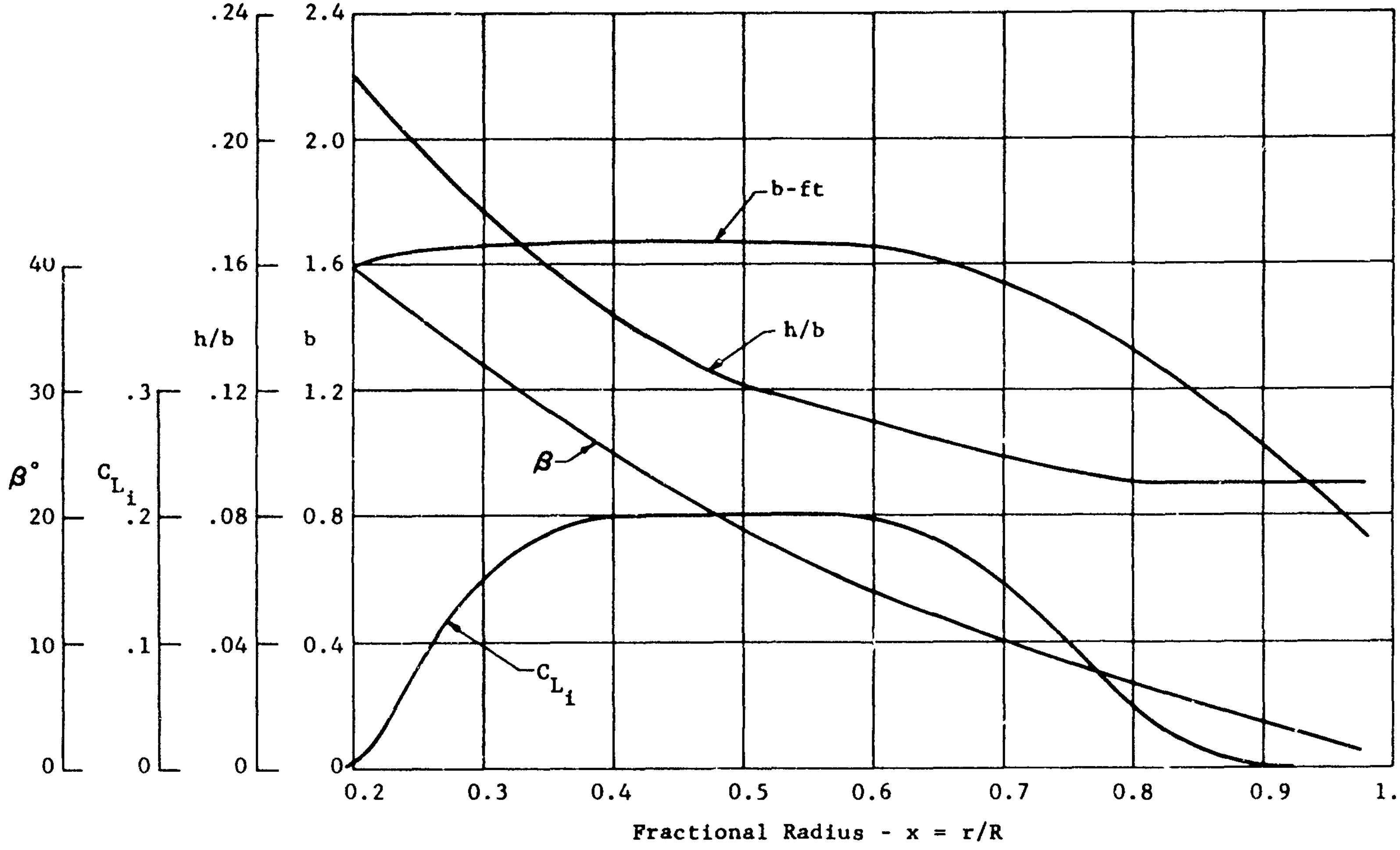

Figure 73. Blade characteristics of the Curtiss-Wright X-100 propeller 3(X100188) blade; Dia. = 10 ft., AF = 188, IC_{L_i} = 0.068.

FURNISHED UNDER UNITED STATES GOVERNMENT CONTRACT No. AF33(615)-3940. SHALL NOT BE EITHER RELEASED OUTSIDE THE GOVERNMENT, OR USED, DUPLICATED, OR DISCLOSED IN WHOLE OR IN PART FOR MANUFACTURE OR PROCUREMENT, WITHOUT THE WRITTEN PERMISSION OF CURTISS-WRIGHT CORPORATION, EXCEPT FOR (I) EMERGENCY REPAIR OR OVERHAUL WORK BY OR FOR THE GOVERNMENT, WHERE THE ITEM OR PROCESS IS NOT OTHERWISE REASONABLY AVAILABLE TO ENABLE TIMELY PERFORMANCE OF THE WORK, OR (II) RELEASE TO A FOREIGN GOVERNMENT, AS THE INTERESTS OF THE UNITED STATES MAY REQUIRE; PROVIDED THAT IN EITHER CASE THE RELEASE, USE, DUPLICATION OR DISCLOSURE HEREOF SHALL BE SUBJECT TO THE FOREGOING LIMITATIONS. THIS LEGEND SHALL BE MARKED ON ANY REPRODUCTION HEREOF IN WHOLE OR IN PART.

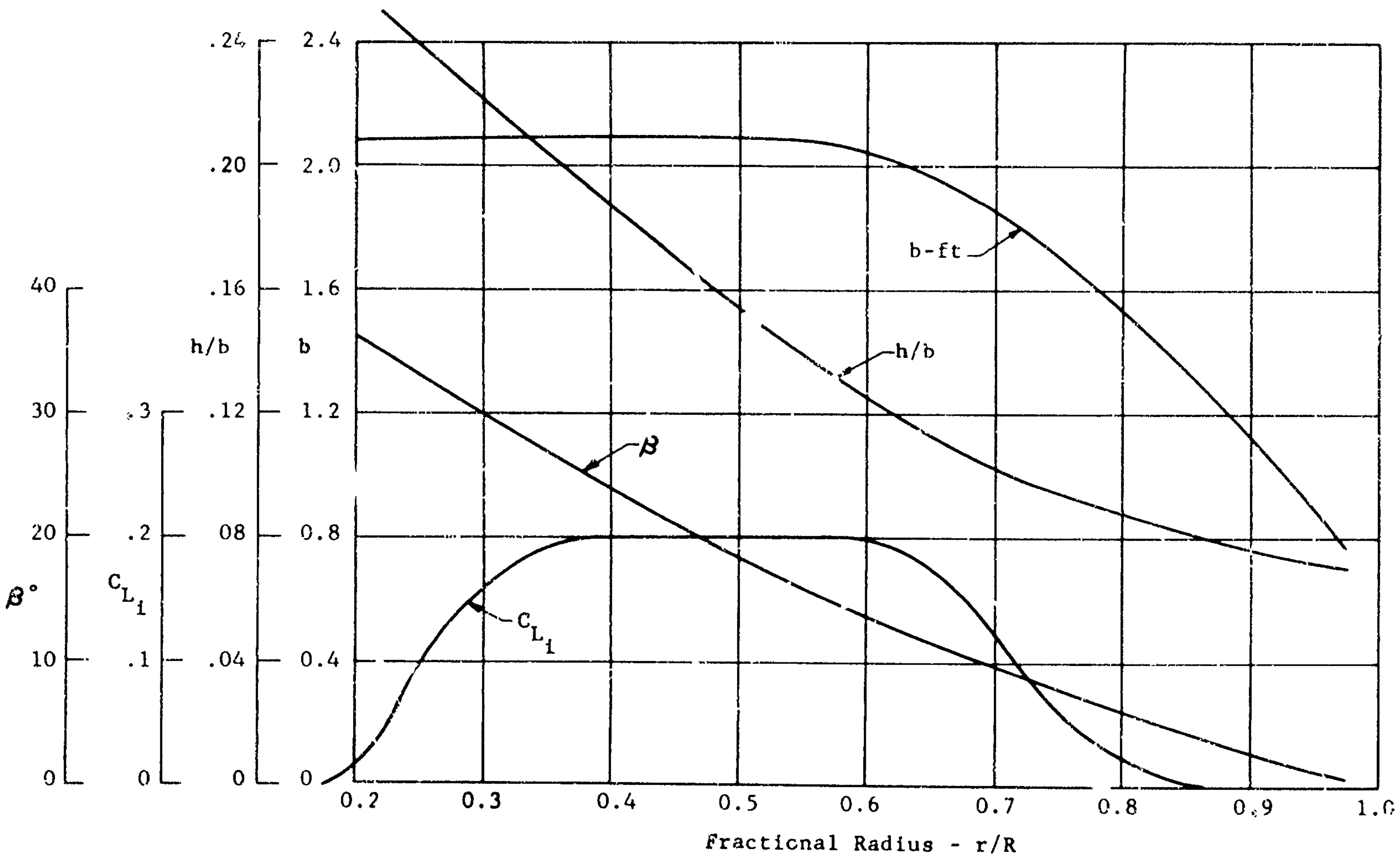

Figure 74. Blade characteristics of the X-19 propeller 3(130168) blade; Dia. = 13 ft., AF = 168, IC_{L_i} = 0.057.

FURNISHED UNDER UNITED STATES GOVERNMENT CONTRACT No. AF33(615)-3940 SHALL NOT BE EITHER RELEASED OUTSIDE THE GOVERNMENT, OR USED, DUPLICATED, OR DISCLOSED IN WHOLE OR IN PART FOR MANUFACTURE OR PROCUREMENT, WITHOUT THE WRITTEN PERMISSION OF CURTISS-WRIGHT CORPORATION, EXCEPT FOR (i) EMERGENCY REPAIR OR OVERHAUL WORK BY OR FOR THE GOVERNMENT, WHERE THE ITEM OR PROCESS IS NOT OTHERWISE REASONABLY AVAILABLE TO ENABLE TIMELY PERFORMANCE OF THE WORK, OR (ii) RELEASE TO A FOREIGN GOVERNMENT, AS THE INTERESTS OF THE UNITED STATES MAY REQUIRE. PROVIDED THAT IN EITHER CASE THE RELEASE, USE, DUPLICATION OR DISCLOSURE HEREOF SHALL BE SUBJECT TO THE FOREGOING LIMITATIONS. THIS LEGEND SHALL BE MARKED ON ANY REPRODUCTION HEREOF IN WHOLE OR IN PART."

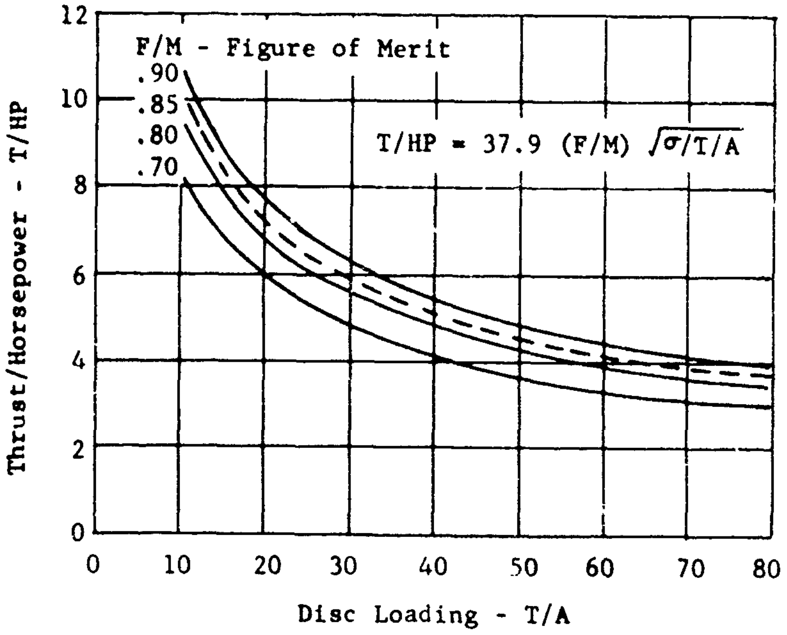

Figure 75. Power loading as a function of disk loading on a static isolated propeller, density ratio $\sigma = 1.0$.

"FURNISHED UNDER UNITED STATES GOVERNMENT CONTRACT No. AF33(615)-3940 SHALL NOT BE EITHER RELEASED OUTSIDE THE GOVERNMENT OR USED DUPLICATED, OR DISCLOSED IN WHOLE OR IN PART FOR MANUFACTURE OR PROCUREMENT, WITHOUT THE WRITTEN PERMISSION OF CURTISS-WRIGHT CORPORATION, EXCEPT FOR (I) EMERGENCY REPAIR OR OVERHAUL WORK BY OR FOR THE GOVERNMENT, WHERE THE ITEM OR PROCESS IS NOT OTHERWISE REASONABLY AVAILABLE TO ENABLE TIMELY PERFORMANCE OF THE WORK OR (II) RELEASE TO A FOREIGN GOVERNMENT, AS THE INTERESTS OF THE UNITED STATES MAY REQUIRE PROVIDED THAT IN EITHER CASE THE RELEASE USE DUPLICATION OR DISCLOSURE HEREOF SHALL BE SUBJECT TO THE FOREGOING LIMITATIONS THIS LEGEND SHALL BE MARKED ON ANY REPRODUCTION HEREOF IN WHOLE OR IN PART."

From Equation (9) it is seen that the blade area can be placed at any station along the blade and still be effective for producing radial force. By distributing the blade chord to minimize the power requirement it is possible to maximize radial force and still obtain high values of efficiency. The resulting blade planform is wide inboard and tapers to a narrow tip.

In the case of the X-100 airplane the blade area, if made rectangular, would have an activity factor of approximately 240 instead of the 188 value obtained with the tapered blade.

As is usual, in the practical design of a propeller, the solidity or activity factor and blade number are established by single point methods of calculation. The distribution of solidity in the case of the X-19 and X-100 aircraft are determined by the radial force lift requirements as well as manufacturing considerations. After the blade planform shape has been determined, the blade thickness ratio is found based on a structural load and weight analysis. The final design characteristics of the blade are then established by an optimization study which determines the best distribution of blade angle and design C_L. This optimization study is generally performed for each operating condition, and then the design C_L and blade angle adjusted so that the best overall propeller characteristics are found for the entire series of flight conditions.

The analysis of optimization for finding the best blade is done using the method of the Calculus of Variations (30). This method determines the best balance of the profile and induced losses to give peak overall performance. At each blade station the characteristics of list versus drag are determined for a range of design C_L, and the locus of the curve represents the best airfoil at any given operating C_L, see Figure 76. With this information available for each station, the distribution of induced losses is found by the method of (30) which gives the best overall performance available. This distribution is different than that which would be found for a frictionless propeller as represented by the well known Betz loading criteria, which gives the best load distribution for the blade operating at zero drag.

It will be noted from Figure 76 that once the operating C_L is obtained for peak performance, the resulting design C_L must be found, and at a given station there are more than one value of design C_L's that can be used and still obtain peak performance. For instance, at the cruise operating C_L, a design C_L of either 0.2 or 0.3 could be used and still obtain the same C_D and L/D. Consideration is therefore given when balancing the blade for all the flight conditions, to choosing the design C_L that is best for all the flight conditions.

If a large difference in design C_L requirements for peak efficiency is encountered between two flight conditions, the design C_L is chosen based on the value required for the most important flight condition. These procedures will give the characteristics required for the best overall propeller. With the X-100 and X-19 airplanes, a fixed design C_L at each station was found to be nearly optimum for all flight conditions.

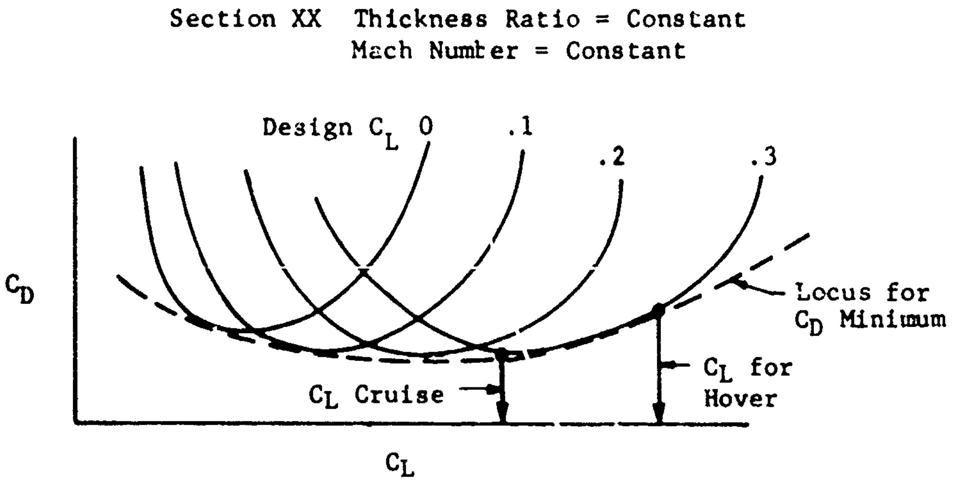

Figure 76. Typical drag polar as a function of design C_L.

The blades for both the X-100 and X-19 aircraft were designed to use NACA 64 series airfoil sections. These sections were chosen as test results indicated slightly higher levels of static thrust are obtained with these blade sections than with the conventional NACA 16 series propeller section. The reason for this improvement is the increased lift drag ratio obtained with the 64 series sections. The blades with 64 series sections operate at better efficiency than equivalent blades with 16 series sections when the power is above the design value as during a control input in hover because of the higher level of maximum lift coefficient available with the "64" series sections.

The blades for the X-19 propeller are very nearly the same as the X-100 propeller blades. The planform of the two blades would be geometrically similar, if the 130166 (X-19) blade were cut back to 12'6" diameter. The extension was made on the blade when it became apparent that the weight of the aircraft had increased 8%. The thickness ratio of the 130166 blade was less outboard, as higher tip section Mach numbers were expected with the X-19, when operating at its design 400 mph cruise condition. With the tip thickness ratio of 7%, the losses due to compressibility are reduced.

In choosing the geometric characteristics of the X-19 blade it was desired to maintain the configuration as near to the X-100 as possible. This was done since the front wing of the X-19 was geometrically similar to that of the X-100. It was preferable to stay close to the experience gained with the X-100 test aircraft.

2. AERODYNAMIC DESIGN

The methods and data for the aerodynamic design of propellers were established between 1948 and 1954. The methods for forward flight conditions were developed using the theory of propellers described by Theodorsen, (24), for calculating the induced velocity at each blade station and thus determining proper section angle of attack and induced efficiency. The strip analysis procedures used for single and dual rotation propellers are completely described in (25) and (26) and are arranged to be used with any set of two dimensional airfoil data.

The airfoil data used in calculating the performance of a propeller is given in (27). This airfoil data is a correlation of all the two dimensional section data then available. Sections with thickness ratio's from 4 to 21% and design lift coefficients from 0 to 0.7 are covered in this report. The data covers a Mach number range from 0 to 1.6 and an angle of attack range through the stall angle.

For sections having a thickness ratio exceeding 21% the data given in (28) are used. The data given in this report covers the Reynolds Number range, of major importance with thick airfoil sections as well as the range of angle attack and Mach number.

The calculated propeller performance, using the methods and airfoil data given in (25) to (27), checks wind tunnel test data closely for the range of flight conditions of the X-100 and the X-19 airplanes. An accuracy of ± 1% can be expected for the case where the propellers are operating at small shaft angles and advance ratio's of 0.5 to 3.5. Only when the propellers are operating at loadings below that for peak efficiency does the calculated performance accuracy deviate more than 1%. In this case errors up to 4% can be expected. Unfortunately, the error between the tests and calculations have been quite inconsistent; therefore the possibility exists that an error is in the test data. This problem has been the subject of considerable investigation, but is yet to be resolved.

The strip analysis procedure used to calculate the performance of propellers at the hover condition is given in (29). This procedure is an extension of the flight strip analysis method, assuming that the inflow velocity determines the pitch of the wake helices. It was necessary to extrapolate the basic Theodorsen curves to determine the inflow velocity on the basis of this assumption. A propeller operating at the hover condition generally has some of the sections stalled. It was found necessary to extend the basic airfoil data of (27) beyond the stall angle so that the working data would be available. The procedure is given in (29). It was noted that to obtain agreement between propeller test and calculations the lift must be much higher than would be measured in two dimensional airfoil tests.

The procedure for determining the optimum design C_L, blade angle or chord distribution to obtain peak efficiency at any blade station is given in (30). This procedure was developed using the Calculus of Variations for balancing the profile and induced losses. It provides the designer with a tool for evaluating the performance with respect to the peak and has been an effective procedure for designing blades.

For initial propeller performance calculations the methods and data of (22) or (23) may be used. These are single point methods of analysis and are useful for sizing the propeller and determining the proper efficiency level. (22) is preferred for this use, as the effort required for the calculations is considerably reduced.

3. HOVER PERFORMANCE AS MEASURED AND CALCULATED

The performance of the propellers used on the X-100 and X-19 VTOL airplanes was measured on several test rigs and in various scale configurations including full scale (See Section IX). The hover performance of the full scale X-100 propeller as measured in the Ames 40 x 80 foot wind tunnel is shown on Figure 77 along with calculated performance and the measured performance of the 15% scale model propeller. The full scale data, (31), was obtained by mounting the propeller in the hover position and measuring the performance without the tunnel operating. The propeller was about three diameters above the floor of the tunnel and therefore was considered out of ground effects. The model data were obtained on a rig that had zero blockage and were run under free air operating conditions. The performance was calculated using the method and data of (29). The X-100 propeller was also tested on Rig No. 2 at Wright Field and the results are given on Figures 78 and 79.

The data given on Figure 77 indicates that calculated performance is much higher than obtained from test. Also, the model results are of little value for finding the overall performance at hover. The calculated performance is high, probably due to the underestimation of the induced losses. It is believed that the induced losses are underestimated rather than the profile losses as the airfoil data used to find the profile losses is also used to find the profile losses in cruise and the calculated performance agrees closely with test data in cruise This has since been the subject of study to determine a theory to correct this difficulty. The model propeller test results do not represent full scale performance because of the low Reynolds Number involved. A comparison of the data from Rig No. 2 and the Ames data, (31) indicate that fair agreement was obtained although the data from the two rigs, when plotted, cross over. Because of the blockage experienced by the propeller on Rig No. 2, it is believed that the Ames data is more representative of the actual performance. It should be pointed out here that because of the difficulty encountered with calculations, only test data were relied upon for predicting static performance of propellers for the X-100, X-19 and other V/STOL aircraft of interest.

The take-off performance of the X-19 was originally determined on the basis of performance measured in the Ames tunnel and shown on Figure 77. Therefore reliable predictions of the hover performance was obtained on the X-19.

Later hover performance characteristics of the X-19 propeller are shown on Figures 80 to 82, as determined on Rig No. 2 at Wright Field. Comparison of these results with the measurements taken from the X-100 propeller indicates the performance of both propellers are nearly identical. The Figure of Merit as determined by these tests peaks at approximately 73.5%.

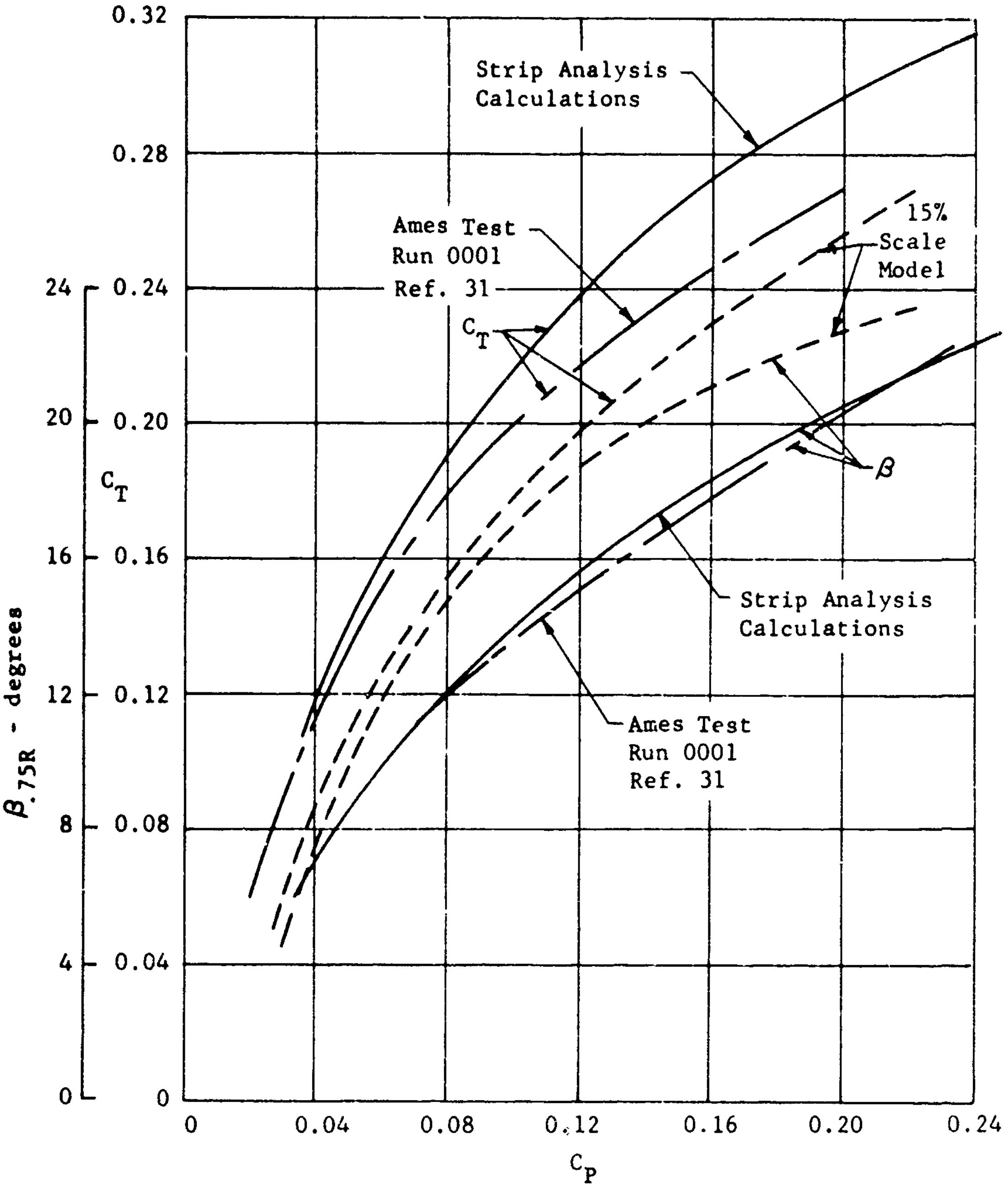

Figure 77. Blade angle and thrust coefficient as a function of power coefficient, static performance, 3(X100188) blade, 500 to 800 πnD

"FURNISHED UNDER UNITED STATES GOVERNMENT CONTRACT No AF33(615)-3940 SHALL NOT BE EITHER RELEASED OUTSIDE THE GOVERNMENT OR USED DUPLICATED, OR DISCLOSED IN WHOLE OR IN PART FOR MANUFACTURE OR PROCUREMENT, WITHOUT THE WRITTEN PERMISSION OF CURTISS-WRIGHT CORPORATION, EXCEPT FOR (I) EMERGENCY REPAIR OR OVERHAUL WORK BY OR FOR THE GOVERNMENT, WHERE THE ITEM OR PROCESS IS NOT OTHERWISE REASONABLY AVAILABLE TO ENABLE TIMELY PERFORMANCE OF THE WORK. OR (II) RELEASE TO A FOREIGN GOVERNMENT, AS THE INTERESTS OF THE UNITED STATES MAY REQUIRE PROVIDED THAT IN EITHER CASE THE RELEASE, USE, DUPLICATION OR DISCLOSURE HEREOF SHALL BE SUBJECT TO THE FOREGOING LIMITATIONS. THIS LEGEND SHALL BE MARKED ON ANY REPRODUCTION HEREOF IN WHOLE OR IN PART."

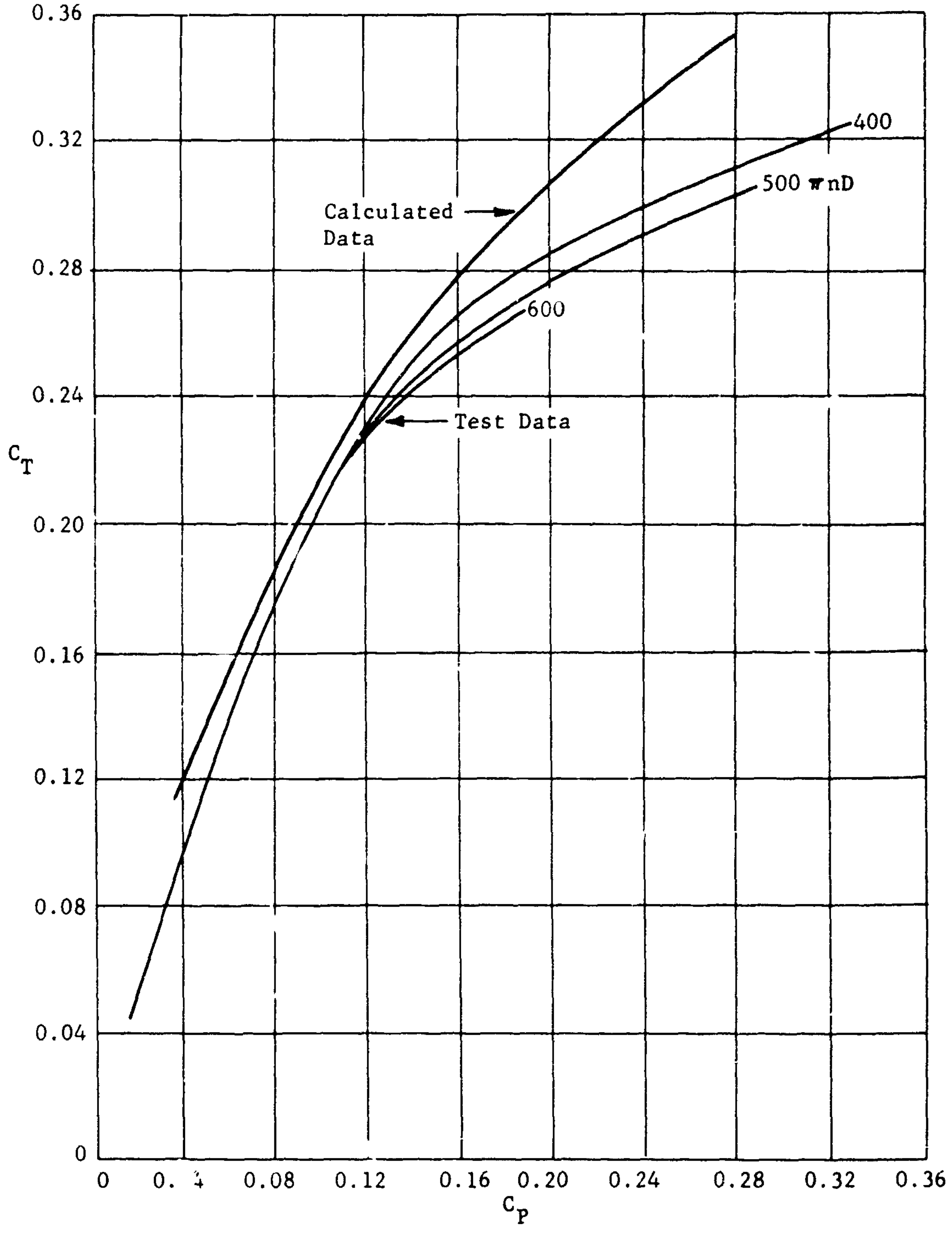

Figure 78. Thrust coefficient as a function of power coefficient, static whirl test dated 7/19/60, Wright-Patterson Air Force Base whirl rig no. 2; model 138592/10188A2F, dia. = 10 ft., AF = 188, IC_{L_i} = 0.068, 1000 horsepower, NACA 64 section series.

"FURNISHED UNDER UNITED STATES GOVERNMENT CONTRACT No. AF33(615)-3940. SHALL NOT BE EITHER RELEASED OUTSIDE THE GOVERNMENT, OR USED, DUPLICATED, OR DISCLOSED IN WHOLE OR IN PART FOR MANUFACTURE OR PROCUREMENT, WITHOUT THE WRITTEN PERMISSION OF CURTISS-WRIGHT CORPORATION, EXCEPT FOR (I) EMERGENCY REPAIR OR OVERHAUL WORK BY OR FOR THE GOVERNMENT, WHERE THE ITEM OR PROCESS IS NOT OTHERWISE REASONABLY AVAILABLE TO ENABLE TIMELY PERFORMANCE OF THE WORK, OR (II) RELEASE TO A FOREIGN GOVERNMENT, AS THE INTERESTS OF THE UNITED STATES MAY REQUIRE. PROVIDED THAT IN EITHER CASE THE RELEASE, USE, DUPLICATION OR DISCLOSURE HEREOF SHALL BE SUBJECT TO THE FOREGOING LIMITATIONS. THIS LEGEND SHALL BE MARKED ON ANY REPRODUCTION HEREOF IN WHOLE OR IN PART."

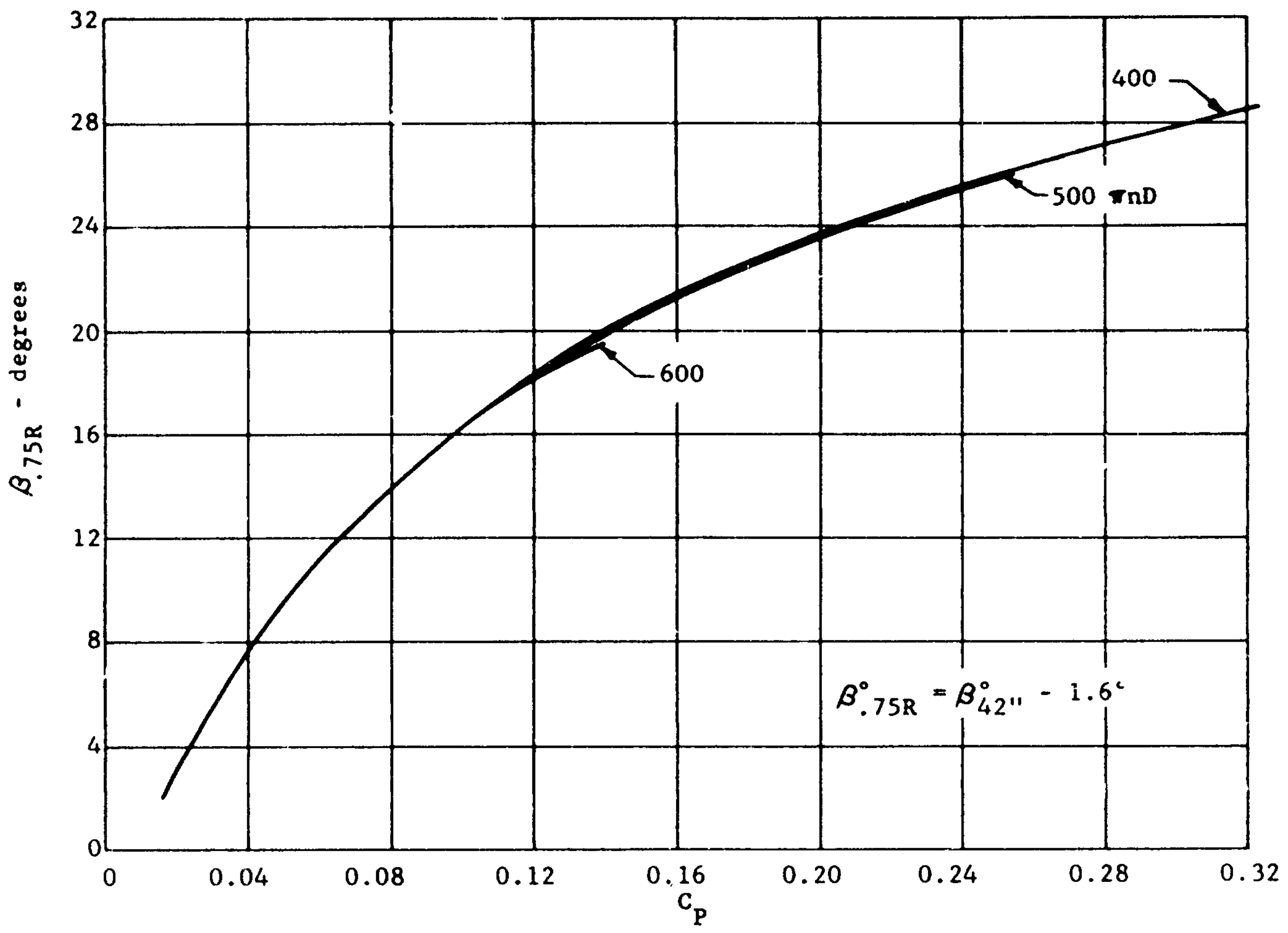

Figure 79. Blade angle as a function of power coefficient, static whirl test dated 7/9/60, Wright-Patterson Air Force Base whirl rig no. 2; model 138542/10188A2F, dia. = 10 ft., AF = 188, IC_{L_i} = 0.068, 1000 horsepower

"FURNISHED UNDER UNITED STATES GOVERNMENT CONTRACT No. AF33(615)-3940 SHALL NOT BE EITHER RELEASED OUTSIDE THE GOVERNMENT OR USED DUPLICATED, OR DISCLOSED IN WHOLE OR IN PART FOR MANUFACTURE OR PROCUREMENT, WITHOUT THE WRITTEN PERMISSION OF CURTISS-WRIGHT CORPORATION, EXCEPT FOR (I) EMERGENCY REPAIR OR OVERHAUL WORK BY OR FOR THE GOVERNMENT, WHERE THE ITEM OR PROCESS IS NOT OTHERWISE REASONABLY AVAILABLE TO ENABLE TIMELY PERFORMANCE OF THE WORK OR (II) RELEASE TO A FOREIGN GOVERNMENT, AS THE INTERESTS OF THE UNITED STATES MAY REQUIRE. PROVIDED THAT IN EITHER CASE THE RELEASE, USE, DUPLICATION OR DISCLOSURE HEREOF SHALL BE SUBJECT TO THE FOREGOING LIMITATIONS. THIS LEGEND SHALL BE MARKED ON ANY REPRODUCTION HEREOF IN WHOLE OR IN PART."

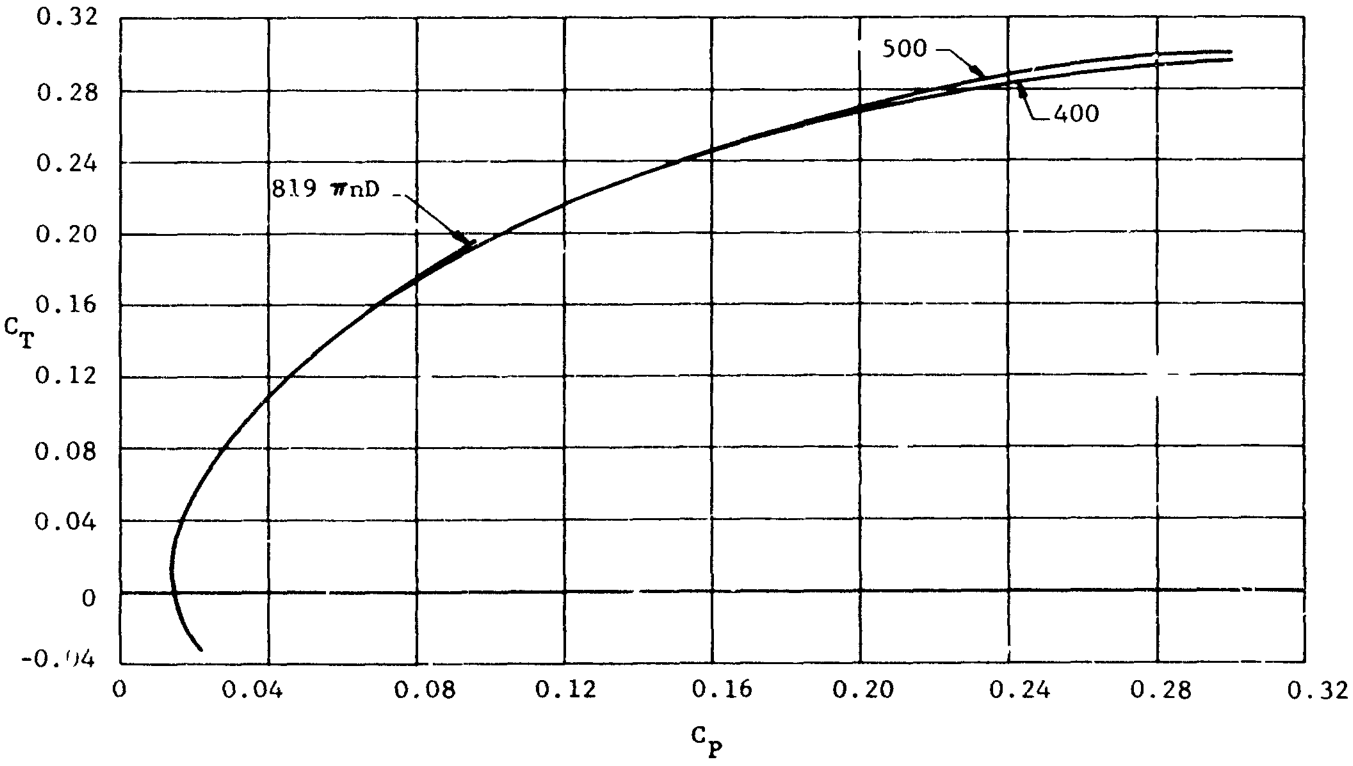

Figure 8C. X-19 thrust coefficient as a function of power coefficient, static, Wright-Patterson Air Force Base whirl rig no. 2; 3(1368A10P3), dia. = 13 ft., AF = 168, IC_{L_i} = 0.057, NACA 64 series sections, 1000 horsepower.

FURNISHED UNDER UNITED STATES GOVERNMENT CONTRACT No. AF33(615)-3940. SHALL NOT BE EITHER RELEASED OUTSIDE THE GOVERNMENT, OR USED, DUPLICATED OR DISCLOSED IN WHOLE OR IN PART FOR MANUFACTURE OR PROCUREMENT, WITHOUT THE WRITTEN PERMISSION OF CURTISS-WRIGHT CORPORATION, EXCEPT FOR (i) EMERGENCY REPAIR OR OVERHAUL WORK BY OR FOR THE GOVERNMENT, WHERE THE ITEM OR PROCESS IS NOT OTHERWISE REASONABLY AVAILABLE TO ENABLE TIMELY PERFORMANCE OF THE WORK, OR (ii) RELEASE TO A FOREIGN GOVERNMENT, AS THE INTERESTS OF THE UNITED STATES MAY REQUIRE; PROVIDED THAT IN EITHER CASE THE RELEASE, USE, DUPLICATION OR DISCLOSURE HEREOF SHALL BE SUBJECT TO THE FOREGOING LIMITATIONS. THIS LEGEND SHALL BE MARKED ON ANY REPRODUCTION HEREOF IN WHOLE OR IN PART."

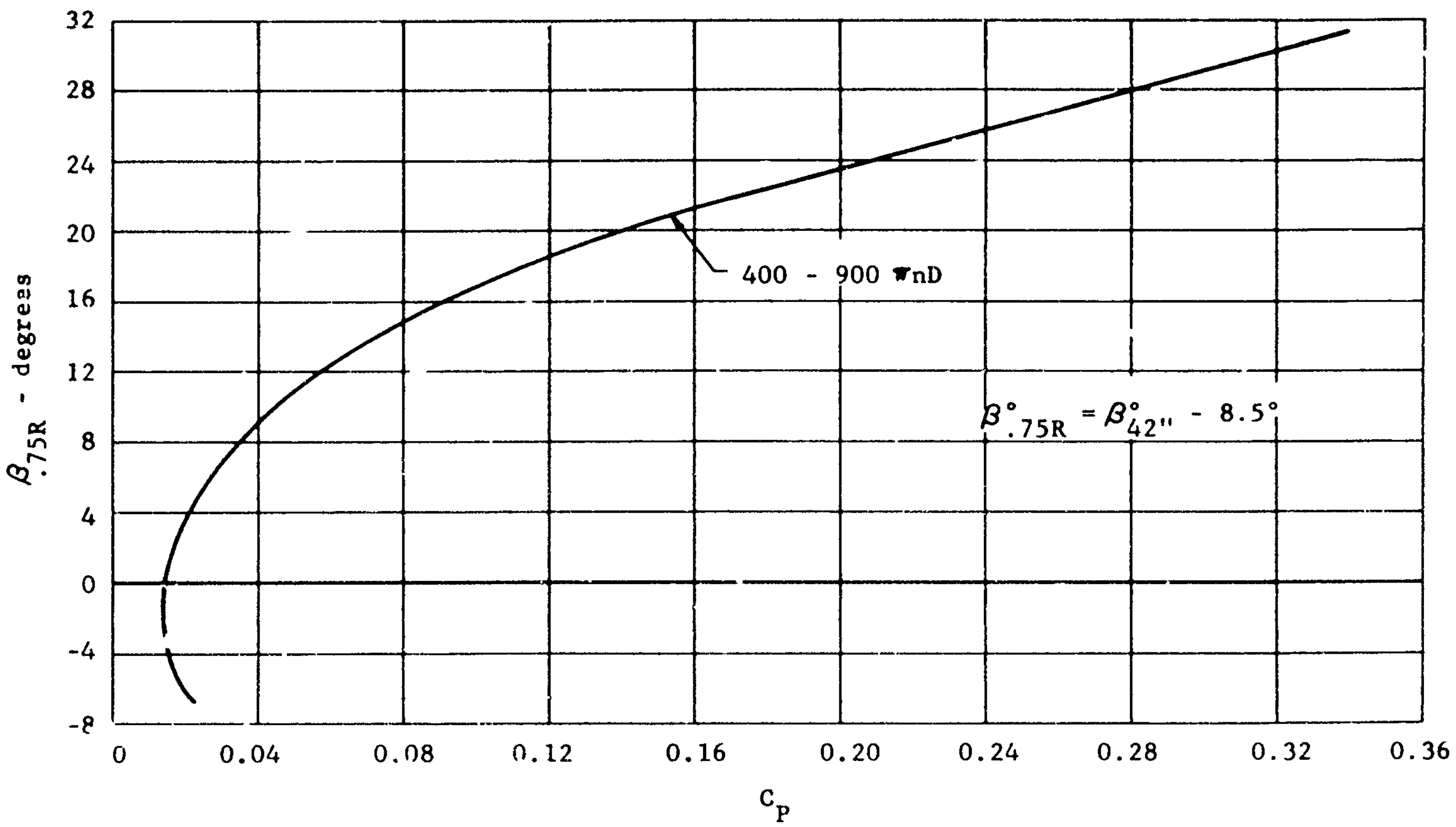

Figure 81. X-19 propeller blade angle as a function of power coefficient, static, Wright-Patterson Air Force Base whirl rig no. 2; 3(13168A10P3), dia. = 13 ft., AF = 168, IC_{L_i} = 0.057, NACA 64 series sections, 1000 horsepower.

FURNISHED UNDER UNITED STATES GOVERNMENT CONTRACT No. AF33(615)-3940 SHALL NOT BE EITHER RELEASED OUTSIDE THE GOVERNMENT, OR USED, DUPLICATED, OR DISCLOSED IN WHOLE OR IN PART FOR MANUFACTURE OR PROCUREMENT, WITHOUT THE WRITTEN PERMISSION OF CURTISS-WRIGHT CORPORATION EXCEPT FOR (i) EMERGENCY REPAIR OR OVERHAUL WORK BY OR FOR THE GOVERNMENT, WHERE THE ITEM OR PROCESS IS NOT OTHERWISE REASONABLY AVAILABLE TO ENABLE TIMELY PERFORMANCE OF THE WORK, OR (ii) RELEASE TO A FOREIGN GOVERNMENT AS THE INTERESTS OF THE UNITED STATES MAY REQUIRE. PROVIDED THAT IN EITHER CASE THE RELEASE, USE, DUPLICATION OR DISCLOSURE HEREOF SHALL BE SUBJECT TO THE FOREGOING LIMITATIONS. THIS LEGEND SHALL BE MARKED ON ANY REPRODUCTION HEREOF IN WHOLE OR IN PART.

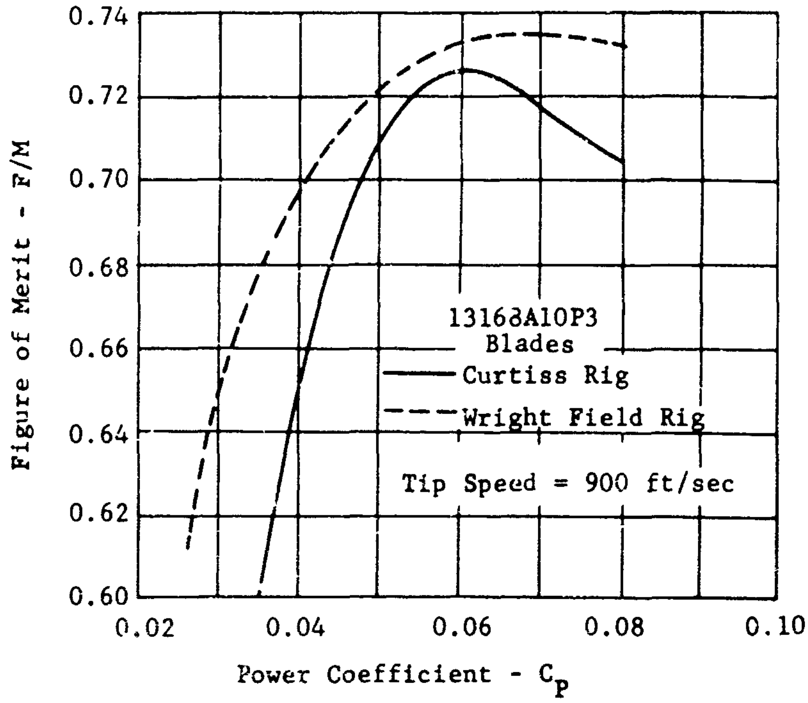

Figure 82. X-19, figure of merit as a function of power coefficient, static, Wright-Patterson Air Force Base whirl rig no. 2; 3(1368A10P3), dia. = 13 ft., AF = 168, IC_{L_i} = 0.057, NACA 64 series sections, 1000 horsepower.

FURNISHED UNDER UNITED STATES GOVERNMENT CONTRACT No AF33(615)-3940 SHALL NOT BE EITHER RELEASED OUTSIDE THE GOVERNMENT, OR USED, DUPLICATED, OR DISCLOSED IN WHOLE OR IN PART FOR MANUFACTURE OR PROCUREMENT, WITHOUT THE WRITTEN PERMISSION OF CURTISS-WRIGHT CORPORATION, EXCEPT FOR (I) EMERGENCY REPAIR OR OVERHAUL WORK BY OR FOR THE GOVERNMENT, WHERE THE ITEM OR PROCESS IS NOT OTHERWISE REASONABLY AVAILABLE TO ENABLE TIMELY PERFORMANCE OF THE WORK, OR (II) RELEASE TO A FOREIGN GOVERNMENT, AS THE INTERESTS OF THE UNITED STATES MAY REQUIRE. PROVIDED THAT IN EITHER CASE THE RELEASE, USE, DUPLICATION OR DISCLOSURE HEREOF SHALL BE SUBJECT TO THE FOREGOING LIMITATIONS. THIS LEGEND SHALL BE MARKED ON ANY REPRODUCTION HEREOF IN WHOLE OR IN PART.'

This compares with a level of 80-plus percent observed from tests of other propellers.

Since the measured static thrust performance is far below the expected level, a research program was undertaken to find ways and means of improving the efficiency. As part of this program a rig was built for measuring the performance without blockage present.

The highlights of the program, including a description of the test rig, are discussed in (32). The static performance of the X-19 propeller was measured on this rig, the results of which are shown on Figures 83 and 84. The data obtained from the Curtiss Rig is 1 to 2 percent lower in Figure of Merit than from Wright Field Rig No. 2. This change is due to blockage and interference from the Wright Field rig and was expected. See (32).

It was found that measurement of the full scale static thrust performance with desired accuracy is extremely difficult. The reason for this is that forces are large and therefore the interaction between thrust force and the torque is difficult to isolate. Furthermore, the propellers must be tested at nearly zero wind conditions to obtain consistent values. As a result, considerable effort is required to obtain satisfactory propeller performance data. The test results presented are believed to accurately describe the propeller hover performance.

4. CRUISE PERFORMANCE MAPS

Performance of the X-100 and X-19 propellers at zero to $\pm 10^{\circ}$ shaft angle flight conditions, can be determined from the efficiency maps, Figures 85 to 91. These maps were calculated based on the methods and data of (25) and (27). For the X-100 propeller, the data covers only operating conditions when the helical tip Mach is less than 0.3. The maps for the X-19 propeller cover conditions up to a forward Mach number of 0.8. As the methods and data given in (25) and (27) have been highly developed, and checked, the data on the maps can be considered to be accurate within $\pm$ 2%.

5. EFFECTS OF TIP SPEED AND BLADE TWIST IN HOVER AND CRUISE

In hover, the effect of changes in tip speed and pitch distribution must be determined by test, as suitable methods and data are not yet available for calculations. With the X-19 and X-100 blades, changes in hover performance with changes in tip speed was not clearly established by the test data, Figures 78, 80 and 83. At the lower loadings it appears that the higher tip speeds result in improvements, whereas at high loadings the reverse is true. The three blade propeller using 109652 blades shown on Figure 92 shows a large improvement in performance with increases of tip speed. The reason for this improvement is probably due to improved load distribution as a result of changes in lift curve slope at the higher tip Mach Number.

The 109652 blade was retwisted as shown on Figure 92. From Figure 94 note that lower values of Figure of Merit are obtained with the retwisted blade, at power coefficients near the peak, than with the original blade.

FURNISHED UNDER UNITED STATES GOVERNMENT CONTRACT No. AF33(615)-3940 SHALL NOT BE EITHER RELEASED OUTSIDE THE GOVERNMENT OR USED DUPLICATED, OR DISCLOSED IN WHOLE OR IN PART FOR MANUFACTURE OR PROCUREMENT, WITHOUT THE WRITTEN PERMISSION OF CURTISS-WRIGHT CORPORATION, EXCEPT FOR (I) EMERGENCY REPAIR OR OVERHAUL WORK BY OR FOR THE GOVERNMENT, WHERE THE ITEM OR PROCESS IS NOT OTHERWISE REASONABLY AVAILABLE TO ENABLE TIMELY PERFORMANCE OF THE WORK OR (II) RELEASE TO A FOREIGN GOVERNMENT, AS THE INTERESTS OF THE UNITED STATES MAY REQUIRE PROVIDED THAT IN EITHER CASE THE RELEASE USE, DUPLICATION OR DISCLOSURE HEREOF SHALL BE SUBJECT TO THE FOREGOING LIMITATIONS. THIS LEGEND SHALL BE MARKED ON ANY REPRODUCTION HEREOF IN WHOLE OR IN PART."

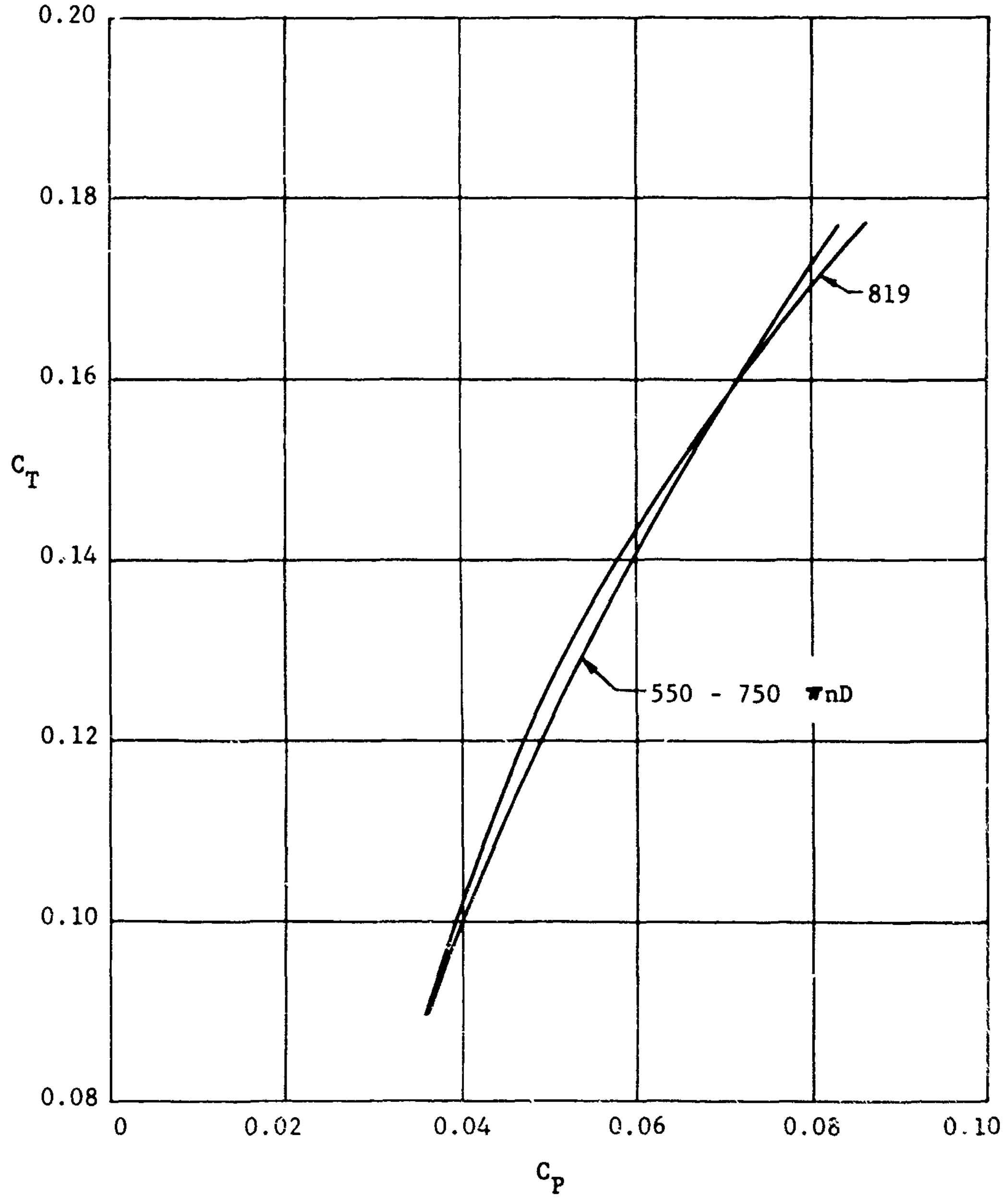

Figure 83. X-19, thrust coefficient versus power coefficient, static; 3(13168A10P3) blade, Curtiss-Wright whirl test rig.

"FURNISHED UNDER UNITED STATES GOVERNMENT CONTRACT No. AF33(615)-3945. SHALL NOT BE EITHER RELEASED OUTSIDE THE GOVERNMENT, OR USED, DUPLICATED OR DISCLOSED IN WHOLE OR IN PART FOR MANUFACTURE OR PROCUREMENT, WITHOUT THE WRITTEN PERMISSION OF CURTISS-WRIGHT CORPORATION EXCEPT FOR (i) EMERGENCY REPAIR OR OVERHAUL WORK BY OR FOR THE GOVERNMENT, WHERE THE ITEM OR PROCESS IS NOT OTHERWISE REASONABLY AVAILABLE TO ENABLE TIMELY PERFORMANCE OF THE WORK. OR (ii) RELEASE TO A FOREIGN GOVERNMENT, AS THE INTERESTS OF THE UNITED STATES MAY REQUIRE. PROVIDED THAT IN EITHER CASE THE RELEASE, USE, DUPLICATION OR DISCLOSURE HEREOF SHALL BE SUBJECT TO THE FOREGOING LIMITATIONS. THIS LEGEND SHALL BE MARKED ON ANY REPRODUCTION HEREOF IN WHOLE OR IN PART."

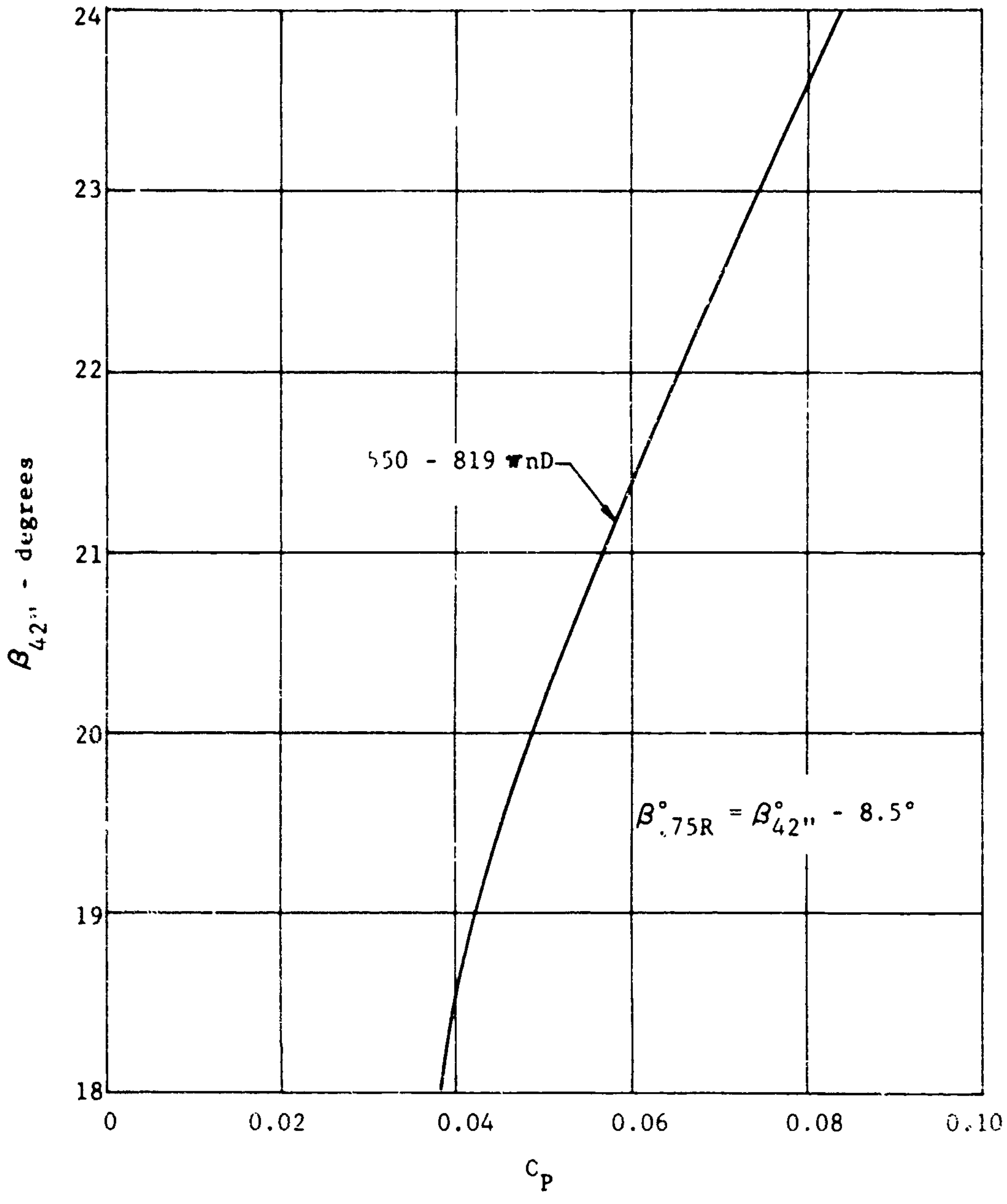

Figure 84. X-19 propeller blade angle versus power coefficient, static; 3(13168A10P3) blade, Curtiss-Wright whirl test rig.

FURNISHED UNDER UNITED STATES GOVERNMENT CONTRACT No AF33(615)-3940 SHALL NOT BE EITHER RELEASED OUTSIDE THE GOVERNMENT, OR USED DUPLICATED, OR DISCLOSED IN WHOLE OR IN PART FOR MANUFACTURE OR PROCUREMENT, WITHOUT THE WRITTEN PERMISSION OF CURTISS-WRIGHT CORPORATION, EXCEPT FOR (i) EMERGENCY REPAIR OR OVERHAUL WORK BY OR FOR THE GOVERNMENT, WHERE THE ITEM OR PROCESS IS NOT OTHERWISE REASONABLY AVAILABLE TO ENABLE TIMELY PERFORMANCE OF THE WORK OR (ii) RELEASE TO A FOREIGN GOVERNMENT AS THE INTERESTS OF THE UNITED STATES MAY REQUIRE. PROVIDED THAT IN EITHER CASE THE RELEASE, USE DUPLICATION OR DISCLOSURE HEREOF SHALL BE SUBJECT TO THE FOREGOING LIMITATIONS THIS LEGEND SHALL BE MARKED ON ANY REPRODUCTION HEREOF IN WHOLE OR IN PART.'

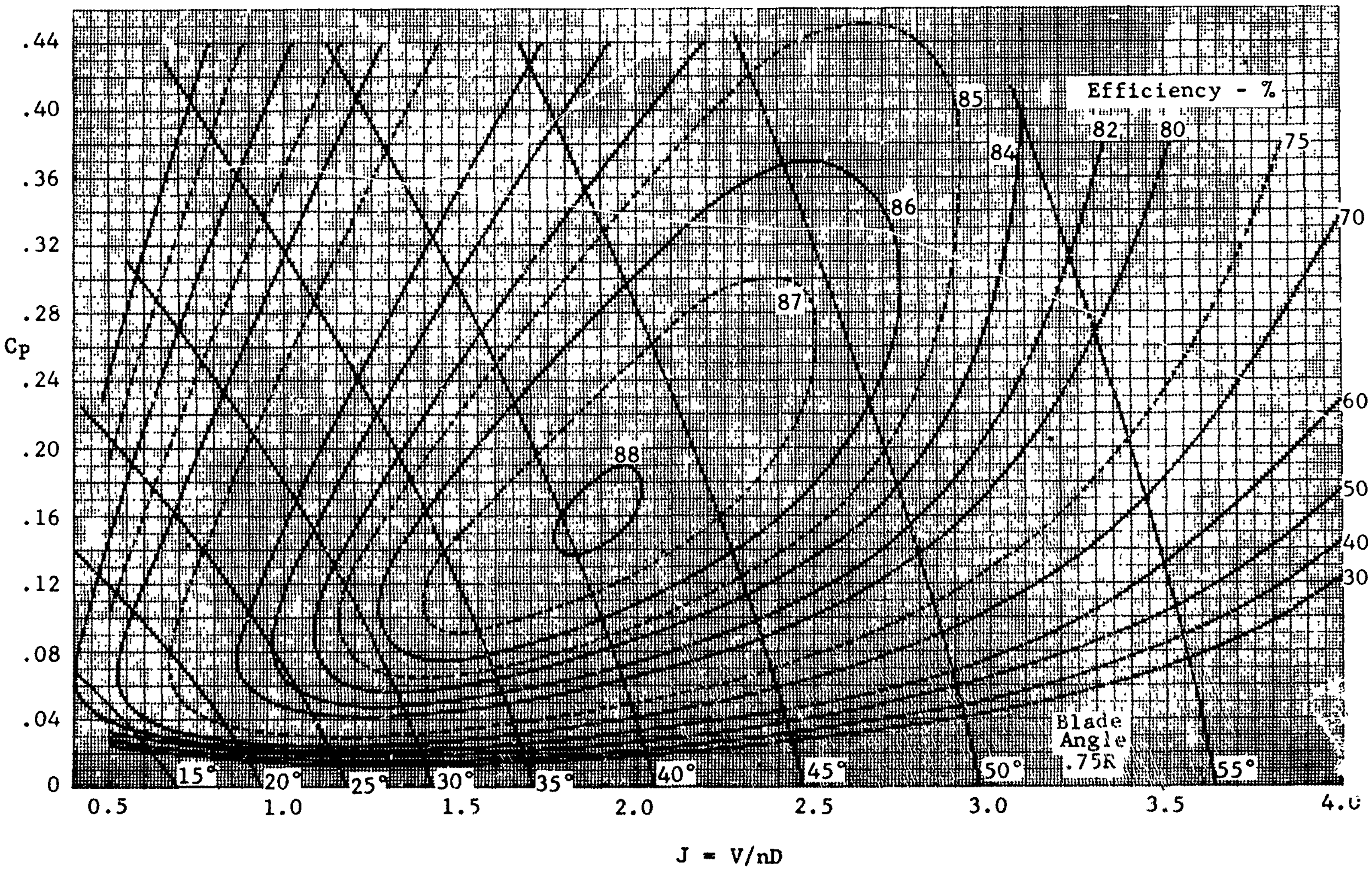

Figure 85. Propeller cruise coefficiency map, Curtiss-Wright X-100 propeller 3(X100188); AF = 188, dia. = 10 ft, IC_{L_i} = 0.067, forward Mach No. = 0.3 or less.

FURNISHED UNDER UNITED STATES GOVERNMENT CONTRACT No. AF33(615)-3940. SHALL NOT BE EITHER RELEASED OUTSIDE THE GOVERNMENT, OR USED DUPLICATED OR DISCLOSED IN WHOLE OR IN PART FOR MANUFACTURE OR PROCUREMENT, WITHOUT THE WRITTEN PERMISSION OF CURTISS-WRIGHT CORPORATION, EXCEPT FOR (i) EMERGENCY REPAIR OR OVERHAUL WORK BY OR FOR THE GOVERNMENT, WHERE THE ITEM OR PROCESS IS NOT OTHERWISE REASONABLY AVAILABLE TO ENABLE TIMELY PERFORMANCE OF THE WORK, OR (ii) RELEASE TO A FOREIGN GOVERNMENT, AS THE INTERESTS OF THE UNITED STATES MAY REQUIRE; PROVIDED THAT IN EITHER CASE THE RELEASE, USE, DUPLICATION OR DISCLOSURE HEREOF SHALL BE SUBJECT TO THE FOREGOING LIMITATIONS. THIS LEGEND SHALL BE MARKED ON ANY REPRODUCTION HEREOF IN WHOLE OR IN PART.

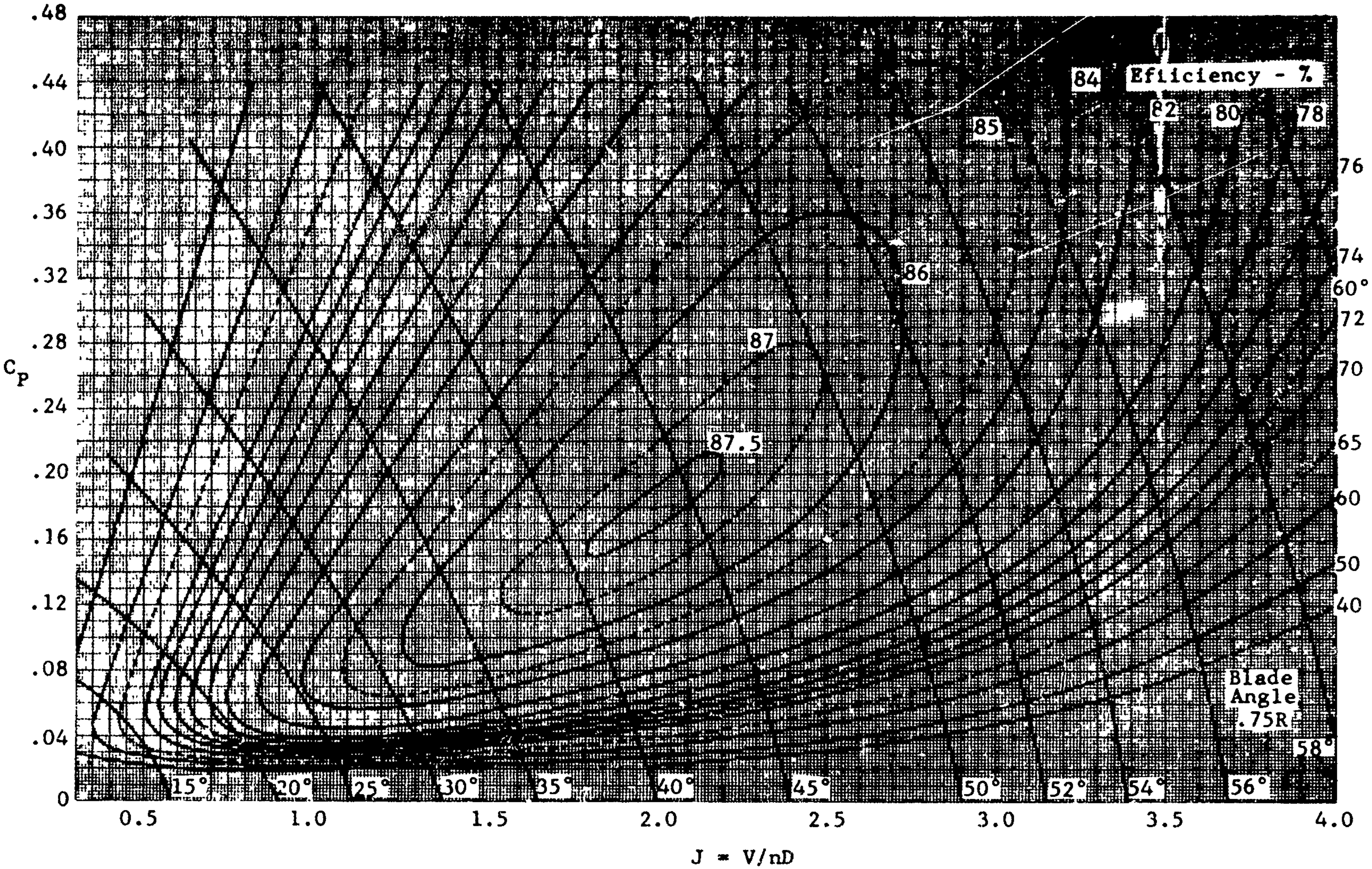

Figure 86. X-19, propeller cruise efficiency map, 3(13168A10P3) blade; AF = 168, dia. = 13 ft, IC_{L_i} = 0.057, forward Mach No. = 0.3 or less.

"FURNISHED UNDER UNITED STATES GOVERNMENT CONTRACT No AF33(615)-3940 SHALL NOT BE EITHER RELEASED OUTSIDE THE GOVERNMENT OR USED DUPLICATED, OR DISCLOSED IN WHOLE OR IN PART FOR MANUFACTURE OR PROCUREMENT, WITHOUT THE WRITTEN PERMISSION OF CURTISS-WRIGHT CORPORATION, EXCEPT FOR (I) EMERGENCY REPAIR OR OVERHAUL WORK BY OR FOR THE GOVERNMENT, WHERE THE ITEM OR PROCESS IS NOT OTHERWISE REASONABLY AVAILABLE TO ENABLE TIMELY PERFORMANCE OF THE WORK OR (II) RELEASE TO A FOREIGN GOVERNMENT, AS THE INTERESTS OF THE UNITED STATES MAY REQUIRE PROVIDED THAT IN EITHER CASE THE RELEASE, USE DUPLICATION OR DISCLOSURE HEREOF SHALL BE SUBJECT TO THE FOREGOING LIMITATIONS. THIS LEGEND SHALL BE MARKED ON ANY REPRODUCTION HEREOF IN WHOLE OR IN PART."

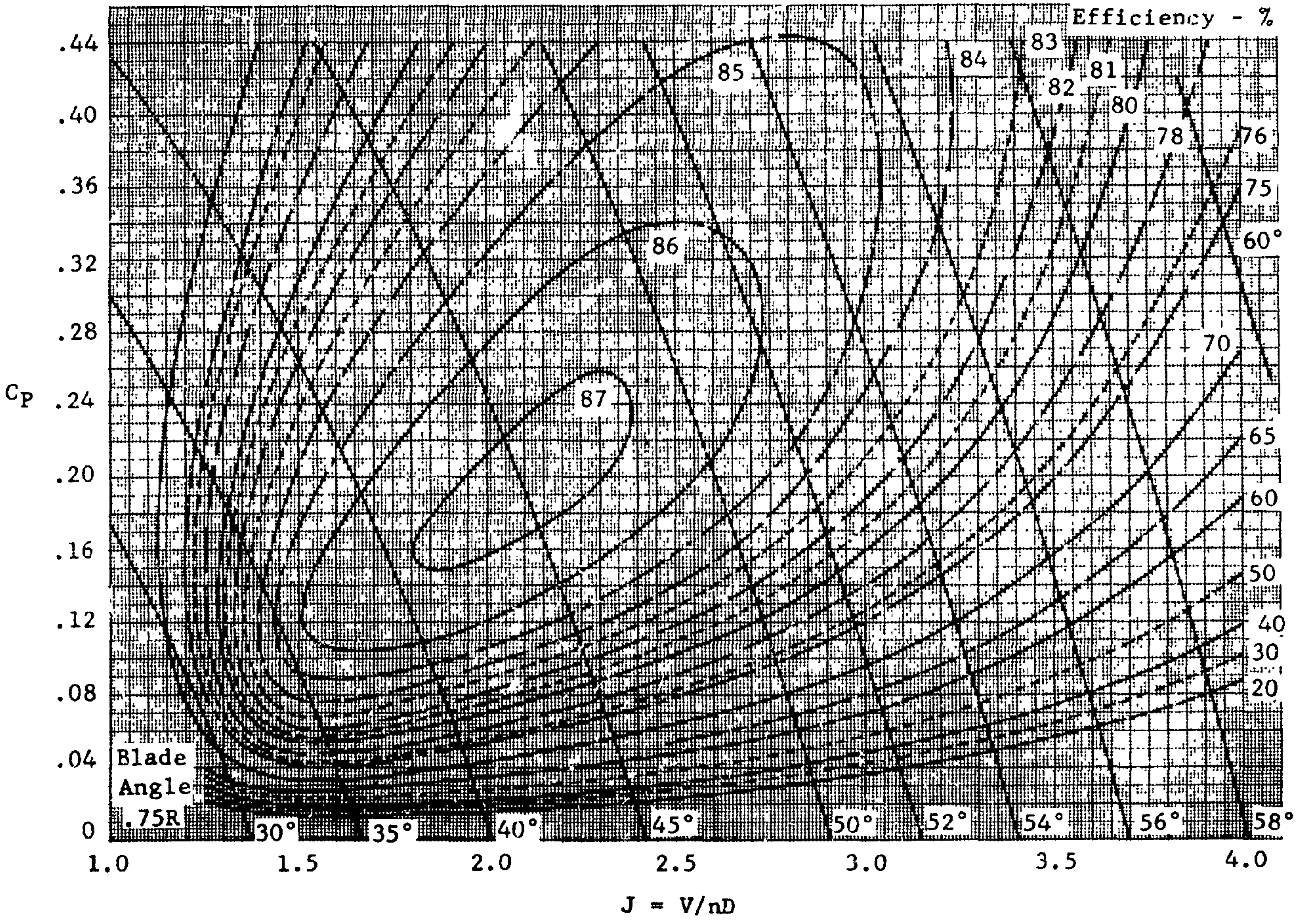

Figure 87. X-19, propeller cruise efficiency map, 3(13168A10P3) blade; AF = 168, dia. = 13 ft, IC_{L_i} = 0.057, forward Mach No. = 0.4 or less.

FURNISHED UNDER UNITED STATES GOVERNMENT CONTRACT No. AF33(615)-3940. SHALL NOT BE EITHER RELEASED OUTSIDE THE GOVERNMENT, OR USED, DUPLICATED, OR DISCLOSED IN WHOLE OR IN PART FOR MANUFACTURE OR PROCUREMENT, WITHOUT THE WRITTEN PERMISSION OF CURTISS-WRIGHT CORPORATION. EXCEPT FOR (I) EMERGENCY REPAIR OR OVERHAUL WORK BY OR FOR THE GOVERNMENT, WHERE THE ITEM OR PROCESS IS NOT OTHERWISE REASONABLY AVAILABLE TO ENABLE TIMELY PERFORMANCE OF THE WORK. OR (II) RELEASE TO A FOREIGN GOVERNMENT, AS THE INTERESTS OF THE UNITED STATES MAY REQUIRE. PROVIDED THAT IN EITHER CASE THE RELEASE, USE, DUPLICATION OR DISCLOSURE HEREOF SHALL BE SUBJECT TO THE FOREGOING LIMITATIONS. THIS LEGEND SHALL BE MARKED ON ANY REPRODUCTION HEREOF IN WHOLE OR IN PART."

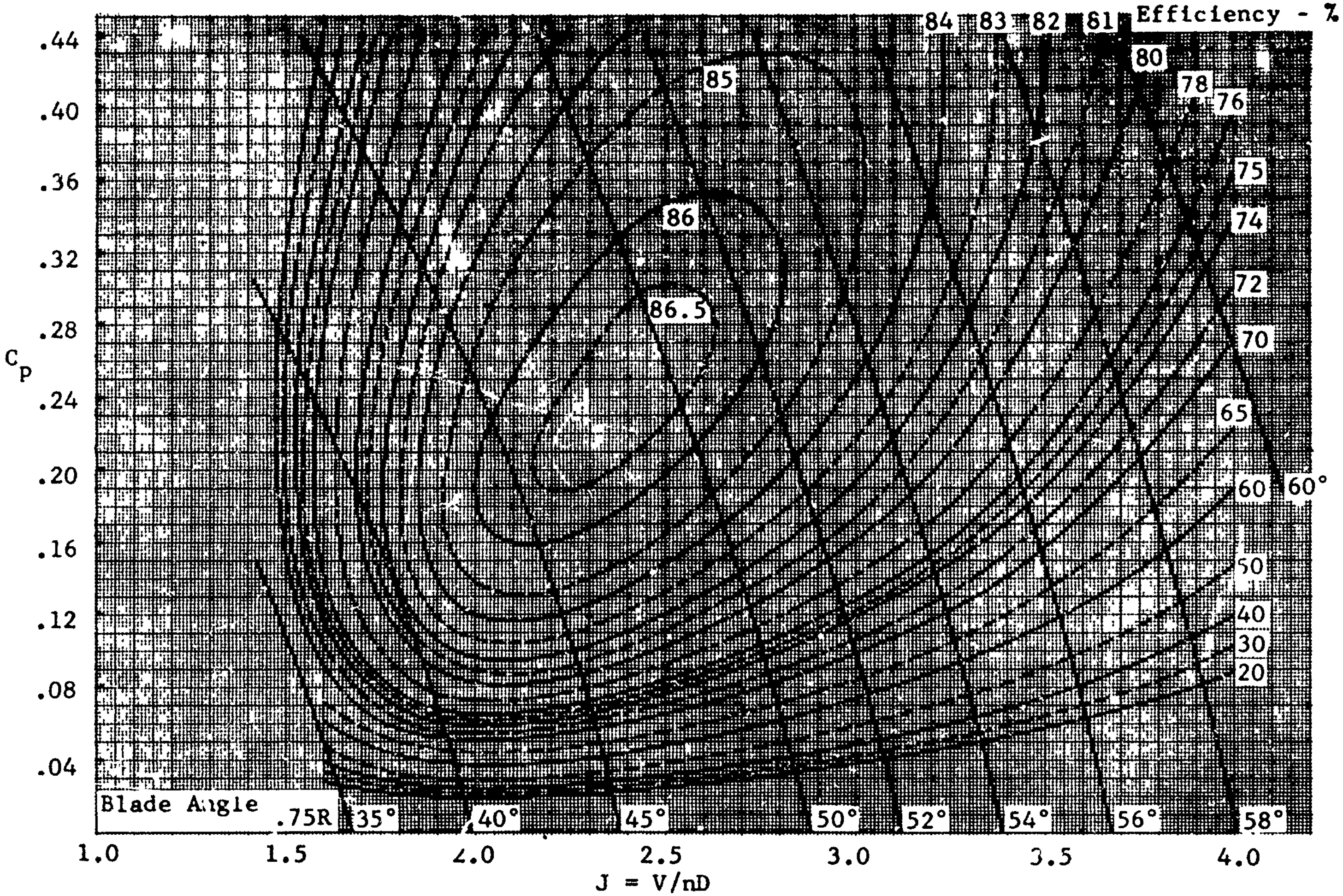

Figure 88. X-19, propeller cruise efficiency map, 3(13168A10P3) blade; AF = 168, dia. = 13 ft, IC_{L_i} = 0.057, forward Mach No. = 0.5 or less.

FURNISHED UNDER UNITED STATES GOVERNMENT CONTRACT No. AF33(615)-3940. SHALL NOT BE EITHER RELEASED OUTSIDE THE GOVERNMENT, OR USED, DUPLICATED, OR DISCLOSED IN WHOLE OR IN PART FOR MANUFACTURE OR PROCUREMENT, WITHOUT THE WRITTEN PERMISSION OF CURTISS-WRIGHT CORPORATION, EXCEPT FOR (I) EMERGENCY REPAIR OR OVERHAUL WORK BY OR FOR THE GOVERNMENT, WHERE THE ITEM OR PROCESS IS NOT OTHERWISE REASONABLY AVAILABLE TO ENABLE TIMELY PERFORMANCE OF THE WORK, OR (II) RELEASE TO A FOREIGN GOVERNMENT, AS THE INTERESTS OF THE UNITED STATES MAY REQUIRE. PROVIDED THAT IN EITHER CASE THE RELEASE, USE, DUPLICATION OR DISCLOSURE HEREOF SHALL BE SUBJECT TO THE FOREGOING LIMITATIONS. THIS LEGEND SHALL BE MARKED ON ANY REPRODUCTION HEREOF IN WHOLE OR IN PART."

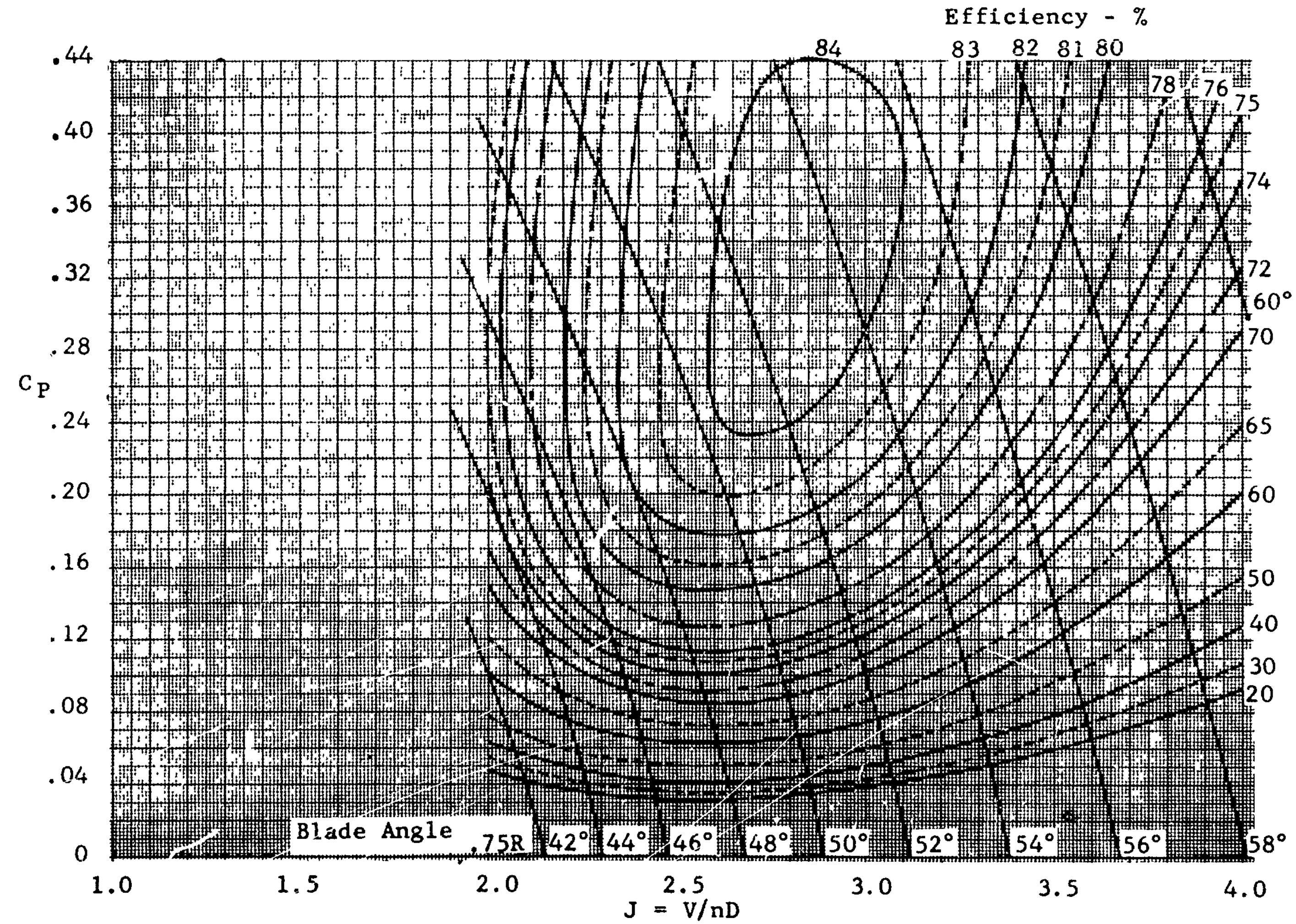

Figure 89. X-19, propeller cruise efficiency map, 3(13168A10P3) blade; AF = 168, dia. = 13 ft, IC_{L_i} = 0.057, forward Mach No. = 0.6 or less.

FURNISHED UNDER UNITED STATES GOVERNMENT CONTRACT No. AF33(615)-3940. SHALL NOT BE EITHER RELEASED OUTSIDE THE GOVERNMENT, OR USED, DUPLICATED, OR DISCLOSED IN WHOLE OR IN PART FOR MANUFACTURE OR PROCUREMENT, WITHOUT THE WRITTEN PERMISSION OF CURTISS-WRIGHT CORPORATION, EXCEPT FOR (i) EMERGENCY REPAIR OR OVERHAUL WORK BY OR FOR THE GOVERNMENT, WHERE THE ITEM OR PROCESS IS NOT OTHERWISE REASONABLY AVAILABLE TO ENABLE TIMELY PERFORMANCE OF THE WORK, OR (ii) RELEASE TO A FOREIGN GOVERNMENT, AS THE INTERESTS OF THE UNITED STATES MAY REQUIRE; PROVIDED THAT IN EITHER CASE THE RELEASE, USE, DUPLICATION OR DISCLOSURE HEREOF SHALL BE SUBJECT TO THE FOREGOING LIMITATIONS. THIS LEGEND SHALL BE MARKED ON ANY REPRODUCTION HEREOF IN WHOLE OR IN PART.

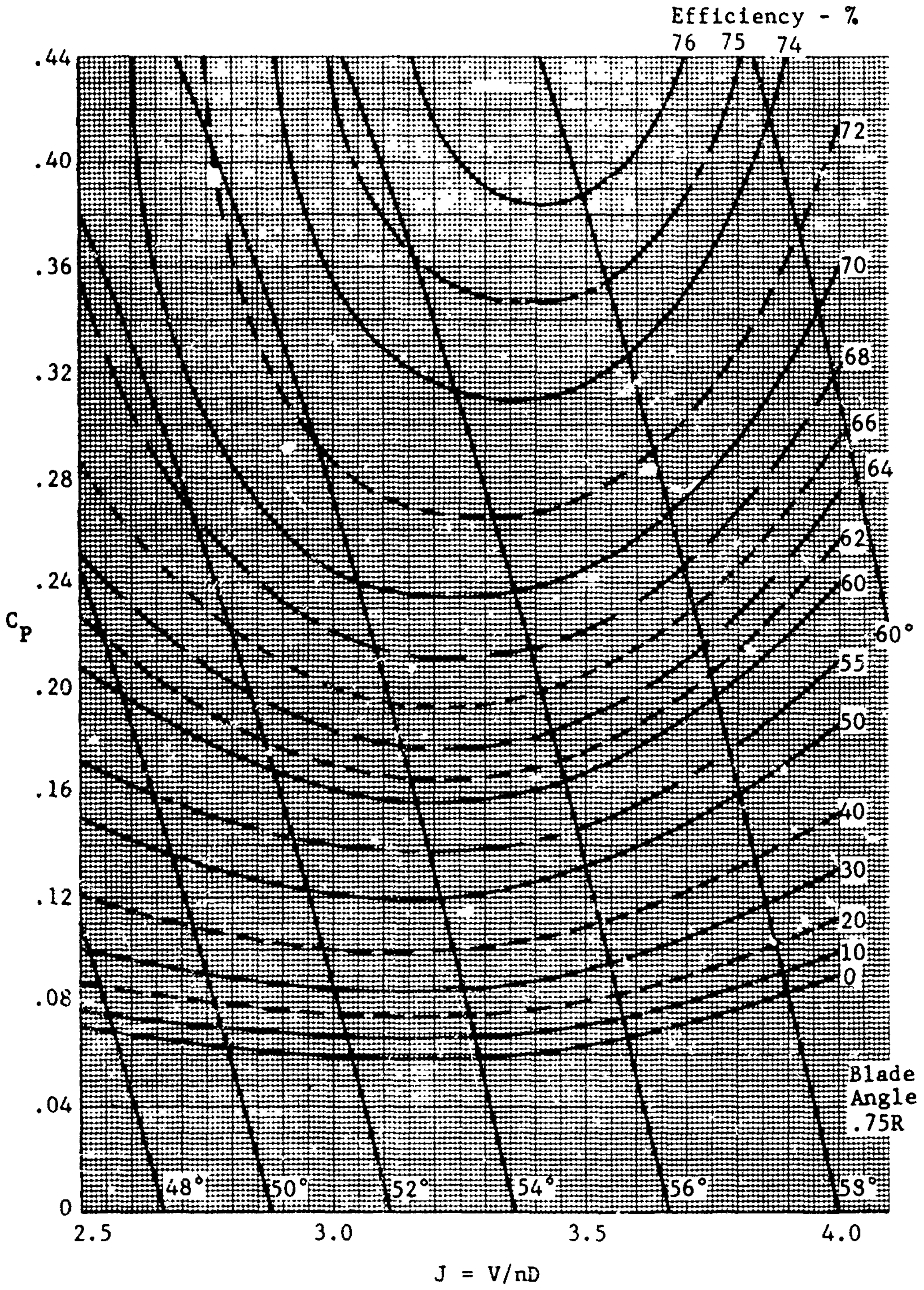

Figure 90. X-19, propeller cruise efficiency map, 3(13168A10P3) blade; AF = 168, dia. = 13 ft, IC_{L_i} = 0.057, forward Mach No. = 0.7 or less.

"FURNISHED UNDER UNITED STATES GOVERNMENT CONTRACT No AF33(615)-1940 SHALL NOT BE EITHER RELEASED OUTSIDE THE GOVERNMENT, OR USED DUPLICATED, OR DISCLOSED IN WHOLE OR IN PART FOR MANUFACTURE OR PROCUREMENT, WITHOUT THE WRITTEN PERMISSION OF CURTISS-WRIGHT CORPORATION, EXCEPT FOR (i) EMERGENCY REPAIR OR OVERHAUL WORK BY OR FOR THE GOVERNMENT, WHERE THE ITEM OR PROCESS IS NOT OTHERWISE REASONABLY AVAILABLE TO ENABLE TIMELY PERFORMANCE OF THE WORK. OR (ii) RELEASE TO A FOREIGN GOVERNMENT, AS THE INTERESTS OF THE UNITED STATES MAY REQUIRE. PROVIDED THAT IN EITHER CASE THE RELEASE, USE, DUPLICATION OR DISCLOSURE HEREOF SHALL BE SUBJECT TO THE FOREGOING LIMITATIONS. THIS LEGEND SHALL BE MARKED ON ANY REPRODUCTION HEREOF IN WHOLE OR IN PART."

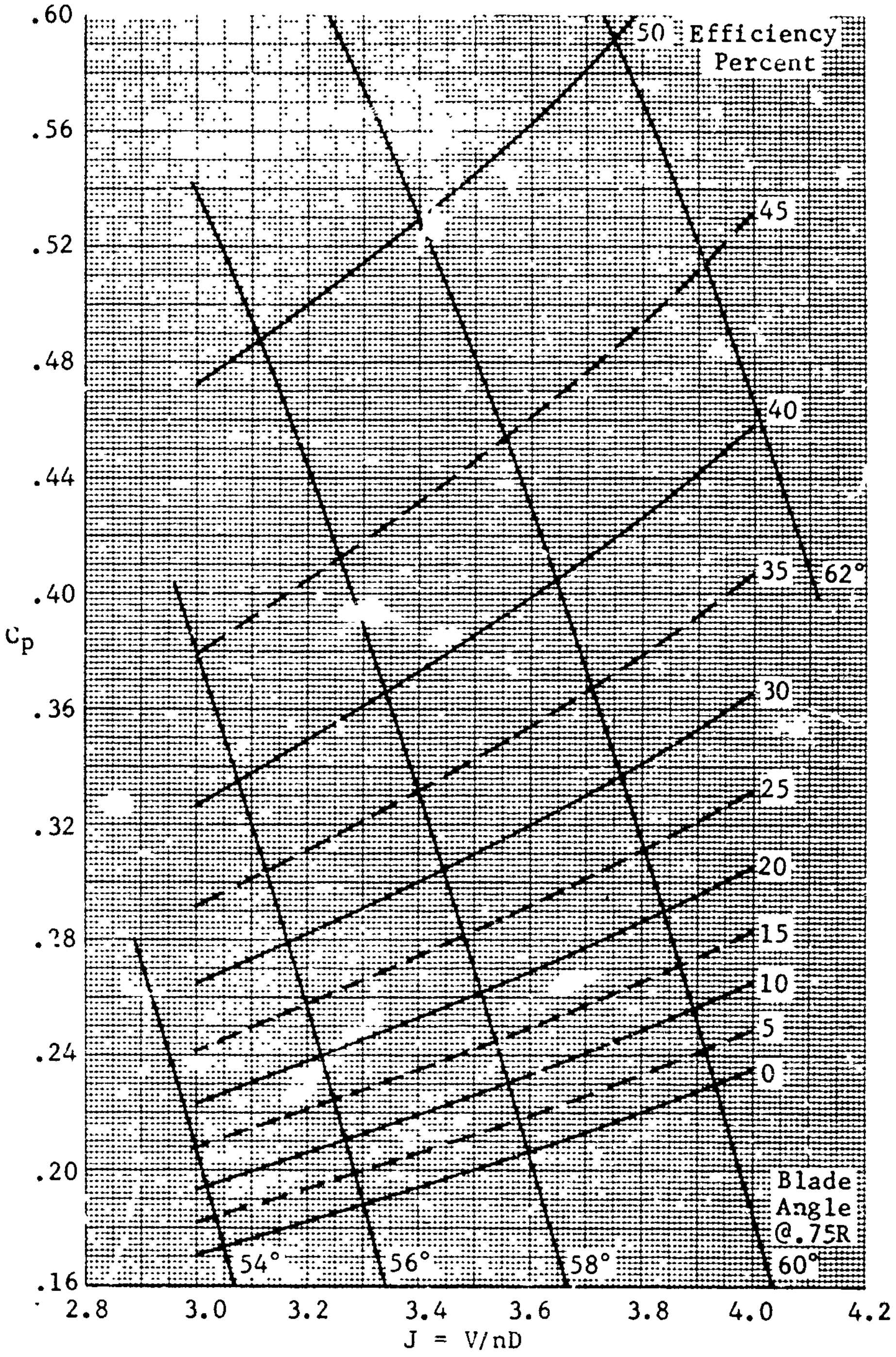

Figure 91. X-19, propeller cruise efficiency map, 3(13168A10P3) blade, AF = 168, dia. = 13 ft, IC_{L_i} = 0.057, forward Mach No. = 0.8 or less.

FURNISHED UNDER UNITED STATES GOVERNMENT CONTRACT No AF33(615)-3940 SHALL NOT BE EITHER RELEASED OUTSIDE THE GOVERNMENT, OR USED, DUPLICATED, OR DISCLOSED IN WHOLE OR IN PART FOR MANUFACTURE OR PROCUREMENT, WITHOUT THE WRITTEN PERMISSION OF CURTISS-WRIGHT CORPORATION EXCEPT FOR (I) EMERGENCY REPAIR OR OVERHAUL WORK BY OR FOR THE GOVERNMENT, WHERE THE ITEM OR PROCESS IS NOT OTHERWISE REASONABLY AVAILABLE TO ENABLE TIMELY PERFORMANCE OF THE WORK, OR (II) RELEASE TO A FOREIGN GOVERNMENT, AS THE INTERESTS OF THE UNITED STATES MAY REQUIRE PROVIDED THAT IN EITHER CASE THE RELEASE, USE, DUPLICATION OR DISCLOSURE HEREOF SHALL BE SUBJECT TO THE FOREGOING LIMITATIONS THIS LEGEND SHALL BE MARKED ON ANY REPRODUCTION HEREOF IN WHOLE OR IN PART."

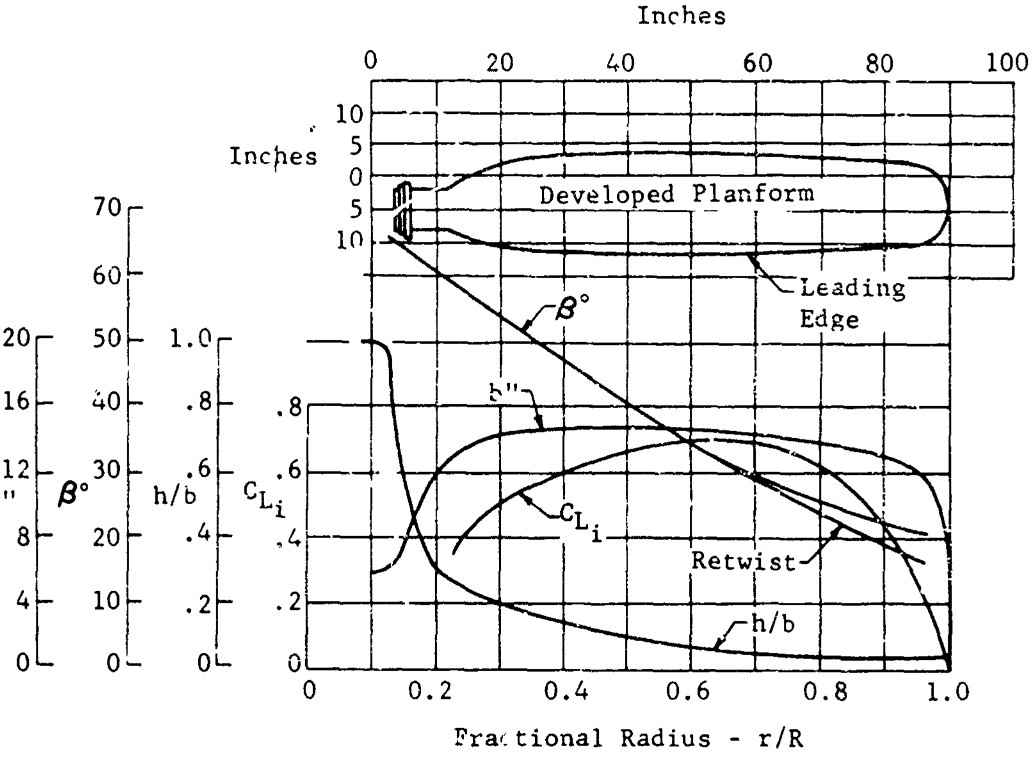

Figure 92. Blade characteristics of the Curtiss-Wright 109652 propeller blade; dia. = 15 ft., AF = 115, IC_{L_i} = 0.5, NACA 65 section series.

FURNISHED UNDER UNITED STATES GOVERNMENT CONTRACT No. AF33(615)-3940. SHALL NOT BE EITHER RELEASED OUTSIDE THE GOVERNMENT, OR USED, DUPLICATED, OR DISCLOSED IN WHOLE OR IN PART FOR MANUFACTURE OR PROCUREMENT, WITHOUT THE WRITTEN PERMISSION OF CURTISS-WRIGHT CORPORATION, EXCEPT FOR (I) EMERGENCY REPAIR OR OVERHAUL WORK BY OR FOR THE GOVERNMENT, WHERE THE ITEM OR PROCESS IS NOT OTHERWISE REASONABLY AVAILABLE TO ENABLE TIMELY PERFORMANCE OF THE WORK; OR (II) RELEASE TO A FOREIGN GOVERNMENT, AS THE INTERESTS OF THE UNITED STATES MAY REQUIRE. PROVIDED THAT IN EITHER CASE THE RELEASE, USE, DUPLICATION OR DISCLOSURE HEREOF SHALL BE SUBJECT TO THE FOREGOING LIMITATIONS. THIS LEGEND SHALL BE MARKED ON ANY REPRODUCTION HEREOF IN WHOLE OR IN PART.

Experience with similar propellers would indicate that if the blade were retwisted in the opposite direction, the performance would also be reduced. This proves the need for an accurate theory and data for predicting static thrust performance.

At the cruise flight condition, peak performance was obtained when the X-19 propeller was operating at a tip speed of 625 to 650 feet per second. This cruise tip speed combined with 820 feet per second for take-off resulted in the best combination of loading at the two operating conditions for the X-19 blading. Test data, using the blading for the X-200 aircraft configuration, are presented in Figure 93 and show a similar cruise tip speed but a higher take-off $\pi n D_p$ value for that earlier aircraft. At the cruise condition 20% reduction in tip speed places the operating point at the power coefficient and advance ratio for peak performance, a further decrease in tip speed has essentially no effect.

The retwisted blade shown on Figure 92 would show a reduction in performance, at the cruise condition of a typical VTOL aircraft as the tip would become underloaded. At the conditions of the X-19 airplane it is estimated that the underloading of the tip would reduce the efficiency more than 5%.

There are many other blade design parameters that can be varied, to influence hover and cruise performance. For instance, instead of wide blades with small values of design C_L, more conventional narrow blades which have large design C_L's can be used. Strictly from propulsion and hover lift considerations, such a blade would exhibit superior performance at these conditions than that obtained from the X-19 propeller. This comparison is valid for propellers stressed to the same loading level. A blade stressed for a lesser level would probably have lower thickness ratio's throughout. This would give the highest performance and thus invalidate the results.

6. HOVER POWER HISTOGRAMS

Two histograms are presented as obtained from flight tests (Figures 95 and 96). The first taken from Flight No. 31 records, demonstrates hover, translation and left turns; this can be considered a hover histogram. As predicted, the front propellers are heavily loaded and are subjected to considerable gear life erosion. The largest percentage of the hover time is spent near 780 HP with very little time spent at the peak power of 1000 HP. The rear propellers are considerably less loaded than the front, with the result that calculated nacelle gear life is much higher.

The second histogram (Figure 96) represents the early transition mode, at which 40 MPH was attained at $\emptyset_F =$ [illegible]. As expected, the front nacelle gear life is greater. Now, the largest percentage of the time is spent at approximately 620 HP. The rear propellers become more highly loaded with the result that life diminishes from in excess of 1000 hours to about 60 hours.

FURNISHED UNDER UNITED STATES GOVERNMENT CONTRACT No. AF33(615)-1940 SHALL NOT BE EITHER RELEASED OUTSIDE THE GOVERNMENT, OR USED, DUPLICATED, OR DISCLOSED IN WHOLE OR IN PART FOR MANUFACTURE OR PROCUREMENT, WITHOUT THE WRITTEN PERMISSION OF CURTISS-WRIGHT CORPORATION, EXCEPT FOR (I) EMERGENCY REPAIR OR OVERHAUL WORK BY OR FOR THE GOVERNMENT, WHERE THE ITEM OR PROCESS IS NOT OTHERWISE REASONABLY AVAILABLE TO ENABLE TIMELY PERFORMANCE OF THE WORK: OR (II) RELEASE TO A FOREIGN GOVERNMENT, AS THE INTERESTS OF THE UNITED STATES MAY REQUIRE: PROVIDED THAT IN EITHER CASE THE RELEASE, USE, DUPLICATION OR DISCLOSURE HEREOF SHALL BE SUBJECT TO THE FOREGOING LIMITATIONS. THIS LEGEND SHALL BE MARKED ON ANY REPRODUCTION HEREOF IN WHOLE OR IN PART."

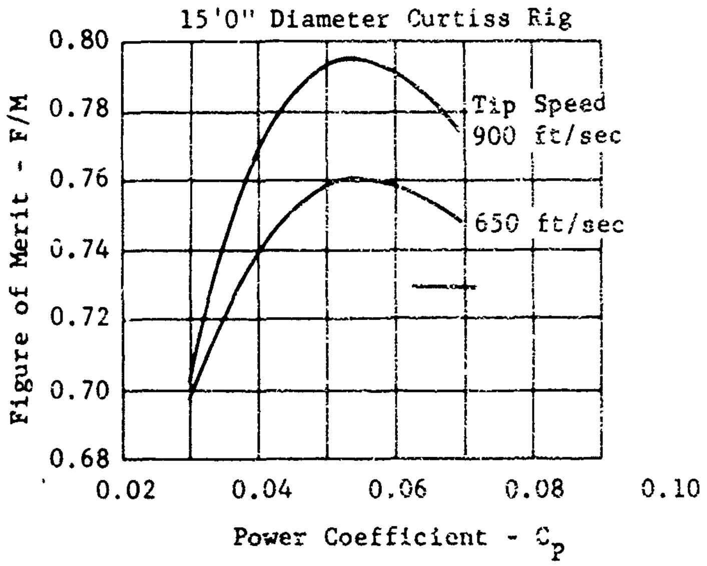

Figure 93. Figure of merit of the Curtiss-Wright 109652 propeller blade as a function of power coefficient, measured on Curtiss-Wright test rig.

"FURNISHED UNDER UNITED STATES GOVERNMENT CONTRACT No. AF33(615)-1940. SHALL NOT BE EITHER RELEASED OUTSIDE THE GOVERNMENT, OR USED, DUPLICATED, OR DISCLOSED IN WHOLE OR IN PART FOR MANUFACTURE OR PROCUREMENT, WITHOUT THE WRITTEN PERMISSION OF CURTISS-WRIGHT CORPORATION, EXCEPT FOR (i) EMERGENCY REPAIR OR OVERHAUL WORK BY OR FOR THE GOVERNMENT, WHERE THE ITEM OR PROCESS IS NOT OTHERWISE REASONABLY AVAILABLE TO ENABLE TIMELY PERFORMANCE OF THE WORK, OR (ii) RELEASE TO A FOREIGN GOVERNMENT, AS THE INTERESTS OF THE UNITED STATES MAY REQUIRE; PROVIDED THAT IN EITHER CASE THE RELEASE, USE, DUPLICATION OR DISCLOSURE HEREOF SHALL BE SUBJECT TO THE FOREGOING LIMITATIONS. THIS LEGEND SHALL BE MARKED ON ANY REPRODUCTION HEREOF IN WHOLE OR IN PART."

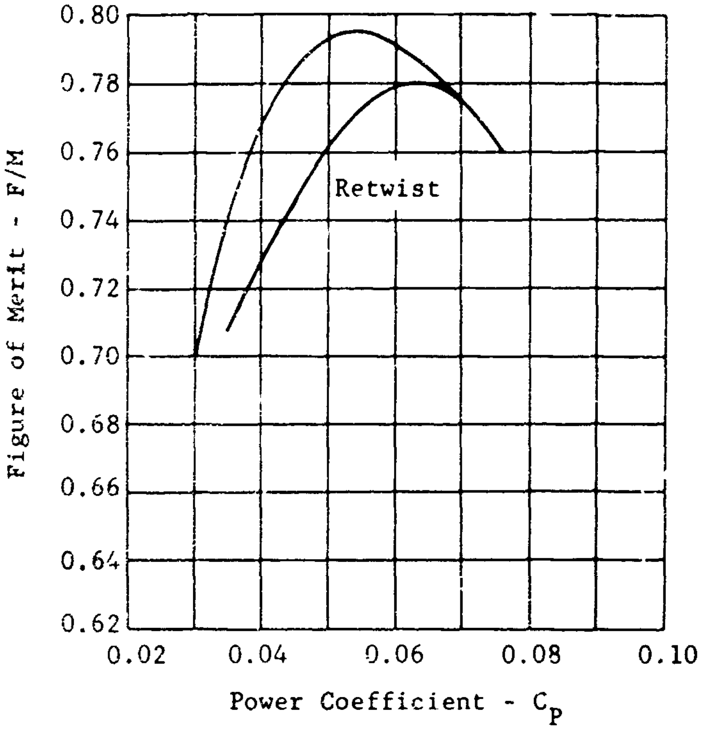

Figure 94 Effect of blade retwist on the figure of merit; 3(109652) blade, 900 πnD, three blades

FURNISHED UNDER UNITED STATES GOVERNMENT CONTRACT No. AF33(6'3)-3940. SHALL NOT BE EITHER RELEASED OUTSIDE THE GOVERNMENT, OR USED, DUPLICATED, OR DISCLOSED IN WHOLE OR IN PART FOR MANUFACTURE OR PROCUREMENT, WITHOUT THE WRITTEN PERMISSION OF CURTISS-WRIGHT CORPORATION EXCEPT FOR (I) EMERGENCY REPAIR OR OVERHAUL WORK BY OR FOR THE GOVERNMENT, WHERE THE ITEM OR PROCESS IS NOT OTHERWISE REASONABLY AVAILABLE TO ENABLE TIMELY PERFORMANCE OF THE WORK, OR (II) RELEASE TO A FOREIGN GOVERNMENT, AS THE INTERESTS OF THE UNITED STATES MAY REQUIRE, PROVIDED THAT IN EITHER CASE THE RELEASE, USE, DUPLICATION OR DISCLOSURE HEREOF SHALL BE SUBJECT TO THE FOREGOING LIMITATIONS. THIS LEGEND SHALL BE MARKED ON ANY REPRODUCTION HEREOF IN WHOLE OR IN PART.

Flight G.W/C.G 12300/43.5, Duration 273 sec

Flight Description: Hover; Translation 15 MPH Foward; Stop; Turn Left 90°; Translate; 10 mph; Turn Left 90°;• Translate; Hover.

Propeller HP/rpm	Transverse Shaft Torque Q (in. lb)	Propeller							
		No. 1		No. 2		No. 3		No. 4	
		A	B	A	B	A	B	A	B
420/1204	7500	99.6	3.6	95.6	48.7	95.6	26.7	100.0	4.0
615	11,000	96.0	21.3	46.9	46.2	68.9	67.1	96.0	16.9
720	12,800	74.7	37.7	0.7	0.7	1.8	1.8	79.1	36.2
780	13,900	37.0	22.2	0		0		42.9	38.5
890	15,840	14.8	14.1					4.4	4.0
975	17,500	0.7	0.7					0.4	0.4
1025	18,250	0						0	

A-% Operating Time Above Q Level Indicated; B-% Operating Time At Increment Of Q Indicated.

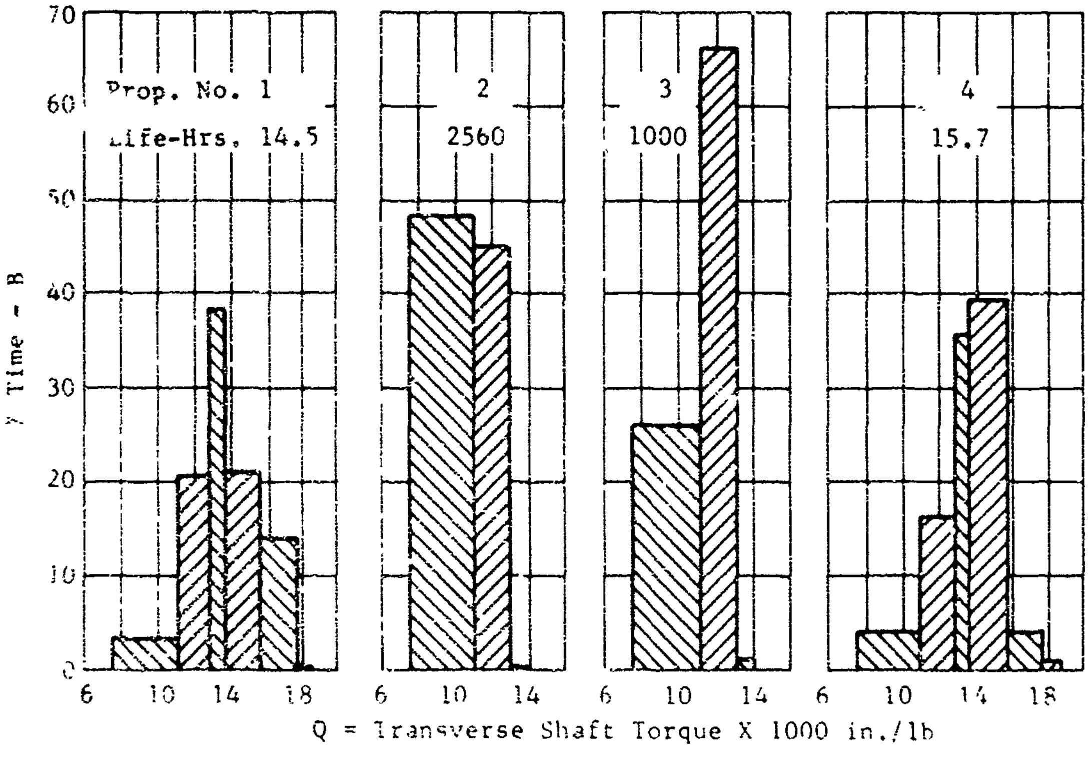

Figure 95 X-19, histogram of transverse shaft loading, flight no. 31, 12/23/64.

67-2046

Flight G.W/C.G 12300/42.8 Duration 137 sec

Flight Description: Hover; Tilt Nacelles To 88°; Accelerate To Foward Flight At 40 MPH; Tilt Nacelles To VTOL Decelerate To Hover

Propeller HP/rpm	Transverse Shaft Torque Q (in. lb)	Propeller							
		No. 1		No. 2		No. 3		No. 4	
		A	B	A	B	A	B	A	B
420/1204	7500	100.0	45.3	100.0	29.9	100.0	31.4	100.0	43.1
620	11,000	54.7	18.9	70.1	47.5	68.6	43.1	56.9	21.1
720	12,840	35.8	20.5	22.6	17.5	25.5	19.7	35.8	19.0
780	13,900	15.3	13.8	5.1	4.4	5.8	5.1	16.8	13.2
860	15,300	1.5	0.8	0.7	0.7	0.7	0	3.6	2.1
900	16,000	0.7	0.7	0		0.7	0.7	1.5	0.8
950	16,900	0				0		0.7	0.7
1000	17,800							0	

A-% Operating Time Above Q Level Indicated; B-% Operating Time At Increment Of Q Indicated.

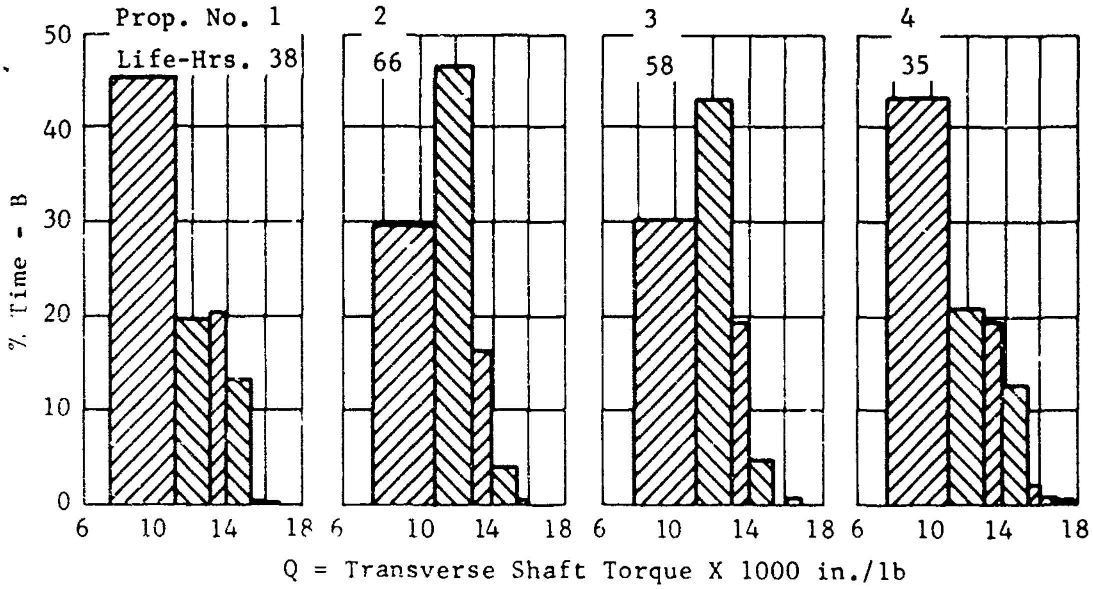

Figure 96 X-19, histogram of transverse shaft loading, flight no. 35, 1/7/65.

This is the result of the variation of aircraft pitch-up moment with velocity and the tilt actuated auto-trim schedule, which makes $(\beta_F - \beta_R)$ more negative. The physical reason for the speed pitch up moment is given in Section III.3.a. under the discussions of wing power effects.

REFERENCES

22. Borst, H. V., A Short Method to Propeller Performance , Curtiss-Wright pamphlet, 1959.

23. Borst, H. V., A Revised Method of Propeller Performance Analysis - Procedure and Data , Curtiss Report C-2700.

24. Theodorsen, T., Theory of Propellers , McGraw-Hill, New York, New York, 1948.

25. Glover, L. S., & Borst, H. V., Application of Theodorsen's Theory to Strip Analysis Procedure for Single Rotating Propellers , Curtiss Report C-2070

26. Glover, L. S., & Borst, H. V., A Method of Strip Analysis for a Dual Rotation Propeller , Curtiss Report C-2085.

27. Borst, H. V., & Enos, L., Aerodynamic Characteristics of NACA 16 Series Airfoils for Application to Propeller Performance Calculations , Curtiss Report C-2000.

28. Warsett, P., & Meyerhoff, L., Application of Thick Airfoils to Propeller Design , Curtiss Report C-1562.

29. Foss, R. L., Strip Analysis Method for Evaluating Static Thrust , Curtiss Report C-2402, 1952.

30. Glover, L., Applications of the Calculus of Variations to the Determination of the Optimum Propeller Data, Curtiss Report C-2342A, December 2, 1954.

31. Yaggy, Paul F., A Wind Tunnel Investigation of Three Propellers Through an Angle-of-Attack Range from 0° to 85°, NASA TN D-318, 1960.

32. Borst, H. V., & Ladden, R. M., "Propeller Testing at Zero Velocity," AVLABS Cornell Conference, June 1966.

SECTION V

PROPELLER STRUCTURE AND CONTROL MECHANISM

SECTION V - NOMENCLATURE

A	=	propeller shaft angle of attack degrees
a	=	slope of the lift curve
b	=	blade section chord
CF		centrifugal force
C_L		lift coefficient
C_m		moment coefficient
C_n		normal force coefficient
C_y		side force coefficient
D		propeller diameter
E		modulus of elasticity
F		force
g		gravity constant
HP		horsepower
h		blade section thickness
I		moment of inertia
J		advance ratio
M		moment
N		normal force
q		dynamic pressure
R		propeller radius total
r		blade radius
S		area
S_n		stress cycles
T		thrust
V		velocity
W		resultant section velocity
X	=	r/R
Y		side force

SECTION V

PROPELLER STRUCTURE AND CONTROL MECHANISM

1. MECHANICAL DESIGN INCLUDING PHILOSOPHY, RELIABILITY, WEIGHT AND MAINTENANCE

a. General Description

The X-19 propellers are three-blade, thirteen foot diameter propellers consisting of a hub, fiberglass blades, a hydromechanical pitch-change power unit, a control valve assembly, and a propeller mounting bearing assembly.

The blades of the four propellers were designed to provide an optimum combination of thrust and radial lift force, the latter being a feature of the Curtiss-Wright V/STOL aircraft flight concept. Blade angle is collectively controlled to achieve thrust variations and differentially controlled for aircraft attitude stability in V/STOL flight configurations. Redundant dual-piston pitch-change actuating systems are employed to assure continual control capability in the event of a single system failure.

The propellers are mounted on the nacelle housings which contain the nacelle bevel gears and the propeller pitch-change mechanism. Shafting, of the power transmission system, interconnects all four propellers to two Lycoming T55-L-5 turbine engines. Either engine is capable of supplying flight power to all four propellers. The spinner and nacelle afterbody fairing complete the propeller/nacelle assembly.

b. Component Descriptions

(1) Hubs

The hubs are made of single piece steel forgings. They are designed to retain the blades by means of two-row, angular-contact bearings and threaded blade nuts. The rear extension of the hub contains the propeller-mounting bearing assembly and the hub drive splines. The power unit is splined directly into the hub and contains the shaft drive spline. The hub construction permits blade installation and removal while the propeller is mounted on the aircraft.

(2) Pitch-Change Mechanism (Figure 97)

The propeller pitch-change system is comprised of a hydraulic power unit which contains two independent nacelle-oil pressure systems. No pressure connections to the aircraft hydraulic systems are required. The power unit assembly includes two tandem pistons, two hydraulic pump assemblies,

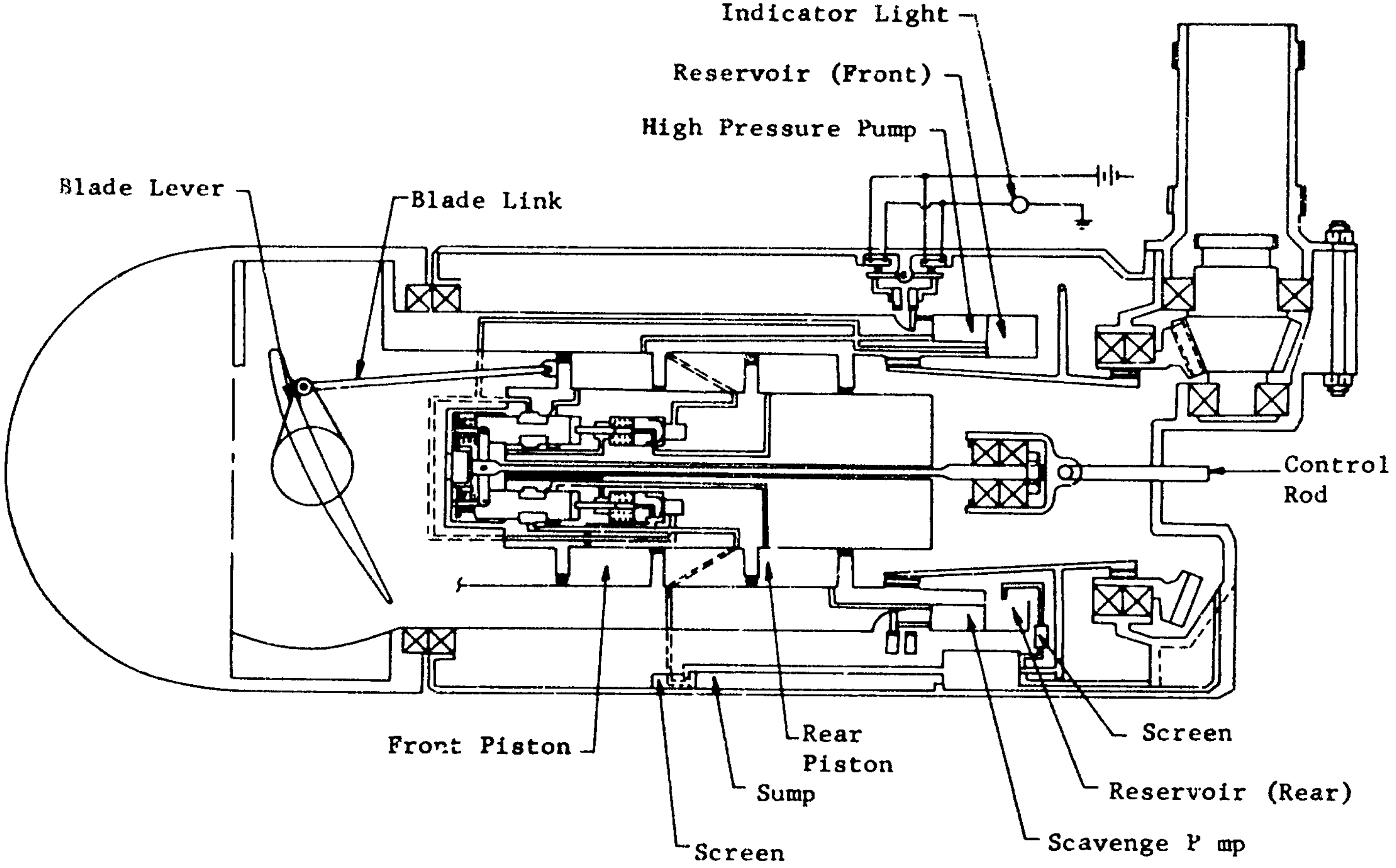
Indicator Light
Reservoir (Front)
High Pressure Pump
Blade Lever
Blade Link
Control Rod
Front Piston
Rear Piston
Sump
Screen
Screen
Reservoir (Rear)
Scavenge Pump

Figure 97. X-19 schematic assembly of the blade pitch change mechanism.

FURNISHED UNDER UNITED STATES GOVERNMENT CONTRACT No. AF33(6[illegible])-3940 SHALL NOT BE EITHER RELEASED OUTSIDE THE GOVERNMENT, OR USED, DUPLICATED OR DISCLOSED IN WHOLE OR IN PART FOR MANUFACTURE OR PROCUREMENT, WITHOUT THE WRITTEN PERMISSION OF CURTISS-WRIGHT CORPORATION, EXCEPT FOR (I) EMERGENCY REPAIR OR OVERHAUL WORK BY OR FOR THE GOVERNMENT, WHERE THE ITEM OR PROCESS IS NOT OTHERWISE REASONABLY AVAILABLE TO ENABLE TIMELY PERFORMANCE OF THE WORK, OR (II) RELEASE TO A FOREIGN GOVERNMENT, AS THE INTERESTS OF THE UNITED STATES MAY REQUIRE; PROVIDED THAT IN EITHER CASE THE RELEASE, USE, DUPLICATION OR DISCLOSURE HEREOF SHALL BE SUBJECT TO THE FOREGOING LIMITATIONS. THIS LEGEND SHALL BE MARKED ON ANY REPRODUCTION HEREOF IN WHOLE OR IN PART.

two oil reservoirs, a dual control valve assembly and suitable arms for attachment of the blade control levers. Planning or adjustment of the blade angle is achieved through a set of differential splines between the blade shank and blade lever. These splines permit blade angle changes in increments of 0.166 degrees. The pitch-change blade lever has a moment arm of 2.60 inches.

Propeller pitch-change is accomplished by two mechanically-coupled single-acting pistons having independent hydraulic systems. Blade angle change results from a transfer of the piston assembly motion, through a link assembly, to a lever which is splined to the blade shank.

The pitch-change hydraulic system is basically a position follow-up mechanism in which the pistons follow valve displacement at approximately the same rate while delivering the force required for pitch-change. Valve displacement corresponds to desired blade angle, and piston displacement corresponds to actual blade angle. The pistons move to balance themselves across the valve ports for any given blade angle until both blade loading and piston pressure are in equilibrium.

Both hydraulic systems operate in the same manner; i.e., at a given control signal, oil flows into each piston from independent high-pressure pump assemblies at a constant rate until the desired blade angle is achieved. Oil is exhausted through the dual control valves to each sump. The valves monitor piston pressures by metering the orifices.

Isolation of the hydraulic systems is obtained in the following manner:

(a) The front piston system functions as follows:

Oil is placed into the hub which acts as the sump for the front piston system. This oil enters the cylinder of the forward hydraulic system through one of the two pump assemblies and is ported through one of the two control valves back into the hub. After being cooled in the hub the oil returns to the rotating sump provided in the pump housing, which feeds the oil back into the pumps.

(b) The rear piston hydraulic system functions as follows:

Oil enters this cylinder from the other pump assembly and is exhausted through its control valve into the nacelle housing where it is cooled. A scavenge and lubrication pump mounted in the nacelle housing delivers oil to the rear piston rotating sump assembly which feeds the pitch-change pumps to complete the hydraulic circuit.

Rotation of both sump assemblies acts to eliminate entrapped air in the oil while serving as a centrifugal pump to supply primed oil to the pitch-change pumps.

The scavenge pump also supplies lubrication to the propeller mounting bearing, the bevel gear set, and retention bearings.

Each pitch-change pump assembly consists of three pumps of vane type which are mounted in a single housing. This housing is mounted in the hub, so it rotates at propeller speed. A pinion gear, which meshes with an internal fixed ring gear, is attached to each pump shaft. Each of the three pumps, in a system, is meshed to one of two fixed ring gears. Power to drive the pumps is obtained from propeller rotation since the pumps and pinion gears revolve as a unit within their respective fixed ring gears.

A pivoted torque-reaction bar, for the two fixed ring gears, is installed in the nacelle together with two micro-switches. A loss of hydraulic pressure in either system will result in an unbalanced reaction-torque on the ring gears causing movement of one gear relative to the other. This gear movement will actuate one of the micro-switches which will close an electrical circuit to the "HYD. PRESS" indicator light.

(3) Controls

Mechanical pitch-change signals are fed from the cockpit to a signal integrator referred to as the coordinator and are received at the propeller as a push pull, blade angle desired, signal (see Figure 157). This signal is transferred through a series of bellcrank linkages and converted into a linear fore-and-aft control rod and valve motion. Each of the two pitch-change control valves is mounted on the end of a differential beam. A mechanically operated relief valve is located aft of each control valve, in the valve assembly. Each relief valve is capable of relieving pressure from one system when actuated by the control valve of the other system. During normal propeller operations, with both pistons and valves operating, there is insufficient movement of either valve to trigger the poppet which actuates the relief valves.

In the event of a "stuck" control valve in one system, the greater movement available to the other control valve due to the differential beam arrangement, allows this valve to actuate the relief valve of the "stuck" system. This results in "dumping" the pressure of the inoperative system. A snap ring type of detent spring on the relief poppet, once actuated, maintains this "dumped" condition until such time as the valve assembly is removed and the relief poppet detent spring reset. This loss of pressure of a single system due to a "stuck" valve is indicated by a tel-light through the reaction-ring gear bar.

A ball-bearing coupling is installed between the non-rotating control rod and the rotating propeller and valve assembly. Two compression springs are installed between the piston and each control valve to eliminate signal backlash and provide a unidirectional signal input force.

Controls that are external to the propeller but which feed into the signal coordinator and then into the propeller pitch-change control rod are as follows:

(a) The governor speed set lever which selects propeller RPM.

(b) The power lever which controls the fuel supply to the engines.

(c) The pilots flight control stick which controls pitch and roll.

(d) The rudder pedals which control yaw.

(e) The SAS system which feeds signals into the coordinator to provide stabilization in pitch and roll.

(f) The tilt switch which controls tilt angles of the nacelles.

(g) The manual propeller pitch-change switch which manually sets collective propeller blade angle.

All these controls feed into the coordinator and result in controlled pitch-change signals to each of the propellers. The coordinator also phases out propeller control of attitude in the transition flight regimes.

(4) Blades

The propellers for the X-19 aircraft are three bladed and 13 feet in diameter, with a 166 Activity Factor. The shell of the blades is of epoxy resin reinforced fiberglass.

The primary load carrying element of the blade is this fiberglass structure which transfers the loads to the steel blade shank on which the fiberglass is molded, Fig. 98. The lightweight rigid foam plastic filling constitutes a sandwich structure with the fiberglass shell to provide the necessary stiffness and load carrying capacity. This type of construction and material was selected to satisfy the structural requirements and at the same time meet the aerodynamic and low blade weight requirements. Detailed description of the blade structural design is given in item 2 of this section.

The propeller spinner is a two-piece design consisting of a fiberglass nose section and a fiberglass foam sandwich rear section. The rear section is bolted to the front of the propeller for support.

The external contour of the spinner is such as to provide smooth airflow over the nacelle outline.

c. Blade Maintenance

(1) Introduction

The purpose of this section is to define the possible types of damage to FRP (fiberglass reinforced plastic) propeller blades and to show methods for repairing such damage, where applicable. In addition, preventive maintenance procedures will be outlined.

(2) Damage

Handling damage is generally confined to the external edges and surfaces including blade shank and fairing. Operational damage could involve the same areas plus the blade and fairing foam fillers.

(a) Fiberglass reinforced plastic (FRP) damage: - Delamination of the cloth plies; breaks or gouges in the surface layers of cloth of the skins, edges or tip without penetration of the full wall thickness or bond line of the blade.

The above types of damage, but to a greater degree, could extend into the interior of the blade.

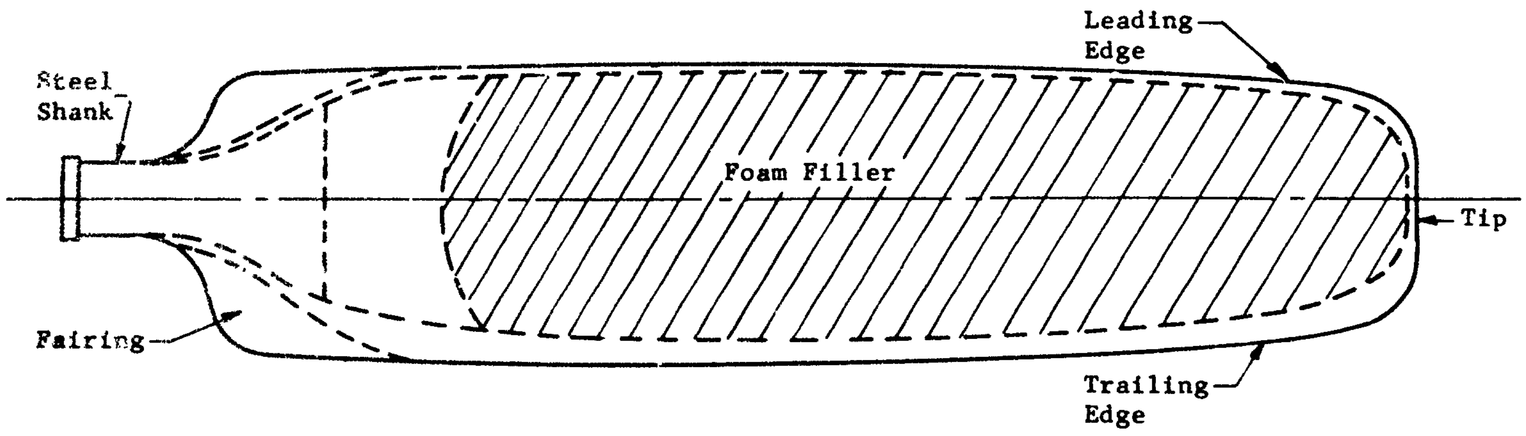
Leading Edge
Steel Shank
Foam Filler
Tip
Fairing
Trailing Edge

Figure 98. Blade schematic illustrating the typical construction of the lightweight fiberglass blade.

(b) Foam damage: - Where separation occurs between the foam and the FRP or where the foam is crushed by a high impact blow.

(c) Protective coating damage: - When damage occurs to the FRP, frequently the protective coating also is affected. Damage to the coating only, is usually due to impingement of stones, sand or similar materials and in most cases will occur at the leading edge and tip of the blade.

(d) Steel shank damage: - Damage to the steel shank would consist of nicks, scratches, abrasion, damaged plating, corrosion, etc.

(3) Determination of Damage

Damage to the FRP portion of the blade is determined by visual inspection except in the case of separation between foam and fiberglass.

The latter is determined by rapping the thrust and camber plates with an item such as a half-dollar or metal washer. Separation will be indicated by a hollow sound whereas a good bond will be indicated by a solid, metallic type of sound. Pressure applied by thumb and knuckles, causing plate deflection, can confirm such separation.

(4) Repair of Damage

Experience in repairing of damage to FRP propeller blades is very limited. Although repairs of extensive damage may eventually be permissible, in this type of blade only relatively minor repairs, as indicated below, were recommended to be made in the field and all others were to be reviewed by the factory. Damage such as shown in Figure 99 may be made in the field:

(a) Provided that not more than 50% of the FRP thickness is involved in making the repair. However, in the case of the inboard fairing skins, gouging of the foam up to one cubic inch, provided the basic blade is not penetrated, may be filled with the designated materials.

(b) Provided that repairs do not extend through the "bond" line of edges or tip.

(c) Provided repair of separation between foam and FRP is compensated for, in propeller balance.

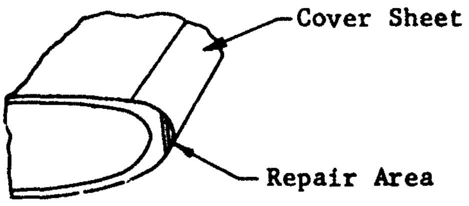
Cover Sheet
Repair Area

Edge Repair

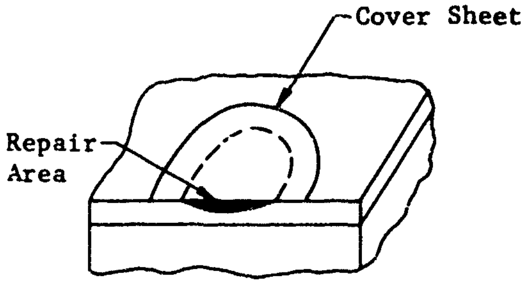
Cover Sheet
Repair Area

Center Repair

Figure 99. Fiberglass blade repair chart illustrating the type of repair that can be performed in the field.

Minor surface damage such as scratches up to 1 to 2 inches long and .005" to .010" maximum depth and areas up to 1/16" diameter and .005" to .010" maximum depth need not be repaired but should be periodically examined. If, however, total area containing such damage exceeds 20 square inches, repairs should be made to the FRP and/or coating.

Repairs to the above types of damage were made as described in the X-19 Utility Maintenance Manual and include the following:

(a) Repair of damage to edges or blade tip.

(b) Repair of damage to blade plate or fairing surface.

(c) Repair of loose or unbonded foam.

(d) Repair of protective coating.

(5) Propeller Balance

All new FRP propeller blades were balanced at the factory to a blade master for a particular design, making such blades interchangeable. Therefore, propeller balance has to be considered when FRP blade repairs are made in the field.

In the case of minor repairs, the propeller balance had to be checked and adjusted.

(6) Preventive Maintenance

The plastic materials used in fabricating the Curtiss-Wright fiberglass propeller blades have been used for many years under various conditions and have been proven to be tough, corrosion resistant, fungus resistant and superior to metals with respect to low notch sensitivity and strength-to-weight ratio.

However, certain preventive maintenance and handling care should be exercised. Blades should be inspected before flight for any external damage to the FRP area and/or steel shank.

Blades should also be checked for the condition of the foam bond by "tap testing".

Any indication of damage should be reviewed and appropriate action taken. Blades should be handled carefully. They should not be lifted with slings or hooks.

The steel shank of the blade should be protected from handling damage and corrosion.

FRP blades should be stored in suitably padded racks when not in use, and, since these blades are foam-filled, they should not be stored in an excessively hot location.

d. Reliability

The X-19 project involved the integration of many components and numerous subsystems into a complete airplane system, and although no numerical reliability requirements had been specified either for the system or its components, it was obvious that the operational reliability goal for the system must be high.

This was dictated by the requirements of aircraft safety and performance, as well as by the necessity of mission success, and was implied in the specified design goal of 10,000 hour service life and 1000 hours time between overhaul of dynamic components.

The project plans for this vehicles did not include reliability demonstration testing as such. The X-19 test program revealed that the proposed testing was primarily intended to assure the functional adequacy of the first flight article. Pre-flight verification is predicated on demonstration in these tests of satisfactory performance of each component and subsystem, where "satisfactory performance" is defined as freedom from failures which would be hazardous in a preliminary flight test program.

The testing of hardware that was initiated during the development phase of the project was essentially a program involving the qualification of the design and quality assurance of the prototype hardware.

In verifying the functional and structural adequacy of the prototype it served to demonstrate compliance with high quality requirements - requirements which result in high reliabilities for mechanical systems.

The experimental program scheduled for the airplane, its subsystems and components is outlined in Figure 100.

In recognition of the fact that the prototype X-19 airplane was an experimental model devoted to extensive flight testing, and that it was the fundamental policy to pursue flight safety and functional adequacy of the system from the earliest possible stage of system utilization, the approach to the problem was to:

(1) Defer formal demonstration of reliability as such until the flight test phase of the program, where the complete system could be tested under a truly operational environment.

(2) Concentrate the reliability effort during the prototype development phase on assuring the functional adequacy and flight safety of the vehicle, rather than on questions of long term failure probabilities.

(a) Make failure analyses of vital subsystems of the airplane, to reveal and eliminate design deficiencies which could result in catastrophic failure or inability to perform expected flight test missions.

(b) Review all pre-flight test programs and results, to detect any failure modes that may be revealed. Despite the fact that reliability measurement during the pre-flight phase is drastically limited by the scope of the test program, where possible the testing was to be directed so as to assure the most meaningful results possible to be obtained from a reliability standpoint.

e. Propeller Weight

The total weight of the complete propeller-nacelle assembly of the X-19 aircraft as assembled for flight testing on the #1 aircraft was 585.9 lbs. The weight breakdown was as follows:

(1) Propeller Assembly	
(a) Assembly less Blades	161.2
(b) Blades	212.4
(2) Nacelle Housing Assembly	31.4
(3) Housing Filling Actuator	162.8
(4) Spinner Afterbody	1.5
(5) Tube and Dam Assembly	8.7
(6) Spinner Assembly	5.4
(7) Miscellaneous Hardware	2.5
Total	585.9

Note: Propeller weight as usually quoted is 373.2 lbs.

2. BLADE STRUCTURAL DESIGN

a. General

The use of fiberglass reinforced plastic as a blade material has been under consideration for many years, the first design studies by Curtiss-Wright having been made in 1943. The main attraction

Sub-System	Component	Description	Test Details
Propeller	Propeller, with blades	Calibration and overspeed on Electric Whirl stand at ASD	Thrust and horse[illegible] calibration Blad[illegible] [illegible] [illegible] [illegible]
	Propeller-Nacelle assembly less blades	Operation of Propeller-Nacelle assembly on CWCD Electric Whirl stand	[illegible] acelle assembly (less blades) [illegible] oading [illegible] vertical [illegible] ler 7° below horizontal
	Blade Retention	Endurance Test 2 Retention fatigue machine	[illegible] 10^6 [illegible] on 2 fiberglass-steel blade shanks to failure
	Blade	Fixed-Root testing to demonstrate structural adequacy and endurance limit of blade under edgewise vibration.	Est. 5 x 10^6 cycles on 1 full-scale blade; to failure
		Free-Free testing to demonstrate structural adequacy and endurance limit of blade under first-mode flapping vibration.	Est. 50 x 10^6 cycles on 1 full-scale blade; to failure
		Torsional testing to demonstrate structural adequacy of blade under flutter stresses, and to establish a torsional endurance limit	Est. 100 x 10^6 cycles on [illegible] full-scale blades; to failure
		1 x P Endurance on CWCD gyro test stand	100 test hours at high 1 x P loading on propeller
Mechanical Transmission System	Shaft coupling & bearing	Torque transmission capacity of crowned splines working against straight splines, in CWCD spline test rig under angular misalignment	Endurance time on straight and crowned splines under torque and misalignment loading
	Nacelle tilt system	Demonstration of operation of nacelle tilt drive systems, including power drive unit, flexible shafting, gear box, bi-directional no-backs, speed reducer, and actuator.	Test cycles on drives: Hydraulic: Full V to Full H and return -- 100x Manual: Full H to Full V -- 25x
	Accessory drive gear box	Endurance test to demonstrate performance at maximum load and speed.	50-hour endurance test, with appropriate drives and power absorbers
Engine-Drive Propeller System	Half-System, simulating front transverse section of the airplane	Verification of the performance, structural adequacy and functioning of the main drive system, its controls, and the accessory drive system of the airplane. Propellers, gear-boxes, shafting, engines	Testing equivalent to 50 hours of normal airplane operation. Blade vibration survey Vibratory torque survey of shafting Stress survey of components 50 hours of scheduled endurance Thrust and torque loads only
Propeller Controls System	Propeller Coordinator	Calibration, overload and endurance testing of coordinator	50-hours of endurance test time
	Stability Augmentation System	Endurance and environmental testing of Dual-Axis Stablizer	Calibration Vibration testing 50-hours endurance
	Engine Speed Control	Calibration and endurance testing on governor test stand.	Vibration survey Calibration 50-hours endurance
Airframe	Castings	Structural proof tests	3 of each
	Minor Components: Fittings Carry-thru structure	 Static and fatigue tests Static and fatigue tests	 7 fittings including 1 splice 500,000 cycles fatigue testing
	Major Components: Landing gear	Drop tests, fore-aft and side loading tests on main gear and nose-wheel	Stress and deflection measurements
Airplane	Entire System	Ground and taxi tests (and ground vibration survey)	Vibration testing of propeller, engine and airframe. At taxi speeds up to 25 mph, check of the various sub-systems of the airplane.
		Flight Tests.	40 hours of flight testing of complete system under flight

		drive system of the airplane. Propellers, gear-boxes, shafting, engines	Stress Survey of components 50 hours of scheduled endurance Thrust and torque loads only
Propeller Controls System	Propeller Coordinator	Calibration, overload and endurance testing of coordinator	50-hours of endurance test time
	Stability Augmentation System	Endurance and environmental testing of Dual-Axis Stabliser	Calibration Vibration testing 50-hours endurance
	Engine Speed Control	Calibration and endurance testing on governor test stand.	Vibration survey Calibration 50-hours endurance
Airframe	Castings	Structural proof tests	3 of each
	Minor Components: Fittings	Static and fatigue tests	7 fittings including 1 splice
	Carry-thru structure	Static and fatigue tests	500,000 cycles fatigue testing
	Major Components: Landing gear	Drop tests, fore-aft and side loading tests on main gear and nose-wheel	Stress and deflection measurements
Airplane	Entire System	Ground and taxi tests (and ground vibration survey)	Vibration testing of propeller, engine and airframe. At taxi speeds up to 25 mph, check of the various sub-systems of the airplane.
		Flight Tests.	40 hours of flight testing of complete system under flight loads and true operating environment.

Note: It should be noted that all testing not pertinent to reliability evaluation has been omitted from the above tabulation. This would include, in general:

1. Functional testing of components and subsystems, such as:
    a. Nacelle Pump, on pump test rig
    b. Electrical System
    c. Hydraulic System
    d. Vacuum System

2. Static Strength testing of components and subsystems, such as:
    a. Static deflection tests of Engine Coupling, Tee, and Nacelle Gearboxes
    b. Load tests on airframe components, such as:
        Front Wing & Carry-thru structure
        Elevator, elevator tab, and supporting structure
        Aft wing, Flaperon [illegible]
        Vertical [illegible]
        Fuselage
        Control Syst[illegible]
        Propeller, Nacelle housings

B

Figure 100. X-19, experimental program as scheduled for the airplane, subsystems and components.

of this material was the favorable strength-to-weight ratio, see Figure 101. Several problem areas were recognized such as the blade retention, adequate filler material, method of fabrication, etc. Serious studies of fiberglass blades were started in 1956 and active development initiated in early 1958 on blades for the X-100 aircraft. The first blades were molded in August of 1958 and installed on the X-100 aircraft in January 1959. Since that time 260 blades have been molded of five different designs in diameters of 10', 13', 13'6" and 15'6" and extensive testing carried out. Three different designs have passed standard military whirl test endurance and overspeed tests at powers up to 4400 horsepower and tip speeds up to 1200 ft/sec. See Figure 102.

b. Blade Design

As finally evolved, the Curtiss fiberglass reinforced plastic blade consists of a hollow monocoque shell molded on a steel shank. The internal cavity is filled with a plastic foam to provide the necessary support and rigidity to the fiberglass plates. This structure is shown in Figure 103. In the establishment of this design several structural characteristics had to be investigated. These were: material layup and properties, steel shank design, and the foam filler requirements.

(1) Fiberglass Material Properties

Following extensive material evaluations, it was determined that a combination of 43 and 181 cloth, in the ratio of 3 layers of 43 to one layer of 181, was best suited to provide the necessary radial and chordwise strength requirements of the blades. It should be noted however, that later full scale testing proved that this combination was marginal with respect to shear strength and shear rigidity.

In the more recent layups, this deficiency had been corrected by adding a layer of 181 cloth at 45° to the principal direction. With the basic layup established, extensive testing was carried out to establish the pertinent material characteristics, i.e. static strength and moduli, fatigue strength, abrasion characteristics, etc. The results of these evaluations are shown in Figures 104-112. From a structural standpoint the most important of the material properties is the Goodman Diagram, Figure 111. As shown, this curve represents the basic material characteristics; however, for design purposes this curve is modified to provide a safe working stress limit. The design curve as derived for the fiberglass blade is given in Figure 112. Other pertinent characteristics evaluated in the fiberglass blade program are given in Figures 113 through 115.

BLANK

Material	UTS F_T(psi)	Fatigue S($\pm$psi)	Notched Fatigue S_N($\pm$ psi)	Density d(lb/in^3)	F_T/d	S/d	S_N/d
CPS5037 CPS5038 Epoxy FRP (43:181 = 3.1)	103,800	12,600 FP	9,800 .010 45°V	.070	1.48	.18	.14
T1.(150A)	143,000	66,000 RRM	23,000 RRM .010 K_t=2.75	.160	.89	.41	.14
Mag. Forg. (ZK60AT-5)	48,000	18.000 Ax.	7,000 Axial .010 K_t=2.80	.065	.74	.28	.11
AL.76S Forg.	70,000	14,300 FP	10,500 RRM 60°V	.101	.69	.14	.10
Ext. Blade Steel (4320)	140,000	52,500 FP	30,800 RRM .010 K_t=2.75	.284	.49	.19	.11

Figure 101. Strength to weight comparison between fiberglass and other common structural materials.

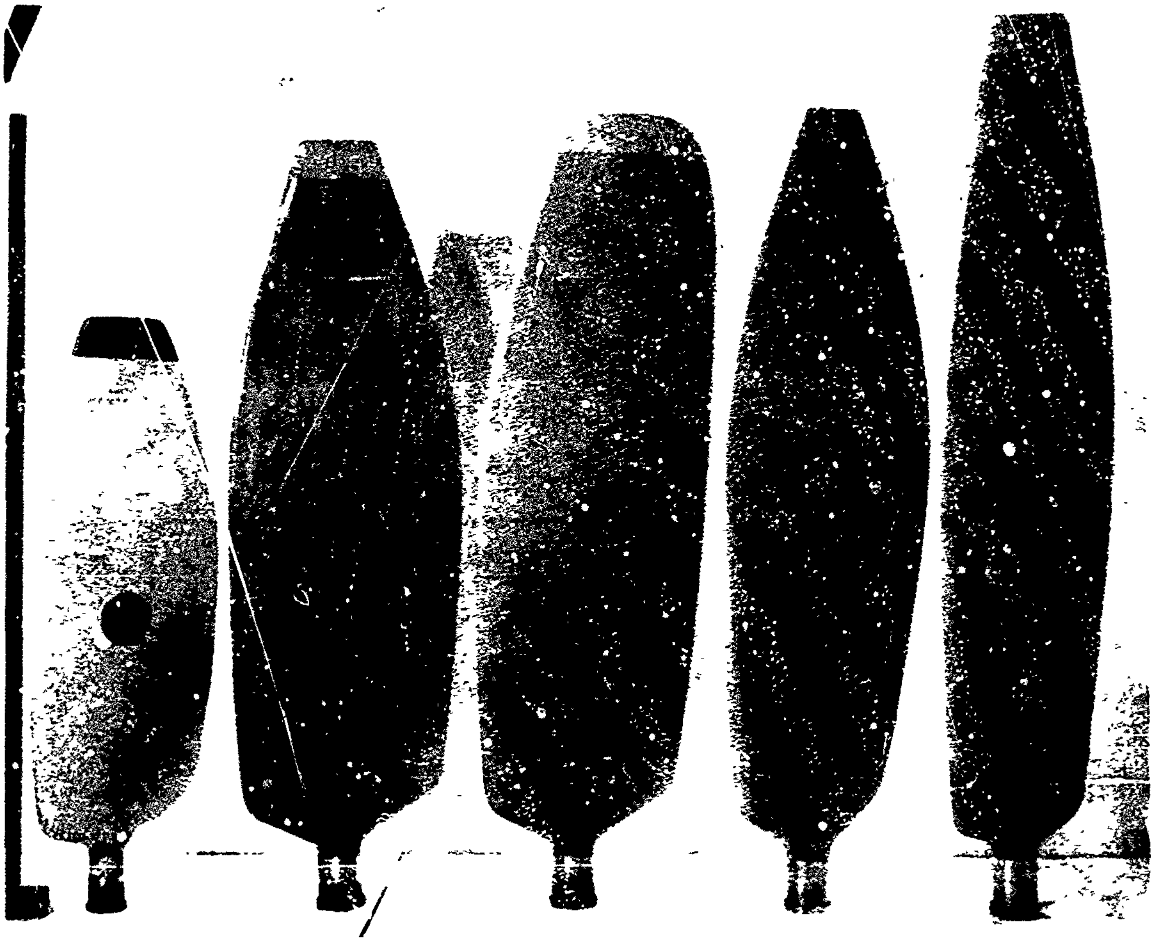

Figure 102. Fiberglass propeller blades which have been built and tested. From left to right: 10'-0" diameter used on X-100 aircraft, 13'-0" diameter used on X-19 aircraft, 13'-6" diameter used in static thrust testing, 13'-6" designed for T-64 engine tested to 4000 hp, 15'-6" designed for T-64 tested to 4400 hp.

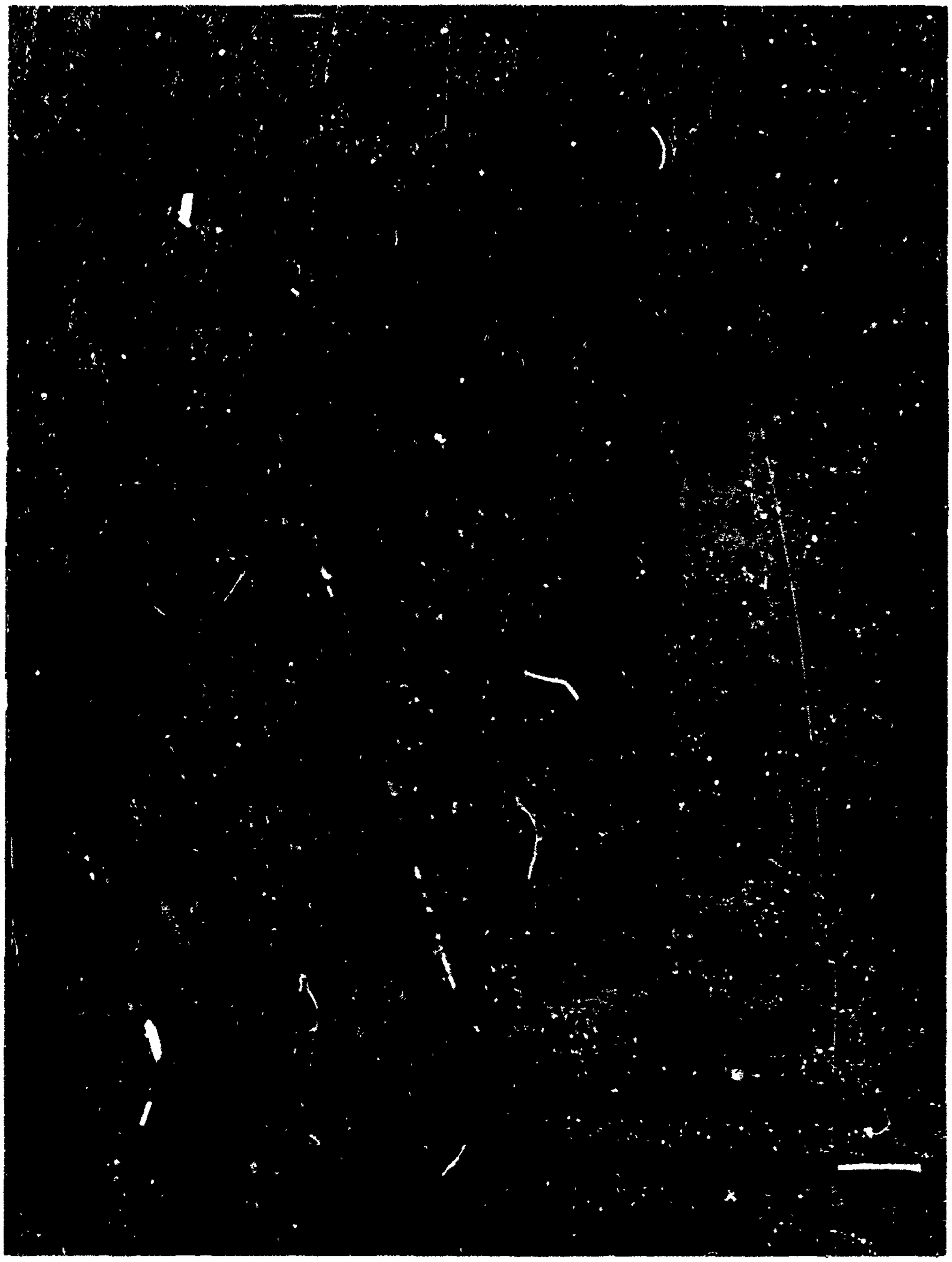

Figure 103. Sectioned fiberglass propeller blade showing the steel shank, fiberglass shell and foam filler.

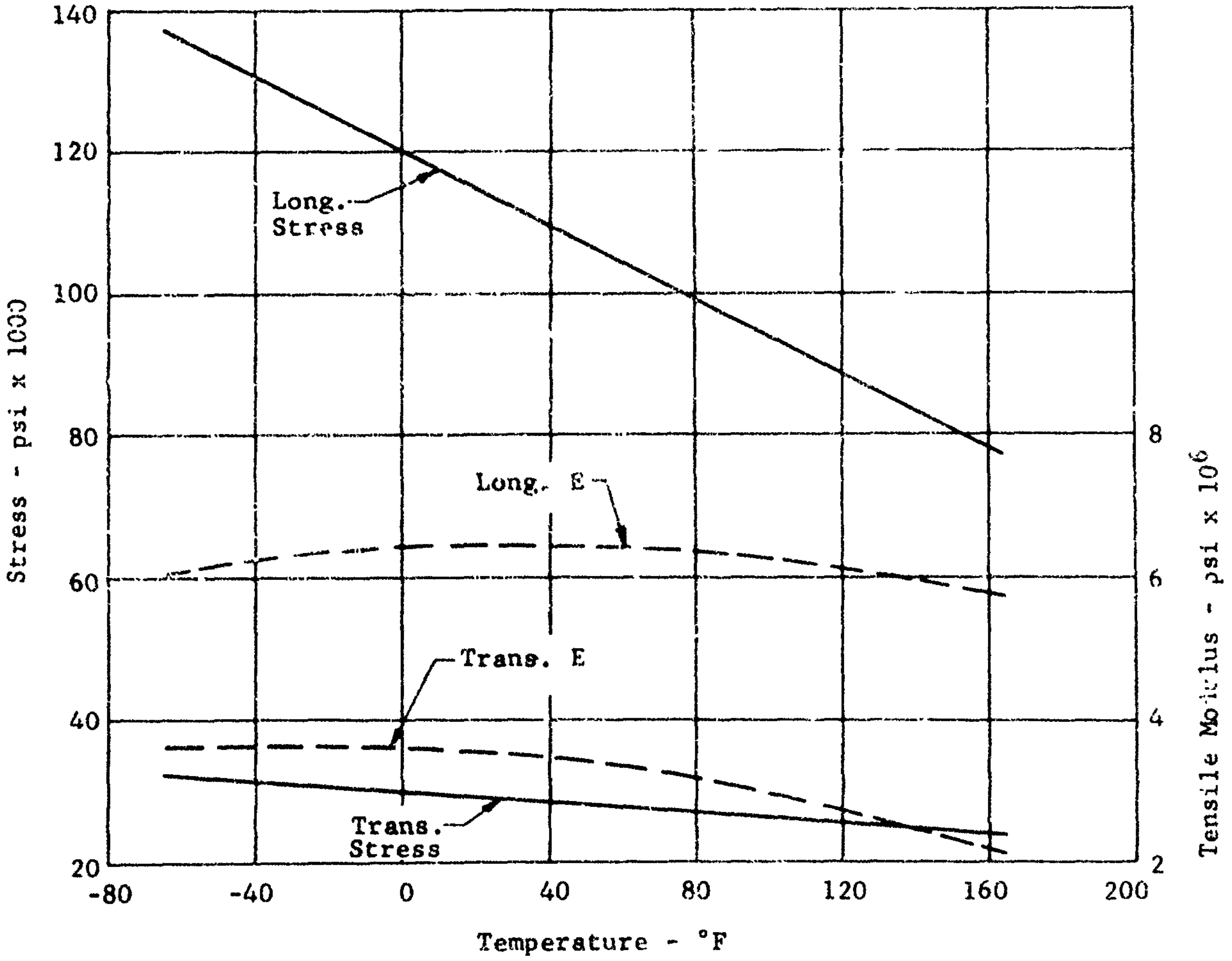

Figure 104. Epoxy fiberglass, ultimate tensile stress and tensile modulus, variation with temperature. One layer Stanpreg Vet 181 per CPS 5037, three layers Stanpreg Vet 43 per CPS 5038, 17 ply thickness: ASTM: D638-60T.

"FURNISHED UNDER UNITED STATES GOVERNMENT CONTRACT No. AF33(615)-3944. SHALL NOT BE EITHER RELEASED OUTSIDE THE GOVERNMENT, OR USED, DUPLICATED, OR DISCLOSED IN WHOLE OR IN PART FOR MANUFACTURE OR PROCUREMENT, WITHOUT THE WRITTEN PERMISSION OF CURTISS-WRIGHT CORPORATION, EXCEPT FOR (i) EMERGENCY REPAIR OR OVERHAUL WORK BY OR FOR THE GOVERNMENT, WHERE THE ITEM OR PROCESS IS NOT OTHERWISE REASONABLY AVAILABLE TO ENABLE TIMELY PERFORMANCE OF THE WORK, OR (ii) RELEASE TO A FOREIGN GOVERNMENT, AS THE INTERESTS OF THE UNITED STATES MAY REQUIRE; PROVIDED THAT IN EITHER CASE THE RELEASE, USE, DUPLICATION OR DISCLOSURE HEREOF SHALL BE SUBJECT TO THE FOREGOING LIMITATIONS. THIS LEGEND SHALL BE MARKED ON ANY REPRODUCTION HEREOF IN WHOLE OR IN PART."

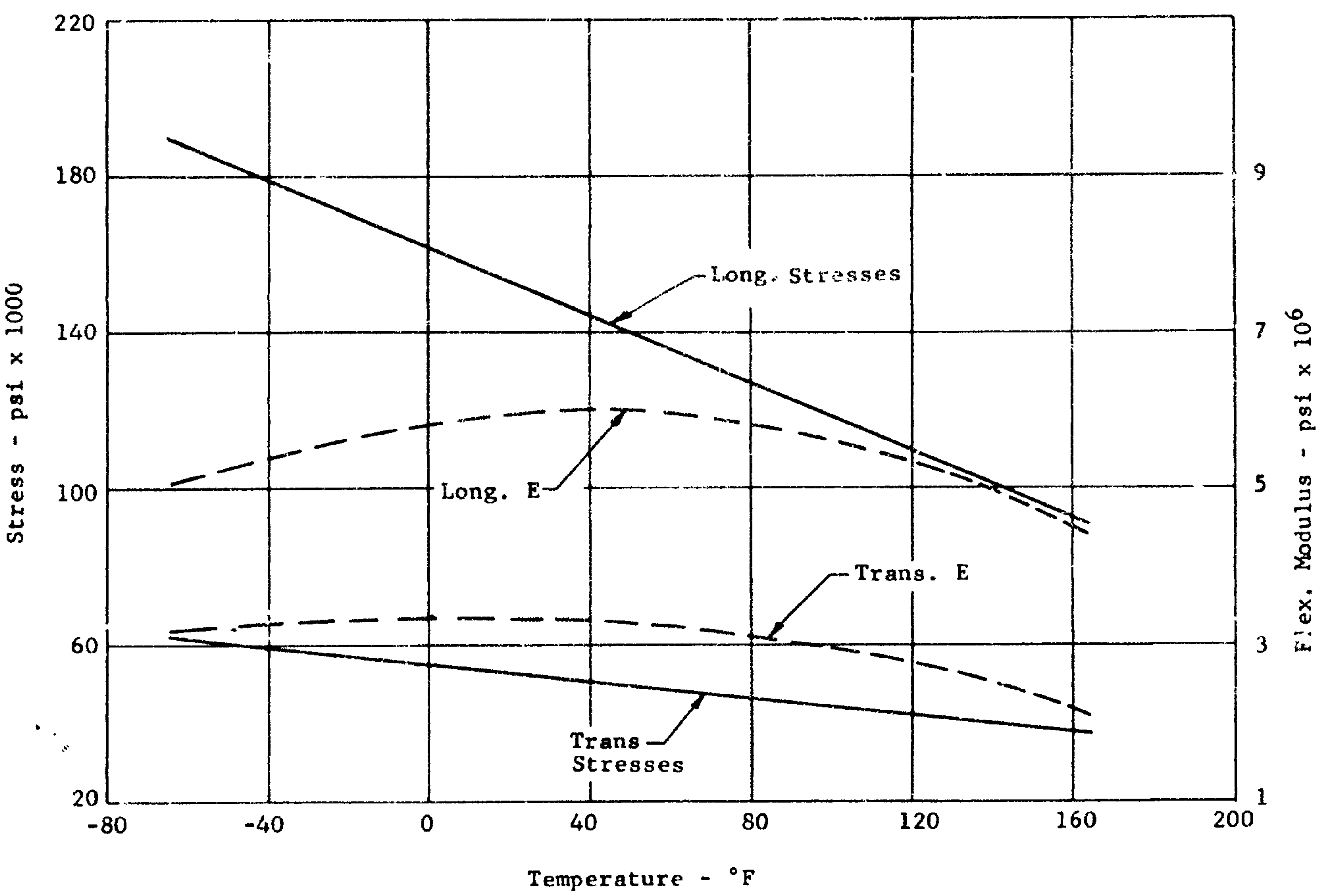

Figure 105. Epoxy fiberglass, ultimate flexural stress and modulus variation with temperature. One layer Stanpreg Vet 181 per CPS 5037, three layers Stanpreg Vet 43 per CPS 5038, 17 ply thickness: ASTM: D790-59T.

"FURNISHED UNDER UNITED STATES GOVERNMENT CONTRACT No. AF33(615)-3940. SHALL NOT BE EITHER RELEASED OUTSIDE THE GOVERNMENT, OR USED, DUPLICATED, OR DISCLOSED IN WHOLE OR IN PART FOR MANUFACTURE OR PROCUREMENT, WITHOUT THE WRITTEN PERMISSION OF CURTISS-WRIGHT CORPORATION, EXCEPT FOR (I) EMERGENCY REPAIR OR OVERHAUL WORK BY OR FOR THE GOVERNMENT, WHERE THE ITEM OR PROCESS IS NOT OTHERWISE REASONABLY AVAILABLE TO ENABLE TIMELY PERFORMANCE OF THE WORK, OR (II) RELEASE TO A FOREIGN GOVERNMENT, AS THE INTERESTS OF THE UNITED STATES MAY REQUIRE. PROVIDED THAT IN EITHER CASE THE RELEASE, USE, DUPLICATION OR DISCLOSURE HEREOF SHALL BE SUBJECT TO THE FOREGOING LIMITATIONS. THIS LEGEND SHALL BE MARKED ON ANY REPRODUCTION HEREOF IN WHOLE OR IN PART."

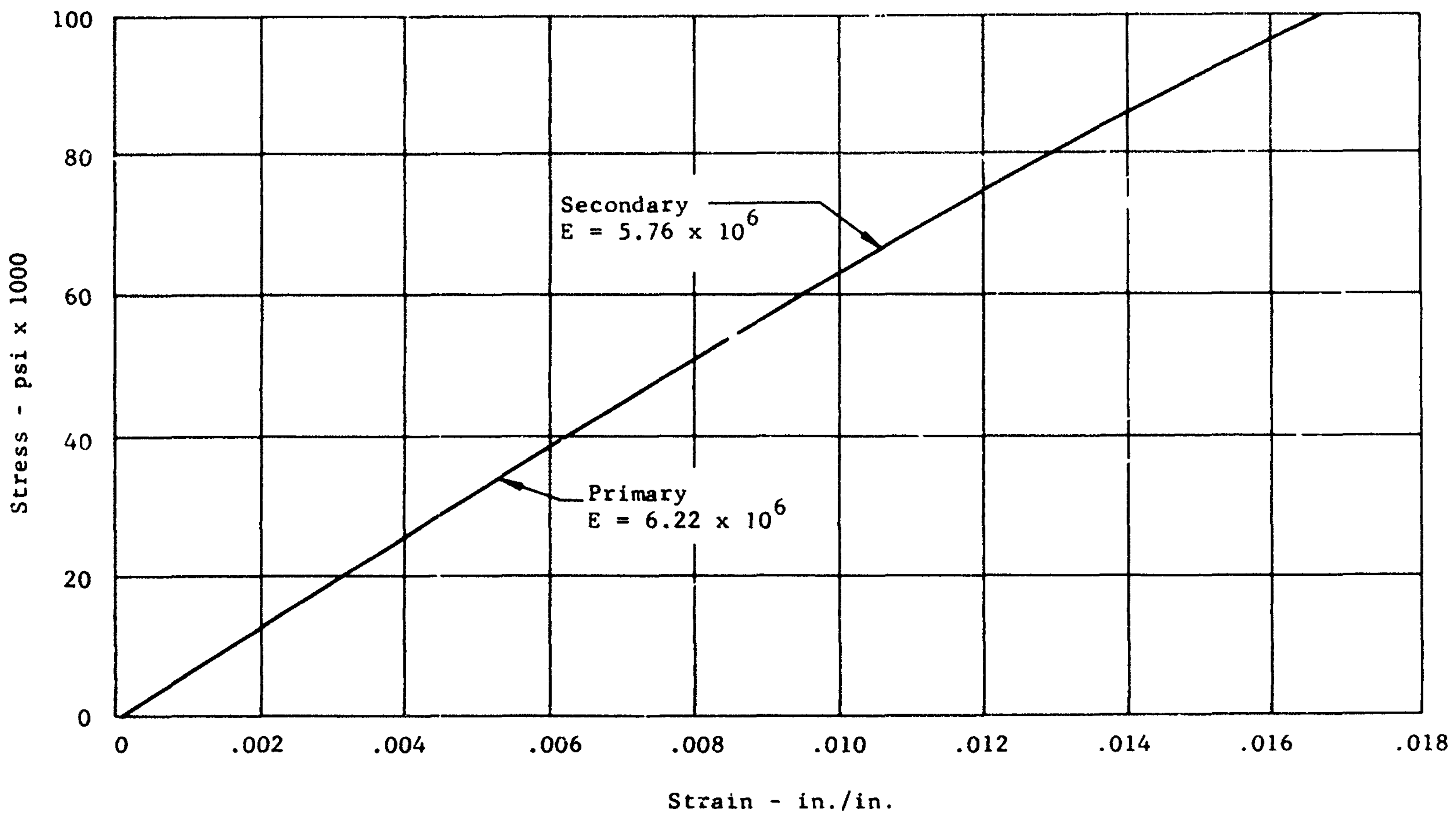

Figure 106. Epoxy fiberglass, typical tensile stress strain curve longitudinal direction. One layer Stanpreg Vet 181 per CPS 5037, three layers Stanpreg Vet 43 per CPS 5038, 17 ply thickness: ASTM: D638-60T.

"FURNISHED UNDER UNITED STATES GOVERNMENT CONTRACT No. AF33(615)-3940. SHALL NOT BE EITHER RELEASED OUTSIDE THE GOVERNMENT, OR USED, DUPLICATED, OR DISCLOSED IN WHOLE OR IN PART FOR MANUFACTURE OR PROCUREMENT, WITHOUT THE WRITTEN PERMISSION OF CURTISS-WRIGHT CORPORATION, EXCEPT FOR (I) EMERGENCY REPAIR OR OVERHAUL WORK BY OR FOR THE GOVERNMENT, WHERE THE ITEM OR PROCESS IS NOT OTHERWISE REASONABLY AVAILABLE TO ENABLE TIMELY PERFORMANCE OF THE WORK: OR (II) RELEASE TO A FOREIGN GOVERNMENT, AS THE INTERESTS OF THE UNITED STATES MAY REQUIRE: PROVIDED THAT IN EITHER CASE THE RELEASE, USE, DUPLICATION OR DISCLOSURE HEREOF SHALL BE SUBJECT TO THE FOREGOING LIMITATIONS. THIS LEGEND SHALL BE MARKED ON ANY REPRODUCTION HEREOF IN WHOLE OR IN PART."

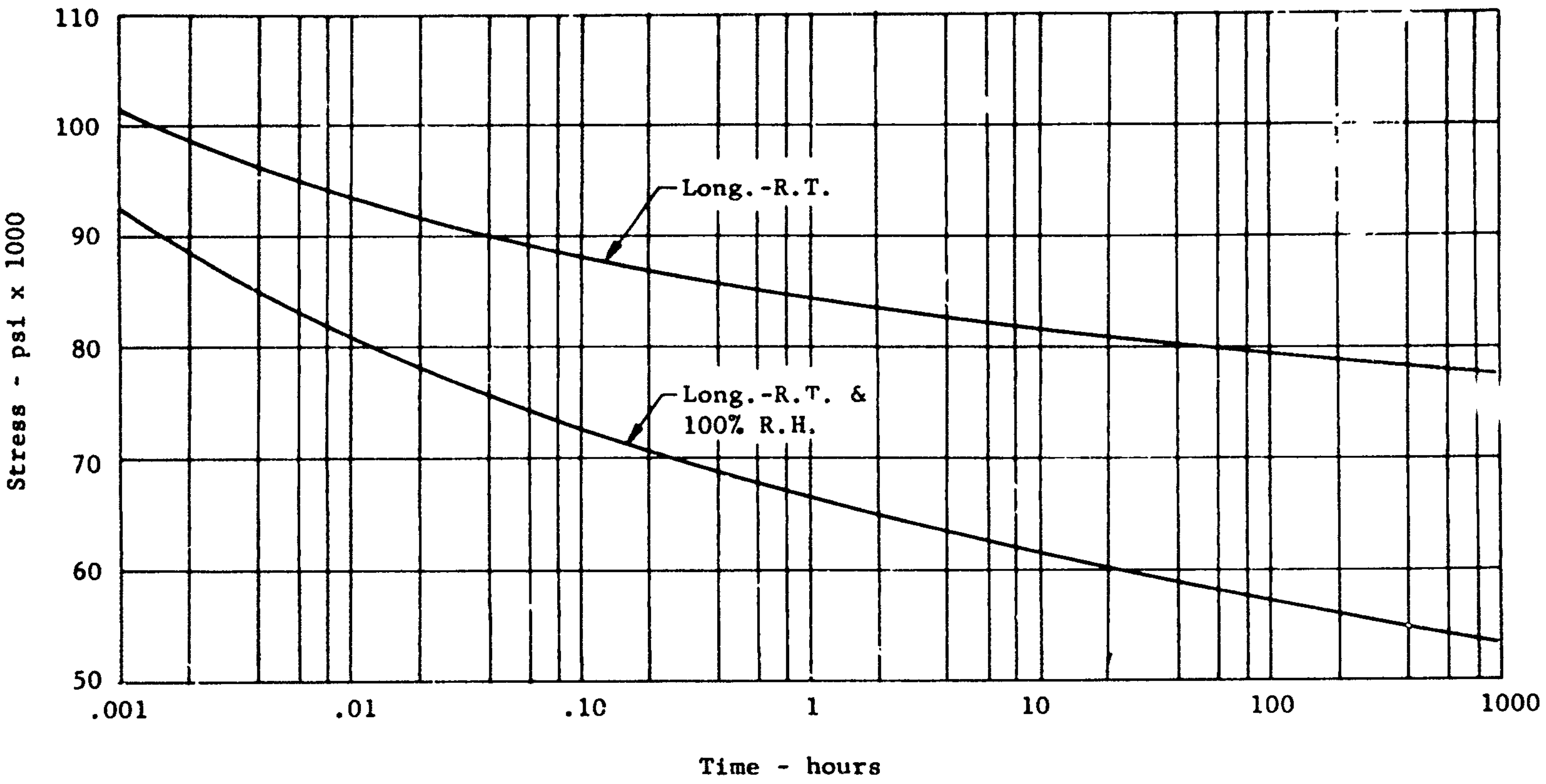

Figure 107. Epoxy fiberglass, tensile stress rupture. Standard room temperature, standard humidity and 100% humidity. One layer Stanpreg Vet 181 per CPS 5037, three layers Stanpreg Vet 43 per CPS 5038, 17 ply thickness: ASTM; D674-56.

FURNISHED UNDER UNITED STATES GOVERNMENT CONTRACT No. AF33(615)-1940. SHALL NOT BE EITHER RELEASED OUTSIDE THE GOVERNMENT, OR USED, DUPLICATED, OR DISCLOSED IN WHOLE OR IN PART FOR MANUFACTURE OR PROCUREMENT, WITHOUT THE WRITTEN PERMISSION OF CURTISS-WRIGHT CORPORATION, EXCEPT FOR (I) EMERGENCY REPAIR OR OVERHAUL WORK BY OR FOR THE GOVERNMENT, WHERE THE ITEM OR PROCESS IS NOT OTHERWISE REASONABLY AVAILABLE TO ENABLE TIMELY PERFORMANCE OF THE WORK. OR (II) RELEASE TO A FOREIGN GOVERNMENT, AS THE INTERESTS OF THE UNITED STATES MAY REQUIRE PROVIDED THAT IN EITHER CASE THE RELEASE, USE, DUPLICATION OR DISCLOSURE HEREOF SHALL BE SUBJECT TO THE FOREGOING LIMITATIONS. THIS LEGEND SHALL BE MARKED ON ANY REPRODUCTION HEREOF IN WHOLE OR IN PART."

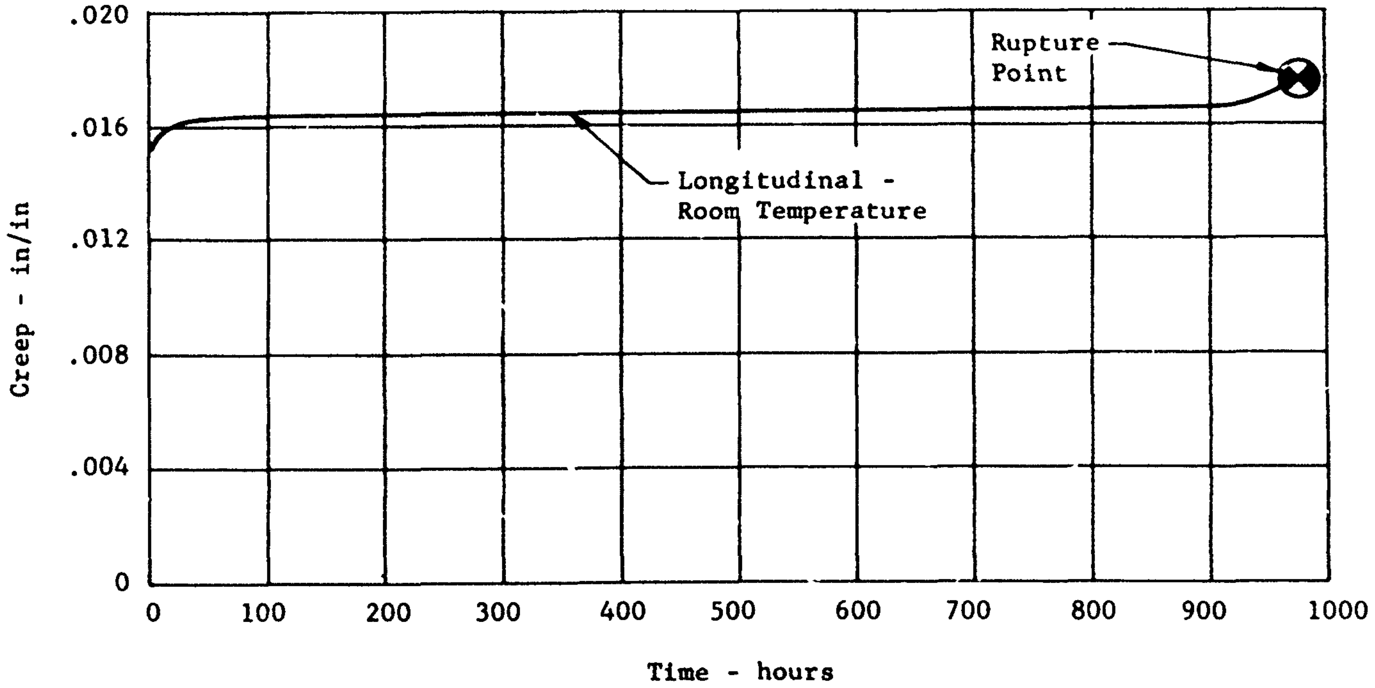

Figure 108. Epoxy fiberglass, creep rupture curve longitudinal tension, tensile stress = 75,000 psi. One layer Stanpreg Vet 181 per CPS 5037, three layers Stanpreg Vet 43 per CPS 5038, 17 ply thickness: ASTM: 674-56.

"FURNISHED UNDER UNITED STATES GOVERNMENT CONTRACT No. AF33(615)-3940. SHALL NOT BE EITHER RELEASED OUTSIDE THE GOVERNMENT, OR USED DUPLICATED, OR DISCLOSED IN WHOLE OR IN PART FOR MANUFACTURE OR PROCUREMENT, WITHOUT THE WRITTEN PERMISSION OF CURTISS-WRIGHT CORPORATION, EXCEPT FOR (i) EMERGENCY REPAIR OR OVERHAUL WORK BY OR FOR THE GOVERNMENT, WHERE THE ITEM OR PROCESS IS NOT OTHERWISE REASONABLY AVAILABLE TO ENABLE TIMELY PERFORMANCE OF THE WORK, OR (ii) RELEASE TO A FOREIGN GOVERNMENT, AS THE INTERESTS OF THE UNITED STATES MAY REQUIRE. PROVIDED THAT IN EITHER CASE THE RELEASE, USE, DUPLICATION OR DISCLOSURE HEREOF SHALL BE SUBJECT TO THE FOREGOING LIMITATIONS. THIS LEGEND SHALL BE MARKED ON ANY REPRODUCTION HEREOF IN WHOLE OR IN PART."

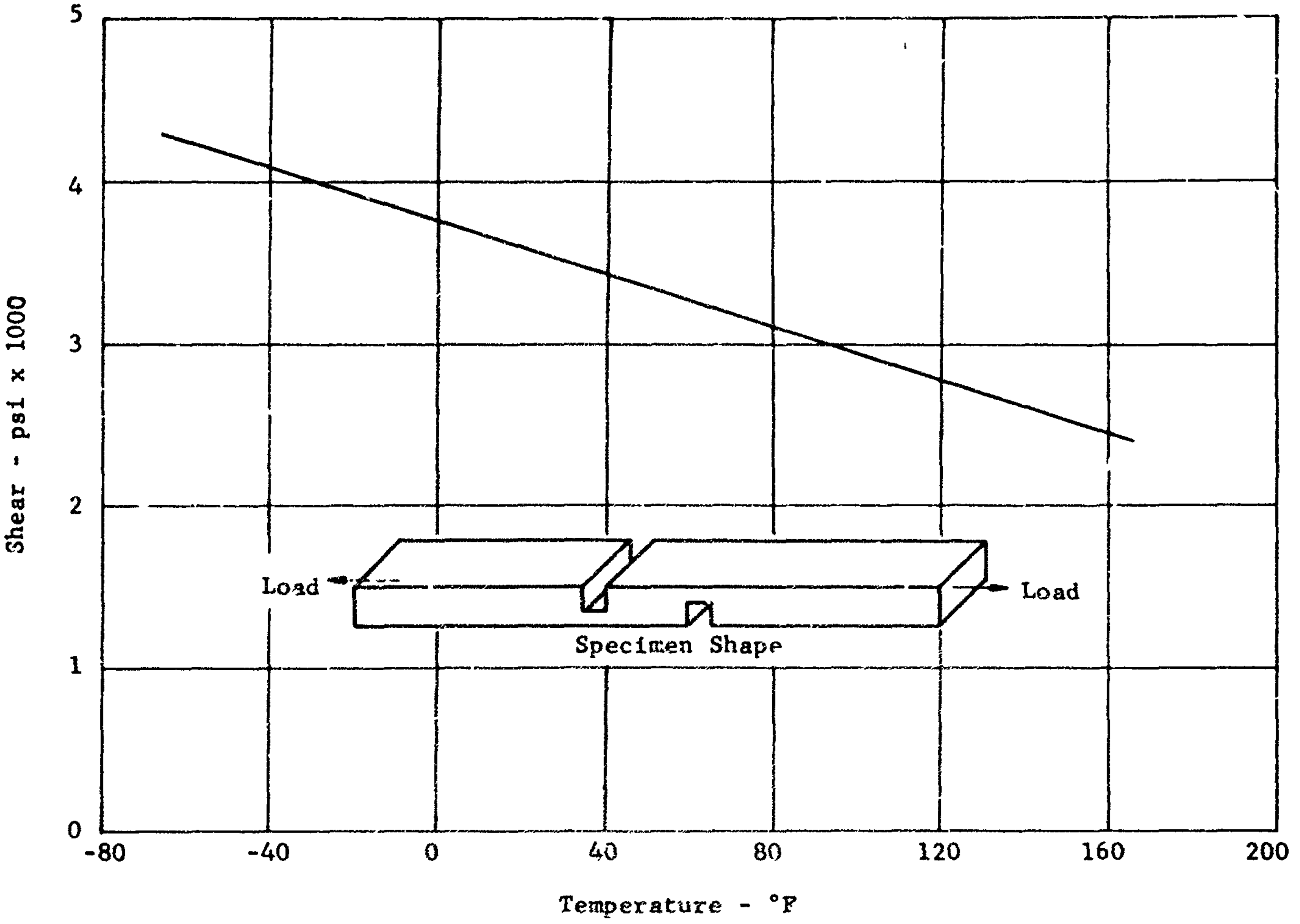

Figure 109. Epoxy fiberglass, interlaminar shear variation with temperature. One layer Stanpreg Vet 181 per CPS 5037, three layers Stanpreg Vet 43 per CPS 5038, 17 ply thickness: Federal Test Method Standard 406.

'FURNISHED UNDER UNITED STATES GOVERNMENT CONTRACT No. AF33(615)-3940 SHALL NOT BE EITHER RELEASED OUTSIDE THE GOVERNMENT, OR USED DUPLICATED, OR DISCLOSED IN WHOLE OR IN PART FOR MANUFACTURE OR PROCUREMENT, WITHOUT THE WRITTEN PERMISSION OF CURTISS-WRIGHT CORPORATION, EXCEPT FOR (I) EMERGENCY REPAIR OR OVERHAUL WORK BY OR FOR THE GOVERNMENT, WHERE THE ITEM OR PROCESS IS NOT OTHERWISE REASONABLY AVAILABLE TO ENABLE TIMELY PERFORMANCE OF THE WORK OR (II) RELEASE TO A FOREIGN GOVERNMENT, AS THE INTERESTS OF THE UNITED STATES MAY REQUIRE. PROVIDED THAT IN EITHER CASE THE RELEASE, USE, DUPLICATION OR DISCLOSURE HEREOF SHALL BE SUBJECT TO THE FOREGOING LIMITATIONS. THIS LEGEND SHALL BE MARKED ON ANY REPRODUCTION HEREOF IN WHOLE OR IN PART.'

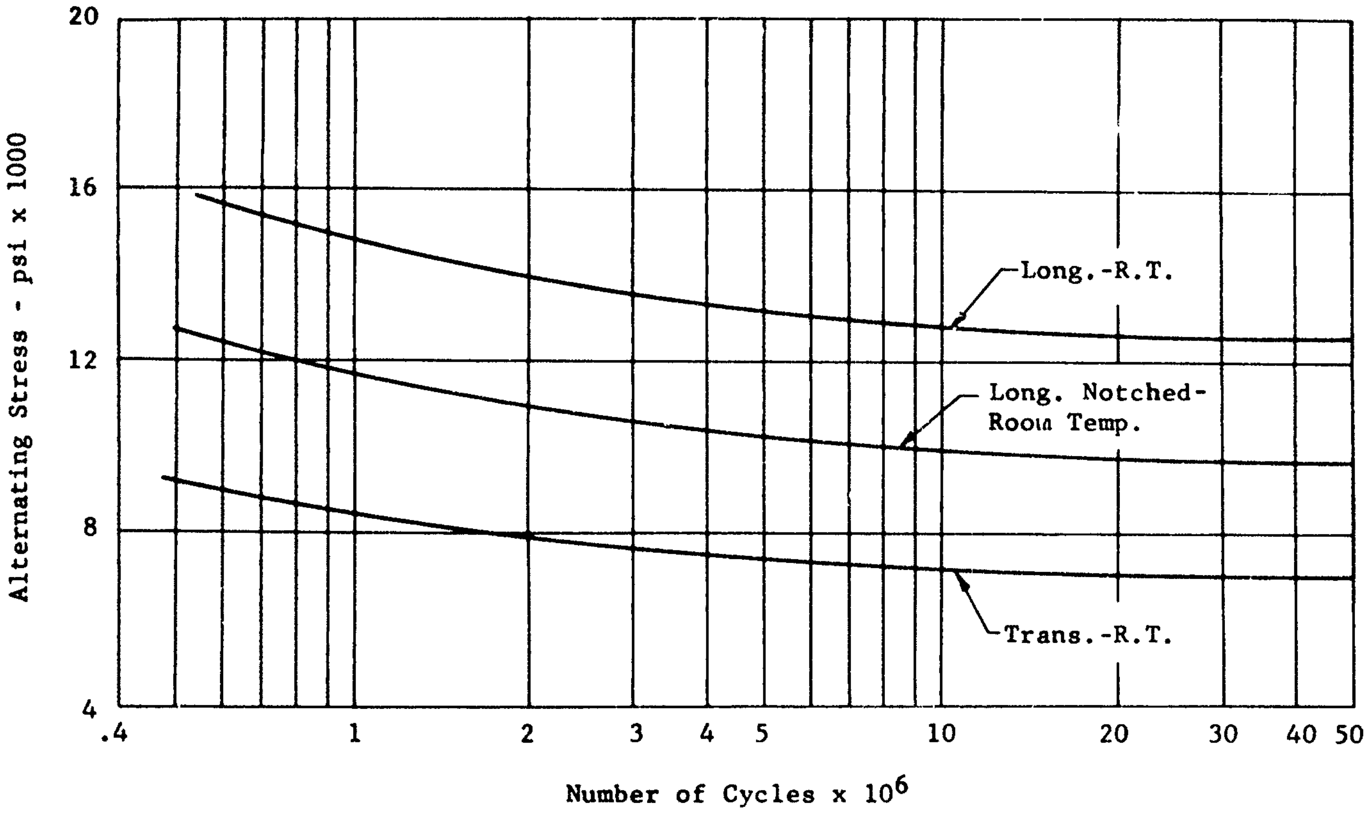

Figure 110. Epoxy fiberglass, flexural fatigue S-N curves for smooth and notched longitudinal specimens and smooth traverse specimens at room temperature. One layer Stanpreg Vet 181 per CPS 5037, three layers Stanpreg Vet 43 per CPS 5038, 17 ply thickness: ASTM: D671-517.

"FURNISHED UNDER UNITED STATES GOVERNMENT CONTRACT No. AF33(615)-3940. SHALL NOT BE EITHER RELEASED OUTSIDE THE GOVERNMENT, OR USED, DUPLICATED, OR DISCLOSED IN WHOLE OR IN PART FOR MANUFACTURE OR PROCUREMENT, WITHOUT THE WRITTEN PERMISSION OF CURTISS-WRIGHT CORPORATION, EXCEPT FOR (I) EMERGENCY REPAIR OR OVERHAUL WORK BY OR FOR THE GOVERNMENT, WHERE THE ITEM OR PROCESS IS NOT OTHERWISE REASONABLY AVAILABLE TO ENABLE TIMELY PERFORMANCE OF THE WORK. OR (II) RELEASE TO A FOREIGN GOVERNMENT, AS THE INTERESTS OF THE UNITED STATES MAY REQUIRE. PROVIDED THAT IN EITHER CASE THE RELEASE, USE, DUPLICATION OR DISCLOSURE HEREOF SHALL BE SUBJECT TO THE FOREGOING LIMITATIONS. THIS LEGEND SHALL BE MARKED ON ANY REPRODUCTION HEREOF IN WHOLE OR IN PART."

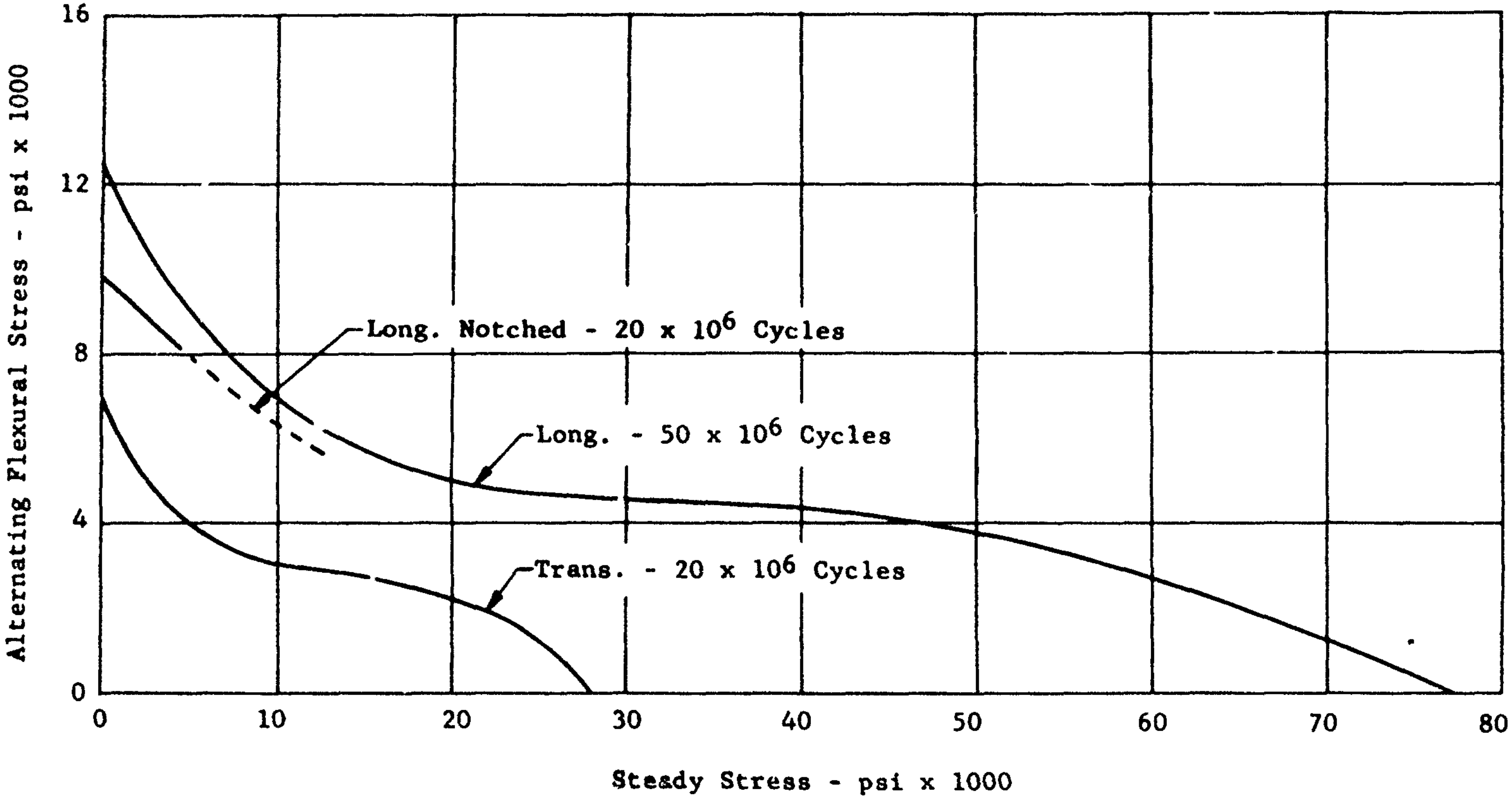

Figure 111. Epoxy fiberglass, modified Goodman diagram in the longitudinal and transverse directions. One layer Stanpreg Vet 181 per CPS 5037, three layers Stanpreg Vet 43 per CPS 5038, 17 ply thickness: ASTM: D671-51T.

FURNISHED UNDER UNITED STATES GOVERNMENT CONTRACT No. AF33(615)-3946. SHALL NOT BE EITHER RELEASED OUTSIDE THE GOVERNMENT, OR USED DUPLICATED, OR DISCLOSED IN WHOLE OR IN PART FOR MANUFACTURE OR PROCUREMENT, WITHOUT THE WRITTEN PERMISSION OF CURTISS-WRIGHT CORPORATION, EXCEPT FOR (I) EMERGENCY REPAIR OR OVERHAUL WORK BY OR FOR THE GOVERNMENT, WHERE THE ITEM OR PROCESS IS NOT OTHERWISE REASONABLY AVAILABLE TO ENABLE TIMELY PERFORMANCE OF THE WORK. OR (II) RELEASE TO A FOREIGN GOVERNMENT, AS THE INTERESTS OF THE UNITED STATES MAY REQUIRE. PROVIDED THAT IN EITHER CASE THE RELEASE, USE, DUPLICATION OR DISCLOSURE HEREOF SHALL BE SUBJECT TO THE FOREGOING LIMITATIONS. THIS LEGEND SHALL BE MARKED ON ANY REPRODUCTION HEREOF IN WHOLE OR IN PART."

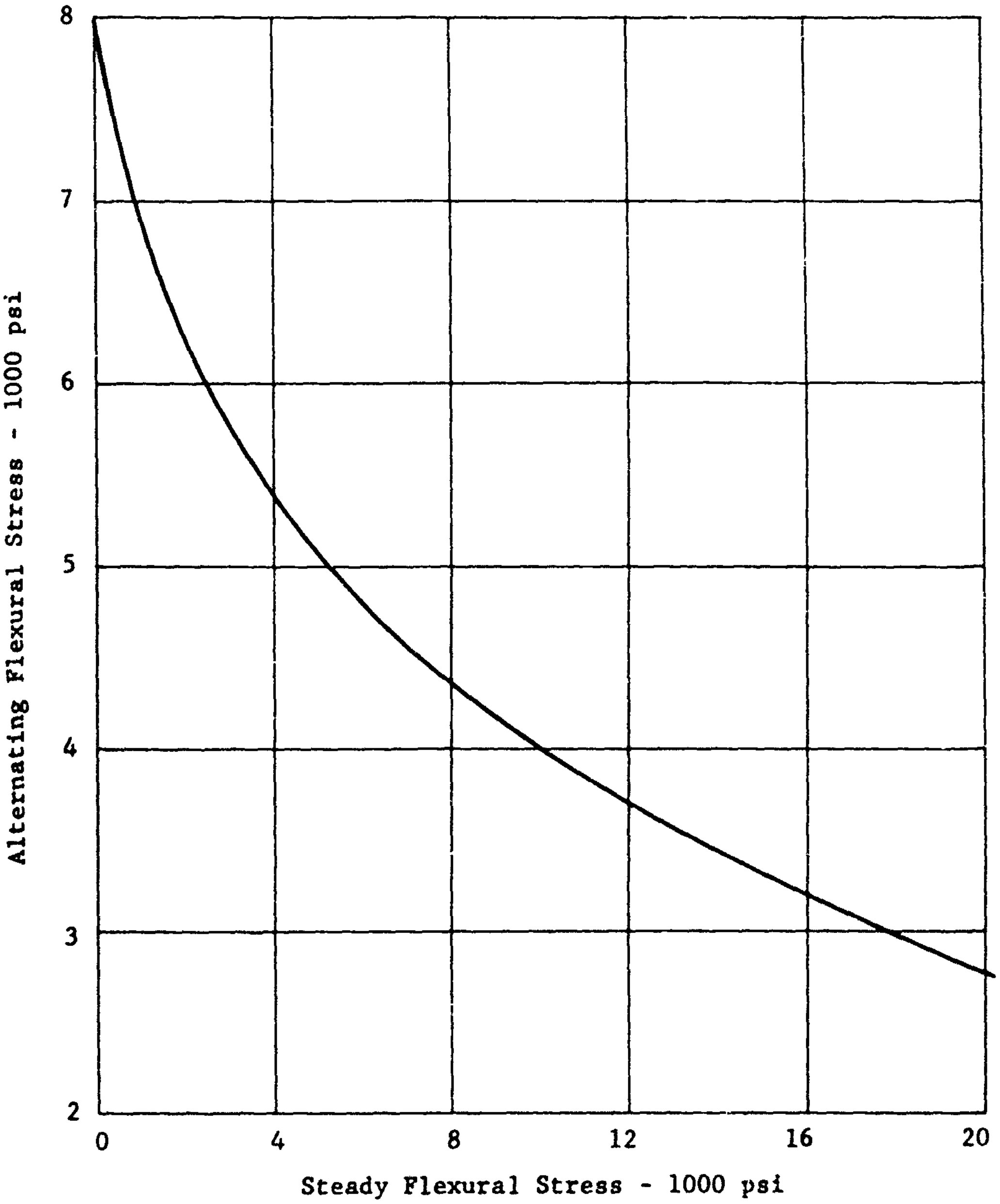

Figure 112. Epoxy fiberglass, design modified Goodman diagram as established for propeller blades. One layer Stanpreg Vet 181 per CPS 5037, three layers Stanpreg Vet 43 per CPS 5038.

"FURNISHED UNDER UNITED STATES GOVERNMENT CONTRACT No. AF33(615)-3940 SHALL NOT BE EITHER RELEASED OUTSIDE THE GOVERNMENT, OR USED, DUPLICATED, OR DISCLOSED IN WHOLE OR IN PART FOR MANUFACTURE OR PROCUREMENT, WITHOUT THE WRITTEN PERMISSION OF CURTISS-WRIGHT CORPORATION, EXCEPT FOR (i) EMERGENCY REPAIR OR OVERHAUL WORK BY OR FOR THE GOVERNMENT, WHERE THE ITEM OR PROCESS IS NOT OTHERWISE RESONABLY AVAILABLE TO ENABLE TIMELY PERFORMANCE OF THE WORK OR (ii) RELEASE TO A FOREIGN GOVERNMENT, AS THE INTERESTS OF THE UNITED STATES MAY REQUIRE. PROVIDED THAT IN EITHER CASE THE RELEASE, USE, DUPLICATION OR DISCLOSURE HEREOF SHALL BE SUBJECT TO THE FOREGOING LIMITATIONS. THIS LEGEND SHALL BE MARKED ON ANY REPRODUCTION HEREOF IN WHOLE OR IN PART."

Coating	Thickness	Specimen	Erosion in./hr
Neoprene	.025	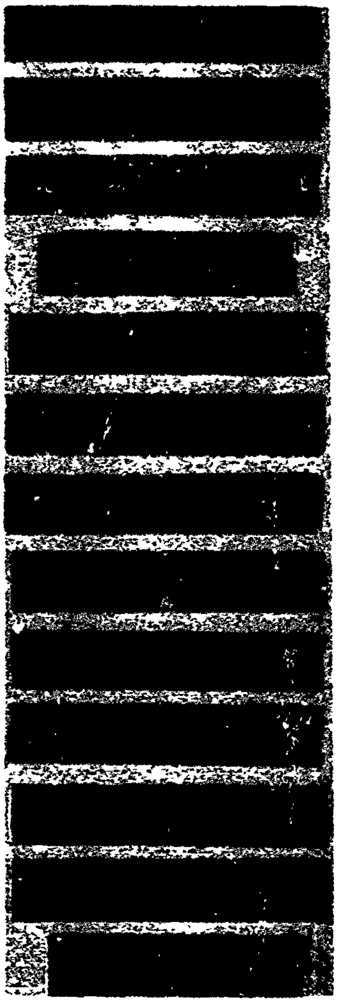	.0022
Uscothane	.040		.0025
Eccocoat IC2	.014		.0027
Stainless Steel	.012		.0036
Proprietary	.019		.0042
Proprietary	.011		.0042
Adiprene LD-315	.020		.0081
Conap	.015		.0086
Adiprene LD-213	.023		.0091
Bostik 435	.007		.0602
Marshall Urethane	.013		.0640
Dayglo 202-14	.005		.0840
Chemglaze Z051	.009		.1441

This chart shows a comparison test run on the Curtiss-Wright erosion test machine. The specimens are listed in order of their rates of erosion. The first two materials are relatively impractical to cover an entire blade because of their weight and need for cement bonding but are useful as leading edge abrasion strips. The Eccocoat is not usable because of its high cure temperature. The stainless steel, while it has a fairly low erosion rate, is not as good as it might appear since it is puckered and full of pinholes. This condition is virtually eliminated when the stainless is coated. The two proprietary coatings therefore are the most satisfactory in current use.

Figure 113. Comparative erosion resistance of various coating materials on fiberglass.

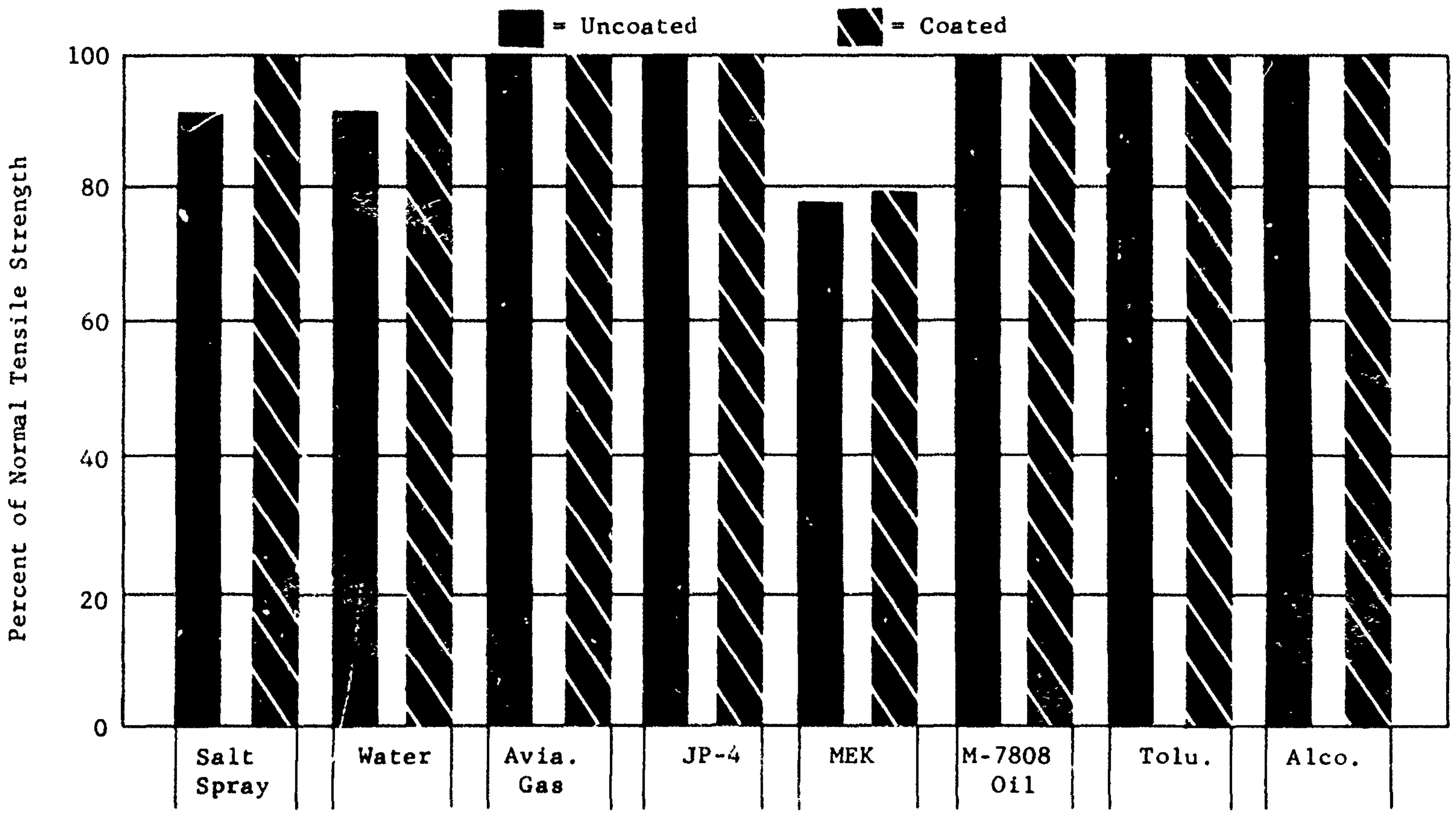

Figure 114. The effect of immersion in various solvents for seven days on the ultimate tensile strength of epoxy fiberglass with and without urethane coating.

Type	Use	Shear Strength (psi)		
		-65°F	R.T.	165°F
Shell VI	Shank Double Wrap Cured FRP to Cured FRP	2700	3800	1250
Angier SWL 164	Stainless to FRP Stainless to Neoprene	——	449	124

		Peel Strength (ppi)		
		-65°F	R.T.	165°F
Angier SWL 164	Neoprene to FRP	——	19.8	7.1

Figure 115. The strength characteristics of the various adhesives selected for use in the manufacture of fiberglass reinforced plastic blades.

(2) Foam Filler

On the basis of the theoretical wall thickness, the hollow fiberglass shell would be completely inadequate as a propeller blade. Because of the high flexibility of the plates, extensive buckling would occur at very low loads. This could obviously be remedied by designing the shell by elastic buckling criteria. However, that approach would result in wall thicknesses which would nullify the fundimental material weight advantage. The other alternative is to support the plates in such a manner as to prevent local plate instability. The developments in foam plastics offered the ideal material for a blade filler. An extensive development program was carried out to select a foam that would have the required characteristics: low density, high strength, good elongation, good bonding to the glass, etc. The foam development extended over a considerable period. Typical characteristics of the initial selections are given in Figure 116. In full scale blade testing and flight testing the foam proved to be the critical area in the design.

All blade failures apparently initiated with a foam separation or foam failure followed by a shell failure. Foam development was a continuing program, and the final blades for the X-19 included a considerably improved variation.

(3) Steel Shank

In the initial blade development studies, it was apparent that the fiberglass material would not be adequate for a conventional Curtiss flanged blade retention. An entirely new system of blade retention would have to be developed for an all fiberglass design. Therefore, in the initial development it would be more expedient to adapt the fiberglass blade to the time proven flanged steel retention, and continue a fiberglass retention development as a separate program.

In establishing the shank design the primary consideration was to provide a fail-safe joint between the glass and steel, i.e. a design which would continue to support the propeller loads in the event of a bond failure.

Several designs were studied, but the final selection was the relatively simple flaired or bell shaped tube, see Figure 117. This design has proven to provide the necessary mechanical interlock between the fiberglass and steel required to transmit the centrifugal, bending, and torsional loads without bonding. In practice, however, the fiberglass is carefully bonded to the steel, and the interlock feature is only provided to prevent catastrophic failure in the event of inadequate bonding.

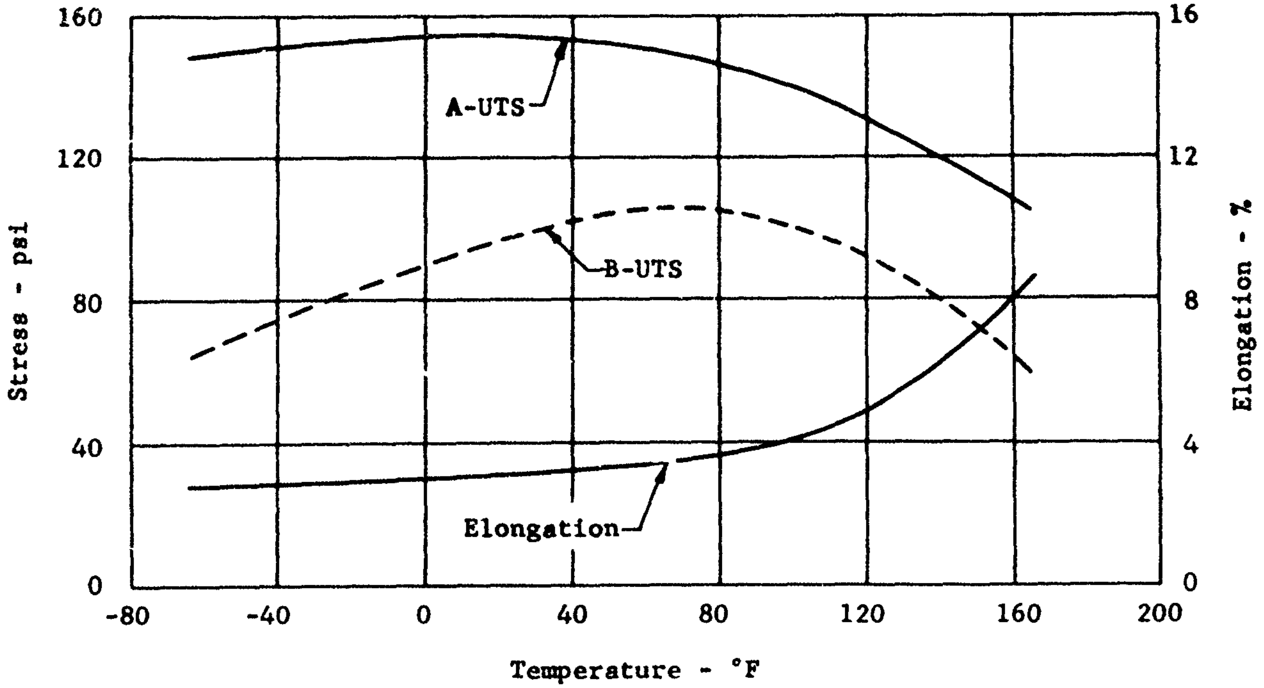

Figure 116. Typical properties of foam plastic filler as used in in the fiberglass foam plastic blade. Polyether base - Freon blown, A = 7.0 pounds per cubic foot, B = 5.0 pounds per cubic foot.

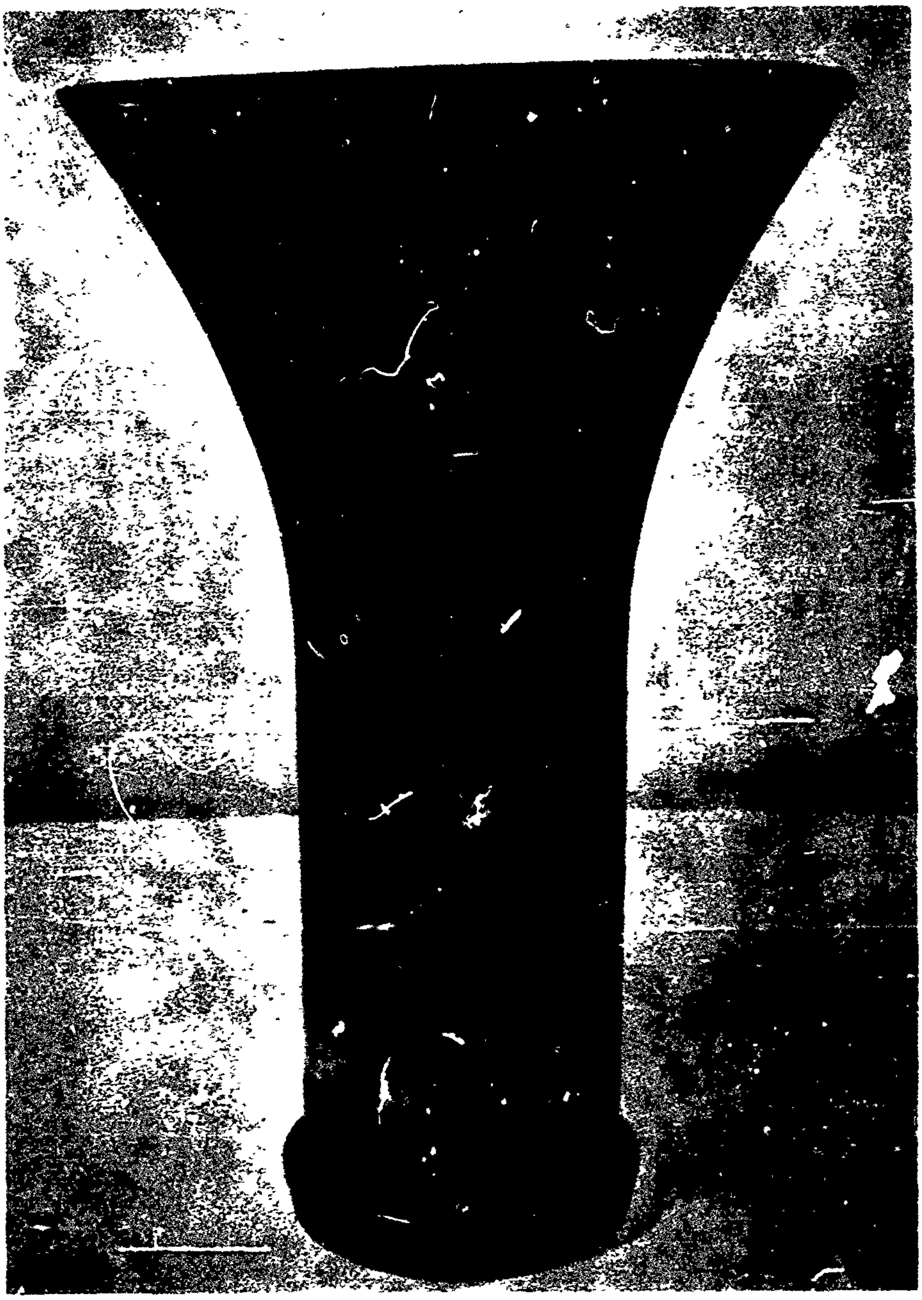

Figure 117. Steel shank as designed for the 13166A10P3 blade. AMS 6415 vacuum melt steel, RC 42-46.

(a) Material - In order to minimize blade weight of the X-19 propeller, the steel shank utilized high strength steel. The material was AMS 6415, RC 42-46. It is obvious that this hardness is bordering on the undesirable brittle range of the material. As a precaution against structural problems, the Metallurgy Department specified special heat-treat procedures for the processing of these shanks. In the initial development some cracking occurred due to hydrogen embrittlement and during the fiberglass molding cycle, Figure 118. This problem was overcome with the improvement of handling and processing techniques.

c. Design Details - 13166A10P3

(1) General Design Data

The 13166A10P3 design blade has a 13'0" installed diameter, has a calculated activity factor of 166 and an integrated design C_L of 0.055. A flange type shank design, having a bearing diameter of 4.4086/4.4078 inches is incorporated in the 13166A10P3 blade. The blade manufacturing centerline distance is 2.193 inches as measured from the butt face of the blade shank and the 2.35 degree blade forward tilt is incorporated by a machining operation starting at the 7-inch station. See Table IV for a complete tabulation of more detailed General Design Data.

(2) External Data

This blade planform is parallel sided from approximately the 15 inch station through the 42 inch station with a chord width of 25 inches. The planform tapers in a slight arc to a chord of 7.95 inches at the tip station. The aerodynamic design of the blade is discussed in Section 4.

The blade section profiles used from the 18 inch station outboard to the tip are NACA series - 64 type. Inboard of the 18 inch station a mathematical fairing profile was calculated to the last round station at 7.5 inch blade radius. See Table V for a tabulation of the Blade External Characteristics Data.

(3) Internal Data

Wall thickness of the steel blade root and the fiberglass cloth lay-up in the 13166A10P3 design blade has been determined to satisfy the structural requirements based on the

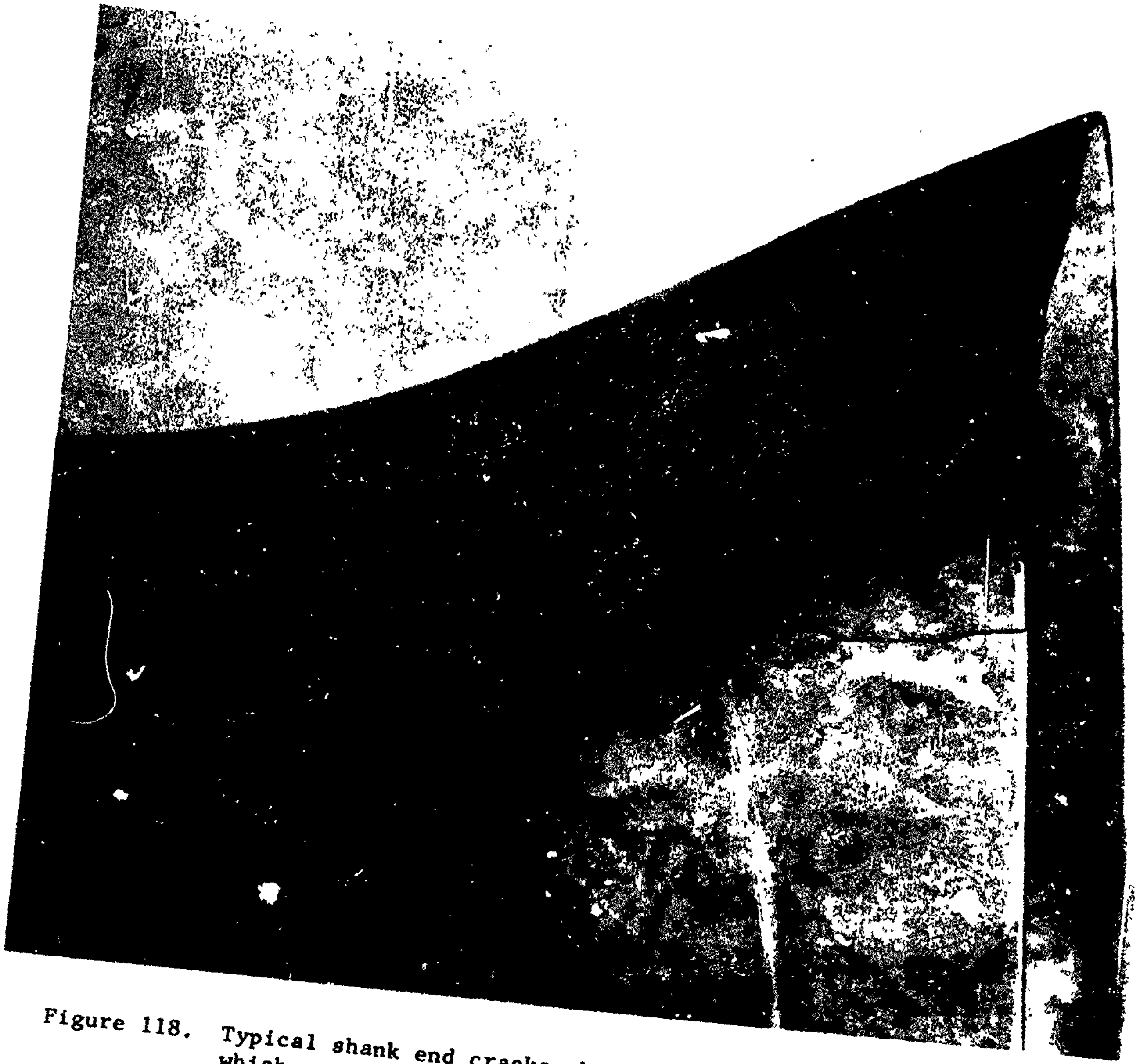

Figure 118. Typical shank end cracks which occured during fabrication and which were attributed to hydrogen embrittlement.

Table IV. Blade design 13166A10P3; general design data and summary.

Blade	Hollow Fiberglass
Design	13166A10P3
Diameter	13 feet
Activity Factor	166
Integrated Design Lift Coefficient	.055
h/b at .25 R	.2400
at .50 R	.1550
at .75 R	.0947
R	78.0"
.75R	58.50"
β 42" sta. - β .75 R	8.50°
b/D Max.	.1603
b Max.	25.00"
Forward Tilt - Origin 7" Sta. β at 42" station -30°	2.35°
External Surface Area from 7.5" Station to tip	3066 sq. in.
Volume of Fiberglass	403 cu. in.
Volume of Foam Filler Blade	1916 cu. in.
Volume of Foam Filler Shank Fairing	590 cu. in.
Total Blade Weight	59.15 lbs.
Total Blade Moment	1457.15 in. lbs.
Blade Center of Gravity - Station	24.65 Station
Edge Unbalance (Leading Edge Heavy)	
Vertical Balance Moment (β 42" Sta.=0°)	-4.10 in. lbs.
Face Unbalance (Camber Face Heavy)	
Vertical Balance Moment (β 42" Sta.=90°)	30.47 in. lbs.
Polar Moment of Inertia	11.21 slug - ft^2
Centrifugal Force Total (1210 rpm)	57,369 lbs.
Centrifugal Stress Max. at 1210 rpm	
Steel	15,000 lbs./in^2
Fiberglass	4,250 lbs./in^2
Station at Max Centrifugal Stress	
Steel	7.5" Station
Fiberglass	42" Station
Centrifugal Twisting Moment at 1210 RPM	
without tilt	23,992 in. - lbs.
with tilt	23,540 in. - lbs.
β 42" Sta. at Max. Centrifugal Twisting Moment -	
without tilt	39.55°
with tilt	38.13°

Table V. Blade design 13166A10P3; blade section characteristics data.

Station r	r/R	h	b	h/b	b/D	C_L	β	Notes
7.5	.096	4.40	4.40	1.0000	.0282	0	79.4	Round
9	.115	5.15	7.40	.6959	.0474	0	77.9	Faired
12	.154	6.49	22.47	.2888	.1440	0	74.9	Faired
15	.192	6.84	24.91	.2746	.1597	.007	71.9	Faired
18	.231	6.23	25.00	.2492	.1603	.063	68.9	NACA Series 64
21	.269	5.81	25.00	.2324	.1603	.125	66.2	NACA Series 64
24	.308	5.48	25.00	.2192	.1603	.165	63.7	NACA Series 64
27	.346	5.16	25.00	.2064	.1603	.190	61.3	NACA Series 64
30	.385	4.85	25.00	.1940	.1603	.200	59.1	NACA Series 64
36	.462	4.20	25.00	.1680	.1603	.200	54.9	NACA Series 64
42	.538	3.55	25.00	.1420	.1603	.200	51.0	NACA Series 64
48	.615	2.91	24.28	.1199	.1556	.194	47.5	NACA Series 64
54	.692	2.34	22.42	.1044	.1437	.130	44.5	NACA Series 64
60	.769	1.81	19.77	.0916	.1267	.050	41.9	NACA Series 64
66	.846	1.34	16.28	.0823	.1044	.002	39.3	NACA Series 64
72	.923	.92	12.34	.0746	.0791	0	36.8	NACA Sreies 64
75	.962	.72	10.18	.0707	.0653	0	35.5	NACA Series 64
77	.987	.59	8.68	.0680	.0556	0	34.7	NACA Series 64
* 78	1.000	.52	7.95	.0654	.0510	0	34.3	NACA Series 64

* Before 1" Corner Radii and Full Thickness Radius

allowable stresses for the fiberglass system and steel selected. The steel blade root is fabricated from a bell-shaped die forging which includes the blade forward tilt requirement. Fabrication consists of a machine turning followed by hot forming and final machining to produce the desired shank shape and spline configuration. In the 13166A10P3 shank configuration, the outboard fiberglass blade is held to the steel shank mechanically without relying on the bonding properties of the fiberglass.

Any bonding realized is considered as an additional factor of safety and is not included in the structural calculations. A lightweight, 8 lbs. per cu. ft. internal foam plastic filler is used in the 13166A10P3 blade for control of plate diaphragming, blade distortion and vibratory stresses. The internal foam also contributes to the stiffness and load carrying capacity of the fiberglass structure.

A 5 lb. per cu. ft. foam is used as an internal filler of the blade shank fairing which extends from the 7.5 to 27 inch station. This shank fairing has a 0.015 inch external fiberglass cover sheet. The total weight of the foam is approximately 10 lb. The shank weighed 18.5 lb. and the fiberglass was approximately 41 lb.

(4) Section Properties

The section properties, for the basic fiberglass blade, foam plastic blade filler, and the steel blade root, were calculated using digital computing equipment. For evaluation of the composite structure, all values for materials other than fiberglass were converted to their respective "fiberglass equivalent" values. Density values for the materials used are as follows:

Internal Foam	0.00463 lbs./cu. in.
Fairing Foam	0.00289 lbs./cu. in.
Fiberglass	0.070 lbs./cu. in.
Steel	0.284 lbs./cu. in.
Urethane Rubber	0.039 lbs./cu. in.

Table VI is a summary of the blade sections properties.

(5) Blade Construction

The 13166A10P3 design blade was fabricated by the following method:

(a) Machine and hot form die forging 162848F to the steel blade root configuration, Dwg. 164206.

Table VI. Blade design 13166A10P3; summary of blade structural & mass section properties (equivalent to fiberglass).

Sta.	Area Struct.	Area Mass	I Min. Struct.	I Min. Mass	I Maj. Mass	y_{c_g}	y_c	b_{c_g}	LEA	I/c_C Struct.	I/c_T Struct.	Z Struct.
7.5	19.55	15.10	41.99	32.50	32.50	0	0	2.200	2.200	19.09	19.09	
9	23.61*	19.38*	52.59*	43.44*	46.29*	0	0	3.696	3.700	21.44*	21.44*	221
	25.30	21.07	57.91	48.76	51.61					22.61	22.61	
12	37.08*	33.25*	106.31*	96.09*	236.31	0	0	11.105	9.500	34.85*	34.85*	5061
	40.56	36.73	122.81	112.59	252.88					38.02	38.02	
15	20.72*	20.62*	94.90*	90.55*	299.55*	.010	.007	11.029	11.160	29.34*	29.58*	8845
	24.66	24.56	118.89	114.54	333.81					35.01	35.28	
18	11.82	13.03	55.47	57.39	301.96	.079	.056	10.991	11.250	17.91	17.97	10058
21	11.22	11.77	47.44	47.95	384.62	.147	.116	11.121	11.250	16.36	16.56	18430
24	10.79	10.91	37.98	38.02	479.37	.173	.160	11.754	11.250	13.72	14.20	35545
27	10.86	14.40	29.47	33.86	669.37	.182	.186	11.626	11.250	11.18	11.83	52835
30	9.26	12.64	22.24	26.01	583.25	.188	.194	11.615	11.250	8.93	9.54	45249
36	6.95	9.96	12.63	15.22	453.65	.184	.194	11.611	11.250	5.81	6.30	34142
42	5.48	8.07	7.13	8.75	369.03	.182	.194	11.689	11.250	3.85	4.24	27450
48	4.31	6.40	3.79	4.67	277.83	.172	.182	11.426	10.925	2.48	2.77	19424
54	3.35	4.90	1.90	2.33	184.62	.106	.113	10.647	10.090	1.56	1.70	11204
60	2.60	3.65	.883	1.05	109.02	.035	.037	9.616	8.895	.96	1.00	5205
66	2.06	2.69	.372	.425	57.95	.002	.002	8.097	7.325	.56	.56	2020
72	1.60	1.90	.126	.137	25.09	0	0	6.321	5.555	.27	.27	539
75	1.41	1.59	.062	.066	14.79	0	0	5.291	4.580	.17	.17	224
77	1.28	1.39	.035	.036	9.44	0	0	3.860	3.920	.12	.12	105
77.8	2.77	2.77	.043	.043	9.25	0	0			.17	.17	68
78	0	0	0	0	0	0	0	3.492	3.600	0	0	0

* Including D.W.

(b) Assemble blade root 164206 with Teflon Bladder filled with clay beads and shape to core mold. Form rigid blade layup mandrel by drawing a vacuum on the bladder.

(c) Layup fiberglass cloth, cut to shape, over steel blade root and bladder mandrel to the specified wall thickness.

(d) Place "part c" assembly into blade mold and place in press. Release vacuum and build up internal pressure in bladder. Heat blade mold to required temperature and cure at 300°-325°F.

(e) Remove blade mold from press and remove internal beads and Teflon bladder. Foam fill blade internally with 8 lb./cu. ft. rigid foam and heat in press to cure foam.

(f) A second wrap, consisting of a fiberglass filament wound operation at a specified tension on a controlled schedule was added and cured at this time for increased hoop strength.

(g) Build up leading edge aerodynamic strip 60 in. station to tip in accordance with W_X dimension shown on finished section detail dwg. L-12953.

(h) Line 13166A10P3 Blade Shank Fairing Mold with 0.015 in. thick fiberglass cloth and assemble fairing mold on the foam fiberglass blade. Fill fairing mold with 5 lb./cu. ft. foam and cure.

(i) Perform all necessary finishing and balance operations.

Propeller balancing of these blades will be accomplished by adjustment of the radial location of the blades in the propeller hub. The total range of radial adjustment possible is 0.140 in.

This movement amounts to approximately 7.5 in. lbs. Blade horizontal balance moment is controlled, during blade fabrication, and is maintained within tolerance of a master balance moment. Note that no balance provisions have been provided for in the blade shank configuration Dwg. No. 164206. Therefore, blade balancing is accomplished by minor variations in the number of layers of cloth or the foam density.

(6) Blade Material

(a) Blade Root

The steel blade root was fabricated from Dwg. No. 162848F die forging. The die forging steel is AMS 6415, fully annealed, Brinell 229 max. After machining, the steel shank is heat treated per CPS 7011 to the desired hardness of Rockwell C 42 - 46.

(b) Fiberglass

Two types of fiberglass fabrics are specified for the structural blade wall thickness. These fabrics are impregnated per CPS 5033 by the Standard Insulation Co. These materials are:

(aa) Stanpreg VET 181, per CPS 5037, bidirectional fabric

(bb) Stanpreg VET 43, per CPS 5038, unidirectional fabric

(cc) Roving 60 End, per CPS 5039, 204 Filaments

The following tabulation presents test values based on repeated tests of the Stanpreg System. A ratio of one layer of VET 181 material to three layers of VET 43 material was used in the fabrication of test specimens to be consistent with the blade fabrication layup. The 60 end roving was used as a double wrap in the shank region with the filament wound at a specified tension on a controlled schedule.

Physical Properties 43:181-3:1

Ultimate Tensile

Longitudinal	79000 to 117000 psi	Avg. 101,700 psi
Transverse	25700 to 31470 psi	Avg. 28,700 psi

Ultimate Flexural

Longitudinal	108,600 to 147,230 psi	Avg. 129,200 psi
Transverse	43,240 to 51,000 psi	Avg. 46,400 psi

Tensile Modulus

Longitudinal

Primary	$(5.4 \text{ to } 7.15) \times 10^6$	Avg. 6.2×10^6
Secondary	$(5.4 \text{ to } 6.01) \times 10^6$	Avg. 5.66×10^6

Transverse

Primary	$(2.8 \text{ to } 5.4) \times 10^6$	Avg. 3.77×10^6
Secondary	$(.85 \text{ to } 1.3) \times 10^6$	Avg. 1.05×10^6

Flexural Modulus

Longitudinal

Primary	$(5.37 \text{ to } 6.38) \times 10^6$	Avg. 5.7×10^6

Transverse

Primary	$(3.36 \text{ to } 3.99) \times 10^6$	Avg. 3.8×10^6

Flexural Endurance Limit SN Curves

Longitudinal	(Infinite Life)	± 13000
Transverse	(Infinite Life)	± 7000

Flexural Endurance From Goodman Curves

Longitudinal	(20×10^6)	8000 psi ± 8500
	(20×10^6)	18000 psi ± 6000

The tested density of the fiberglass laminate, with a 30% approximate resin content, is 0.070 lb/cu. in.

(c) Fiberglass Roving

This material is a glass roving, per CPS 5039 impregnated with an epoxy resin, per CPS 5033.

(d) Blade Internal Foam

The blade cavity was filled with an 8 lb./cu. ft., rigid, self bonding foam plastic filler.

(e) Fairing Internal Foam

The fairing cavity was filled with a 5 lb./cu. ft. rigid, self bonding foam plastic filler.

(f) Urethane Rubber Coating

To protect the blade against erosion and abrasion damage a coating of Elastomeric Urethane was applied to the entire external fiberglass blade surface.

d. Design Details - 13166A12P3 Design

In the later phases of the X-19 program the 13166A10P3 blade was modified to incorporate an improved foam filler and the fiberglass layup was modified to provide better shear strength. This revised design was designated the 13166A12P3 blade. This design was phased into the airplane program in the summer of 1965. The design was adequately proven by testing prior to acceptance for flight. However, formal analyses of the design was not initiated prior to temination of operations. The section details are given in Table VII for comparison purposes.

e. Structural Analysis

A complete structural analysis has been made for the 13166A10P3 design and pertinent factors, are presented in this report.

(1) Design Loads

The initial design loads for the 13166A10P3 were established from the early aerodynamic considerations (33) for 12,300 lbs gross weight aircraft. A total of six flight conditions were selected to cover the load spectrum of the blades. These conditions together with the resultant propeller loads are shown in Table VIII.

Subsequently the X-19 flight loads were revised as the state of the art advanced and a review of that data shows that the maximum loads during transition were changed to some extent. With the higher gross weight, the airplane design load factors were reduced from 3.0 to 2.7 and therefore the high speed maneuver loads were essentially the same. The revised loads are also shown in Table VIII. Preliminary analysis indicated that with respect to the blades the initial loads were slightly conservative and these conditions were retained for detailed blade design purposes.

(2) Stress Analysis

The detailed analysis of this blade has been made using the methods of analysis developed over the years for metal blades. Strictly speaking, these procedures are not completely applicable due to the anisotropic characteristics of the fiberglass material. However, during the FRP blade development program, extensive static and fatigue testing was carried out on specimens, panels, and full scale blades. This testing proved that the directional characteristics of the material were small and conventional theory was generally applicable.

Table VII. Blade design 13166A12P3; summary of blade structural & mass section properties (equivalent to fiberglass).

Sta.	Area Struct.	Area Mass	I Min. Struct	I Min. Mass	I Maj. Mass	y_{c_g}	y_c	b_{c_g}	LEA	X_{c_g}	I/cc Struct	I/c$_T$ Struct	Z Struct
7.5	23.898	15.190	50.732	32.246	32.246	0	0	2.200	2.200	0	23.060	23.060	161
9	27.175 28.882*	21.209	59.247 64.615*	48.512	53.019	0	0	3.697	3.700	- .003	24.182	24.182	223
12	40.715 44.159*	38.518	112.370 128.490*	115.340	335.270	0	0	9.484	9.500	-1.751	37.519	37.519	462
15	21.057 25.025*	26.390	97.494 122.040*	119.300	434.090	.009	.007	11.034	11.160	-1.421	30.410	30.240	1574
17.5	17.567 10.757	18.738 14.409	80.967 52.278	78.560 60.325	436.070 380.840	.083		11.187 11.174	11.250	-1.323 -1.326	26.917 17.380	25.926 16.740	5337 3484
18	10.622	14.253	51.256	59.328	380.170	.082	.056	11.086	11.250	-1.414	17.082	16.513	3571
21	10.247	12.331	44.150	48.458	433.950	.155	.116	11.177	11.250	-1.323	15.266	15.367	12395
24	9.963	11.046	35.168	38.057	495.340	.176	.160	11.768	11.250	- .732	12.714	13.132	30678
27	9.948 11.643	9.948 15.140	28.976 31.061	28.976 35.373	536.590 695.760	.180 .184	.186	12.218 11.955	11.250	- .282 - .545	10.984 11.792	11.637 11.454	51268 54899
30	10.602	13.928	25.179	28.818	632.950	.190	.194	11.963	11.250	- .537	10.120	10.788	49151
36	8.797	11.724	15.986	18.423	524.460	.188	.194	11.982	11.250	- .518	7.370	7.953	39782
42	7.370	9.897	9.685	11.200	442.920	.187	.194	12.060	11.250	- .440	5.241	5.741	33352
48	6.013	8.071	5.371	6.200	341.880	.177	.182	11.767	10.925	- .373	3.522	3.909	24231
54	4.693	6.250	2.704	3.106	228.040	.109	.113	10.925	10.090	- .285	2.229	2.416	13928
60	3.509	4.675	1.192	1.370	133.030	.037	.037	9.816	8.895	- .069	1.298	1.345	6268
66	2.670	3.478	.474	.540	69.382	.001	.002	8.171	7.325	+ .031	.709	.711	2296
72	2.114	2.582	.162	.178	30.328	0	0	6.244	5.555	+ .074	.353	.353	601
75	1.818	2.082	.078	.083	17.110	0	0	5.173	4.580	+ .083	.218	.218	239
77.75	1.570	1.725	.042	.044	10.466	0	0	4.425	3.920	+ .085	.144	.144	108
77.75	3.500	3.500	.065	.065	15.215	0	0	3.964		- .376	.223	.223	141
78	0	0	0	0	0	0	0	3.492	3.600	0	0	0	0

* Including D.W.

Table VIII. Design propeller loads 13166A10P3 blade, X-19 aircraft.

	Condition	HP	rpm	Knots	Thrust lb	Pitching Moment in-lb	Yawing Moment in-lb	Normal Force lb
Initial Design Conditions 12300 lb Gross Weight	Hover	1200	1204	0	5400	--	--	--
	Transition	650	1065	80	2440	56400	42000	510
	Transition 30'/sec Gust	650	1065	80	2670	74100	46400	187
	Pitch in Transitions	927	1065	80	3400	53400	53400	672
	Climb	470	955	218	585	18000	46800	923
	High Speed Load Factor 3.0	475	955	252	373	38000	70300	3120
Revised Conditions 13660 lb Gross Weight	Transition 30'/sec Gust	527	1065	50	3484	79500	34000	155
	Acceleration Transition	526	1065	50	2670	32000	55300	1018
	Roll in Transition	550	1065	50	3195	66000	37100	70
	Pitch in Transition	733	1065	85	3085	35500	58700	579

The transition area of the fiberglass to the steel shank, i.e., from 7.5 in. to the 17.5 in. radii involves a complex load transfer analysis which is not amenable to the simple or conventional approach.

The structural adequacy of this section has been substantiated by test and has included static and fatigue testing in the laboratory plus full scale propeller testing on the Curtiss gyroscopic test stand and on the ASD whirl rig. This testing is discussed in more detail in Section V,2.f.

The exact manner of load transfer and precise stress distribution in this bi-material section is subject to further investigation. Additional analytical study and experimental verification is required to yield a precise theoretical procedure for analyzing this blade area.

(a) Steady and First Order Loads and Stresses

Using the loads as previously defined, the resulting blade stresses, retention loads, and shaft loads are given in Table VIII. For reference purposes typical blade stress distributions are plotted in Figures 119 and 120.

These data (blade stresses, retention and shaft loads) as given in Table IX were based upon the computed flight characteristics of a 12,300 lb. design gross weight airplane. They were considered to be the design values for the 13166A10P3 blade and associated propeller components. Note that the shaft loads of Table IX give a vibratory component. This is based upon the results of the Ames tunnel test of the X-100 airplane which indicated extraneous blade vibration of 2xP and 4xP frequency. These will be felt by the propeller shaft as a 3xP vibration. It was further observed in blade manufacturing that there was a variation in the tilt between blades. The tilt difference between blades is due to the change in shank position within the die during manufacturing. This effect produced a rotating couple or unbalance on the propeller shaft which varied with blade angle setting and RPM. Through selective blade assembly for the propeller, this unbalance moment was held to a maximum of 4400 in.-lbs.

The blade stresses as given in Table IX are considered satisfactory except for continued operation at high speed maneuver condition (n = 3) where the stresses exceed the fatigue strength on both the steel shank and the outboard fiberglass.

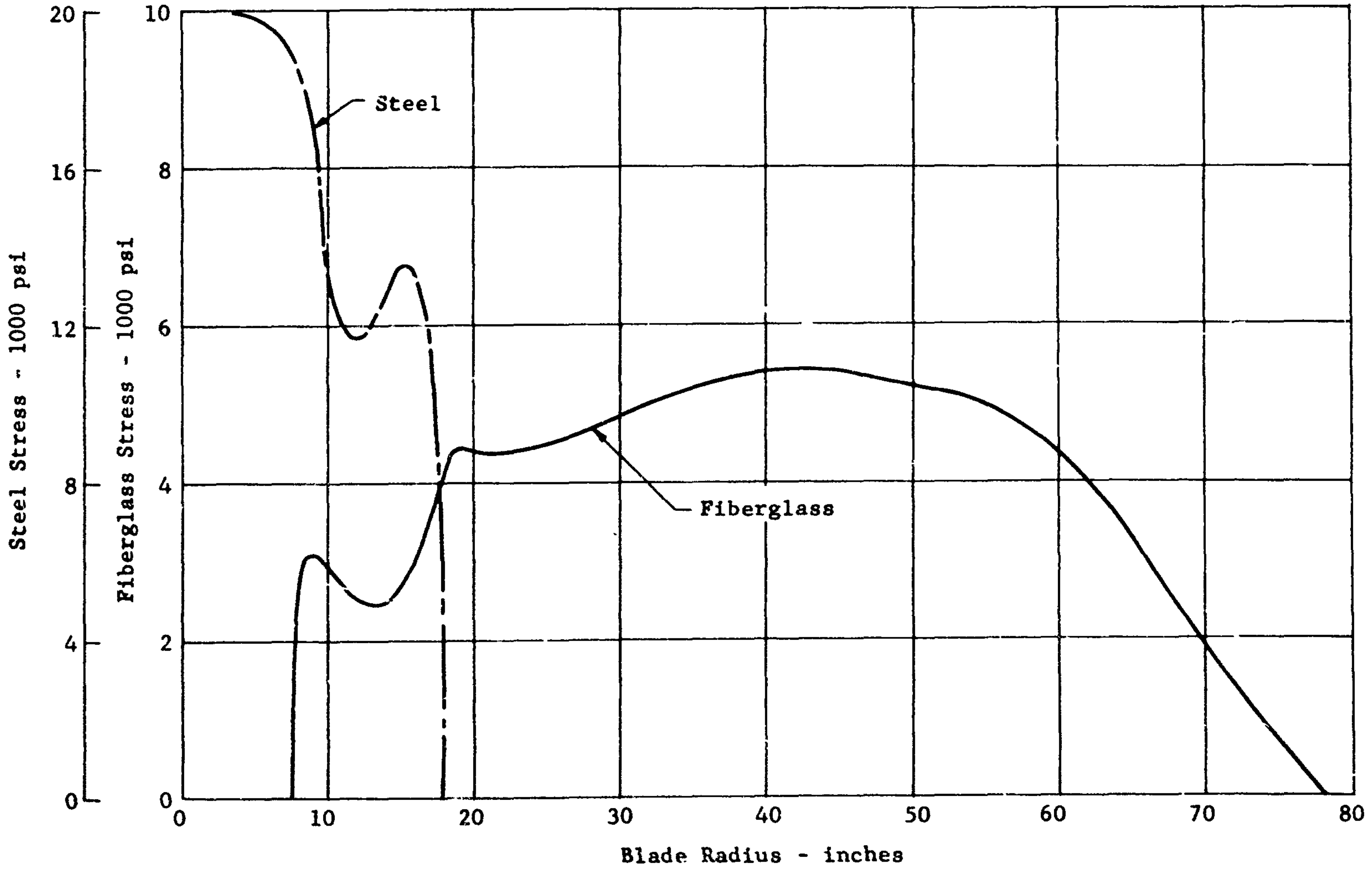

Figure 119. The 13166A10P3 blade steady stress distribution for a pitching maneuver during transition flight; 927 hp, 1065 rpm, 80 knots.

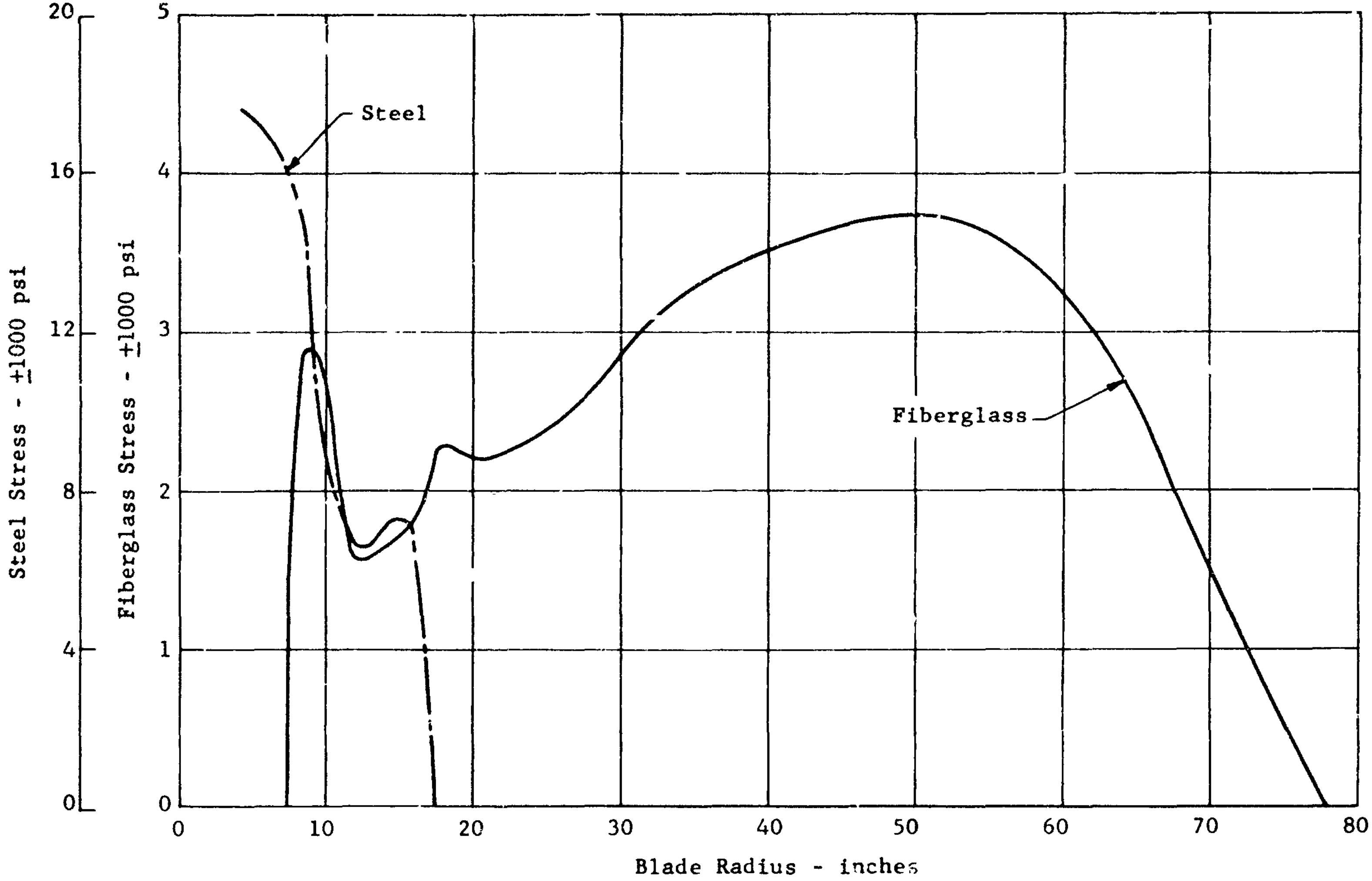

Figure 120. The 13166A10P3 blade vibratory stress distribution for a pitching manuever during transition flight; 927 hp, 1065 rpm, V = 80 knots.

Table IX. Summary of structural analysis; 13166A10P3 blade design, design loads for 12,300 lb airplane gross weight.

Polar Moment of Inertia, I_p = 11.2 slug ft^2

Centrifugal Twisting Moment, $Q_{r_{max}}$ = 23,400 in. lb at 1204 rpm, $\beta_{42''}$ = 41°

Centrifugal Force, CF = 56,900 lb at 1204 rpm

	Condition					
Item	Hover	Equil. Trans.	Trans. + Gust	Man. Trans.	Climb	High Speed Maneuver (n = 3)
HP	1,200	650	650	927	470	475
rpm	1,204	1,065	1,065	1,065	955	955
V - knots	0	80	80	80	218	252
Blade Stress - psi						
Shank - 5" Sta.	29,500	14,700 ± 16,300	15,500 ± 19,100	19,940 ± 17,500	12,850 ± 14,200	12,670 ± 40,000
Outboard	8,660	4,660 ± 3,830	4,010 ± 4,840	5,790 ± 3,740	3,740 ± 2,930	3,550 ± 7,050
Location - in.Sta.	48	48	54	48	42	42
Retention Loads						
CF - lb	56,900	44,500	44,500	44,500	35,700	35,700
M_s - in. lb at blade butt	58,900	14,860	17,600	38,020	14,400	13,400
M_v - in lb at blade butt	----	± 61,500	± 74,000	± 1,800	± 54,600	± 142,500
M_s - in. lb at bearing stack	56,020	13,180	15,060	31,900	13,500	12,300
M_v - in. lb at bearing stack	---	± 60,300	± [illegible] 300	± 66,000	± 52,800	± 139,000
θM_s - degrees	13	29.0	24.6	21.0	29.4	26.6
θM_v - degrees	----	18.1	7.8	20.8	43.0	63.7
Shaft Loads						
T - Thrust - lb	5,400	2,440	2,670	3,400	585	373
N - Normal Force - lb	----	510	187	672	923	3,120
Y - Side Force - lb	----	84	113	56	246	795
M_p - Pitch Moment - in. lb	----	56,400	74,100	53,400	18,000	38,000
M_y - Yawing Moment - in. lb	----	42,000	46,400	53,400	46,800	70,300
*M_v - Shaft Vibratory Moment - in lb	----	± 17,600	± 21,800	± 18,800	± 10,000	± 16,000

* This moment is based upon the preliminary reduction of data taken on the full scale tests of the X-100 airplane in the Ames 40 × 80 tunnel. The frequency with respect to the propeller support will be 3XP. In addition, the propeller will generate a rotating couple due to differential tilt between blades which will have a magnitude on the order of [illegible] 400 inch pounds.

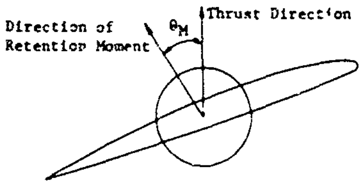

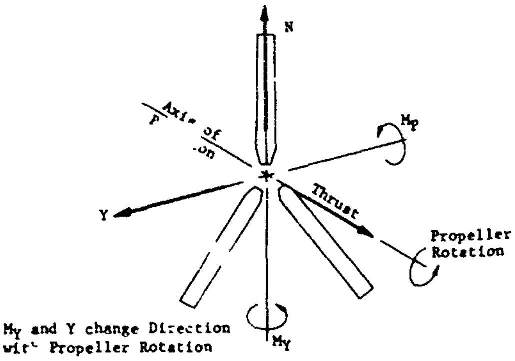
N
Axis of Propeller Rotation
M_p
Y
Thrust
Propeller Rotation
M_Y and Y change Direction with Propeller Rotation
M_Y

The blade stress analysis further indicated that the design vibratory stresses of the blade material would be exceeded at load factors greater than 1.7. A life of 6 hours was computed for a blade operating at loads corresponding to a load factor of 3.0. In view of the original design decision to regard operation at this load factor as an emergency or demonstration condition which is transient in occurrence a calculated blade life of 6 hours was considered satisfactory.

Between the 7.5 and 17.5 in radii, the stresses as shown in Figures 119 and 120 are nominal values computed on the assumption that conventional beam theory was applicable. For this bi-material region such an assumption served only for qualitive comparison of the resulting stresses. Since a rigorous theoretical solution was not possible, the structural adequacy of this area was verified by experimental means. Stress magnitudes and distributions typical of the steel-fiberglass junction area at test loads corresponding to the maneuvering transition condition are given in Figures 121 and 122.

(b) Resonant Frequencies and Flutter

The computed fixed-root frequencies of the 13166A10P3 blade are shown in Figure 123. These curves show both a 3xP excited flapping and 4xP excited edgewise resonance close to the cruise RPM, and only slightly removed from the transition speed. However, by virtue of the material damping characteristics of the fiberglass propeller blades and for the anticipated magnitude of the excitation no serious blade stress problem was anticipated as a result of these proximites to resonances. In cruise flight, based on conventional airplane experience, 3xP and 4xP excitations of sufficient strength to produce excessive stress would not be expected. In transition where these higher ordered excitations may be more significant, a low blade response is expected. This contention was based upon experimental evidence obtained in laboratory testing, on the gyroscopic whirl rig, and during WPAFB calibration testing which have all demonstrated high damping characteristics of the laminated glass blade design and a corresponding low response at resonant conditions. However, these potential blade resonant problems were to be carefully investigated by analysis of the strain gage data during the aircraft flight test program.

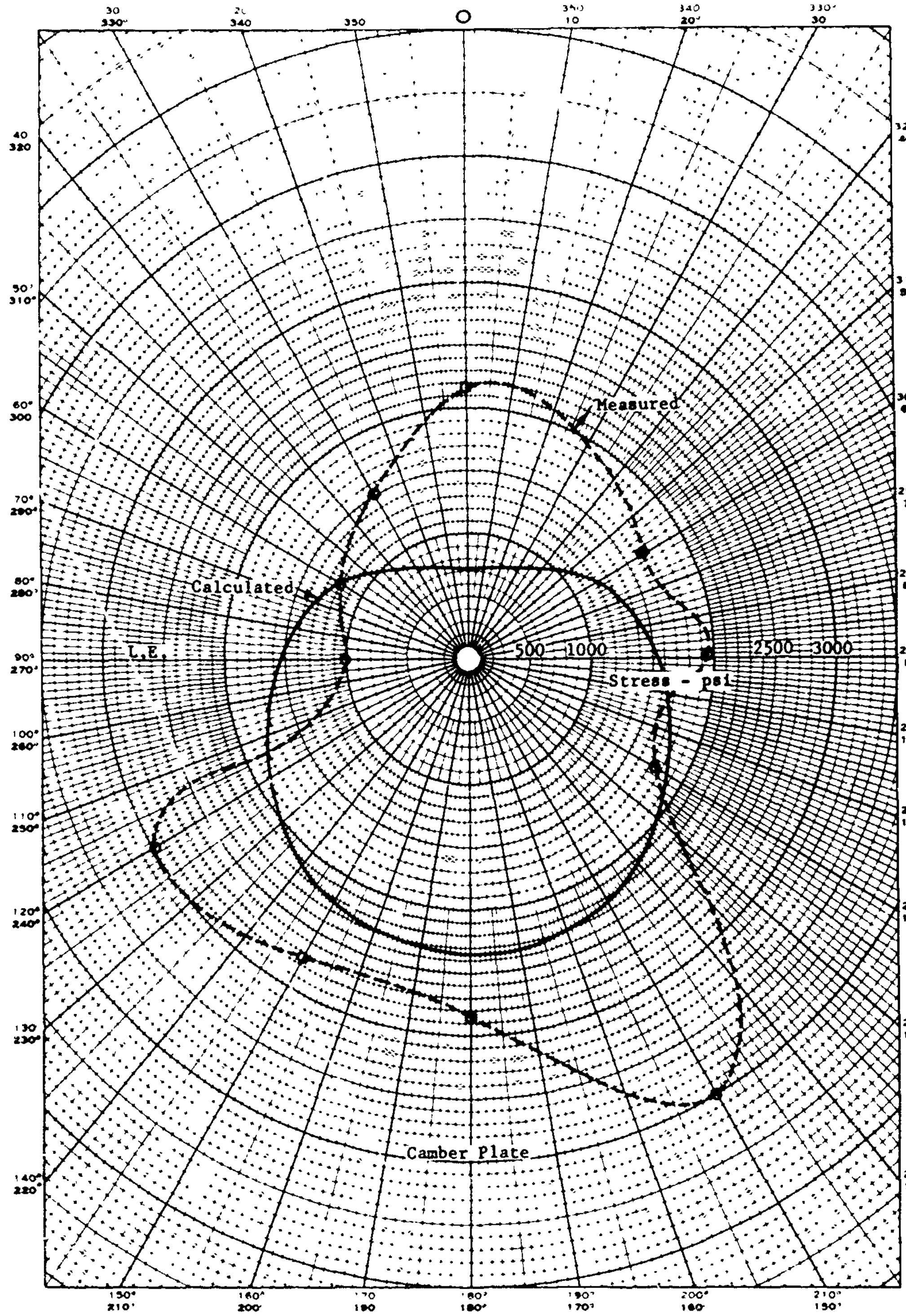

Figure 121. Comparison of the calculated and measured steady stress distribution around the 11 inch station on the 13166A10P3 blade. Centrifugal load = 46,000 pounds, bending moment = 24,000 inch-pounds.

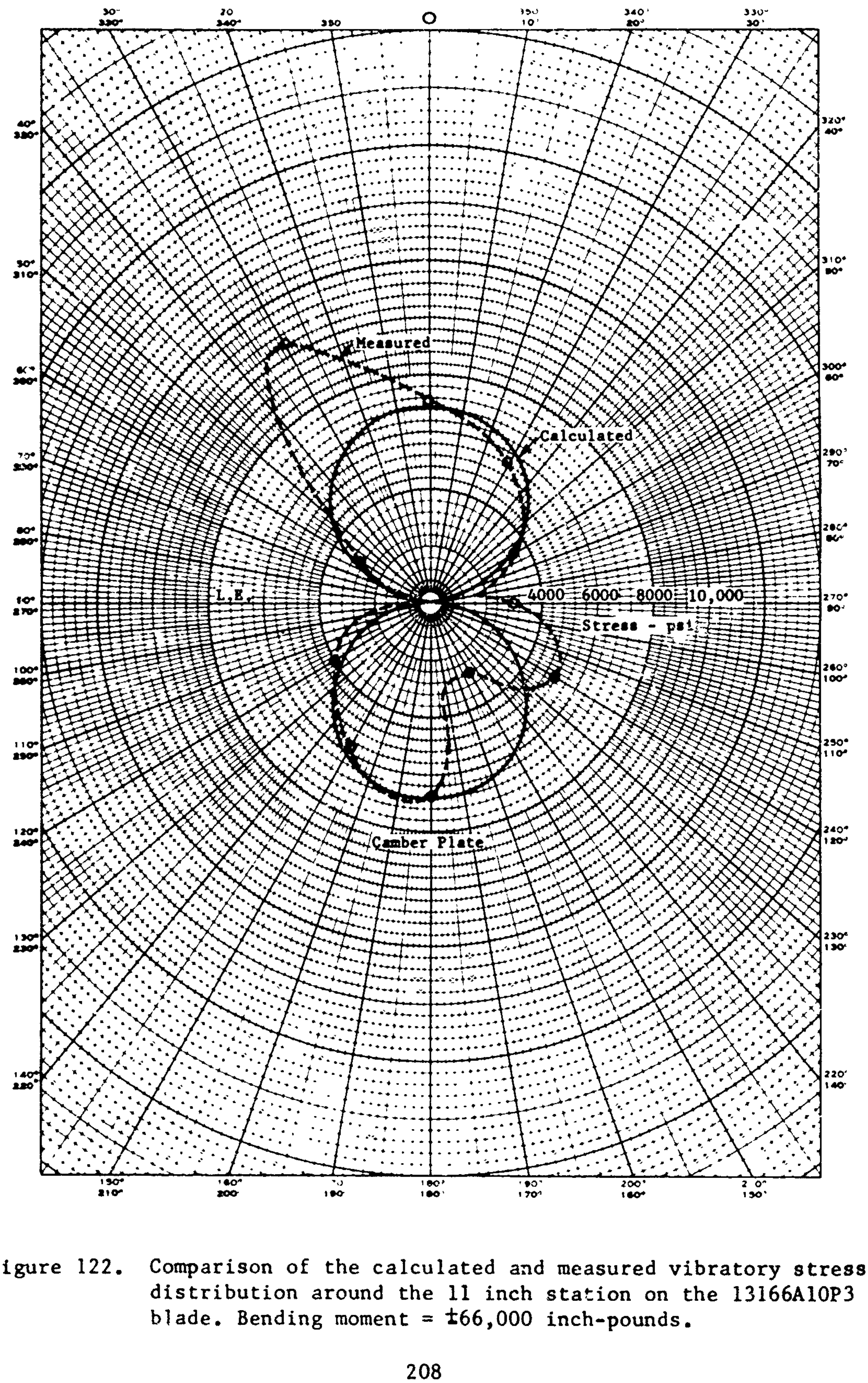

Figure 122. Comparison of the calculated and measured vibratory stress distribution around the 11 inch station on the 13166A10P3 blade. Bending moment = ±66,000 inch-pounds.

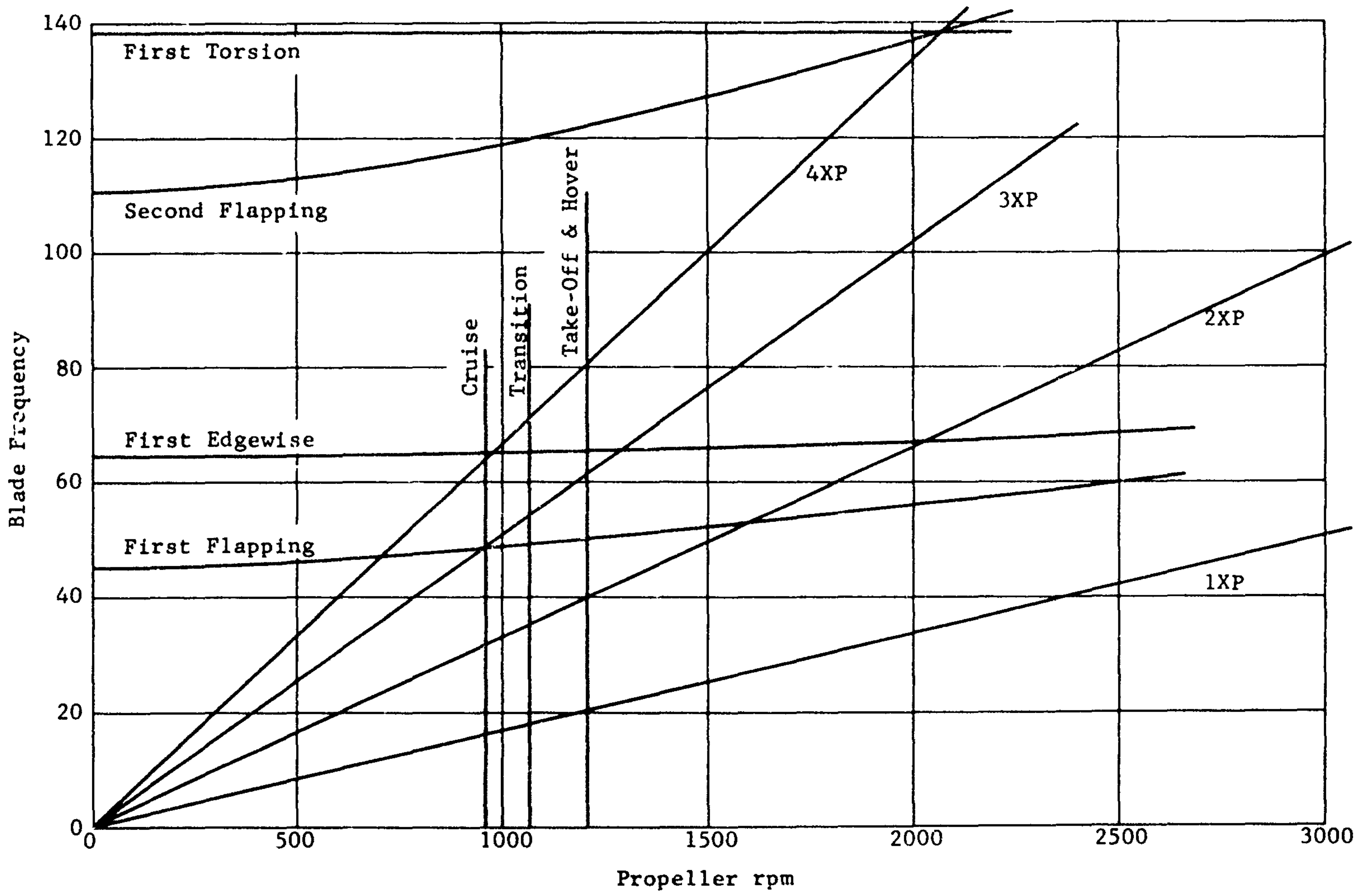

Figure 123. Calculated fixed root resonant frequencies of the 13166A10P3 fiberglass propeller blade.

The calculated stall flutter characteristics of the 13166A10P3 blade indicate a flutter-free design. This was experimentally demonstrated by ASD of WPAFB up to 1400 horsepower which is well beyond the take-off requirements of the X-19 aircraft. The major factor in evaluating stall flutter is the "reduced frequency". The natural torsional frequency of these fiberglass blades is considerably higher than with past metal blades. For example, in hollow steel blades the fundamental torsional frequency ranged from 50 to 80 cps, on solid dural blades the general range was from 90 to 120 cps. However, on the fiberglass test blades the torsional frequency was measured at approximately 230 cps. This significantly higher frequency is directly reflected in the reduced frequency parameter which was sufficiently high that a stall flutter-free condition was shown by calculation. It is to be further noted that theoretical stall flutter studies have shown that high camber and tapered planform are flutter deterents, and both of these features have been included in these fiberglass blades. High camber is a stall flutter deterent only because the maximum lift coefficient is higher than a low camber design and if the solidities of blades compared are identical.

f. Full Scale Blade Testing

This section presents the details and summary of the results of full scale testing on the propeller blades as component items. Other full scale testing pertinent to the blade development and qualifications, but which included the testing of the entire propeller assembly, are discussed in Section V,7.

(1) Free-free Testing

The purpose of this test was to establish the endurance limit of the outboard portion of the full scale, as manufactured, blade. For this test the blade, instrumented to measure longitudinal vibratory strains, was suspended vertically by a clamp at the shank end, Figure 124. The blade was excited in its fundamental flapping mode and a vibratory stress survey made. Endurance testing was then continued while monitoring the maximum flexural stress. The actual endurance running was made in steps of increasing stress, and running each value for ten million cycles or until failure. A summary of test results pertinent to the X-19 blades is given in Table X.

A typical blade failure is shown in Figure 125. Testing of this type has established as flexural endurance limit for the 13166A10P3 blade of ± 9900 psi.

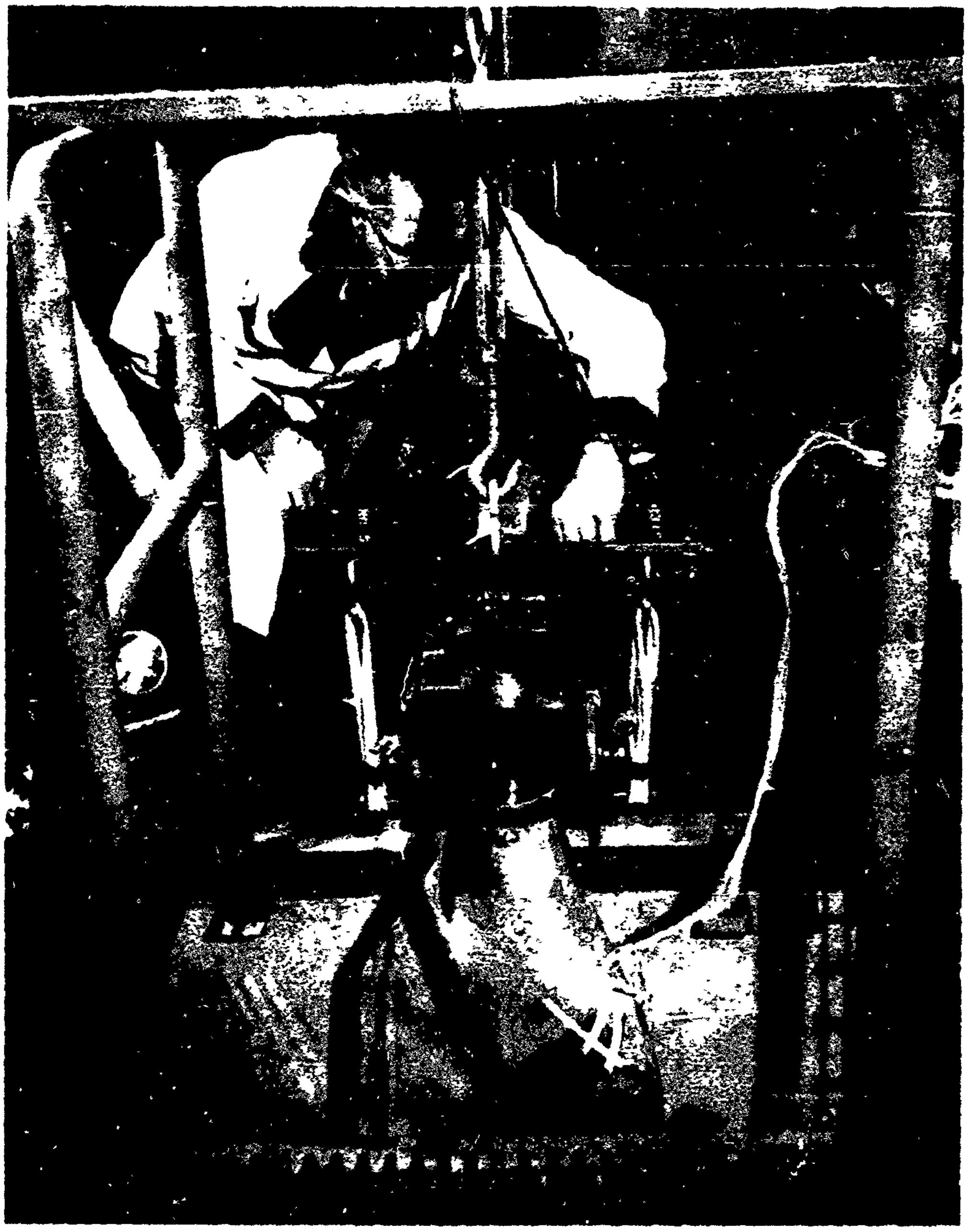

Figure 124. Laboratory test set-up for endurance testing propeller blades in the free-free mode.

Table X. Tabulation of endurance history; 13166A10P3 blades.

Blade	Stress Level psi	Endurance Cycles		Remarks
		At Level	Total	
P-176-4	± 8000 ± 9000	11.7×10^6 $.53 \times 10^6$	11.7×10^6 12.2×10^6	Failure was a delamination of glass at 62 - 63" Sta. T.E. Camber. Foam cracked at c.g. about 65" Sta.
P-127-2	± 8000 ± 9000	10×10^6 $.147 \times 10^6$	10×10^6 10.147×10^6	Failure was a delamination at 70" Sta. Camber. Foam cracked at c.g. extending 4" inboard and 2" from T.E.
P-191-3	± 8000 ± 9000 ± 10000	10×10^6 10×10^6 $.63 \times 10^6$	10×10^6 20×10^6 20.63×10^6	Failure was in crack at 60" sta. camber. Foam cracked in failure area.
P-[illegible]6-4	± 8000 ± 9000 ± 10000	10×10^6 10×10^6 1.25×10^6	10×10^6 20×10^6 21.25×10^6	Failure was a crack at 61" Sta. thrust. Foam cracked in area of failure.
P-132-3	± 8000 ± 9000 $\pm 10,000$	10×10^6 10×10^6 $.455 \times 10^6$	10×10^6 20×10^6 20.45×10^6	Failure was a series of cracks at at approx. 70" Sta. Foam cracked in area of failure.

Table X. Concluded.

Blade	Stress Level psi	Endurance Cycles		Remarks
		At Level	Total	
P-127-4	± 1405 ± 1580	10.28×10^6 $.46 \times 10^6$	10.28×10^6 10.74×10^6	Failure was a foam crack at section c.g. located 64" Sta. to 67" static No fiberglass failure.
P-140-6	± 1405 ± 1580 ± 1755	10×10^6 10×10^6 72,500	10×10^6 20×10^6 20.07×10^6	Failure was a transverse crack at 60" station. Foam O.K. at crack area but had large charred area at the 30" Sta. with some cracks noted.
P-155	± 1580	846,000	846,000	Failure was a transverse crack at 60" station. Foam O.K. at crack area but had large shrinkage area at inboard end. Investigation of sectioned blade indicates the shrinkage extended outboard to approximately 44" station.

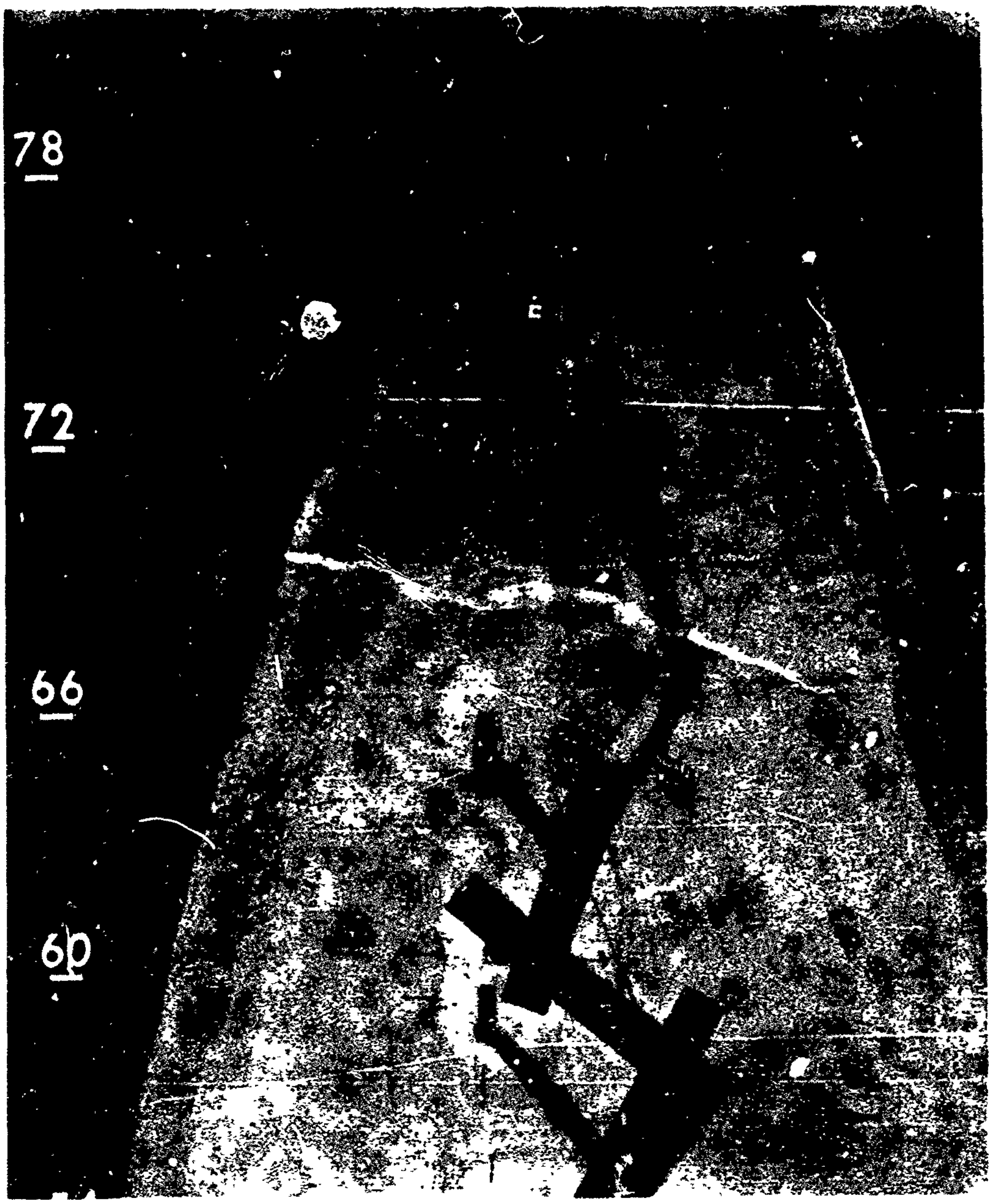

Figure 125. Typical blade failure obtained in free-free endurance testing. This blade completed 10 x 10^6 cycles at each of ±8000, ±9000, ±10,000 and ±11,000 psi. Failure occured at 1.2 x 10^6 cycles at the ±12,000 psi level.

(2) Fixed - Root Testing

This particular type of blade testing was designed to establish the fatigue strength of the inboard end of the blade. For this testing the blade was clamped at the shank and an exciting force was applied outboard and in the chordwise direction, see Figure 126. As was customary in this type of testing, strain gages were installed and the areas of maximum stress were located and monitored throughout the endurance testing. In the X-19 program, test blade Serial No. P-68-2, completed vibratory stress surveys at ± 4,000 and ± 6,000 psi levels. Endurance testing was initiated at ± 6,000 psi vibratory stress level and run for 20 x 10^6 cycles. Following this, the stress level was increased in ± 1,000 psi increments and run for 10 x 10^6 cycles at each level until failure.

Stress Level	Cycles at Level	Total Cycles
± 6,000	20 x 10^6	20 x 10^6
± 7,000	10 x 10^6	30 x 10^6
± 8,000	10 x 10^6	40 x 10^6
± 9,000	0.2 x 10^6	40.2 x 10^6

After 0.2 x 10^6 cycles were completed at ± 9,000 psi level, the test was terminated due to failure. Typical failures obtained from this type of testing is shown in Figure 127.

The results obtained in this test demonstrated a blade endurance limit (based on 50 x 10^6 cycles) in the edgewise direction of ± 7,900 psi. This is significantly above the established design stress of ± 6,000 psi, thus substantiating the use of that value for design purposes.

(3) Blade Torsion

The blade torsion test was essentially the same basic set-up as the free-free test previously discussed except that the blade was excited in the fundamental torsion mode by two exciters 180° out of phase. This test set-up is shown in Figure 128.

For the X-19 program two blades were run as follows:

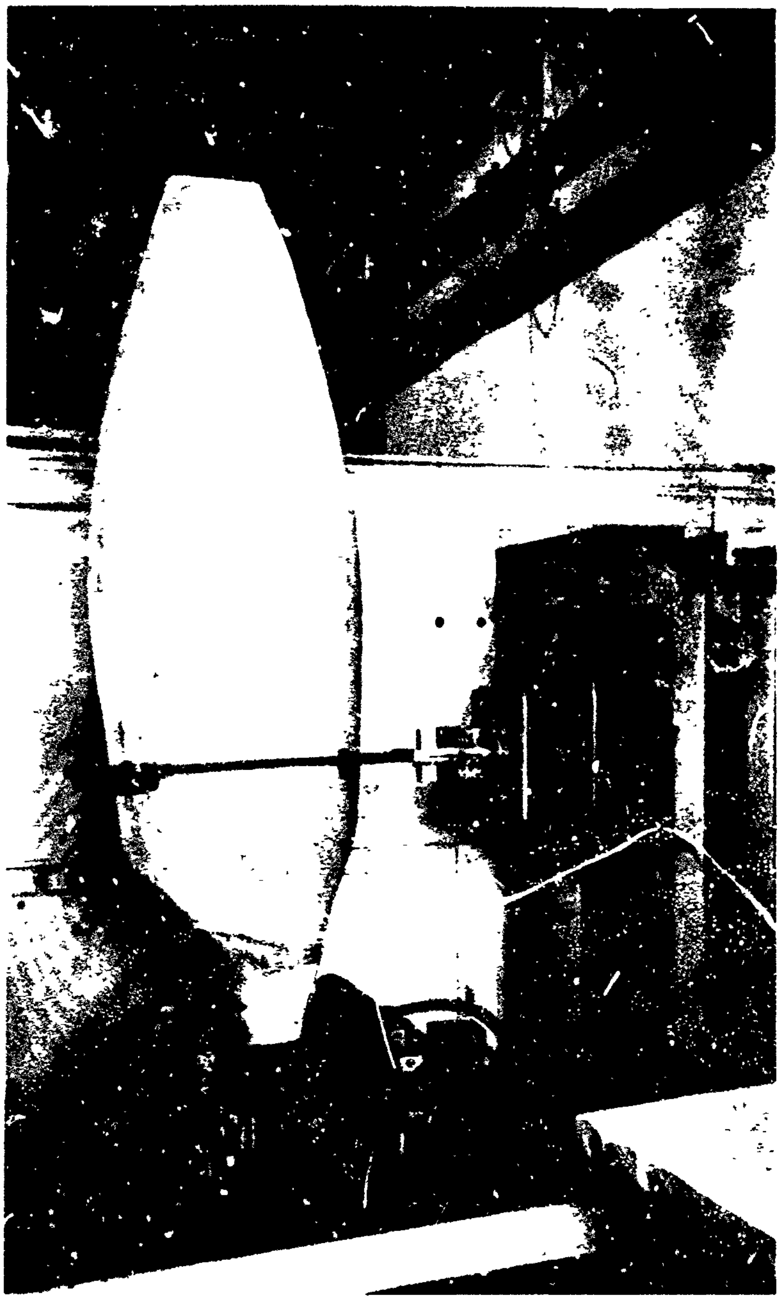

Figure 126. Laboratory test set-up for fixed root endurance testing of propeller blades.

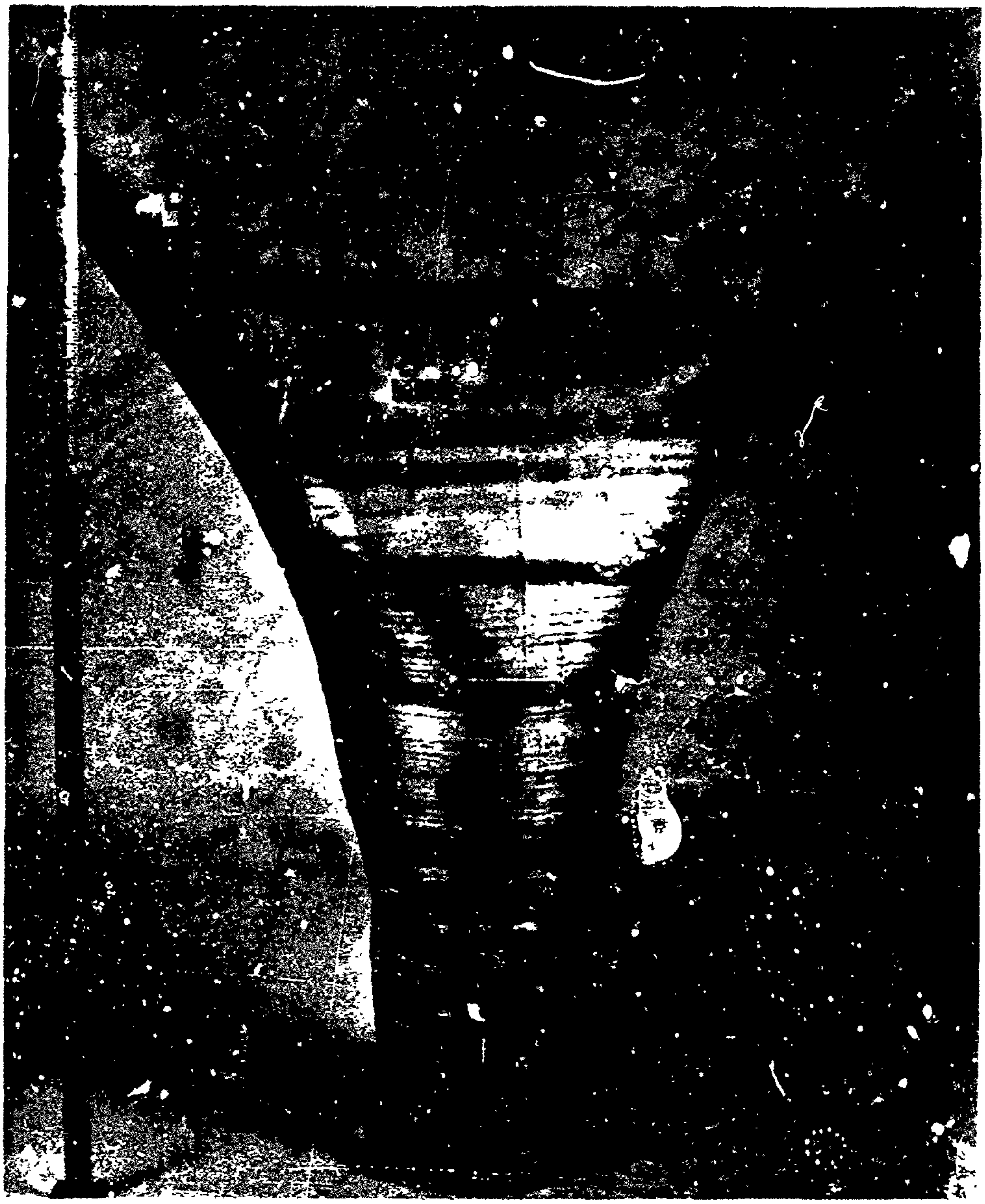

Figure 127. Typical blade fatigue failure obtained during fixed root endurance testing of the X-19 propeller blade.

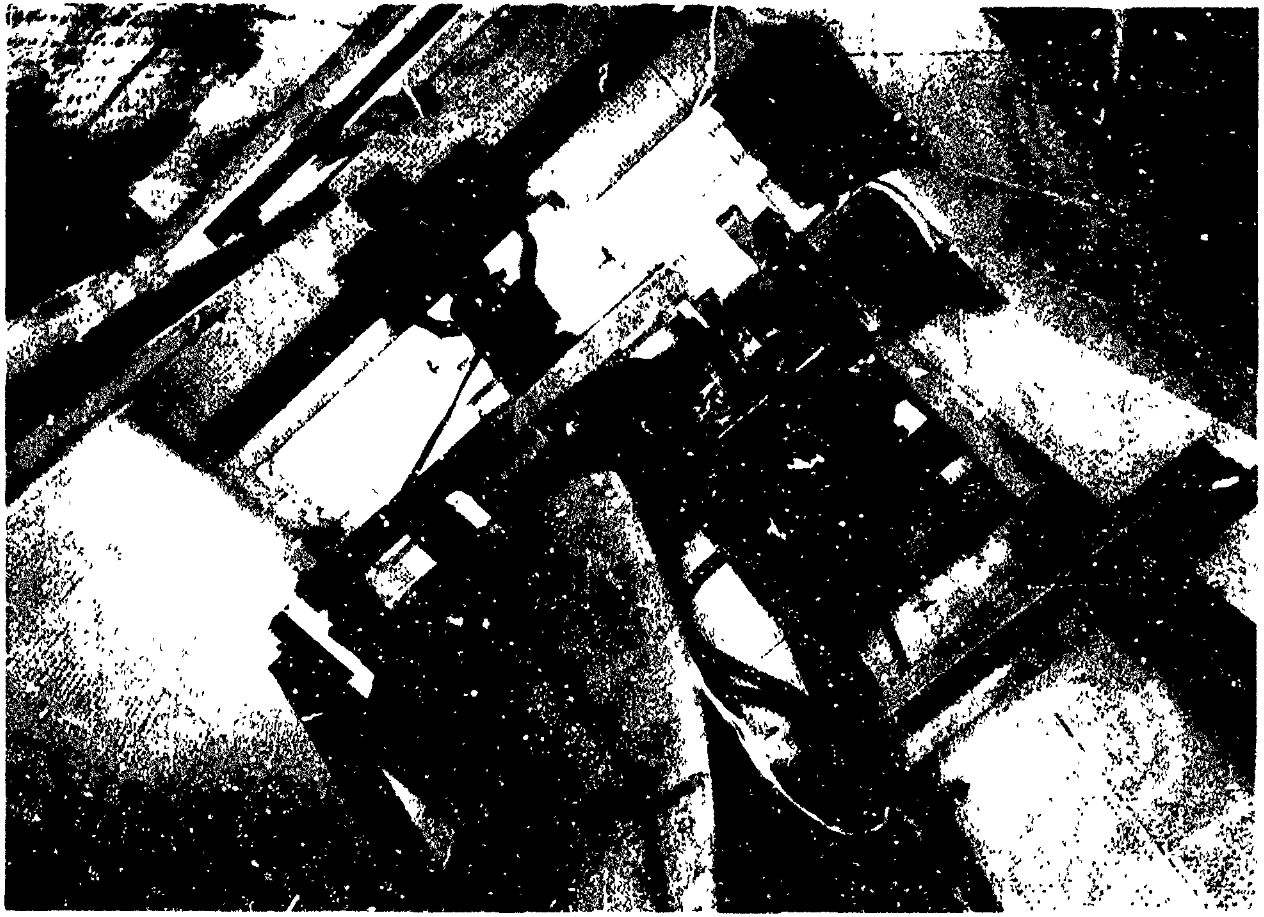

Figure 128. Laboratory test set-up for free-free torsion endurance testing of propeller blades.

Blades P-41 (-4)

Shear Stress Level - PSI	Cycles at Level	Total Cycles at or above Design Level
± 445	20×10^6	-
± 582	10×10^6	-
± 730	10×10^6	-
± 845	10×10^6	10×10^6
± 935	2×10^6	12×10^6
± 1,000	$.6 \times 10^6$	12.6×10^6
± 1,000	$.3 \times 10^6$	12.9×10^6

The test was terminated at this point due to increasing temperature and inability of the vibrator drive system to supply the required power to continue the test.

Blade P-42 (-6)

Shear Stress Level - PSI	Cycles at Level	Total Cycles at or above Design Level
± 1,000	20×10^6	20×10^6
± 1,300	1×10^6	21×10^6

After 1×10^6 cycles at ± 1,300 psi level, a rupture in the fiberglass appeared at the 32.5 inch radius, 12.25 inches from the lead edge on the thrust face, see Figure 129.

The results of these tests would indicate a torsional endurance limit between ± 1,000 and ± 1,300 psi shear stress. Since this was well above the maximum anticipated flight value of ± 300 to ± 500 psi, it was considered that an adequate margin had been demonstrated.

(4) Retention Testing

Two types of retention testing were conducted on the X-19 blade retentions; a static test to failure and the retention fatigue test.

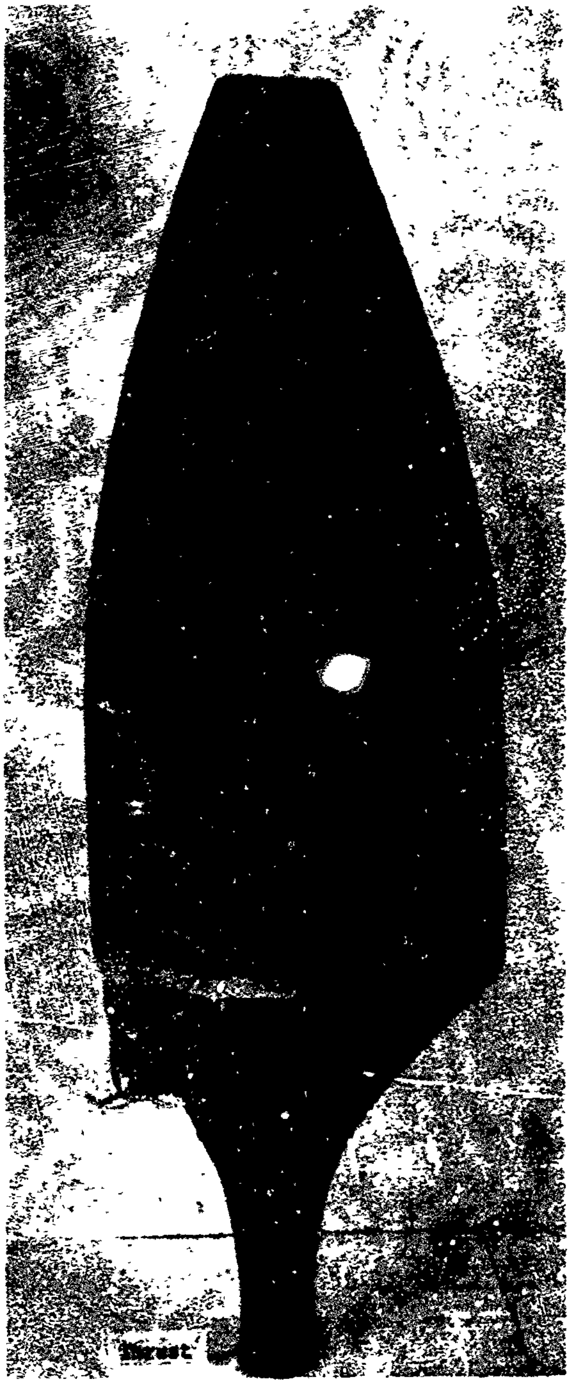

Figure 129. Fatigue failure on blade P42-6 after 1.0 x 10^6 cycles of torsional endurance testing.

(a) Static Test

The purpose of this test was to demonstrate the ultimate centrifugal load capacity of the 13166A10P3 blade without bonding between the steel shank and fiberglass.

For this purpose a special inboard portion of the blade was fabricated using the standard steel shank and fiberglass layups outboard to about the 30" radius. Modifications were then made to adapt the part to the test machine. In making this piece, the steel shell was carefully waxed to prevent bonding of the fiberglass to the steel. This shank portion was placed in the tension test machine, see Figure 130, and subjected to a pure tension load simulating propeller centrifugal force. Failure occurred at 128,000 lbs. as compared with the maximum operating blade CF of 56,900 lbs. The resultant failure is shown in Figure 131.

(b) Retention Fatigue Tests

It was the purpose of this testing to establish the fatigue strength of the blade retention. For this purpose the blade retention including the blade nut, the blade bearing, blade shank and special collet, which simulates the hub barrel, were installed in a test rig which was capable of imposing centrifugal force and both steady and vibratory bending loads along with bearing oscillation to simulate pitch change on the complete blade retention system, see Figure 132. The test blade shank was a full scale blade inboard section consisting of the steel shank and fiberglass lay-up. The actual blade profile and lay-up was maintained to the 21" sta. with modifications outboard, 21" - 31.5", to adapt the piece to the test machine such that the test loads were applied to the simulated fiberglass blades. Endurance testing was conducted monitoring all loads by means of wire strain gages mounted on the steel shank and test rig components.

The two steel blade shanks were run as follows:

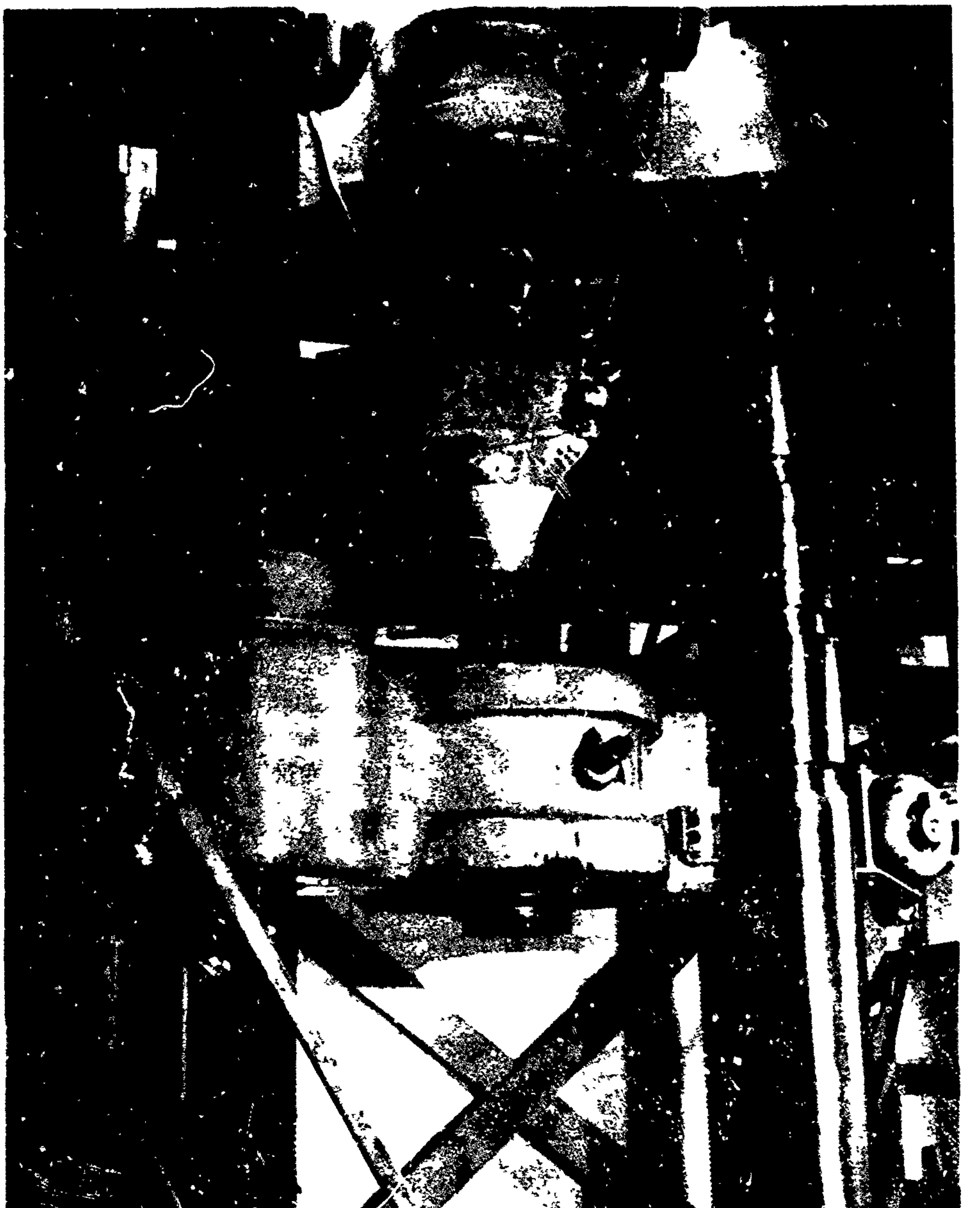

Figure 130. Laboratory test set-up for static tension test of the X-19 propeller unbonded blade shank.

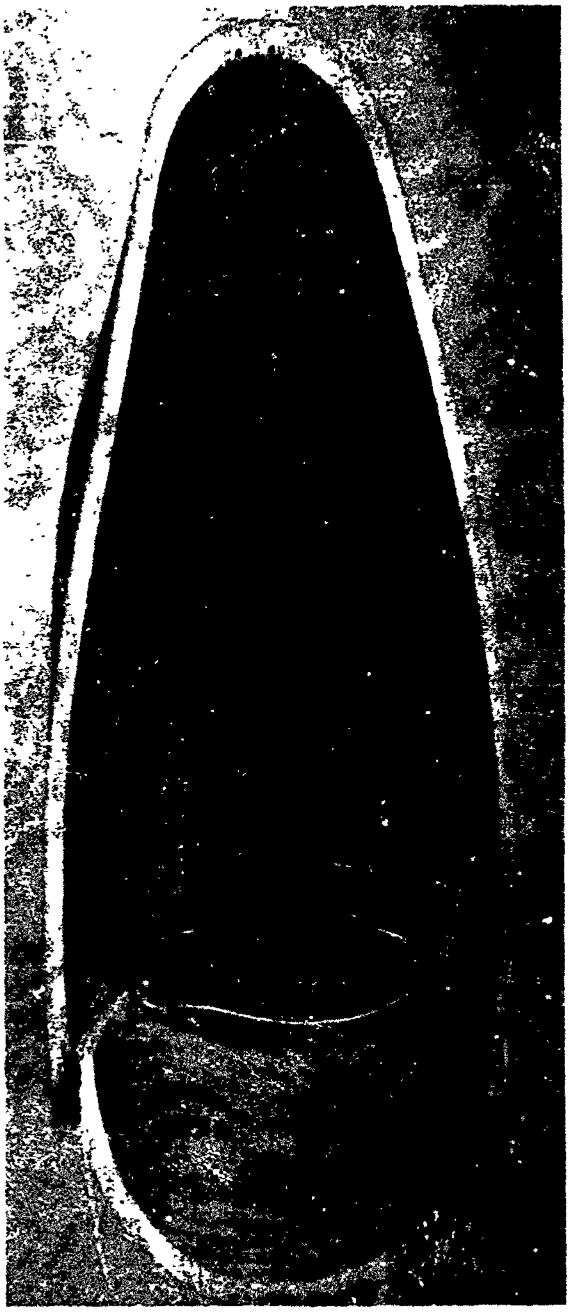

Figure 131. X-19, propeller unbonded blade shank failure. Ultimate load was 128,000 pounds.

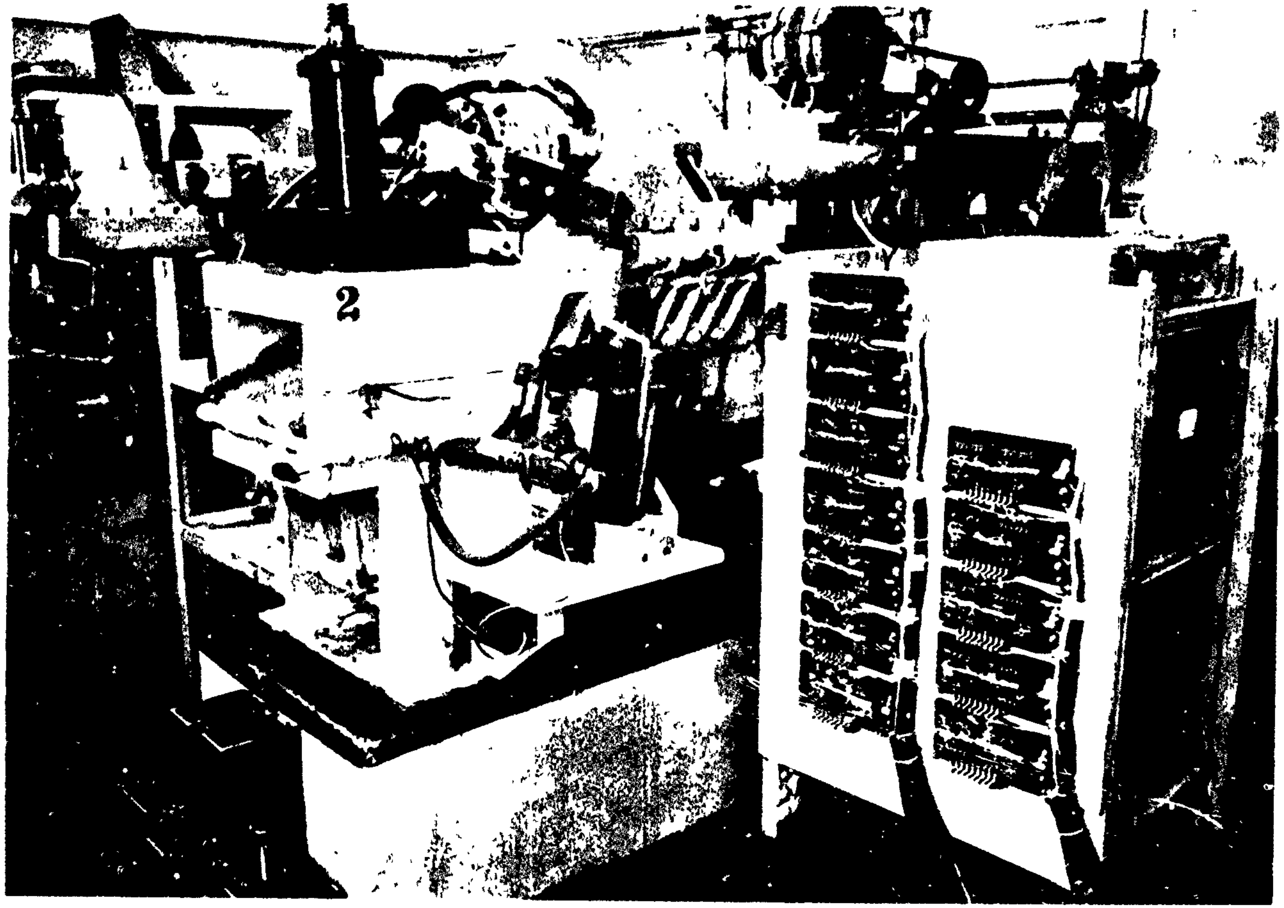

Figure 132. Blade retention laboratory fatigue test set-up. This facility simultaneously applies centrifugal force, steady bending moment and vibratory bending moment.

(aa) Shank P-69 (p/n 164206)

Vibratory Bending Load-lb. in.	Centrifugal Load-lbs.	Steady Bending Load-lb. in.	Cycles at Level	Total Cycles at or above Design Level
* ± 66000	46000	24000	10 x 10^6	10 x 10^6
± 77000	52800	27600	6.4 x 10^6	16.4 x 10^6

The test was terminated after 16.4 x 10^6 cycles when a shank failure occurred. The failure was a spiral type crack in the steel shank originating at approximately the 5.5" station, camber side. The failure was analyzed and found to originate in a rust pit, a direct result of internal corrosion. This was caused by the presence of water which leaked from the test rig cooling system and the lack of the plating which was inadvertently omitted from the test part but which was specified in the flight component. Because of the lack of protective plating on the test piece and the vulnerability of the part to corrosion, the failure was not representative of the flight component.

One retention bearing, P/N 162563 S/N 96, was used for the complete test of 16.4 x 10^6 stress reversal cycles and was in perfect condition when removed except for two small spall marks on one inner race.

(bb) Shank P-171 (P/N 164206)

Vibratory Bending Load-lb. in.	Centrifugal Load-lbs.	Steady Bending Load-lb. in.	Cycles at Level	Total Cycles at or above Design Level
± 72300	44500	21400	4.9 x 10^6	4.9 x 10^6
± 72300	69000	29400	5.1 x 10^6	10.0 x 10^6
± 70000	81000	18000	10.0 x 10^6	20.0 x 10^6
± 83200	51200	21000	5.01 x 10^6	25.01 x 10^6
± 90500	86300	36800	0.19 x 10^6	25.2 x 10^6
± 90500	55600	22900	2.96 x 10^6	28.16 x 10^6
± 90500	55600	22900	0.45 x 10^6	28.61 x 10^6

* Transition design loads corresponding to V = 80 KTS, HP = 927, RPM = 1065, for the 12,300 lb. aircraft gross weight.

The test was terminated after 28.61 x 10^6 cycles when a shank failure occurred. The crack extended approximately 300° around the steel shank in the flange radius. The failure was fatigue in nature with the origin in the flange fillet radius at the location of maximum applied loading. (Figure 133).

A fatigue life analysis was made of the above test data and the minimum demonstrated fatigue strength of the retention was shown to be ± 91,500 in-lbs. vibratory bending moment for the 12,300 lb. design G.W. steady loads of transition flight which are CF = 44,500 lbs. and M = 16,060 in-lbs. An ample margin of safety was thereby shown to exist with respect to the anticipated vibratory bending moment of ± 72,300 in-lbs. for the 12,300 lb. aircraft.

(5) Additional Full Scale Blade and Sample Testing

Considerable additional testing of blades and blade material were accomplished in the course of the blade development program which was pertinent to the qualification of the strength or life of the structure. These tests are simply listed for completeness:

(a) Water spray (Full scale)

(b) Sand and gravel abrasion (Full scale and samples)

(c) Fungus (Samples)

(d) Impact, Bird and bullet (Full scale)

(e) Weathering (Samples)

(f) Lightning (Full scale)

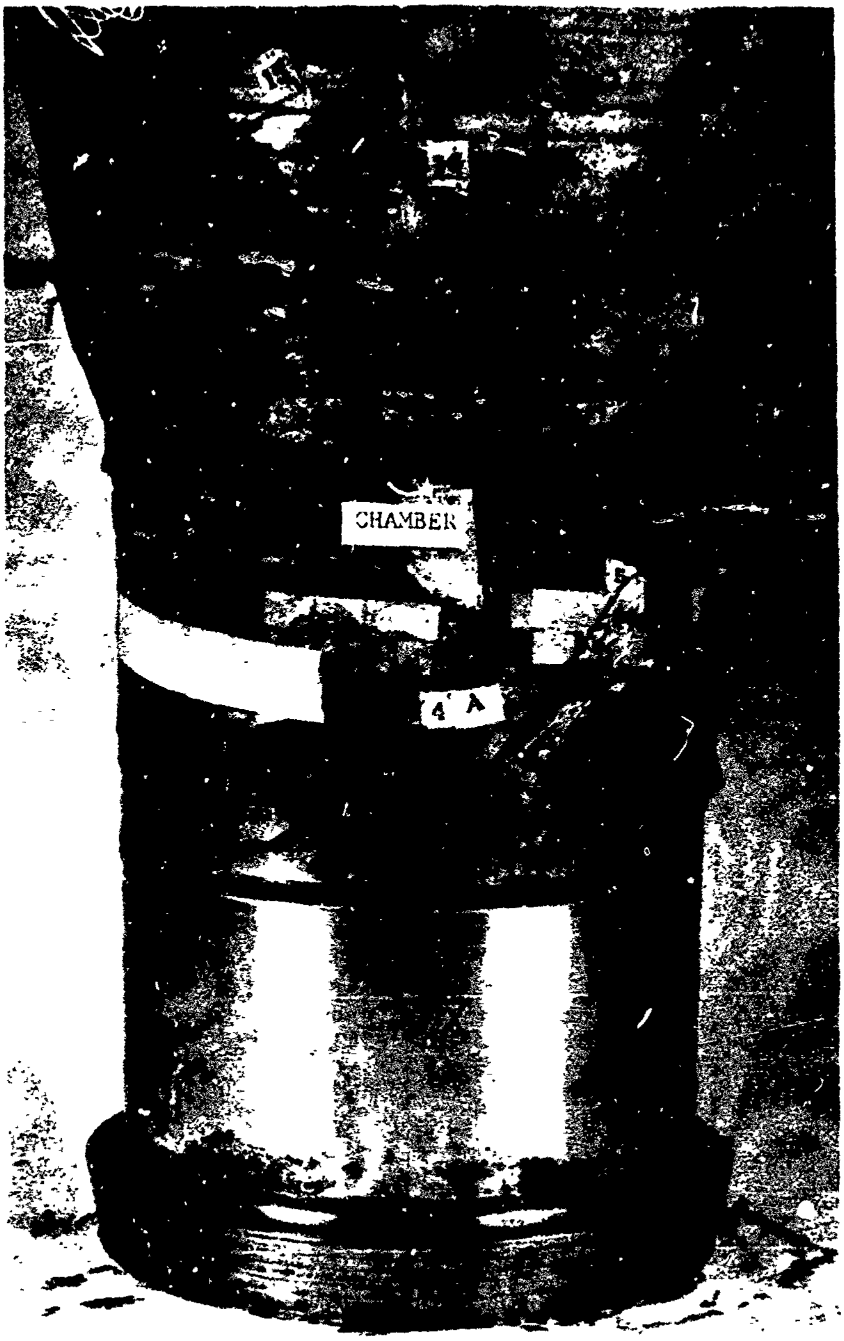

Figure 133. Typical fatigue failure of the X-19 blade shank.

3. PROPELLER DESIGN LOADING THEORY AND TEST

a. General

With respect to the airframe, the rotating propeller generates six basic load components. These are shown in Figure 134. These forces and moments represent the summation at the propeller shaft of the aerodynamic lift and drag components developed by each of the rotating blades. From the viewpoint of the air-frame designer, it is only these resultant loads which are of concern and these are readily obtained by wind tunnel testing and generally presented in coefficient form (33). The propeller designer, however, also required the loading of the individual blade, and for this theoretical developments are generally used.

b. Theoretical Propeller Loading

The flow through the disk of an aircraft propeller is generally quite complex. In simplest form, it might be considered as though the propellers were operating at some angle of attack, A, with respect to the flow field, Figure 134. The angle of attack results from several factors, e.g., the attitude of the aircraft, geometry of the aircraft, wing circulation, influence of the fuselage and other surfaces, etc.

For analysis purposes, this flow can be considered in the two components, normal and parallel to the disk. It is quite obvious that with these velocities, any given blade section, as it passes through one revolution. will experience a uniform velocity on which is superimposed a sinusoidal harmonic having a frequency equal to the rotational speed or the commonly called 1XP frequency. The aerodynamic forces will also reflect this uniform plus sinusoidal variation. The uniform or steady components produce the propeller thrust and torque. The 1XP vibratory blade loads produce the shaft moments and normal forces.

The thrust and torque forces are readily determined. The so called strip analysis methods are well established within the propeller industry, and were developed from a background of many years of propeller testing. The first order, or 1XP, blade loads are not so well defined:

(1) First Order, or 1XP Blade Loading

For the conventional aircraft, the 1XP propeller blade loading is accurately predictable.

Because of the very low propeller angle-of-attack (0° to 20°), a relatively simple development gives the 1XP lift force at a given blade station as:

$$\Delta L_{1XP} = q/2 \sin 2A \left[ab + 2bC_L \mathrm{Cot}\ \phi_o \right] \Delta r \sin \omega t \qquad (1)$$

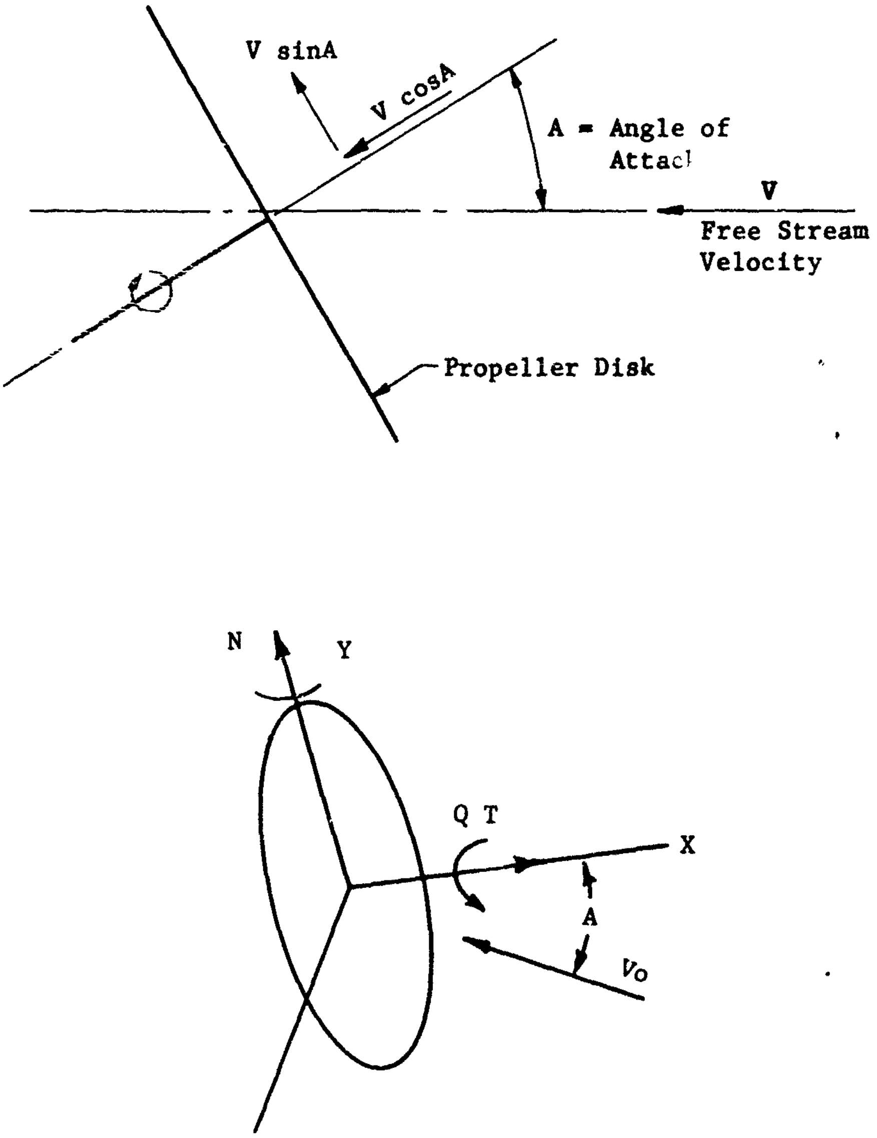
V sinA
V cosA
A = Angle of Attack
V
Free Stream Velocity
Propeller Disk
N
Y
Q T
X
A
Vo

Figure 134. Basic velocity components at the disk of a tilted propeller.

which for small angles becomes

$$\Delta L_{1XP} \doteq Aq \left[ab + 2bC_L \text{Cot } \phi_o \right] \Delta r \sin \omega t \tag{2}$$

where: A = propeller angles of attack

q = free stream dynamic pressures, lb/ft^2

a = slope of the lift curve

b = section chord, ft

C_L = operating lift coefficient

ϕ = apparent wind angle at the given station

Δr = incremental radius, ft

ωt = propeller rotational angle, radians

This development is well known and the propeller forces obtained from this simple expression have been substantiated by considerable flight testing. However, the above expression becomes quite inaccurate as A becomes greater than 20°, and is therefore not applicable to the tilt nacelle or tilt wing propeller driven VTOL airplane.

Recognizing this fact, a more generalized development ([illegible]) was undertaken in order to more accurately predict propeller loads for the high angle region. From this development the basic 1XP blade force at a given station was shown to be:

$$\begin{aligned}(\Delta L/\Delta r)_{1XP} = q/2 \Big\{ \sin 2A \Big[bC_L \text{Cot } \phi \Big(2 - \frac{V_o}{\alpha W} \cos \phi\Big) + ba \Big] \\ + 3/4\, ab\frac{V}{W} \cos^3 A \sin \phi \Big\} \sin \omega t \\ - qab \sin A \left[\frac{V_1 r}{VR} (\text{Cot } \phi - 2\alpha) \right] \cos \omega t\end{aligned} \tag{3}$$

where, in addition to terms previously defined,

V_o and V_1, are components of induced velocity, ft/sec

W = resultant velocity at a given section, ft/sec

V = free stream velocity, ft/sec

α = propeller section angle of attack, radians

r = radius to a given station, ft

R = tip radius, ft

If a propeller is considered to be operating at an angle-of-attack that is in a pure pitch-up direction, referring to Figure 189, it can be shown that the summation of the blade IXP loads will produce the following forces and moments:

Force Component Eq (3)	Force	Moment
	See Figure 189	
Sin ωt	N	Y
Cos ωt	S	M

Equation (3) was generally used to evaluate blade loadings in the X-19 program. The major problem in its application was the evaluation of the induced velocities, and for this purpose considerable use of helicopter rotor data was used (35), (36), (37) and (38). It became apparent quite early in the X-19 program that the propeller forces generated by Equation (3) did not agree satisfactorily with data derived by the Aerodynamics Department from wind tunnel testing. The expedient solution was therefore taken for design purposes. The blade load distribution as computed by Equation (3) was retained but the load magnitude was modified as necessary to agree with the wind tunnel derived data.

(2) Higher Order Load Components.

The previous section has been concerned only with the first order of 1XP component of the propeller blade load which is a major factor. However, as previously stated the actual flow through the propeller disk is nonuniform which gives rise to higher harmonics.

On the conventional aircraft these harmonics were of no concern except at those rotational speeds where they coincide with a resonant propeller frequenty. In those cases it was only necessary to keep the operating speeds sufficiently removed from the natural frequencies of the system. In the VTOL aircraft there may be certain propeller attitudes where these higher harmonics may be significant. At termination of the Curtiss VTOL activity this was under theoretical study, but no definite conclusions had been reached. Allowance for the effects of these higher harmonics was generally made in propeller analysis and was based on past flight test or propeller test history.

(3) Continued Theoretical Blade Loading

In recognition of the short comings of the available theoretical methods for predicting propeller loads and blade loadings, a more detailed study of propeller load analysis was undertaken as an R & D effort by the VTOL Division, and this work was continuing at the time of termination. In principle the approach consisted basically of defining the propeller flow field as a mathematical function of radius and rotational angle.

Then with the known airfoil characteristics the force on any given blade element could be determined as a function of the rotational angle. A Fourier Analysis was then applied to this function to separate the various harmonic components. Obviously the major problem was the definition of the flow field to include the many influencing factors.

The induced velocity distribution during the high angle-of-attack operation of a propeller has a large effect on the loadings. Unfortunately, this velocity distribution is known only approximately at this time. It is possible, in principle, to calculate this distribution, as has been done for flapping rotor helicopters, (39). Such a calculation has not been carried out as yet for a rigid propeller. Another possible source for such data is a rather elaborate experimentation, to give the velocity close to the propeller at a large number of points. This experimental data could then be converted to a double Fourier series.

The present source of the inflow velocity distribution is a combination of theoretical and test data. The method that has been used previously to estimate the inflow velocity distribution for an isolated propeller is given below:

Simple momentum considerations give:

$$v_{1_{nom}} = V_1/2 - \sqrt{V_1^2/4 + T/2\rho\pi R^2} \qquad (4)$$

where V_1 is the forward velocity component of the propeller parallel to the shaft, T is thrust, R is the propeller radius, and ρ is the air density. The radial distribution of V_1 has been based on some static test data taken on the X-100 propeller, which has been subject to a Fourier analysis.

It has been found, however, that the interference of a nearby wing, fuselage, or other propeller can have major effects on the propeller loading. The rear propellers of the X-19 aircraft are subject to this effect, as demonstrated by wind tunnel model testing. No simple method of estimating the interference velocities exists at present, however, there is no basic obstacle to a reasonable estimate which can be had by superimposing certain known classical solutions for flow about simple bodies. A discussion of this is given in section III where fuselage flow effects upon the rear wing are defined.

The program therefore was developed in terms of symmetrical flow about an aircraft configuration with two horizontal lifting surfaces and two nacelles per side, with a central fuselage. The positions of the above components are otherwise arbitrary. Provision was made for variable nacelle angle in pitch with respect to the wing and variable aircraft angle-of-attack with respect to the remote velocity. The wings were simulated by a large number of the usual bound and trailing vortex segments. The strengths of these segments were in accordance with a given spanwise lift distribution and an assumed chordwise distribution. The fuselage and nacelles were simulated by a combination of sources and doublets on their centerlines. The strengths of the sources and doublets were defined in terms of simplified boundary conditions for the isolated bodies, with provision made for variations in wing upwash or downwash along their lengths. The velocity distributions for all vortices, sources, and doublets were superimposed without attempting to satisfy flow boundary conditions strictly for the whole configuration.

The accuracy of the total distribution found in this way was expected to be acceptable. The velocity components in three dimensions are calculated at a large number of points in each propeller, with special provision made for points close to a trailing vortex sheet. Certain refinements were contemplated. The most important of these would be propeller blade trailing and shed vortex sheets, with trajectories given by the velocity distribution of the present program, superimposed on the remote velocity and estimated propeller induced velocity. Another provision could be variable chordwise lift distribution, given by the local angle of attack. Finally, the resulting velocity distribution could be used to compute new values of local angles of attack and vortex sheet trajectories. This information could be used in a new cycle of computations with the expectation that the results would be of greater accuracy.

c. Propeller Test Loads

As stated in the previous section, the design propeller loads were established on the basis of wind tunnel testing.

In the case of the blades, theoretical distribution of loading were used but modified in magnitude to agree with the test data. It was the intent that during the X-19 flight test program, sufficient propeller instrumentation would be installed to permit a correlation between design loads and flight loads.

(1) Wind tunnel tests

The basic propeller loads used for design were determined from wind tunnel testing of free-propellers, models, and the X-100 aircraft. This testing is fully discussed in Section IX. In the course of the blade loading development, correlation was made between theoretical and test data. Typical comparisons are shown in Figures 135 and 136.

(2) Flight Test

The limited preliminary flight testing of the X-19 did not provide the opportunity to verify the accuracy of the 1XP propeller design loads. However, calculations were made for an equilibrium transition flight and it was possible to compare the calculated blade stresses measured during flight. A typical comparison is given in Figure 137. The correlation is considered good and this very limited data would imply that the 1XP propeller loads as used were realistic for the airplane.

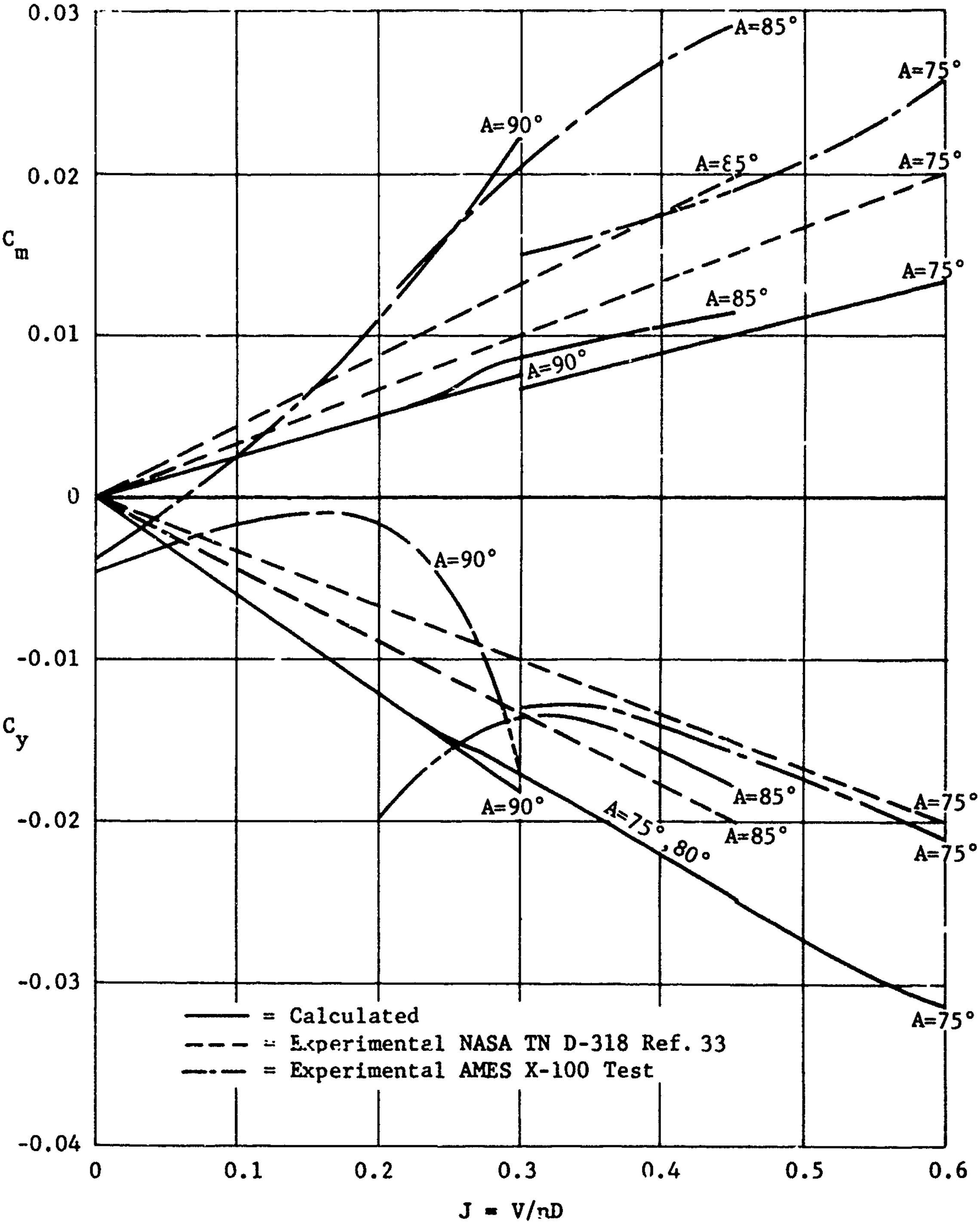

Figure 135. Comparison of the propeller yawing and pitching moment coefficients at flow angularities close to 90°, and at low advance ratios, $\beta_{.75R}$ = 15°.

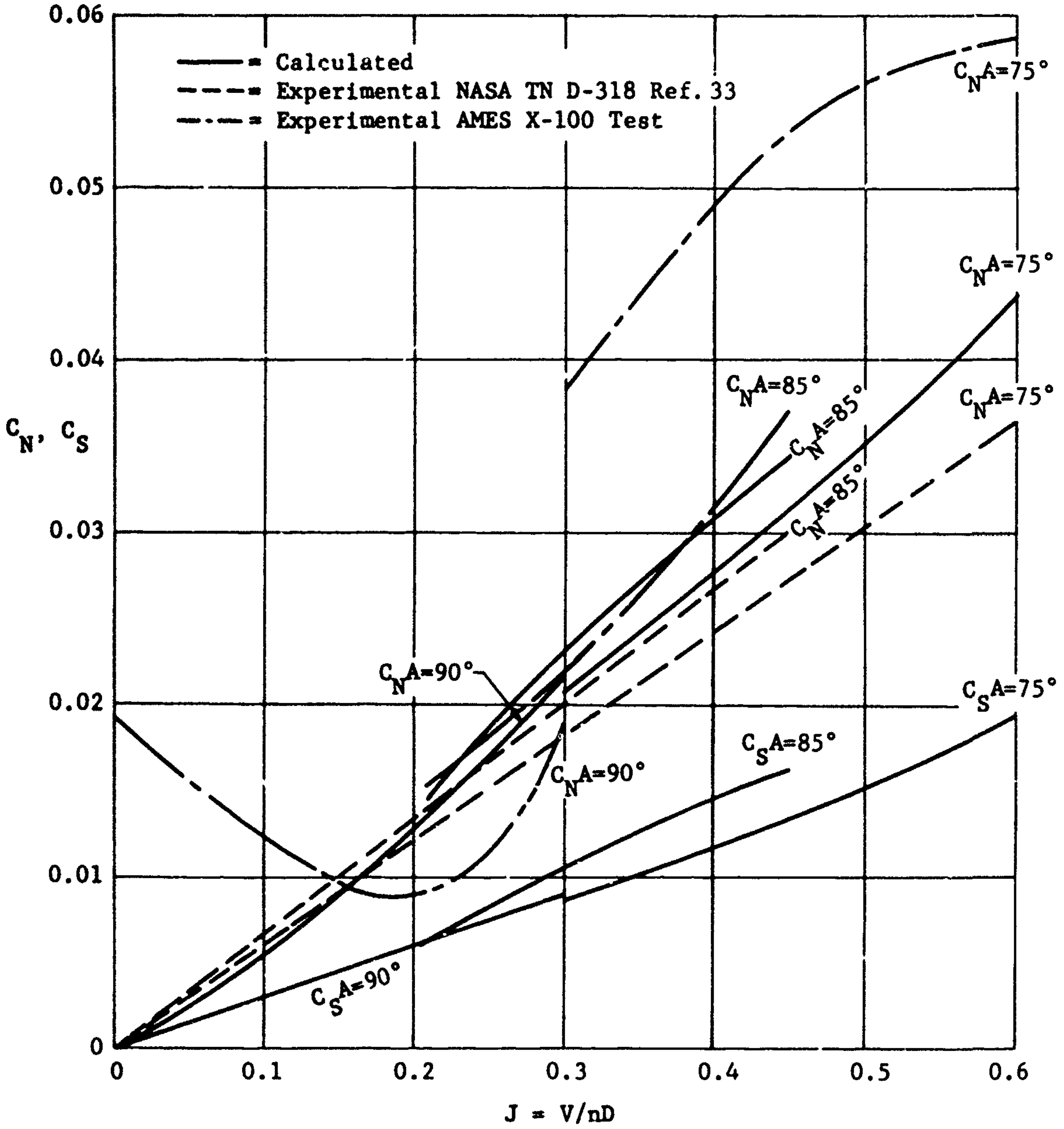

Figure 136. Comparison of propeller normal and side force coefficients at flow angularities close to 90° at low advance ratios, $\beta_{.75R} = 15°$.

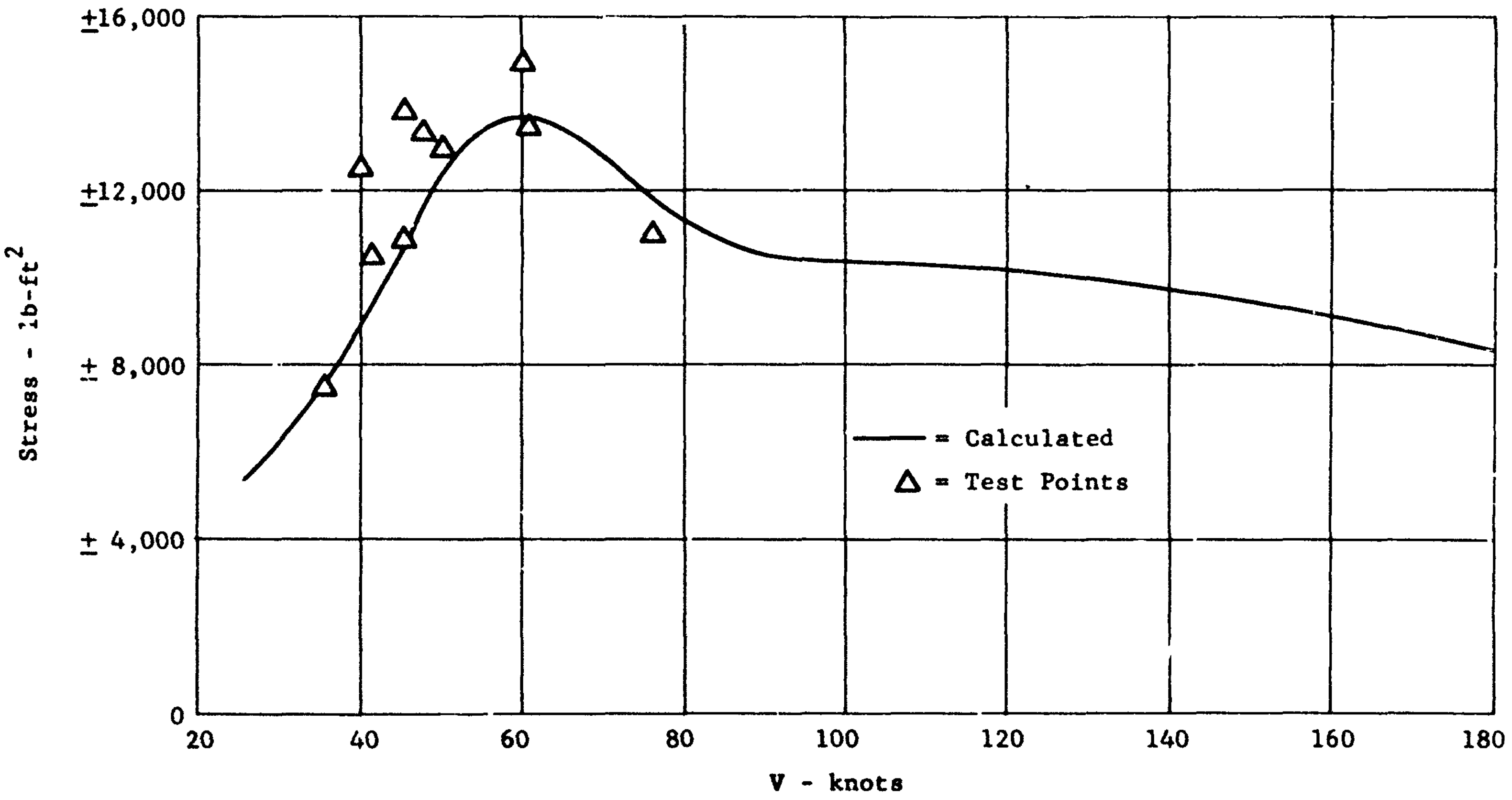

Figure 137. Comparison of calculated and measured blade vibratory shank stress for equilibrium transition flight of the X-19 aircraft.

4. WEIGHT COMPARISON OF 19 FIBERGLASS PROPELLER

Early in the concept studies of VTOL aircraft, it was recognized that the propulsion system would be a significant portion of the total aircraft weight and a considerable effort went into weight reduction studies of this system. Accordingly, the propeller blade received early design emphasis since a reduction in blade weight would be multiplied by 12, the total number of blades, and would reflect to some extent a comparable saving in the weight of hub and other components. A summary of this work is as follows:

a. Blade Weight Studies

General studies were made in the selection of a lightweight propeller blade design considering both fiberglass and the lightweight metals (40). The results of these studies showed a definite advantage in favor of the fiberglass design and these studies considered both VTOL/STOL and conventional turbo-prop installations. Typical results of these studies are shown in Figures 138 and 139 which show a blade weight comparison of several types of blade construction for a specific airplane installation. In these charts, reference is made to the composite blade.

This type of design consisted of a metal structural center spar which was generally elliptical in cross section and was formed as closely as possible to the required airfoil shape. The airfoil section was then completed by bonding a preformed leading and trailing edge strip to the spar. Abrasion resistance was provided by a thin stainless steel sheath.

It is well known that the major factor in the structural design of a propeller is the 1XP vibratory blade load. Referring to Equation (2), page 226, it is seen that this loading is proportional to the Aq factor. A review of several operational propellers having hollow steel blades, resulted in an average weight vs. Aq curve as shown in Figure 140. For a more generalized fiberglass weight comparison, typical turbo-prop installations were selected and an equivalent fiberglass blade was designed. The weight advantage in fiberglass is clearly shown in Figure 140. The final weight of the 13166A12P3 blade is 70.6 lbs. No direct comparison has been made between the X-19 blade and comparable blades in other materials. It is estimated, however, that an aerodynamically equivalent hollow steel version would have a weight of approximately 132 lbs.

b. Hub Weight Studies

The propeller hub design is governed by the blade loads; and, a reduced weight blade therefore offers hub weight advantages. However, this contribution was not a major one in the conventional

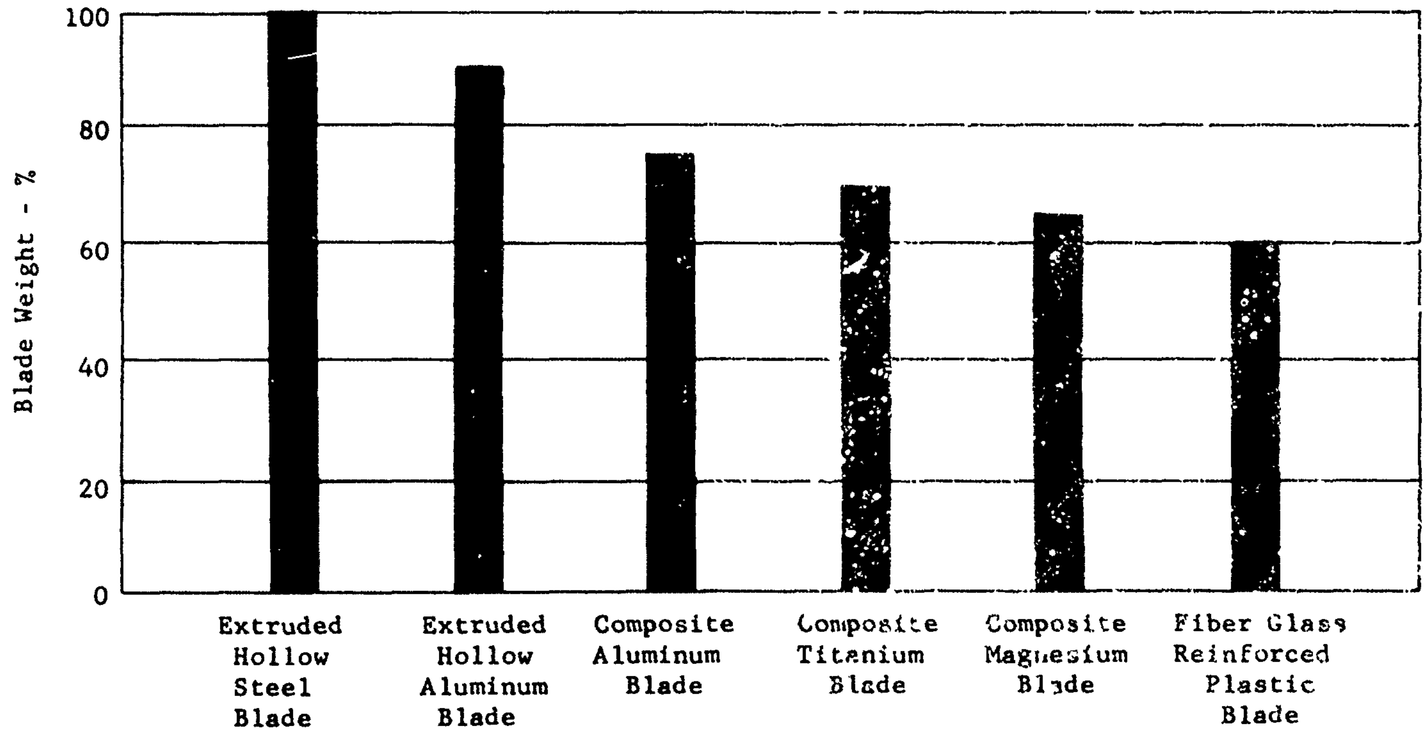

Figure 138. Relative blade weight comparison considering various materials for the design of a hypothetical VTOL/STOL propeller; 15'-0" diameter, 120 AF, 1000 hp at 1146 rpm.

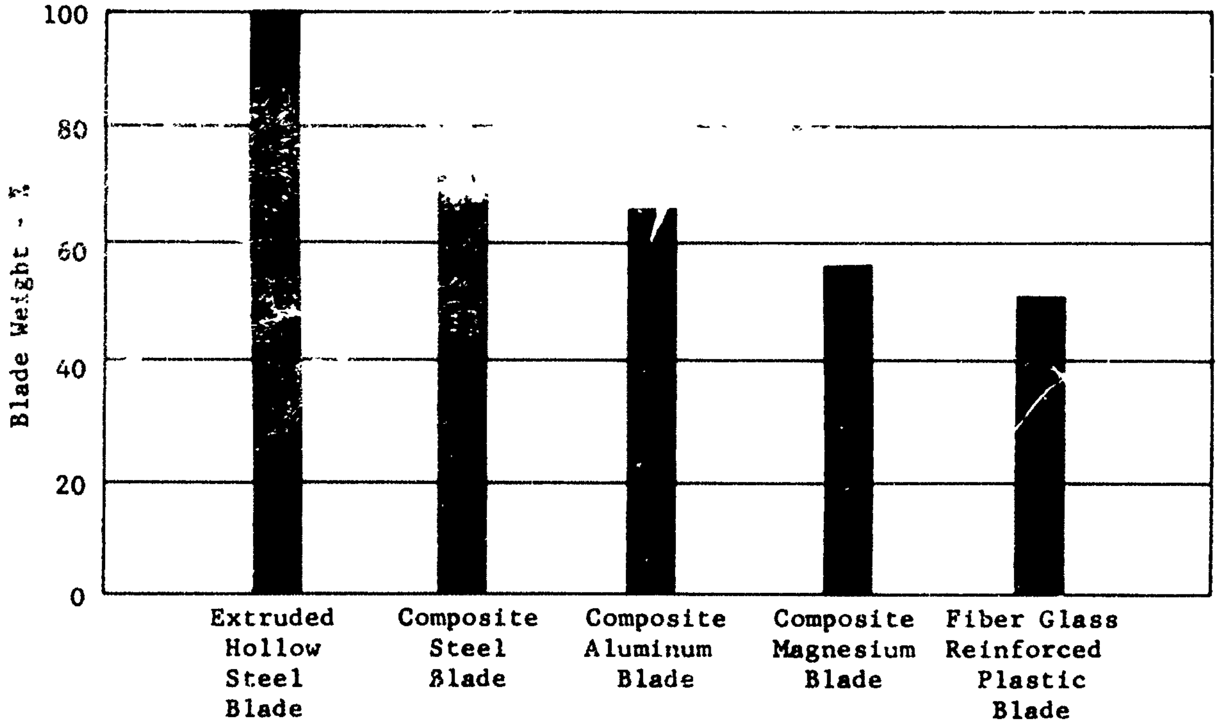

Figure 139. Relative blade weight comparison considering various materials for the design of a turbo-prop installation; 13'-6" diameter, 150 AF, 4000 hp at 1160 rpm.

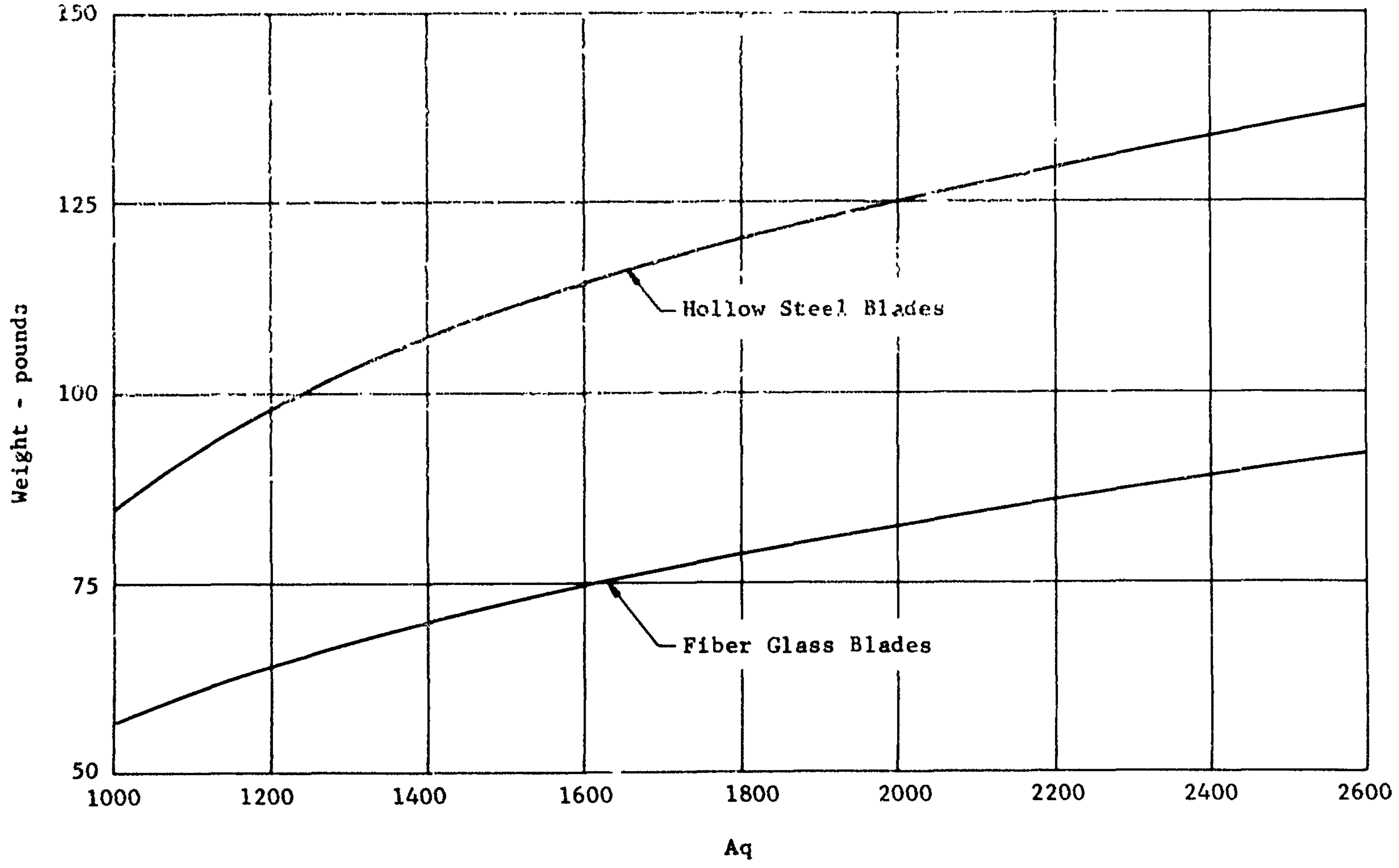

Figure 140. Variation of blade weight with 1 x P excitation factor, Aq, for hollow steel and fiberglass blades on a typical turboprop installation; 13'-6" diameter, 165 AF, 4500 hp at 1200 rpm.

hub design and the desirability of a more efficient hub structure was recognized. For this reason considerable design effort went into the redesign of the hub assembly for the X-100 aircraft. As finally evolved for the X-19 aircraft, the 162595 hub is, in general, a scaled-up version of the 138034 hub used for the X-100 vehicle. Although there is an external resemblance to the conventional Curtiss Electric Propeller hub, the internal differences are many, including the absence of an integral inner structure. The conventional nut-and-cone shaft mounting was replaced by a large, 2-row nose-mount bearing on the rear extension. The self-contained pitch-change mechanism consisted of a hydraulic piston operating inside the rear extension and connected by linkages to cranks on the blade butts. The torque drive was through short internal splines at the extreme aft end of the rear extension. The design differences resulted in an unusual geometry which combines, in one hub, a shank size less than #2 (115 mm) with a rear extension larger than that for a standard S.A.E. #60 splined shaft.

The resulting total propeller, less blades weight, for the X-19 was 161.2 lbs. Again there is no direct comparison with a conventional propeller hub assembly designed for the X-19 installation. However, a similar sized Curtiss Electric Propeller would have a propeller (less blades) weight of approximately 200 lbs.

5. PROPELLER STRUCTURAL PROBLEMS

Through the development and testing of the X-19, a number of structural problems were encountered in the propeller system. These problems varied in importance and are described as follows:

a. Blades

There were two basic problems with the propeller blades; one was associated with the foam filler and the second was with the steel shank.

(1) Foam Filler

In the course of operating the No. 1 X-19 for a total of 114 hours, foam separations were encountered in five blades. Three of the separations were repaired and the blades were returned to aircraft testing and separations occurred a second time, thus accounting for eight cases of separation. Upon subsequent X-ray inspection, it was found that four of these five blades also showed cracks in the foam. On 31 January 1965, during a maintenance ground run, a sixth blade experienced foam shifting and resultant tip bulging as a result of foam bond failure or foam separation. Detailed inspection of these six blades disclosed a consistent pattern of sound foam and fiberglass but poor bonding between the two elements.

A review of the foam bonding technique employed in these blades, in the light of the current state-of-the-art, disclosed several factors which could potentially contribute to the lack of bond including:

(a) The use of a cleaner containing methylene chloride to clean the fiberglass blade shell prior to foaming may result in deterioration of the foam bond.

(b) The use of an epoxy primer (Rexton) may result in lower bond strengths than obtainable with a urethane primer.

(c) Storage of the "T" component of the Nopco H-106 foam at temperatures below 60°F before use in the blades may have caused separation of its TDI constituent.

(d) Temperature and humidity control was not optimized during the priming and foaming operations.

An extensive investigation was initiated to review and/or modify the Curtiss Process Specifications CPS 6266 (Molded Fiberglass Reinforced Plastic Blades) and CPS 5065 (Foam Plastic-Rigid-Freon-Blown, Low Density). This analysis and specimen testing was performed at the Curtiss Division and Redel, Inc. California.

This investigation program was extensive and involved studies of surface preparation, types of foam, chemistry variations, curing cycles, and evaluation of the foam material properties. A total of 27 full scale blades were built and fatigue tested using the more promising developments. Based upon these tests the foam system developed was a considerable improvement and the 13166A12 blades which incorporated this new foam were considered structurally satisfactory for the flight test program.

However, the foam problem was not considered completely solved to satisfy high service life, and this still remains an area which needs further development in the light-weight blade program.

b. Blade Shank

As previously mentioned the X-19 shanks were made of AMS 6415 steel heat treated to RC 42-46. This is bordering on the brittle range. Although the metallurgy department had set up special procedures (double bake immediately after plating) for processing these shanks, certain problems developed in the initial development.

(1) Longitudinal Cracks in Outboard End of Shank

There were three instances of cracking in the outboard end of the shank (Fig. 118) prior to blade fabrication, and therefore before any application of operational or test loads. In addition, a similar crack found during examination of a blade which failed on a fixed-root test could not definitely be attributed to fatigue and may have originated as a static crack.

It was theorized that cracking of this type, during or soon after manufacture, may have been associated with residual stress from the forming process, and/or with hydrogen embrittlement of the steel. In either case, a time factor appeared to have been operating, which may have resulted in deferred failures.

(a) At Shank Fabrication

Two completed shanks, which had been approved after magnaflux, were found at final inspection to be cracked. The normal time interval between magnaflux and final inspection was reportedly less than two weeks; that between plating and baking was variable, a critical factor where hydrogen embrittlement is involved.

(b) At Blade Fabrication

Blade P-120 had unsatisfactory fiberglass during initial blade fabrication. The fiberglass was therefore stripped, at which time examination disclosed similar cracks in the shank outboard end.

(c) During Test

Blade P-68(-2) failed after 42 x 10^6 cycles of fixed-root testing. Examination of the blade after failure showed branching cracks at the shank outboard end. As previously mentioned; these may well have originated as static failures. As a result of these failures, the Metallurgy and Blade Design Departments set-up rigid processing controls. Further incidences were not found and this problem appeared to have been solved.

(2) Fatigue Failures in Inboard Portion of Shank

Two retention tests of the X-19 type shank failed at low total cycles by reason of fatigue failures originating at areas of internal shank corrosion. As a result of the first failure, precautions were taken to prevent rust formation during testing of the second shank. Inasmuch as failure of the second shank was subsequently attributed to a corrosion origin, it was concluded that the blade shank was insufficiently cleaned prior to application of the protective coatings. These fatigue failures indicated the possibility of a high notch sensitivity such as would be expected with a material of low ductility.

Following discussions among Metallurgy, Blade Design, and Structures, the internal surface all steel shanks were carefully cleaned, the bore was shot-peened and a suitable protective coating was applied. No further incidences of shank corrosion were found.

c. Hubs

There were no structural deficiencies of the propeller hub itself. However, in the hub assembly, it was found that under load there was a harmonic drive type of action which tended to rotate the inner race of the nose mount bearing with respect to the hub. This tendency to turn would also tend to tighten the bearing preload nut, P/N 169564. In the original design, the lug which was provided to lock the bearing preload nut was inadequate to restrain this motion. Lug failures were experienced after relatively short periods of operation which in turn permitted the nut to tighten. This action resulted in failure of the hub rear extension in one of the early endurance test runs. A spline type lock was designed which proved adequate. It was noted, however, in subsequent testing under high vibratory load that considerable galling and wear was produced between the nose mount bearing race and the hub shoulder and between the bearing race and the nut face.

Since galling is a potential origin for fatigue failure, redesign of the hub rear extension was recommended, and preliminary studies of this problem had been initiated at the time of termination of the project.

d. Blade Pitch Control

Early in the functional testing of the propeller, it became apparent that the blade link, P/N 168267, which transmits the pitch change force from the hydraulic piston to the blade butt, was marginal with respect to the anticipated loads. This was corrected by a simple strengthening of the part.

During airplane ground testing, it was found that the propeller control push-rods inside the wing were being subjected to a significant vibration. This caused a fatigue type failure of some of the rod ends and certain cast aluminum hangers.

In order to determine the magnitude of the vibratory forces, strain gages were installed in the system. On the basis of the measured data, the rod end size was increased and redesigned hangers were machined from aluminum bar stock.

After considerable development testing on the half system rig, a failure was found in one of the pitch change pistons. Examination indicated that this was a fatigue type failure; however, the cause of this failure was never satisfactorily explained. As a precaution, the part was redesigned to provide a heavier section and more generous fillet radii.

e. Propeller Housing

This housing, P/N 166464, provided the support or mounting of the propeller to the nacelle gear box housing which was attached to the wing structure through the trunnion of the tilt mechanism. It consisted of a cast magnesium shell (AMS 4434 commonly designated AZ92A-T6) reinforced for stiffness by internal longitudinal ribs. The forward portion was a conical section which faired into a cylindrical shell about 9 inches aft of the propeller. This structure was not adequate to transmit the encountered magnitude of 2xP vibratory propeller loads for the period of aircraft flight testing and the failure of this housing in flight resulted in the loss of the No. 1 X-19 aircraft.

The investigation which followed the crash of the aircraft revealed that the failure was the result of a combination of factors.

(1) The vibratory load level reacted on the nacelle housings during later airplane operation was considerably higher than had been anticipated in the establishment of the original design criteria. More specifically, the strain gage data that was evaluated from flights Nos. 32 to 50, most of which were accomplished at NAFEC, indicated that the 2xP component (vibratory on the nacelle) during conversion (tilt translation) flying was of the same magnitude as the 1xP component which is a steady load on the nacelle.

(2) Just prior to ultimate failure, an emergency maneuver was executed which produced steady loads significantly higher than design values.

(3) A strain gage survey showed that the actual stress gradient in the rib/transition area was twice the value used in the theoretical analysis based on a limited Stresscoat survey. Also, sand pits in the rib tips added to the stress concentration and the intolerance of the area to fatigue loading.

As a result of the above described investigation, the housing was completely redesigned, P/N 174988. At the termination of the contract, this housing had been completely static tested. Plans for fatigue testing the entire nacelle assembly under simulated propeller steady and vibratory loading were being made. A laboratory test facility was designed to accommodate the entire nacelle gear box and attaching propeller housing with all subsystems intact with the exception of the blades and tilt mechanism.

6. PROPELLER INDUCED LOADS

The loads on the airframe induced by the propeller, can be of both a steady and vibratory nature. The six basic steady load components consisting of thrust, torque moments and normal forces have been discussed under Sub-part 3 of this Section. It is the purpose of this part to briefly discuss the other theoretical loads and also to present those airframe loadings which were observed during testing of the X-19 airplane.

a. Theoretical Loads

As previously noted in Section V, 3., the flow through the propeller may be considered as being made up of a uniform flow upon which are superimposed many harmonic components 1XP, 2XP, 3XP etc. Each of these velocity components will generate a corresponding load component, and it is the summation of the blade load harmonics at the propeller centerline that is reflected on the airframe. The nature of the reaction on the aircraft depends upon the number of blades, and the order of vibrations.

By a relatively simple mathematical procedure it can be shown that the shaft thrust and moment due to a blade harmonic force are:

$$T = F_n \cos(n\omega t), \quad n = mB$$

$$T = 0, \quad n \neq mB$$

$$M = M_n \frac{B}{2} \left\{ \cos \ (n+1)\,\omega t \right\}, \quad \frac{n+1}{B} = \text{integer}$$

$$M = M_n \frac{B}{2} \left\{ \cos \ (n-1)\,\omega t \right\}, \quad \frac{n-1}{B} = \text{integer}$$

where:

T = total shaft thrust due to a given harmonic blade force, lb.

M = total shaft moment due to a given harmonic blade force, in.-lb.

F_n = Maximum value of the blade harmonic thrust force, lb.

M_n = Maximum value of the blade moment at the shaft centerline due to the harmonic force, in.-lb.

B = number of blades

n = order of vibration

m = integer

t = time, sec.

ω = blade rotational frequency, rad./sec.

$n\omega$ = harmonic frequency, rad./sec.

Considering these equations with respect to a 3-way propeller, such as was used on the X-19 airplane, the following shaft reactions are obtained:

(1) A 1XP blade harmonic is thrust reactionless but produces a steady shaft moment.

(2) A 2XP blade excitation is thrust reactionless but produces a vibratory shaft moment having a frequency of 3XP.

(3) The 3XP blade harmonic, will produce a 3XP thrust component and will be moment reactionless.

(4) The 4XP blade load will be thrust reactionless, but it will produce a vibratory shaft moment at 3XP frequency.

The 1XP load component has been more fully discussed in Sub-part 3 of this section. The forcing function of the higher harmonics, 2XP, 3XP etc., cannot by the present state-of-the-art be calculated with any reliable degree of accuracy. Flight test was generally relied upon to evaluate the severity of these components and to establish rpm restrictions. Generally these excitations have been sufficiently low that they were of little concern in conventional aircraft except at resonant speeds. Care was therefore exercised in the propeller design to be certain that the propeller natural frequencies did not coincide with the higher harmonic frequencies at operating speeds.

There is evidence in theoretical work and the limited flight test data which indicated that both the 2XP and 3XP blade harmonics may become significant in certain portions of the transition flight on the VTOL-type aircraft. It must be noted that any propeller blade harmonic which produces a shaft reaction dynamically couples the propeller to the airframe. The propeller and propeller forces must be considered in any airframe dynamic study. These are controlling loading criteria in the design of the propeller, nacelle housings, tilt mechanism and possibly the wing structure in a V/STOL aircraft.

b. Airframe Test Results

In the limited testing of the X-19 aircraft, certain vibrations were obtained in the aircraft which were attributed to the propeller. These occurred both on the ground and in flight.

(1) Ground test

The initial ground testing of the X-19 aircraft was conducted on a tie down rig. Essentially, this consisted of restraining the aircraft against vertical motion by rigid supports or columns at each of the four wing tips. Fore-aft motion was prevented by stops at the main landing gear. Running on this rig produced a strong vibration throughout the airframe at 1XP frequency and 3XP frequency. The 1XP component was found to be due to propeller unbalance, and was eliminated by a careful matching of both the horizontal and vertical balance between blades. Previously, only horizontal balance had been carefully controlled. The 3XP component was found to vary with nacelle attitude, being more severe in the hover position and decreasing in severity as the nacelle tilted down to the cruise position. This vibration was believed to be due to blade passage over the wing. It was also found that this vibration was sensitive to the manner of aircraft support. With the aircraft on the tie down rig, where the main support was at the wing tips, the response was quite strong. With the aircraft supported on the ground through the landing gears in a normal manner, the 3XP vibration was considerably less, and once the aircraft became airborne this response was significantly reduced. In other words, the natural modes of the airframe structure changed as the manner of support was changed and the response to the 3XP blade passage excitation reflected this change in the natural modes.

(2) Flight Test

Propeller blade strain data recorded during flight testing of No. 1 X-19 showed an unexpectedly high percentage of 2XP stress, which was reflected as 3XP on the nacelle and its supporting structure. When blade vibratory stress was plotted with respect to rpm, a magnification similar to a resonant condition was observed, see Figure 141.

In an attempt to substantiate the apparent resonant trend, a stress-rpm survey was made in conjunction with the green running on the second X-19 aircraft. A good harmonic analysis of the records had been made, and the analysis showed that for the conditions of the test there was a noticeable 2XP stress amplification between 950 and 1150 rpm.

The data, however, did not show a well defined resonant speed. This is shown in Figure 142. Further, a qualitative analysis of this test data indicated that the stresses on the nacelle and trunnion were being significantly influenced by a 3XP thrust component. A review was then made of the 13166A12P3 blade frequency calculations. Although correct

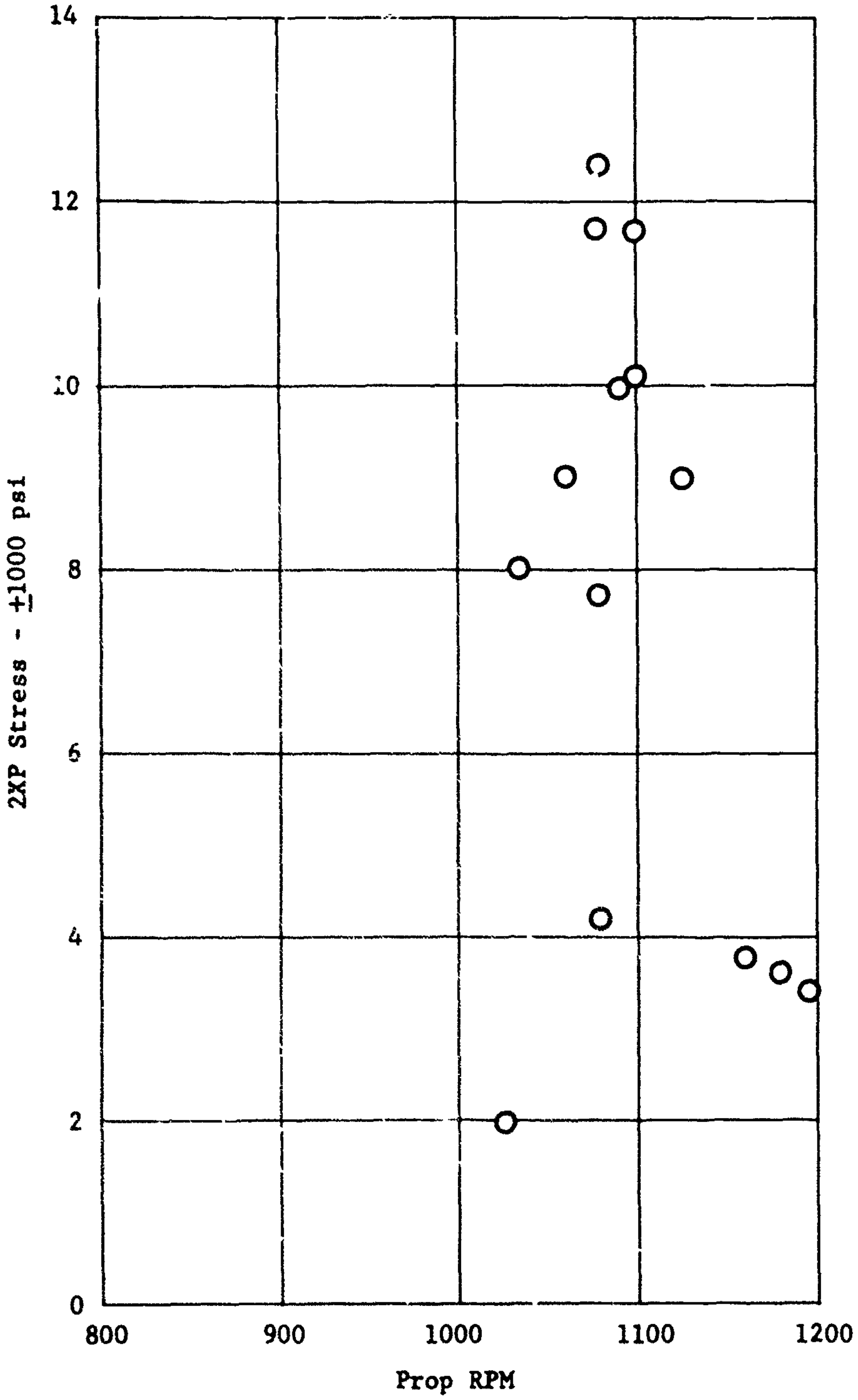

Figure 141. The 2XP component of blade stress as measured during flight test on the X-19 aircraft showing a resonant trend with rpm.

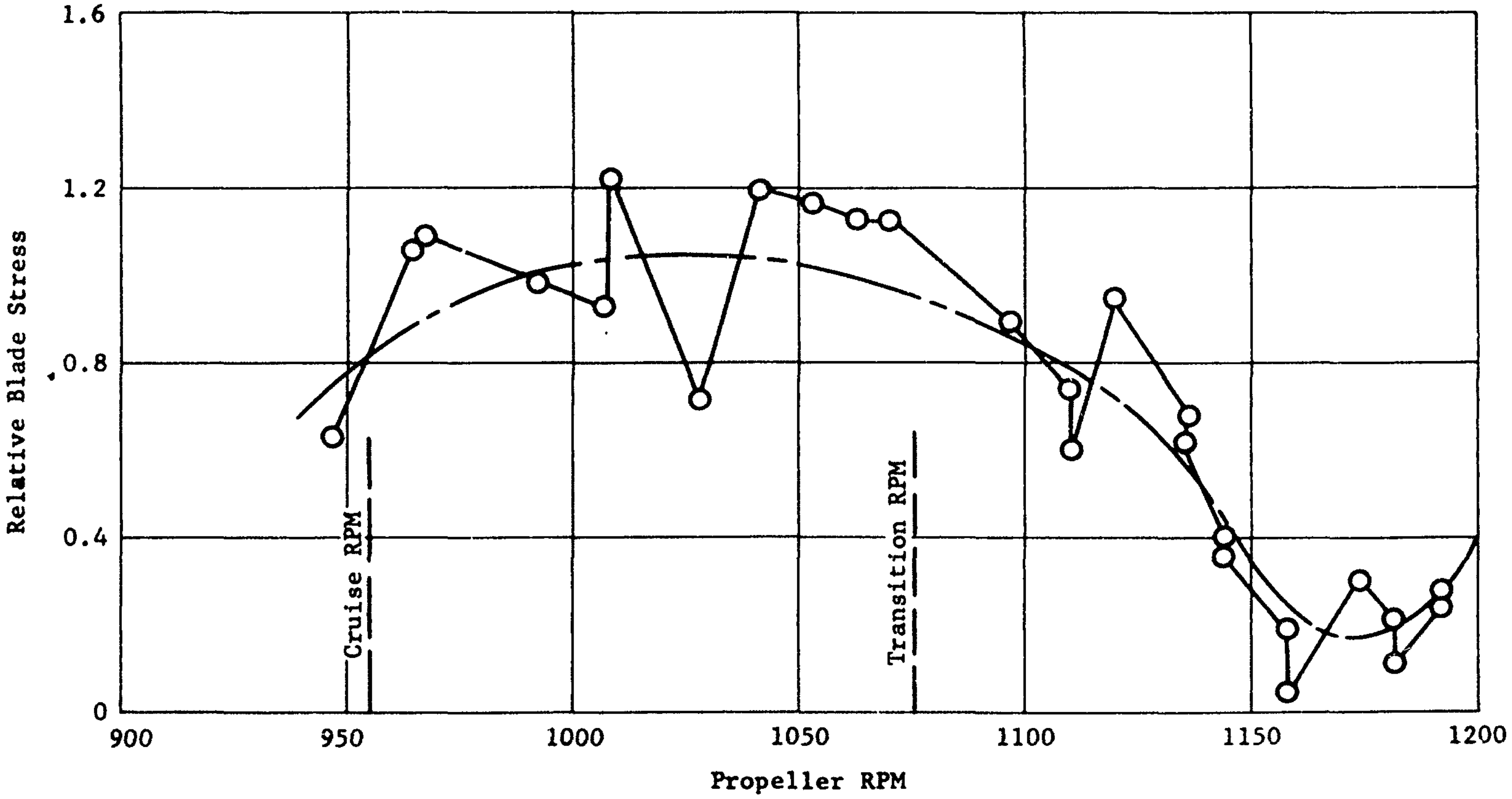

Figure 142. Variation of the 2XP blade stress component with rpm as measured during a ground vibration survey on the X-19 aircraft.

for the input used, it was found that the blade mass distribution calculated from the preliminary properties was 18% lower than the "as manufactured" blade weight. This would reduce the calculated frequency from 1480 to 1350 rpm. On this basis, a lower installed propeller resonance would be expected since the 2XP excitation on a 3-way propeller is not moment reactionless on the shaft which would produce a coupling with a nacelle structure. However, this would normally not be expected to reduce the resonant rpm to the 1150 shown in Figure 142.

These factors tended to weaken the resonance theory and promote the possibility of a stronger than anticipated 2XP aerodynamic excitation during the transition flight. An elementary analysis had shown that the 2XP excitation would be a function of:

$$(V \sin A)^2 \sin \beta$$

where V = aircraft forward velocity

A = the propeller angle of attack

β = propeller blade angle setting.

In order to determine the degree of correlation, the velocity, blade angle and tilt angle were obtained from the flight records for further analysis. The tilt angle was used as a first approximation of propeller angle of attack and the above expression was evaluated for several flight conditions. The corresponding 2XP vibratory stress as measured on the blade was then plotted against this parameter. This plot and an apparent correlation is shown in Figure 143. At the time of termination, this problem of 2XP blade resonance or high 2XP propeller aerodynamic loading had not been completely resolved.

The reasons for the high loadings encountered on the nacelle of the X-19 during conversion that led to its failure must be found so that proper design loads can be determined, as these loads could have a major influence on the nacelle structure of any new tilt rotor or tilt wing airplane. There are many reasons for the high loads, for instance they could have been developed as a result of flow conditions from the front wing, influencing high loading on the aft propeller, or by the start of nacelle whirl, or could be just a function of an airframe resonance condition. The question can be answered by testing an isolated X-19 propeller at the same conditions encountered prior to the loss of the propeller to find if excessive 2 x P stresses are induced on the blade. If not, the high stress levels were induced by conditions peculiar to the X-19 in which case the question is adequately

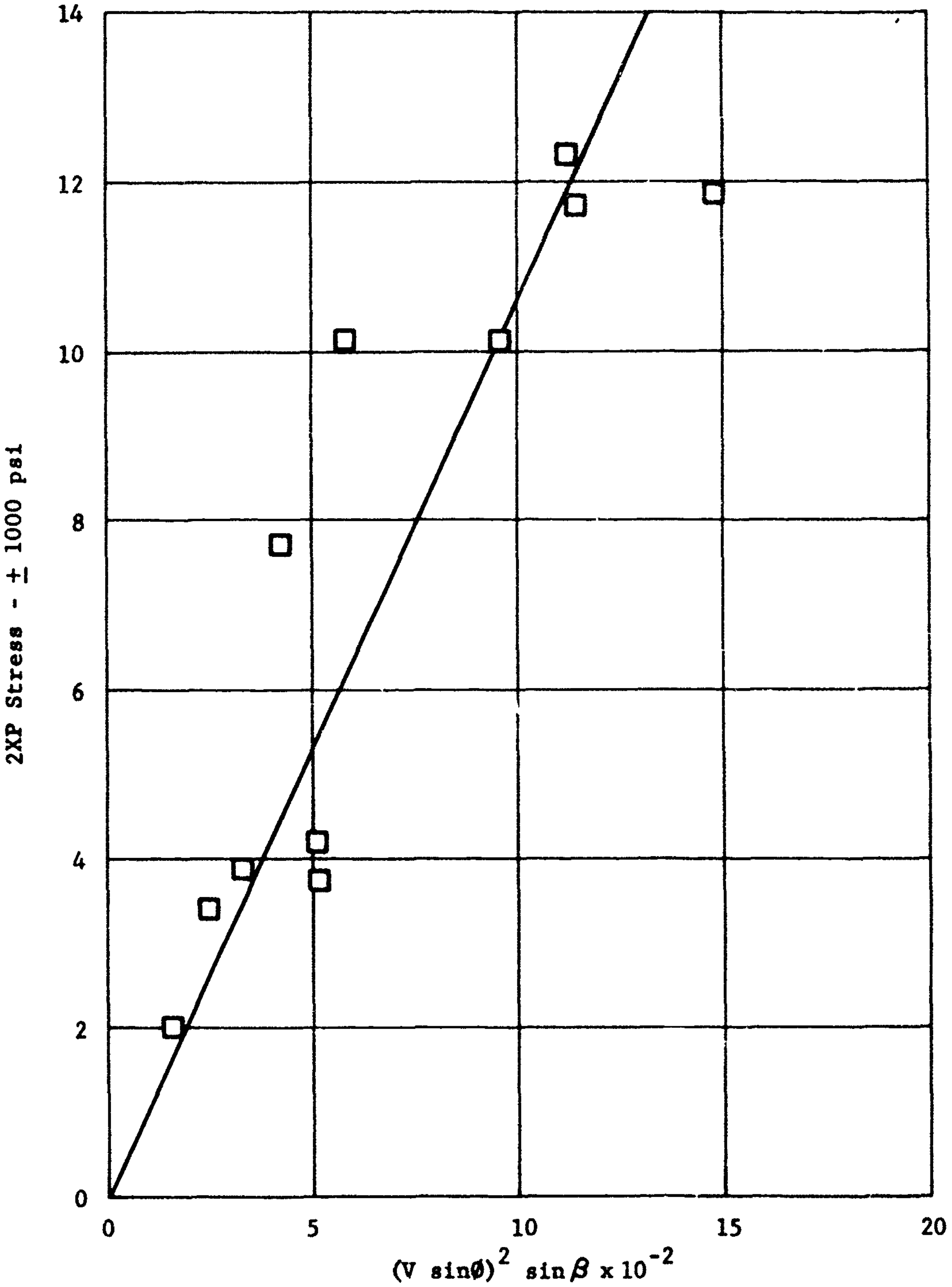

Figure 143. Variation of the 2XP blade stress as measured during flight test of the X-19 aircraft as a function of the theoretical 2XP parameters, $(V \sin \phi)^2 \sin \beta$.

answered. Otherwise, if the high stresses were generated by isolated propeller, further theoretical and experimental work will be required to develop the necessary solution.

7. PROPELLER TESTING

Except for the development testing of the fiberglass blades which is presented in Section V, 2., this section covers the details of the testing accomplished to qualify the X-19 propeller for flight.

a. Propeller Hub Static Test

The 162595 hub employed in the propeller of the X-19 aircraft, although utilizing well-proven design principles, differs in numerous ways from those heretofore built by this company. The absence of an integral inner structure, the replacement of a conventional nut-and-cone shaft mounting by a large, 2-row nose-mount bearing on the rear extension, the self-contained pitch-change mechanism consisting of a hydraulic piston operating inside the rear extension and connected by linkages to cranks on the blade butts, and the torque drive through short internal splines at the extreme aft end of the rear extension are all design differences which differentiate this propeller from its predecessors.

(1) Design Loads

Propeller components are commonly stress-analyzed for the maximum propeller loads predicted for service operation, on the assumption that during the life of the airplane the accumulated stress cycles at the higher loads will be sufficient to constitute an endurance condition. Because of the complex flight maneuvers possible with this vehicle, normal operating loads cover a wide range of centrifugal force as well as symmetrical and unsymmetrical bending moments. Loads given in Table IX for the transition plus gust, maneuver transition, and high speed conditions were selected as representing the heaviest loading on the hub and were utilized as major design criteria.

(2) Test Procedure

The propeller hub was mounted on a specially designed tension machine, Figure 144, in such a manner as to simulate the aircraft mounting. The blades were replaced by special test shanks which were retained in the hub by means of the design blade retention.

The centrifugal and bending loads were applied simultaneously to each barrel by means of hydraulic jacks, and a static simulation of the vibratory loads were superimposed in the correct phasing. Because of the highly redundant nature of the hub structure, the testing was done in two phases:

(a) Stresscoat Test

The initial effort consisted of a qualitative stress survey with brittle lacquer to determine the locations

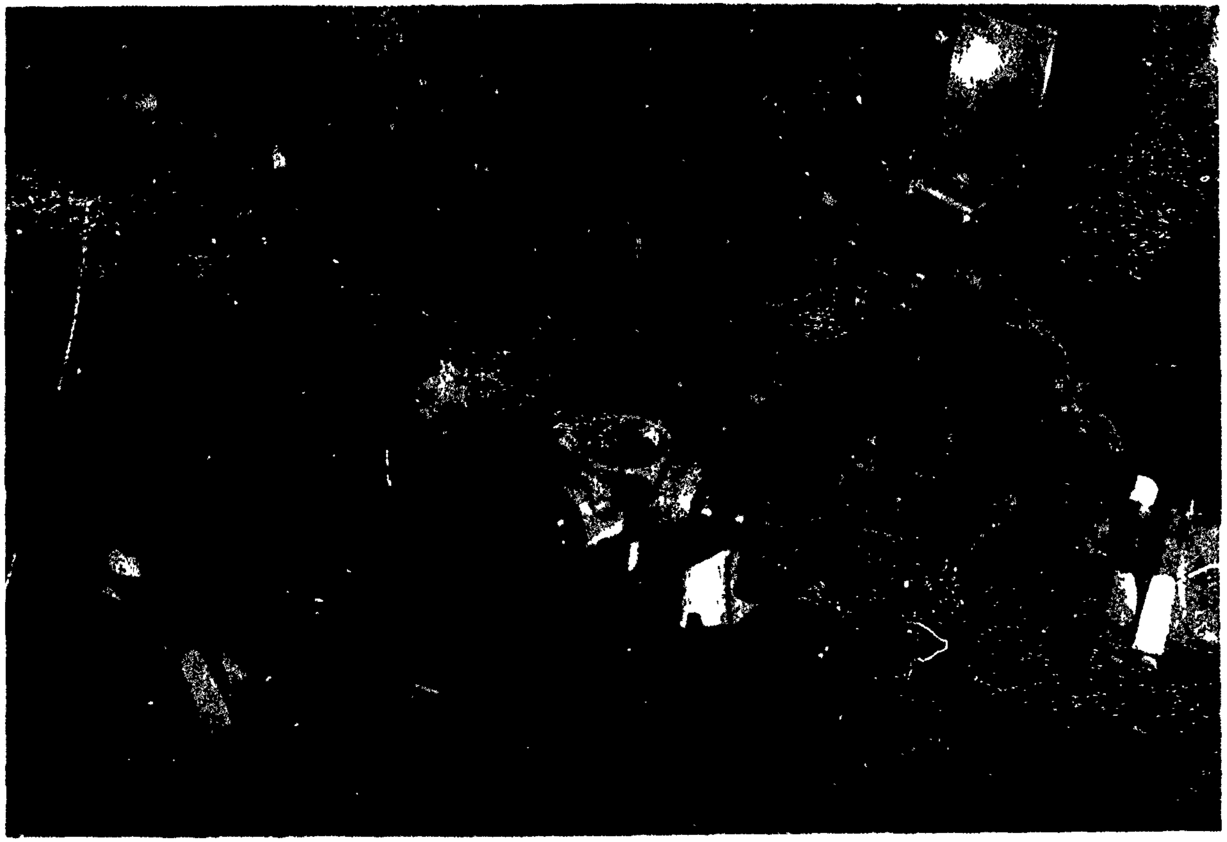

Figure 144. Laboratory test facility for the static testing of propeller hubs.

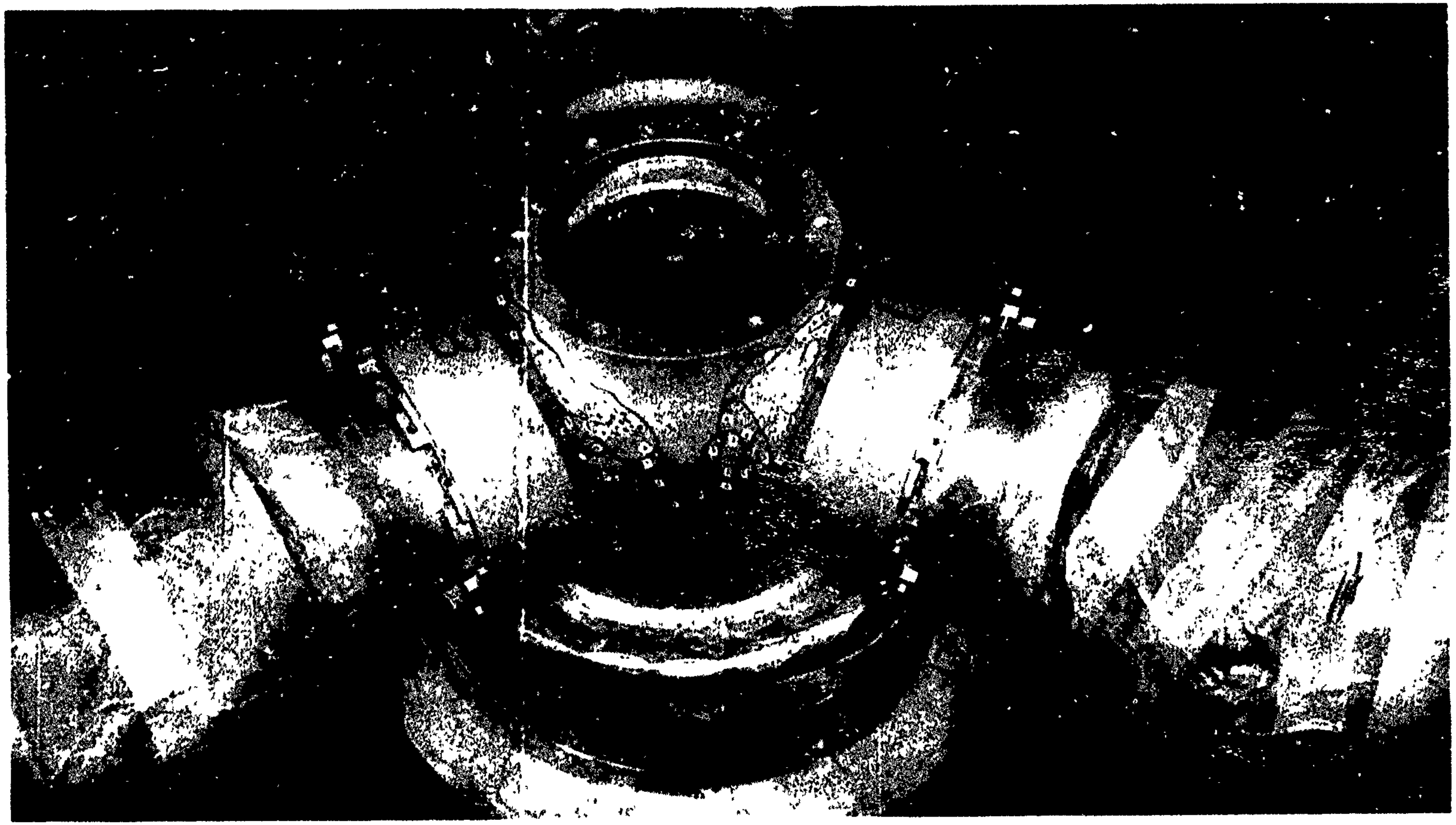

Figure 145. Stress coat patterns appearing on the X-19 propeller hub under a simulated design steady/vibratory load condition.

of stress concentrations and directions of principal tensile strain, see Figure 145. Results of this test phase were used to assist in properly orienting resistance wire strain gages for the definitive phases of the test program.

(b) Wire Strain Gage Test

In view of the limitations of Stresscoat for quantitatively exact work, the definitive stress evaluation was based upon the use of a wire strain gage survey. During the second phase of the investigation, therefore, quantitative measurement of apparent stress was accomplished by means of these gages and conventional strain gage instrumentation.

On the X-19 hub a total of 129 strain gages were installed. The pertinent locations are illustrated in Figures 146, 147, 148 and 149.

(3) Results

An extensive analysis of the data from 129 strain gages and three loading conditions was made, and the pertinent results indicating the locations and stress magnitudes of the more highly stressed areas are given in table XI. It is seen that for the design loads the minimum factor of safety is 1.28, and for the most part the factors were well in excess of 2.0. The testing therefore indicated that the 162595 hub was adequate for the anticipated flight loads of the X-19 aircraft.

b. Laboratory Whirl Test

This is a standard propeller test used in the development and qualification testing of the functional aspect of the propeller-nacelle assembly.

(1) Description

This test was performed in the C-W, Curtiss Division laboratory to demonstrate operation of the complete propeller-nacelle assembly. This assembly was whirled on an electrically driven whirl stand utilizing test shanks and counterweights to simulate the blade loads, Figure 150. Testing was performed at speeds, blade angles, rate of pitch change, and net twisting moments (centrifugal and aerodynamic twisting moments), that were predicted for normal operation of the aircraft. In addition, simulated governing and power transients which would require propeller pitch change excursions during the various phases of aircraft operation were demonstrated.

(2) Test Program

The endurance qualification and assurance testing of the X-19 was initially performed to the 50 hour level. Upon completion of the 50 hour qualification test and subsequent

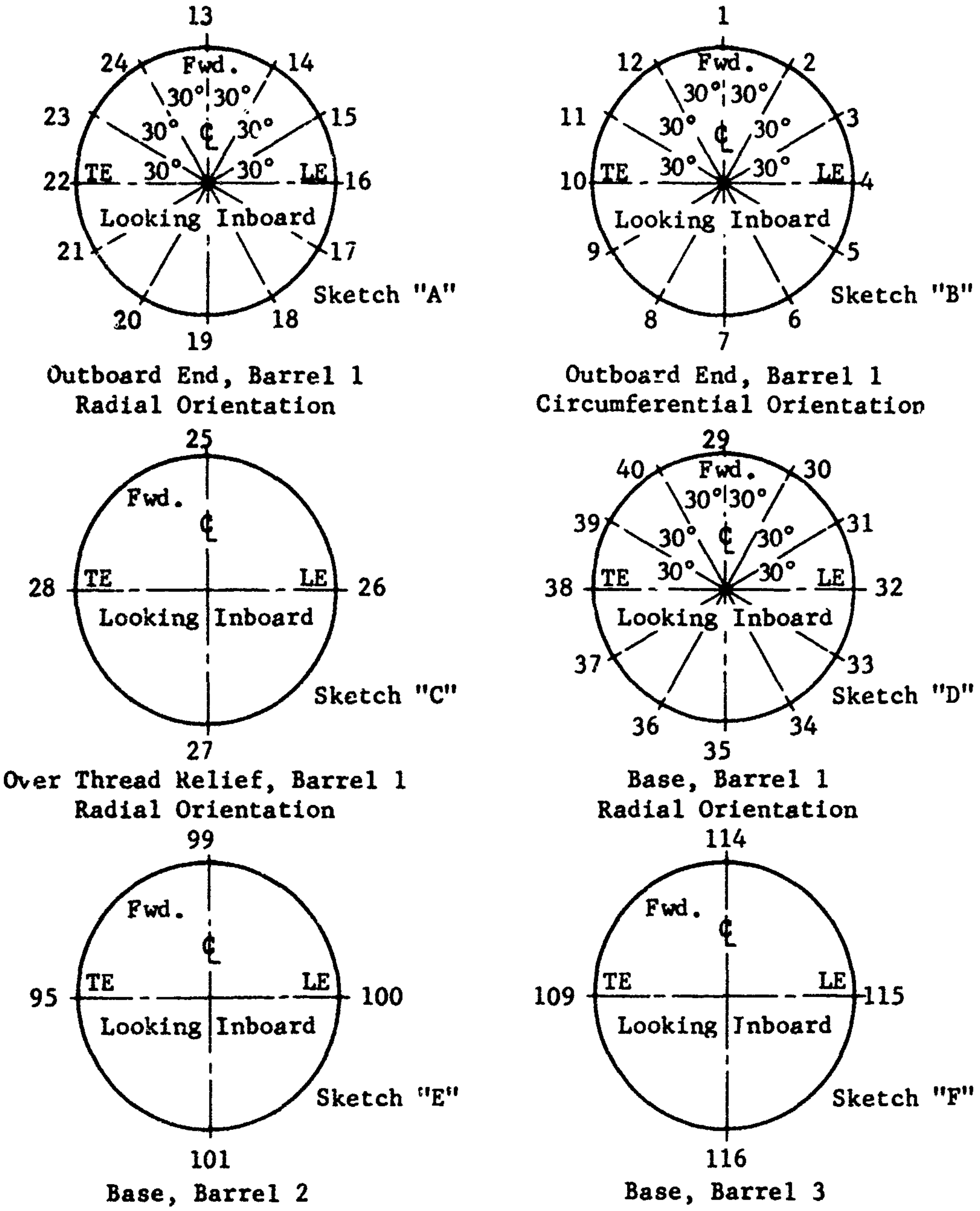
13
24
14
Fwd.
30°
23
15
¢
22
TE
LE
16
Looking Inboard
21
17
Sketch "A"
20
18
19
1
12
2
11
3
10
4
9
5
Sketch "B"
8
6
7
25
28
26
Sketch "C"
27
29
40
30
39
31
38
32
37
33
Sketch "D"
36
34
35
99
95
100
Sketch "E"
101
114
109
115
Sketch "F"
116

Outboard End, Barrel 1
Radial Orientation

Outboard End, Barrel 1
Circumferential Orientation

Over Thread Relief, Barrel 1
Radial Orientation

Base, Barrel 1
Radial Orientation

Base, Barrel 2
Radial Orientation

Base, Barrel 3
Radial Orientation

Figure 146. Location of wire strain gages around outer circumference of barrels of X-19 propeller hub 162595 during static testing in hub tension machine.

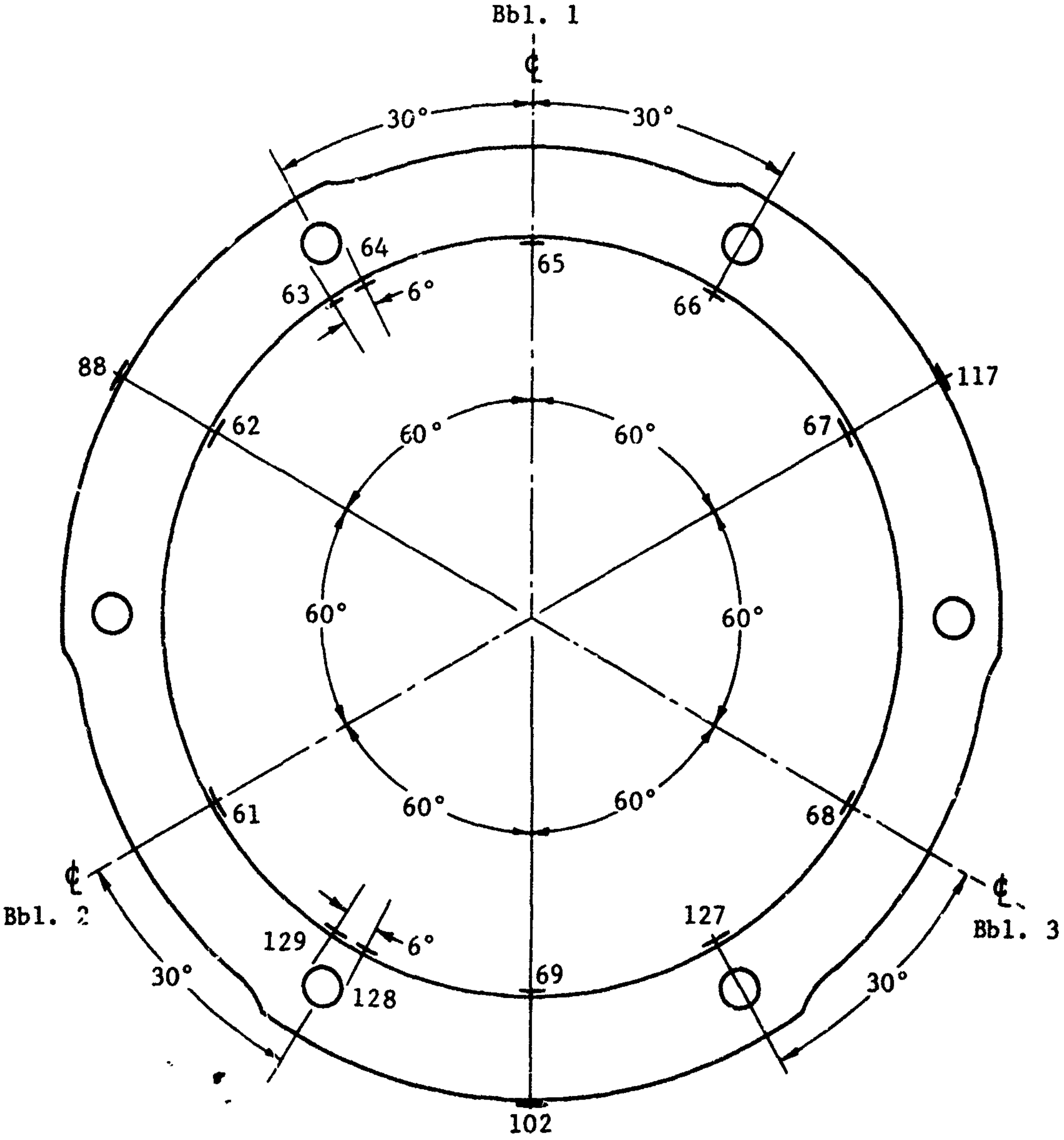
Bbl. 1
30°
30°
64
65
63
6°
66
88
117
62
67
60°
60°
60°
60°
60°
60°
61
68
Bbl. 2
Bbl. 3
129
6°
127
30°
69
30°
128
102

Note: Gages oriented circumferentially.
Gages 127, 128, 129 are A-19.
All others are A-8.

Figure 147. Location of wire strain gages around inner and outer periphery of front ring of X-19 propeller hub 162595 during static testing in hub tension machine.

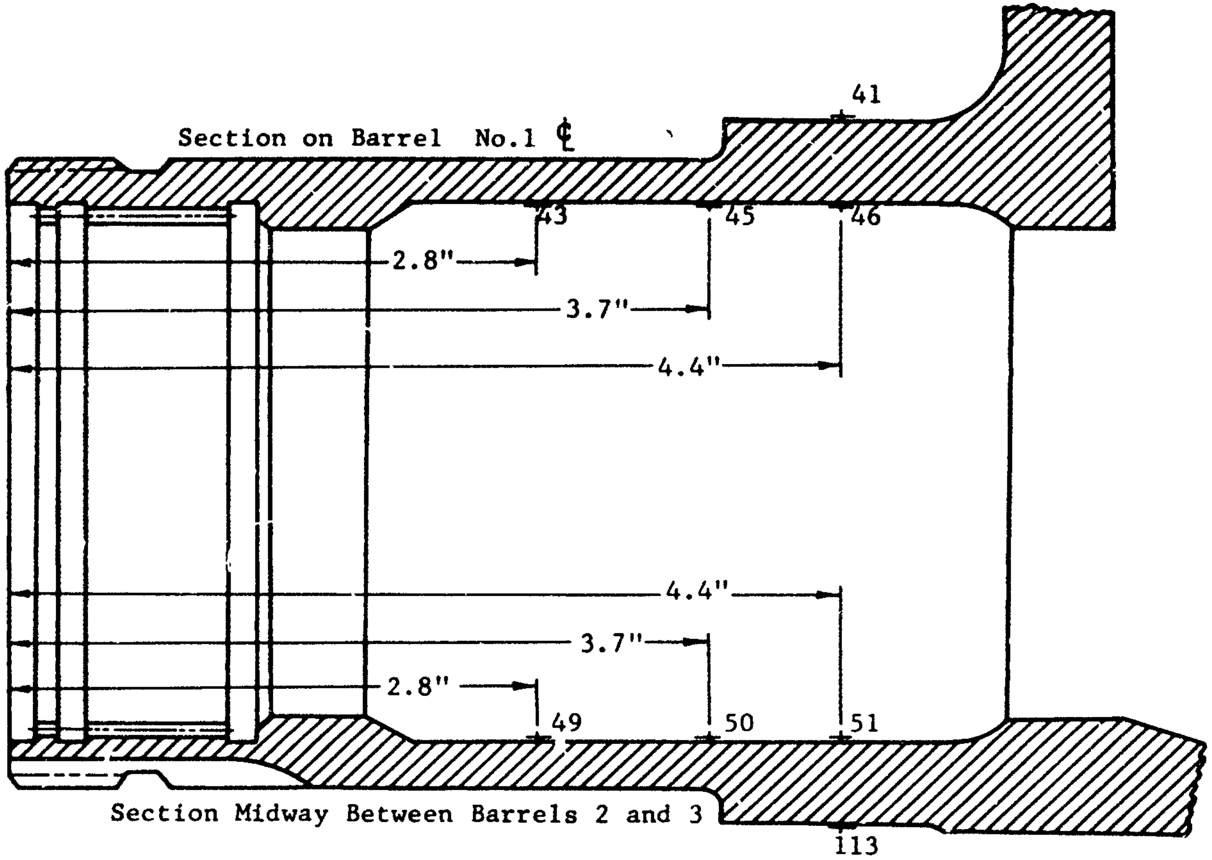
Section on Barrel No.1 ℄
41
43
45
46
2.8"
3.7"
4.4"
4.4"
3.7"
2.8"
49
50
51
Section Midway Between Barrels 2 and 3
113

Figure 148. Location of wire strain gages on inner and outer surfaces of rear extension of X-19 propeller hub 162595 during static testing in hub tension machine.

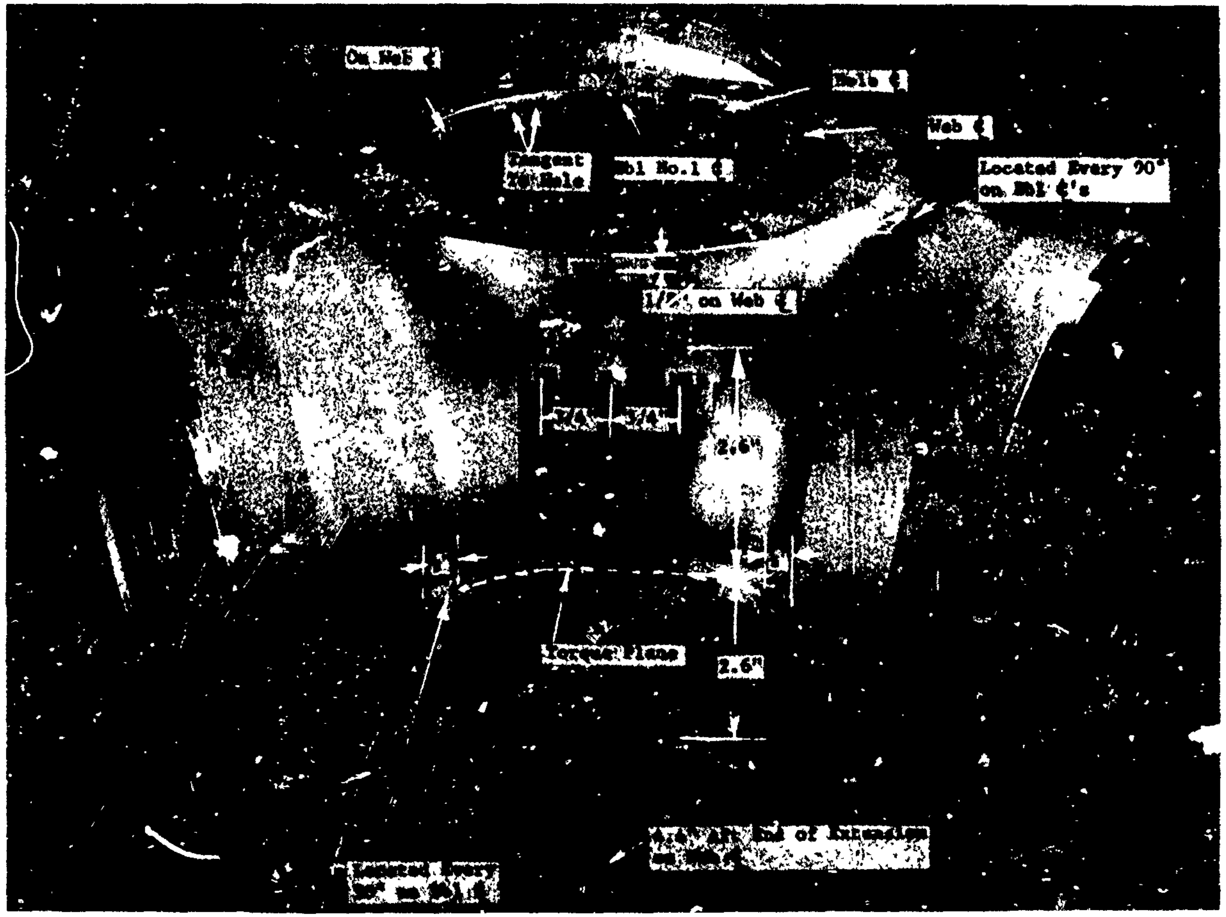
On Web ℄
Hub ℄
Web ℄
Located Every 90°
on Bbl ℄'s
Tangent
Hole
Bbl No.1 ℄
1/4 on Web ℄
3/4
3/4
2.6"
Torque Plane
2.6"

Figure 149. X-19, propeller hub showing typical location of strain gages during static test.

Table XI. Maximum composite stresses in X-19 propeller hub 162595.

Structural Element	Load	Stress psi	Factor of Safety	Gage No.	Gage Location (See Figs. 139-142)
Barrel	III	5733 ± 21826	2.52	35	Bbl. outer surface @ base; radial
	IV	21467 ± 19033	2.61	34	Ditto
	VI	12357 ± 28607	1.85	34	Ditto
Front Ring	III	6364 ± 22189	2.47	69	Front ring inner surface; circumferential
	IV	1589 ± 20026	2.82	69	Ditto
	VI	2785 ± 43948	1.28	63	Ditto
Rear Extension	III	103 ± 10864	5.24	43	Extension inner surface, a bbl; longitudinal
	IV	101 ± 9715	5.86	43	Ditto
	VI	135 ± 8155	6.98	41	" outer " " " "
Hub Shell Between Barrels	III	-5144 ± 9400	6.06	126	Shell outer surface; fore-aft
	IV	8535 ± 11871	4.56	123	Shell outer surface; torquewise
	VI	7139 ± 38436	1.42	123	Shell outer surface; torquewise
Summary; minimum F.S., entire structure	III	6364 ± 22189	2.47	69	Front ring inner surface; circumferential
	IV	21467 ± 19033	2.61	34	Bbl. outer surface @ base; radial
	VI	2785 ± 43948	2.15	63	Front ring inner surface; circumferential

Figure 150. Laboratory whirl test facility for qualifying the propeller-nacelle assembly under simulated loading.

inspection, the components were reassembled on the test stand and assurance testing continued to a total of 150 hours. Test cycles, of one hour duration each, were conducted. Each cycle was performed according to the following schedule:

(a) Take-off and Hover Condition - 8 minutes per cycle

With the nacelles at the hover tilt stop position and the propeller at 1204 rpm, the pitch change system was operated to cycle the blade angle as follows: The counterweight angle was set equivalent to the take-off condition (approximately 9° at 0.75R) and the pitch change was oscillated ± 1° at a frequency of 1.5 cycles per second.

(b) Climb and Transition Condition - 12 minutes per cycle

While tilting the nacelle down to the cruise stop position, at a rate of 2.5 to 3 degrees per second, in steps of approximately 15 to 20 degrees of tilt, the propeller speed was gradually decreased to 957 cruise rpm. The pitch change system was operated so as to cycle the blade angle at varying pitch change cycling rates, i.e., 1.2, 0.9, 0.6, 0.3 cycles per second with the amplitude of blade angle change compatible with the nacelle tilt gain change schedule.

(c) Cruise Condition - 21 minutes per cycle

With the nacelle at the cruise stop position and the propeller speed at 957 rpm, the pitch change system was operated such as to cycle the blade angle at 0.33 cycles per second with a blade angle change amplitude of approximately ± 3°.

(d) Descent and Transition Condition - 12 minutes per cycle

While tilting the nacelle up to the hover stop position, at a rate of 2.5 to 3 degrees per second, in steps of approximately 15 to 20 degrees of tilt, propeller rpm was gradually increased from 957 to 1204 and the pitch change system was operated to cycle blade angle in reverse order of that defined in Section (c) above.

(e) High Speed Descent and Shutdown - 7 minutes per cycle

With the nacelle at the hover stop position and the propeller speed at 1204 rpm, the pitch change system was operated to cycle the blade angle as described in Sub section (a) above.

(f) Single Piston Operation

During the course of the test, two one-hour cycles were accomplished per 50 hour of endurance using single piston operation; one hour using the front piston and one hour using the rear piston.

(g) Data recorded

The following data were monitored and recorded at the start, twice during, and again at the end of, each 50 hour endurance period:

(1) Lube pump pressure.

(2) Lube oil temperature.

(3) Rate of pitch change.

(4) Control Response - (Blade angle input signal vs actual blade angle vs time).

(5) Input control forces required to obtain pitch change for each of the five conditions defined in the test program.

(3) Results

Following completion of the initial fifty hours of qualification testing, the propeller nacelle assembly was reassembled for continued testing under the "assurance" phase of the program. This one hundred hours of assurance testing was successfully completed, which concluded the total one hundred and fifty hours of qualification and assurance testing.

Satisfactory single piston operation after 50 hours and again at the conclusion of 100 hours of assurance testing proved the integrity of the dual piston system together with the dual piston monitoring system.

At the completion of the test program all parts were visually inspected, magnetic particle and/or Zyglo inspected, as applicable, with no discrepancies reported.

c. Electric Motor Whirl Test of X-19 Propeller

The objective of this test was to obtain basic aerodynamic data and to fulfill the propeller qualification requirements of specification MIL-P-26366, on the Wright Field Electric Motor Whirl Test Rig at Dayton, Ohio.

The program covered aerodynamic thrust and horsepower calibration, a flutter boundary test, and one hour over speed test and the 20 hour endurance test.

(1) Test Program

The test program run on the ASD-WPAFB whirl stand was as follows:

(a) Thrust and horsepower calibration

Aerodynamic calibration of thrust and horsepower was obtained at speeds of 600, 800, 1000, 1200, 1400 rpm to a limit of 1400 horsepower, at the following blade angles +8°, +10°, +12°, +14°, +16°, +18°, +20°, +22°, +24°. +27°, +30°, as measured at the 0.75 radius.

(b) Flutter boundary survey

Although the propeller blades had been designed to be flutter-free on the X-19 installation, a flutter boundary survey was made to verify the design.

(c) Overspeed run and endurance

The original intention of this test was to meet the requirements of the Curtiss Division X-19 Model Specification which called for a one hour overspeed run at a blade angle at which 730 horsepower would be absorbed at a speed of 1491 rpm. This speed is 140% of maximum continuous (transition) speed. However, at the recommendation of ASD, the program was changed to meet the interpretation of the requirements of MIL-P-26366 for propeller qualification as follows:

	Horsepower	RPM	Blade Angle @ 42 in. Radius
One Hour Overspeed	1075	1491	19.5°
20 Hour Endurance	1612	1230-1245	26.4°

The rating for the one hour overspeed was based on the propeller absorbing normal rated propeller power (2150 x 0.5) at 120 percent of the maximum rated propeller rpm (1204 x 1.20).

The rating for the endurance condition was based on absorbing 150 percent of normal rated power possible from the two X-19 engines (2150 x 2 x 1.5)/4 divided among the four propellers at a blade angle setting at which the propeller absorbs normal rated propeller power at normal rated rpm (2150 x 0.5 @ 1204 rpm).

For comparison, the operational ratings of the X-19 propellers are given below for the 13,660 lb gw A/C.

Take-off and Hover	860 HP @ 1204 rpm
Cruise	563 HP @ 957 rpm

(d) Instrumentation and Limitations

In order to define and monitor the magnitude of blade stresses during the whirl testing, the propeller blades were completely instrumented and this gaging is shown in Table XII. The output of these gages was recorded or monitored throughout the major portion of the testing. At the conclusion of the basic test program, the gages were stripped and a short calibration run was made to determine the aerodynamic interference effect, if any, of the gage installation on the static thrust. No change was noted. In order to assure safe operation of the propeller, the following limitations were established:

(1) Flexural Stress

(aa)	Steel	± 18,000 psi
(bb)	Fiberglass	± 4,000 psi

(2) Shear Stress

(aa)	Steel	± 6,000 psi
(bb)	Fiberglass	± 1,000 psi

(3) Propeller rpm not to exceed 1491.

(e) Blade stresses

Blade vibratory stresses were recorded during the aerodynamic calibration and endurance runs. A series of stress surveys was conducted utilizing these gages and typical maximum composite blade stress curves of the results as shown in Figures 151, 152. From the results of these surveys, a group of gages was selected and monitored throughout the calibration and endurance runs.

Maximum stresses encountere were as follows:

Table XII. Gage layout.

Location	Blade		
	1	2	3
Gages radially mounted 0.5 chord, Camber Plate			
12" Sta.	X	-	-
18" Sta.	X	-	-
24" Sta.	X	-	-
30" Sta. (rectangular rosette)*	X	-	X
36" Sta.	X	-	-
42" Sta.	X	X	X
48" Sta. (rectangular rosette)*	X	-	-
54" Sta.	X	X	X
60" Sta. (rectangular rosette)*	X	-	-
66" Sta.	X	-	-
Gages radially mounted, Camber Plate			
15" Sta. (2" from L.E.)	-	-	X
15" Sta. (1" from T.E.)	-	-	X
48" Sta. (2" from L.E.)	-	-	X
54" Sta. (2" from L.E.)	X	X	-
Shank gages mounted radially, 6.25" Sta.			
0° (rectangular rosette)*	X	X	X
22° (flexural gage)	X	-	-
45° (rectangular rosette)*	X	X	X
67° (flexural gage)	X	-	-
90° (rectangular rosette)*	X	X	X
112° (flexural gage)	X	-	-
Gages transversely mounted 0.5 chord, Thrust Plate			
18" Sta.	X	-	-
4" Sta.	X	X	-
30" Sta.	-	X	-
36" Sta.	-	-	X
42" Sta.	-	-	X

* The rectangular rosette gages were oriented such as to have the center leg in the radial direction. The two remaining legs were used as a shear bridge.

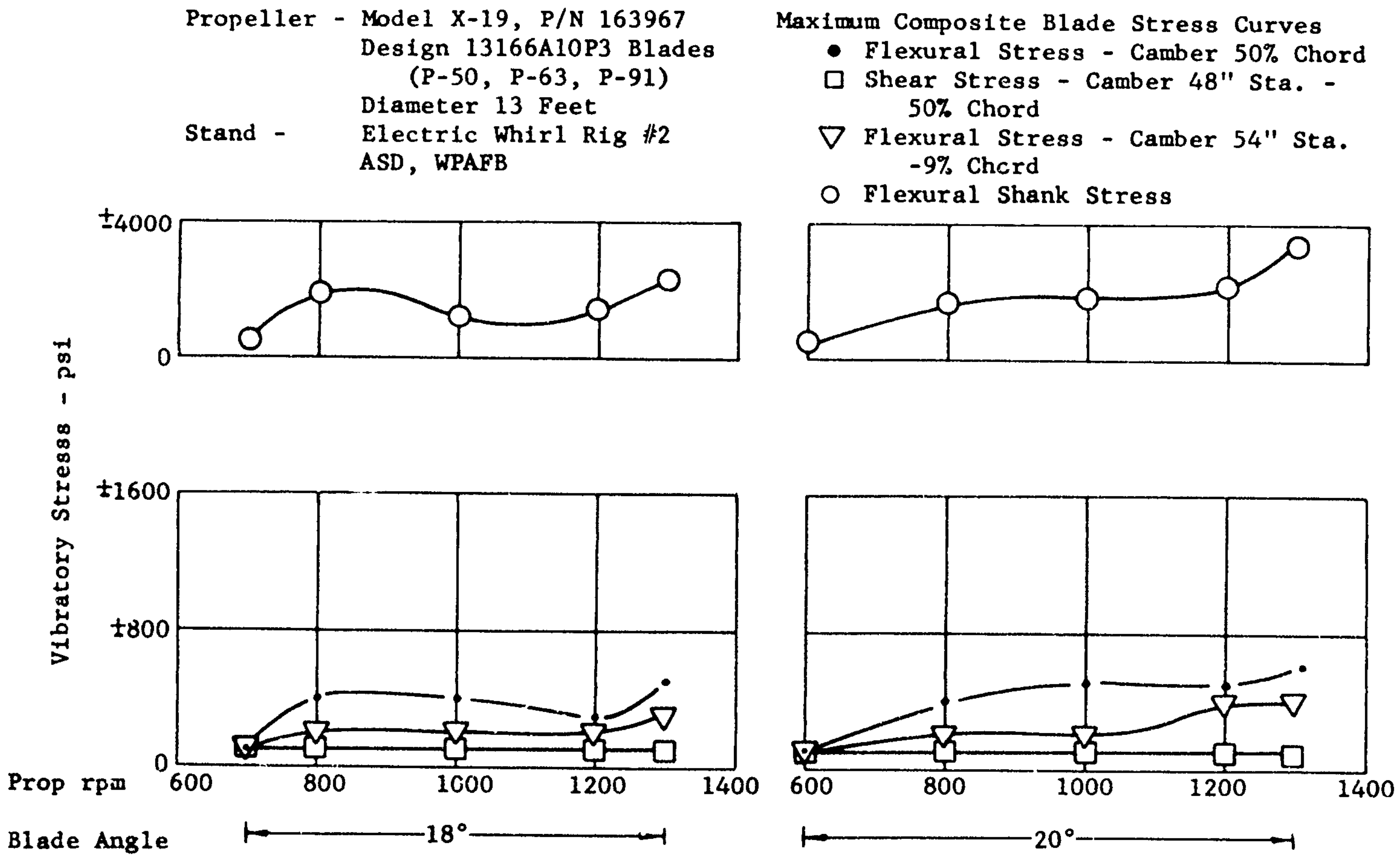

Figure 151. Maximum composite blade stress taken during propeller thrust calibration on WPAFB electric whirl rig.

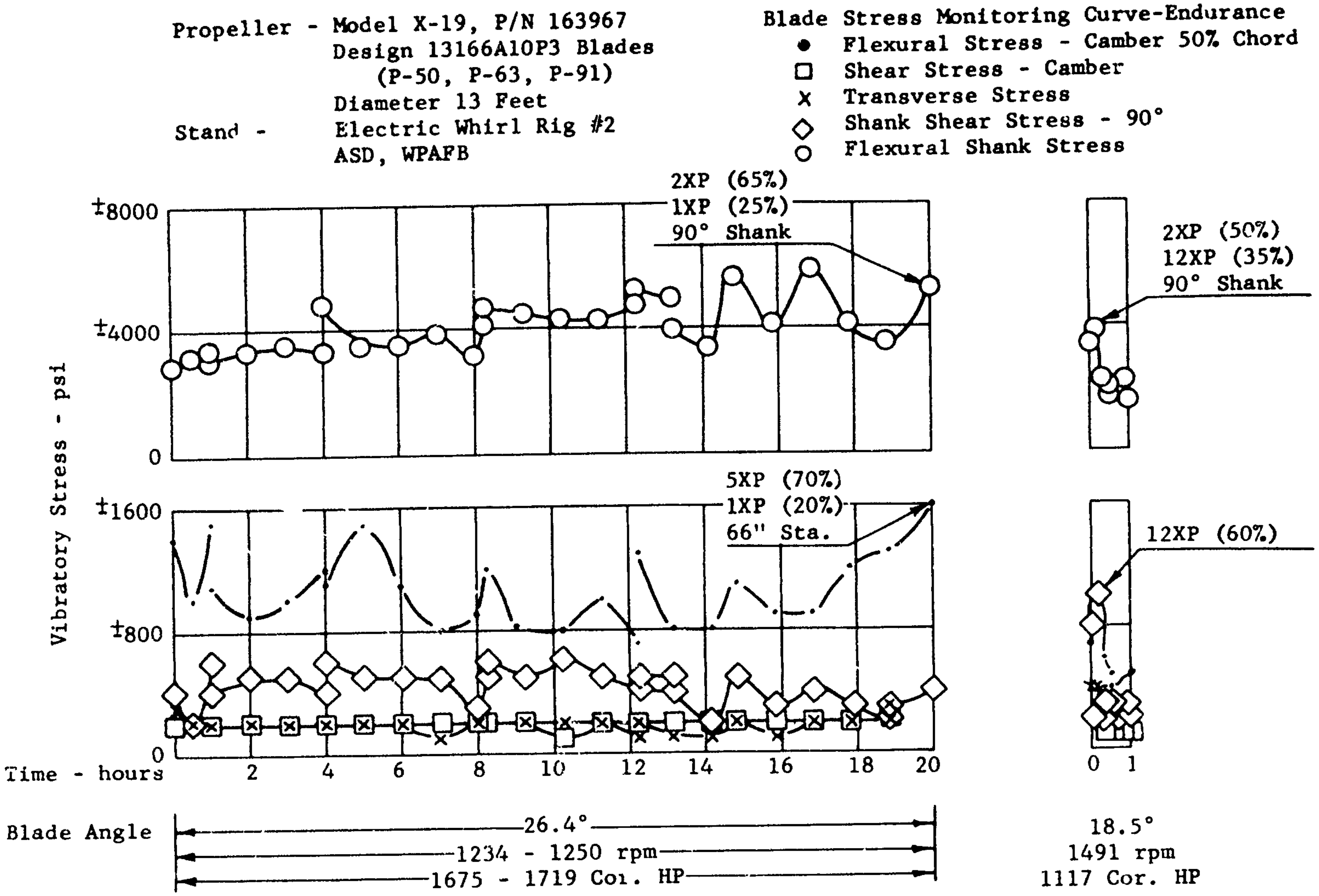

Figure 152. Blade stress monitored curve taken during propeller endurance test on WPAFB electric whirl rig.

	Vibratory Stress ± psi	RPM	Blade Angle (Deg. at 42" sta.)
Steel Shank			
Radial	7100	1300	5
Shear	1300	1290	24.4
Fiberglass			
Radial	1900	1300	5
Transverse	800	840	40.2
Shear	300	1300	5

In summary, the blade vibratory stresses encountered during the aerodynamic calibration and endurance running were low with no indication of blade flutter or resonance.

On the basis of theoretical analysis, indications of resonance would have been expected at about 800 and 1350 RPM, see Figure 123, but these points were obscured by the high damping of the system. Laboratory testing had shown that the internal material damping of these fiberglass blades is relatively high as compared with the former metal blades. This has been evident in the power requirements necessary to obtain adequate stress levels in endurance testing and in preliminary logarithmic decrement evaluation. Therefore, it had been contended that these fiberglass blades would show significantly lower response characteristics than had been experienced in the past. However, examination of the stress curves, Figures 151 and 152, could indicate that a resonance is being approached at about 1200 - 1300 rpm.

It is to be noted that the plots represent a maximum value, and a study of the stress records indicate that the increase in stress at this speed is due to a beat frequency which appears to be power sensitive. Further, stress records taken in the 1300 to 1400 rpm range were not speed sensitive as would be expected with a well defined resonance.

The X-19 Propeller with 13166A10P3 design fiberglass foam filled blades has successfully completed a whirl test required in the X-19 Model Specification and the overload requirements of MIL-P-26366. Structural strength of the blade design was proven.

(f) Propeller Inspection

Following the testing the propellers were shipped back to the Curtiss Division where a detailed inspection was made.

All steel and aluminum parts were magnafluxed and zygloed. All parts passed Magnaflux and Zyglo inspection.

Visual examination showed all parts to be in excellent condition except for the P/N 162563 blade bearings which had false Brinell marks. The P/N 162843 block had spline tooth markings on it from contact with the piston. The P/N 13166A10P3 design blades S/N P-50, P-63, and P-91 were in very good condition except for a foam separation on blade S/N P-91. X-Ray examination and visual inspection showed no internal cracks in any of the blades.

The bearings were inspected metallurgically, and found to be within drawing specifications with a hardness of R_C 62 and correct microstructure. The race curvatures were measured and found to be within specifications.

The false Brinelling of the bearing races noted was the result of subjecting the bearings to abnormal loads due to high centrifugal loading and poor lubrication conditions resulting from fixed pitch (no blade oscillation). This condition is conducive to fretting corrosion of the races as the contact area becomes dry.

d. 1XP Gyroscopic Endurance

The gyroscopic rig was developed to provide a relatively simple means of endurance-testing a full sized propeller at its design vibratory and steady loads. In this testing the blade first order aerodynamic loading is simulated by the 1XP gyroscopic or inertia loading of the precessing propeller.

(1) Rig Description

The gyroscopic test rig, Figure 153, is an assembly of an R-2800 propeller driven engine, a special propeller mounting provision and an electric motor/Reeves precessional drive system, all of which is mounted on a circular track turntable. The turntable can be rotated at speed from 0 to 25 rpm. Adaptations have been made to the R-2800 nose section to permit a direct or geared propeller drive depending upon the rpm and horsepower requirements of the test propeller. The entire propeller-engine assembly is enclosed in

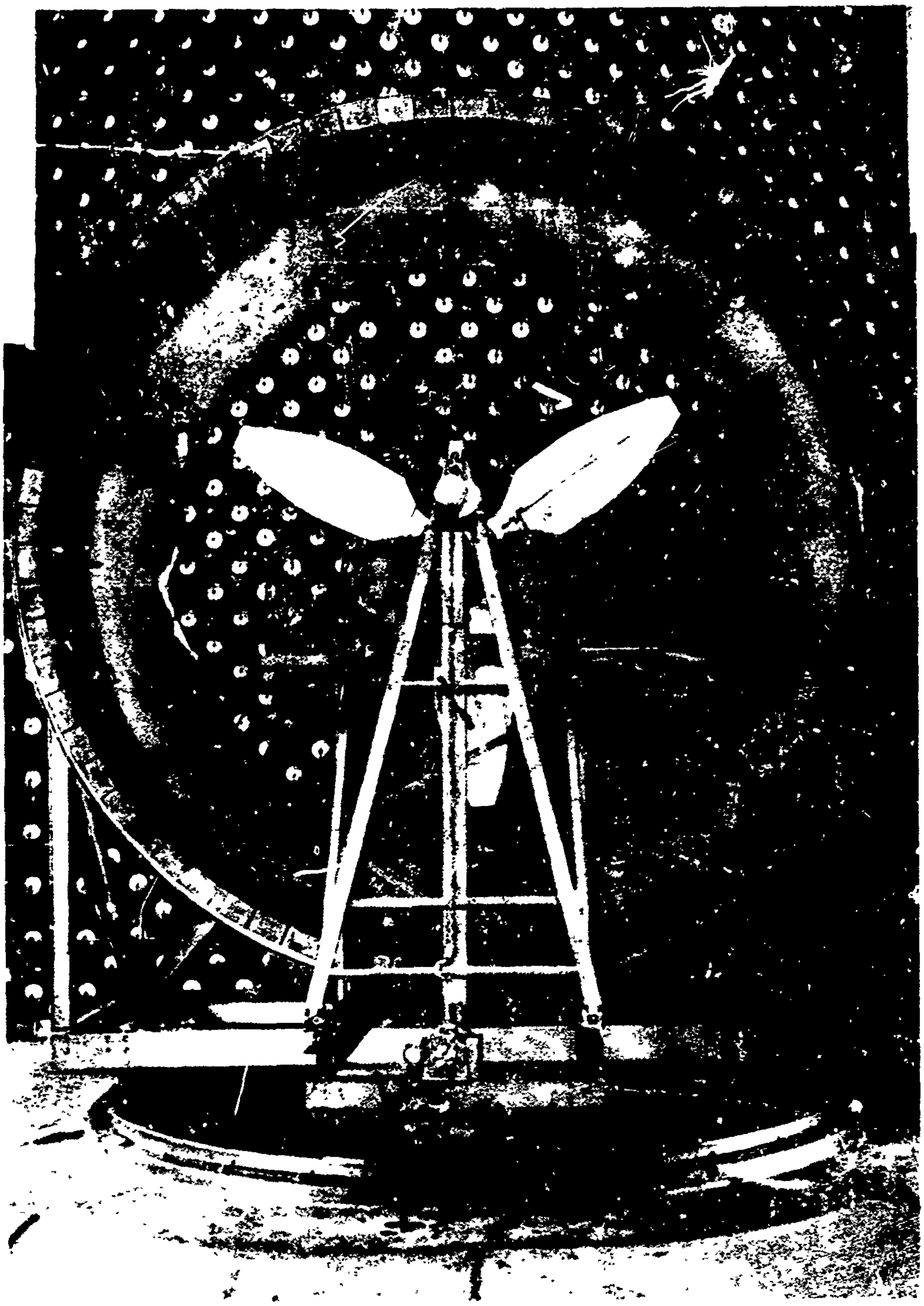

Figure 153. Curtiss gyroscopic test facility for qualifying full scale propellers under simulated steady and vibratory loading.

protective shroud, and a baffle ring is provided to provide a somewhat better airflow through the propeller disk.

(2) Test Program

As previously stated the gyroscopic test is designed to provide endurance testing of the assembled propeller; (blades, hub, and propeller mounting), at the combined steady and 1XP vibratory design loads. The centrifugal loads are exactly simulated by driving the propeller at its design rpm. The steady static aerodynamic bending loads are simulated by adjusting blade angles, i.e. power and thrust until the desired blade stress level is obtained. The 1XP vibratory loading is generated by the inertia forces resulting from the precession of rotation of the rig and the desired magnitude established by the variation of rig speed. In the course of the development of the X-19 blade design, several propellers were run on the gyroscopic facility. With the design loads thus simulated the testing is continued for a specified number of hours. The final test on using the 13166A12P3 blades, is generally typical and is presented in detail.

(a) X-19 Propeller Gyroscopic test

The 13166A12P3 blades (S/N P154-6, P190-4 and P193-4), were strain gaged similar to the layout shown in Table XV. The propeller was then mounted on the test rig which had been modified to incorporate the nacelle housing so that the propeller mounting and drive would duplicate the aircraft installation. Stress surveys were then made at 800, 900, 1,000, 1100 and 1204 propeller rpm without rig precession, and a 10, 11, and 12 rig rpm and 1204 propeller rpm. For this propeller, the endurance condition was set up to duplicate the 30 ft/sec gust at a 50 knots transition for the 13,660 lbs. aircraft, see Table VIII. For this condition the maximum blade stresses were computed to be 4500 ± 2900 psi.

The stress surveys showed that at the desired propeller speed of 1204 rpm, operational limitations of the R-2800 direct drive engine caused abnormally low blade engine angle operation which resulted in a blade steady stress of approximately 10,000 psi. This was considerably above the desired value, and an equivalent condition was selected.

This is illustrated in Figure 134 which shows the desired point with respect to the material design Goodman curve. To maintain the same relationship to this curve at 10,000 psi steady stress requires a

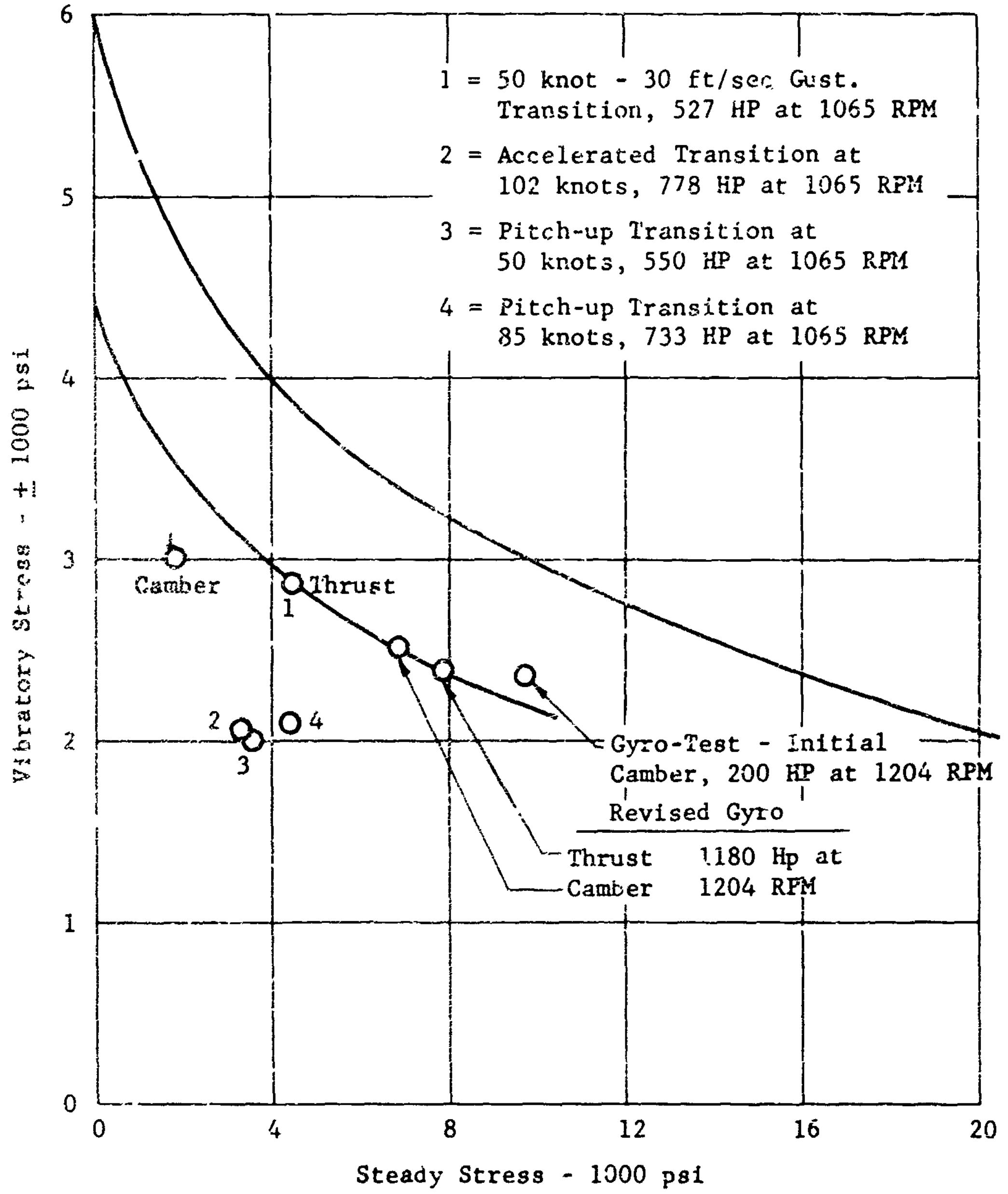

Figure 154. X-19 blade modified Goodman diagram showing design and gyroscopic test points.

vibratory stress of ± 2200 psi. Endurance was therefore set up for blade stress levels of 10,000 ± 2200 psi, psi, or 1204 propeller rpm, 12.4 rig rpm, and B_{42} = 12°. Later analysis of the stress records indicated actual stress levels were 10,000 ± 2300 psi. See Table XVI.

At the end of 3 hours running under these loads, a small area of foam separation was suspected on blade P-190, and at the completion of 4 hours this separation was definitely confirmed and the testing was stopped for blade repair. During this interim, it was suggested that the propeller drive be changed from direct drive to an 0.45 gear ratio which would improve the operation of the R-2800 drive engine and permit a better simulation of operating blade angle and steady blade loading. These changes were made and the testing resumed. Stress surveys were retaken and it was found that the steady stress could be reduced to 7000 psi.

From the Goodman curves this required increasing the vibratory stress level to ± 2500 psi, Figure 154. Endurance was continued at this load level for an additional 36.5 hours at which time the test was terminated due to a separation of the foam in blade P-190.

(b) Results X-19 Gyro Test

The stresses measured on the X-19 propeller blade during gyroscopic testing are given in Table XIII and Figure 155. Following the testing the propeller was completely disassembled and inspected. This inspection showed that except for the foam separation on blade P-190 and brinelling of the blade retention bearings all parts were in good condition. The brinelling of the bearing races is common in fixed pitch operation. Based upon the 40.5 hours endurance, the propellers were considered satisfactory for flight test purposes provided that a blade inspection for foam separation was made after each flight.

e. Half Systems Rig Testing

The half systems rig was designed and built primarily for development and qualification testing of the X-19 power transmission system. This test facility, Figure 156, duplicated the forward half of the X-19 transmission system; engines, gearboxes, shafting, and propellers. The power which would normally be delivered to the rear propellers was absorbed by a water brake. Although not intended as a propeller test, per se, it did provid extensive operational experience under a wide range of horsepower,

Table XIII. Vibratory and steady stress summary, X-19 blades.

Blade Design 13166A12P3 change A (F100 Foam)
Blade No.1 - P 154
Blade No.2 - P 190
Blade No.3 - P 193

Modulus, Shank - 29.9 x 10^6
Modulus, Fiberglass - (30" Station) - 5.2 x 10^6

Date: July 6, 1965

Vibratory Stress Summary														
Blade Angle β	Prop rpm	Rig rpm	90° Shank			18.5"TE	24" RC	30" RC			36" RC	48" RC	60" RC	Remarks
			B1 ±psi	B2 ±psi	B3 ±psi	B1 ±psi	B1 ±psi	B1 ±psi	B2 ±psi	B3 ±psi	B1 ±psi	B1 ±psi	B1 ±psi	
12°	1204	10	13,300	13,300	14,600	1,130	1,710	1,940	2,100	1,810	2,040	1,640	1,575	Investigation
12°	1204	12	15,200	15,200	15,200	1,180	1,870	2,230	2,360	2,300	2,230	1,770	1,640	Investigation
12°	1204	11	14,400	14,400	14,400	1,130	1,740	2,100	2,300	2,165	2,100	1,710	1,640	Investigation
12°	1204	12	15,200	15,600	15,900	1,180	1,900	2,260	2,420	2,360	2,300	1,770	1,670	Endur. Begin
12°	1204	12	15,200	15,600	15,900	1,180	1,900	2,260	2,420	2,360	2,300	1,770	1,670	End of 1st Hr
12°	1204	12.1	15,200	15,600	15,400	1,180	1,900	2,300	2,460	2,400	2,300	1,770	1,670	End of 2nd Hr
12°	1204	12.05	15,200	15,600	15,200	1,180	1,900	2,300	2,420	2,360	2,300	1,770	1,670	End of 3rd Hr
12°	1204	12	15,100	15,100	15,100	1,180	1,900	2,260	2,400	2,300	2,300	1,770	1,670	End of 4th Hr
Steady Stress Summary														
12°	1000	0	26,300	27,000	25,700	7,640	6,400	7,670	7,910	7,500	7,860	6,170	5,500	Investigation
12°	1100	0	32,000	31,500	29,400	8,940	7,500	8,950	9,050	8,600	9,150	7,000	6,280	Investigation
12°	1204	0	35,200	36,000	33,900	11,250	8,350	9,850	10,300	9,950	10,600	8,200	7,000	Investigation
12°	1204	12	34,500	34,400	32,100	9,740	8,260	9,200	10,450	9,100	9,970	7,360	6,250	Endur. Cond.

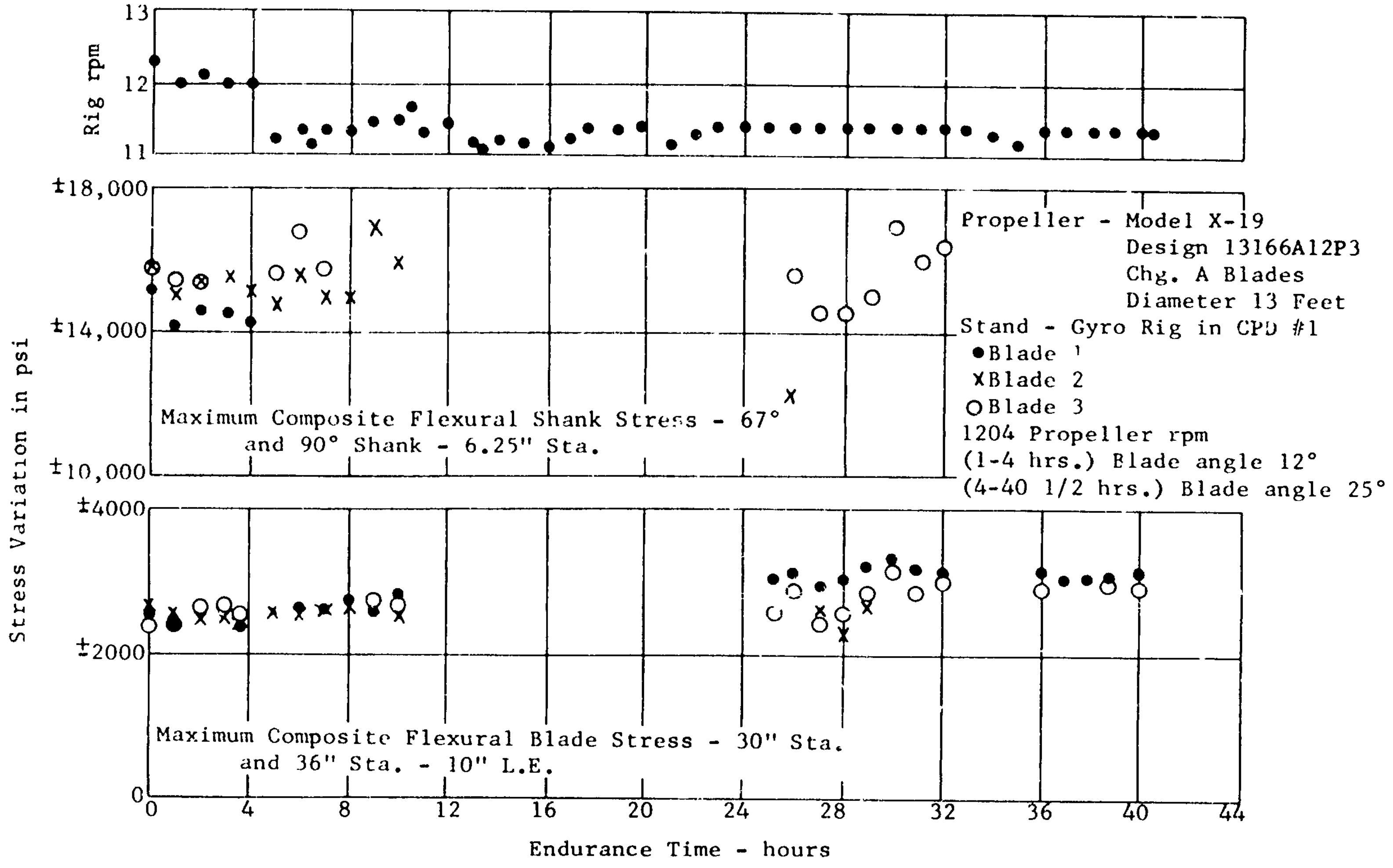

Figure 155. X-19 blade vibratory stresses as monitored during the gyroscopic endurance testing.

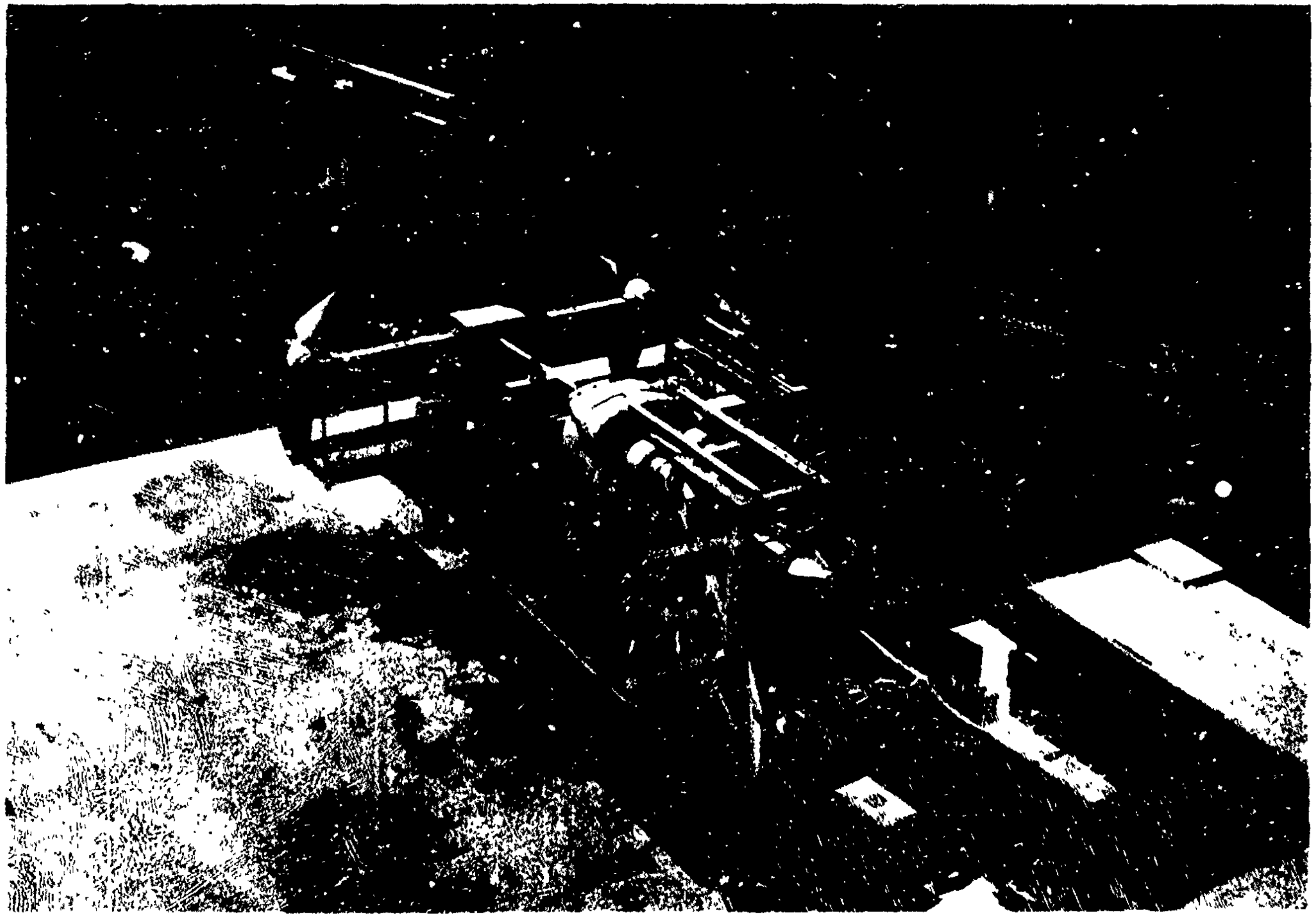

Figure 156. Curtiss half system test rig for qualifying the propulsion system of the X-19.

rpm, and propeller tilt angle which simulated aircraft operation. Further, the half systems rig was in the open and was operated year round under all normal weather conditions, and thus provided a limited degree of environmental testing.

A typical load spectrum used during half system running is given in Table XIV. Throughout the half systems testing the same set of propellers was used, and they accumulated over 400 hours of total running time. The only blade repair necessary during that operation was repair of leading edge erosion following a run made during a heavy rain. A heavy urethane protection strip was installed which prevented recurrence of that problem.

Table XIV. X-19 PFVT, 13,660 lb gross weight flight cycle.

Fifteen cycles of ten hours duration were conducted. Each test cycle was performed according to the following schedule:

	Time		Prop	Prop HP		Water Brake		Engine	Tilt	Total Horsepower in Transverse and Rear Longitudinal Shafts
	min	sec	rpm	No.1	No.4	HP	rpm	rpm	Angle	
Take-Off Hover and Differential Pitch										
R	16	0	1204	860	860	1280	4950	15,100	96.5°	3000 **
	1	0	1204	1100	1100	1280	4950	15,100	96.5°	3430
R*	3	0	1204	604	1100	1280	4950	15,100	96.5°	2984
R*	3	0	1204	1100	604	1280	4950	15,100	96.5°	2984
	5	0	1204	890	719	1280	4950	15,100	96.5°	2889
	5	0	1204	719	890	1280	4950	15,100	96.5°	2889
Up and Down Transition - Climb and Descent										
	3	0	1066	825	825	790	4400	13,400	73.0°	2440
	12	0	1066	767	767	786	4400	13,400	50.0°	2320
	15	0	1066	652	652	1356	4400	13,400	3.0°	2660
Maximum Speed Cruise										
	504	0	957	563	563	1126	3940	12,000	3.0°	2252
Landing										
	30	0	1204	860	860	1280	4950	15,100	96.5°	3000
Emergency - 1 Engine Out										
	3	0	1204	730	730	740	4950	15,100	96.5°	2200
	600	0	= 10 Hours							

* Twice during each ten hour cycle, this point was set by holding 1250 HP for 15 seconds on the right propeller and 863 HP on the left propeller and vice versa.

Inspections were made as required during this qualification testing.

** Since the engine torquemeter has an accuracy of ± 4% of normal rated power, (.04 x 1850 = 74 HP) it was almost impossible to guarantee the input horsepower using the engine torquemeter. Therefore, the power supplied to the E.C.G.B. was the total HP in the shafts plus the losses due to Tee Box and E.C.G.B. efficiency.

REFERENCES

(33) P. F. Yaggy and V. L. Rogallo, A Wind Tunnel Investigation of Three Propellers Through an Angle of Attack Range From 0° to 85°, NASA TND-318, dated May 1960.

(34) Lehman, F. G. and Burke, P. R., General Dynamic Analysis of STOL/VTOL Propeller Blades, WADC TR 58-371, 1958.

(35) Coleman, R. P., Feingold, A. M. and Stempen, C. W., Evaluation of the Induced-Velocity Field of an Idealized Helicopter Rotor, NACA WRL-126, 1945.

(36) Castles, Walter J. and DeLeeuw, J. H., The Normal Components of the Induced Velocity in the Vicinity of a Lifting Rotor and Some Examples of its Application, NACA Rep. 1184, 1954.

(37) Heyson, H. H., Analysis of Comparison With Theory of Flow-Field Measurements Near a Lifting Rotor in the Langley Full Scale Tunnel, NACA TN 3691, 1956.

(38) Heyson, H. H., and Katzoff, S., Normal Component of Induced Velocity in the Vicinity of a Lifting Rotor With a Non-Uniform Disk Loading, NACA TN 3690, 1956.

(39) Miller, R. M., Rotor Blade Harmonic Blade Loading, IAS Preprint No. 62-82, January 1960.

(40) Amatt, W. and Griffin, D. K., Light Weight Abrasion Resistant Propeller Blades for STOL/VTOL Aircraft, WADC T.R. 58-372, 1958.

SECTION VI

AIRCRAFT CONTROL BY PROPELLER THRUST MODULATION

SECTION VI - NOMENCLATURE

A	propeller angle of attack ($\phi + \alpha$) degrees	
b	wing span	ft
C_D	= $\frac{D}{qS}$	
C_L	= $\frac{L}{qS}$	
$C_{l_{\delta_a}}$	= $\partial(L/qSb_F)/\partial\delta_a$	
C_m	airplane pitching moment coefficient about c.g. = $M/qS\bar{c}$	
$C_{n_{\delta_a}}$	- $\partial(N/qSb_F)/\partial\delta_a$	
C.P.	control power	
C_P	total power coefficient, $\frac{550\ HP}{\rho n^3 D^5}$	
D_P	propeller diameter,	ft
D	drag,	lb
J	propeller advance ratio, $\frac{V}{nD}$	
K_θ	height control anticipator gain, rpm (prop)/deg	
L	rolling moment = $qSC_l b$	ft-lb
L	lift = qSC_L	lb
L_v	rolling moment due to lateral velocity, ft-lb/ft/sec	
M	pitching moment	ft-lb
N	yawing moment,	ft-lb
$\bar{N}$	height control anticipator signal	
N_v	rate of change of yawing moment with lateral velocity, ft-lb/ft/sec	
Q	= $2\pi n$ (550 HP) torque	ft-lb
q	= $\frac{1}{2}\rho V^2$ dynamic pressure	lb/ft^2
S	wing area	ft^2
SAS	stability augmentation system	
STOL	short take-off and landing	
T	thrust	lb
V	forward velocity,	ft/sec
W	aircraft weight,	lb
X	moment arm	ft
Y	propeller yawing moment	ft-lb
β	propeller blade angle	degrees
δ_a	aileron deflection ($\delta_{a_R} - \delta_{a_L}$)	degrees
δ_r	rudder deflection	degrees
θ	power lever rotation	degrees
ϕ_F	front propeller tilt angle	degrees
ρ	density	$slug/ft^3$
τ	height control anticipator wash-out time constant, sec	

Subscripts

F	Front propeller
R	Rear propeller
1,2,3,4	Propeller number
W	Wing

Propeller Numbering System

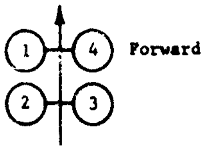

SECTION VI

AIRCRAFT CONTROL BY PROPELLER THRUST MODULATION

1. INTRODUCTION

The statement of work does not specifically call for a discussion of the thrust modulation technique. However it is felt this section would be incomplete without such a description. For this reason, the introduction will be devoted to an understanding of the control mechanism as it relates control inputs to propeller blade angle.

A block diagram of the control system is given in Figure 157. The system behaves in the following manner. The pilot inserts various signals into the coordinator by moving the control stick, tilting the nacelles and changing throttle or the pilot manual trim. The aircraft reacts and sets up various motions. The pitch and roll SAS sense respective angular rates thereby adding new inputs to the coordinator. In general, the stick or SAS motion feed additively into the coordinator; i.e., either stick or SAS are governed by Figures 158 or 160 with the following restrictions. (1) SAS has 30% authority of the stick, (2) Sum of SAS and stick do not exceed maximum $\gamma^{(i)}$ shown in curves 158 and 160. Changes in throttle or power will be sensed as RPM changes in the governor system which in turn alters the output of the coordinator collectively.

The output of the coordinator in response to pilot, SAS, or governor action, is given by the following expression:

$$\gamma_1 = G_1^{(P)}\left[\gamma_1^{(1)}\ (S_{pitch}) + \gamma_1^{(1)}(\nu_{pitch})\right] + \gamma_1^{(2)} + G_1^{(R)}\left[\gamma_1^{(3)}\ (S_{roll})\right.$$

$$\left. + \gamma_1^{(3)}\ (\nu_{roll})\right] + G_1^{(y)}\ \gamma_1^{(4)} + \gamma_1^{(5)} + \gamma_1^{(6)}$$

where:

S_{pitch} = stick position From Fig. 158 readout: $\gamma_1^{(1)}, \ldots, \gamma_4^{(1)}$

Δ_{pitch} = pilot pitch trim From Fig. 159 readout: $\gamma_1^{(2)}, \ldots, \gamma_4^{(2)}$

ν_{pitch} = SAS position From Fig. 158 readout: $\gamma_1^{(1)}, \ldots, \gamma_4^{(1)}$

S_{roll} = stick position From Fig. 160 readout: $\gamma_1^{(3)}, \ldots, \gamma_4^{(3)}$

ν_{roll} = SAS position From Fig. 160 readout: $\gamma_1^{(3)}, \ldots, \gamma_4^{(3)}$

S_{yaw} = pedal position From Fig. 161 readout: $\gamma_1^{(4)}, \ldots, \gamma_4^{(4)}$

ϕ_F = front tilt angle From Fig. 162 readout: $\gamma_1^{(5)}, \ldots, \gamma_4^{(5)}$

FURNISHED UNDER UNITED STATES GOVERNMENT CONTRACT No. AF33(615)-3340 SHALL NOT BE EITHER RELEASED OUTSIDE THE GOVERNMENT, OR USED, DUPLICATED, OR DISCLOSED IN WHOLE OR IN PART FOR MANUFACTURE OR PROCUREMENT, WITHOUT THE WRITTEN PERMISSION OF CURTISS-WRIGHT CORPORATION, EXCEPT FOR (I) EMERGENCY REPAIR OR OVERHAUL WORK BY OR FOR THE GOVERNMENT, WHERE THE ITEM OR PROCESS IS NOT OTHERWISE RESONABLY AVAILABLE TO ENABLE TIMELY PERFORMANCE OF THE WORK. OR (II) RELEASE TO A FOREIGN GOVERNMENT, AS THE INTERESTS OF THE UNITED STATES MAY REQUIRE. PROVIDED THAT IN EITHER CASE THE RELEASE, USE DUPLICATION OR DISCLOSURE HEREOF SHALL BE SUBJECT TO THE FOREGOING LIMITATIONS THIS LEGEND SHALL BE MARKED ON ANY REPRODUCTION HEREOF IN WHOLE OR IN PART "

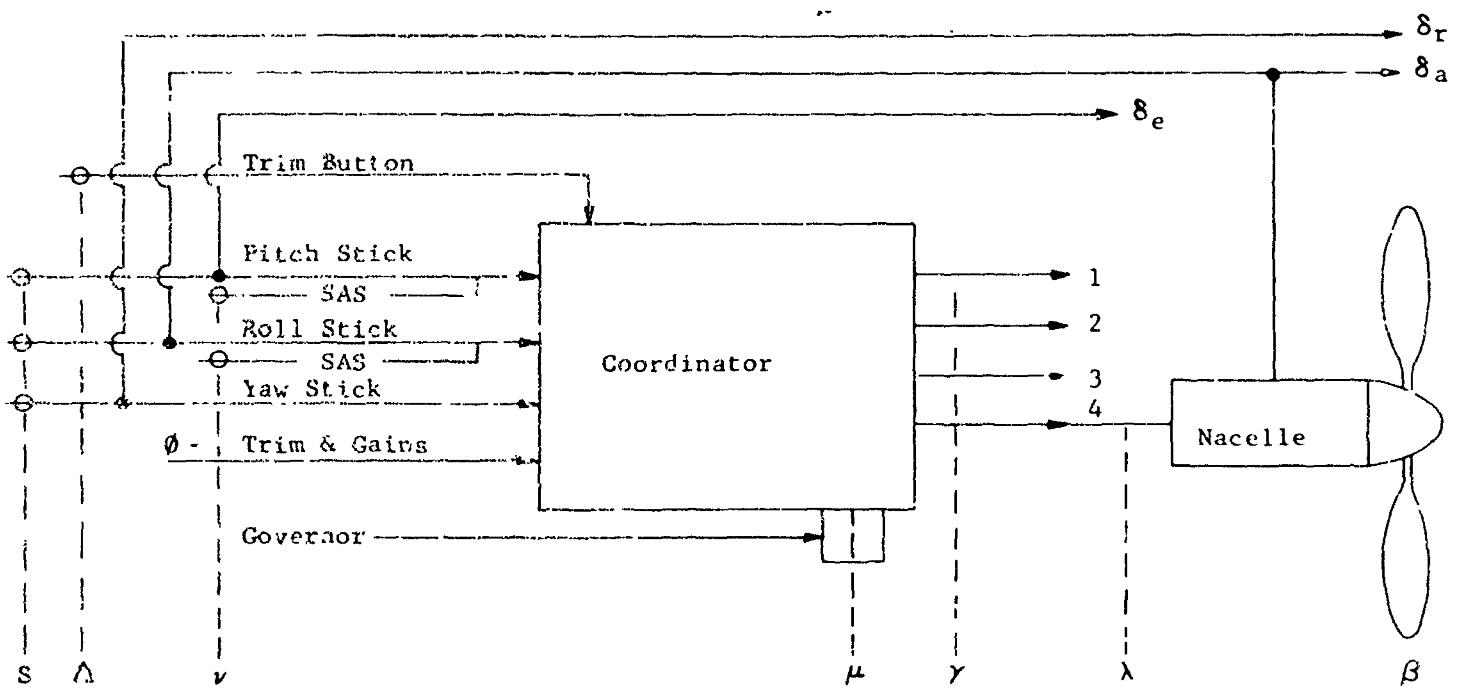
Trim Button
Pitch Stick
SAS
Roll Stick
SAS
Yaw Stick
ϕ - Trim & Gains
Governor
Coordinator
1
2
3
4
Nacelle
δ_r
δ_a
δ_e
S
Λ
ν
μ
γ
λ
β

Figure 157. X-19, block diagram of the propeller thrust modulation system.

FURNISHED UNDER UNITED STATES GOVERNMENT CONTRACT No. [illegible] SHALL NOT BE EITHER RELEASED OUTSIDE THE GOVERNMENT, OR USED, DUPLICATED, OR DISCLOSED IN WHOLE OR IN PART FOR MANUFACTURE OR PROCUREMENT, WITHOUT THE WRITTEN PERMISSION OF CURTISS-WRIGHT CORPORATION, EXCEPT FOR (1) EMERGENCY REPAIR OR OVERHAUL WORK [illegible] FOR THE GOVERNMENT, WHERE THE ITEM OR PROCESS IS NOT OTHERWISE REASONABLY AVAILABLE TO ENABLE TIMELY PERFORMANCE OF THE WORK [illegible] RELEASE TO A FOREIGN GOVERNMENT AS THE INTERESTS OF THE UNITED STATES MAY REQUIRE, PROVIDED THAT IN EITHER CASE THE RELEASE [illegible] DUPLICATION OR DISCLOSURE HEREOF SHALL BE SUBJECT TO THE FOREGOING LIMITATIONS. THIS LEGEND SHALL BE MARKED ON ANY REPRODUCTION HEREOF IN WHOLE OR IN PART.

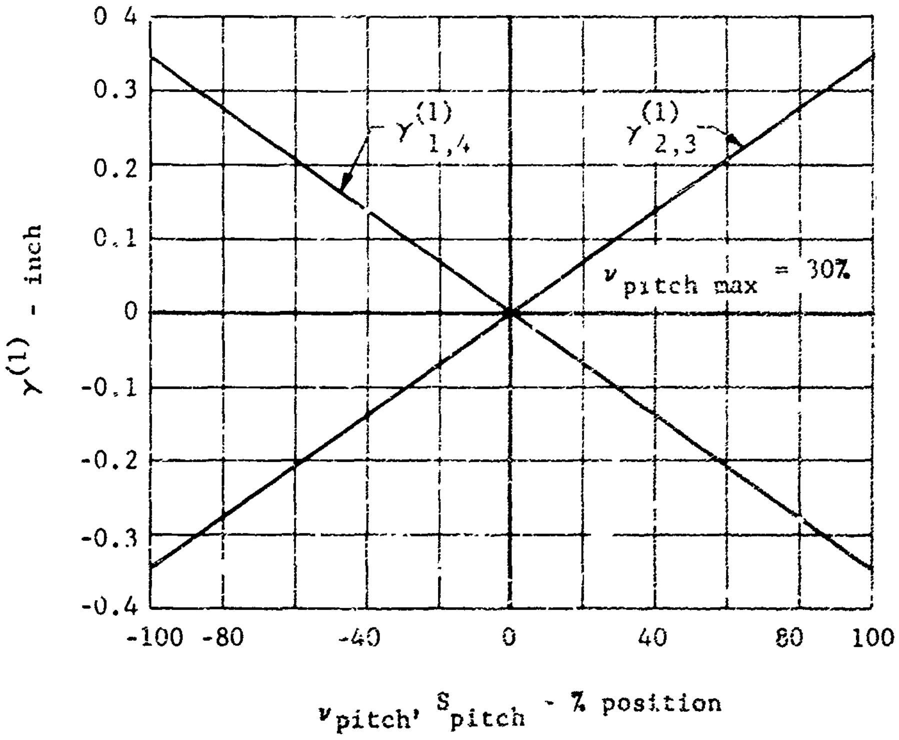

Figure 158. X-19, coordinator output stroke as a function of pitch control deflection or SAS motion.

"FURNISHED UNDER UNITED STATES GOVERNMENT CONTRACT No. AF33(615)-3940. SHALL NOT BE EITHER RELEASED OUTSIDE THE GOVERNMENT, OR USED, DUPLICATED, OR DISCLOSED IN WHOLE OR IN PART FOR MANUFACTURE OR PROCUREMENT, WITHOUT THE WRITTEN PERMISSION OF CURTISS-WRIGHT CORPORATION, EXCEPT FOR (I) EMERGENCY REPAIR OR OVERHAUL WORK BY OR FOR THE GOVERNMENT, WHERE THE ITEM OR PROCESS IS NOT OTHERWISE REASONABLY AVAILABLE TO ENABLE TIMELY PERFORMANCE OF THE WORK, OR (II) RELEASE TO A FOREIGN GOVERNMENT, AS THE INTERESTS OF THE UNITED STATES MAY REQUIRE. PROVIDED THAT IN EITHER CASE THE RELEASE, USE, DUPLICATION OR DISCLOSURE HEREOF SHALL BE SUBJECT TO THE FOREGOING LIMITATIONS. THIS LEGEND SHALL BE MARKED ON ANY REPRODUCTION HEREOF IN WHOLE OR IN PART."

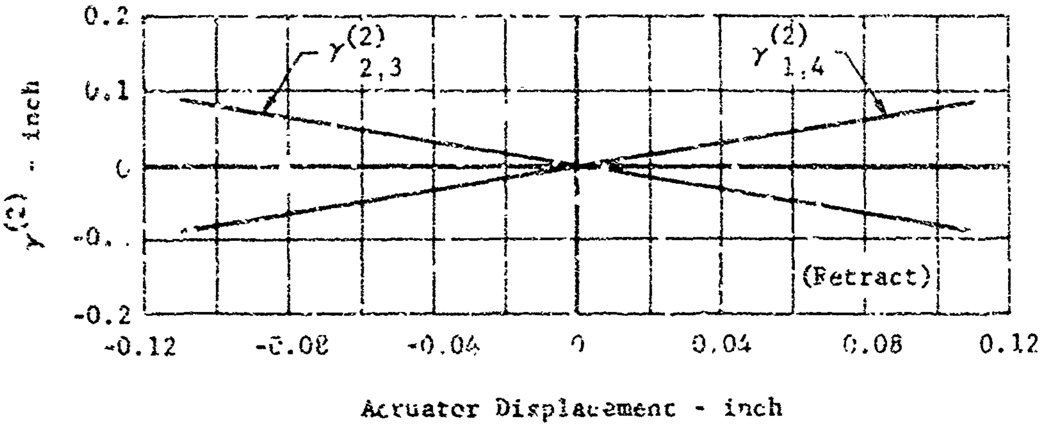

Figure 159. X-19, coordinator output stroke as a function of pilot pitch trim actuator displacement.

FURNISHED UNDER UNITED STATES GOVERNMENT CONTRACT NO. AF33(6[illegible]) [illegible]. SHALL NOT BE EITHER RELEASED OUTSIDE THE GOVERNMENT, OR USED, DUPLICATED, OR DISCLOSED IN WHOLE OR IN PART FOR MANUFACTURE OR PROCUREMENT, WITHOUT THE WRITTEN PERMISSION OF [illegible]RTISS-WR[illegible] CORPORATION, EXCEPT FOR (I) EMERGENCY REPAIR OR OVERHAUL WORK BY OR FOR THE GOVERNMENT, WHERE THE ITEM OR PROCESS IS NOT OTHERWISE REASONABLY AVAILABLE TO ENABLE TIMELY PERFORMANCE OF THE WORK; OR (II) RELEASE TO A FOREIGN GOVERNMENT, AS THE INTERESTS OF THE UNITED STATES MAY REQUIRE; PROVIDED THAT IN EITHER CASE THE RELEASE, USE, DUPLICATION OR DISCLOSURE HEREOF SHALL BE SUBJECT TO THE FOREGOING LIMITATIONS. THIS LEGEND SHALL BE MARKED ON ANY REPRODUCTION HEREOF IN WHOLE OR IN PART.

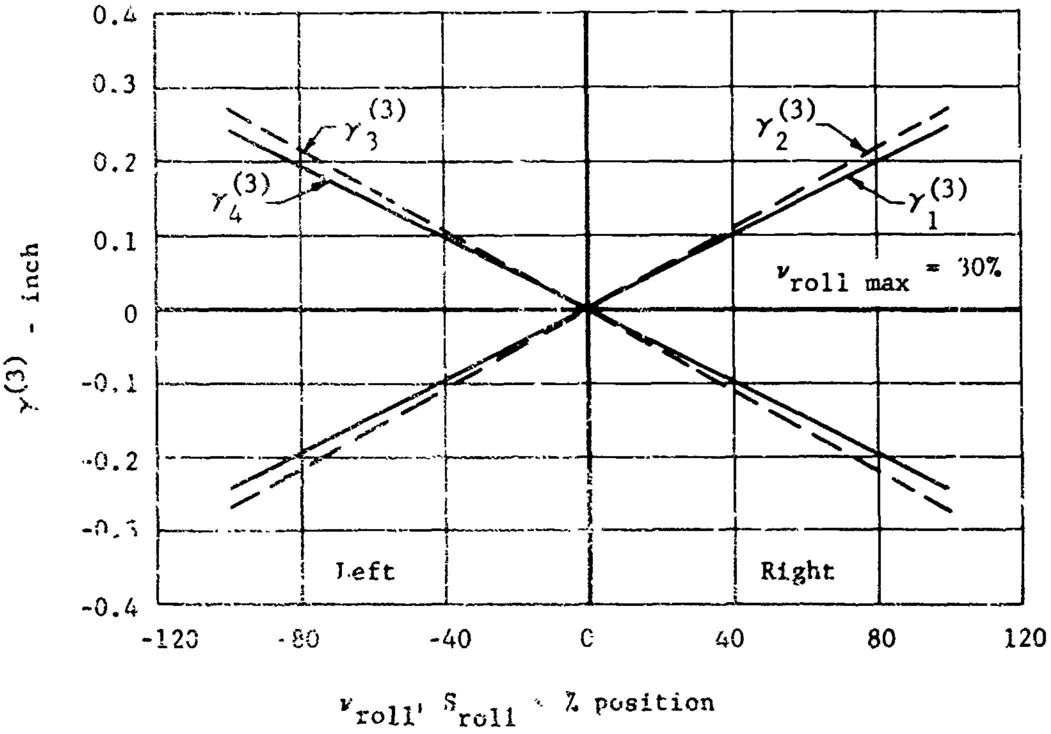

Figure 160. X-19, coordinator output stroke as a function of roll control deflection or SAS motion.

"FURNISHED UNDER UNITED STATES GOVERNMENT CONTRACT No. AF33(615)-3940. SHALL NOT BE EITHER RELEASED OUTSIDE THE GOVERNMENT, OR USED, DUPLICATED, OR DISCLOSED IN WHOLE OR IN PART FOR MANUFACTURE OR PROCUREMENT, WITHOUT THE WRITTEN PERMISSION OF CURTISS-WRIGHT CORPORATION, EXCEPT FOR (I) EMERGENCY REPAIR OR OVERHAUL WORK BY OR FOR THE GOVERNMENT, WHERE THE ITEM OR PROCESS IS NOT OTHERWISE REASONABLY AVAILABLE TO ENABLE TIMELY PERFORMANCE OF THE WORK, OR (II) RELEASE TO A FOREIGN GOVERNMENT, AS THE INTERESTS OF THE UNITED STATES MAY REQUIRE; PROVIDED THAT IN EITHER CASE THE RELEASE, USE, DUPLICATION OR DISCLOSURE HEREOF SHALL BE SUBJECT TO THE FOREGOING LIMITATIONS. THIS LEGEND SHALL BE MARKED ON ANY REPRODUCTION HEREOF IN WHOLE OR IN PART."

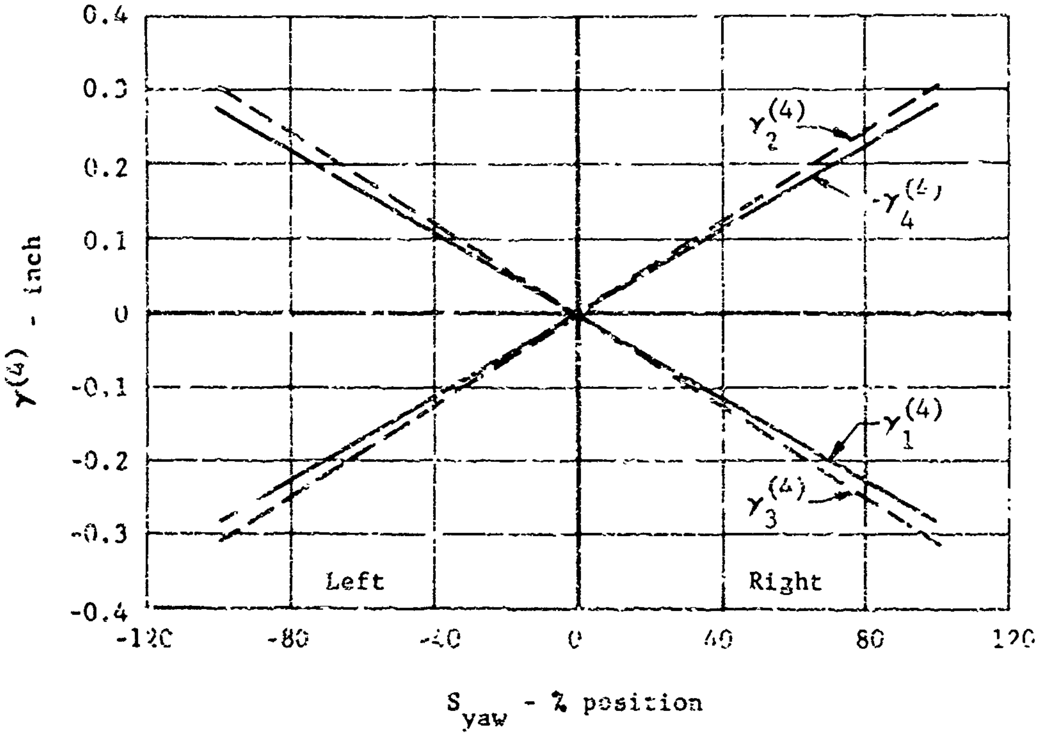

Figure 161. X-19, coordinator output stroke as a function of yaw control (pedal) deflection.

FURNISHED UNDER UNITED STATES GOVERNMENT CONTRACT No. [illegible] SHALL NOT BE EITHER RELEASED OUTSIDE THE GOVERNMENT, OR USED, DUPLICATED, OR DISCLOSED IN WHOLE OR IN PART FOR MANUFACTURE OR PROCUREMENT, WITHOUT THE WRITTEN PERMISSION OF CURTISS-WRIGHT CORPORATION, EXCEPT FOR (I) EMERGENCY REPAIR OR OVERHAUL WORK BY OR FOR THE GOVERNMENT, WHERE THE ITEM OR PROCESS IS NOT OTHERWISE REASONABLY AVAILABLE TO ENABLE TIMELY PERFORMANCE OF THE WORK, OR (II) RELEASE TO A FOREIGN GOVERNMENT, AS THE INTERESTS OF THE UNITED STATES MAY REQUIRE, PROVIDED THAT IN EITHER CASE THE RELEASE, USE, DUPLICATION OR DISCLOSURE HEREOF SHALL BE SUBJECT TO THE FOREGOING LIMITATIONS. THIS LEGEND SHALL BE MARKED ON ANY REPRODUCTION HEREOF IN WHOLE OR IN PART.

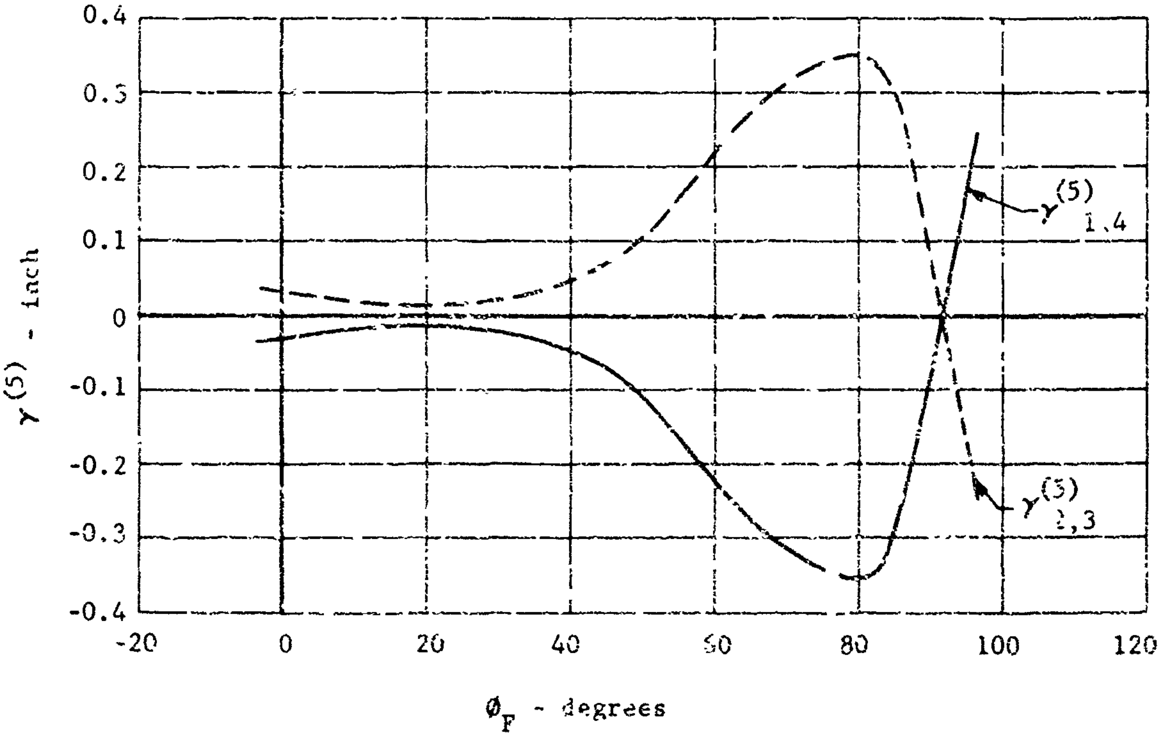

Figure 162. X-19, coordinator output stroke as a function of tilt angle (auto-trim schedule).

"FURNISHED UNDER UNITED STATES GOVERNMENT CONTRACT No. AF33(615) 3940. SHALL NOT BE EITHER RELEASED OUTSIDE THE GOVERNMENT, OR USED, DUPLICATED, OR DISCLOSED IN WHOLE OR IN PART, FOR MANUFACTURE OR PROCUREMENT, WITHOUT THE WRITTEN PERMISSION OF CURTISS-WRIGHT CORPORATION, EXCEPT FOR (I) EMERGENCY REPAIR OR OVERHAUL WORK BY OR FOR THE GOVERNMENT, WHERE THE ITEM OR PROCESS IS NOT OTHERWISE REASONABLY AVAILABLE TO ENSURE TIMELY PERFORMANCE OF THE WORK, OR (II) RELEASE TO A FOREIGN GOVERNMENT, AS THE INTERESTS OF THE UNITED STATES MAY REQUIRE; PROVIDED, THAT IN EITHER CASE THE RELEASE, USE, DUPLICATION OR DISCLOSURE HEREOF SHALL BE SUBJECT TO THE FOREGOING LIMITATIONS. THIS LEGEND SHALL BE MARKED ON ANY REPRODUCTION HEREOF IN WHOLE OR IN PART."

ϕ_F	=	front tilt angle	From Fig. 163 readout:	$G_1^{(P)}, \dots, G_4^{(P)}$
ϕ_F	=	front tilt angle	From Fig. 164 readout:	$G_1^{(R)}, \dots, G_4^{(R)}$
ϕ_F	=	front tilt angle	From Fig. 165 readout:	$G_1^{(y)}, \dots, G_4^{(y)}$
μ	=	collective shaft position	From Fig. 166 readout:	$\gamma_1^{(6)}, \dots, \gamma_4^{(6)}$

and

S	- stick position	percent
Δ	- pilot pitch trim position	inches
ν	- SAS position	percent
μ	- Collective shaft position	inches
γ_i	- Coordinator output position = $\gamma_i^{(1)} + \cdots + \gamma_i^{(6)}$	inches
λ_i	- nacelle input position	degrees
$\beta_{.75R}$	- propeller blade angle (pitch)	degrees
ϕ_F	- front tilt angle	degrees

Subscripts

i = 1,2,3,4, - relate to propeller no.

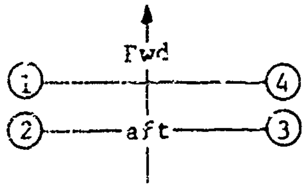

Superscripts -

$\gamma^{(1)}$ coordinator output due to stick or SAS - (pitch plane)

$\gamma^{(2)}$ coordinator output due to pilot manual trim button

$\gamma^{(3)}$ coordinator output due to stick or SAS - (roll plane)

$\gamma^{(4)}$ coordinator output due to pedals - (yaw plane)

$\gamma^{(5)}$ coordinator output due to auto-trim schedule

$\gamma^{(6)}$ coordinator output due to governor collective motion

The output of the coordinator is transmitted by a push-pull linkage through the fuselage and wings to the nacelle input arm. The gearing of this linkage is given in Figure 167. The nacelle contains a gain changer

FURNISHED UNDER UNITED STATES GOVERNMENT CONTRACT No. [illegible] SHALL NOT BE EITHER RELEASED OUTSIDE THE GOVERNMENT, OR USED, DUPLICATED, OR DISCLOSED IN WHOLE OR IN PART FOR MANUFACTURE OR PROCUREMENT, WITHOUT THE WRITTEN PERMISSION OF CURTISS-WRIGHT CORPORATION, EXCEPT FOR: (1) EMERGENCY REPAIR OR OVERHAUL WORK BY OR FOR THE GOVERNMENT, WHERE THE ITEM OR PROCESS IS NOT OTHERWISE REASONABLY AVAILABLE TO ENABLE TIMELY PERFORMANCE OF THE WORK; OR (2) RELEASE TO A FOREIGN GOVERNMENT, AS THE INTERESTS OF THE UNITED STATES MAY REQUIRE; PROVIDED THAT IN EITHER CASE THE RELEASE, USE, DUPLICATION OR DISCLOSURE HEREOF SHALL BE SUBJECT TO THE FOREGOING LIMITATIONS. THIS LEGEND SHALL BE MARKED ON ANY REPRODUCTION HEREOF IN WHOLE OR IN PART.

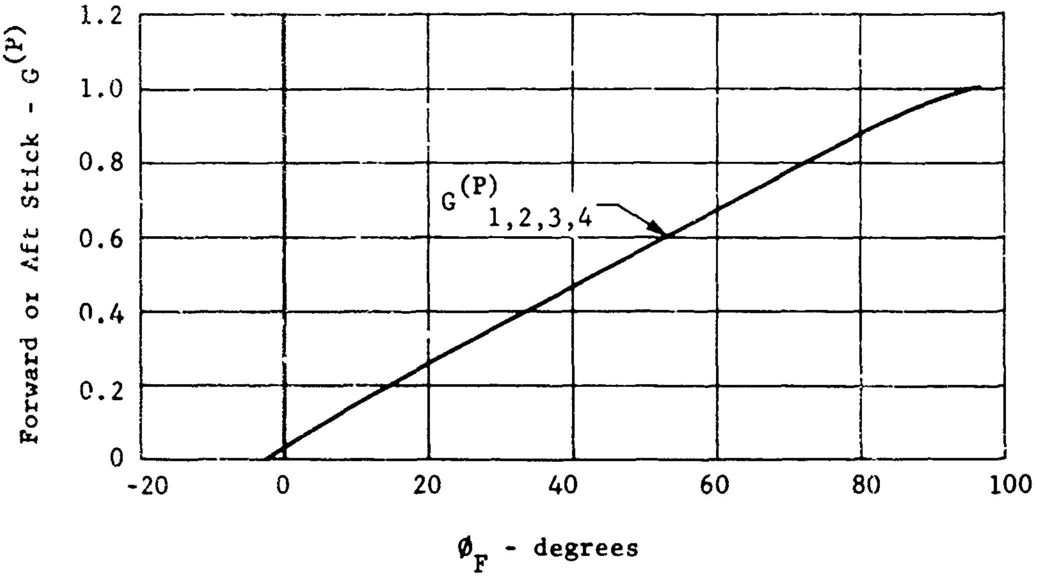

Figure 163. X-19, propeller pitch control gain as a function of tilt angle (pitch-gain schedule).

"FURNISHED UNDER UNITED STATES GOVERNMENT CONTRACT No. AF33(615)-3940. SHALL NOT BE EITHER RELEASED OUTSIDE THE GOVERNMENT, OR USED, DUPLICATED, OR DISCLOSED IN WHOLE OR IN PART FOR MANUFACTURE OR PROCUREMENT, WITHOUT THE WRITTEN PERMISSION OF CURTISS-WRIGHT CORPORATION, EXCEPT FOR (i) EMERGENCY REPAIR OR OVERHAUL WORK BY OR FOR THE GOVERNMENT, WHERE THE ITEM OR PROCESS IS NOT OTHERWISE REASONABLY AVAILABLE TO ENABLE TIMELY PERFORMANCE OF THE WORK, OR (ii) RELEASE TO A FOREIGN GOVERNMENT, AS THE INTERESTS OF THE UNITED STATES MAY REQUIRE: PROVIDED THAT IN EITHER CASE THE RELEASE, USE, DUPLICATION OR DISCLOSURE HEREOF SHALL BE SUBJECT TO THE FOREGOING LIMITATIONS. THIS LEGEND SHALL BE MARKED ON ANY REPRODUCTION HEREOF IN WHOLE OR IN PART."

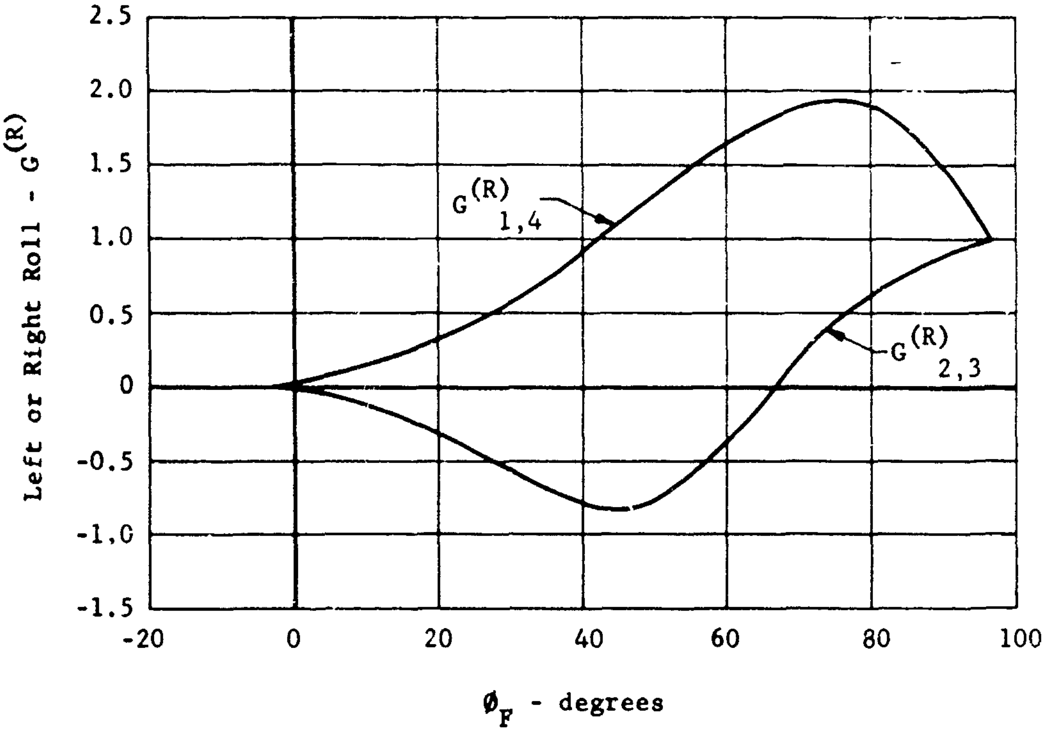

Figure 164. X-19, propeller roll control gain as a function of tilt angle (roll-gain schedule).

FURNISHED UNDER UNITED STATES GOVERNMENT CONTRACT No AF33(615)-3940 SHALL NOT BE EITHER RELEASED OUTSIDE THE GOVERNMENT, OR USED, DUPLICATED, OR DISCLOSED IN WHOLE OR IN PART FOR MANUFACTURE OR PROCUREMENT, WITHOUT THE WRITTEN PERMISSION OF CURTISS WRIGHT CORPORATION, EXCEPT FOR (I) EMERGENCY REPAIR OR OVERHAUL WORK BY OR FOR THE GOVERNMENT WHERE THE ITEM OR PROCESS IS NOT OTHERWISE REASONABLY AVAILABLE TO ENABLE TIMELY PERFORMANCE OF THE WORK, OR (II) RELEASE TO A FOREIGN GOVERNMENT, AS THE INTERESTS OF THE UNITED STATES MAY REQUIRE. PROVIDED THAT IN EITHER CASE THE RELEASE, USE, DUPLICATION OR DISCLOSURE HEREOF SHALL BE SUBJECT TO THE FOREGOING LIMITATIONS. THIS LEGEND SHALL BE MARKED ON ANY REPRODUCTION HEREOF IN WHOLE OR IN PART.

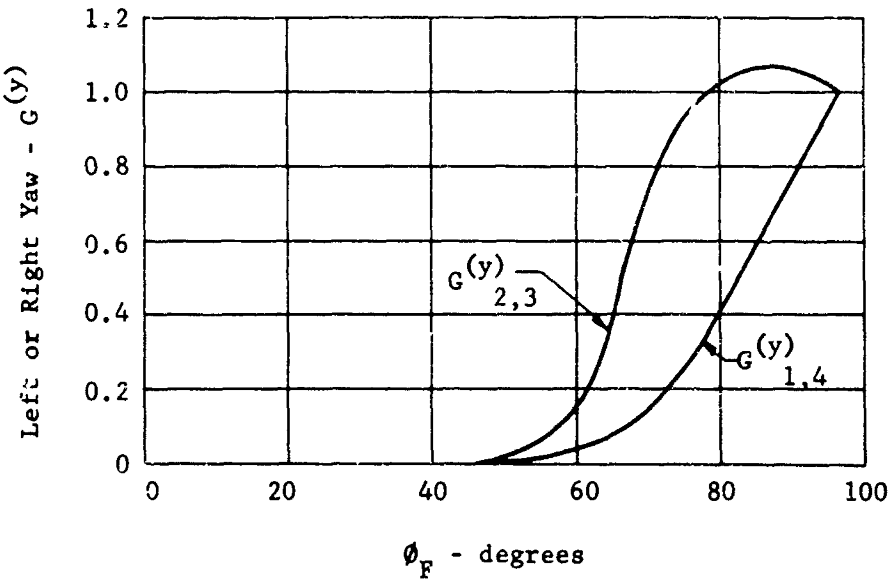

Figure 165. X-19, propeller yaw control gain as a function of tilt angle (yaw-gain schedule).

"FURNISHED UNDER UNITED STATES GOVERNMENT CONTRACT No. AF33(615)-3940 SHALL NOT BE EITHER RELEASED OUTSIDE THE GOVERNMENT OR USED, DUPLICATED, OR DISCLOSED IN WHOLE OR IN PART FOR MANUFACTURE OR PROCUREMENT, WITHOUT THE WRITTEN PERMISSION OF CURTISS-WRIGHT CORPORATION, EXCEPT FOR (i) EMERGENCY REPAIR OR OVERHAUL WORK BY OR FOR THE GOVERNMENT, WHERE THE ITEM OR PROCESS IS NOT OTHERWISE REASONABLY AVAILABLE TO ENABLE TIMELY PERFORMANCE OF THE WORK. OR (ii) RELEASE TO A FOREIGN GOVERNMENT, AS THE INTERESTS OF THE UNITED STATES MAY REQUIRE. PROVIDED THAT IN EITHER CASE THE RELEASE, USE, DUPLICATION OR DISCLOSURE HEREOF SHALL BE SUBJECT TO THE FOREGOING LIMITATIONS. THIS LEGEND SHALL BE MARKED ON ANY REPRODUCTION HEREOF IN WHOLE OR IN PART."

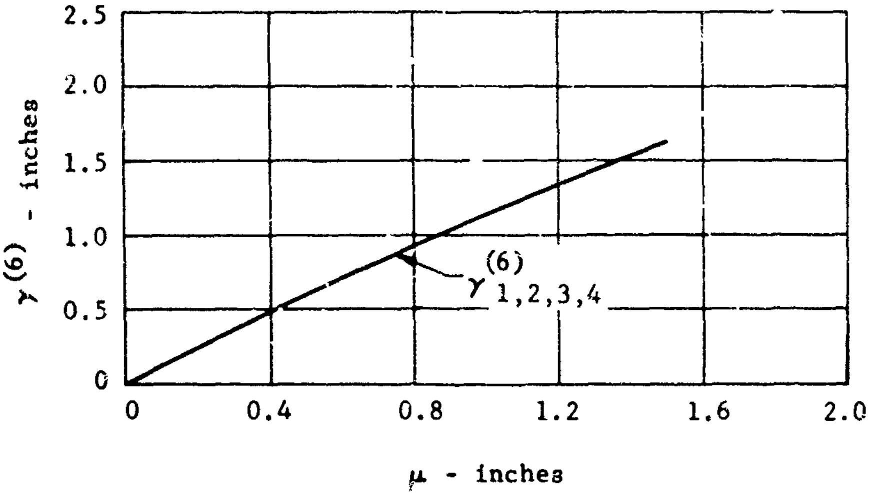

Figure 166. X-19, coordinator output stroke as a function of governor collective shaft displacement.

FURNISHED UNDER UNITED STATES GOVERNMENT CONTRACT No AF33(615)-1940 SHALL NOT BE EITHER RELEASED OUTSIDE THE GOVERNMENT OR USED, DUPLICATED, OR DISCLOSED IN WHOLE OR IN PART FOR MANUFACTURE OR PROCUREMENT, WITHOUT THE WRITTEN PERMISSION OF CURTISS-WRIGHT CORPORATION, EXCEPT FOR (I) EMERGENCY REPAIR OR OVERHAUL WORK BY OR FOR THE GOVERNMENT, WHERE THE ITEM OR PROCESS IS NOT OTHERWISE REASONABLY AVAILABLE TO ENABLE TIMELY PERFORMANCE OF THE WORK. OR (II) RELEASE TO A FOREIGN GOVERNMENT, AS THE INTERESTS OF THE UNITED STATES MAY REQUIRE PROVIDED THAT IN EITHER CASE THE RELEASE, USE, DUPLICATION OR DISCLOSURE HEREOF SHALL BE SUBJECT TO THE FOREGOING LIMITATIONS THIS LEGEND SHALL BE MARKED ON ANY REPRODUCTION HEREOF IN WHOLE OR IN PART."

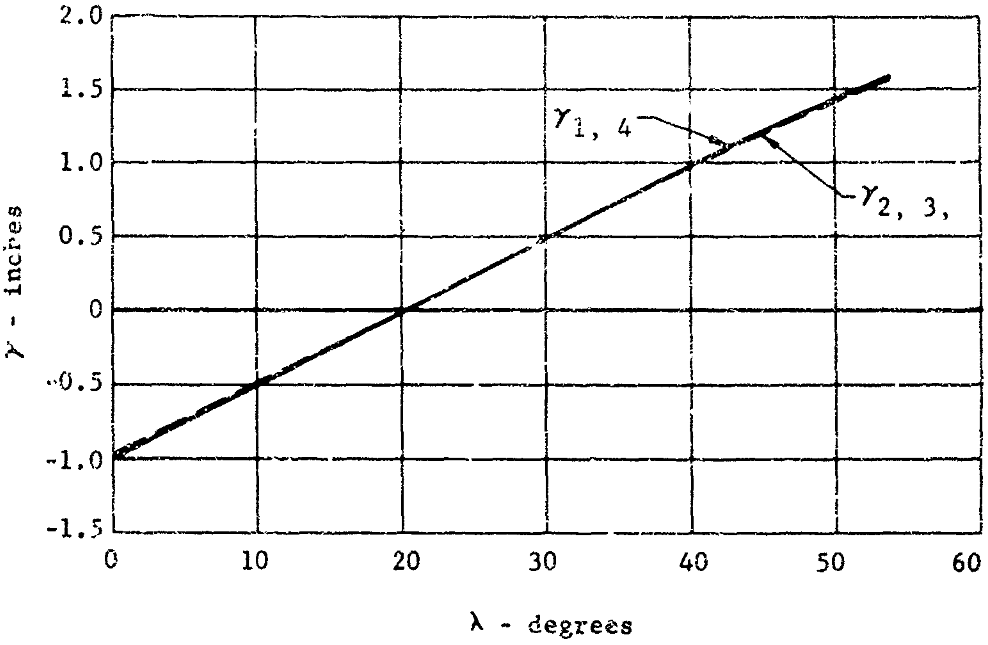

Figure 167. X-19, nacelle input arm position, λ, as a function of coordinator output stroke, γ.

"FURNISHED UNDER UNITED STATES GOVERNMENT CONTRACT NO. AF33(615)-3940. SHALL NOT BE EITHER RELEASED OUTSIDE THE GOVERNMENT, OR USED, DUPLICATED, OR DISCLOSED IN WHOLE OR IN PART FOR MANUFACTURE OR PROCUREMENT, WITHOUT THE WRITTEN PERMISSION OF CURTISS-WRIGHT CORPORATION, EXCEPT FOR (I) EMERGENCY REPAIR OR OVERHAUL WORK BY OR FOR THE GOVERNMENT, WHERE THE ITEM OR PROCESS IS NOT OTHERWISE REASONABLY AVAILABLE TO ENABLE TIMELY PERFORMANCE OF THE WORK; OR (II) RELEASE TO A FOREIGN GOVERNMENT, AS THE INTERESTS OF THE UNITED STATES MAY REQUIRE. PROVIDED THAT IN EITHER CASE THE RELEASE, USE, DUPLICATION OR DISCLOSURE HEREOF SHALL BE SUBJECT TO THE FOREGOING LIMITATIONS. THIS LEGEND SHALL BE MARKED ON ANY REPRODUCTION HEREOF IN WHOLE OR IN PART.

which is sensitive to tilt angle and the input arm position. The output of the nacelle is fed into the propeller servo control, from which a propeller blade angle is generated.

The relationship between nacelle input arm, tilt angle and blade angle is given in Figure 168. At a given flight condition, the propeller blade angle determines the torque absorption for a horsepower input. Obviously, as the four propeller blade angles change, the aerodynamic torque is altered and the system changes RPM. The governor senses this change and automatically adjusts the collective shaft position, μ , to maintain fixed RPM. This alters the output of the coordinator sending an equal stroke to each of the four propellers.

2. CONTROL POWERS.

The following are the design hover control powers.

The maximum angular accelerations quoted are for a W = 12,300 lb. airplane:

Axis	Max. Control Power ft. lb.	Max. Angular Acceleration, rad/sec^2
Pitch	± 27,000	± 0.68
Roll	± 20,000	± 1.75
Yaw	± 5,600	± 0.12

3. TIME CONSTANT FOR PROPELLER FORCES

Time response of hover pitch, roll or yaw control moments to pilot commanded step control inputs are shown in Figure 169. Common factors in pitch, roll and yaw systems are, (1) an assumed dead time due to system linkage "slop", etc., of 0.2 seconds following control application, and (2) the propeller blade angle actuator with a time constant of 0.085 seconds. The pitch and roll systems both include hydraulic boosters which introduce a further system lag. It was not possible to determine the boosters' time constant at the time of writing, so a representative time constant of 0.1 seconds was assumed for both. There is no boost in the yaw control system.

Thrust growth or decay time following a propeller blade angle change was computed to be 0.0065 seconds. This is based on the following: (1) hover propeller speed of 819 πnD; (2) 0.7R blade station; and (3) the lift change is developed in two chord lengths of passage. This lag was considered negligibly small and hence omitted. No SAS effects are included in data given on Figure 169.

FURNISHED UNDER UNITED STATES GOVERNMENT CONTRACT No. AF33(616)-3940. SHALL NOT BE EITHER RELEASED OUTSIDE THE GOVERNMENT, OR USED, DUPLICATED, OR DISCLOSED IN WHOLE OR IN PART FOR MANUFACTURE OR PROCUREMENT, WITHOUT THE WRITTEN PERMISSION OF CURTISS-WRIGHT CORPORATION, EXCEPT FOR (I) EMERGENCY REPAIR OR OVERHAUL WORK BY OR FOR THE GOVERNMENT, WHERE THE ITEM OR PROCESS IS NOT OTHERWISE REASONABLY AVAILABLE TO ENABLE TIMELY PERFORMANCE OF THE WORK, OR (II) RELEASE TO A FOREIGN GOVERNMENT, AS THE INTERESTS OF THE UNITED STATES MAY REQUIRE. PROVIDED THAT IN EITHER CASE THE RELEASE, USE, DUPLICATION OR DISCLOSURE HEREOF SHALL BE SUBJECT TO THE FOREGOING LIMITATIONS. THIS LEGEND SHALL BE MARKED ON ANY REPRODUCTION HEREOF IN WHOLE OR IN PART.

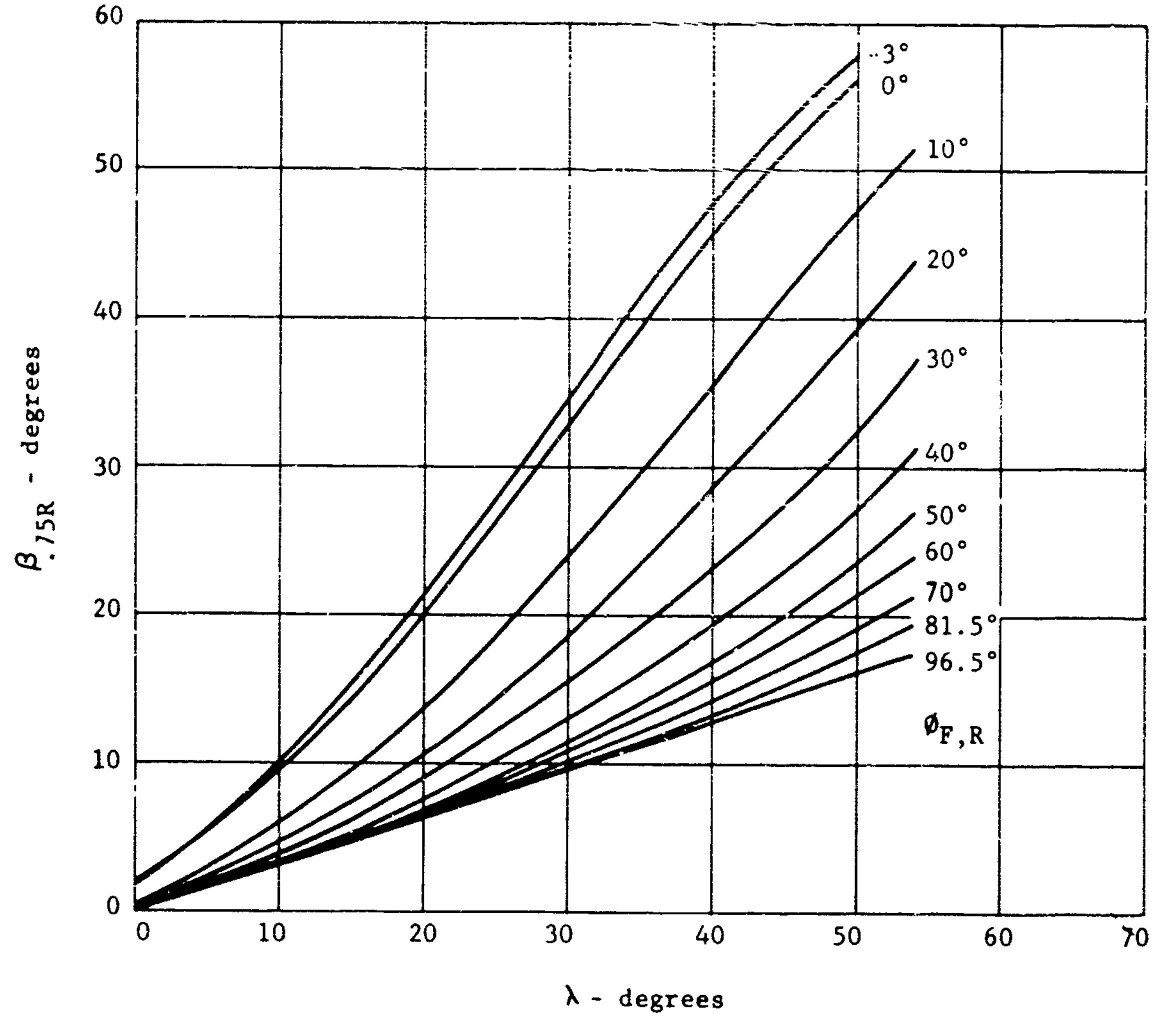

Figure 168. X-19, propeller blace angle β .75R as a function of nacelle input arm position, λ .

FURNISHED UNDER UNITED STATES GOVERNMENT CONTRACT No. AF33(615)-3940 SHALL NOT BE EITHER RELEASED OUTSIDE THE GOVERNMENT, OR USED, DUPLICATED, OR DISCLOSED IN WHOLE OR IN PART FOR MANUFACTURE OR PROCUREMENT, WITHOUT THE WRITTEN PERMISSION OF CURTISS-WRIGHT CORPORATION, EXCEPT FOR (I) EMERGENCY REPAIR OR OVERHAUL WORK BY OR FOR THE GOVERNMENT, WHERE THE ITEM OR PROCESS IS NOT OTHERWISE REASONABLY AVAILABLE TO ENABLE TIMELY PERFORMANCE OF THE WORK. OR (II) RELEASE TO A FOREIGN GOVERNMENT, AS THE INTERESTS OF THE UNITED STATES MAY REQUIRE: PROVIDED THAT IN EITHER CASE THE RELEASE, USE, DUPLICATION OR DISCLOSURE HEREOF SHALL BE SUBJECT TO THE FOREGOING LIMITATIONS. THIS LEGEND SHALL BE MARKED ON ANY REPRODUCTION HEREOF IN WHOLE OR IN PART.

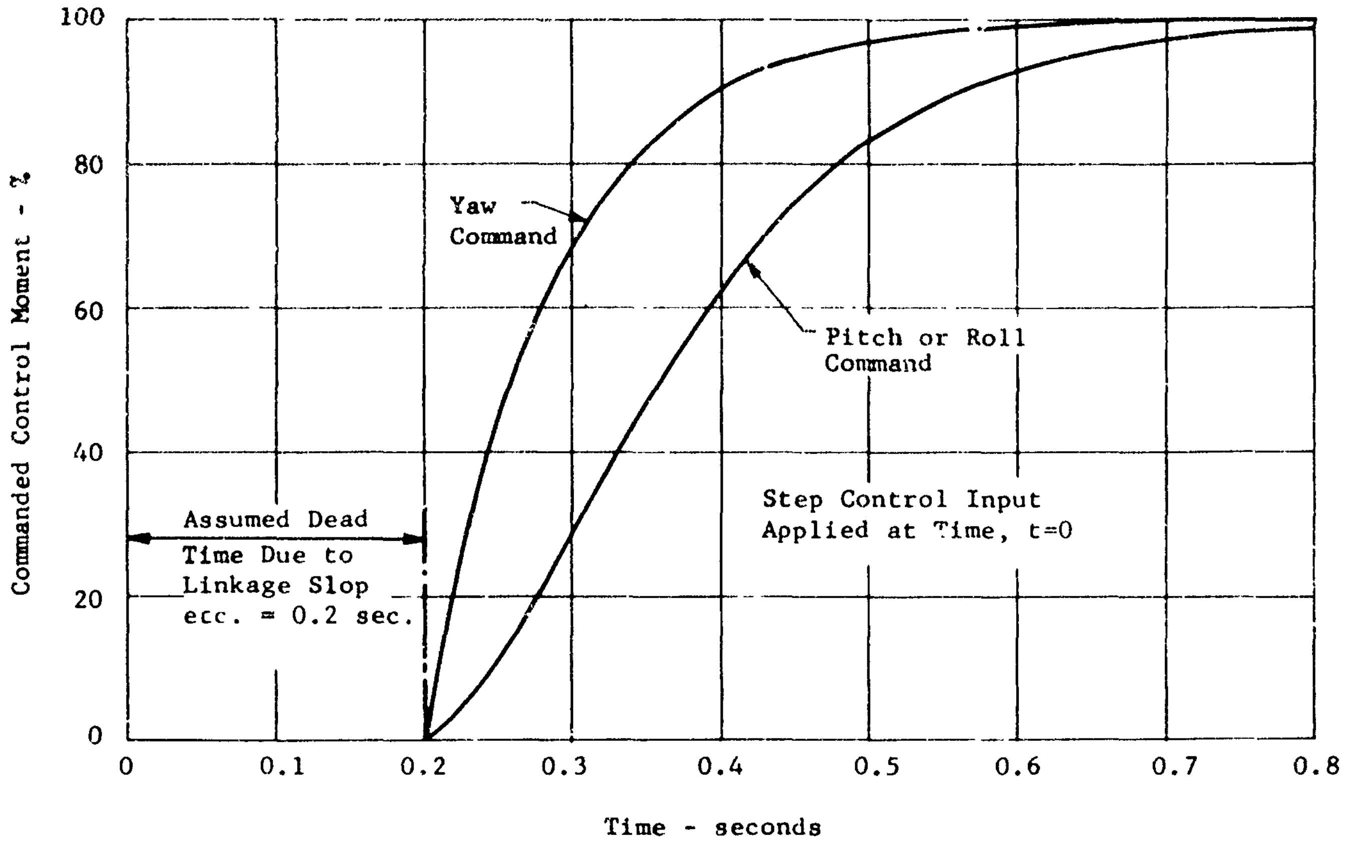

Figure 169. X-19, hover control moment response due to a pilot commanded step input of pitch, roll or yaw control.

4. PROPELLER POWER INCREMENTS DUE TO CONTROL APPLICATION

The power increments due to control deflections depends on the coordinator gain schedules. One can obtain this information from the introduction of this section. However a more convenient form is plotted in the Figure of Section VII, 7.c. These figures show directly the stick-imposed propeller blade angle increments (maximum) as a function of tilt angle. Using these curves, and specifying the recommended tilt-velocity schedule, weight, steady state conditions, density, RPM and center of gravity one can obtain the power increments due to control applications.

5. CONTROL COUPLING AND RESPONSE

Aerodynamic characteristics of the propeller control system are described herein. The blade angle of each of the four propellers as a function of control stick input is given on Figure 170. The blade angle change will give force components depending on the operating J, A and wash conditions. The forces add vectorially about the center of gravity, to obtain resultant control moments. In addition, the aerodynamic control surfaces which function in parallel with the propellers blade angle changes contribute their share to the moments. Lastly, the propeller power effects upon the wings are added into the moments. The equations governing the forces are given below for a wind axis system.

Roll

$$\begin{aligned}\Sigma L = {} & \left[(C_{L_1} - C_{L_4})X_F + (C_{L_2} - C_{L_3})X_R\right] qS + (Q_1 - Q_4)\cos A_F + \\ & (Q_3 - Q_2)\cos A_R + (Y_1 - Y_4)\sin A_F + (Y_3 - Y_2)\sin A_R + \\ & C_{l_{\delta_r}} Sb_F q\delta_r + C_{l_{\delta_a}} Sb_F q\delta_a + \left[(C_{L_{W_1}} - C_{L_{W_4}})X_{F_W} + \right. \\ & \left.(C_{L_{W_2}} - C_{L_{W_3}})X_{R_W}\right] qS\end{aligned}$$

Yaw

$$\begin{aligned}\Sigma N = {} & \left[(C_{D_4} - C_{D_1})X_F + (C_{D_3} - C_{D_2})X_R\right] qS + (Q_4 - Q_1)\sin A_F + \\ & (Q_2 - Q_3)\sin A_R + (Y_1 - Y_4)\cos A_F + (Y_3 - Y_2)\cos A_R + \\ & C_{n_{\delta_a}} Sb_F q\delta_a + C_{n_{\delta_r}} Sb_F q\delta_r\end{aligned}$$

The pitching moment equation is omitted because of the symmetry in the lateral plane.

The means of eliminating the lateral coupling was as follows. Assume that a roll signal is applied. Select some front blade angles according to the relationships set forth in Figure 170. Then select a set of rear blade angles in similar manner. Obtain the propeller forces which result from the blade increments and solve in the yaw equation, by reiterating on the rear propeller blade angle increments until yaw moment is zero.

"FURNISHED UNDER UNITED STATES GOVERNMENT CONTRACT No. AF33(615)-3946. SHALL NOT BE EITHER RELEASED OUTSIDE THE GOVERNMENT, OR USED, DUPLICATED, OR DISCLOSED IN WHOLE OR IN PART FOR MANUFACTURE OR PROCUREMENT, WITHOUT THE WRITTEN PERMISSION OF CURTISS-WRIGHT CORPORATION, EXCEPT FOR (i) EMERGENCY REPAIR OR OVERHAUL WORK BY OR FOR THE GOVERNMENT, WHERE THE ITEM OR PROCESS IS NOT OTHERWISE REASONABLY AVAILABLE TO ENABLE TIMELY PERFORMANCE OF THE WORK; OR (ii) RELEASE TO A FOREIGN GOVERNMENT, AS THE INTERESTS OF THE UNITED STATES MAY REQUIRE; PROVIDED THAT IN EITHER CASE THE RELEASE, USE, DUPLICATION OR DISCLOSURE HEREOF SHALL BE SUBJECT TO THE FOREGOING LIMITATIONS. THIS LEGEND SHALL BE MARKED ON ANY REPRODUCTION HEREOF IN WHOLE OR IN PART."

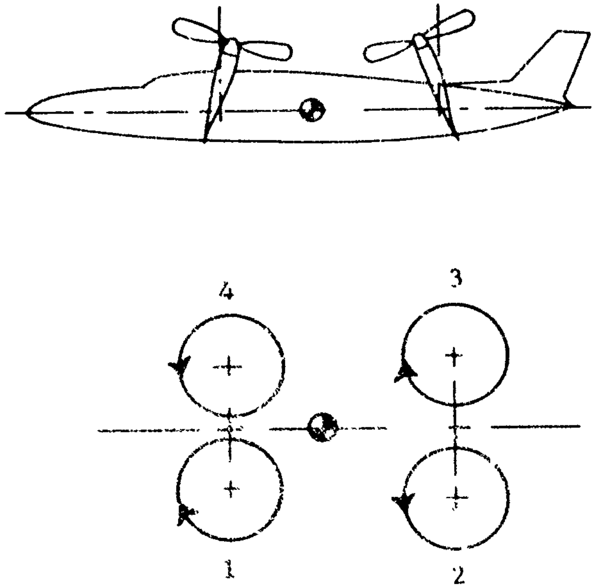

Typical Blade Angle Buildup For A Positive Control Moment

			Pitch	Roll	Yaw
β_1	=	$\beta_{F.\ \mathrm{Trim}}$	$+ \Delta\beta_1$	$+ \Delta\beta_1$	$- \Delta\beta_1$
β_2	=	$\beta_{R.\ \mathrm{Trim}}$	$- \Delta\beta_2$	$+ \Delta\beta_2$	$+ \Delta\beta_2$
β_3	=	$\beta_{R.\ \mathrm{Trim}}$	$- \Delta\beta_3$	$- \Delta\beta_3$	$- \Delta\beta_3$
β_4	=	$\beta_{F.\ \mathrm{Trim}}$	$+ \Delta\beta_4$	$- \Delta\beta_4$	$+ \Delta\beta_4$

Where

	Front	Rear
Pitch	$+ \Delta\beta_1 = + \Delta\beta_4$	$= - \Delta\beta_2 = - \Delta\beta_3$
Roll	$+ \Delta\beta_1 = - \Delta\beta_4$	$; + \Delta\beta_2 = - \Delta\beta_3$
Yaw	$- \Delta\beta_1 = + \Delta\beta_4$	$; + \Delta\beta_2 = - \Delta\beta_3$

Figure 170. X-19, propeller blade angle relationships due to control column application.

FURNISHED UNDER UNITED STATES GOVERNMENT CONTRACT No. AF33(615)-1940. SHALL NOT BE EITHER RELEASED OUTSIDE THE GOVERNMENT, [illegible] DUPLICATED, OR DISCLOSED IN WHOLE OR IN PART FOR MANUFACTURE OR PROCUREMENT, WITHOUT THE WRITTEN PERMISSION OF CURTISS-WRIGHT CORPORATION, EXCEPT FOR (I) EMERGENCY REPAIR OR OVERHAUL WORK BY OR FOR THE GOVERNMENT, WHERE THE ITEM OR PROCESS IS NOT OTHERWISE REASONABLY AVAILABLE TO ENABLE TIMELY PERFORMANCE OF THE WORK, [illegible] STATES MAY REQUIRE; PROVIDED THAT IN EITHER CASE THE RELEASE [illegible] LIMITATIONS. THIS LEGEND SHALL BE MARKED ON ANY REPRODUCTION HEREOF IN WHOLE OR IN PART.

Then knowing the fore and aft blade angles which give zero yaw, substitute into the roll equation to determine the magnitude of the roll moment. Then select new front blade angles and repeat the process until the desired range of rolling moment for zero yaw coupling is established. A similar procedure is used to obtain the uncoupled yaw input. This procedure was performed on a digital computer, where uncoupled lateral-directional moments resulted, at the full stick deflection. For partial stick deflections a small coupling was permitted. The results are shown in Figure 171 for the case of the yawing input. The coupling at ϕ_F = 20° and 40° is entirely due to the rudder induced roll, as the propellers are phased out. Yaw induced by the roll control was insignificant.

The pitch coupling created by a roll or yaw signal in the hover regime is shown in Figure 172. For a full roll or yaw signal, a negative pitch coupling of 2100 ft-lbs. is induced. This is less than ten percent of the pitch control capability. It was reasoned that if a full roll signal was inserted, the pilot might easily generate an inadvertent ten percent pitch signal (one half inch of the stick motion) without realizing it. Consequently, this degree of pitch coupling was permitted.

Experience, in flying the X-19, apparently has justified this philosophy. No complaints were registered, concerning the control systems coupling characteristics. Further, it should be borne in mind that this discussion relates to pure aerodynamic coupling. Any small alignment problems existing in the region of flight experience could only have compounded the problem.

Figures 173 and 174 have been included to illustrate the various forces contributing to the uncoupled control inputs. The front propeller has been held constant throughout the range of tilt angles as a matter of convenience. Therefore these buildups do not conform directly with the system roll and yaw gains. However, they point up the unusual interchange of the forces as they contribute to a control moment while nullifying the coupling moment.

6. PROPELLER CONTRIBUTION TO STEADY STATE AIRCRAFT MOMENTS DURING TRANSITION

Figures 175, 176, 177, 178 show the aircraft pitching moment characteristics at four propeller tilt angles in transition. Shown in these Figures are the propeller and airframe contributions to the total. These data have been extracted from the wind tunnel data of (41).

At each tilt angle shown the propellers are operating at fixed advance ratio and total power coefficient as given below:

"FURNISHED UNDER UNITED STATES GOVERNMENT CONTRACT No. AF33(615)-3966. SHALL NOT BE EITHER RELEASED OUTSIDE THE GOVERNMENT, OR USED, DUPLICATED, OR DISCLOSED IN WHOLE OR IN PART FOR MANUFACTURE OR PROCUREMENT, WITHOUT THE WRITTEN PERMISSION OF CURTISS-WRIGHT CORPORATION, EXCEPT FOR (I) EMERGENCY REPAIR OR OVERHAUL WORK BY OR FOR THE GOVERNMENT, WHERE THE ITEM OR PROCESS IS NOT OTHERWISE REASONABLY AVAILABLE TO ENABLE TIMELY PERFORMANCE OF THE WORK; OR (II) RELEASE TO A FOREIGN GOVERNMENT, AS THE INTERESTS OF THE UNITED STATES MAY REQUIRE. PROVIDED THAT IN EITHER CASE THE RELEASE, USE, DUPLICATION OR DISCLOSURE HEREOF SHALL BE SUBJECT TO THE FOREGOING LIMITATIONS. THIS LEGEND SHALL BE MARKED ON ANY REPRODUCTION HEREOF IN WHOLE OR IN PART."

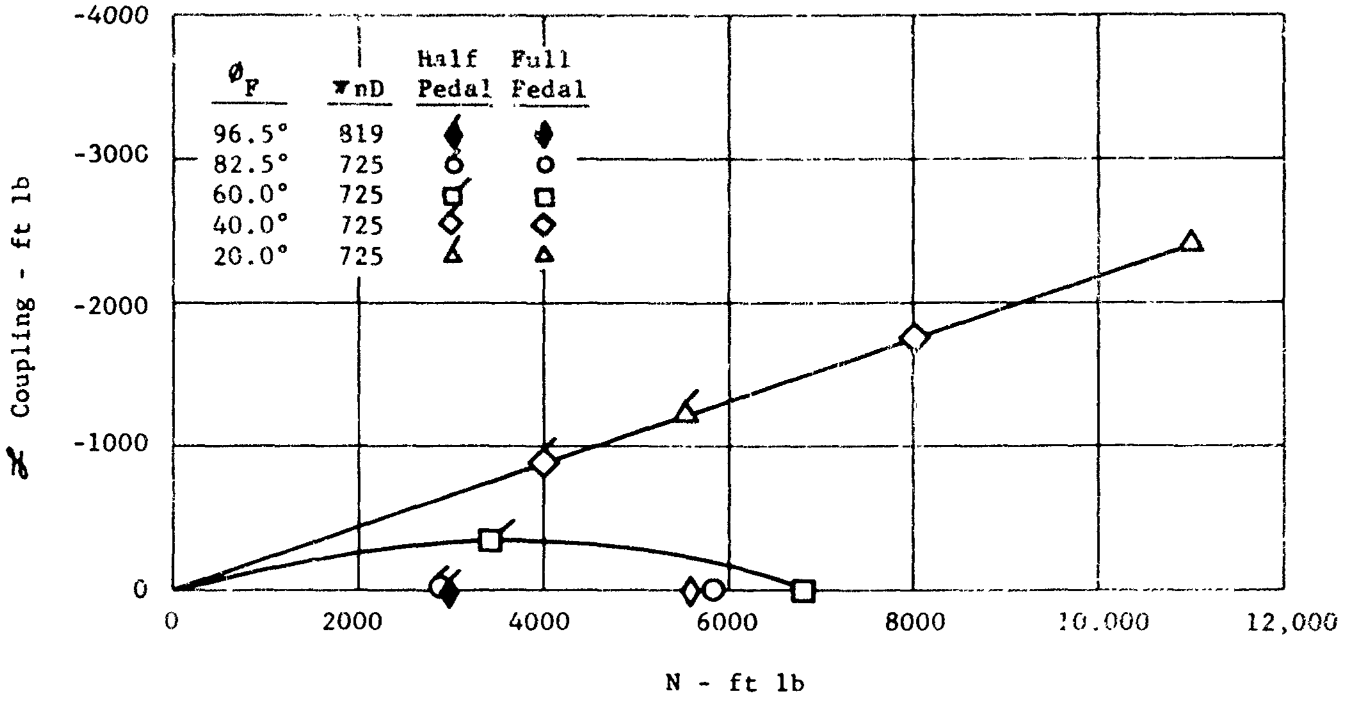

Figure 171. X-19, roll coupling generated by a yaw control input.

FURNISHED UNDER UNITED STATES GOVERNMENT CONTRACT No. AF33[illegible] SHALL NOT BE EITHER RELEASED OUTSIDE THE GOVERNMENT, OR USED, DUPLICATED, OR DISCLOSED IN WHOLE OR IN PART FOR MANUFACTURE OR PROCUREMENT, WITHOUT THE WRITTEN PERMISSION OF CURTISS-WRIGHT CORPORATION, EXCEPT FOR (i) EMERGENCY REPAIR OR OVERHAUL WORK BY OR FOR THE GOVERNMENT, WHERE THE ITEM OR PROCESS IS NOT OTHERWISE REASONABLY AVAILABLE TO ENABLE TIMELY PERFORMANCE OF THE WORK, OR (ii) RELEASE TO A FOREIGN GOVERNMENT, AS THE INTERESTS OF THE UNITED STATES MAY REQUIRE; PROVIDED THAT IN EITHER CASE THE RELEASE, USE, DUPLICATION OR DISCLOSURE HEREOF SHALL BE SUBJECT TO THE FOREGOING LIMITATIONS. THIS LEGEND SHALL BE MARKED ON ANY REPRODUCTION HEREOF IN WHOLE OR IN PART.

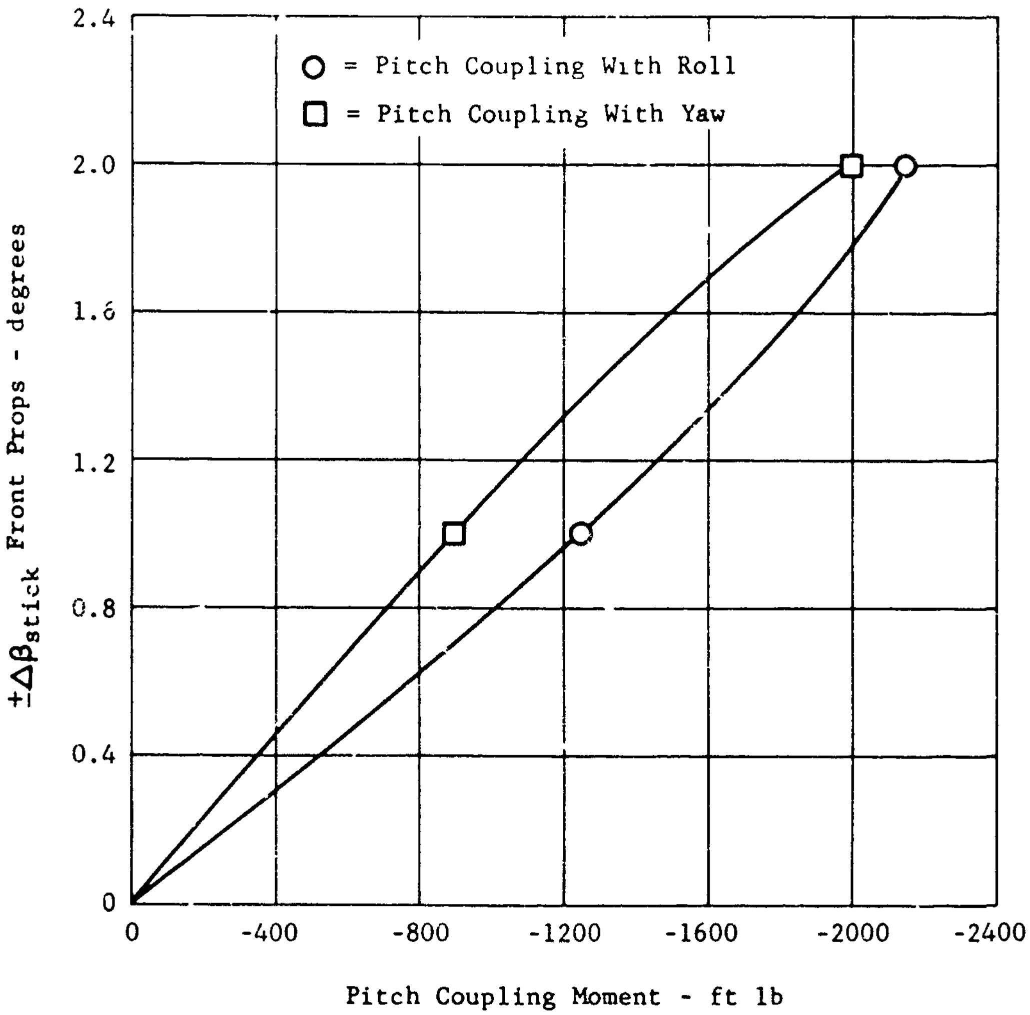

Figure 172. X-19, pitch coupling generated by roll or yaw control input; V = 0 fps.

"FURNISHED UNDER UNITED STATES GOVERNMENT CONTRACT No. AF33(615)-3940. SHALL NOT BE EITHER RELEASED OUTSIDE THE GOVERNMENT, OR USED, DUPLICATED, OR DISCLOSED IN WHOLE OR IN PART FOR MANUFACTURE OR PROCUREMENT, WITHOUT THE WRITTEN PERMISSION OF CURTISS-WRIGHT CORPORATION, EXCEPT FOR (i) EMERGENCY REPAIR OR OVERHAUL WORK BY OR FOR THE GOVERNMENT, WHERE THE ITEM OR PROCESS IS NOT OTHERWISE RESONABLY AVAILABLE TO ENABLE TIMELY PERFORMANCE OF THE WORK; OR (ii) RELEASE TO A FOREIGN GOVERNMENT, AS THE INTERESTS OF THE UNITED STATES MAY REQUIRE; PROVIDED THAT IN EITHER CASE THE RELEASE, USE, DUPLICATION OR DISCLOSURE HEREOF SHALL BE SUBJECT TO THE FOREGOING LIMITATIONS. THIS LEGEND SHALL BE MARKED ON ANY REPRODUCTION HEREOF IN WHOLE OR IN PART."

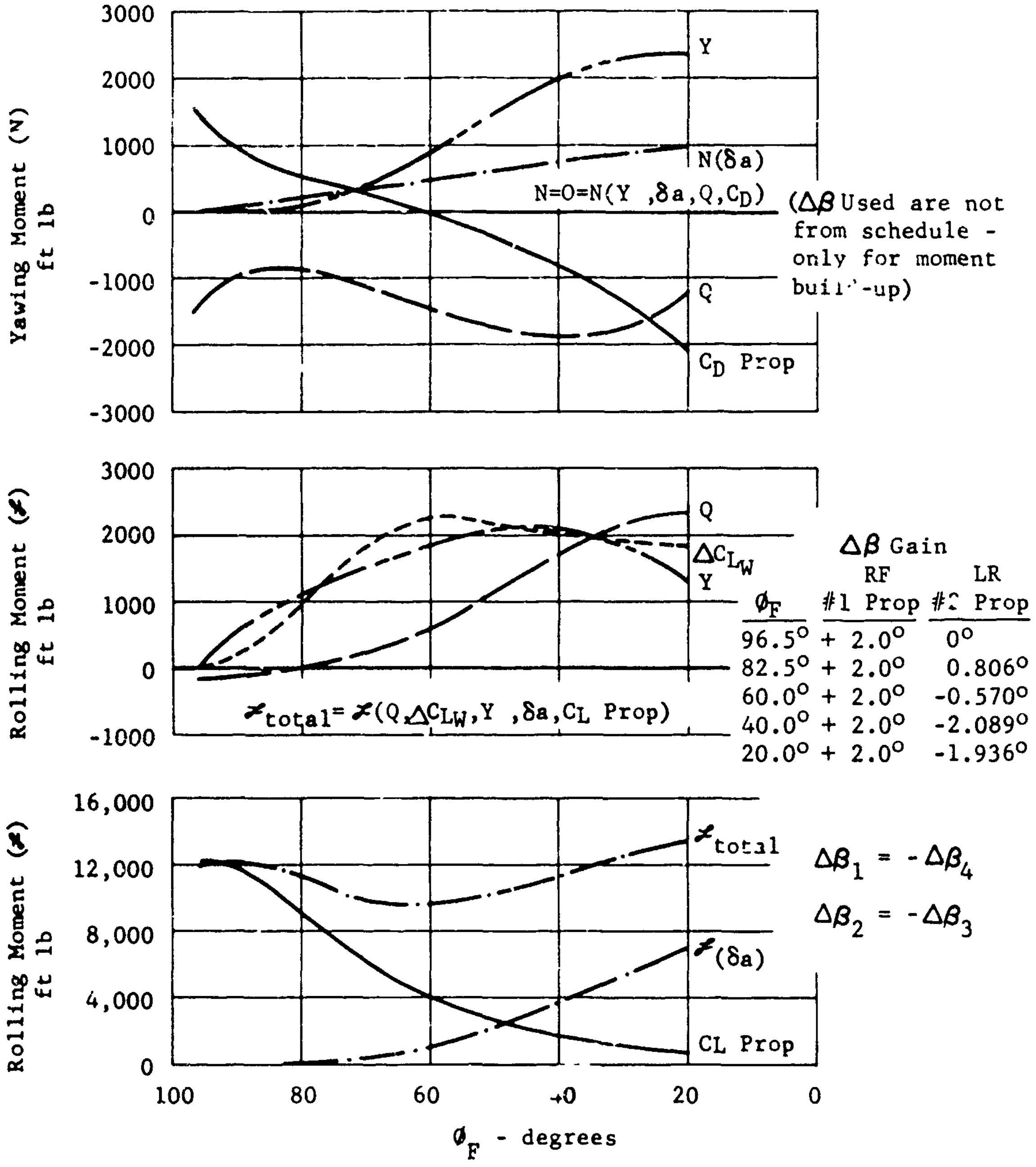

Δβ Gain

$Ø_F$	RF #1 Prop	LR #2 Prop
96.5°	+ 2.0°	0°
82.5°	+ 2.0°	0.806°
60.0°	+ 2.0°	-0.570°
40.0°	+ 2.0°	-2.089°
20.0°	+ 2.0°	-1.936°

$\Delta\beta_1 = -\Delta\beta_4$

$\Delta\beta_2 = -\Delta\beta_3$

Figure 173. X-19, distribution of forces due to a roll control input (maximum aileron).

FURNISHED UNDER UNITED STATES GOVERNMENT CONTRACT No. AF33(657)-3940. SHALL NOT BE EITHER RELEASED OUTSIDE THE GOVERNMENT, OR USED, DUPLICATED, OR DISCLOSED IN WHOLE OR IN PART FOR MANUFACTURE OR PROCUREMENT, WITHOUT THE WRITTEN PERMISSION OF CURTISS-WRIGHT CORPORATION, EXCEPT FOR (i) EMERGENCY REPAIR OR OVERHAUL WORK BY OR FOR THE GOVERNMENT, WHERE THE ITEM OR PROCESS IS NOT OTHERWISE REASONABLY AVAILABLE TO ENABLE TIMELY PERFORMANCE OF THE WORK, OR (ii) RELEASE TO A FOREIGN GOVERNMENT, AS THE INTERESTS OF THE UNITED STATES MAY REQUIRE; PROVIDED THAT IN EITHER CASE THE RELEASE, USE, DUPLICATION OR DISCLOSURE HEREOF SHALL BE SUBJECT TO THE FOREGOING LIMITATIONS. THIS LEGEND SHALL BE MARKED ON ANY REPRODUCTION HEREOF IN WHOLE OR IN PART.

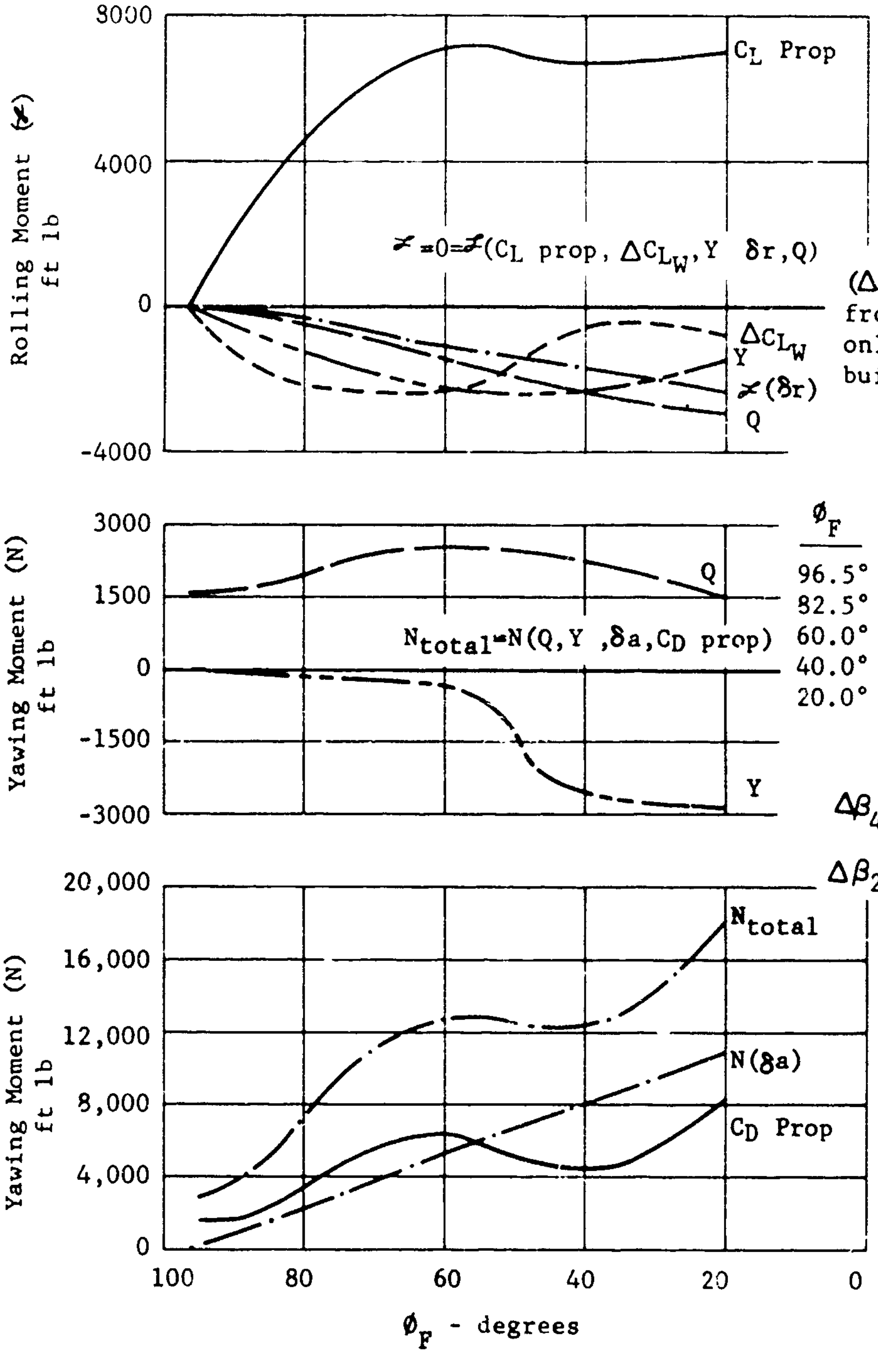

($\Delta\beta$ Used are not from schedule - only for moment build-up)

$\Delta\beta$ Gain

ϕ_F	RF #4 Prop	LR #2 Prop
96.5°	+1.0°	+1.1°
82.5°	+1.0°	+2.474°
60.0°	+1.0°	+3.067°
40.0°	+1.0°	+4.054°
20.0°	+1.0°	+3.678°

$$\Delta\beta_4 = -\Delta\beta_1$$

$$\Delta\beta_2 = -\Delta\beta_3$$

Figure 174. X-19, distribution of forces due to a yaw control input (maximum rudder).

"FURNISHED UNDER UNITED STATES GOVERNMENT CONTRACT No. AF33(615)-3940. SHALL NOT BE EITHER RELEASED OUTSIDE THE GOVERNMENT, OR USED, DUPLICATED, OR DISCLOSED IN WHOLE OR IN PART FOR MANUFACTURE OR PROCUREMENT, WITHOUT THE WRITTEN PERMISSION OF CURTISS-WRIGHT CORPORATION, EXCEPT FOR (I) EMERGENCY REPAIR OR OVERHAUL WORK BY OR FOR THE GOVERNMENT, WHERE THE ITEM OR PROCESS IS NOT OTHERWISE REASONABLY AVAILABLE TO ENABLE TIMELY PERFORMANCE OF THE WORK, OR (II) RELEASE TO A FOREIGN GOVERNMENT, AS THE INTERESTS OF THE UNITED STATES MAY REQUIRE: PROVIDED THAT IN EITHER CASE THE RELEASE, USE, DUPLICATION OR DISCLOSURE HEREOF SHALL BE SUBJECT TO THE FOREGOING LIMITATIONS. THIS LEGEND SHALL BE MARKED ON ANY REPRODUCTION HEREOF IN WHOLE OR IN PART."

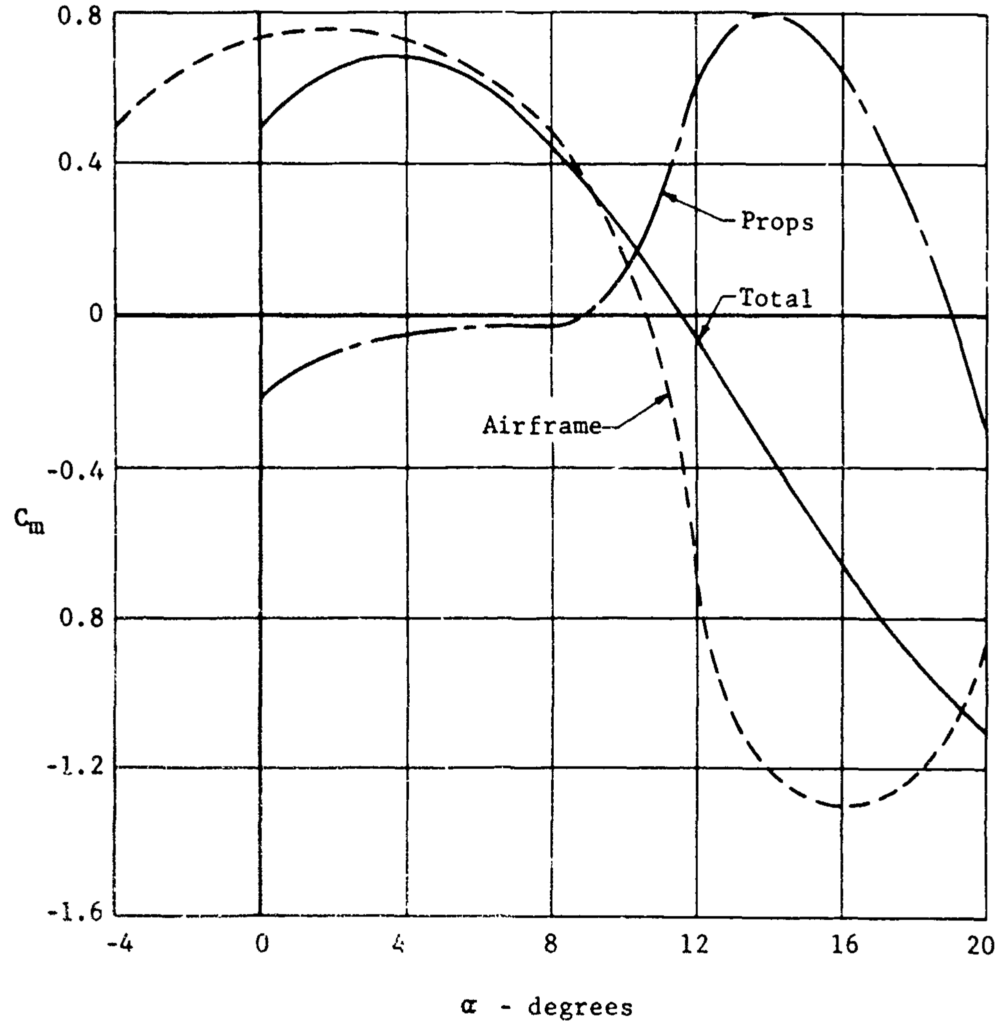

Figure 175. X-19, aircraft pitching moment characteristics at ϕ_F = 20°, including airframe and propeller contributions; c.g. = 42.8% lift chord.

FURNISHED UNDER UNITED STATES GOVERNMENT CONTRACT No. AF33(615)-3940 SHALL NOT BE EITHER RELEASED OUTSIDE THE GOVERNMENT, OR USED, DUPLICATED, OR DISCLOSED IN WHOLE OR IN PART FOR MANUFACTURE OR PROCUREMENT, WITHOUT THE WRITTEN PERMISSION OF CURTISS-WRIGHT CORPORATION EXCEPT FOR (i) EMERGENCY REPAIR OR OVERHAUL WORK BY OR FOR THE GOVERNMENT, WHERE THE ITEM OR PROCESS IS NOT OTHERWISE REASONABLY AVAILABLE TO ENABLE TIMELY PERFORMANCE OF THE WORK OR (ii) RELEASE TO A FOREIGN GOVERNMENT AS THE INTERESTS OF THE UNITED STATES MAY REQUIRE PROVIDED THAT IN EITHER CASE THE RELEASE, USE, DUPLICATION OR DISCLOSURE HEREOF SHALL BE SUBJECT TO THE FOREGOING LIMITATIONS THIS LEGEND SHALL BE MARKED ON ANY REPRODUCTION HEREOF IN WHOLE OR IN PART
]

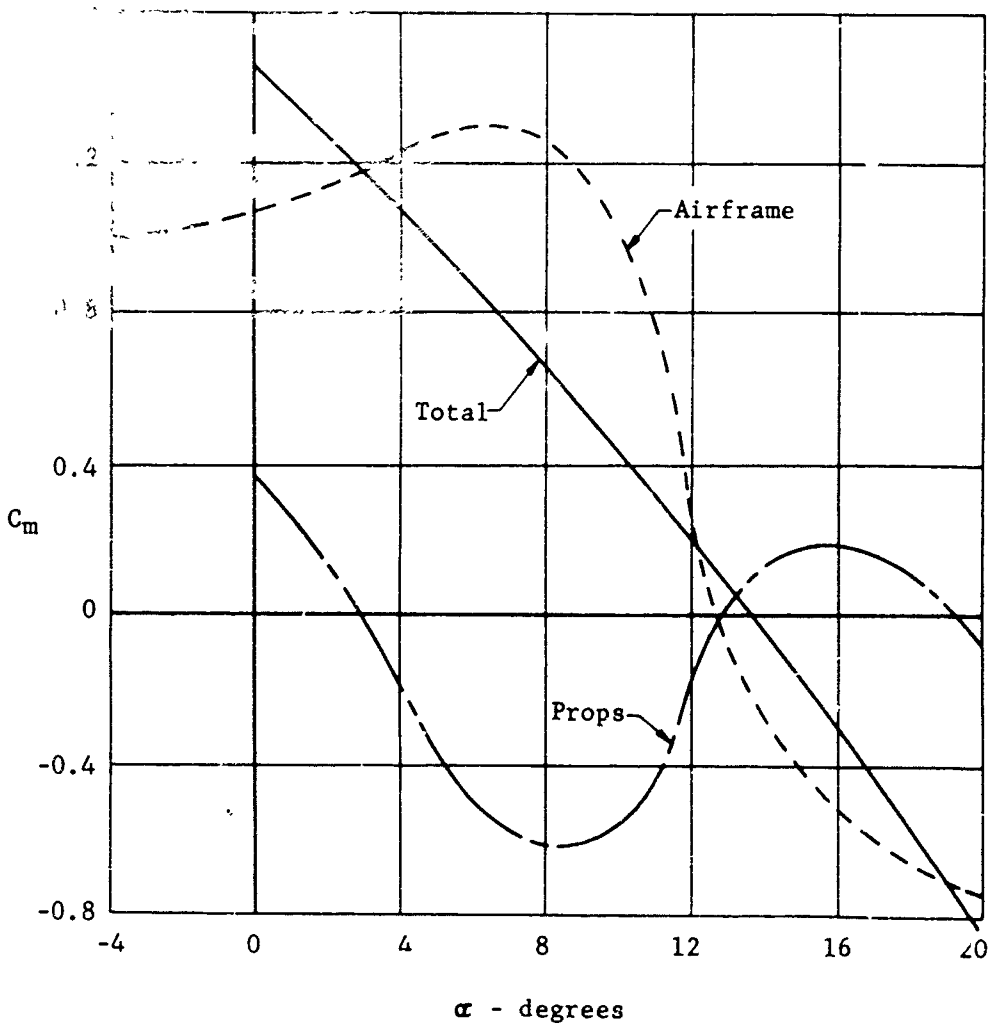

Figure 176. X-19, aircraft pitching moment characteristics at $\emptyset_F$ = 40°, including airframe and propeller contributions; c.g. = 42.8% lift chord.

"FURNISHED UNDER UNITED STATES GOVERNMENT CONTRACT No AF33(615)-3940. SHALL NOT BE EITHER RELEASED OUTSIDE THE GOVERNMENT, OR USED, DUPLICATED, OR DISCLOSED IN WHOLE OR IN PART FOR MANUFACTURE OR PROCUREMENT, WITHOUT THE WRITTEN PERMISSION O CURTISS-WRIGHT CORPORATION, EXCEPT FOR (I) EMERGENCY REPAIR OR OVERHAUL WORK BY OR FOR THE GOVERNMENT, WHERE THE ITEM OR PROCESS IS NOT OTHERWISE REASONABLY AVAILABLE TO ENABLE TIMELY PERFORMANCE OF THE WORK; OR (II) RELEASE TO A FOREIGN GOVERNMENT, AS THE INTERESTS OF THE UNITED STATES MAY REQUIRE. PROVIDED THAT IN EITHER CASE THE RELEASE, USE, DUPLICATION OR DISCLOSURE HEREOF SHALL BE SUBJECT TO THE FOREGOING LIMITATIONS. THIS LEGEND SHALL BE MARKED ON ANY REPRODUCTION HEREOF IN WHOLE OR IN PART."

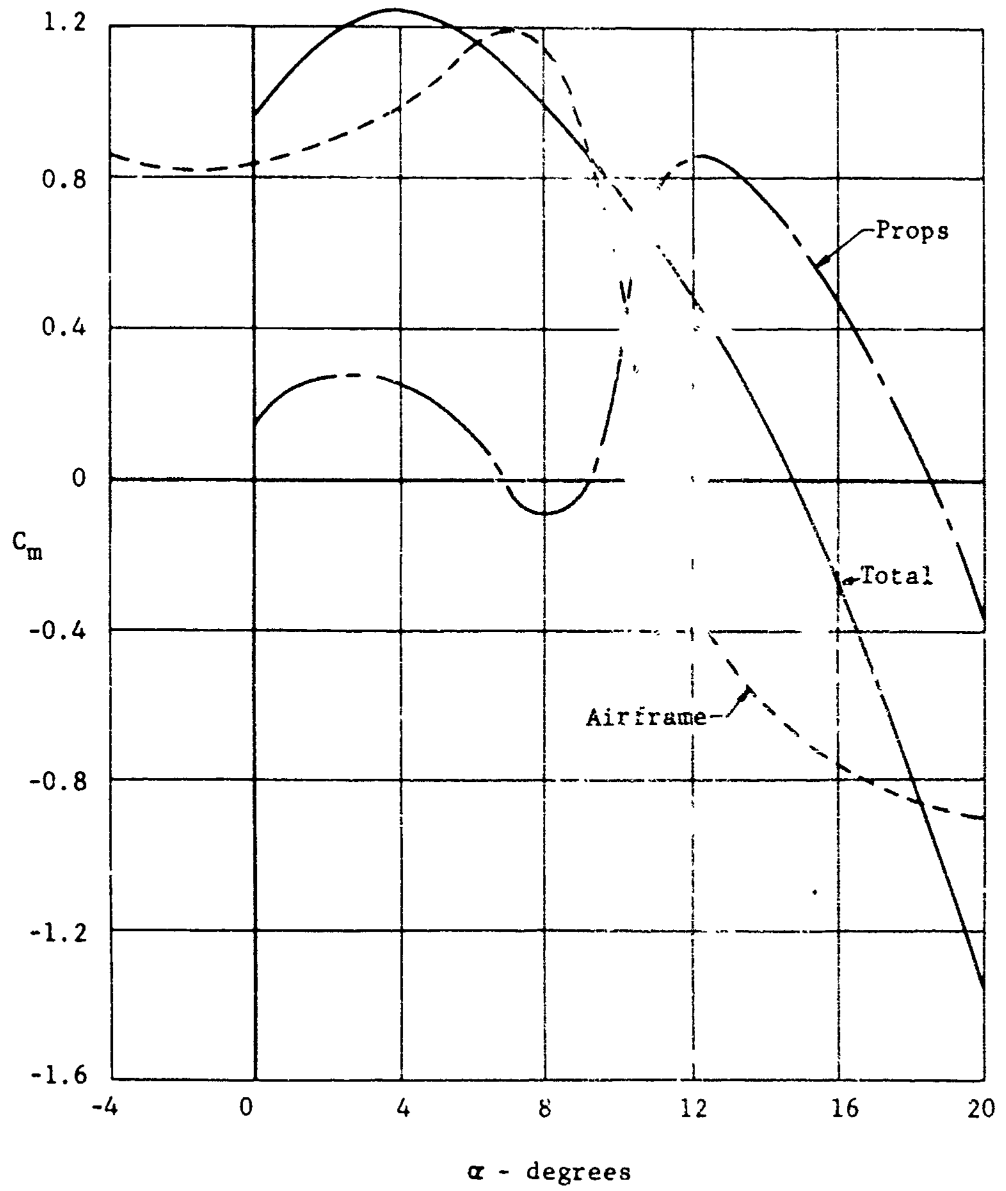

Figure 177. X-19, aircraft pitching moment characteristics at ϕ_F = 60°, including airframe and propeller contributions; c.g. = 42.8% lift chord.

FURNISHED UNDER UNITED STATES GOVERNMENT CONTRACT No. AF33(615)-1940. SHALL NOT BE EITHER RELEASED OUTSIDE THE GOVERNMENT, OR USED, DUPLICATED, OR DISCLOSED IN WHOLE OR IN PART FOR MANUFACTURE OR PROCUREMENT, WITHOUT THE WRITTEN PERMISSION OF CURTISS-WRIGHT CORPORATION, EXCEPT FOR (i) EMERGENCY REPAIR OR OVERHAUL WORK BY OR FOR THE GOVERNMENT, WHERE THE ITEM OR PROCESS IS NOT OTHERWISE REASONABLY AVAILABLE TO ENABLE TIMELY PERFORMANCE OF THE WORK, OR (ii) RELEASE TO A FOREIGN GOVERNMENT, AS THE INTERESTS OF THE UNITED STATES MAY REQUIRE; PROVIDED THAT IN EITHER CASE THE RELEASE, USE, DUPLICATION OR DISCLOSURE HEREOF SHALL BE SUBJECT TO THE FOREGOING LIMITATIONS. THIS LEGEND SHALL BE MARKED ON ANY REPRODUCTION HEREOF IN WHOLE OR IN PART.

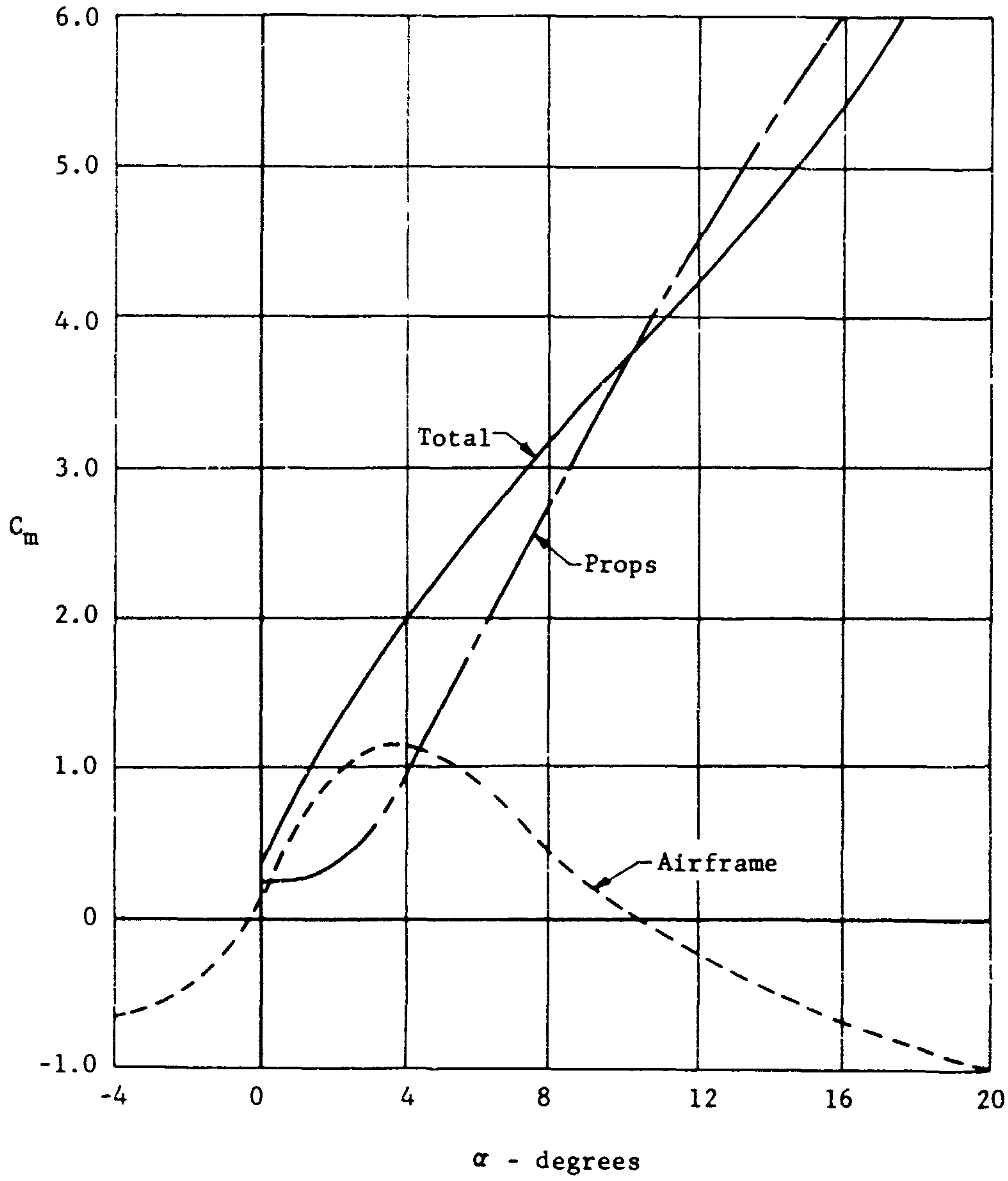

Figure 178. X-19, aircraft pitching moment characteristics at ϕ_F = 82.5%, including airframe and propeller contributions; c.g. = 42.8% lift chord.

"FURNISHED UNDER UNITED STATES GOVERNMENT CONTRACT No. AF33(615)-3940. SHALL NOT BE EITHER RELEASED OUTSIDE THE GOVERNMENT, OR USED, DUPLICATED, OR DISCLOSED IN WHOLE OR IN PART FOR MANUFACTURE OR PROCUREMENT, WITHOUT THE WRITTEN PERMISSION OF CURTISS-WRIGHT CORPORATION, EXCEPT FOR (I) EMERGENCY REPAIR OR OVERHAUL WORK BY OR FOR THE GOVERNMENT, WHERE THE ITEM OR PROCESS IS NOT OTHERWISE REASONABLY AVAILABLE TO ENABLE TIMELY PERFORMANCE OF THE WORK, OR (II) RELEASE TO A FOREIGN GOVERNMENT, AS THE INTERESTS OF THE UNITED STATES MAY REQUIRE. PROVIDED THAT IN EITHER CASE THE RELEASE, USE, DUPLICATION OR DISCLOSURE HEREOF SHALL BE SUBJECT TO THE FOREGOING LIMITATIONS. THIS LEGEND SHALL BE MARKED ON ANY REPRODUCTION HEREOF IN WHOLE OR IN PART."

ϕ_F °	J	Total C_P
20	.879	.199
40	.747	.202
60	.619	.236
80	.358	.236

The above C_P values are those required for equilibrium flight with an aircraft weight of 12,300 lbs. It should be noted that the propeller contributions to C_m were obtained merely by subtracting the "propellers off" curves from the "power on" curves so that any propeller interference effects on the airframe are included.

The effect of c.g. location is conventional, namely, the further forward the c.g. the more stable the value of C_m. The effect of increasing power at ϕ_F = 20°, 40°, 60° is slightly destabilizing; at ϕ_F = 82.5° increasing power is slightly stabilizing. No strictly theoretical estimates of propeller contributions to pitching moments in transition were made.

7. CONTROL DEFICIENCIES AND ACTIONS

a. Increased Low Speed Roll Control

Flight test experience with a number of jet-lift VTOL types had indicated a need for higher roll power, than was predicted by many of the published low speed handling qualities criteria. Results with these aircraft showed the need for providing an available roll acceleration of approximately 1.5 to 1.8 rad/sec^2. This corresponds to maximum rolling moments of 17,100 and 20,600 ft-lb, respectively, when referred to the X-19 airplane. The original design roll control moment for the X-19 was specified at 13,000 ft-lb, yielding an available roll acceleration of 1.14 rad/sec^2.

The need for higher roll power has been evidenced with jet-lift VTOL's during lateral maneuvering at low airspeeds, and appears to be a function of the airplane's roll response to lateral velocity at large sideslip angles.

Data obtained by NASA Ames with the X-14A vehicle maneuvering in the speed range from zero to 40 knots resulted in their recommending maximum roll acceleration capability of 1.8 rad/sec^2 for normal operation of fighter type aircraft. This Ames proposal seems to have merit considering recent incidents with several of the jet-lift vehicles which many investigators attribute, in part, to their low roll control powers.

Although the X-19 differs from most jet-lift VTOL types by virtue of having positive dihedral effect, it appeared desirable to provide X-19 with a roll acceleration capability of about 1.8 rad/sec^2 at low speeds pending sufficient operational flight experience. In addition, the aircraft would be capable of hovering in 90 degree cross winds of 35 knots.

On the above basis it was decided to specify a maximum roll control power of 20,000 ft. lb., yielding a maximum roll acceleration of 1.75 rad/sec^2 for a 12,300 lb. airplane.

The lateral translational speed capability, based on the value of the derivative L_V obtained from early flight test data, was estimated to be accomplished with approximately 75% of full roll control. Later flight test data revealed however that L_V was somewhat higher than the earlier results had indicated, with the result that full roll control was required to reach 35 knots lateral velocity (with the roll SAS off). With the roll SAS on, the lateral velocity capability is further reduced.

b. Yaw Control

The X-19's low hover yaw control power of 0.12 radians/sec^2 has been the subject of discussion since the design was first conceived. The argument that the aircraft is unresponsive in yaw to external disturbances (i.e. $N_V \simeq o$) and thus requires little control power to maintain a particular heading does have merit; but nevertheless, precise pilot commanded heading changes are difficult to effect. This is due to the low yaw damping as well as the low control power. The time constant in yaw (inertia/damping) is on the order of 14 seconds, thus giving an acceleration control rather than the preferred rate control. No problems arose during flight testing that could be attributed to the above deficiencies. It is recognized, however, that most of the flight testing was conducted under favorable calm air weather conditions.

While retaining the same tandem configuration there are a number of ways in which to improve the yaw control system. However, none of these measures had been enacted at the time of the project termination. They are:

(1) Increase propeller blade angle excursions at the expense of running high powers on the nacelle gear-boxes. (Very limited improvement)

(2) Increase forward and aft nacelle "toe-in" at the expense of some lift loss and the necessity for a new transition tilt schedule. (Very limited improvement).

(3) Provide differential fore and aft tilting of the port and starboard propellers. This method seems promising and the numerous analyses conducted confirmed that it is a feasible solution. It is indeed the only one which would comply with the yaw angular displacement requirement of AGARD 408 and possibly that of MIL-H-8501A.

(4) Install a yaw damper. This would result in: a lower time constant in yaw (the desirable rate control system) as well as compliance with the yaw damping requirement of AGARD 408 and MIL-H-8501A. The addition of some form of yaw damper to the existing system (C.P. = .12 rad/sec^2) would afford some improvement but a control power increase as well is highly desirable.

c. Height Control

With the original X-19 height control system, propeller thrust response to power lever commands was quite slow. This resulted in pilot induced aircraft height oscillations during one particular flight. However, it never did produce overly adverse pilot criticism. The slow response was a result of the thrust being developed downstream of the significant time lag caused by the engine propeller dynamics. Specifically, a power lever command resulted in the following sequence of events:

(1) A change in gas producer speed,

(2) A change in engine torque,

(3) A change in propeller speed,

(4) A change in propeller blade angle (and hence thrust) through the propeller speed governor.

The objective of the modified system was to provide faster thrust response with a minimum of modification. This was achieved by introducing an appropriate power lever signal downstream of the engine-propeller lag, namely at the input to the propeller speed governor. This signal is in addition to the already existing command to the engine. This addition to the system was called an "anticipator".

A comprehensive fixed base analog simulation was performed, both open and closed loop, to determine the optimum characteristics of the anticipator and hence the whole height control system.

The optimum anticipator transfer function was determined as:

$$\frac{N(S)}{\theta(S)} = -\frac{K_\theta S}{S + 1/\tau}$$

where $\bar{N}$ is the anticipator signal

θ is the power lever position

K_θ is the anticipator gain with the units of $\frac{\text{r.p.m. (propeller)}}{\text{deg (power lever)}}$

τ is the anticipator wash-out time constant. The value of τ governs the rate at which the anticipator signal is "washed-out" as a function of time.

The optimum values for these parameters were found to be: K_θ = 35 r.p.m./deg. and τ = 0.5 sec. Figure 179 shows a comparison between thrust response to a step power lever input for the modified system with the above values of K_θ, τ, and for the original system. Upon observation of the thrust response with these anticipator settings, one may query the reason for the large overshoot and the relatively poor damping. It is emphasized that this system was described as "optimum" by three experienced evaluation pilots on the flight simulator. The hardware item however included the provision for independent adjustment of the two parameters.

Unfortunately, it is not known how precisely the flight hardware item duplicated the desired characteristics.

The available data indicated that the modified system had the desired characteristic, see flight test results section 12.

d. Miscellaneous

It is mentioned briefly that during the course of flight testing the control stick breakout forces were changed on a number of occasions at the pilot's request. These changes were felt to be a part of the pilot's learning processes in the airplane and not necessarily because of initial deficiencies.

8. PROPELLER POWER PENALTIES DUE TO CONTROL INPUT DEVIATIONS

A considerable effort was expended in the area of propeller controls and alignment. Several tests were run in the tie-down rig to establish rigging and alignment procedures. The final technique which evolved resulted in alignments between the coordinator, nacelle gain changer, and propeller, to be accomplished at the cruise tilt angle. The reason for this was that nacelle gain is large at the cruise tilt angle, see Figure 168. Therefore any alignment error introduced at this point would be diminished at the higher tilt angles.

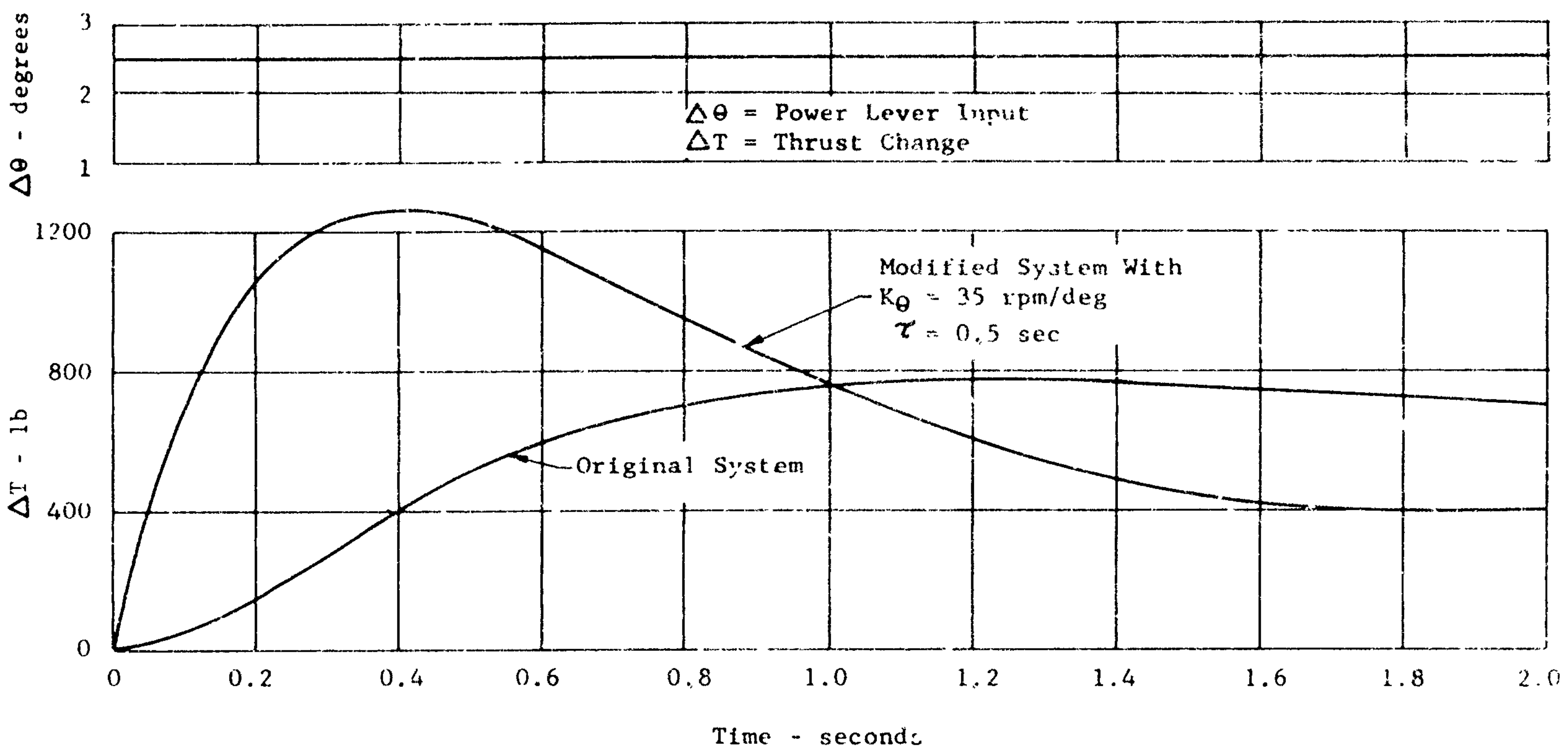

Figure 179. X-19, time history of hover thrust response to a step power lever input, original and modified system.

Alignment tests fell into two categories. Those involving control deflections, and those involving linkage at neutral control position. In general, the tests involving control deflections indicated few problems. The propeller-to-stick gearing was relatively close to that required, at all of the tilt angles tested. In cruise, it was found that control deflections induced no propeller blade angle changes, thus indicating the proper phaseout of the propeller. There were indications of small amounts of sticking which appeared as scatter in the results. However, the normal vibrations of the aircraft in operation presumably eliminated this characteristic, as the pilot always had response to small stick deflections.

The second part of the testing appeared to yield less satisfactory results. This testing consisted of determining the absolute blade angle on each propeller for neutral stick position as a function of tilt angle. The requirements are that the two front and the two rear blade angles of the propeller always be equal in magnitude. However, the difference between the front and rear propeller blade angles must equal the auto-trim schedule shown in Figure 214. It was found that the auto-trim schedule was reasonably close at the high tilt angles, and was generally too negative at tilt angles below $\phi_F = 40^\circ$. It was shown that this was the result of the nacelle gain change linkage deviating from the design schedule shown in Figure 168. This would have introduced some nose down moment. However, it would not have been a control problem as the moment would have been small. Also, this was correctable through the use of the pilot manual trim button. It would however have represented a torque imbalance in the cruise mode, requiring corrective action by the pilot, again through use of the pilot manual trim button.

This test also indicated that left and right side propeller blade angles were not symmetrical. At the high tilt angles this was a small effect. However the lateral deviation of blade angle grew as cruise tilt angle was approached. There was always a question as to how large this deviation was. The test was accomplished without the benefit of normal aircraft vibration. It was felt that some of the rough points would be washed out under flight conditions. However, the general trend could not be overlooked. For this reason, the lateral trim devices were installed. These permitted the pilot to adjust lateral blade angle deviations by monitoring a differential torque indicator. Once again, it appeared that the nacelle gain changer might be at fault. Some studies had been initiated to establish the alignment restrictions upon the gain linkage. It was felt that a large portion of this problem could be eliminated through more careful alignment procedures in this mechanism.

The significance of these problems can be reasonably demonstrated. First of all there appeared to be few problems associated with the control deflections. As the tested excursions were close to the design schedule, one did not anticipate unusual deviations from the control power or the loads throughout the system.

The lateral deviation does not represent much of a problem at the high tilt angles either, for the following reason. Any lateral deviation which might exist would have been sensed by the pilot as a moment about the center of gravity. Consequently, he would correct the motion through a stick deviation. Thus the effect of either a lateral or longitudinal (auto-trim) deviation is to shift the stick and pedals from their predetermined position. The loads throughout would then be consistent with the predicted values. If for some reason the pilot requires a full stick or pedal deflection, it is possible the control moment would differ from the prescribed value by the initial stick deviation. It is conceivable that deviations in the loads could result from this. However, in the flying accomplished throughout the program, it was found that little stick or pedal deviation actually occurred about an equilibrium position. As this was the case, from hover to about $\phi_F = 60°$, it can be concluded that alignment problems in this regime were of small proportions.

The region from about $\phi_F = 50^o$ down to cruise was the one which generated the most concern with respect to the control system deviation. As the aircraft did not fly in this regime one cannot discuss "actual problems." Instead some comments will be made concerning what the problems might have been. It was pointed out that lateral and longitudinal deviations in blade angle grew as the tilt angle approached cruise. It was further pointed out that the pilot had available a lateral and longitudinal trim device for use in eliminating the uncalled for moments. The policy formulated for flight in this regime was to approach cautiously, so as not to be caught unaware by an upsetting moment. This was a conservative approach, inasmuch as the upsetting moments at the low tilt angles are small. In cruise the pitch and roll moments are essentially zero.

Of greater concern was the torque distribution. It was recognized that the pilot would concentrate on controlling his flight path. The torque distribution would fall out as required, in order to meet this requirement. As the tilt angle approaches cruise, it was found that blade angle deviations on the order of two degrees might be expected. This was found from tie-down rig tests.

What this means in torque is as follows: Assume that one of the propellers is two degrees higher in blade angle than the others. At intermediate cruise speeds, a propeller absorbs about 300 horsepower per degree of blade angle. Assume further that the cruise condition requires a total of 1600 shaft horsepower. If properly aligned, each propeller would absorb 400 horsepower. In this case however, the off propeller would want to absorb 1000 horsepower. This cannot exist as the aerodynamic torque would be greater than the engine torque. The system would slow down, triggering the governor circuit, and the collective blade angle would be decreased sufficiently to make the aerodynamic torque equal to 1600 horsepower at the governed R.P.M. In this case the final distribution of torque would consist of three propellers at 250 horsepower and the overloaded propeller at 850 horsepower. For this particular alignment, the governor assures that the overloaded propeller absorbs three-fourths, rather than all of the blade angle overload.

It is for numbers of this order that the longitudinal and lateral trim switches were installed. The pilot is required to monitor his torque distribution instruments. By proper manipulation of the trim switches he can equalize the torque distribution and preserve the life of the transmission components.

The major problem therefore, was that of torque distribution. The continued efforts to solve the nacelle gain change alignments would have eliminated any concern for the control problem. Until that solution was obtained however, the pilot would have been obligated to closely monitor his instruments for torque equalization.

REFERENCES

41. Low Speed Wind Tunnel Tests of a 0.12 Scale Model of the Curtiss-Wright M-200 VTOL Airplane to Evaluate Longitudinal, Lateral and Directional Stability Characteristics, North American Aviation, Inc., Columbus Division, Report No. NA62H-719, October 1962, (NACAL No. 93).

42. Wind Tunnel Tests of Three Curtiss-Wright Propellers from 0 to 180 Degrees, University of Maryland Test No. 418, September 196[illegible].

43. Curtiss-Wright Corporation, Model X-200T Tandem, Front and Rear Propeller -Nacelle- Wing Characteristics in the Presence of the Fuselage, MIT Wind Tunnel Report No. 1003, October 1960.

44. P. F. Yaggy & F. Rogallo, A Wind Tunnel Investigation of Three Propellers Through an Angle of Attack Range from 0° to 85°, NASA TND-318, May 1960.

Unclassified

Security Classification

DOCUMENT CONTROL DATA - R&D

(Security classification of title body of abstract and indexing annotation must be entered when the overall report is classified)

1 ORIGINATING ACTIVITY (Corporate author)

Curtiss-Wright Corporation
VTOL Systems Division
Caldwell, New Jersey

2a REPORT SECURITY CLASSIFICATION
Unclassified

2b GROUP
----

3 REPORT TITLE

THE X-19 V/STOL TECHNOLOGY - A CRITICAL REVIEW

4 DESCRIPTIVE NOTES (Type of report and inclusive dates)

Final Report

5 AUTHOR(S) (Last name first name initial)

Fluk, Harold

6 REPORT DATE May 1967	7a TOTAL NO OF PAGES 619	7b NO OF REFS 98

8a CONTRACT OR GRANT NO AF 33(615)-3940	9a ORIGINATOR'S REPORT NUMBER(S) AFFDL-TR-66-195
b PROJECT NO	
c	9b OTHER REPORT NO(S) (Any other numbers that may be assigned this report)
d	WAD R864 F

10 AVAILABILITY/LIMITATION NOTICES Each transmittal of this document outside the agencies of the U.S. Government must have prior approval of the Air Force Flight Dynamics Laboratory, V/STOL Technology Division (FDV).

11 SUPPLEMENTARY NOTES

----

12 SPONSORING MILITARY ACTIVITY

AF Flight Dynamics Laboratory (RTD)
Attn: FDV
Wright-Patterson AFB, Ohio

13 ABSTRACT This report contains a condensed description of the X-19 V/STOL Technology. The broad categories discussed include in Section I a review of the developments leading up to the X-19 program. Sections II through VI are devoted entirely to the propellers and the considerations involved in design. The radial force principle is postulated in Section II. Interference effects on the wings due to the propellers are discussed in Section III. The propeller aerodynamic design in hover and cruise is presented in Section IV. Section V is devoted to the structure and control mechanisms of the propeller. Section VI relates to the use of propellers as in airplane control device. The tandem wing principle is discussed in Section VII, covering stability, control, and drag. Section VIII is devoted solely to ground effects. The wind tunnel research activity leading up to the X-19 is presented in Section IX. The structural loads in hover, transition and cruise are discussed in Section X. Section XI presents information pertinent to landing procedures in hover or cruise in the event of power failure. A summary of the flight test program is given in Section XII, including aircraft and hardware performance characteristics. Finally, Section XIII is devoted to a general discussion and assessment of the aircraft's unorthodox features.

DD FORM 1 JAN 64 1473

Unclassified

Security Classification

Security Classification

14 KEY WORDS	LINK A		LINK B		LINK C	
	ROLE	WT	ROLE	WT	ROLE	WT
X-19 V/STOL Technology						
Radial Force Propeller						
Propeller - Airplane Control						
Tandem Wing Concept						
Tilting Propellers						
Flight Test Results of X-19						
Wing - Propeller Interference Effects						
Wind Tunnel Experiments of X-19						
Power Transmission System						
Utility Transport						

INSTRUCTIONS

1. ORIGINATING ACTIVITY: Enter the name and address of the contractor, subcontractor, grantee, Department of Defense activity or other organization *(corporate author)* issuing the report.

2a. REPORT SECURITY CLASSIFICATION: Enter the overall security classification of the report. Indicate whether "Restricted Data" is included. Marking is to be in accordance with appropriate security regulations.

2b. GROUP: Automatic downgrading is specified in DoD Directive 5200.10 and Armed Forces Industrial Manual. Enter the group number. Also, when applicable, show that optional markings have been used for Group 3 and Group 4 as authorized.

3. REPORT TITLE: Enter the complete report title in all capital letters. Titles in all cases should be unclassified. If a meaningful title cannot be selected without classification, show title classification in all capitals in parenthesis immediately following the title.

4. DESCRIPTIVE NOTES: If appropriate, enter the type of report, e.g., interim, progress, summary, annual, or final. Give the inclusive dates when a specific reporting period is covered.

5. AUTHOR(S): Enter the name(s) of author(s) as shown on or in the report. Enter last name, first name, middle initial. If military, show rank and branch of service. The name of the principal author is an absolute minimum requirement.

6. REPORT DATE: Enter the date of the report as day, month, year; or month, year. If more than one date appears on the report, use date of publication.

7a. TOTAL NUMBER OF PAGES: The total page count should follow normal pagination procedures, i.e., enter the number of pages containing information.

7b. NUMBER OF REFERENCES: Enter the total number of references cited in the report.

8a. CONTRACT OR GRANT NUMBER: If appropriate, enter the applicable number of the contract or grant under which the report was written.

8b, 8c, & 8d. PROJECT NUMBER: Enter the appropriate military department identification, such as project number, subproject number, system numbers, task number, etc.

9a. ORIGINATOR'S REPORT NUMBER(S): Enter the official report number by which the document will be identified and controlled by the originating activity. This number must be unique to this report.

9b. OTHER REPORT NUMBER(S): If the report has been assigned any other report numbers *(either by the originator or by the sponsor)*, also enter this number(s).

10. AVAILABILITY/LIMITATION NOTICES: Enter any limitations on further dissemination of the report, other than those imposed by security classification, using standard statements such as:

(1) "Qualified requesters may obtain copies of this report from DDC."

(2) "Foreign announcement and dissemination of this report by DDC is not authorized."

(3) "U. S. Government agencies may obtain copies of this report directly from DDC. Other qualified DDC users shall request through

____."

(4) "U. S. military agencies may obtain copies of this report directly from DDC. Other qualified users shall request through

____."

(5) "All distribution of this report is controlled. Qualified DDC users shall request through

____."

If the report has been furnished to the Office of Technical Services, Department of Commerce, for sale to the public, indicate this fact and enter the price, if known.

11. SUPPLEMENTARY NOTES: Use for additional explanatory notes.

12. SPONSORING MILITARY ACTIVITY: Enter the name of the departmental project office or laboratory sponsoring *(paying for)* the research and development. Include address.

13. ABSTRACT: Enter an abstract giving a brief and factual summary of the document indicative of the report, even though it may also appear elsewhere in the body of the technical report. If additional space is required, a continuation sheet shall be attached.

It is highly desirable that the abstract of classified reports be unclassified. Each paragraph of the abstract shall end with an indication of the military security classification of the information in the paragraph, represented as *(TS)*, *(S)*, *(C)*, or *(U)*.

There is no limitation on the length of the abstract. However, the suggested length is from 150 to 225 words.

14. KEY WORDS: Key words are technically meaningful terms or short phrases that characterize a report and may be used as index entries for cataloging the report. Key words must be selected so that no security classification is required. Identifiers, such as equipment model designation, trade name, military project code name, geographic location, may be used as key words but will be followed by an indication of technical context. The assignment of links, rules, and weights is optional.

Unclassified
Security Classification